ISSN 2313–5891 (Online)
ISSN 2304–974X (Print)

Ukrainian Food Journal

Volume 15, Issue 2
2026

Kyiv **Київ**

2026

Ukrainian Food Journal is an international scientific periodical journal that publishes articles by specialists in the field of food science, engineering and technology, chemistry, economics and management.

Ukrainian Food Journal – міжнародне наукове періодичне видання для публікації результатів досліджень фахівців у галузі харчової науки, техніки та технології, хімії, економіки і управління.

Ukrainian Food Journal is abstracted and indexed by scientometric databases:

Ukrainian Food Journal індексується наукометричними базами:

Index Copernicus (2012)
EBSCO (2013)
Google Scholar (2013)
UlrichsWeb (2013)
CABI full text (2014)
Online Library of University of Southern Denmark (2014)
Directory of Open Access scholarly Resources (ROAD) (2014)
European Reference Index for Humanities and Social Sciences (ERIH PLUS) (2014)
Directory of Open Access Journals (DOAJ) (2015)
InfoBase Index (2015)
Chemical Abstracts Service Source Index (CASSI) (2016)
FSTA (Food Science and Technology Abstracts) (2018)
Web of Science (Emerging Sourses Citaton Index) (2018)
Scopus (2022)

Ukrainian Food Journal включено у перелік наукових фахових видань України з технічних наук, категорія А (Наказ Міністерства освіти і науки України № 358 від 15.03.2019)

Editorial office address:

National University
of Food Technologies
68 Volodymyrska str.
Kyiv 01601, **Ukraine**

Адреса редакції:

Національний університет
харчових технологій

вул. Володимирська, 68
Київ 01601, **Україна**

e-mail: **ufj_nuft@meta.ua**

© NUFT, 2026

© НУХТ, 2026

Ukrainian Food Journal is an open-access, peer-reviewed scientific journal published by the National University of Food Technologies (Kyiv, Ukraine). The journal accepts original research articles, short communications, review papers, news, and literature reviews across all areas of food science, including food technology, engineering, nutrition, food chemistry, economics, and management.

Manuscripts must present novel findings, demonstrate a clear connection to food science, and be of broad interest to the international scientific community.

Topics covered by the journal include:

- Food engineering
- Food chemistry
- Food microbiology
- Food quality and safety
- Food processes
- Automation of food processes
- Food packaging
- Economics
- Food nanotechnologies
- Economics and management

Please note that the journal does not consider the following types of submissions:

Articles containing medical claims or involving studies on humans or animals, as these topics fall outside the journal's scope.

Articles lacking scientific novelty or significance, including those focused solely on solving routine practical or engineering problems.

Ukrainian Food Journal is published quarterly, with four issues released each year in March, June, September, and December.

Reviewing a Manuscript for Publication

Upon receiving a manuscript, the Editor-in-Chief first evaluates its content to ensure it aligns with the journal's scope. The Editor-in-Chief also reviews the article's formatting, style, and illustrative materials, may offer recommendations for improvement, and decides whether to forward the manuscript for peer review.

All manuscripts submitted to the Ukrainian Food Journal undergo a double-blind peer review process. Each submission is reviewed by at least two independent experts: one member of the Editorial Board and one reviewer who is external to both the Editorial Board and the publisher. This ensures an objective and balanced evaluation of the manuscript's scientific quality.

The full Guide for Authors is available on our website:

http://ufj.nuft.edu.ua

International Editorial Board

Editor-in-Chief:

Olena Stabnikova, Dr., *National University of Food Technologies, Ukraine*

Members of Editorial Board:

Sonia Amariei, PhD, Prof., *University "Ştefan cel Mare" of Suceava, Romania*
Eirin Marie Skjøndal Bar, PhD, Assoc. Prof., *Norwegian University of Science and Technology, Trondheim, Norway*
Yurii Bilan, PhD, Prof., *Tomas Bata University in Zlin, Czech Republic*
Kirsten Brandt, PhD, *Newcastle University, United Kingdom*
Moisés Burachik, PhD, *Institute of Agricultural Biotechnology of Rosario* (*INDEAR*), *Bioceres Group, Rosario, Argentina*
Stanka Damianova, PhD, Prof., *Ruse University "Angel Kanchev", branch Razgrad, Bulgaria*
Yuliya Dzyazko, PhD, Prof., *Institute of General and Inorganic Chemistry of the National Academy of Sciences of Ukraine*
Yun-Hwa Peggy Hsieh, PhD, Prof. Emerita, *Florida State University, USA*
Lelieveld Huub, PhD, *Global Harmonization Initiative Association, The Netherlands*
Sheila Kilonzi, PhD, *Karatina University, Kenya*
Jasmina Lukinac, PhD, Assoc. Prof., *University of Osijek, Croatia*
Dora Marinova, PhD, Prof., *Curtin University Sustainability Policy Institute, Curtin University, Australia*
Rana Mustafa, PhD, *Global Institute for Food Security, University of Saskatchewan, Canada*
Godwin D. Ndossi, PhD, Prof., *Hubert Kairuki Memorial University, Dar es Salaam, Tanzania*
Umezuruike Linus Opara, PhD, Prof., *Stellenbosch University, Cape Town, South Africa*
Semih Otles, PhD, Prof., *Ege University, Turkey*
Octavio Paredes-López, PhD, Prof., *The Center for Research and Advanced Studies of the National Polytechnic Institute, Guanajuato, Mexico*
Tetiana Pirog, PhD, Prof., *National University of Food Technologies, Ukraine*
Cristina Popovici, PhD, Assoc. Prof., *Technical University of Moldova*
Agota Giedrė Raišienė, PhD, *Lithuanian Institute of Agrarian Economics, Lithuania*
Egon Schnitzler, PhD, Prof., *State University of Ponta Grossa, Ponta Grossa, Brazil*
Oleksandr Shevchenko, PhD, Prof., *National University for Food Technologies, Ukraine*
Cristina Luisa Miranda Silva, PhD, Assoc. Prof., *Portuguese Catholic University – College of Biotechnology, Portugal*
Stefan Stefanov, PhD, Prof., *University of Food Technologies, Bulgaria*
Yordanka Stefanova, PhD, Assist. Prof., *University of Plovdiv "Paisii Hilendarski", Bulgaria*
María S. Tapia, PhD, Prof., *Central University of Venezuela, Caracas, Venezuela; COR MEM of the Academy of Physical, Mathematical and Natural Sciences of Venezuela*
Bảo Thy Vương, PhD, *Mekong University, Vietnam*

Managing Editor:

Oleksii Gubenia, PhD, Assoc. Prof., *National University of Food Technologies, Ukraine*

Contents

Food Technology……..……..…….. 271

Tatiana Capcanari, Eugenia Covaliov, Nikoleta Țurea, Oxana Radu, Violina Popovici
Fermentation-assisted valorisation of hemp-derived ingredients for functional pasta development…… 271

Gaolin Hu, Tamara Nosenko, Serhii Stankevych, Tetiana Ovsiannikova
Influence of membrane lipid composition on the stability of encapsulated DNA under oxidative stress…….. 293

Atipan Saimmai, Sutanate Saelao, Aem Nuylert, Suppasil Maneerat
ε-Poly-L-lysine extends the ambient shelf life of pickled Ma-muang Bao by suppressing yeast growth…….. 308

Olena Stabnikova, Andrii Marynin, Viktor Stabnikov, Roman Svyatnenko, Valeriy Demchenko
Plant essential oils for food shelf-life extension and active packaging systems……... 323

Loredana-Mariana Huțuțui, Sonia Amariei, Dana Huțu
Polyphenolic phytochemical compounds from *Sambucus nigra* L. and *Rubus fruticosus* L. for food freshness indicators…….. 361

Sergij Shulga, Oksana Shulga
Modification of potato starch by acylation with acetyllactic acid chloride for food and packaging applications…….. 390

Sutapa Laha, Annalakshmi Chatterjee
Active coating based on longan seed starch and pomelo peel pectin for extending shelf life of tomatoes……. 401

Iryna Huzova, Diana Kindzera, Oleksandr Shevchenko, Oleksandr Bessarab
Energy-efficient saturation and drying of pumpkin pieces…… 418

Galyna Khomych, Tetiana Lebedenko, Galina Krusir, Lali Elanidze
Enhancement of bakery product quality using chokeberry processing by-products…….. 436

Microbiology, Biotechnology..... 455

Oksana Skrotska, Pavlo Holubiev
Biological synthesis of copper nanoparticles using plants, microorganisms and other natural resources..... 455

Iryna Kovshar, Viktor Udymovych, Viktor Stabnikov
Utilization of plant biomass and agro-industrial waste for low-cost biocementation processes..... 503

Hanna Bondar, Viktoriia Krasinko
Iron accumulation in yeast under different cultivation conditions..... 518

Olena Gudzenko, Liudmyla Varbanets, Liudmyla Butsenko, Lidiia Pasichnyk
Soil-derived *Bacillus* strains producing proteolytic enzymes for food industry applications..... 532

Processes and Equipment and Control Systems..... 550

Andriy Pogrebnyak, Iryna Perkun, Volodymyr Pogrebnyak, Maxim Korneyev, Svitlana Haponenko, Yehor Beliaiev, Olena Yudina
Mathematical modeling of water-polymer jet cutting for frozen food products..... 550

Economics and Management..... 566

Ali Kılıç, Müge Hendek, Damla Uslu
Bibliometric analysis of artificial intelligence applications in food quality control and safety..... 566

Instructions for authors..... 588

Fermentation-assisted valorisation of hemp-derived ingredients for functional pasta development

Tatiana Capcanari, Eugenia Covaliov, Nikoleta Țurea, Oxana Radu, Violina Popovici

Technical University of Moldova, Chisinau, Republic of Moldova

Keywords:

Hemp
Cannabis sativa
Seed
Meal
Inflorescence
Lactic acid
Fermentation
Functionality
Pasta
Bioactive
Antioxidant

Article history:

Received 29.10.2025
Received in revised form 27.02.2026
Accepted 30.06.2026

Corresponding author:

Tatiana Capcanari
E-mail: tatiana.capcanari@toap.utm.md

DOI:
10.24263/2304-974X-2026-15-2-3

Abstract

Introduction. Hemp seed meal and hemp inflorescence are underutilised by-products of industrial hemp (*Cannabis sativa* L.) processing, rich in bioactive compounds yet hampered by antinutritional factors that limit their direct use in food formulation. This study aimed to evaluate lactic acid bacteria fermentation as a strategy for their valorisation and to develop functional pasta enriched with the optimally fermented substrates.

Materials and methods. Hemp seed meal and hemp inflorescence were fermented separately with *Lactiplantibacillus plantarum*, *Lacticaseibacillus casei*, and *Streptococcus thermophilus* at 35 °C for 22 h. Phytic acid, condensed tannins, total polyphenol content (TPC), total flavonoid content (TFC), and antioxidant activity (DPPH, ABTS) were determined before and after fermentation. Based on these results, *L. plantarum* was selected for pasta development. Two product series were prepared by replacing wheat flour with fermented hemp seed meal (PM) or fermented hemp inflorescence (PI) at substitution levels of 5-30% and were evaluated for technological quality, CIELAB colourimetric parameters, bioactive composition, and sensory acceptability.

Results and discussion. *L. plantarum* achieved the greatest reduction in phytic acid (79.9% in hemp seed meal; 76.1% in hemp inflorescence) and condensed tannins (63.1%; 65.0%), while generating the highest gains in TPC, TFC, and antioxidant activity. In the finished pasta, the content of bioactive substances increased dose-dependently, with the PI series reaching substantially higher values than PM at matching substitution levels. Technological parameters remained within acceptable limits up to 20% substitution. CIELAB analysis confirmed progressive darkening in both series (ΔE up to 55.92 in PI30). Sensory evaluation identified 5-20% as the most acceptable range for the PM series and 5-15% for the PI series.

Conclusions. Fermentation with *L. plantarum* effectively reduced antinutritional compounds and enhanced the bioactive profile of both hemp-derived substrates. Incorporation at 5–20% substitution produced functional pasta combining measurable nutritional enrichment with acceptable technological quality and consumer acceptability, supporting circular bioeconomy objectives through valorisation of hemp processing residues.

Introduction

Reducing the volume of agri-food residues generated along the production chain has become one of the defining challenges of a sustainable food system. According to the Food and Agriculture Organisation of the United Nations, around 14% of the food produced worldwide is lost between harvest and retail, a figure that does not even account for additional losses that occur once raw materials enter processing facilities (FAO, 2019). At the consumer end of the chain, the United Nations Environment Programme estimates a further 19% of available food is wasted at retail, food service, and household levels, bringing the combined share of food lost or wasted globally to roughly a third of total production (UNEP, 2024). The circular bioeconomy approach, which treats processing residues not as waste but as a starting point for new ingredients, has gained particular traction in the food industry, since converting such residues into functional ingredients can simultaneously reduce environmental burden and create added economic value (Marcelli et al., 2025; Pal et al., 2024; Shilev et al., 2025; Stabnikova et al., 2023a, b).

Industrial hemp (*Cannabis sativa* L.) is a clear example of a crop whose processing still leaves considerable biomass unexploited. The protein content in hemp seeds is rather high being 55.4±0.26%, fat content – 14.5±0.13% which makes it good raw material for pressing oil (Blazhenko et al., 2024). After cold-pressing hemp seeds for oil, a solid residue, commonly referred to as hemp seed meal or hemp seed cake, remains, retaining most of the seed's original protein, fibre, and mineral content (Capcanari et al., 2023, 2025). However, it remains primarily directed toward animal feed rather than human food applications (Hossain et al., 2026; Rajasekhar et al., 2021). A second, even less studied stream is hemp inflorescence, generated as a threshing residue wherever the plant is cultivated for fibre, seed, or cannabinoid extraction. Only in recent years this material has begun to be examined as a potential novel food and a source of flavonoids and other phenolic compounds, rather than being discarded as field residue (Spampinato et al., 2024; Spano et al., 2022).

The nutritional exploitation of both materials, however, is constrained by the presence of antinutritional compounds typical of plant-derived raw materials. Phytic acid and condensed tannins both bind divalent and trivalent minerals, as well as dietary proteins, forming complexes that resist digestion and reduce the bioavailability of these nutrients once consumed (Arsov et al., 2024; Salim et al., 2023). This limitation has so far restricted the direct incorporation of hemp seed meal and hemp inflorescence into food matrices at nutritionally meaningful levels, since simply adding the raw materials would also add their antinutrient load.

Fermentation with lactic acid bacteria offers a way around this constraint without requiring specialised equipment or significant investment. The acidification produced by the bacteria activates endogenous and microbial phytases, while bacterial esterases and glycosidases release polyphenols otherwise bound to the cell wall matrix, a combination that has been shown to lower antinutrient content while raising bioactive compound levels and antioxidant activity across a range of plant-based substrates (Erem and Kilic-Akyilmaz, 2024). The extent of these changes depends strongly on the bacterial strain and the substrate involved, which is why a comparative screening across strains is a necessary step before a fermented material can be confidently used in food formulation.

Pasta is widely consumed across different cultures and age groups, possesses a long shelf life, and its manufacturing process readily accommodates the incorporation of dry powdered ingredients without requiring major modifications to conventional production lines, making it a practical carrier for delivering bioactive compounds from agri-food by-products without disrupting established consumer habits (Carpentieri et al., 2022). For the same reasons, pasta has become one of the most frequently studied matrices for the valorisation of agro-industrial residues, although the technological and sensory outcomes of such fortification depend strongly on the type and proportion of by-product used.

The aim of the present study was to evaluate the effect of fermentation with three lactic acid bacteria strains, *Lactiplantibacillus plantarum, Lacticaseibacillus casei*, and *Streptococcus thermophilus*, on the antinutritional and bioactive profile of hemp seed meal and hemp inflorescence, to select the most efficient strain based on these results, and to develop and characterise pasta enriched with the resulting fermented ingredients at increasing substitution levels.

Materials and methods

Materials and fermentation procedure

Hemp seed meal (Figure 1a) and hemp inflorescence (Figure 1b) were obtained from the Association of Hemp Cultivators, Breeders and Processors of the Republic of Moldova (ACAPC), harvest 2025, within the framework of a collaborative study on the valorisation of hemp-derived food residues in the context of the circular bioeconomy. Both raw materials were accompanied by quality certificates confirming compliance with toxicological and microbiological safety requirements. Prior to use, the materials were ground to a fine powder and sieved through a 250 μm mesh sieve (ROTH Rotilabo, Germany), packed in airtight containers, and stored under light-protected conditions until further analysis.



a **b**

Figure 1. Hemp seed meal (a) and hemp inflorescence (b)

Three lactic acid bacteria strains were used as starter cultures: *Lactiplantibacillus plantarum* (probiotic supplement, 20 × 10^9 CFU/capsule, DRcaps, BioForm), *Lacticaseibacillus casei* (probiotic culture, 10^{11} CFU/g, powder, VitaMatic), and *Streptococcus thermophilus*, obtained from a commercial vegan yoghurt starter culture (Maiele Lactice Vegan Iaurt, Vivo).

Because hemp seed meal and hemp inflorescence powder are inherently low in free fermentable carbohydrates, an exogenous glucose source was added to provide the lactic acid bacteria with a readily metabolizable carbon source sufficient to support acidification toward the target pH. A pharmaceutical-grade sterile glucose solution for infusion (10%, w/v; 100 mg/mL, 250 mL) was used to obtain a final glucose concentration of 1% (w/v) in each fermentation mixture. The liquid phase volume was adjusted based on each raw material's water absorption capacity to ensure adequate hydration and homogeneous mixing. Accordingly, the hemp seed meal substrate was prepared using 400 g of powder and 600 mL of liquid phase, whereas the hemp inflorescence substrate consisted of 500 g of powder and 500 mL of liquid phase.

The inoculum was prepared by rehydrating the respective bacterial preparation in 20-30 mL sterile distilled water at 35-37 °C, followed by gentle mixing and activation for 15-20 min. The target inoculation level was 10^7 CFU/g of hydrated substrate, corresponding to ½ capsule of *L. plantarum* per kg of substrate, and 0.1 g of *L. casei* powder per kg of substrate. The *S. thermophilus* inoculum was prepared from the vegan yoghurt starter culture according to the manufacturer's instructions at an equivalent concentration. The activated bacterial suspension was then added to the hydrated hemp matrix and homogenised for 1-2 min.

Fermentation was carried out at 35 °C for 22 h under controlled conditions, with pH monitored at 0, 4, 8, 12, 16, 20, and 22 h. Upon reaching the target pH of 4.5, the fermented substrates were pasteurised at 70 °C for 30 min. The pasteurised substrates were then dried to a moisture content of approximately 14.5%, comparable to that of wheat flour, and ground into a

fine powder to enable homogeneous incorporation into the flour matrix. The resulting fermented hemp-derived powder was stored at 21±2 °C until further use.

Premium-quality wheat flour (Băneasa, Romania), eggs, salt, and potable water were used to prepare pasta. Wheat flour was partially replaced with fermented hemp-derived powder at substitution levels of 5, 10, 15, 20, 25, and 30 g per 100 g total flour weight, with egg (50 g per 100 g flour) and salt (2 g per 100 g flour) kept constant across all formulations, as detailed in Table 1.

Methods

Phytic acid content. Phytate content in the hemp inflorescence and hemp seed meal samples, before and after fermentation with the three lactic acid bacteria strains (*Lactiplantibacillus plantarum, Lacticaseibacillus casei*, and *Streptococcus thermophilus*), was determined spectrophotometrically using the Wade reagent method, based on the colourimetric reaction between ferric ions and phytic acid (Zhang and Bai, 2014).

The principle of the method relies on the strong and selective affinity of phytic acid for ferric ions (Fe^{3+}). The sample is first extracted with a dilute hydrochloric acid solution to solubilise phytates, and the resulting extract is clarified by centrifugation and filtration. When the clarified extract is mixed with the Wade reagent – a solution of ferric chloride ($FeCl_3 \cdot 6H_2O$) and sulfosalicylic acid – phytic acid preferentially binds the available Fe^{3+} ions, removing them from the iron-sulfosalicylate complex responsible for the reagent's colour. As phytate concentration increases, the colour intensity of the remaining iron complex decreases proportionally. After a second centrifugation step to remove any precipitate, the absorbance of the supernatant is measured spectrophotometrically at $\lambda = 500$ nm against a distilled water blank, and the decrease in absorbance is converted to phytic acid equivalent concentration using a calibration curve built from standard phytic acid solutions. Results are expressed as mg phytic acid equivalents per 100 g dry weight (mg PA/100 g DW).

Tannin content. Tannins are polyphenolic antinutritional compounds that bind dietary proteins and minerals, thereby reducing their digestibility and bioavailability. Condensed tannin content was determined using the vanillin-HCl colourimetric method (Palacios et al., 2021). The principle of the method is based on the reaction of vanillin, under strongly acidic conditions, with the flavan-3-ol units of condensed tannins, producing a stable red-coloured chromophore. The extracted sample is mixed with an acidified vanillin reagent and incubated to allow full colour development, after which absorbance is measured spectrophotometrically ($\lambda = 500$ nm) against a reagent blank. Tannin concentration is calculated from a calibration curve constructed using a catechin standard and expressed as mg catechin per 100 g dry weight (mg CE/100 g DW).

Total polyphenol content (TPC). Total polyphenol content was determined spectrophotometrically using the Folin-Ciocalteu method (Pérez et al., 2023). The principle relies on the reduction of the phosphomolybdic-phosphotungstic acid complex contained in the Folin-Ciocalteu reagent by phenolic hydroxyl groups under alkaline conditions, producing a blue-coloured chromophore proportional to the total phenolic content of the sample. After a defined incubation period in the dark to allow colour stabilisation, absorbance was measured spectrophotometrically ($\lambda = 760$ nm) against a blank. Total polyphenol content was calculated from a calibration curve built with gallic acid as the reference standard and expressed as mg gallic acid equivalents per 100 g dry weight (mg GAE/100 g DW).

Total flavonoid content (TFC). Total flavonoid content was determined using the aluminium chloride ($AlCl_3$) colorimetric method (Shraim et al., 2021). The principle is based on the formation of a stable complex between Al^{3+} ions (in the presence of sodium nitrite and sodium

hydroxide) and the hydroxyl/keto groups of flavonoids, yielding a coloured chromophore whose intensity is proportional to flavonoid content. The extract was sequentially reacted with sodium nitrite, aluminium chloride, and sodium hydroxide solutions, and absorbance was measured spectrophotometrically (λ = 510 nm) against a blank. Total flavonoid content was calculated from a calibration curve constructed with catechin as the reference standard and expressed as mg catechin equivalents per 100 g dry weight (mg CE/100 g DW).

DPPH radical scavenging activity. Antioxidant activity was assessed by the DPPH free radical scavenging assay (Munteanu and Apetrei, 2021). The principle is based on the ability of antioxidant compounds to donate a hydrogen atom to the stable, purple-coloured DPPH (2,2-diphenyl-1-picrylhydrazyl) radical, converting it to its pale-yellow reduced form (DPPH-H) and thereby decreasing absorbance proportionally to the antioxidant activity of the sample. Absorbance was measured spectrophotometrically (λ = 515 nm) before and after reaction with the extract, against a methanol blank. Rather than expressing the result as a simple percentage of inhibition, radical scavenging activity was quantified against a Trolox calibration curve, constructed by plotting the percentage inhibition of Trolox standard solutions at known concentrations, and the results were expressed as mg Trolox equivalents per 100 g dry weight (mg Trolox/100 g DW).

ABTS radical scavenging activity. Antioxidant activity was assessed by the ABTS radical cation decolourisation assay (Munteanu and Apetrei, 2021). The principle is based on the generation of the blue-green $ABTS^{\bullet+}$ radical cation by oxidation of ABTS [2,2′-azino-bis(3-ethylbenzothiazoline-6-sulfonic acid)] with potassium persulfate; in the presence of hydrogen-donating antioxidants, the radical is reduced, and its characteristic absorbance decreases proportionally to the antioxidant capacity of the sample. Absorbance was measured spectrophotometrically (λ = 734 nm) before and after the addition of the extract. Results were calculated against a Trolox calibration curve and expressed as mg Trolox equivalents per 100 g dry weight (mg Trolox/100 g DW).

Pasta making procedure. Pasta samples were prepared using wheat flour, eggs, salt, and fermented hemp-derived ingredients as functional components. Two experimental series were developed: one based on fermented hemp seed meal (fHSM) and the other on fermented hemp inflorescence (fHI). In both series, wheat flour was partially replaced with fermented hemp material at levels of 5, 10, 15, 20, 25, and 30%, while a control sample (P0) was produced without hemp addition (Table 1).

Table 1

Formulation of pasta samples enriched with different levels of fermented hemp flour

Ingredients (g)	P0	P5	P10	P15	P20	P25	P30
Wheat flour	100.0	95.0	90.0	85.0	80.0	75.0	70.0
Fermented hemp flour*	0.0	5.0	10.0	15.0	20.0	25.0	30.0
Egg	50.0	50.0	50.0	50.0	50.0	50.0	50.0
Salt	2.0	2.0	2.0	2.0	2.0	2.0	2.0

P0 – control pasta sample prepared without hemp ingredient; P5-P30 – pasta samples containing 5-30% fermented hemp flour as partial replacement of wheat flour. *Fermented hemp flour refers to either fermented hemp seed meal (fHSM) or fermented hemp inflorescence (fHI), depending on the experimental series.

The required quantities of wheat flour and fermented hemp ingredient were first dry-mixed to ensure uniform distribution of the functional component. Eggs and salt were subsequently

added, and all ingredients were kneaded until a homogeneous dough was obtained. The dough was allowed to rest for 30 min at room temperature to promote hydration and gluten relaxation.

After resting, the dough was sheeted with a laboratory roller to achieve a uniform thickness, then cut into thin pasta strands. The prepared pasta samples were thermally processed by boiling in water until fully cooked, then cooled in cold water to halt further thermal treatment.

Colour evaluation. The colourimetric parameters of pasta samples were determined using a portable spectrophotometric colourimeter (ColorReader Max, China) operating in the CIELAB colour space. The coordinates L* (lightness), a* (redness/greenness), and b* (yellowness/blueness) were recorded at three different locations on each sample and averaged. The total colour difference (ΔE) relative to the control sample (P0) was calculated according to Equation (1):

$$\Delta E = \sqrt{(L_{sample} - L_0)^2 + (a_{sample} - a_0)^2 + (b_{sample} - b_0)^2} \quad (1)$$

where (L_0), (a_0), and (b_0) represent the colour coordinates of the control sample (Giusti et al., 2024).

Sensory evaluation. Sensory evaluation of the cooked pasta samples was conducted by a panel of 114 untrained consumers aged 18-60 years, of both genders, representative of the general public. The evaluation was conducted across multiple sessions with 15-20 participants each to ensure consistent conditions throughout the assessment. Four sensory attributes were evaluated: colour, odour, taste, and overall acceptability, using a nine-point hedonic scale anchored at 1 (dislike extremely) and 9 (like extremely).

All thirteen pasta samples were served freshly cooked at a serving temperature of 60-65 °C, consistent with the typical consumption temperature of hot main dishes, presented in coded white porcelain bowls labelled with three-digit random numbers, and offered in a randomised order to minimise carry-over and positional bias. Panellists were provided with still water and instructed to rinse their mouths between consecutive samples to minimise sensory fatigue and flavour carry-over.

The study was conducted in accordance with the ethical standards applicable to research involving human participants, and all panellists provided informed consent prior to participation.

Physicochemical and technological quality parameters of pasta. The physicochemical and technological properties of pasta samples were assessed on both dried (uncooked) and cooked products, as specified below.

Titratable acidity was determined on dried pasta samples by potentiometric titration with 0.1 N NaOH solution to an endpoint of pH 8.5, monitored with a pH meter, and expressed as degrees of acidity, corresponding to the volume in mL of 0.1 N NaOH required to neutralise the acids contained in 100 g of product.

Moisture content of dried pasta samples was determined gravimetrically by drying at 105±2 °C to constant weight and expressed as a percentage of the initial sample mass (%). Both parameters were compared against the maximum values stipulated by the Technical Regulation for bakery and pasta products in the Republic of Moldova (Technical Regulation Decision No. 775, 2007).

Optimal cooking time was determined by cooking samples in boiling water and extracting them at 15-second intervals, with up to three pieces pressed between two glass slides and visually inspected for the disappearance of the white, ungelatinized core. The time at which no white core was visible in any of the tested pieces was recorded as the optimal cooking time (AACC., 2012).

Swelling index (SI) and water absorption index (WAI) were determined by cooking 20 g of pasta in 200 mL of boiling water for the previously established optimal cooking time. After

draining, the cooked pasta was weighed (Wcd) and then dried at 105±2 °C to a constant weight (Wd). The weight of the uncooked pasta before boiling was recorded as Wr. SI and WAI were calculated according to Gull et al. (2018) using the following equations:

$$SI = \frac{Wcd - Wd}{Wd} \text{ (g } H_2O/\text{g)} \quad (2)$$

$$WAI = \frac{Wcd - Wr}{Wr} \text{ (g/100 g)} \quad (3)$$

Cooking loss (CL) was determined by evaporating the cooking water remaining after draining in an oven at 100±2 °C until a constant weight was reached. The residue was weighed and expressed as a percentage of the initial dry pasta weight, representing the total soluble solids lost into the boiling water during cooking (AACC, 2012).

Statistical analysis

All experimental determinations were carried out in triplicate, and results are expressed as mean±standard deviation (SD). Statistically significant differences among samples were assessed using one-way analysis of variance (ANOVA), with pairwise comparisons performed using Tukey's honestly significant difference (HSD) and Duncan's multiple range post hoc tests at a significance level of $p \leq 0.05$. Statistically homogeneous groups are indicated in the tables and figures by superscript letters. All analyses were performed using XLStat software (version 7.5.2, Addinsoft, Paris, France).

Results and discussion

Fermentation-induced improvement of the nutritional and functional quality of hemp-derived substrates

To evaluate the suitability of *Lactiplantibacillus plantarum*, *Lacticaseibacillus casei*, and *Streptococcus thermophilus* for the bioprocessing of hemp-derived food residues, the dynamics of active acidity (pH) were monitored throughout fermentation of the hemp inflorescence and hemp seed meal substrates. Active acidity was selected as the primary process indicator because it reflects bacterial metabolic activity in real time and directly governs the activation of endogenous and microbial enzymes that degrade antinutritional compounds, as well as the technological and microbiological stability of the final fermented matrix (Figure 2).

Among the three lactic acid bacteria evaluated, *S. thermophilus* and *L. casei* consistently displayed the fastest acidification kinetics in both hemp substrates, lowering the pH below 5.5 within the first 8 h of fermentation, whereas *L. plantarum* required a longer period to reach comparable values. This pattern is consistent with comparative trials of lactobacilli in plant-derived doughs, where *L. casei* achieved the lowest pH and the highest lactate accumulation among the three strains tested, while *L. plantarum* acidified more slowly yet displayed the highest measured phytase activity and the largest reduction in phytic acid content, indicating that acidification speed and antinutrient-hydrolysing efficiency are not necessarily coupled within the same strain (Hashemi et al., 2019). A similar dissociation between acidification speed and functional output has been reported for hemp-based matrices, where lactic acid fermentation of hemp flour with *L. plantarum* required an extended fermentation period, yet was associated with a marked increase in organic acids, polyphenols, and free amino acids over the fermentation course (Di Biase et al., 2025).

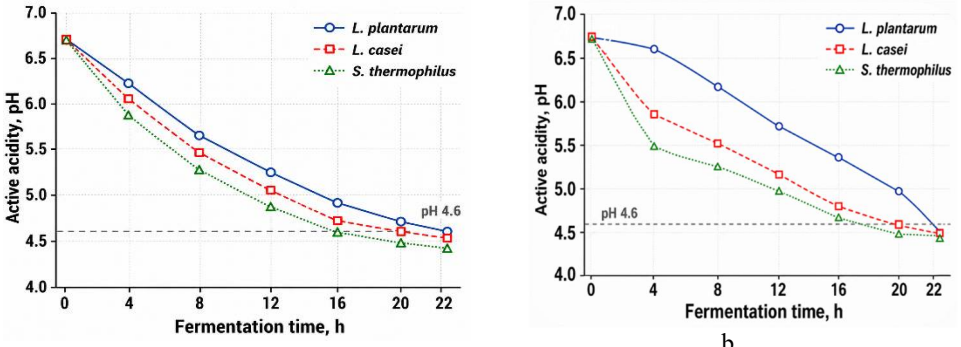

Figure 2. Dynamics of active acidity (pH) during the fermentation of (a) hemp seed meal and (b) hemp inflorescence substrates

The progressive decline in pH toward 4.5 across both matrices is functionally relevant at two complementary levels. From a food-safety perspective, an equilibrium pH at or below 4.6 is the internationally recognised boundary below which *Clostridium botulinum* spores cannot germinate or produce toxin, and regulatory practice requires that finished equilibrium pH values for acidified foods not exceed 4.6 (U.S. FDA, 2026). This is corroborated by microbiological risk assessments confirming that population growth and toxin production by proteolytic *C. botulinum* are prohibited at or below pH 4.6 under otherwise optimal conditions (ACMSF, 2023). The final pH of 4.5-4.6 was reached after 20-22 h of fermentation in both hemp matrices, therefore, placing the fermented substrates within the technological stability range expected of a shelf-stable functional ingredient.

The shape of the acidification curve itself helps explain the efficacy of fermentation in reducing antinutritional compounds. Lactic acid bacteria generally lack strong intrinsic phytase activity; instead, their main contribution is to create the mildly acidic environment that activates endogenous and microbial phytases, whose activity in plant matrices has been shown to peak around pH 5.5, with degradation strongly dependent on this pH window and largely lost when endogenous phytases are inactivated beforehand (Reale et al., 2007). In the present fermentations, all three strains transit gradually through the pH 5.5-6.0 range between 4 and 12 h before reaching the terminal plateau near pH 4.5, providing an adequate window for phytase-mediated hydrolysis ahead of the final, microbiologically safe stabilisation. This two-phase pattern is consistent with reports on hempseed fermentation, where lactic acid bacteria simultaneously decreased anti-nutrient levels (tannins, saponins, phytic acid, trypsin inhibitors) while increasing total polyphenols, flavonoids, and antioxidant scavenging capacity (Okomo Aloo et al., 2023), and with hemp bioprocessing studies where lactic acid bacteria fermentation was found to be the most effective method for improving the antioxidant potential of hemp, through intense proteolysis releasing bioactive peptides (Pontonio et al., 2020).

The fermentation time required to approach the 4.5-4.6 pH range in this study (16-22 h) is longer than reported for simpler plant-based liquid matrices. A single rice-based matrix fermented with comparable lactobacilli decreased pH from 7.18 to 4.74 within just 6 h, while extreme acidity is generally required for plant-based drinks (below pH 4), in contrast with dairy yoghurt fermented to pH 4.6 (Nissen et al., 2020). This difference is attributable to the higher buffering capacity and structural complexity (fibre, protein, residual lipids) of hemp inflorescence and seed meal compared with liquid cereal-based substrates, rather than to any inherent limitation of the selected starter cultures.

The practical relevance of fermentation for the nutritional upgrading of hemp-derived by-products was further assessed by evaluating its effects on the two principal antinutritional compounds reported in plant-based raw materials, phytic acid and tannins, both of which impair mineral and protein bioavailability through chelation and complexation mechanisms. The antinutritional profile of the two hemp-derived substrates before and after fermentation with the three lactic acid bacteria strains is presented in Table 2.

Table 2

Fermentation effect on antinutritional factors of hemp-derived substrates

Sample	Phytic acid (mg PA/100 g DW)	Tannins (mg CE/100 g DW)
HSM	6347.32±13.43^{d}	171.40±1.12^{d}
HSM-LP	1274.42±12.16^{a}	63.28±1.14^{a}
HSM-LC	1867.75±11.52^{b}	75.42±1.86^{b}
HSM-ST	2646.33±17.25^{c}	112.56±2.11^{c}
HI	314.64±4.43^{D}	757.15±4.63^{D}
HI-LP	75.22±2.15^{A}	264.61±2.26^{A}
HI-LC	108.46±2.22^{B}	328.72±1.11^{B}
HI-ST	137.82±3.34^{C}	412.35±2.04^{C}

Results indicate the mean value of three independent determinations and are expressed as mean±standard deviation (SD). Different superscript letters within each substrate group indicate statistically significant differences between samples ($p \leq 0.05$): lowercase letters (a-d) refer to hemp seed meal samples, whereas uppercase letters (A-D) refer to hemp inflorescence samples. No statistical comparison was performed between the two substrate groups due to their different compositional profiles. HSM – hemp seed meal; HI – hemp inflorescence; LP – *L. plantarum*; LC – *L. casei;* ST – *S. thermophilus.*

The unfermented hemp seed meal (HSM) exhibited a phytic acid content of 6347.32±13.43 mg PA/100 g DW, a value in close agreement with previously reported levels for hempseed meal, where Russo and Reggiani (2013) recorded phytic acid concentrations of 6120-7540 mg/100 g DW across Italian and French hemp varieties, confirming that hemp seed by-products retain a substantial phosphorus reserve in the form of phytate, as commonly observed in oilseed meals following defatting, which proportionally concentrates non-lipid seed components Russo and Reggiani (2013). In contrast, the unfermented hemp inflorescence (HI) showed a markedly lower phytic acid content (314.64±4.43 mg PA/100 g DW), approximately twenty-fold lower than in HSM. This difference is consistent with the known biological localisation of phytic acid, which is synthesised and stored predominantly in the seed as the main organic phosphorus reserve for germination, rather than in vegetative or floral tissue (Lott et al., 2000). The residual phytic acid detected in the inflorescence samples is most likely attributable to the presence of small amounts of immature seed and bract material retained in harvested industrial hemp inflorescence.

Tannin content followed an opposite trend between the two matrices: HI showed a markedly higher tannin concentration (757.15±4.63 mg CE/100 g DW) than HSM (171.40±1.12 mg CE/100 g DW). This pattern aligns with the recognised richness of hemp inflorescence in polyphenolic compounds, including flavanols such as catechin and epicatechin, which have been identified as major constituents of the hemp inflorescence polyphenolic fraction (Izzo et al., 2020), in contrast with hemp seed tissue, where phenolic compounds are comparatively less abundant and antinutritional load is dominated instead by phytic acid.

Fermentation with all three lactic acid bacteria strains significantly reduced both phytic acid and tannin content in both substrates ($p \leq 0.05$). In HSM, phytic acid decreased by 79.9%, 70.6%, and 58.3% following fermentation with *L. plantarum, L. casei*, and *S. thermophilus*, respectively, while tannin content decreased by 63.1%, 56.0%, and 34.3% for the same strains. A similar hierarchy was observed in HI, with phytic acid reductions of 76.1%, 65.5%, and 56.2%, and tannin reductions of 65.0%, 56.6%, and 45.5% for *L. plantarum, L. casei*, and *S. thermophilus*, respectively.

This efficacy ranking is the inverse of the acidification kinetics shown in Figure 3, in which L. plantarum exhibited the slowest pH decline among the three strains, whereas *S. thermophilus* acidified fastest. This apparent discrepancy is consistent with previous comparative findings on lactobacilli fermentation of plant-based matrices, in which *L. casei* achieved the lowest pH and fastest acidification, whereas *L. plantarum* exhibited the highest phytase activity and the largest

reduction in phytic acid content among the three strains tested (Hashemi et al., 2019). Taken together, these results indicate that the rate of acidification and the efficiency of antinutrient hydrolysis are governed by partially independent strain-specific traits, with *L. plantarum's* comparatively slower but more prolonged metabolic activity translating into superior phytase- and tannase-mediated degradation of antinutritional compounds in both hemp inflorescence and hemp seed meal.

The same fermented samples were further analysed for their bioactive composition and antioxidant capacity, presented in Table 3.

Table 3

Fermentation effect on bioactive composition and antioxidant activity of hemp-derived substrates

Sample	TPC (mg GAE/100 g DW)	TFC (mg CE/100 g DW)	DPPH (mg Trolox/100 g DW)	ABTS (mg Trolox/100 g DW)
HSM	647.32±2.43^{a}	181.16±4.28^{a}	510.44±3.32^{a}	596.71±1.36^{a}
HSM-LP	1016.26±4.85^{d}	285.37±5.72^{d}	893.64±1.82^{d}	1087.52±6.25^{d}
HSM-LC	925.53±3.71^{c}	254.46±5.11^{c}	811.42±1.74^{c}	962.44±4.62^{c}
HSM-ST	843.75±2.92^{b}	231.12±4.87^{b}	728.64±1.33^{b}	876.18±3.75^{b}
HI	3386.41±5.28^{A}	1282.55±4.64^{A}	1726.37±4.52^{A}	2448.33±3.41^{A}
HI-LP	4315.83±4.16^{D}	1674.74±2.53^{D}	2346.58±2.66^{D}	3488.41±2.82^{D}
HI-LC	3872.62±3.75^{C}	1552.61±2.74^{C}	2182.46±2.35^{C}	3292.53±3.44^{C}
HI-ST	3654.28±3.14^{B}	1428.22±1.86^{B}	2075.32±2.81^{B}	2875.64±1.17^{B}

Results indicate the mean value of three independent determinations and are expressed as mean±standard deviation (SD). Different superscript letters within each substrate group indicate statistically significant differences between samples ($p \leq 0.05$): lowercase letters (a-d) refer to hemp seed meal samples, whereas uppercase letters (A-D) refer to hemp inflorescence samples. No statistical comparison was performed between the two substrate groups due to their different compositional profiles. HSM – hemp seed meal; HI – hemp inflorescence; LP – *L. plantarum*; LC – *L. casei;* ST – *S. thermophilus*.

Fermentation with all three lactic acid bacteria strains significantly increased TPC, TFC, DPPH, and ABTS values in both hemp matrices ($p \leq 0.05$; Table 4), following the inverse pattern of the antinutrient reduction reported above, with the largest gains observed for *L. plantarum*, followed by *L. casei* and *S. thermophilus*.

In hemp seed meal, this increase is consistent with the recognised phenolic richness of the hull fraction retained in seed cake after oil extraction, which has been reported to substantially raise the phenolic content of food matrices upon incorporation (Feng et al., 2022). In hemp inflorescence, the considerably higher baseline TPC, TFC, and antioxidant values compared with seed meal reflect the well-documented accumulation of flavonoids and phenolic acids in hemp flower tissue, the magnitude of which varies substantially with genotype and growing season (Beleggia et al., 2023).

The fermentation-induced increase observed for all four parameters can be explained by the enzymatic activity of lactic acid bacteria (LAB) on the plant cell wall matrix. During fermentation, LAB strains secrete polyphenol-associated enzymes, including β-glucosidases and esterases, that hydrolyse ester and glycosidic bonds linking phenolic compounds to cell wall polysaccharides and proteins, releasing them into a free, spectrophotometrically detectable and more bioaccessible form; strains with higher glycosidase and esterase activity have been shown to achieve a correspondingly greater release of bound phenolics during fermentation (Zhang et al., 2025). This mechanism is consistent with the comparatively larger relative increase in TPC observed in hemp seed meal fermented with *L. plantarum*, of approximately 57%, compared with approximately 27% in hemp inflorescence under the same treatment, since seed meal phenolics are predominantly present in bound, esterified forms requiring enzymatic liberation, whereas hemp inflorescence already contains a substantial pool of free, readily extractable polyphenols prior to fermentation.

Quality attributes and functional properties of pasta enriched with fermented hemp-derived ingredients

Consumer-relevant quality attributes of hemp-enriched pasta. Based on the results obtained for antinutritional factor reduction and enhancement of bioactive composition, *L. plantarum* was selected as the most suitable starter culture for the further development of hemp-enriched pasta products. Among the three tested strains, *L. plantarum* demonstrated the highest efficiency in both matrices, achieving the greatest reductions in phytic acid and tannin content, while simultaneously providing the most pronounced increases in total polyphenol and total flavonoid content, as well as antioxidant activity.

Specifically, fermentation with *L. plantarum* reduced phytic acid by 79.9% and tannins by 63.1% in hemp seed meal, while in hemp inflorescence the reductions reached 76.1% and 65.0%, respectively. The same fermentation treatment resulted in the highest accumulation of bioactive compounds and antioxidant capacity, confirming this strain's superior metabolic potential for valorising hemp-derived substrates. Only the optimally fermented substrates, namely HSM-LP and HI-LP, were selected as functional ingredients for pasta formulation. Two experimental pasta series were subsequently developed: one enriched with fermented hemp seed meal and the other with fermented hemp inflorescence, both incorporated at substitution levels ranging from 5 to 30% of wheat flour (Figure 3).

Clear differences in colour and surface characteristics were observed as the incorporation level of hemp-derived substrates increased. The control sample (P0) exhibited the typical bright yellow colour characteristic of conventional wheat-based pasta, with a smooth and uniform surface.

The incorporation of fermented hemp seed meal progressively altered the pasta's visual characteristics, resulting in a gradual transition from yellow to darker olive-brown tones as the substitution level increased from 5% to 30%. Samples PM5-PM15 retained relatively good visual uniformity and acceptable appearance, whereas higher incorporation levels (PM20-PM30) showed noticeably darker colouration and a rougher surface texture, likely due to the increased presence of fibrous particles originating from the hemp hull fraction. A similar concentration-dependent effect was observed in pasta enriched with fermented hemp inflorescence (PI). However, compared to the PM series, the PI samples displayed lighter greenish-olive hues, particularly at lower substitution levels (PI5-PI15), reflecting the presence of chlorophylls and other plant pigments naturally abundant in hemp floral tissue. At higher inclusion levels (PI20-PI30), the samples became progressively darker and more heterogeneous in appearance, although the strand structure remained well preserved.

The visual changes described above were further confirmed by instrumental chromatic analysis, which provided objective quantification of colour differences among the pasta formulations (Table 4).

The control sample showed the highest lightness value ($L^* = 89.00$), confirming the typical bright yellow appearance of wheat-based pasta. In both enriched series, L^* decreased progressively with increasing substitution level, reaching 47.26 in PM30 and 46.32 in PI30. This indicates a pronounced darkening of the pasta matrix resulting from replacing wheat flour with pigment- and fibre-rich hemp ingredients. A similar reduction in lightness was reported by (Biernacka et al., 2022) in pasta enriched with dried leek powder, where cooked pasta L^* decreased from 75.51 in the control to 67.29 at the highest enrichment level.

The a^* coordinate shifted from negative values in the control sample (−4.00), indicating a greenish tone, toward positive values in the enriched samples. In the PM series, a^* increased to 1.92 in PM30, while in the PI series, it reached 1.08 in PI30. This shift reflects the progressive modification of pasta colour from the original yellow-green tone toward darker olive-brown shades. Similar transitions from negative or low a^* values toward more positive values have been reported in pasta enriched with vegetable or fruit by-products, where natural pigments such as chlorophyll derivatives, carotenoids and oxidised phenolic compounds strongly modify the red-green balance of the product (Pasini et al., 2025).



Figure 3. Visual appearance of pasta samples enriched with fermented hemp-derived ingredients

P0 – control pasta sample; PM5-PM30 – pasta samples enriched with 5-30% hemp seed meal fermented with *L. plantarum*; PI5-PI30 – pasta samples enriched with 5-30% hemp inflorescence fermented with *L. plantarum*

Table 4

Chromatic parameters of pasta samples enriched with fermented hemp-derived ingredients

Sample	*L**	*a**	*b**	*ΔE*
P0	89.00±0.72^{gG}	-4.00±0.05^{aA}	54.00±0.31^{gG}	-
PM5	86.12±0.68^{f}	-3.86±0.04^{b}	32.44±0.28^{f}	21.75±0.42^{a}
PM10	74.36±0.56^{e}	-0.24±0.06^{c}	31.28±0.33^{e}	27.29±0.55^{b}
PM15	65.21±0.81^{d}	0.14±0.08^{d}	26.52±0.41^{d}	36.58±0.64^{c}
PM20	64.38±0.63^{c}	0.32±0.07^{e}	27.14±0.36^{c}	36.69±0.59^{c}
PM25	63.42±0.52^{b}	0.86±0.09^{f}	27.06±0.44^{b}	37.47±0.62^{d}
PM30	47.26±0.77^{a}	1.92±0.11^{g}	26.22±0.52^{a}	50.49±0.91^{e}
PI5	76.14±0.66^{F}	-0.92±0.05^{B}	31.12±0.26^{F}	26.43±0.48^{A}
PI10	72.25±0.59^{E}	0.08±0.06^{c}	26.42±0.35^{E}	32.52±0.54^{B}
PI15	61.18±0.74^{D}	0.82±0.07^{D}	24.86±0.39^{D}	40.57±0.73^{C}
PI20	54.36±0.81^{C}	0.94±0.08^{E}	22.84±0.41^{C}	46.85±0.84^{D}
PI25	49.18±0.76^{B}	1.02±0.09^{F}	19.26±0.47^{B}	53.08±0.88^{E}
PI30	46.32±0.88^{A}	1.08±0.10^{G}	18.22±0.51^{A}	55.92±0.95^{F}

Results indicate the mean value of three independent determinations and are expressed as mean±standard deviation (SD). Different superscript letters within each experimental series indicate statistically significant differences between samples ($p \leq 0.05$): lowercase letters (a-g) correspond to the P0-PM series, whereas uppercase letters (A-G) correspond to the P0-PI series. No statistical comparison was performed between the PM and PI series due to differences in substrate composition. P0 – control pasta sample; PM5-PM30 – pasta samples enriched with 5-30% hemp seed meal fermented with *L. plantarum*; PI5-PI30 – pasta samples enriched with 5-30% hemp inflorescence fermented with *L. plantarum*

The *b** coordinate, associated with yellowness, decreased substantially from 54.00 in P0 to 26.22 in PM30 and 18.22 in PI30. This decline indicates a loss of the characteristic yellow tone of wheat pasta and confirms the dominant influence of hemp-derived pigments and fibrous particles. The decrease in *b** was stronger in the PI series, suggesting that fermented hemp inflorescence contributed more intensively to colour darkening than fermented hemp seed meal. This behaviour is consistent with the visual appearance of the samples and with the higher content of phenolic and pigment-associated compounds previously observed in hemp inflorescence.

The total colour difference (*ΔE*) confirmed that all enriched samples were clearly distinguishable from the control. *ΔE* increased from 21.75 in PM5 to 50.49 in PM30 and from 26.43 in PI5 to 55.92 in PI30. These values largely exceed the perceptibility threshold of $\Delta E > 3$, which is generally considered visible to consumers. Pasini et al. (2025) also emphasised that *ΔE* values above 3 in enriched pasta are readily perceived by consumers, although acceptance depends on product familiarity and expectations.

Prior to physicochemical and technological characterisation, the acceptability of the fortified pasta formulations was assessed from the consumer perspective, as sensory acceptance represents a primary criterion for the viability of any novel food product (Figure 4).

The control (P0) achieved the highest scores for every attribute, with values ranging from 8.10 to 8.30, reflecting strong consumer preference for the colour, odour, and taste of plain durum wheat pasta. In the PM series, scores remained above 7.0 across all three attributes up to PM15, placing these formulations within the range conventionally associated with positive consumer liking on a nine-point hedonic scale. At PM20, scores fell slightly below 7.0 for colour and taste (6.70 and 6.60, respectively), while odour remained at 6.80, indicating that the olfactory profile of the seed meal ingredient was somewhat better tolerated by consumers than its visual and gustatory impact. At PM25 and PM30, all attributes dropped into the 5.2-6.2 range, still above the midpoint of the scale but no longer conveying clear positive acceptance.

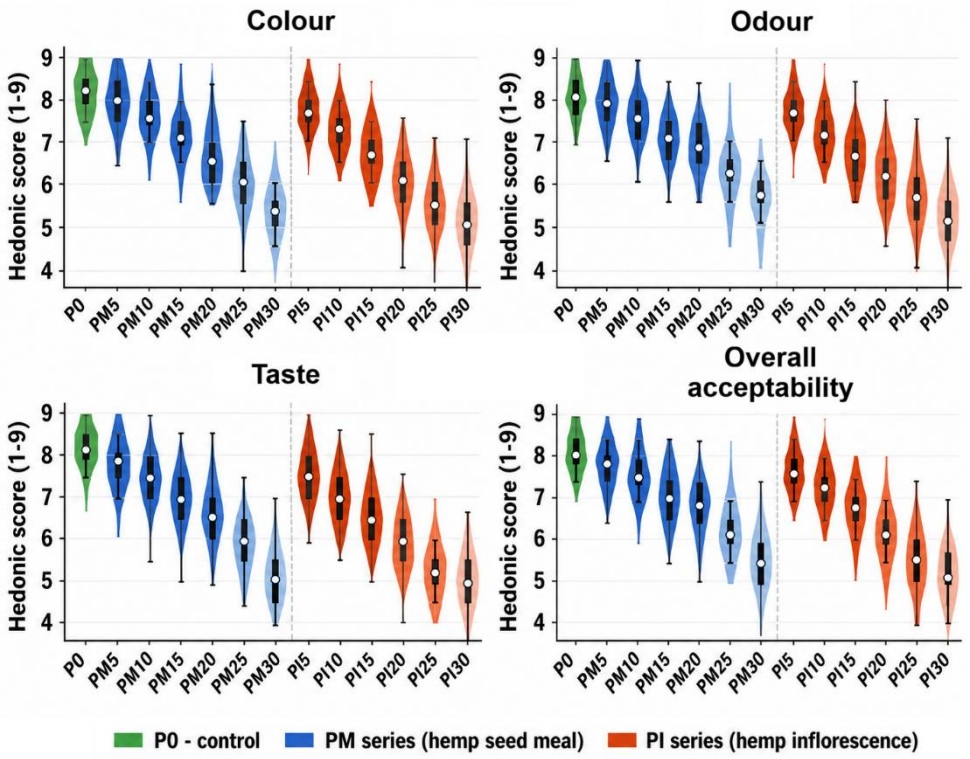

Figure 4. Hedonic score distribution of pasta samples enriched with fermented hemp-derived ingredients.

White dots indicate mean values; central black boxes represent interquartile ranges. A dashed vertical line separates the hemp seed meal (PM) and hemp inflorescence (PI) series.

The PI series declined more steeply. PI5 scored comparably to PM5 across all attributes (7.60-7.80), but from PI10 onward, the inflorescence series lagged behind the seed meal series at every matching substitution level. This gap was most pronounced for taste and colour: at 20% substitution, PI20 scored 5.90 for taste against 6.60 for PM20, a difference that traces directly to the stronger and more unusual flavour profile of the inflorescence material, which consumers found increasingly intrusive at higher concentrations. Colour divergence between the two series was equally clear to panellists, consistent with the CIELAB data in Table 4, which showed that the PI series exhibited a steeper drop in L^* and a distinct greenish hue not present in the PM series.

The general pattern of declining hedonic scores with increasing substitution level observed in both series aligns with findings reported for pasta enriched with beet stalk powder at 5-20% substitution, where a dose-dependent decrease in consumer acceptability was equally pronounced and scores showed wider individual variation at higher substitution levels, reflecting growing consumer disagreement about acceptability as the organoleptic profile of the product moves further from the familiar wheat pasta baseline (Solomakou et al., 2025). This divergence in consumer response at higher substitution levels is consistent with the broader observation that novel ingredients derived from food industry by-products tend to generate more heterogeneous hedonic responses as their sensory contribution becomes more perceptible, particularly when colour and flavour deviate markedly from the expected reference (Scheibenzuber et al., 2025).

The hedonic scores recorded across both series suggest that consumer acceptability of the fortified pasta was maintained within a practically relevant range up to moderate substitution levels, with the PM series proving more sensorially compatible with the wheat pasta matrix than the PI series at matching incorporation rates.

Technological quality and functional value of pasta enriched with fermented hemp-derived ingredients. The technological behaviour of the resulting pasta during cooking was evaluated to determine whether incorporating fermented hemp seed meal and hemp inflorescence preserved the quality attributes expected of a wheat-based pasta product. Titratable acidity, moisture content, optimal cooking time, swelling index, water absorption index (WAI), and cooking loss were assessed across the full substitution range (5-30%) for both ingredients, as these parameters jointly describe the structural and textural changes induced by fortification during the gelatinisation and hydration process. The results are presented in Table 5.

Table 5

Physicochemical and technological quality parameters of pasta samples enriched with fermented hemp-derived ingredients

Sample	Titratable acidity (degrees)	Moisture (%)	Optimal cooking time (min)	Swelling index (g H_2O/g)	Water absorption index (g/100 g)	Cooking loss (%)
P0	1.22 ± 0.04^{aA}	9.85 ± 0.11^{aA}	6.5 ± 0.1^{eE}	2.34 ± 0.05^{eE}	1.84 ± 0.03^{aA}	3.18 ± 0.12^{aA}
PM5	1.41 ± 0.05^{b}	10.02 ± 0.08^{a}	6.2 ± 0.1^{d}	2.21 ± 0.04^{d}	1.89 ± 0.03^{b}	4.02 ± 0.14^{b}
PM10	1.47 ± 0.03^{b}	10.14 ± 0.12^{ab}	6.0 ± 0.1^{c}	2.12 ± 0.03^{c}	1.92 ± 0.03^{b}	4.84 ± 0.17^{c}
PM15	1.62 ± 0.06^{c}	10.26 ± 0.10^{b}	5.8 ± 0.1^{c}	2.05 ± 0.04^{c}	1.98 ± 0.03^{c}	5.65 ± 0.19^{d}
PM20	1.68 ± 0.04^{c}	10.38 ± 0.13^{b}	5.5 ± 0.1^{b}	1.94 ± 0.03^{b}	2.05 ± 0.04^{d}	6.42 ± 0.21^{e}
PM25	2.13 ± 0.07^{d}	10.52 ± 0.09^{bc}	5.2 ± 0.1^{a}	1.88 ± 0.03^{a}	2.12 ± 0.03^{e}	7.18 ± 0.24^{f}
PM30	2.24 ± 0.05^{d}	10.67 ± 0.12^{c}	5.0 ± 0.1^{a}	1.81 ± 0.03^{a}	2.18 ± 0.04^{f}	8.02 ± 0.27^{g}
PI5	1.45 ± 0.04^{B}	10.08 ± 0.10^{A}	6.1 ± 0.1^{D}	2.18 ± 0.04^{D}	1.91 ± 0.03^{B}	4.25 ± 0.15^{B}
PI10	1.82 ± 0.06^{C}	10.22 ± 0.08^{AB}	5.9 ± 0.1^{C}	2.06 ± 0.03^{C}	1.97 ± 0.03^{C}	5.11 ± 0.18^{C}
PI15	2.17 ± 0.05^{D}	10.37 ± 0.11^{B}	5.7 ± 0.1^{C}	1.99 ± 0.03^{C}	2.04 ± 0.04^{D}	5.86 ± 0.20^{D}
PI20	2.66 ± 0.08^{E}	10.54 ± 0.13^{BC}	5.4 ± 0.1^{B}	1.91 ± 0.03^{B}	2.11 ± 0.04^{E}	6.74 ± 0.23^{E}
PI25	3.21 ± 0.09^{F}	10.72 ± 0.09^{C}	5.2 ± 0.1^{A}	1.84 ± 0.03^{A}	2.17 ± 0.04^{F}	7.51 ± 0.26^{F}
PI30	3.67 ± 0.11^{G}	10.94 ± 0.14^{C}	5.0 ± 0.1^{A}	1.76 ± 0.02^{A}	2.24 ± 0.05^{G}	8.33 ± 0.28^{G}

Results indicate the mean value of three independent determinations and are expressed as mean±standard deviation (SD). Different superscript letters within each experimental series indicate statistically significant differences between samples ($p \leq 0.05$): lowercase letters (a-g) correspond to the P0-PM series, whereas uppercase letters (A-G) correspond to the P0-PI series. No statistical comparison was performed between the PM and PI series due to differences in substrate composition. P0 – control pasta sample; PM5-PM30 – pasta samples enriched with 5-30% hemp seed meal fermented with *L. plantarum*; PI5-PI30 – pasta samples enriched with 5-30% hemp inflorescence fermented with *L. plantarum*

All measured parameters changed progressively and significantly ($p \leq 0.05$) with increasing substitution level in both the hemp seed meal and hemp inflorescence series and were compared with the values stipulated in national regulations (Technical Regulation Decision No. 775, 2007). Titratable acidity rose from 1.22 in the control to 2.24 degrees in PSM30 and 3.67 in PI30; against the regulated maximum of 3.5 degrees, every formulation remained compliant except PI30, which

exceeded the limit only marginally. This trend reflects the residual organic acid content carried over from the fermentation step, and is markedly more pronounced in the inflorescence series, consistent with the higher tannin and polyphenol load already noted for HI relative to HSM in Tables 2 and 3, since these compounds, alongside lactic acid, also contribute to the titratable acidity of plant-based matrices (Capcanari and Covaliov, 2025; Tolve et al., 2020). Moisture content of the dried pasta increased moderately with substitution level, from 9.85% in P0 to 10.67% in PSM30 and 10.94% in PI30; against the regulated maximum of 13% for this parameter, all thirteen formulations remained below the ceiling, indicating that, unlike titratable acidity, moisture was not a limiting factor for any of the substitution levels tested.

Axentii et al. (2023) reported a comparable dose-dependent rise in titratable changes and cooking losses when wheat flour was replaced with non-fermented hemp seed meal at levels of up to 20% in rigatoni pasta, where cooking loss increased alongside substitution level while remaining within an acceptable technological range, a pattern that closely matches what was observed here for the PM series up to the same substitution level. The slightly steeper increase recorded in the present study for the fermented PM series, compared with the non-fermented hemp seed meal used by those authors, is consistent with the additional organic acid content generated by lactic acid fermentation, which is not present in unfermented hemp ingredients.

Optimal cooking time decreased with substitution level in both series, from 6.5 min in the control to 5.0 min in both PM30 and PI30, while the swelling index fell from 2.34 g H_2O/g in P0 to 1.81 g H_2O/g in PM30 and 1.76 g H_2O/g in PI30, and water absorption index moved in the opposite direction, rising to 2.18-2.24 g/g at the highest substitution levels. This combination, shorter cooking time, lower swelling index, and higher WAI, indicates that the starch-gluten network responsible for water retention during gelatinization was progressively replaced by fibre-rich, non-starch material from the hemp ingredients (Camelo-Méndez et al., 2018; Wang et al., 2024), which binds water more readily but does not contribute to the structured swelling typical of starch granules, a mechanism also described for wheat-based pasta and noodles where non-starch components compete with starch for available water during cooking (Bianchi et al., 2021; Masiala et al., 2024).

Cooking loss increased with substitution level across both series, from 3.18% in the control to 8.02% in PM30 and 8.33% in PI30, placing the two highest-substitution samples at or just above the 8 g/100 g threshold generally regarded as the upper limit of acceptable cooking loss for fortified durum pasta, a limit also confirmed for durum pasta enriched with broccoli leaf powder at comparable cooking loss values (Drabińska et al., 2022).

Comparing the two series at equivalent substitution levels, hemp inflorescence consistently produced a more pronounced effect on titratable acidity, moisture, optimal cooking time, swelling index, WAI, and cooking loss than hemp seed meal. Taken together with the regulatory comparison above, these results indicate that substitution levels up to approximately 20% for both hemp ingredients keep the pasta within the technological and, where applicable, regulatory limits considered for wheat-based pasta products, whereas the 25-30% levels, particularly for hemp inflorescence, approach or exceed these limits for titratable acidity and cooking loss.

The functional value of the pasta was assessed beyond its physicochemical and technological quality parameters by measuring total polyphenol and total flavonoid content, and antioxidant activity (DPPH and ABTS assays), to verify whether the bioactive gains documented for the raw substrates carried over into the finished product (Table 6).

All bioactive and antioxidant parameters were determined in pasta samples after cooking at their optimal cooking time to ensure a realistic assessment of the compounds available in the consumed product. Both experimental pasta series exhibited a progressive and statistically significant enhancement in bioactive composition with increasing substitution level ($p \leq 0.05$), although the magnitude of enrichment differed markedly depending on the incorporated hemp-derived ingredient.

Table 6

Bioactive composition and antioxidant activity of cooked pasta samples enriched with fermented hemp-derived ingredients

Sample	TPC (mg GAE/100 g product)	TFC (mg CE/100 g product)	DPPH (mg Trolox/100 g product)	ABTS (mg Trolox/100 g product)
P0	34.82±1.14^{aA}	10.26±0.42^{aA}	18.42±0.73^{aA}	26.74±0.91^{aA}
PM5	52.44±1.52^{b}	15.64±0.55^{b}	31.82±0.94^{b}	44.16±1.12^{b}
PM10	68.75±1.84^{c}	20.52±0.62^{c}	45.74±1.12^{c}	62.35±1.43^{c}
PM15	86.14±2.05^{d}	26.43±0.74^{d}	61.82±1.43^{d}	82.54±1.76^{d}
PM20	102.46±2.31^{e}	31.72±0.82^{e}	78.53±1.74^{e}	104.38±2.12^{e}
PM25	118.72±2.64^{f}	37.65±0.94^{f}	96.44±2.05^{f}	128.64±2.41^{f}
PM30	135.84±2.88^{g}	43.26±1.02^{g}	114.72±2.24^{g}	154.82±2.73^{g}
PI5	96.24±2.42^{B}	32.84±0.86^{B}	56.52±1.26^{B}	88.63±1.92^{B}
PI10	164.38±3.11^{C}	58.72±1.14^{C}	101.44±1.94^{C}	158.72±2.61^{C}
PI15	228.56±3.82^{D}	82.64±1.62^{D}	148.54±2.42^{D}	236.84±3.12^{D}
PI20	294.62±4.25^{E}	108.34±2.05^{E}	198.44±2.84^{E}	322.42±3.84^{E}
PI25	362.84±4.86^{F}	136.22±2.44^{F}	251.32±3.15^{F}	415.63±4.52^{F}
PI30	434.16±5.22^{G}	166.54±2.82^{G}	306.44±3.62^{G}	516.84±5.11^{G}

Results indicate the mean value of three independent determinations and are expressed as mean±standard deviation (SD). Different superscript letters within each experimental series indicate statistically significant differences between samples ($p \leq 0.05$): lowercase letters (a-g) correspond to the P0-PM series, whereas uppercase letters (A-G) correspond to the P0-PI series. No statistical comparison was performed between the PM and PI series due to differences in substrate composition. P0 – control pasta sample; PM5-PM30 – pasta samples enriched with 5-30% hemp seed meal fermented with *L. plantarum*; PI5-PI30 – pasta samples enriched with 5-30% hemp inflorescence fermented with *L. plantarum*

In the hemp seed meal series, TPC increased from 34.82 mg GAE/100 g in the control sample to 135.84 mg GAE/100 g in PM30, corresponding to an approximately fourfold increase. A similar trend was observed for TFC, which rose from 10.26 to 43.26 mg CE/100 g. These results indicate that fermented hemp seed meal contributed measurable amounts of phenolic compounds to the pasta matrix, despite the dilution effects of wheat flour and water uptake during cooking. Comparable enrichment trends have been reported in other functional pasta systems fortified with phenolic-rich plant ingredients. Abinaya et al. (2025) observed a marked increase in TPC (59.05-280.01 mg GAE/100 g) and TFC (30.09-250.48 mg/100 g) in pasta enriched with onion peel colour extract. The steeper increase reported in that study is expected, since onion peel extract represents a highly concentrated phenolic fraction, whereas fermented hemp seed meal is a whole-food ingredient containing proteins, dietary fibre, and structural polysaccharides that dilute the relative phenolic density.

A substantially stronger enrichment effect was observed in pasta containing fermented hemp inflorescence. At the highest substitution level (PI30), TPC reached 434.16 mg GAE/100 g, while TFC reached 166.54 mg CE/100 g, representing values approximately three to four times higher than those recorded in the corresponding seed meal formulations. This difference is primarily explained by the intrinsic composition of the incorporated substrate rather than fermentation efficiency, since hemp inflorescence exhibited considerably higher baseline concentrations of polyphenols and flavonoids than hemp seed meal, as previously demonstrated in Table 3. This observation is consistent with phytochemical profiling studies of *Cannabis sativa* inflorescences, which reported substantial accumulation of phenolic compounds and flavonoids in floral tissues (Izzo et al., 2020).

Antioxidant activity followed the same overall pattern as TPC and TFC, confirming that the enrichment in phenolic compounds translated into improved radical-scavenging capacity. In the PM series, DPPH increased from 18.42 to 114.72 mg Trolox/100 g and ABTS from 26.74 to 154.82 mg Trolox/100 g. In the PI series, the increase was even more pronounced, reaching 306.44 mg Trolox/100 g (DPPH) and 516.84 mg Trolox/100 g (ABTS) in PI30, corresponding to approximately 16.6-fold and 19.3-fold increases relative to the control, respectively.

When interpreting these results, the effect of cooking must be carefully considered, since thermal processing may simultaneously reduce and enhance the measurable bioactive fraction. Water-soluble phenolics may be partially lost through leaching into cooking water, whereas heat-induced disruption of plant cell wall structures can promote the release of previously bound compounds, thereby increasing extractability. This dual behaviour has been demonstrated by Di Matteo et al. (2025), who reported cultivar-dependent changes in total polyphenol content in cooked *Asparagus officinalis*, with reductions of 12-28% in some samples due to leaching, while others showed moderate increases of 5-15% due to enhanced release of bound phenolics. Similar observations were reported by Kosewski et al. (2025), who showed that thermal processing significantly modified both phenolic availability and antioxidant capacity through structural changes in plant matrices. Therefore, the antioxidant activity measured in the cooked pasta samples should be interpreted as the net result of these competing phenomena rather than as a direct carry-over of the antioxidant potential of the raw ingredients.

Across all formulations, ABTS values were consistently higher than the corresponding DPPH values, a trend already observed in the raw fermented substrates. This difference is generally attributed to the broader reactivity spectrum of the ABTS assay, which detects both hydrophilic and lipophilic antioxidant compounds, whereas the DPPH assay is more selective toward specific radical-scavenging molecules. Similar analytical behaviour was reported by Thaipong et al. (2006), who demonstrated that ABTS generally yields higher antioxidant estimates in complex plant matrices due to its broader sensitivity across diverse antioxidant classes.

Conclusions

This study demonstrated that lactic acid bacterial fermentation is an effective, low-cost strategy for the valorisation of two underutilised hemp-derived by-products. All measured parameters changed progressively and significantly ($p \leq 0.05$) with increasing substitution level of hemp seed meal and hemp inflorescence – as functional ingredients for pasta enrichment.

Among the three strains evaluated, *Lactiplantibacillus plantarum* proved the most effective starter culture for both substrates, achieving the greatest reduction in phytic acid and condensed tannins while simultaneously generating the highest gains in total polyphenol content, total flavonoid content, and antioxidant activity as measured by both DPPH and ABTS assays. This outcome confirmed that the rate of acidification and antinutrient-hydrolysing efficiency are governed by partially independent, strain-specific mechanisms, with *L. plantarum* demonstrating superior metabolic adaptability to hemp-derived matrices despite its comparatively slower acidification kinetics. All three strains reached the technologically and microbiologically safe pH threshold of 4.5 after 20-22 h of fermentation in both substrates, validating the process from a food safety perspective.

The incorporation of the optimally fermented substrates into durum wheat pasta at substitution levels of 5-30% produced formulations with clearly distinct physicochemical, colourimetric, bioactive, and sensory profiles. Technological quality parameters remained within technically acceptable limits up to 20% substitution for both hemp seed meal and hemp inflorescence, with only the 30% inflorescence sample marginally exceeding the regulated titratable acidity ceiling of 3.5 degrees. The progressive darkening of pasta colour with increasing substitution level, more pronounced in the inflorescence series and with a distinct olive-green undertone, was consistent with the polyphenol and chlorophyll contents of the respective ingredients and was reflected in the CIELAB parameters. Bioactive content of the cooked pasta increased dose-dependently across both series, confirming that

the functional gains achieved through fermentation were retained through dough mixing, drying, and boiling, with the inflorescence series consistently reaching higher absolute values of TPC, TFC, DPPH, and ABTS than the seed meal series at matching substitution levels.

Sensory evaluation indicated that the most sensorially viable substitution range was 5-20% for hemp seed meal and 10-15% for hemp inflorescence, beyond which the increasingly pronounced colour and flavour contribution of the hemp ingredients reduced hedonic scores to borderline acceptable levels. Taken together, these findings suggest that a substitution level of 15-20% fermented hemp seed meal or 10-15% fermented hemp inflorescence represents the optimal balance between functional enrichment and consumer acceptability for this type of fortified pasta.

From a broader perspective, the results confirm that lactic acid fermentation can serve as a practical bridge between agri-food residue management and functional food development, converting two currently underexploited streams of hemp-derived materials into ingredients that simultaneously reduce antinutritional load, enhance bioactive content, and deliver measurable antioxidant potential to a widely consumed staple food. Future research should address the in vitro bioaccessibility of bioactive compounds in finished pasta, mineral bioavailability as a direct outcome of phytate reduction, and the shelf-life behaviour of fermented ingredients under different storage conditions.

Acknowledgment. The research was supported by the Moldovan Government within the project of Young Researchers 25.80012.5107.11TC **BIO-FERM** - Valorization of bioactive compounds from alternative plant sources for the development of functional fermented foods, running at the Technical University of Moldova

References

AACC (2012), *Approved Methods of Analysis*, 11th ed., Method 66-50.01: Optimum Cooking Time for Pasta, American Association of Cereal Chemists International, St. Paul, MN, USA

Abinaya S., Panghal A., Chhikara N., Bishnoi P., Tanwar R., Gupta R. (2025), Onion peel color extract incorporation in pasta and effect on functional, phytochemical, structural, thermal, and storage stability, *Food Chemistry Advances,* 6, 100934, https://doi.org/10.1016/j.focha.2025.100934

ACMSF (2023), *Report on Botulinum Neurotoxin-Producing Clostridia, Advisory Committee on the Microbiological Safety of Food*, UK Food Standards Agency, Food Standards Agency, https://doi.org/10.46756/sci.fsa.ozk974

Arsov A., Tsigoriyna L., Batovska D., Armenova N., Mu W., Zhang W., Petrov K., Petrova P. (2024), Bacterial degradation of antinutrients in foods: The genomic insight, *Foods,* 13(15), 2408, https://doi.org/10.3390/foods13152408

Axentii M., Stroe S.-G., Codină G.G. (2023), Development and quality evaluation of rigatoni pasta enriched with hemp seed meal, *Foods,* 12(9), 1774, https://doi.org/10.3390/foods12091774

Beleggia R., Menga V., Fulvio F., Fares C., Trono D. (2023), Effect of genotype, year, and their interaction on the accumulation of bioactive compounds and the antioxidant activity in industrial hemp (*Cannabis sativa* L.) inflorescences, *International Journal of Molecular Sciences,* 24(10), 8969, https://doi.org/10.3390/ijms24108969

Bianchi F., Tolve R., Rainero G., Bordiga M., Brennan C.S., Simonato B. (2021), Technological, nutritional and sensory properties of pasta fortified with agro-industrial by-products: a review, *International Journal of Food Science and Technology,* 56(9), pp. 4356-4366, https://doi.org/10.1111/ijfs.15168

Biernacka B., Dziki D., Gawlik-Dziki U. (2022), Pasta enriched with dried and powdered leek: Physicochemical properties and changes during cooking, *Molecules,* 27(14), 4495, https://doi.org/10.3390/molecules27144495

Blazhenko M., Falendysh N., Shpak V. (2024), Effect of hemp seed by-products on wheat dough fermentation, *Ukrainian Food Journal*, 13(4), pp. 737–752, https://doi.org/10.24263/2304-974X-2024-13-4-8

Camelo-Méndez G.A., Tovar J., Bello-Pérez L.A. (2018), Influence of blue maize flour on gluten-free pasta quality and antioxidant retention characteristics, *Journal of Food Science and Technology,* 55, pp. 2739-2748, https://doi.org/10.1007/s13197-018-3196-9

Capcanari T., Covaliov E. (2025), Development of clean-label protein- and fiber-enriched dry pretzels using hemp seed by-products, *Foods,* 14(22), 3925, https://doi.org/10.3390/foods14223925

Capcanari T., Covaliov E., Negoiță C. (2025), Harnessing hemp (*Cannabis sativa* L.) seed cake proteins: From concentrate production to enhanced choux pastry quality, *Foods,* 14(4), 567, https://doi.org/10.3390/foods14040567

Capcanari T., Covaliov E., Negoiță C., Siminiuc R., Chirsanova A., Reșitca V., Țurcanu D. (2023), Hemp seed cake flour as a source of proteins, minerals and polyphenols and its impact on the nutritional, sensorial and technological quality of bread, *Foods,* 12(23), 4327, https://doi.org/10.3390/foods12234327

Carpentieri S., Larrea-Wachtendorff D., Donsì F., Ferrari G. (2022), Functionalization of pasta through the incorporation of bioactive compounds from agri-food by-products: Fundamentals, opportunities, and drawbacks, *Trends in Food Science & Technology,* 122, pp. 49-65, https://doi.org/10.1016/j.tifs.2022.02.011

Di Biase M., Scicchitano D., Valerio F., Lonigro S.L., Cifarelli V., Ostante G., D'Antuono I., Candela M., Ferrara M. (2025), Microbial ecology and nutritional features in liquid sourdough containing hemp flour fermented by lactic acid bacterial strains, *Foods,* 14(3), 469, https://doi.org/10.3390/foods14030469

Di Matteo A., Paolillo A., Ciriaco L., Silva J.L.D., Pascale S.D., Izzo L. (2025), Effect of cooking and in vitro digestion on the polyphenols and antioxidant properties of *Asparagus officinalis* L. cultivars, *Foods,* 14, 2367, https://doi.org/10.3390/foods14132367

Drabińska N., Nogueira M., Szmatowicz B. (2022), Valorisation of broccoli by-products: Technological, sensory and flavour properties of durum pasta fortified with broccoli leaf powder, *Molecules,* 27(15), 4672, https://doi.org/10.3390/molecules27154672

Erem E., Kilic-Akyilmaz M. (2024), The role of fermentation with lactic acid bacteria in quality and health effects of plant-based dairy analogues, *Comprehensive Reviews in Food Science and Food Safety,* 23(4), e13402, https://doi.org/10.1111/1541-4337.13402

FAO (2019), *The State of Food and Agriculture 2019. Moving Forward on Food Loss and Waste Reduction*, Food and Agriculture Organization of the United Nations, Rome

Feng X., Sun G., Fang Z. (2022), Effect of hempseed cake (*Cannabis sativa* L.) incorporation on the physicochemical and antioxidant properties of reconstructed potato chips, *Foods,* 11(2), 211, https://doi.org/10.3390/foods11020211

Giusti M.M., Gordillo B., González-Miret M.L. (2024), Color analysis, In: Ismail B.P., Nielsen S.S. (Eds.), *Nielsen's Food Analysis*, pp. 509-522, Food Science Text Series, Springer International Publishing, Cham, https://doi.org/10.1007/978-3-031-50643-7_31

Gull A., Prasad K., Kumar P. (2018), Nutritional, antioxidant, microstructural and pasting properties of functional pasta, *Journal of the Saudi Society of Agricultural Sciences,* 17(2), pp. 147-153, https://doi.org/10.1016/j.jssas.2016.03.002

Hashemi S.M.B., Gholamhosseinpour A., Mousavi Khaneghah A. (2019), Fermentation of acorn dough by lactobacilli strains: Phytic acid degradation and antioxidant activity, *LWT – Food Science and Technology,* 100, pp. 144-149, https://doi.org/10.1016/j.lwt.2018.10.054

Hossain L., Whitney K., Simsek S. (2026), Hemp seed as an emerging source of nutritious functional ingredients, *Critical Reviews in Food Science and Nutrition,* 66, pp. 933-949, https://doi.org/10.1080/10408398.2025.2534839

Izzo L., Castaldo L., Narváez A., Graziani G., Gaspari A., Rodríguez-Carrasco Y., Ritieni A. (2020), Analysis of phenolic compounds in commercial *Cannabis sativa* L. inflorescences using UHPLC-Q-Orbitrap HRMS, *Molecules,* 25(3), 631, https://doi.org/10.3390/molecules25030631

Kosewski G., Chanaj-Kaczmarek J., Dziedzic K., Jakubowski K., Lisiak N., Przysławski J., Drzymała-Czyż S. (2025), Changes in polyphenolic profile and antioxidant properties of selected raw and processed vegetables under different cooking methods, *Applied Sciences,* 15, 4677, https://doi.org/10.3390/app15094677

Lott J.N.A., Ockenden I., Raboy V., Batten G.D. (2000), Phytic acid and phosphorus in crop seeds and fruits: a global estimate, *Seed Science Research,* 10(1), pp. 11-33, https://doi.org/10.1017/S0960258500000039

Marcelli A., Osimani A., Aquilanti L. (2025), Vegetable by-products from industrial processing: From waste to functional ingredient through fermentation, *Foods,* 14(15), 2704, https://doi.org/10.3390/foods14152704

Masiala A., Vingadassalon A., Lemoyne S., Pejcz E., Wojciechowicz-Budzisz A., Olędzki R., Aurore G., Harasym J. (2024), Sustainable valorization of breadfruit (*Artocarpus altilis* leaves) as a pasta ingredient, *Sustainability,* 16(24), 11030, https://doi.org/10.3390/su162411030

Munteanu I.G., Apetrei C. (2021), Analytical methods used in determining antioxidant activity: A review, *International Journal of Molecular Sciences,* 22(7), 3380, https://doi.org/10.3390/ijms22073380

Nissen L., Di Carlo E., Gianotti A. (2020), Prebiotic potential of hemp blended drinks fermented by probiotics, *Food Research International,* 131, 109029, https://doi.org/10.1016/j.foodres.2020.109029

Okomo Aloo S., Park S., Oh D.H. (2023), Impacts of germination and lactic acid bacteria fermentation on anti-nutrients, bioactive compounds, and selected functional properties of industrial hempseed (*Cannabis sativa* L.), *Food Chemistry,* 428, 136722, https://doi.org/10.1016/j.foodchem.2023.136722

Pal P., Singh A.K., Srivastava R.K., Rathore S.S., Sahoo U.K., Subudhi S., Sarangi P.K., Prus P. (2024), Circular bioeconomy in action: Transforming food wastes into renewable food resources, *Foods,* 13, 3007, https://doi.org/10.3390/foods13183007

Palacios C.E., Nagai A., Torres P., Rodrigues J.A., Salatino A. (2021), Contents of tannins of cultivars of sorghum cultivated in Brazil, as determined by four quantification methods, *Food Chemistry,* 337, 127970, https://doi.org/10.1016/j.foodchem.2020.127970

Pasini G., Arp C.G., De Leo S., Brandolini A., Estivi L., Hidalgo A. (2025), Technological and nutritional characteristics of gluten-free pasta enriched with tomato and linseed by-products, *Food Science & Nutrition,* 13, e71105, https://doi.org/10.1002/fsn3.71105

Pérez M., Dominguez-López I., Lamuela-Raventós R.M. (2023), The chemistry behind the Folin-Ciocalteu method for the estimation of (poly)phenol content in food: Total phenolic intake in a Mediterranean dietary pattern, *Journal of Agricultural and Food Chemistry,* 71(46), pp. 17543-17553, https://doi.org/10.1021/acs.jafc.3c04022

Pontonio E., Verni M., Dingeo C., Diaz-de-Cerio E., Pinto D., Rizzello C.G. (2020), Impact of enzymatic and microbial bioprocessing on antioxidant properties of hemp (*Cannabis sativa* L.), *Antioxidants,* 9(12), 1258, https://doi.org/10.3390/antiox9121258

Rajasekhar K., Fausto S., Byron S., Frank C., Chris B., Rodney C., Eric W. (2021), Characterization of the nutritional and safety properties of hemp seed cake as animal feed ingredient, *International Journal of Livestock Production,* 12(2), pp. 53-63, https://doi.org/10.5897/IJLP2020.0750

Reale A., Konietzny U., Coppola R., Sorrentino E., Greiner R. (2007), The importance of lactic acid bacteria for phytate degradation during cereal dough fermentation, *Journal of Agricultural and Food Chemistry,* 55(8), pp. 2993-2997, https://doi.org/10.1021/jf063507n

Russo R., Reggiani R. (2013), Variability in antinutritional compounds in hempseed meal of Italian and French varieties, *Plant,* 1(2), pp. 25-29, https://doi.org/10.11648/j.plant.20130102.13

Salim R., Nehvi I.B., Mir R.A., Tyagi A., Ali S., Bhat O.M. (2023), A review on anti-nutritional factors: Unraveling the natural gateways to human health, *Frontiers in Nutrition,* 10, 1215873, https://doi.org/10.3389/fnut.2023.1215873

Scheibenzuber S., Pucci E., Presenti O., Serafini G., Nobili C., Zoani C., Duta D.E., Mihai A.L., Criveanu-Stamatie G.D., Belc N., Falch E., Rustad T., Rychlik M. (2025), Consumers acceptance of new food ingredients from the food industry's by-products — a focus group study, *Frontiers in Nutrition,* 12, 1509833, https://doi.org/10.3389/fnut.2025.1509833

Shilev S., Neykova I., Petrova S. (2025), Valorization of agricultural residues to valuable products: A circular bioeconomy approach, In: Bayer T., Kircher M. (Eds.), *Biowaste to Value-Added Products, Advances in Biochemical Engineering/Biotechnology*, Springer Nature Switzerland, Cham, https://doi.org/10.1007/10_2025_286

Shraim A.M., Ahmed T.A., Rahman M.M., Hijji Y.M. (2021), Determination of total flavonoid content by aluminum chloride assay: A critical evaluation, *LWT – Food Science and Technology,* 150, 111932, https://doi.org/10.1016/j.lwt.2021.111932

Solomakou N., Fotiou D., Goula A.M. (2025), The use of agricultural waste in developing nutrient-rich pasta: The use of beet stalk powder, *Recycling,* 10(6), 217, https://doi.org/10.3390/recycling10060217

Spampinato G., Candeliere F., Amaretti A., Paris R., Montanari M., Virzì N., Strani L., Citti C., Cannazza G., Rossi M., Raimondi S. (2024), A three-years survey of microbial contaminants in industrial hemp inflorescences from two Italian cultivation sites, *Journal of Cannabis Research,* 6(1), 31, https://doi.org/10.1186/s42238-024-00241-z

Spano M., Di Matteo G., Ingallina C., Sobolev A.P., Giusti A.M., Vinci G., Cammarone S., Tortora C., Lamelza L., Prencipe S.A., Gobbi L., Botta B., Marini F., Campiglia E., Mannina L. (2022), Industrial hemp (*Cannabis sativa* L.) inflorescences as novel food: The effect of different agronomical practices on chemical profile, *Foods,* 11(22), 3658, https://doi.org/10.3390/foods11223658

Stabnikova O., Shevchenko O., Stabnikov V., Paredes-López O. (Eds.), (2023a), *Bioconversion of Waste to Value-added Products*, CRC Press, Boca Raton, London, New York, https://doi.org/10.1201/9781003329671

Stabnikova O., Shevchenko A., Stabnikov V., Paredes-López O. (2023b), Utilization of plant processing wastes for enrichment of bakery and confectionery products, *Ukrainian Food Journal*, 12(2), pp. 299-308, https://doi.org/10.24263/2304-974X-2023-12-2-11

Technical Regulation, Decision No. 775, 2007. "Bakery and Pasta Products" (Hotărârea Guvernului nr. 775 din 03.07.2007 cu privire la aprobarea Reglementării tehnice "Produse de panificație și paste făinoase"), Official Monitor of the Republic of Moldova.

Thaipong K., Boonprakob U., Crosby K., Cisneros-Zevallos L., Hawkins Byrne D. (2006), Comparison of ABTS, DPPH, FRAP, and ORAC assays for estimating antioxidant activity from guava fruit extracts, *Journal of Food Composition and Analysis,* 19(6-7), pp. 669-675, https://doi.org/10.1016/j.jfca.2006.01.003

Tolve R., Pasini G., Vignale F., Favati F., Simonato B. (2020), Effect of grape pomace addition on the technological, sensory, and nutritional properties of durum wheat pasta, *Foods,* 9(3), 354, https://doi.org/10.3390/foods9030354

UNEP (2024), Food Waste Index Report 2024: Think Eat Save. Tracking Progress to Halve Global Food Waste, United Nations Environment Programme, Nairobi

U.S. FDA (2026), 21 CFR Part 114 – Acidified foods, Electronic Code of Federal Regulations, U.S. Government Publishing Office, https://www.ecfr.gov/current/title-21/chapter-I/subchapter-B/part-114

Wang J., Li Y., Guo X., Zhu K., Wu Z. (2024), A review of the impact of starch on the quality of wheat-based noodles and pasta: From the view of starch structural and functional properties and interaction with gluten, *Foods,* 13(10), 1507, https://doi.org/10.3390/foods13101507

Zhang H.W., Bai X.L. (2014), Optimization of extraction conditions for phytic acid from rice bran using response surface methodology and its antioxidant effects, *Journal of Food Science and Technology,* 51(2), pp. 371-376, https://doi.org/10.1007/s13197-011-0521-y

Zhang L., Li A., Liu H., Mo Q., Zhong Z. (2025), Effects of lactic acid bacteria fermentation on the release and biotransformation of bound phenolics in Ma bamboo shoots (*Dendrocalamus latiflorus* Munro), *Foods,* 14(15), 2573, https://doi.org/10.3390/foods14152573

Cite:

Capcanari, T., Covaliov, E., Țurea, N., Radu, O., & Popovici, V. (2026). Fermentation-assisted valorisation of hemp-derived ingredients for functional pasta development. *Ukrainian Food Journal, 15*(2), 271–292. https://doi.org/10.24263/2304-974X-2026-15-2-3

Influence of membrane lipid composition on the stability of encapsulated DNA under oxidative stress

Gaolin Hu[1], Tamara Nosenko[2], Serhii Stankevych[3], Tetiana Ovsiannikova[4]

1 – Chinasoft International Ltd, Shanghai, China
2 – National University of Food Technologies, Kyiv, Ukraine
3 – State Biotechnological University, Kharkiv, Ukraine
4 – National Technical University «Kharkiv Polytechnic Institute», Kharkiv, Ukraine

Keywords:

DNA
Encapsulation
Liposomes
Oxidative stress
Protection
Lipid saturation
Hydrogen peroxide
Membrane stability

Article history:

Received 21.12.2025
Received in revised form 26.03.2026
Accepted 30.06.2026

Corresponding author:

Gaolin Hu
E-mail: green_hu@aliyun.com

DOI:
10.24263/2304-974X-2026-15-2-4

Abstract

Introduction. The aim of research is to establish the patterns of influence of the fatty acid composition of lipid membranes (using the example of liposomes) on the resistance of encapsulated DNA to oxidative degradation.

Materials and methods. The objects of the study are liposomes from tristearin, triolein and their 1:1 mixture; total *E. coli* DNA. DNA isolation was carried out by phenol-chloroform extraction. Liposomes were obtained by thin-film hydration with extrusion. Encapsulation was assessed by fluorescence method (PicoGreen). Oxidative stress was simulated by H_2O_2 (1 mM, 37 °C, 120 min). DNA degradation was analyzed by agarose electrophoresis with densitometry (ImageJ).

Results and discussion. The efficiency of DNA encapsulation was similar for all liposome types, ranging from 28.4±3.2% for tristearin-based liposomes to 31.7±2.9% for triolein-based liposomes and 29.6±3.5% for the 1:1 lipid mixture. The protective capacity of liposomes against oxidative stress strongly depended on the degree of saturation of lipid acyl chains.

The amount of intact DNA retained after 120 min of incubation with 1 mM H_2O_2 at 37 °C was 82.3±2.4% for tristearin-based liposomes, 58.4±1.6% for the 1:1 mixture, and 38.1±1.1% for triolein-based liposomes, whereas free DNA retained only 6.3±2.1%. At earlier time points, the same trend was observed: after 30 min, DNA preservation was 94.5±3.2% for tristearin, 83.6±3.9% for the 1:1 mixture, and 72.8±4.8% for triolein, compared with 41.2±5.1% for free DNA. After 60 min, the corresponding values were 88.7±4.0%, 71.2±4.4%, 54.3±5.2%, and 18.6±3.8%, respectively.

A clear linear relationship was observed between the degree of lipid unsaturation (Dun) and the amount of protected DNA (ADNAp). The regression equations describing the kinetic behavior were as follows: at 30 min, $ADNAp = -12.5 \cdot Dun + 107.07$ ($R^2 = 0.9888$); at 60 min, $ADNAp = -16.9 \cdot Dun + 105.67$ ($R^2 = 0.9954$); and at 120 min, $ADNAp = -20.35 \cdot Dun + 98.867$ ($R^2 = 0.9981$).

These results demonstrate that saturated lipids provide superior protection against oxidative DNA damage due to their tightly packed bilayer structure and higher phase transition temperature, whereas unsaturated lipids form more membranes that are fluid in which double bonds are more susceptible to oxidative attack.

Conclusions. A quantitative linear relationship exists between triacylglycerol unsaturation and liposome-protected DNA stability under oxidative stress; saturated lipids (tristearin) are the most suitable matrix for stable food-industry DNA calibrators.

Introduction

Oxidative damage to nucleic acids is a key challenge in modern biotechnology and analytical quality control. This issue concerns not only fundamental research (e.g., ageing and mutagenesis), but also applied fields such as the stability of reference materials for PCR, preservation of genetic material in biobanks (Cordsmeier et al., 2022), and quality control of food raw materials for GMO detection (Shin et al., 2025). In all these areas, DNA degradation induced by oxidative stress represents a major limitation.

DNA calibrators and standard reference samples used in PCR-based food authentication and GMO analysis require high stability, as their integrity directly affects measurement accuracy (Benamara et al., 2025). However, long-term storage often leads to oxidative damage, resulting in DNA fragmentation and potentially underestimated analytical results. A similar challenge exists in biobanking, where maintaining genetic integrity over extended periods is critical (Cordsmeier et al., 2022).

Recent studies have shown that oxidation of unsaturated lipids in nanoparticle systems can lead not only to degradation of the lipid matrix but also to the formation of covalent adducts between lipid oxidation products and nucleic acids (Estabrook et al., 2025). This indicates that lipid systems are not merely passive carriers but may actively influence DNA stability. However, the underlying mechanisms remain insufficiently understood, particularly the role of lipid fatty acid composition in protecting encapsulated DNA. Given the growing demand for stable DNA calibrators in PCR-based food analysis, this topic is of significant practical relevance.

Although lipid-based systems for nucleic acid protection have been widely studied, most research has focused on cationic liposomes for gene delivery or on encapsulation of low-molecular-weight antioxidants. Regarding DNA protection itself, several key questions remain unresolved. Estabrook et al. (2025) demonstrated that oxidative degradation of unsaturated lipids within nanoparticles generates electrophilic products capable of reacting with adjacent siRNA molecules. This finding highlights a direct link between lipid composition and nucleic acid stability. However, their study focused on chemically modified lipids and did not systematically address how varying degrees of unsaturation in neutral lipid bilayers influence nucleic acid degradation. This gap persists because most studies are oriented toward efficient gene delivery, where cargo release is desirable, rather than long-term stabilization of genetic material for analytical applications (Gardea-Gutiérrez et al., 2025; Burger et al., 2025).

Additional studies have shown that lipid structure can influence DNA condensation (Thongbamrer et al., 2025), but these systems are typically designed for ROS-triggered release rather than protection, reflecting the different objectives of pharmacology (delivery) versus biobanking and analytical metrology (preservation). Solid lipid nanoparticles have also been investigated for protecting biological materials during cryopreservation (Asadi et al., 2025), but the observed effects are mainly attributed to encapsulated antioxidant compounds (e.g., linalool), while the lipid matrix itself is considered chemically inert. Thus, the intrinsic physicochemical properties of the lipid matrix (such as saturation degree and phase behavior) and their contribution to DNA protection remain unclear.

Therefore, a clear research gap exists: there is a lack of systematic quantitative studies addressing how the degree of fatty acid unsaturation in neutral liposomes affects the oxidative stability of encapsulated DNA. This necessitates the use of simplified model liposome systems without additional antioxidants or charged components.

The aim of this study is to elucidate the influence of lipid membrane fatty acid composition (using liposomes as a model system) on the resistance of encapsulated DNA to oxidative degradation. The results are expected to support the rational design of lipid matrices for stable DNA calibrators and reference materials used in PCR-based food quality control.

Materials and methods

Test materials used in the experiment

The following materials were used in this study: tristearin (Sigma-Aldrich, T4887, China), chemically pure grade, CAS 555-43-1; triolein (Sigma-Aldrich, T7140, China), chemically pure grade, CAS 122-32-7; and a 1:1 (w/w) mixture of the two lipids, prepared immediately prior to use.

Total DNA isolated from *Escherichia coli* K-12 (strain CGMCC 1.3373) was used without further fractionation.

Research procedure

The study was performed in several consecutive stages. At the first stage, liposomal vesicles of three types were prepared – based on tristearin, triolein and their mixture in a 1:1 ratio. In parallel, total DNA was isolated from *Escherichia coli* cells.

At the second stage, the obtained DNA was encapsulated in liposomes of the indicated compositions. After that, the efficiency of encapsulation was assessed by quantitative fluorescence method using the PicoGreen dye.

At the third stage, the resistance of encapsulated DNA to oxidative stress was studied. For this, the samples were incubated with 1 mM H_2O_2 at 37 °C, taking aliquots after 0, 30, 60 and 120 minutes. The degree of DNA degradation was analyzed by agarose electrophoresis followed by densitometric analysis in the ImageJ program.

At the fourth stage, based on the obtained quantitative data, graphs were constructed of the dependence of the preserved DNA on the degree of lipid unsaturation and a correlation analysis was performed.

Preparation of liposomal vesicles

Liposome formation was performed using a classical approach, namely the thin-film hydration method, which was further supplemented with an extrusion procedure to standardize the vesicle size (Zhang, 2023). Three lipid mixtures with different compositions were prepared for the experiments. In the first case, 10 mg of fully saturated tristearin was used, the second sample consisted of 10 mg of unsaturated triolein. The third option was a combined system, where both lipids were taken in equal mass ratios. Each mixture was dissolved in 5 ml of chloroform. The solution was transferred to a 50 ml round-bottom flask. On a rotary evaporator at a temperature of 50 °C (for triolein) or 60 °C (for tristearin and the mixture) and reduced pressure, the solvent was removed by rotating the flask until a thin transparent film was formed on the walls. The flask was left in a vacuum desiccator for 2 hours to remove solvent residues. Then, 10 ml of HEPES buffer (4-[(2-hydroxyethyl)-1-piperazinyl]-ethanesulfonic acid – 20 mM, pH 7.4, NaCl – 150 mM) was added, preheated to a temperature above the phase transition temperature of the corresponding lipid. The flask was gently shaken manually until the film was completely separated from the walls, forming a suspension of multilamellar liposomes. To obtain small unilamellar vesicles, the suspension was passed through an extruder with polycarbonate membranes of successively decreasing pore diameter: 11 times through a 200 nm membrane, then 11 times through a 100 nm membrane, and finally 11 times through a 50 nm membrane. For samples containing tristearin, extrusion was performed on a heating block at 60 °C. The obtained liposomes were stored at 4 °C for no more than 7 days.

Isolation of total DNA from *Escherichia coli*

DNA was isolated from an overnight culture of *Escherichia coli* K-12 (strain CGMCC 1.3373) grown on Luria-Bertani medium (Cheng et al., 2004). 5 ml of the culture was removed and centrifuged for 10 min at 5000 g. The supernatant was discarded. 500 µl of cell lysis buffer (100 mM Tris-HCl pH 8.0, 50 mM EDTA, 1% SDS) and proteolytic enzyme (10 µl of proteinase K (20 mg/ml)) were added to the pellet. The mixture was then incubated for 1 h at 55 °C, during which it was stirred periodically.

After lysis, 500 µl of a mixture of phenol: chloroform: isoamyl alcohol (25:24:1) was added to the system. Then the resulting substance was shaken vigorously until an emulsion was formed and centrifuged for 10 min at 10000 g. The upper (aqueous) phase was transferred to a clean tube carefully enough not to touch the interphase. The extraction was repeated twice.

The aqueous phase after two extractions was combined and 600 µl of cold isopropanol was added to it. The resulting mixture was stirred and left for 20 min at a temperature of -20 °C. After exposure, the mixture was separated by centrifugation for 15 min at 12000 g. The precipitate formed was washed twice with 500 µl of cold 70% ethanol. Moreover, each time after adding ethanol, centrifugation was carried out for 5 min at 12000 g. The precipitate was dried in air for 15-20 min. The dried precipitate was dissolved in 100 µl of TE-buffer (10 mM Tris-HCl pH 8.0, 1 mM EDTA). The concentration of the isolated DNA was determined spectrophotometrically at a wavelength of 260 nm. The purity of the isolated total DNA was assessed by the ratio of the optical density A260/A280. Samples were considered acceptable for further studies if they had a value of 1.8–2.0. The obtained total DNA samples were stored at -20 °C.

Encapsulation of DNA into liposomes

For encapsulation, freshly prepared liposomes (according to p. 2. 3) and a solution of total *E. coli* DNA (p. 2. 4) with a concentration of 1 mg/ml were used. 1 ml of liposome suspension (5 mg/ml in lipids) was mixed with 200 µl of DNA solution (DNA:lipid ratio 1:10 by weight). The mixture was incubated for 30 min at room temperature, periodically gently mixing (without vortexing). To stabilize the formed lipoplexes, the mixture was passed once through an extruder with a 100 nm membrane. Encapsulation was carried out separately for three types of liposomes: based on tristearin, triolein and their 1:1 mixture. A control sample was also used – DNA without liposomes, treated similarly (Burger et al., 2025).

Purification of liposomes from unencapsulated DNA and determination of encapsulation efficiency

The obtained liposomes were purified by gel filtration. A 10 ml column was prepared (a syringe filled with Sepharose CL-4B, equilibrated with TE buffer). 0.5 ml of the liposome-DNA mixture was applied to the column. Elution was performed with TE buffer, collecting 0.5 ml fractions. The cloudy fractions (first 2–3 ml) – liposomes with encapsulated DNA – were combined. The clear fractions contained free DNA. The encapsulation efficiency was determined using the Quant-iT PicoGreen dsDNA Assay Kit (ThermoFisher, USA). A calibration curve was prepared using standard DNA samples (0–1000 ng/ml). The purified liposomes were diluted 300 times with TE buffer.

The fluorescence of two series of samples was measured:

1) 100 µl of diluted liposomes + 100 µl of TE buffer;

2) 100 µl of diluted liposomes + 100 µl of TE buffer with 1% Triton X-100 (final Triton concentration 0.5%).

After 10 min of incubation at room temperature, 100 µl of PicoGreen solution (Invitrogen, USA), a fluorescent dye for quantitative determination of double-stranded DNA in solution, diluted 1:200 in TE buffer, was added. Incubation was carried out for 5 min in the dark. Fluorescence was measured at λ_{ex}=480 nm and λ_{em}=520 nm on a ST-360 plate reader (KHB, China). The DNA concentration was determined from the calibration curve (Saxena, 2023). The encapsulation efficiency E_e was calculated by the formula:

$$E_e = \frac{(C_{lis} - C_{unlyz})}{C_{lis}}, \% \quad (1)$$

where C_{lis} is the concentration of DNA in lysed liposomes (total DNA),

C_{unliz} is the concentration of DNA in unlysed liposomes (external DNA).

Resistance of encapsulated DNA to oxidative degradation

Oxidative degradation was initiated by adding hydrogen peroxide. Its concentration (1 mM) was selected based on the results of previous experiments: under these conditions, free DNA was moderately damaged, i.e., it was not destroyed instantly, but gradually, which allowed recording the kinetics of the process for 120 minutes (Qing et al., 2006). In each tube containing 200 µl of sample (liposomes of one of the three types or free DNA), H_2O_2 was added to the final concentration indicated above. All samples were incubated at 37 °C. After 0, 30, 60, and 120 minutes, 50 µl aliquots were taken, which were immediately mixed with 10 µl of sample loading buffer. Buffer composition: 40% glycerol, 0.25% bromophenol blue, 50 mM EDTA (pH 8.0). Control samples, to which H_2O_2 was not added, underwent the same incubation and selection procedure.

Electrophoretic fractionation of samples was performed in a 1.5% agarose gel. The buffer system was a TAE solution (composition: 40 mM Tris, 20 mM sodium acetate, 1 mM EDTA; pH adjusted to 8.0). Aliquots of 20 µl of each sample were added to the prepared gel wells. Separation was performed at a constant voltage of 100 volts for 40 minutes. After completion of electrophoresis, the gel was transferred to a solution of SYBR Green I dye (dilution 1:10,000 in the same TAE buffer) and incubated for 20 minutes in the absence of light. Detection of fluorescent bands was performed using a transilluminator equipped with a blue LED source with a wavelength of 490 nm. The gel image was recorded with a digital camera.

Quantitative analysis of DNA degradation

Gel photographs were processed in the ImageJ 1.54f program (public domain, NIH, USA). A brightness profile was constructed for each lane, which allows us to see exactly where the DNA bands are located on the gel. Next, the area of the peak corresponding to high-molecular-weight (i.e., non-degraded) DNA was measured. If degradation was visible in the lane, a slightly different approach was used: the total area under the entire profile curve was measured, from the beginning to the end of the lane (full-lane quantification gives a more accurate picture when DNA breaks down into small fragments). The percentage of retained DNA was calculated relative to a control sample to which H_2O_2 was not added. This control sample was conventionally taken as 100% retained DNA (Schneider et al., 2012).

Statistical data processing

All experiments were performed in triplicate. Data are presented as mean±standard deviation (M±SD). Statistical analysis was performed using GraphPad Prism 9.0 (GraphPad Software, USA). Two-tailed Student's t-test was used to compare two groups. One-way analysis of variance (ANOVA) was used for multiple comparisons, followed by Tukey's post hoc test. Differences between groups were considered statistically significant at $p < 0.05$. Microsoft Excel 2016 (Microsoft, USA) was used to construct graphs.

Results and discussion

Encapsulation of total *E. coli* DNA into liposomes of different fatty acid composition

At the first stage of the work, it was necessary to assess how effectively triacylglycerols of different degrees of saturation are able to form liposomes and include total DNA isolated from E. coli. For this purpose, three types of liposomes were prepared – based on tristearin (fully saturated), triolein (unsaturated) and their mixture in a 1:1 ratio. Free DNA, which was not encapsulated, served as a control.

After encapsulation and purification of liposomes from unbound DNA, the efficiency of inclusion of genetic material was determined. The measurement results are given in Table 1.

Table 1

Efficiency of encapsulation of total *E. coli* DNA in liposomes of different composition

Liposome type	Encapsulation efficiency, %
Tristearin	28.4±0.8
Triolein	31.7±1.0
1:1 Mixture	29.6±0.9

As can be seen from Table 1, all three types of liposomes provide similar encapsulation efficiencies ranging from 28 to 32%. Statistical analysis did not reveal significant differences between groups. Thus, the degree of unsaturation of the fatty acid chains in the lipid bilayer has virtually no effect on the ability of liposomes to capture DNA during passive loading. A typical elution profile on a Sepharose CL-4B column for a tristearin-based liposome sample is shown in Figure 1. Liposomes were eluted from the column in fractions 2–5 (eluate volume 1.0–2.5 ml), which corresponds to the free volume of the column. Free unbound DNA was eluted later in fractions 9–12 (volume 4.5–6.0 ml). Fluorescence in the fractions containing liposomes increased 3–4-fold after addition of Triton X-100 compared to unlysed samples, indicating successful incorporation of DNA into the internal volume of vesicles based on the studied lipid raw material.

The obtained efficiency values (about 30%) are in good agreement with the literature data for passive loading of DNA into neutral liposomes. In the works (Estabrook et al., 2025; Thongbamrer et al., 2025) 25–40% incorporation for such systems is reported. Slightly higher rates (up to 60–70%) are achieved when using cationic liposomes or active encapsulation (Gardea-Gutiérrez et al., 2025; Burger et al., 2025), but this was not part of the objectives of this study. It is important to emphasize that total DNA isolated from *E. coli* is a mixture of

fragments of different lengths – from several hundred to tens of thousands of base pairs. Such heterogeneity will likely affect the incorporation efficiency, since long molecules are more difficult to "pack" inside the vesicle. Nevertheless, the results obtained indicate that encapsulation occurs in a comparable manner for all three types of liposomes. This allows for a correct comparison of their ability to protect DNA from oxidative damage in the next step. If the encapsulation efficiency were significantly different, any differences in protection could be explained simply by the different amounts of DNA inside the liposomes, rather than by the qualitative properties of the membrane.

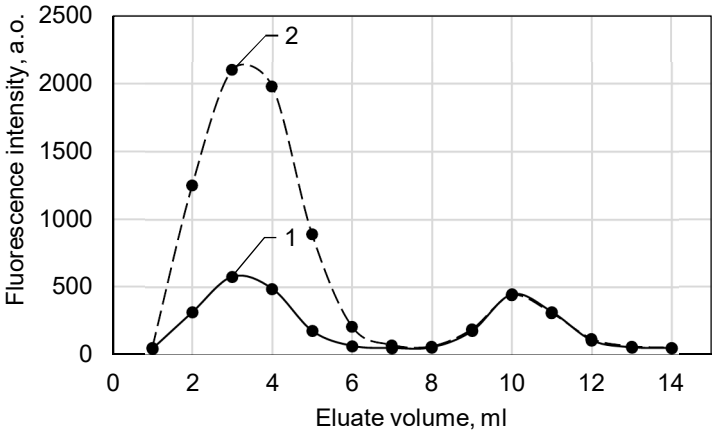

Figuure 1. Elution profile of tristearin-based liposomes on a Sepharose CL-4B column after incubation with DNA:
1 – PicoGreen fluorescence in unlysed liposomes (external DNA);
2 – fluorescence after addition of Triton X-100 (total DNA)

The results obtained indicate that liposomes based on both saturated and unsaturated lipids can be used to create DNA calibrators and standard samples for PCR control in the food industry. The encapsulation efficiency will be comparable. This is important from the point of view of technological flexibility, because the production of standard samples can be adjusted using more accessible or technological lipid raw materials without losing the yield of the target product.

It is necessary to note certain limitations of the described method. The use of total DNA rather than plasmid or size-defined fragmented DNA may introduce additional variability and, consequently, affect reproducibility between different DNA isolation batches. In addition, the passive loading approach used in this study does not allow control over the amount of DNA encapsulated per vesicle or its spatial organization within liposomes. However, these limitations do not affect the main conclusion that no significant differences in encapsulation efficiency were observed between the studied formulations.

Since the encapsulation efficiency was found to be the same for all three types of liposomes, the next logical step is to investigate the protective properties of these systems under oxidative stress conditions (see sections 3.2 and 3.3). In addition, it seems promising to study the effect of adding cholesterol to the composition of liposomes on the stability of encapsulated DNA, since cholesterol is known to increase the mechanical stability of the lipid bilayer (Boonnoy et al., 2024).

Resistance of encapsulated DNA to oxidative stress depending on fatty acid composition of liposomes

The next stage of the work was to find out whether the degree of saturation of fatty acid chains in the composition of liposomes affects their ability to protect encapsulated DNA from oxidative degradation. For this, samples of liposomes of three types (tristearin, triolein, 1:1 mixture) with encapsulated DNA were incubated with hydrogen peroxide (1 mM) at 37 °C. Free DNA, which was not encapsulated but underwent the same treatment, served as a control. The results of the quantitative analysis are shown in Figure 2 and Table 2.

Table 2

Retained intact DNA (%) after incubation with H_2O_2

Sample Type	Time of incubation, min		
	30	60	120
Free DNA (control)	41.2±0.8	18.6±0.5	6.30±0.03
Tristearin	94.5±2.7	88.1±2.6	78.0±2.4
Triolein	68.8±2.1	54.3±1.6	37.3±1.1
1:1 Mixture	83.6±2.4	73.2±2.1	59.2±1.6

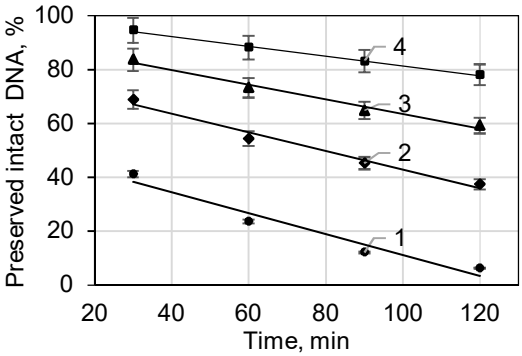

Figure 2. Dependence of the degree of preservation of intact DNA in samples (in % of the initial amount) on the incubation time with H_2O_2: 1 – free DNA (control); 2 – tristearin (saturated); 3 – triolein (unsaturated); 4 – mixture 1:1

From the data in Table 2 and Figure 2 it is clear that after 2 hours of incubation in a solution of H_2O_2, no more than 6% of free DNA remains intact. Encapsulation of DNA in liposomes changes the situation radically. The best protected DNA was found in liposomes from tristearin, the degree of preservation there reached more than 80%. Triolein liposomes, on the contrary, showed weak protection, because after 120 minutes of incubation, less than 40% of the genetic material remained intact. For a 1:1 mixture, an intermediate value was obtained – less than 60%.

As can be seen from Figure 2, the amount of intact DNA decreases over time for all types of samples, but the rate and extent of this decrease are markedly different depending on the liposome composition. For free DNA (curve 1), the most rapid degradation is observed: after 120 minutes, only a small fraction of the initial DNA remains intact. Encapsulation in liposomes significantly retards the degradation process, with the protective

effect being greatest for tristearin-based liposomes (curve 2) and least pronounced for triolein-based ones (curve 3). The 1:1 mixture (curve 4) shows intermediate behaviour, confirming the gradual transition of protective properties with changing lipid unsaturation.

The kinetic curves are well described by linear regression equations (Figure 2). The coefficients of determination (R^2) for all curves exceed 0.95, indicating a good fit of the data to a linear model within the studied time interval (0–120 min). The slope of the curves reflects the rate of DNA degradation: the steepest decline is observed for free DNA (slope -11.62), while the gentlest slope corresponds to tristearin liposomes (slope -5.46). The slopes for triolein and the 1:1 mixture are intermediate (-8.16 and -10.36, respectively). This indicates that the saturated lipid matrix provides the slowest degradation rate, whereas the unsaturated matrix accelerates DNA loss. The calculated regression equations, coefficients of determination, Pearson correlation coefficients (r) and significance of correlation (p) for the dependence of the amount of preserved DNA A_{DNAp}, % (amount of DNA protected) on the time τ, min for each sample type are summarised in Table 3.

Table 3

Linear regression parameters for DNA degradation kinetics

Sample type	Regression equation	R^2	Pearson correlation coefficient	Significance of correlation
Free DNA (control)	$A_{DNAp} = -11.62\ \tau + 49.845$	0.9506	-0.9750	0.005
Tristearin (saturated)	$A_{DNAp} = -5.46\ \tau + 99.55$	0.9962	-0.9981	0.002
Triolein (unsaturated)	$A_{DNAp} = -10.36\ \tau + 77.3$	0.9785	-0.9892	0.003
Mixture 1:1	$A_{DNAp} = -8.16\ \tau + 90.6$	0.9829	-0.9914	0.002

The slope values clearly demonstrate that the encapsulation of DNA in liposomes alters the degradation kinetics: while free DNA loses integrity rapidly, the liposomal formulations provide a substantial protective effect. Among the liposomes, tristearin (fully saturated) exhibits the lowest degradation rate, while triolein (unsaturated) shows the highest rate, indicating a strong relationship between lipid saturation and protective capacity. The mixture 1:1 gives an intermediate degradation rate, which is consistent with its intermediate unsaturation level. These results suggest that the protective ability of liposomes can be tuned by adjusting the ratio of saturated to unsaturated lipids, providing a basis for designing liposomal carriers with controlled DNA stability.

The results obtained can be explained by the different structural organization of the liposome shell. Saturated tristearin chains are able to pack tightly, forming a membrane with a high phase transition temperature (about 55 °C). Such a membrane is poorly permeable, which prevents the diffusion of H_2O_2 and free radicals into the interior of the vesicle. Unsaturated triolein chains in liposomes behave differently. The double bonds in them themselves act as targets for oxidative damage. In addition, the membrane formed by them is more liquid, its phase transition temperature is about -20 °C. Due to this structure, it is noticeably easier for oxidant molecules to penetrate the vesicle. A mixture of the initial components in liposomes provides an intermediate option: a homogeneous bilayer with an average packing density is formed, which, apparently, determines its properties.

Our finding that saturated lipids provide superior protection aligns with the concept that bilayer structure dictates permeability and oxidative stability. This is consistent with molecular dynamics simulations showing that cholesterol, which orders the bilayer, inhibits oxygen permeation and reduces oxidative damage to unsaturated lipids (Boonnoy et al., 2024). However, that study focused solely on oxygen dynamics, whereas our work directly demonstrates protection of an encapsulated macromolecule – DNA.

The importance of lipid structure for nucleic acid interactions is further supported by studies on ROS-sensitive nanoparticles, where lipid chain length and structure affect DNA condensation efficiency (Thongbamrer et al., 2025; Zhao et al., 2024). These systems, however, are designed for ROS-triggered release, not for long-term preservation – a distinction driven by the differing goals of pharmacology versus biobanking and metrology.

Similarly, solid lipid nanoparticles have been used to protect cells during cryopreservation, but the observed effects are attributed to encapsulated antioxidants (e.g., linalool), while the lipid matrix itself is treated as an inert carrier (Asadi et al., 2025). Our study, by using pure lipids without additives, reveals that the matrix itself contributes significantly to protection, a role that has been overlooked in previous studies.

The obtained data are in good agreement with the literature data. In the works (Das et al., 2016; Mathews et al., 2024) it is shown that liposomes based on saturated phospholipids (DPPC) provide higher stability of encapsulated antioxidants than liposomes based on unsaturated ones (DOPC). Our study confirms this pattern for another system – DNA encapsulation in neutral triacylglycerol vesicles, and also demonstrates the possibility of quantitatively predicting protective properties based on the degree of unsaturation of the lipid components. The obtained results are directly related to the development of stable DNA calibrators for the food industry. To ensure the maximum shelf life of standard samples under conditions that simulate oxidative stress (for example, long-term storage at room temperature and in the presence of oxygen), it is advisable to use liposomes based on saturated fatty acids (tristearin). They provide more effective DNA preservation. For situations where the cost of the raw material is critical, rather than maximum protection, a mixture of saturated and unsaturated lipids (ratio 1:1) can be used, which provides an intermediate level of stability (about 58% after 120 min). Triolein and more unsaturated raw materials in pure form for the creation of long-term calibrators are not recommended due to the low protective capacity. In addition, the proposed model system (encapsulation of DNA in liposomes with subsequent oxidative stress) can be used as a rapid screening test to assess the antioxidant capacity of various lipid matrices. Instead of studying the oxidation of the lipids themselves by complex analytical methods, one can assess the preservation of the DNA reporter, which is much simpler and cheaper.

However, it is worth noting that the experiments were conducted on a model system (phosphate-saline buffer, constant temperature 37 °C) and do not take into account other factors that may affect DNA stability in real storage conditions (variable temperature, humidity, presence of other oxidants, microbial contamination). It is also worth noting that the work used total DNA, which is heterogeneous in length, which could affect the absolute values of degradation. The revealed pattern needs to be confirmed on other types of lipids (for example, with different chain lengths or with the addition of cholesterol). In addition, it is promising to study the protective properties of liposomes under real long-term storage conditions (weeks and months) at different temperatures, as well as in food matrices (oils, emulsions, fatty sauces). The next logical step will be to quantitatively establish a correlation between the degree of lipid unsaturation and the degree of DNA protection.

Relationship between the degree of unsaturation of liposomal lipids and the degree of DNA protection from oxidative degradation

To establish a quantitative relationship between the composition of the lipid matrix and its ability to protect encapsulated DNA, the data obtained in section 3.2 were used. Each type of liposome was assigned a numerical value for the degree of unsaturation. For tristearin, which does not contain double bonds in fatty acid chains, this value was taken as 0. For triolein, each chain of which has one double bond (i.e., three double bonds per molecule), it was taken as 1. For a 1:1 mixture, the degree of unsaturation was calculated as the arithmetic mean – 0.5. This approach is simplified, but acceptable for establishing a general pattern.

The percentage of intact DNA preserved after 60 minutes of incubation with H_2O_2 was chosen as an indicator of protection against oxidative DNA destruction. This time interval was chosen because by 60 minutes, the degradation of free DNA is already significant (less than 20% is retained), but for triolein-based liposomes the signal level is still significantly higher than the background, which allows for a quantitative comparison with acceptable accuracy. For each time interval (30, 60 and 120 min), a graph of the dependence of the retained DNA on the degree of unsaturation of the liposomal lipids was constructed. The results are shown in Figure 3.

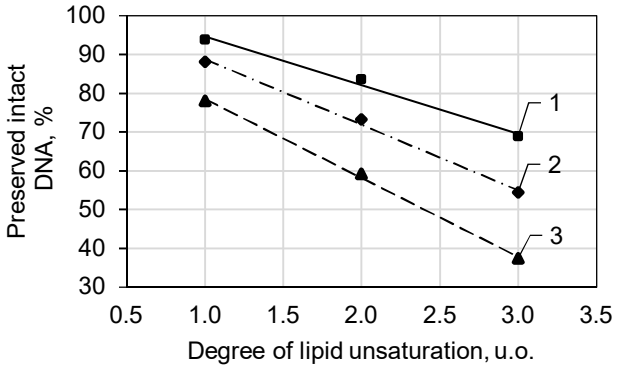

Figure 3. Dependence of preserved intact DNA (%) on the degree of unsaturation of liposome lipids after 30, 60 and 120 minutes of incubation with H_2O_2 (1 mM, 37 °C): 1 – 30 min; 2 – 60 min; 3 – 120 min.

As can be seen from Figure 3, a linear relationship is observed between the degree of lipid unsaturation and the amount of preserved DNA at all three time intervals. An increase in the content of unsaturated fatty acid chains in the composition of liposomes is accompanied by a deterioration in their ability to prevent oxidative degradation of encapsulated DNA. Pearson correlation coefficients (r) and linear regression equations for the dependence of the amount of preserved DNA A_{DNAp}, % (amount of DNA protected) on the degree of unsaturation of liposomal lipids D_{un}, u. o.(degree of unsaturation) for each time interval are given in Table 4.

For all three time intervals, the coefficient of determination R^2 exceeds 0.98, indicating a very close linear relationship. The slope (regression coefficient) increases with time: after 30 minutes it is -10.9, after 60 minutes – -30.5, and after 120 minutes – -41.7. This means that with increasing incubation time, the effect of unsaturation becomes more pronounced.

Therefore, with increasing duration of oxidative stress, the contribution of unsaturation of the lipid matrix to DNA degradation becomes increasingly significant.

Table 4

Linear regression parameters for the dependence of the amount of DNA retained on the degree of unsaturation of liposomal lipids

Incubation time, min	Regression equation	R^2	Pearson correlation coefficient	Significance of correlation
30	A_{DNAp} = -12.5 D_{un} + 107.07	0.9888	-0.9944	0.004
60	A_{DNAp} = -16.9 D_{un} + 105.67	0.9954	-0.9977	0.004
120	A_{DNAp} = -20.35 D_{un} + 98.867	0.9981	-0.9990	0.003

The results obtained allow us to formulate a simple quantitative rule: an increase in the degree of unsaturation by 0.1 units (i.e. by 10% when going from pure saturated lipid to a mixture with 10% unsaturated) leads to a decrease in the preserved DNA after 60 minutes by approximately 3%. After 120 minutes, this effect is even stronger – a decrease of approximately 4.2% for every 0.1 unit of unsaturation. Although only three values of the degree of unsaturation (0; 0.5; 1) were investigated in this work, the high linearity of the dependence ($R^2 > 0.98$) allows us to assume with a high probability that this pattern will also be observed for intermediate compositions (e.g., 70/30 or 30/70). This is important from a practical point of view, since it allows us to predict the protective properties of liposomes for any ratio of saturated to unsaturated triacylglycerols without conducting additional experiments.

The established linear relationship is the basis for the rational design of lipid matrices for DNA calibrators. The manufacturer of standard samples can be guided by a simple rule: the greater the required storage stability, the lower the degree of unsaturation of the lipid matrix should be. The regression equations given below can be used to quantitatively predict the shelf life of calibrators under conditions simulating oxidative stress. In addition, the proposed approach (using DNA as a molecular probe) can be used to assess the oxidative stability of various lipid systems. Instead of measuring peroxide and anisidine numbers by complex methods, one can assess the stability of the DNA reporter, which is much simpler and requires only electrophoresis equipment and basic software. It should be noted that the established linear relationship was obtained for three points, which is a minimally sufficient number to assume linearity, but not to prove it unambiguously. For a more reliable conclusion, additional experiments with intermediate compositions (e.g., 75/25 and 25/75) are needed.

The observed linear relationship between unsaturation degree and DNA protection also has implications for understanding membrane stability under stress. Changes in fatty acid composition, e.g., under herbicide exposure, are known to disrupt membrane integrity (Li et al., 2024). Our quantitative model provides a framework for predicting how variations in unsaturation affect the protective capacity of lipid bilayers, which may be relevant for designing more stable membrane systems for various applications.

The next step should be to expand the study to other ratios of saturated and unsaturated lipids, as well as to other types of fatty acids (e.g., linoleic, linolenic). In addition, it is promising to study the protective properties of liposomes under different storage conditions (temperature, humidity, lighting). It is also worth checking whether the established linear relationship holds for other types of encapsulated molecules (e.g., RNA, proteins, and small molecules).

Conclusions

The efficiency of total DNA encapsulation is 28–32% for all three types of liposomes – based on tristearin (28.4±3.2%), triolein (31.7±2.9%) and their 1:1 mixture (29.6±3.5%). No statistically significant differences between the compositions were found. The degree of unsaturation of fatty acid chains does not affect the passive inclusion of DNA into the internal volume of liposomes. This is explained by the fact that at the stage of hydration of the lipid film, the formation of vesicles and the capture of dissolved DNA occurs mainly due to physicochemical processes (hydration, swelling, twisting of the bilayer), which weakly depend on the acyl composition of triacylglycerols. Any type of lipid raw material can be used to create DNA calibrators without loss of yield of the target product. This allows the choice of matrix based on cost, availability, or the required level of protection.

After 120 minutes of incubation with 1 mM H_2O_2, the DNA preservation was: for liposomes based on tristearin – 78.0±2.4%, for a 1:1 mixture – 59.2±1.6%, for triolein – 37.3±1.1%. In free (unencapsulated) DNA, only 6.30±0.03% was preserved after the same time. Saturated lipids, in particular tristearin, form a densely packed bilayer with a high phase transition temperature. This structure makes it difficult for hydrogen peroxide and free radicals to diffuse to the encapsulated DNA. Unsaturated lipids, on the contrary, create a looser packing, and the presence of double bonds makes them additional targets for oxidation. As a result, the penetration of oxidants is facilitated and the degradation of genetic material is accelerated.

For the development of stable DNA calibrators with a long shelf life, it is advisable to use liposomes based on saturated lipids (tristearin). They ensure the preservation of more than 80% of encapsulated DNA after 120 minutes of oxidative stress. In cases where the priority is cost, rather than maximum protection, an acceptable compromise is a mixture of saturated and unsaturated lipids in a 1:1 ratio, which allows preserving about 59% of DNA. Pure triolein is not recommended due to its low protective capacity – less than 40% after 120 minutes. In addition, the proposed model can be used as a rapid screening test to assess the antioxidant capacity of lipid matrices.

A linear relationship was established between the degree of lipid unsaturation and the amount of preserved DNA. An increase in the degree of unsaturation by 0.1 (i.e., by 10% when going from pure saturated lipid to a mixture) leads to a decrease in preserved DNA by approximately 1.3% after 30 min, by 1.7% after 60 min, and by 2.0% after 120 min. The increase in the effect over time indicates that unsaturated lipids not only protect DNA worse, but also undergo oxidation themselves, which further destabilizes the system. The established linear dependence allows us to predict the protective properties of liposomes for any ratio of saturated to unsaturated triacylglycerols without conducting additional experiments. This creates a basis for the rational design of lipid matrices with a given level of stability. In addition, the proposed approach can be used as a quantitative method for assessing the oxidative stability of lipid systems by the preservation of a DNA reporter, which is a simpler alternative to traditional methods (peroxide and anisidine numbers).

References

Asadi Z., Aghaz F., Rahimi Z., Arkan E., Vaisi-Raygani A. (2025), Do linalool-loaded solid lipid nanoparticles improve the quality of naval medical research institute mouse sperm during freezing/thawing and handling processes?, *Biopreservation and Biobanking*, Advance online publication, https://doi.org/10.1089/bio.2024.0156

Benamara S., Sbartai I., Sbartai H., Moroté F., Cohen-Bouhacina T., Grauby-Heywang C. (2025), Different propensity to oxidation and responses to compression of unsaturated mono- and di-galactosyldiacylglycerol Langmuir monolayers: Possible role of polymorphic transitions in lipid phase in the context of energy-converting membranes, *Chemistry and Physics of Lipids*, 270, 105506, https://doi.org/10.1016/j.chemphyslip.2025.105506

Boonnoy P., Janlad M., Bagheri B., Dias C., Karttunen M., Wong-Ekkabut J. (2024), Cholesterol inhibits oxygen permeation through biological membranes: mechanism against double-bond peroxidation, *RSC Advances*, 14(40), pp. 29113-29121, https://doi.org/10.1039/d4ra04846f

Burger M., Brigger F., Mantella V., Leroux J.C. (2025), Encapsulation of protein/DNA complexes into unilamellar liposomes via annexin-mediated membrane recruitment and sonication, *Cell Reports Methods*, 5(6), 101073, https://doi.org/10.1016/j.crmeth.2025.101073

Cheng L., Li T.Y., Zhang Y. (2004), Rapid preparation of total nucleic acids from E. coli for multi-purpose applications, *Journal of Biochemistry and Molecular Biology*, 37(3), pp. 351–355, https://doi.org/10.5483/bmbrep.2004.37.3.351

Cordsmeier L., Hahn M.B. (2022), DNA stability in biodosimetry, pharmacy and DNA based data-storage: Optimal storage and handling conditions, *ChemBioChem*, 23(23), e202200391, https://doi.org/10.1002/cbic.202200391

Das A., Adhikari C., Chakraborty A. (2016), Lipoplex-mediated deintercalation of doxorubicin from calf thymus DNA–doxorubicin complex, *Langmuir*, 32(35), pp. 8889–8899, https://doi.org/10.1021/acs.langmuir.6b01860

Estabrook D.A., Huang L., Lucchese O.R., Charland D.J., Yu Z., Sayyed F.B., Buser J.Y., Oh Y., Liu X., Johnson H.A., Rodriguez K.G., Wambolt N.A., Corba S.A., Nash G.T., Yang D., Wang T. (2025), Buffer optimization of siRNA-lipid nanoparticles mitigates lipid oxidation and RNA-lipid adduct formation, *Nature Communications*, 16, 8380, https://doi.org/10.1038/s41467-025-63651-4

Gardea-Gutiérrez D., Román-Aguirre M., Oseguera-Guerra B.E., Loera-Valencia R., Montes-Fonseca S.L. (2025), Improved application of the inverse emulsion method for generating flexible asymmetric liposomes for DNA plasmid delivery, *Journal of Liposome Research*, 35(4), pp. 446-454, https://doi.org/10.1080/08982104.2025.2521067

Li J., Zhang Q., Chen H., Xu D., Chen Z., Wen Y. (2024), Dynamic changes of fatty acids and (R)-dichlorprop toxicity in *Arabidopsis thaliana*: correlation, mechanism, and implications, *Environmental Science and Pollution Research International*, 31(43), pp. 55522-55534, https://doi.org/10.1007/s11356-024-34888-1

Mathews P.D., Gama G.S., Megiati H.M., Madrid R.R.M., Garcia B.B.M., Han S.W., Itri R., Mertins O. (2024), Flavonoid-labeled biopolymer in the structure of lipid membranes to improve the applicability of antioxidant nanovesicles, *Pharmaceutics*, 16(1), 141, https://doi.org/10.3390/pharmaceutics16010141

Saxena V. (2023), Preparation and physical characterization of DNA binding cationic liposomes, In: D'Souza, G.G., Zhang, H. (Eds.), Liposomes. *Methods in Molecular Biology*, 2622, pp. 121–126, Humana Press, https://doi.org/10.1007/978-1-0716-2954-3_10

Schneider C.A., Rasband W.S., Eliceiri K.W. (2012), NIH Image to ImageJ: 25 years of image analysis, *Nature Methods*, 9, pp. 671–675, https://doi.org/10.1038/nmeth.2089

Shin J., Jaruga P., Dizdaroglu M., Kool E.T. (2025), DNA content and DNA damage in raw and heat-processed foods, *Journal of Agricultural and Food Chemistry*, 73(45), pp. 29069–2908, https://doi.org/10.1021/acs.jafc.5c08138

Thongbamrer C., Kunkeaw N., Nguitragool W., Roobsoong W., Sattabongkot J., Pengnam S., Opanasopit P., Yingyongnarongkul B.E. (2025), Enhancing transfection efficiency of

spermine-based cationic lipids with a lysine-based spacer, *Chemistry – An Asian Journal*, 20(11), e202401751, https://doi.org/10.1002/asia.202401751

Yang Q., Xu J., Qian X., Zhang K., Lei X. (2006), Eliminating nucleic acids contaminants by hydrogen peroxide-induced free radicals during the preparation of proteins, *Biochemical Engineering Journal*, 29(1-2), pp. 23–26, https://doi.org/10.1016/j.bej.2005.02.022

Zhang H. (2023), Thin-film hydration followed by extrusion method for liposome preparation, In: D'Souza, G.G., Zhang, H. (Eds.), *Liposomes. Methods in Molecular Biology*, 2622, pp. 57–63, Humana, New York, NY, https://doi.org/10.1007/978-1-0716-2954-3_4

Zhao R.M., Zhang Q.F., Tian X.L., Chen J.J., Yu X.Q., Zhang J. (2024), ROS-Responsive bola-lipid nanoparticles as a codelivery system for gene/photodynamic combination therapy, *Molecular Pharmaceutics*, 21(4), pp. 2012-2024, https://doi.org/10.1021/acs.molpharmaceut.4c00053

Cite:

Hu, G., Nosenko, T., Stankevych, S., & Ovsiannikova, T. (2026). Influence of membrane lipid composition on the stability of encapsulated DNA under oxidative stress. *Ukrainian Food Journal, 15*(2), 293–307. https://doi.org/10.24263/2304-974X-2026-15-2-4

ε-Poly-L-lysine extends the ambient shelf life of pickled Ma-muang Bao by suppressing yeast growth

Atipan Saimmai, Sutanate Saelao, Aem Nuylert, Suppasil Maneerat

Prince of Songkla University, Songkhla, Thailand

Keywords:

ε-Poly-L-lysine
Picked
Ma-muang Bao
Yeast growth inhibition
Biopreservation
Shelf-life

Article history:

Received 17.01.2026
Received in revised form 24.04.2026
Accepted 30.06.2026

Corresponding author:

Atipan Saimmai
E-mail: atipan.s@psu.ac.th

DOI:
10.24263/2304-974X-2026-15-2-5

Abstract

Introduction. This study aimed to evaluate ε-poly-L-lysine (ε-PL) as a natural biopreservative for inhibiting yeast spoilage and extending the ambient shelf life of pickled Ma-muang Bao without compromising product quality or safety.

Materials and methods. Microbiological and physicochemical changes in retail-packaged pickled Ma-muang Bao stored at 32 °C were investigated. The antimicrobial activity of ε-PL was determined using a broth microdilution assay. The preservative efficacy of ε-PL was compared with that of potassium sorbate by monitoring microbial counts, pH, titratable acidity, sugar content, ethanol formation, texture, and shelf life over a 30-day storage period.

Results and discussion. Yeasts were identified as the predominant spoilage microorganisms in pickled Ma-muang Bao, with counts exceeding 7 $\log_{10}$ CFU/g during storage at 32 °C. Their rapid proliferation resulted in the fermentation of sugars, ethanol production, off-odour development, and visible package swelling, all of which are characteristic manifestations of spoilage in acidified fruit-based products.

ε-Poly-L-lysine exhibited strong antimicrobial activity against both bacterial and yeast populations, with minimum inhibitory concentrations (MICs) of 25 mg/L for bacteria and 50–100 mg/L for yeasts. Compared with potassium sorbate, ε-PL demonstrated broader and more consistent antimicrobial activity, particularly in inhibiting yeast growth under high-temperature storage conditions. In the product challenge test, ε-PL applied at 200 mg/kg effectively suppressed total aerobic bacteria, lactic acid bacteria, and yeasts throughout the storage period. In addition, ε-PL significantly reduced ethanol accumulation, which is directly associated with yeast metabolic activity, thereby preventing gas formation and package swelling. At the same time, key physicochemical parameters, including sugar content, titratable acidity, pH stability, and texture firmness, were better preserved in ε-PL-treated samples compared with the control and potassium sorbate-treated samples.

Notably, ε-PL treatment slowed down the overall deterioration kinetics of the product, resulting in a more stable sensory profile and delayed onset of spoilage-related changes. This effect was reflected in both microbiological stability and physicochemical integrity, indicating that ε-PL acts not only as an antimicrobial agent but also indirectly contributes to quality preservation by suppressing fermentation-driven

Conclusion. ε-Poly-L-lysine at 200 mg/kg effectively controlled yeast spoilage, preserved the physicochemical quality, and extended the shelf life of pickled Ma-muang Bao under ambient storage conditions.

Introduction

Mango is widely cultivated in Thailand. One indigenous cultivar native to Songkhla Province, known as Ma-muang Bao, is traditionally processed into pickled Ma-muang Bao (Mamuang Bao Chae-Im), a regional specialty that has become popular among tourists throughout Thailand. The pickling process involves soaking the fruit in salt and sugar solutions, which reduces free water activity and limits the growth of certain microorganisms. However, the product has a short shelf life of up to three days at 32 °C, often accompanied by package swelling and an unpleasant ethanol-like odor that negatively affects consumer acceptability. These issues have been largely attributed to high yeast populations (>6 $\log_{10}$ CFU/g) in products from Songkhla (Indrati et al., 2022).

Thermal treatment at 100 °C for 10 seconds extends shelf life only up to three days at 25 °C (Kaewthong et al., 2025), which may still be insufficient for distribution to distant regions or export to international markets. As a result, some manufacturers apply preservatives such as benzoic acid and its salts, which are inexpensive, do not significantly alter sensory properties, and exhibit antifungal activity (Islam et al., 2024). However, excessive intake of these compounds may cause irritation of the gastrointestinal tract and other tissues, including the liver and kidneys, while benzoic acid has also been reported to exhibit mutagenic and teratogenic effects (Hartwig and Commission, 2025).

As safer alternatives, bioactive antimicrobials such as nisin and ε-poly-L-lysine (ε-PL) are increasingly used in foods and are recognized as safe by the U.S. Food and Drug Administration (FDA) due to their digestibility in humans and the absence of toxic residues (Wang et al., 2024). ε-PL is a water-soluble, colorless, and odorless polypeptide produced by *Streptomyces albulus*. It exhibits broad-spectrum antimicrobial activity against Gram-positive and Gram-negative bacteria, as well as yeasts and molds. It is approved by the FDA as a food-grade preservative for microbial control (Li et al., 2022) and remains stable over a wide pH range (2–9) with high thermal resistance (80–120 °C) (Shifrin et al., 2025).

Based on these properties, this study aimed to evaluate ε-poly-L-lysine as a natural preservative for inhibiting yeast growth and extending the ambient shelf life of pickled Ma-muang Bao, with the goal of reducing reliance on synthetic preservatives while maintaining product quality and safety.

Materials and methods



Figure 1. Pickled Ma-muang Bao samples

Materials

Pickled Ma-muang Bao products were procured from a retail shop in Hat Yai District (Songkhla Province, Thailand) (Figure 1).

ε-PL was purchased from Punature Food ingredient, China. Potassium sorbate and sodium benzoate were obtained from Ajex Finechem, Australia. All reagents were analytical grade.

Methods

Changes in microbial counts of pickled Ma-muang Bao during storage

At storage days 1, 2, 4, 7, 10, and 14, 25 g of pickled Ma-muang Bao were aseptically transferred into 225 mL of 0.1% peptone water, homogenized with a stomacher (Seward, UK), and serially diluted ten-fold to appropriate levels. Total aerobic bacteria were enumerated by spread-plating onto Plate Count Agar (PCA, Hi-Media, India) and incubated at 37 °C for 48 h; lactic acid bacteria (LAB) were determined similarly on De Man, Rogosa and Sharpe (MRS, Hi-Media, India) agar supplemented with 0.04% (w/v) bromocresol purple and incubated at 37 °C for 48 h. Yeasts were enumerated by spread-plating on Potato Dextrose Agar (PDA, Hi-Media, India) acidified with 1 mL tartaric acid per 100 mL medium and incubated at 30 °C for 2-5 days. For all determinations, plates with 30-300 colonies were counted and results expressed as CFU /g following Pasrija and Kumari (2025). Morphologically distinct bacterial, LAB, and yeast colonies were purified by 2-3 rounds of re-streaking on respective medium and preserved in liquid respective medium containing 30% (v/v) glycerol at -20 °C for subsequent analyses.

Determination of minimum inhibitory concentrations (MIC and MIC_{90}) of ε-poly-L-lysine and potassium sorbate against bacterial and yeast isolates from pickled Ma-muang Bao

Six bacterial isolates recovered from pickled Ma-muang Bao (three non-LAB from PCA and three LAB) and six yeast isolates were evaluated by a broth microdilution assay in 96-well microplates. Non-LAB were grown in 10 mL nutrient broth (NB, Hi-Media, India) at 32 °C for 24 h; LAB were cultured in 10 mL MRS broth at 32 °C for 24 h; and yeasts were cultivated in 10 mL PDB at 32 °C for 24 h with shaking at 150 rpm. Stock solutions of ε-PL and potassium sorbate were prepared in the corresponding test broths (NB for non-LAB bacteria, MRS for LAB, PDB for yeasts), adjusted to pH 5.5, and sterile-filtered (0.45 μm). For each assay well, 100 μL of standardized inoculum was dispensed to yield a final inoculum of 10^5 CFU/mL, followed by 100 μL of antimicrobial solution to achieve final ε-PL concentrations of 6.25, 12.5, 25, 50, 100, 200, and 400 mg/L, or potassium sorbate concentrations of 12.5, 25, 50, 100, 200, 400, and 800 mg/L. Plates were incubated at 32 °C for 24 h. Positive growth controls comprised NB, MRS, or PDB containing the respective inocula without antimicrobial, while negative controls were uninoculated broths. After incubation, turbidity was measured at 660 nm using a microplate reader (Thermo Fisher Scientific, USA)). The MIC was defined as the lowest concentration at which no growth was detected (OD_{660} comparable to the negative control), and the MIC_{90} as the lowest concentration producing ≥90% growth inhibition relative to the positive control; MIC_{90} values were subsequently used in subsequent experiments.

Comparative evaluation of commercial preservatives and ε-PL **for shelf-life extension of pickled Ma-muang Bao at different temperatures**

Pickled Ma-muang Bao batches (500 g per treatment) were prepared under five conditions: ε-PL at 1× and 2× the MIC_{90} (as determined in Section 2), sodium benzoate at 200 or 400 mg k/g, potassium sorbate at 200 or 400 mg k/g, and an untreated control. Treated products were stored at 4 °C and 32 °C for 30 days. Samples were collected on days 1, 2, 4, 7, 10, 15, 20, and 30 for microbiological analyses (total aerobic bacteria, LAB, and yeasts) as described above, and for physicochemical measurements including pH, titratable acidity, total sugars, ethanol content, and texture (texture analyser). The preservative efficacy of ε-PL versus the commercial preservatives across storage temperatures was evaluated.

Physicochemical analyses of pickled Ma-muang Bao

pH. Samples (10 g) were homogenized in 100 mL of distilled water using a stomacher, filtered through Whatman No. 4 paper, and the filtrate pH was measured with a calibrated pH meter (Mettler Toledo, Switzerland) (Beak and Kim, 2026).

Titratable acidity as lactic acid. Samples (20 g) were homogenized in 20 mL of distilled water, filtered through cheesecloth, and centrifuged (10,000 rpm, 10 min, 4 °C). The supernatant (aliquot) was titrated with 0.1 N NaOH to a phenolphthalein endpoint (1% w/v in ethanol) (Tosif et al., 2025).

Total sugars (phenol-sulfuric acid method). Samples (20 g) were homogenized in 80 mL of distilled water, filtered through cheesecloth, and centrifuged (10,000 rpm, 10 min, 4 °C). The supernatant was appropriately diluted. For color development, 1.0 mL of diluted sample was mixed with 1.0 mL of 5% (w/v) phenol and then 5.0 mL of concentrated H_2SO_4 was added. After 10 min at room temperature, absorbance (Thermo, USA) was read at 480 nm, and total sugars were quantified against a glucose calibration curve (Kumar et al., 2026).

Reducing sugars (DNS method). From the same diluted sample preparation as in Section 4.3, 1.0 mL of diluted sample solution was combined with 1.0 mL of 3,5-dinitrosalicylic acid (DNS) reagent, boiled for 10 min, and rapidly cooled in an ice-water bath for 5 min. Absorbance was read at 540 nm and reducing sugars were determined from a glucose standard curve (de Oliveira Silva et al., 2025).

Ethanol by gas chromatography (GC-FID). A 20 g sample was homogenized with 20 mL distilled water, followed by filtration through cheese cloth and centrifugation (10,000 rpm, 10 min, 4 °C). The filtrate was further filtered using a membrane filter (0.20 µm). One milliliter was placed into the GC vial, and 2 µL was injected onto an HP 6890 GC (HP, USA) fitted with a HP-INNOWax column and flame ionization detector (FID). The oven temperature was kept constant at 150 °C for 6 minutes. Ethanol content was calculated using a standard curve made with ethanol standards and expressed as mg/L (mg/kg).

Statistical analyses

The statistical analysis was done using IBM SPSS Statistics. The significance of difference among treatments was analysed using one-way analysis of variance (ANOVA) test; whenever ANOVA test was significant ($p<0.05$), the mean values were compared using Duncan's Multiple Range Test (DMRT).

Results and discussion

Microbiological and chemical changes in pickled Ma-muang Bao during storage at 32 °C (14 days)

The initial pH of the product was 2.30±0.02 at 32 °C and exhibited minimal variability during a 14-day period. Titratable acidity (expressed in terms of lactic acid equivalents) rose from 1.92±0.10% (day 0) to 2.43±0.10% (day 4), but then decreased to 2.04±0.10% after day 14 (Figure 2a). The initial population of total aerobic bacteria was low (3.6±0.1 $\log_{10}$ CFU/g) and decreased to below the detectable level after day 10. In contrast, the LAB population was high initially (6.6±0.1 $\log_{10}$ CFU/g), reached its maximum value on day 2 (7.6±0.1 $\log_{10}$ CFU/g), and decreased to 3.8±0.1 $\log_{10}$ CFU/g after day 14 (Figure 2b).

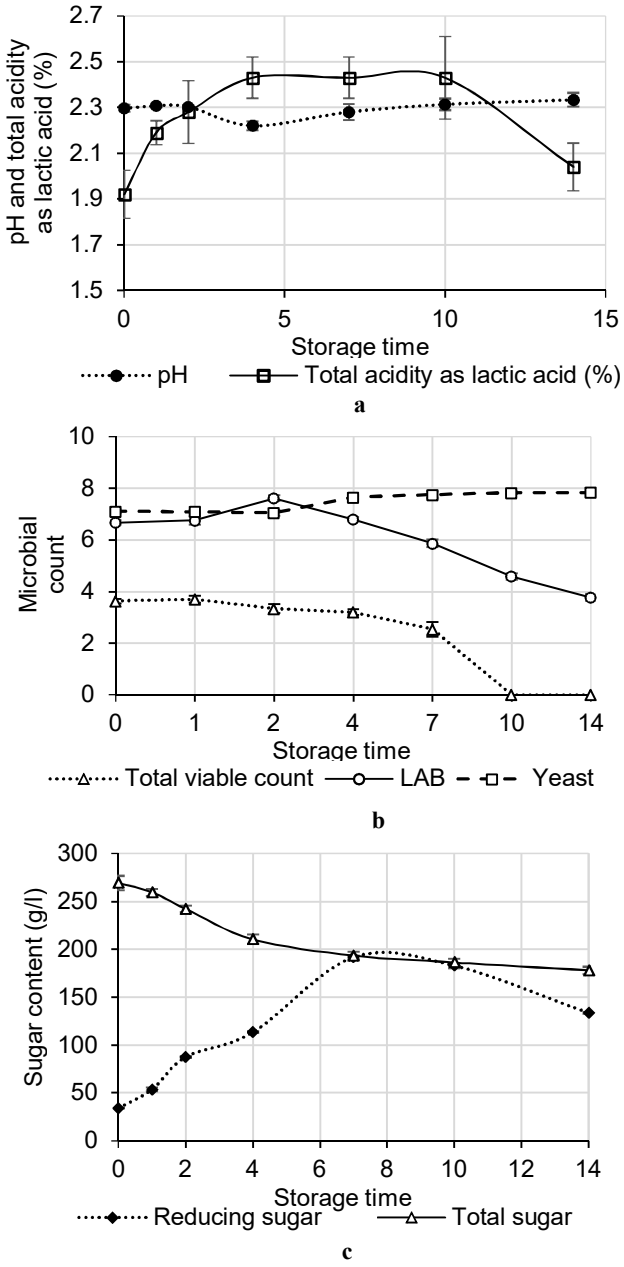

Figure 2. **pH, total acidity (a), microbial counts (b) and reducing sugar and total sugar contents (c) in pickled *Ma*-muang Bao during storage at 32 °C for 14 days**

The inhibition of total aerobes is supported by the synergistic action of low pH and relatively high organic acids. Organic acids that are not dissociated can enter bacterial cells and inhibit transport and cell physiology, ultimately killing the bacteria (Yu et al., 2026).

Similarly, concentrations of organic acids greater than 0.77% have been found to be inhibitory towards bacterial growth (Sorathiya et al., 2025). The range of LAB content reported for fermented mango samples from Songkhla Province is less than 1.0-5.8 $\log_{10}$ CFU/g based on processing methods (Indrati et al., 2022); the presence of high levels of LABs detected in this study is indicative of the use of the conventional method of fermentation with back-slopping. Yeasts were present at high initial levels (7.1±0.2 $\log_{10}$ CFU/g) and continued to be so until the end of storage, while no molds were observed. Notably, yeast levels were above the standard for pickled fruits (≤10^3 CFU/g). This finding is plausible because yeasts can grow when $a_w < 0.80$ in such sugar-rich, low aw conditions (Bayarri Fernández et al., 2025). Carbohydrate trends support active yeast metabolism: reducing sugars rose from 34.03±0.75 g/L (day 0) to 193.45±1.98 g/L (day 7) and then decreased to 133.56±1.13 g/L (day 14), while total sugars declined from 269.34±7.51 g/L to 178.03±3.72 g/L over the same period (Figure 2c). The simultaneous build-up of metabolic products of fermentation (organic acids, ethanol, and CO_2) resulted in increasing fermented or alcoholic off-odors that would be undesirable for the consumers (Yee et al., 2025), and also package inflation within 14 days, most likely from CO_2, creating practical problems during shipping. In summary, these data imply that under warm conditions, the yeasts are the main microorganisms responsible for sugar metabolism in the product, making the isolates suitable candidates for testing of biopreservation.

Minimum inhibitory concentrations of ε-poly-L-lysine against bacteria and yeasts isolated from pickled Ma-muang Bao

Yeast-driven spoilage was evident for this product, consistent with the high-sugar/low-pH matrix that favours yeast growth, off-odour development, and package swelling from metabolically produced gas, ultimately shortening shelf life. To identify an effective biopreservative level that does not alter texture or flavor, we determined the minimum inhibitory concentration (MIC) of ε-PL against bacterial and yeast isolates by a broth microdilution assay using 6.25-400 mg/L ε-PL (Table 1).

Table 1

Minimum inhibitory concentration (MIC) of ε-poly-L-lysine ad potassium sorbate against yeast isolated from pickled Ma-muang Bao

Isolates	Minimum inhibition concentration (MIC)	
	ε-Polylysine (mg/L)	Potassium sorbate (mg/L)
MGB01	25	800
MGB02	25	800
MGB03	25	800
MGLC01	25	>800
MGLC02	25	>800
MGLC03	25	>800
MGY01	50	200
MGY02	50	200
MGY03	100	200
MGY04	50	200
MGY05	100	200
MGY06	100	200

All six bacterial isolates (MGB01, MGB02, MGB03, MGLC01, MGLC02, MGLC03) were inhibited at 25 mg/L ε-PL; among the six yeasts, MGY01, MGY02, and MGY04 had MIC 50 mg/L, while MGY03, MGY05, and MGY06 required 100 mg/L. For comparison with a common commercial preservative, potassium sorbate showed substantially higher MICs against the bacteria: 800 mg/L for MGB01-MGB03 and >800 mg/L for MGLC01-MGLC03; all six yeasts had MIC 200 mg/L. Thus, ε-PL exhibited greater antimicrobial potency than potassium sorbate against the product-associated bacterial panel and comparable or better activity against the yeasts. On this basis, ε-PL at 100 mg/L inhibited all 12 isolates and was selected for downstream preservation trials.

Mechanistically, ε-PL is a bioactive cationic polypeptide produced by *Streptomyces albulus* with broad activity against spoilage and pathogenic bacteria, yeasts, and molds; reported modes of action include disruption of cell-wall biogenesis and interference with nucleic-acid synthesis, leading to loss of barrier function and cell death (Lou et al., 2025). Its safety for human consumption has been recognized by the U.S. FDA (Berman et al., 2025). Supporting efficacy from prior food applications: 0.1-0.4 g/L of ε-PL inhibited microbes on fresh-cut brassica in 12 days (Faisal et al., 2025), whereas 0.1% ε-PL inhibited *Aliivibrio* spp., *Pseudoalteromonas* spp. and *Psychromonas* spp. on shrimp at 0 °C for up to 7 days (Hu et al., 2025). The limited ability of potassium sorbate as an antibacterial due to lower concentrations is attributed to lower rates of transport of weak acid molecules across cell envelopes. As concentration increases, homeostasis of intracellular pH is compromised, resulting in death of bacterial cells (Arroyo-López et al., 2008).

Comparison of the efficacy of commercial preservatives and ε-poly-L-lysine in pickled Ma-muang Bao during storage at 32 °C for 30 days

Pickled Ma-muang Bao was prepared under five treatments: an untreated control; potassium sorbate at 200 and 400 mg/kg (S200 and S400); and ε-poly-L-lysine (ε-PL) at 100 and 200 mg/kg (P100 and P200). Microbial counts, pH, titratable acidity (TA), sugar content, ethanol concentration, and texture were monitored during 30 days of storage at 32 °C.

Microbiological changes

In the control experiment, aerobic bacteria, LAB, and yeasts started out at 3.7±0.2, 5.5±0.1, and 7.1±0.1 $\log_{10}$ CFU/g, respectively (Figures 3a-3c). The total number of aerobes reached undetectable levels within 10 days; LAB increased to 7.2±0.1 $\log_{10}$ CFU/g before dropping to undetectable levels after 14 days, while yeasts peaked at 8.3±0.2 $\log_{10}$ CFU/g after seven days before declining to 3.1±0.1 $\log_{10}$ CFU/g after day 30 (Figure 3a). With potassium sorbate (S200, S400), initial totals and yeasts were lower than control (totals 3.2±0.1 and 2.7±0.4 log10 CFU/g; LAB 5.7±0.2 and 5.1±0.1 log10 CFU/g; yeasts 4.9±0.1 and 2.9±0.1 log10 CFU/g, respectively), and both totals and yeasts declined to undetectable by day 22; LAB increased to 6.5±0.1 (S200) and 6.7±0.1 (S400) log10 CFU/g. In case of ε-PL, both P100 and P200 had undetectable levels of total aerobes and LAB from day 1 onwards. Yeasts in the product ranged from 4.1±0.14 (P100) and 2.7±0.1 (P200) log10 CFU/g initially and decreased to undetectable levels on days 18 and 22, respectively. While MIC90 values obtained through broth tests offered an initial guide, in-product higher concentrations proved to be better due to the diffusion and binding limitations associated with the fruit-based system and relatively high yeast levels (>7 log10 CFU/g), factors usually encountered in solid/ high sugar-content foods (Turantaş et al., 1999; Tango et al., 2016; Wang et al., 2017) (Figs. 3a-3c).

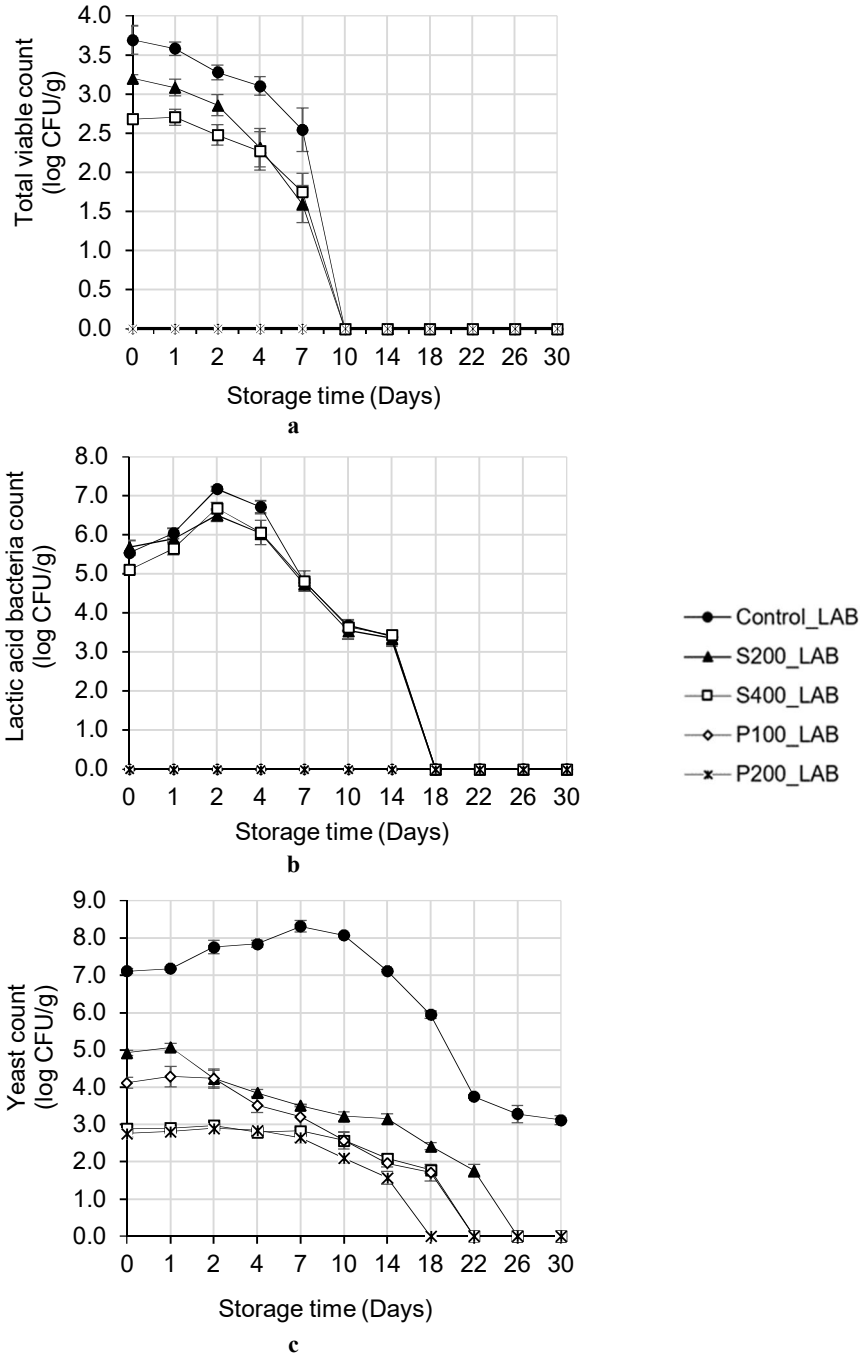

Figure 3. Counting of total bacteria (a), lactic acid bacteria (b) and yeasts (c) determined in pickled *Ma*-muang Bao with or without potassium sorbate or ε-poly-L-lysine supplementation for 30 days of storage at 32 °C

Physicochemical changes

Regardless of treatment, pH values remained between 2.30 and 3.25, which is within the range generally considered acceptable for pickled fruit products (≤3.5) (Figure 4).

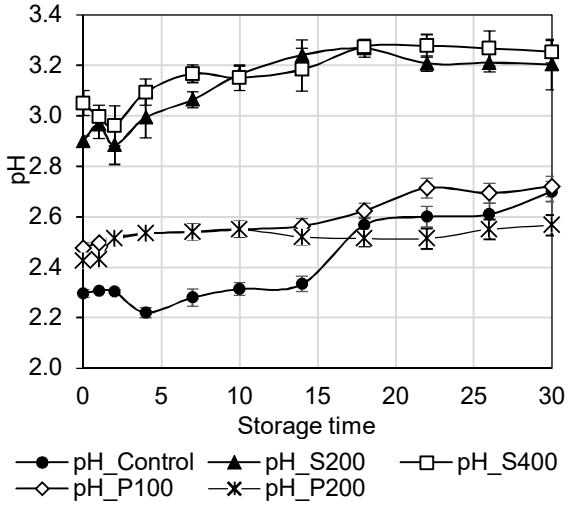

Figure 4. Changes in pH of pickled *Ma*-muang Bao treated with or without potassium sorbate or ε-poly-L-lysine during storage at 32 °C for 30 days

In the control treatment, pH was lower initially (2.30±0.10) and declined during the first week when there was an increase in TA (equivalent to lactic acid), reaching its peak of 2.43±0.09% by the fourth day and declining further to 1.35±0.16% by the thirty day (Figure 5).

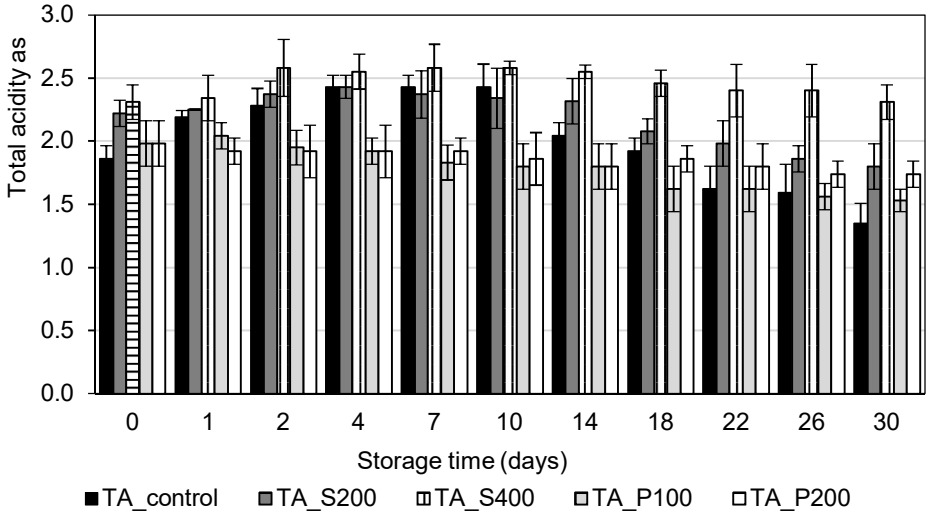

Figure 5. Changes in titratable acidity, expressed as lactic acid, of pickled *Ma*-muang Bao treated with or without potassium sorbate or ε-poly-L-lysine during storage at 32 °C for 30 days

On the other hand, P100 treatment showed an increase in pH while TA decreased to 1.53±0.09%. For S200 and S400, pH increased from ~2.9-3.0 to 3.20-3.25 by day 30; TA began at ~2.20-2.31%, peaked on day 4 (2.43±0.09% and 2.58±0.15%, respectively), then declined to 1.80±0.18% (S200) and 2.31±0.14% (S400). The changes in pH and TA observed in sorbate-treated samples may be associated with the buffering effect of weak-acid salts and microbial metabolic activity during storage (Figs. 4-5); while the activities of the yeast (acetaldehyde production, around 4-5; organic acids oxidation) might have caused the increase of pH and decrease of TA (Middelhoven et al., 1983; Savard et al., 2002; Singla et al., 2012; Vilela-Moura et al., 2008) (Figures 4-5).

Reducing sugars began similarly across treatments (32.55-36.18 g/L) and increased by day 7, with the control reaching 191.73±1.98 g/L; S200, S400, P100, and P200 were lower at 101.02±4.70, 56.94±6.88, 86.93±5.71, and 40.83±4.08 g/L, respectively (Figure 6).

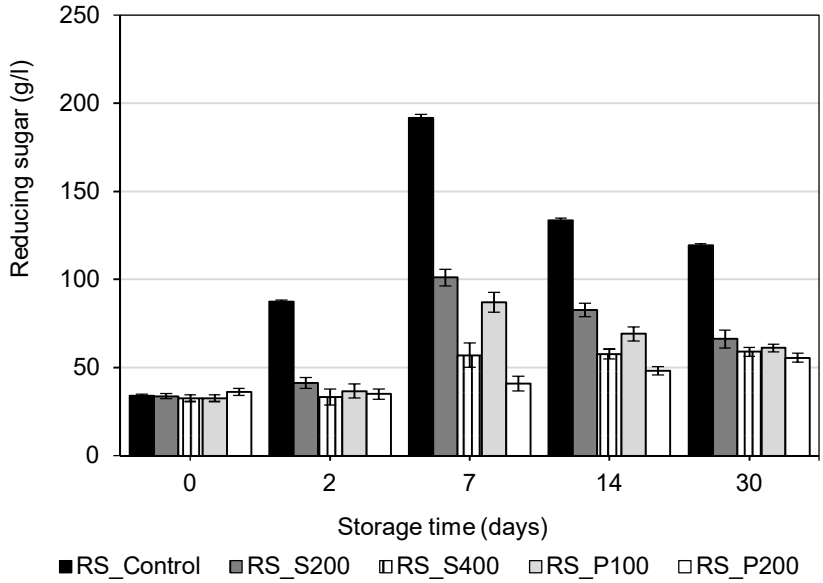

Figure 6. Changes in reducing sugar content of pickled *Ma*-muang Bao treated with or without potassium sorbate or ε-poly-L-lysine during storage at 32 °C for 30 days

Thereafter, reducing sugars declined to 119.23±1.13, 66.09±5.21, 58.79±2.50, and 61.06±2.22 g/L for control, S200, S400, and P100 by day 30 (values for P200 continued to track lowest change among treatments). Total sugars started at ~259.9 g/L and fell to 181.40±8.72 (control), 220.4±5.38 (S200), 243.5±4.59 (S400), 227.6±8.21 (P100), and 231.8±10.75 g/L (P200) (Figure 7). Ethanol was initially low (0.12-0.48 g/L) but in the control rose sharply to 24.91±1.61 g/L by day 14, whereas S400 and P200 remained low (1.81±0.10 and 1.84±0.12 g/L on day 14) and increased only slowly thereafter (Figure 8). Ethanol trends mirrored yeast counts, consistent with glycolytic conversion of sugars to ethanol and CO_2 (Africa, 2025) and with prior observations in pickled Ma-muang Bao products (Guadalupe-Daqui et al., 2023) (Figures 6–8.)

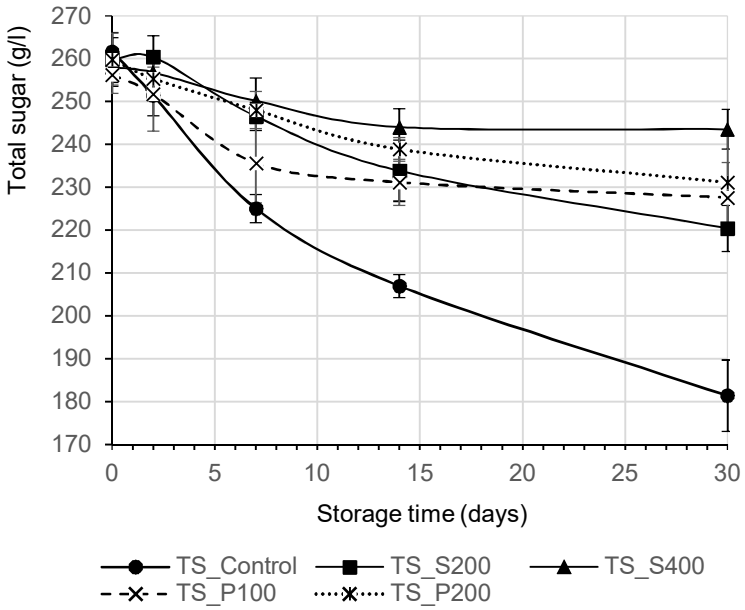

Figure 7. Changes in total sugar content of pickled *Ma*-muang Bao treated with or without potassium sorbate or ε-poly-L-lysine during storage at 32 °C for 30 days

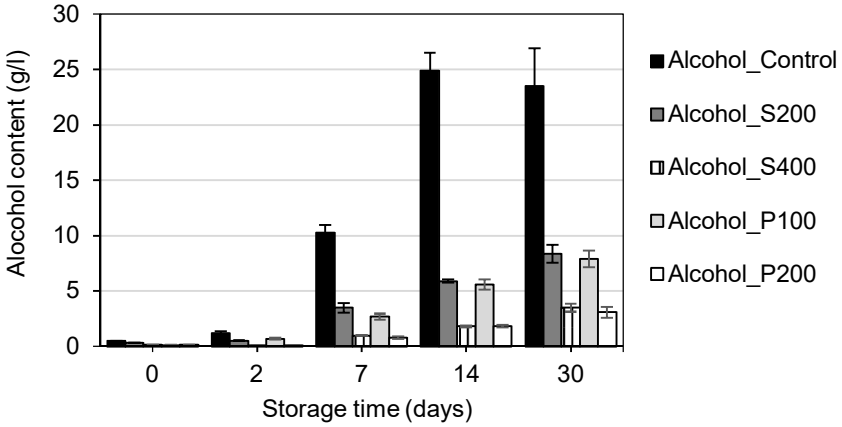

Figure 8. Changes in ethanol content of pickled *Ma*-muang Bao treated with or without potassium sorbate or ε-poly-L-lysine during storage at 32 °C for 30 days

Firmness (N) generally increased during storage in all treated groups, whereas the control became unmeasurable from day 10 because of severe softening and tissue disintegration, likely resulting from yeast gas production (causing tissue porosity) and the activity of cell wall-degrading enzymes that depolymerize pectin and cellulose (Li et al., 2026). Treated samples lost measurable firmness later (14-18 days), with values differing by treatment and storage time ($p < 0.05$) (Table 2).

Table 2

Firmness of pickled *Ma*-muang Bao with added preservatives and bioactive compounds during 30 days of storage at 32 °C

Days	Experiments				
	Control	S200	S400	P100	P200
0	2.47 ± 0.11^{aA}	2.38 ± 0.13^{aA}	2.43 ± 0.23^{aA}	2.42 ± 0.23^{aA}	2.43 ± 0.24^{aA}
2	2.43 ± 0.15^{aA}	2.40 ± 0.18^{aA}	2.39 ± 0.12^{aA}	2.37 ± 0.21^{aA}	2.39 ± 0.13^{aA}
4	2.59 ± 0.14^{bA}	2.43 ± 0.16^{aA}	2.45 ± 0.13^{aA}	2.40 ± 0.11^{aA}	2.41 ± 0.13^{aA}
7	2.74 ± 0.14^{bB}	2.52 ± 0.12^{aB}	2.47 ± 0.13^{aA}	2.54 ± 0.15^{aB}	2.52 ± 0.11^{aA}
10	ND	2.61 ± 0.14^{aB}	2.63 ± 0.17^{aB}	2.69 ± 0.15^{aB}	2.65 ± 0.14^{aB}
14	ND	2.83 ± 0.21^{aC}	2.80 ± 0.14^{aC}	2.82 ± 0.12^{aC}	2.84 ± 0.14^{aC}
18	ND	ND	3.03 ± 0.13^{aC}	ND	2.94 ± 0.15^{aC}
22	ND	ND	ND	ND	ND
26	ND	ND	ND	ND	ND
30	ND	ND	ND	ND	ND

Note: Different lowercase letters within the same row indicate statistically significant differences at the 95% confidence level ($p < 0.05$). Different uppercase letters within the same column indicate statistically significant differences at the 95% confidence level ($p < 0.05$). ND: Not determined; S200: the pickled mango was treated with 200 mg/kg of potassium sorbate, S400: the pickled mango was treated with 400 mg/kg of potassium sorbate, P100: the pickled mango was treated with 100 mg/kg of ε-polylysine and P200: the pickled mango was treated with 200 mg/kg of ε-polylysine.

Both preservatives were effective as compared to the control in terms of microbial as well as quality preservation, where the maximum effect was provided by the treatment with ε-PL at 200 mg/kg (P200) in terms of m

aximum inhibition (total aerobes, LAB, yeasts), least changes in sugar content and ethanol content, and better maintenance of texture; while for S400, it was effective against yeast but showed limited inhibition against LAB. The ε-PL treatment helped in preventing pH/TA variability, reduced ethanol production, and increased shelf life by about 10 days more than that of the control (Figs. 3-8; Table 2).

Conclusions

Yeast was predominant in the microbial population (>7.0 $\log_{10}$ CFU/g at the onset of the experiment) and increased upon storing the samples at 32 °C, coupled with increasing pH levels and decreasing titratable acidity. The broth microdilution method determined that all the isolated yeasts had an MIC of 100 mg/L of ε-PL. In product challenge experiments, ε-PL 200 mg/kg and potassium sorbate 400 mg/kg resulted in decreased yeasts levels to 2.76 and 2.89 $\log_{10}$ CFU/g, respectively, with minimal change in pH levels, total acidity, ethanol formation, and changes in texture consistency. Both treatments extended the shelf-life period by over 7 days compared to the control sample; ε-PL 200 mg/kg exhibited the broadest and most potent antimicrobial effects.

Acknowledgment. This work was financially supported by Food Innovation Research Institute, Research and Development Office, Prince of Songkla University (Contract No. FIRIn 2561/019), Thailand.

References

Shifrin V.A., Geetha P.S., Kabilan M., Kanchana S., Sabarinathan K.G., Mini M.L., Pasupathi E. (2025), A comprehensive review of potent antimicrobial agent, *Annals of Phytomedicine*, 14(1), pp. 412-421, https://doi.org/10.54085/ap.2025.14.1.39

Bayarri Fernández S., Maza Rubio M.T., Serrano González A., Duarte Pac R., Pinilla Navarro V., Lorán Ayala S., Iriarte Goñi J.I. (2025), *Zero Waste: Awareness for the Rduction of Food Waste*, Instituto Agroalimentario de Aragón IA2, Zaragoza, https://doi.org/10.26754/uz.978-84-10169-68-5

Beak U.B., Kim H.Y. (2026), Physicochemical and microbial changes in raw beef meat induced by radiation, *Food Science of Animal Resources*, 46(1), 56, https://doi.org/10.1007/s44463-026-00060-1

Berman T.A., Ben-Arye E., Kienle G.S., Master V., Huston A., Paller C.J. (2025), Integrating botanicals into oncology care: consideration of FDA regulation of botanical products and botanical clinical trials, *Clinical Cancer Research*, 31(9), pp. 1566-1572, https://doi.org/10.1158/1078-0432.CCR-24-3419

de Oliveira Silva M., Macedo B.E., de Castro R.J.S. (2025), Revealing the phenolic profile and antioxidant and antidiabetic properties of enzymatically hydrolyzed seriguela, *Journal of Future Foods*, 6, pp. 1-10, https://doi.org/10.1016/j.jfutfo.2024.11.026

Faisal M., Arshad N., Wang H., Li C., Ma J., Kong X., Yu L. (2025), Recent advances in technologies for preserving fresh-cut fruits and vegetables, *Foods*, 14(16), 2769, https://doi.org/10.3390/foods14162769

Guadalupe-Daqui M., Goodrich-Schneider R.M., Sarnoski P.J., Carriglio J.C., Sims C.A., Pearson B.J., MacIntosh A.J. (2023), The effect of CO_2 concentration on yeast fermentation, *Journal of Industrial Microbiology and Biotechnology*, 50(1), kuad001, https://doi.org/10.1093/jimb/kuad001

Arroyo-López F.N., Bautista-Gallego J., Durán-Quintana M.C., Garrido-Fernández A. (2008), Modelling the inhibition of sorbic and benzoic acids on a native yeast cocktail from table olives, *Food Microbiology*, 25(4), pp. 566-574, https://doi.org/10.1016/j.fm.2008.02.007

Hartwig A., MAK Commission. (2025), Benzoic acid and alkali benzoates, *The MAK Collection for Occupational Health and Safety*, 3(4), pp. 1758-1828, https://doi.org/10.34865/mb6585e6318_w

Hu J., Xie K., Zhu H., Giusti A., Li M., Zheng Y., Deng S. (2025), Effects of atmospheric cold plasma treatment mode on muscle quality and bacterial community of red shrimp during cold storage, *Food Research International*, 207, 116051, https://doi.org/10.1016/j.foodres.2025.116051

Indrati N., Phonsatta N., Poungsombat P., Khoomrung S., Sumpavapol P., Panya A. (2022), Metabolic profiles alteration of Southern Thailand traditional sweet pickled mango during the production process, *Frontiers in Nutrition*, 9, 934842, https://doi.org/10.3389/fnut.2022.934842

Islam F., Saeed F., Imran A., Shehzadi U., Ali R., Nosheen F., Ojukwu M. (2024), Bio-preservatives and essential oils as an alternative to chemical preservatives in the baking industry: a concurrent review, *Journal of Food Science and Technology*, 61(4), pp. 609-620, https://doi.org/10.1007/s13197-023-05762-8

Kaewthong P., Petcharat T., Kangsanant S., Puttarak P., Srirak T., Quan T.H., Chantakun K. (2025), Acidification and pasteurization affect quality and storage characteristics of low-salt Southern Thai sour curry paste, *ES Food and Agroforestry*, 20, 1523, https://doi.org/10.30919/esfa1523

Kumar R.R., Hasija S., Kumar A., Gampa M., Goswami S., Kumar S., Jha G.K. (2026), Carbon isotope signature decodes the synergistic effect of flag leaf and ear in providing assimilates

for grain-filling in wheat under tissue-specific light exclusion, *Plant Stress*, 101233, https://doi.org/10.1016/j.stress.2026.101233

Li J., Zhang S., Lyu J., Zhou W., Bi J. (2026), Differential roles of thermal versus cryo-mechanical forces in tailoring pectin and cellulose structure: a study on solute-enhanced drying of peach, *Food Hydrocolloids*, 179, 112771, https://doi.org/10.1016/j.foodhyd.2026.112771

Li S., Mao Y., Zhang L., Wang M., Meng J., Liu X., Guo Y. (2022), Recent advances in microbial ε-poly-L-lysine fermentation and its diverse applications, *Biotechnology for Biofuels and Bioproducts*, 15(1), 65, https://doi.org/10.1186/s13068-022-02166-2

Lou Z., Cheng X., Dong J., Dai W., Chen X., Wang H. (2025), The antibacterial mechanism and cell damage mechanism of natural antibacterial agents and their applications in food, *Journal of Food Measurement and Characterization*, 20, pp. 1362-1386, https://doi.org/10.1007/s11694-025-03794-6

Middelhoven W.J., Roskam J.H., Hoogkamer-te Niet M.C. (1983), Enzyme systems dehydrogenating ethanol and acetaldehyde in *Acetobacter aceti*, *FEMS Microbiology Letters*, 16, pp. 273-276, https://doi.org/10.1111/j.1574-6968.1983.tb00308.x

Pasrija R., Kumari D. (2025), Counting colony forming units (CFU) to estimate viable fungal cells in a sample, in *Protocols for Studying Pathogenic Fungi*, pp. 53-61, https://doi.org/10.1007/978-981-96-7047-5_3

Savard T., Beaulieu C., Gardner N.J., Champagne C.P. (2002), Characterization of spoilage yeasts isolated from fermented vegetables, *Food Microbiology*, 19(4), pp. 363-373, https://doi.org/10.1006/fmic.2002.0483

Singla A., Paroda S., Dhamija S.S., Goyal S., Shekhawat K., Amachi S., Inubushi K. (2012), Bioethanol production from xylose: problems and possibilities, *Journal of Biofuels*, 3(1), pp. 39-49, https://doi.org/10.5958/j.0976-3015.3.1.004

Sorathiya K.B., Melo A., Hogg M.C., Pintado M. (2025), Organic acids in food preservation: exploring synergies, molecular insights and sustainable applications, *Sustainability*, 17(8), 3434, https://doi.org/10.3390/su17083434

Tango C.N., Khan I., Park Y.S., Oh D.H. (2016), Growth of *Staphylococcus aureus* in cooked ready-to-eat ground fish as affected by potassium sorbate, *LWT - Food Science and Technology*, 71, pp. 400-408, https://doi.org/10.1016/j.lwt.2016.03.048

Tosif M.M., Bains A., Chawla P., Paul S., Kumari P., Dhull S.B., Goksen G. (2025), Optimizing starch-free arabinogalactan-rich taro nanomucilage: green experimental design, structural elucidation, amino acid profiling and biological properties, *Food Chemistry*, 479, 143731, https://doi.org/10.1016/j.foodchem.2025.143731

Turantaş F., Göksungur Y., Dinçer H.A., Ünlütürk A., Güvenç U., Zorlu N. (1999), Effect of potassium sorbate and sodium benzoate on microbial population and fermentation of black olives, *Journal of the Science of Food and Agriculture*, 79(9), pp. 1197-1202, https://doi.org/10.1002/(sici)1097-0010(199907)79:9<1197:aid-jsfa355>3.0.co;2-s

Vilela-Moura A., Schuller D., Mendes-Faia A., Côrte-Real M. (2008), Reduction of volatile acidity of wines by selected yeast strains, *Applied Microbiology and Biotechnology*, 80(5), pp. 881-890, https://doi.org/10.1007/s00253-008-1616-x

Wang C., Yang J., Zhu X., Lu Y., Xue Y., Lu Z. (2017), Effects of *Salmonella* bacteriophage, nisin and potassium sorbate on safety and shelf life of fresh chilled pork, *Food Control*, 73, pp. 869-877, https://doi.org/10.1016/j.foodcont.2016.09.034

Wang Z., Wang Z., Tan Z., Cui J., Jia S. (2024), Application of ε-poly-L-lysine in improving food quality and safety, In: Z. Lu, Y. Lu (Eds.), *Bio-Based Antimicrobial Agents to Improve Agricultural and Food Safety*, pp. 221-255, https://doi.org/10.2174/9789815256239124010 1

Yee C.S., Zahia-Azizan N.A., Abd Rahim M.H., Mohd Zaini N.A., Raja-Razali R.B., Ushidee-Radzi M.A., Wan-Mohtar W.A.A.Q.I. (2025), Smart fermentation technologies: microbial

process control in traditional fermented foods, *Fermentation*, 11(6), 323, https://doi.org/10.3390/fermentation11060323

Yu H., Liu X., Zhang S., Lei Y., Zou B., Xie P., Zang M. (2026), Advances in antibacterial strategies of organic acids coupled with cold sterilization methods for controlling bacterial contamination in beef carcasses and cuts, *Critical Reviews in Food Science and Nutrition*, 66(4), pp. 843-858, https://doi.org/10.1080/10408398.2025.2534162

Cite:

Saimmai, A., Saelao, S., Nuylert, A., & Maneerat, S. (2026). ε-Poly-L-lysine extends the ambient shelf life of pickled Ma-muang Bao by suppressing yeast growth. *Ukrainian Food Journal, 15*(2), 308–322. https://doi.org/10.24263/2304-974X-2026-15-2-5

Plant essential oils for food shelf-life extension and active packaging systems

Olena Stabnikova[1], Andrii Marynin[1], Viktor Stabnikov[1], Roman Svyatnenko[1], Valeriy Demchenko[2]

1 – National University of Food Technologies, Kyiv, Ukraine
2 – E.O. Paton Electric Welding Institute, the NAS of Ukraine, Ukraine

Keywords:

Essential oils
Food preservation
Antimicrobial activity
Antioxidant activity
Active packaging
Nanoemulsions

Article history:

Received 12.09.2025
Received in revised form 14.01.2026
Accepted 30.06.2026

Corresponding author:

Olena Stabnikova
E-mail: stabstab6@gmail.com

DOI: 10.24263/2304-974X-2026-15-2-6

Abstract

Introduction. Essential oils are natural bioactive compounds that are widely studied as alternatives to synthetic preservatives in food systems and as functional components in active packaging materials. Their antimicrobial and antioxidant activities make them promising candidates for enhancing food safety and extending product shelf life.

Materials and methods. Essential oils are natural bioactive compounds that are widely studied as alternatives to synthetic preservatives in food systems and as functional components in active packaging materials. Their antimicrobial and antioxidant activities make them promising candidates for enhancing food safety and extending product shelf life.

Results and discussion. Essential oils contain a complex mixture of volatile compounds responsible for their biological activity. Their antimicrobial effects are associated with disruption of microbial cell membranes, leakage of intracellular components, inhibition of enzymatic systems, and interference with genetic material, enabling control of a wide range of foodborne pathogens, including bacteria, yeasts, and molds. Antioxidant activity is mainly attributed to phenolic compounds acting as radical scavengers and inhibitors of lipid oxidation, while effectiveness depends on chemical composition influenced by plant species, geographical origin, and extraction method; phenol-rich oils generally show stronger activity. Direct application in foods has demonstrated potential to reduce microbial load and delay spoilage in meat, dairy, bakery products, and fresh produce, but high volatility, low water solubility, and strong aroma limit practical use. To overcome these limitations, modern delivery systems have been developed, including edible coatings, biodegradable films, nanoemulsions, encapsulation, and active packaging, which improve stability, enable controlled release, and reduce sensory impact. However, their application requires careful control of concentration and formulation due to possible effects on sensory quality and safety concerns related to toxicity and migration from packaging materials.

Conclusions. Essential oils are effective natural preservatives with strong antimicrobial and antioxidant properties. Their incorporation into advanced delivery systems, including active packaging, improves stability and performance; however, further optimization and safety assessment are required for their practical application.

Introduction

Essential oils (EOs) are concentrated extracts composed of complex mixtures of volatile compounds obtained from various morphological parts of aromatic plants, including leaves, flowers, fruits, seeds, peels, stems, roots, and bark**.** Although over 3,000 essential oils have been described, their application in the food industry is restricted to only a few dozen. Representative examples include flowers of lavender (*Lavandula angustifolia L.*) (Kajjari et al., 2022); flower buds of clove (*Syzygium aromaticum* L.) (Liñán-Atero et al., 2024); leaves of peppermint (*Mentha piperita* L.) (Radivojac et al., 2021), spearmint (*Mentha piperita* L.) (Hudz et al., 2023), lemon balm (*Melissa officinalis* L.) (Stojanović et al., 2024), laurel (*Laurus nobilis* L.) (Nikovska et al., 2017), and basil (*Ocimum basilicum* L.) (El-Soud et al., 2015); peels of lemon (*Citrus limon* L.) (Kačániová et al., 2014), sweet orange (*Citrus sinensis* L.) (Nascimento et al., 2025), and pomegranate (*Punica granatum* L.) (Ara and Raofie, 2016); umbels of fennel (*Foeniculum vulgare* Mill.) (Šunić et al., 2023); bark of several species in the *Cinnamomum* genus (Guo et al., 2024); the rhizomes (underground stems) of turmeric (*Curcuma longa* L.) (Ibáñez and Blázquez, 2021) and ginger (*Zingiber officinale* Roscoe) (Funk et al., 2016); roots (together with rhizomes) of valerian (*Valeriana officinalis* L.) (Muhetaer et al., 2025); seeds of grape (*Vitis vinifera* L.) (Martin et al., 2020), black cumin (*Nigella sativa* L.) (Shevchenko et al., 2025), dill (*Anethum graveolens* L.) (Kostova et al.,2014), and coriander (*Coriandrum sativum* L.) (Chandrakala et al., 2024); the underground bulbs of garlic (*Allium sativum* L.) (Verma et al., 2023) and others. It was shown that all parts of oregano (*Origanum vulgare* L.), a perennial herb, including leaves, flowers, roots, and stems can be used for essential oil production (Han et al, 2017). Flowers and leaves of an aromatic plant rosemary formerly known as *Rosmarinus officinalis* but now classified as *Salvia rosmarinus* are employed for extraction of essential oil (Sahu and Sahu, 2024). In certain plants, including thyme, oregano, sage, mint, lemon balm, yarrow, and basil, essential oils are typically extracted from the aerial parts (stems, leaves, and flowers) (Aburigal et al., 2013; Bozzini at al., 2023; Carramiñana et al., 2008; Damyanova et al., 2016; Dong et al., 2023; Hudz et al., 2023; Raal et al., 2024; Stojanović et al., 2013). Some popular plants for essential oil production are shown in Figure 1.

Steam distillation is the most common extraction method for essential oils, whereas mechanical pressing is commonly used for citrus species. Steam distillation is preferred due to its relatively low cost, efficiency in producing highly pure oils without solvents, and suitability for large-scale production. The process occurs at relatively moderate temperatures, which helps preserve subtle aromatic compounds. During distillation, steam passes through the plant material, vaporizing the essential oil components; the steam mixture then condenses, and the oil is separated from the aqueous phase. Due to its efficiency, relative simplicity, and lack of organic solvents, steam distillation is considered a safe, environmentally friendly, and easily scalable method (Machado et al., 2022). Mechanical pressing (cold pressing) is a specialized method used primarily to extract essential oils from the rinds of citrus fruits like lemon, orange, and bergamot. Unlike heat-based methods, this cold-process technique uses pressure, rasping, or scratching to rupture oil glands, preserving natural aroma and preventing degradation to citrus species, helps preserve thermolabile compounds and maintain the characteristic fresh aroma (Çakaloğlu et al., 2018). In addition to these conventional methods, alternative techniques such as solvent extraction, supercritical CO_2 extraction, and microwave- or ultrasound-assisted extraction are increasingly used to improve yield, reduce processing time, and better preserve bioactive constituents (Bakhshabadi et al., 2025; Ivanov et al., 2021).

Essential oils (EOs) contain a variety of polar and non-polar, lipophilic volatile organic compounds, including ketones, aldehydes, phenols, phenolic ethers, lactones, and organic acids. The main constituents of EOs are terpenes — unsaturated hydrocarbons with the general formula $(C_5H_8)_n$, where $n \geq 2$ — and terpenoids, which are modified terpenes containing various functional groups, typically including oxygen.

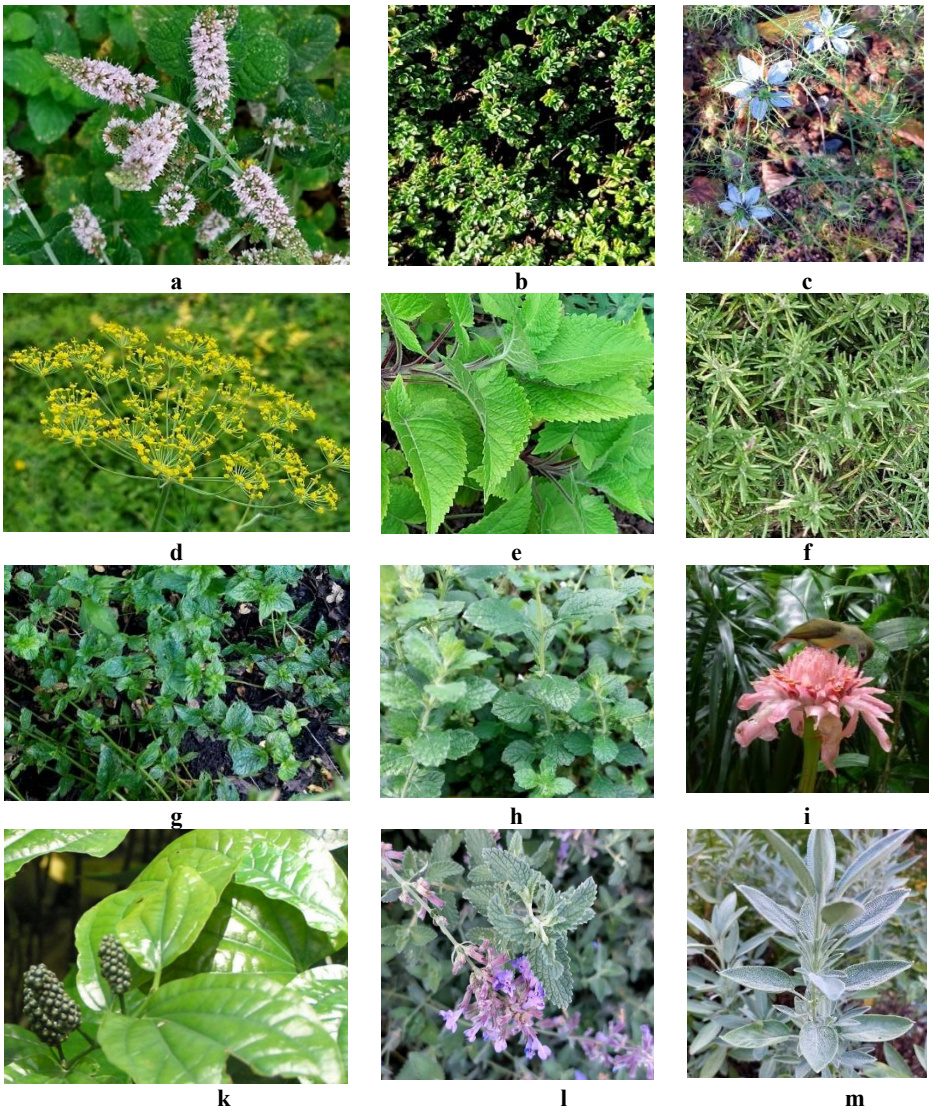

Figure 1. Some popular plants for essential oil production:
a, wild mint (*Mentha longifolia*); b, creeping thyme (*Thymus praecox*); c, love-in-a-mist (*Nigella damascena*); d, umbel of dill weed (*Anethum graveolens*); e, lemon balm (*Melissa officinalis*); f, rosemary (*Salvia rosmarinus*); g, peppermint (*Mentha piperita*), h, spearmint (*Mentha spicata*); i, torch ginger (*Etlingera elatior*); k, black pepper (*Piper nigrum*); l, catmint (*Nepeta racemosa*); m, Spanish sage (*Salvia officinalis* subsp. *lavandulifolia*). (Photo O. Stabnikova)

These compounds exhibit a wide range of biological activities, such as antimicrobial, antifungal, antioxidant, and anti-inflammatory effects (Masyita et al., 2022; Pezantes-Orellana et al., 2024; Sadgrove et al., 2022). Monoterpenes commonly found in essential oils include α-pinene, γ-terpinene, limonene, camphene, myrcene, and p-cymene (Zuzarte et al., 2024), while the most abundant monoterpenoids (oxygenated monoterpenes) include carvacrol, eugenol,

geraniol, thymol, menthol, and 1,8-cineole (Masyita et al., 2022). Sesquiterpenes, composed of three isoprene units ($C_{15}H_{24}$), occur in essential oils as hydrocarbon sesquiterpenes (e.g., β-caryophyllene, α-humulene, germacrene D) and as oxygenated derivatives (e.g., caryophyllene oxide, nerolidol, bisabolol), which contribute significantly to the biological activity of EOs.

Due to their complex chemical composition and pronounced biological activity, EOs are widely applied in different fields: in the food industry as natural flavorings and preservatives; in pharmaceuticals and medicine as antiseptic, anti-inflammatory, spasmolytic, and sedative agents, as well as in aromatherapy; in cosmetics and perfumery as functional ingredients of creams, shampoos, soaps, and perfumes; in household chemistry as components of cleaning and disinfecting products, air fresheners, and candles; and in agriculture as natural pesticides, repellents, and components of biopreparations for plant protection (Bolouri et al., 2022; Inobeme and Adetunji, 2024; Saeed et al., 2020).

The present review focuses on the applications of essential oils (EOs) in the food industry, with particular emphasis on their use in preserving food products and extending their shelf life.

Literature search method

The literature search covered the PubMed, Scopus, Web of Science, and Google Scholar databases, focusing on studies published between 2018 and 2026. The main search term was "essential oil," combined with keywords related to food preservation, including antimicrobial and antioxidant activities, chemical composition, spoilage and pathogenic microorganisms, shelf life, oxidation, as well as edible coatings and packaging materials. Relevant full-text articles were selected for detailed analysis, and additional sources were identified by examining the reference lists of selected research and review papers.

Chemical composition and antibacterial activity of essential oils

The chemical composition of essential oils is influenced by numerous factors, including the plant species, its phenological stage, the geographical origin, climatic conditions, soil type, harvest period, and the method of oil extraction. Thus, the analysis of the chemical composition of essential oils obtained from 12 plant species of the genus *Thymus* revealed substantial variation in the content, %, of individual compounds: thymol, 0.2-55.8; carvacrol, 0.3-81.2; linalool, 0-13; γ-terpinene, 0.5-15.0; p-cymene-0.2-22.8 (Vassiliou et al., 2023). However, essential oils obtained from the same plant species cultivated in different countries frequently exhibit similar predominant components in their composition. Thus, geranial and neral were identified as the major constituents of *Cymbopogon citratus* essential oil, with their contents ranging from 20.9 to 45.95% and 16.2 to 35.3%, respectively, in plants harvested across 12 regions worldwide (Majewska et al., 2019).

The extraction method also influences the chemical composition of essential oils. The content of the main components in black pepper (*Piper nigrum* L.) essential oil obtained using the supercritical carbon dioxide (SC-CO_2) technique, compared with hydrodistillation, was as follows (%): β-caryophyllene (25.38 vs. 18.64), limonene (15.64 vs. 14.95), sabinene (13.63 vs. 13.19), 3-carene (9.34 vs. 8.56), β-pinene (7.27 vs. 9.71), and α-pinene (4.25 vs. 7.96). The essential oils also exhibited different radical scavenging activities, expressed as EC_{50} values: 103.28 μg/mL for the oil obtained by SC-CO_2 extraction and 316.27 μg/mL for the oil obtained by hydrodistillation (Bagheri et al., 2014).

Although essential oils comprise numerous chemical constituents, often exceeding 100, their biological activity is largely governed by just a few predominant components (typically two or three) present at high concentrations, whereas the remaining compounds occur only at low levels

(Schneider et al., 2023). For instance, monoterpene carvacrol was the major constituent of *Satureja montana* EO (70.5%) and *Thymus vulgaris* EO (40.6%) (Carramiñana et al., 2008); menthol was the major component of *Mentha piperita* (peppermint) EO (47.0%) (de Rapper et al., 2013); linalyl acetate (35.6%) and linalool (32.8%) dominated in *Lavandula angustifolia* (lavender) EO (Orchard et al., 2016).

One of the most serious current health challenges is the rapid spread of antimicrobial-resistant microorganisms, largely driven by the excessive use of antibiotics, which has reduced their therapeutic effectiveness. Pathogens such as *Escherichia coli* O157:H7, which causes approximately 2100 hospitalizations and 20 deaths annually; multidrug-resistant *Staphylococcus aureus*, responsible for both mild and life-threatening infections in humans and animals; and various *Candida* species cause severe infections worldwide, including systemic bloodstream infections, with *Candida albicans* remaining the predominant causative agent (Razzouk et al., 2022).

It is well known that essential oils exhibit broad antimicrobial activity and have very low minimum inhibitory concentrations (MIC) and minimum bactericidal concentrations (MBC) against various opportunistic pathogens, including *Escherichia coli, Klebsiella pneumonia, Pseudomonas aeruginosa, Staphylococcus aureus, Enterococcus faecalis, Proteus vulgaris* estimated as 0.05–60 μg/ml (Aumeeruddy-Elalfi et al., 2015; Bajera et al., 2017). Essential oils could inhibit the growth of different foodborne pathogens, including *Listeria monocytogenes*, which is of major safety concern in both meat and fish products (Lambrechts and Rip, 2024; Matle et al., 2020). Thus, MIC and MBC of thyme essential oil against *Salmonella* Typhimurium were 0.25 mg/mL and 0.5 mg/mL, respectively, which demonstrated its high antimicrobial activity (Lin et al., 2019). The mechanisms underlying the antimicrobial action of essential oils involve several complementary pathways. Essential oils can disrupt the structure and function of bacterial cell membranes, thereby increasing membrane permeability and causing leakage of ions and metabolites such as potassium ions, ATP, and carboxyfluorescein. They can also inhibit protein and nucleic acid synthesis, preventing cell replication; reduce ATP production by disturbing lipid–protein interactions within the membrane; and induce oxidative stress, ultimately leading to cellular damage and death (Bouhdid et al., 2010; Bozzini et al., 2023; Hyldgaard et al., 2012; Nazzaro et al., 2013). Moreover, essential oils exert antimicrobial effects by directly interacting with bacterial genetic material. Their active constituents, particularly phenolic compounds, can penetrate cells and interact directly with bacterial DNA, causing structural damage and inhibition of replication and transcription, ultimately suppressing bacterial growth (Falleh, 2025).

The biological activity of essential oils is largely determined by their dominant constituents, including cinnamaldehyde (cinnamon), eugenol (clove), carvacrol and thymol (thyme and savory), limonene (citrus oils), and linalool/linalyl acetate (lavender and sage). For example, the minimum inhibitory concentration (MIC) values against 14 strains of *Escherichia coli* ranged from 0.68–0.82 mg/mL for cinnamon oil and from 0.55–0.72 mg/mL for its major component cinnamaldehyde. Similarly, the MIC values of clove oil and its principal component eugenol varied from 0.75–0.923 mg/mL and 0.44–0.56 mg/mL, respectively (Mishra et al., 2022). Therefore, in general, a higher content of phenolic compounds is associated with stronger antimicrobial activity (Alirezalu et al., 2020; Ji et al., 2023).

Table 1 summarizes the chemical composition and antimicrobial activity of selected widely used essential oils, demonstrating their effectiveness against a broad spectrum of Gram-positive and Gram-negative bacteria, as well as yeasts and molds.

Table 1

Chemical composition and antimicrobial activity of some popular essential oils

Essential oil from plant	Major constituents, % of total content	Active against	Reference
Black pepper (*Piper nigrum*)	Caryophyllene, 60.7; cyclohexene, 6.2; D-3-carene, 6.2; limonene, 4.6; (−)-spathulenol, 4.6	MIC and MFC, mg/mL: 2 and 16 for *Candida albicans* ATCC 64547; 4 and 16 for *Aspergillus flavus* CGMCC 3.06434	Li et al., 2020
Cardamon (*Elettaria cardamomum*)	31.8-cineole, 55.4; α-terpinyl acetate, 28.6; 4-terpineol, 4.3; α-terpineol; limonene, 2.5; sabinene, 1.5	MIC, μg/mL*:* 48 for *Bacillus subtilis* ATCC 6633, *E. faecalis* ATCC 29212, *E. coli* ATCC 25922, *P. aeruginosa* ATCC 27853, *Salmonella Typhimurium* ATCC 14028, *Shigella flexenerii* ATCC 12022, *Serratia marcescens*, *Vibrio cholerae* ATCC 9459	Noumi et al., 2018
Cinnamon (*Cinnamomum zeylanicum*)	Cinnamaldehyde, 79.3; eugenol, 11.9	*Paenibacillus larvae*, MIC 25-100 μg/mL; MBC 125-250 μg/mL	Gende et al., 2008
Cinnamon (*Cinnamomum cassia*)	Cinnamaldehyde, 92.8; cinnamyl acetate, 2.5	MIC, μg/mL: 4.88 for *E.* coli ATCC 25922 and *S. aureus* ATCC 25923; 30.5 for *P. aeruginosa* ATCC 27853	El Atki et al., 2019; Do et al., 2024
Clove (*Syzygium aromaticum*)	Eugenol, 82.16; acetyleugenol, 16.25; caryophyllene, 0.79	MIC, μg/mL: 1.25 for *E. coli* ATCC 35214, *K. pneumoniae* CIP 104727; *L. monocytogenes* ATCC 19115; *P. aeruginosa* ATCC 27853; *S. aureus* ATCC 29213; *B. cereus* ATCC 14579, *Aspergillus niger* CCMM M100; 2.5 for *C. albicans* CCMM L4	Razzouk et al., 2022
Cumin (*Cuminum cyminum*)	Limonene, 36.77; carvone, 57.94; α-pinene, 1.58; trans-dihydrocarvone, 1.66	MIC, μg/mL: 1 for *Streptococcus pyogenes;* 2 for *L. monocytogenes* and *B. subtilis*; 16 for *Enterobacter aerogenes*; 4 for *Salmonella enterica* serovar Typhimurium; 8 for *Shigella dysentery*	Noshad et al., 2023
Dill weed (*Anethum graveolens*)	Carvone, 32.26; α-phellandrene, 20.11; limonene, 18.78; Dill ether, 9.06; p-cymene, 4.40	*Salmonella abony* NTCC 6017; *E. coli* ATCC 8739; *P. aeruginosa* ATCC 9027; *S. aureus* ATCC 6538; *B. subtilis* ATCC 6633; *C albicans* ATCC 1023; *A. brasiliensis* ATCC 16404	Kostova et al., 2020
Fennel (*Foeniculum vulgare*) seeds	Estragole, 66.1–85.2; fenchone, 5.2–23.1; limonene, 4.3–10.3	*E. coli, P. aeruginosa, Salmonella enterica, S. aureus, C. albicans,* and *Aspergillus niger* with MIC from 2.5 to 7.5 mg/mL	Khammassi et al., 2018
Garlic (*Allium sativum*)	Dodecanoic acid, 1,2,3-propanetriyl ester, 92.64	MIC, μg/mL: 11,3 for *E. aerogenes*; 14.8 for *B. subtilis*; 19.1 for *P. aeruginosa*; 7.5 for *A. niger*; 6.5 for *A. flavus*	Arasu et al., 2019
Grapefruit (*Citrus paradise*)	Limonene, 73.5; linalool, 4.7; linalool oxide, 4.2	MIC, mg/mL: 0.14 for *B. cereus* ATCC 14579; 0.21 for *L. monocytogenes*; 0.12 for *Micrococcus flavus* ATCC 10240; 0.14 for *P. aeruginosa* ATCC 27853; 0.16 for *S. aureus* ATCC 6538	Mahmoud, 2017

Ginger (*Zingiber officinale*)	α-curcumeme, 37.6; himachalene, 14.4; ar curcumene, 8.6; himachalene, 14.4	MIC, mg/mL: 1.80 for E. coli ATCC 25922; 1.00 for *P. aeruginosa* ATCC 27858; 2.00 for *Propionibacterium acnes* ATCC 11827 and *C. albicans* ATCC 10231	Orchard et al., 2016
Lavender (*Lavandula angustifolia*)	Linalyl acetate, 36.7; linalool 31.4; terpinen-4-ol, 14.9	MIC, mg/mL: 2 for *S. aureus* ATCC 6538; *P. aeruginosa* ATCC 27853; *E. faecalis* ATCC 51299; 1.5 for *K. pneumoniae* ATCC 13883; 3.0 for *C. albicans* ATCC 10231	de Rapper et al., 2013
Lavender (*Lavandula angustifolia*)	Linalyl acetate, 35.6; linalool, 32.8; β-caryophyllene, 10.2	MIC, mg/mL: 2.00 for *E. coli* ATCC 25922 and *P. acnes* ATCC 11827; 1.00 for *P. aeruginosa* ATCC 27858 and *C. albicans* ATCC 10231	Orchard et al., 2016
Lemon (*Citrus limon*)	β-pinene, 7.2; limonene, 74.9	MIC, mg/mL: 2.00 for *E. coli* ATCC 25922 and *P. acnes* ATCC 11827; 1.00 for *P. aeruginosa* ATCC 27858; 4.00 for *C. albicans* ATCC 10231	Orchard et al., 2016
Lemongrass (*Cymbopogon citratus*)	Neral, 39.0; geranial, 33.3; limonene, 5.8; geranyl acetate, 4.2	MIC, μl/mL: 0.5 for *E. coli*, *C. albicans*, *B. cereus, Salmonella* Typhimurium	Vazirian et al., 2012
Lemongrass (*Cymbopogon citratus*) leaves	Geranial, 38.5; neral, 28.7; D-limonene, 6.9; geraniol, 4.4; citronellyl acetate, 4.3; linalool, 1.6; β-caryophyllene, 1.4	MIC varied from 0.019 to 1.25 mg/mL for *S. aureus, S. epidermidis,* and *C. albicans*	Majewska et al., 2019
Muscatel sage (*Salvia sclarea*)	Linalyl acetate, 72.9; linalool 11.9	MIC, mg/mL: 0.88 for *C. albicans* ATCC 10231; 3.50 for *P. aeruginosa* ATCC 27858; 2.00 for *S. aureus* ATCC 6538	de Rapper et al., 2013
Orange (*Citrus sinensis*)	Limonene, 93.5	MIC, mg/mL: 2.00 for *E. coli* ATCC 25922, *P. acnes* ATCC 11827, *C. albicans* ATCC 10231; 1.00 for *P. aeruginosa* ATCC 27858	Orchard et al., 2016
Oregano (*Origanum vulgare*)	Carvacrol, 85.7; o-cymene, 5.0; γ-terpinene, 1.83; thymol, 1.65; myrcene, 0.51	MIC, 0.125 mg/mL, for *S. aureus* ATCC 6538, *B. cereus* ATCC 10876, *B. subtilis* ATCC 6633, *S. epidermidis* ATCC 12228, and *S.* Typhimurium ATCC 14028; 0.5–1 mg/mL for *P. aeruginosa* ATCC 27853 and *E. faecalis* ATCC 29212	Walasek-Janusz et al., 2024
Peppermint (*Mentha piperita*)	Menthol, 47.5; menthone, 18.6	MIC, mg/mL: 2.0 for *C. albicans* ATCC 10231 and *P. aeruginosa* ATCC 27858; 4.0 for *S. aureus* ATCC 6538	de Rapper et al., 2013
Peppermint (*Mentha piperita*)	Menthol, 47.0; menthone, 18.8%	MIC, mg/mL: 2.00 for *E. coli* ATCC 25922; 1.00 for *P. acnes* ATCC 11827, *P. aeruginosa* ATCC 27858, *C. albicans* ATCC 10231	Orchard et al., 2016
Rosemary (*Rosmarinus officinalis*)	1,8-cineole, 48.0	MIC, mg/mL: 2.0 for *C. albicans* ATCC 10231 and *P. aeruginosa* ATCC 27858; 4.0 for *S. aureus* ATCC 6538	de Rapper et al., 2013

Rosemary (*Rosmarinus officinalis*)	Camphor, 19.1; α-pinene, 14.7; verbenone, 12.3; bornyl acetate, 12.2; 1,8-cineole, 6.9; camphene, 5.0	MIC, mg/mL: 2.00 for *E. coli* ATCC 25922 and *P. aeruginosa* ATCC 27858; 1.67 for *P. acnes* ATCC 11827; 1.00 for *C. albicans* ATCC 10231	Orchard et al., 2016
Spanish sage (*Salvia officinalis* subsp. *lavandulifolia*) aerial parts	Epi-manool, 13.4; α-humulene, 9.7; camphor, 7.2; 1,8-cineole 5.2; juneol , 3.9; spathulenol, 3.5; β-caryophyllene, 3.0; camphene, 3.0; δ-cadinene, 3.0	MIC, 5.92 mg/mL, and MBC, 11.84 mg/mL, for *L. monocytogenes* ATCC 7644	Bozzini at al., 2023
Thyme (*Thymus vulgaris*) stems and flowers	Carvacrol, 40.6; p-cymene. 10.9; thymol, 6.1; γ-terpinene, 5.9; 1,8-cineole, 4.9; linalool, 4.6	*Listeria monocytogenes*	Carramiñana et al., 2008
Thyme (*Thymus vulgaris*)	Thymol, 54.21, p-cymene 20.64, γ-terpinene 6.01, linalool, 2.15, myrcene, 1.28; carvacrol, 2.90	*Pseudomonas aeruginosa*	Pandur et al., 2022
Thyme (*Thymus vulgaris*)	p-cymene, 39.9; thymol, 20.7; γ-terpinene, 8.3	MIC, mg/mL: 1.00 for *C. albicans* ATCC 10231; 2.00 for *P. aeruginosa* ATCC 27858; 3.33 for *S. aureus* ATCC 6538	Rapper et al., 2013
Nutmeg (*Myristica fragrans*)	β-elemene, 18.44; o-cymene, 11.54; 1,2-dimethoxy-4-(2-methoxy-1-propenyl) benzene, 10.32; γ-terpinene 9.34	MIC 15 µL/mL against *S. aureus* ATCC 25923, E. coli ATCC 25922, *L. monocytogenes* ATCC 19111, and *S.* Typhimurium ATCC 14028	Moirangthem et al., 2024
Wild sour (*Hibiscus surattensis*), calyces	β-caryophyllene, 11.68; menthol, 9.44; methyl salicylate, 8.32; camphor, 8.47; germacrene D, 5.13	MIC and MBC, µl/mL: 0.038 and 0.020 *E. coli* ATCC 25922; 0.156 and 0.083 for *L. monocytogenes* ATCC 51774; 0.109 and 0.012 for *Shigella flexneri* ATCC 12022; 0.124 and 0.015 for *S.* Typhimurium ATCC 14028; 0.077 and 0.015 for *Enterobacter aerogenes* ATCC 13048; 0.054 and 0.018 for *S. aureus* ATCC 6538	Akarca, 2019
Winter savory (*Satureja montana*), aerial parts and leaves	Carvacrol, 70.5; β-caryophyllene, γ-terpinene, 2.2; α-pinene, 1.2; p-cymene, 10; borneol, 1.9	*Listeria monocytogenes*	Carramiñana et al., 2008

n.a., not applicable; MIC, the minimum inhibitory concentration; MFC, the minimum fungicidal concentration; ATTC, American Type Culture Collection.

Essential oils exhibit significant antimicrobial, antibacterial, and antifungal properties due to their complex, lipophilic nature, which enables them to disrupt microbial cell membranes. Although their antimicrobial activity is largely determined by chemical composition, establishing a direct correlation between composition and biological activity remains challenging due to synergistic interactions among multiple constituents. Their efficacy varies considerably depending on specific chemical composition, which is influenced by plant origin and extraction methods, as well as by the inherent resistance or susceptibility of target microorganisms. The lowest minimum inhibitory concentration (MIC) values are typically observed for oils rich in phenolic compounds (such as carvacrol, thymol, and eugenol), highlighting their strong potential as natural antimicrobial and preservative agents in food systems.

In some cases, the use of combinations of essential oils is advisable due to potential synergistic effects. A comparative study evaluated individual essential oils of Shirazi thyme (*Zataria multiflora*), cinnamon (*Cinnamomum zeylanicum*), and clove (*Syzygium aromaticum*), as well as their combinations, against *Pseudomonas fluorescens*. The triple combination exhibited the strongest synergistic effect, enabling the use of lower concentrations while maintaining high antimicrobial efficacy. This combination resulted in a 6–8-fold reduction in minimum inhibitory concentration (MIC) compared to individual oils. Specifically, the MIC values for Shirazi thyme, clove, and cinnamon against *P. fluorescens* were 2.25, 2.75, and 2.50 mg/mL, respectively, whereas in combination they decreased to 0.560, 0.042, and 0.078 mg/mL, corresponding to 1/4, 1/32, and 1/64 of the initial values, respectively (Fractional Inhibitory Concentration Index, FICI, = $0.3 \leq 0.5$), indicating a synergistic interaction (Chaichi et al., 2021).

It should be noted that the application of essential oils as food preservatives is constrained by the relatively high concentrations often required to achieve effective antimicrobial activity. Their efficacy may be influenced by temperature, pH, microbial contamination level, and interactions with food components such as starch, fats, and proteins, which can reduce antimicrobial performance in complex food matrices (Zubair et al., 2022). In addition, the strong aroma of essential oils may negatively affect the sensory properties of foods. To address these challenges, essential oils are increasingly incorporated into active packaging systems, edible coatings, films, and encapsulation materials, enabling controlled release and improved preservation efficiency while minimizing undesirable sensory effects (Stabnikova et al., 2026).

Antioxidant activity of essential oils

An important characteristic of essential oils for their applications in food industry is their antioxidant activity (AA), which enables their use as natural alternatives to synthetic preservatives for extending the shelf life of food products. Antioxidant activities of different essential oils measured by the DPPH (2,2-diphenyl-1-picrylhydrazyl) radical scavenging activity assay are shown in Table 2.

In antioxidant evaluation methods based on radical inhibition, including the DPPH assay, IC_{50} and EC_{50} values are commonly applied as indicators of antioxidant effectiveness and are frequently treated as equivalent parameters. Lower values of IC_{50} or EC_{50} correspond to greater antioxidant capacity because lower concentrations are needed to achieve 50% radical scavenging activity. To improve comparability of DPPH results, Scherer and Godoy (2009) introduced the Antioxidant Activity Index (AAI), defined as the ratio between the initial DPPH concentration and the EC_{50} value. Based on this index, antioxidant activity is classified as poor (AAI < 0.5), moderate (0.5–1.0), strong (1.0–2.0), or very strong (AAI ≥ 2.0). Using this approach, clove essential oil was categorized as having very strong antioxidant activity (AAI = 2.2), while oregano essential oil exhibited strong antioxidant properties (AAI = 1.7) (Teixeira et al., 2013). Similarly, high antioxidant activity of clove, cinnamon, and thyme essential oils was reported by Chen et al. (2023).

Table 2

Antioxidant activity of some essential oils measured by the DPPH assay

Essential oil	Antioxidant activity		Reference
	IC_{50}, mg/mL	EC_{50}, mg/mL	
Basil (*Ocimum basilicum*)	12.00	n.a	Cichoski et al., 2011
Catnip (*Nepeta ciliaris*)	80.62	n.a	Ashrafi et al., 2019
Celery seed (*Apium graveolens*)	n.a	10.04±0.39	Teixeira et al. 2013
Cinnamon (*Cinnamomum zeylanicum*)	9.53±0.20	n.a	Živković et al., 2025
Cinnamon	n.a	0.03±0.00	Chen et al., 2023
Citronella (*Cymbopogon nardus*)	n.a	1.18±0.02	Teixeira et al. 2013
Clove (*Eugenia* spp.)	n.a	0.04±0.00	Teixeira et al. 2013
Clove	n.a	0.05±0.01	Chen et al., 2023
Clove (*Syzygium aromaticum*) buds	0.109	n.a	Alfikri et al., 2020
Citrus hybrid	n.a	86.17 ± 4.87	Yang and Park, 2025
Fennel (*F. vulgare*) seeds (from 16 localities of Tunisia)	12.00±0.28 - 38.13±0.66	n.a	Khammassi et al., 2018
Lavender	n.a	12.1±2.16	Chen et al., 2023
Lemongrass (*Cymbopogon citratus*)	5.13 ± 0.13	n.a	Baranová et al., 2025
Origanum (*Thymus capitatus*)	n.a	0.05±0.00	Teixeira et al. 2013
Parsley (*Petroselinum sativum*)	n.a	7.23±0.16	Teixeira et al. 2013
Peppermint	n.a	33.9±5.64	Chen et al., 2023
Tarragon (*Artemisia dracunculus*)	n.a	8.81±0.10	Teixeira et al. 2013
Thyme (*Thymus vulgaris*)	n.a	0.25±0.01	Teixeira et al. 2013
Thyme	n.a	0.14±0.05	Chen et al., 2023
Thyme(*Thymus vulgaris*)	0.16±0.01	n.a	Gedikoğlu et al., 2023
Clove (*Syzygium aromaticum*) fruit	0.38	0.02	Viuda-Martos et al., 2010
Oregano (*Oringanum vulgare*) flowers	3.90	0.02	
Rosemary (*Rosmarinus officinalis*) entire plant	17.00	52.55	
Sage (*Salvia officinalis*) leaves and flowers	4.20	35.56	
Thyme (*Thymus vulgaris*) leaves	1.1	0.09	
Ascorbic acid	0.42	7.98	
BHT	0.53	0.001	
BHT	0.01	n.a	Živković et al., 2025
BHT	0.02	n.a	Teixeira et al. 2013

Note: IC_{50} is the half-maximal inhibitory concentration, i.e., the concentration required to inhibit 50% of radical activity or oxidative reactions; EC_{50} is the half-maximal effective concentration, i.e., the concentration that produces 50% of the maximal antioxidant effect (e.g., 50% radical scavenging); BHT, butylated hydroxytoluene (a synthetic antioxidant); n.a. – not applicable.

However, many essential oils, including basil (*Ocimum basilicum*) leaves, carrot (*Daucus carota*) seed, coriander (*Coriandrum sativum*), garlic (biological source not specified), grapefruit (Citrus paradise), lemon (*Citrus limon*), marjoram (*Thymus mastichina*), onion (*Allium cepa*), rosemary (*Rosmarinus officinalis*), and sage (*Salvia officinalis*) (Teixeira et al., 2013), fennel (*Foeniculum vulgare*) seeds (Khammassi et al., 2018), as well as lavender and peppermint (Chen et al., 2013), exhibited low antioxidant activity. It was shown that antioxidant activity of essential oil is depended from its chemical composition, and correlates with the AA of the mail compound present in it. Thus, phenol-rich essential oils (such as cinnamon, thyme, and clove) exhibited the strongest antioxidant activities, whereas non-phenolic oils (lavender and peppermint) demonstrated very weak

antioxidant activity, likely due to the low antioxidant potential of their main components, linalool and menthol (Chen et al., 2023).

The antioxidant activity of essential oils depends on numerous factors, including geographic origin, harvest time, and the plant's phenological stage (Alfikri et al., 2020), plant species (Yang and Park, 2025) as well as the plant part used for extraction (Yang et al., 2025) and the extraction method employed (Gedikoğlu et al., 2019; Priss et al., 2025). Thus, DPPH assay results revealed that thyme essential oil obtained via microwave-assisted extraction exhibited significantly higher antioxidant activity (IC_{50} = 93.77 μg/mL) compared to oil obtained by hydrodistillation (IC_{50} = 159.59 μg/mL) (Gedikoğlu et al., 2019).The antioxidant activity of essential oils from roots, stems, leaves, and pericarp of *Zanthoxylum nitidum* (shiny-leaf prickly ash), determined by the DPPH assay as scavenging rate (%), was 57.37, 24.63, 100.00, and 44.38, respectively (Yang et al., 2025).

Essential oils in food products

The consumption of food contaminated with harmful microorganisms causes foodborne diseases that affect millions of people annually, and can sometimes result in severe or even fatal outcomes (WHO, 2024). Representatives of the genera *Campylobacter* and *Salmonella*, as well as enterohaemorrhagic *Escherichia coli*, are among the most common foodborne pathogenic bacteria. *Campylobacter* species are mainly found in raw milk and raw or undercooked poultry. Outbreaks of salmonellosis are typically linked to contaminated eggs, poultry, and other animal-derived products. Foodborne illnesses caused by *Escherichia coli* often occur after the consumption of unpasteurized milk, undercooked meat, or contaminated fresh fruits and vegetables. Bacteria of the genus *Listeria*, capable of growing at refrigeration temperatures, are found in unpasteurized dairy products, meat, and fish products, including various ready-to-eat foods, and are responsible for one of the most severe foodborne infections with the high case-fatality rate around 20 percent (FAO and WHO, 2022). *Vibrio cholerae* can infect humans through contaminated raw vegetables and different types of raw or undercooked seafood.

Several fungal species can lead to food spoilage, which is typically associated with visible surface growth and the formation of metabolites responsible for sensory changes. In addition to the deterioration of sensory properties, spoilage molds belonging to the genera *Penicillium* and *Aspergillus* can also produce mycotoxins that cause diseases known as mycotoxicoses. These fungi have been detected on dry-cured meats and fermented sausages (Ji et al., 2021), bread and bakery products (Diowksz et al., 2024; György and Laslo, 2024), dairy products (Garnier et al., 2017), nuts (Buonsenso et al., 2025), as well as dried (Miliordos et al., 2025) and fresh (Zakaria, 2024) fruits and vegetables.

Essential oils have proven highly effective in preventing bread spoilage caused by filamentous fungi, particularly *Aspergillus niger*. For example, star anise essential oil was reported to impair the energy metabolism of *A. niger* by decreasing ATP content and inhibiting the NAD biosynthesis pathway, leading to cell death (Zhao et al., 2022). Strong antifungal activity against *A. niger* was also observed when citral and eugenol were used in combination, demonstrating a synergistic effect: citral affected metabolic pathways and membrane potential, whereas eugenol disrupted membrane integrity, causing leakage of intracellular contents (Ju et al., 2020; Wang et al., 2024).

While synthetic compounds were previously widely employed for this purpose, increasing consumer demand for natural alternatives has shifted attention toward plant-derived substances, particularly essential oils (Stabnikova et al., 2021). Essential oils have long been used as flavoring agents in the food industry; however, their application requires careful consideration. Specifically, it is important to verify whether a given essential oil is included in the U.S. Food and Drug Administration list of substances classified as GRAS (Generally Recognized as Safe) (GRAS List FDA, 2025). It should be noted that GRAS status applies only to low, food-grade concentrations

rather than therapeutic doses. Thus, even when approved, essential oils should be used in food products only at trace levels. Some examples of the effect of direct essential oil addition into food products on spoilage and pathogenic microorganisms are shown in Table 3.

Table 3

Effect of essential oil addition in food products on spoilage and pathogenic microorganisms

Essential oil, dosage	Product	Effect of EO application	Reference
Winter savory (*Satureja montana*) EO, 2.5 µg/g of minced pork	Minced pork	After 7 d at 4 °C: *L. monocytogenes* 4.49 vs 5.16 (control) $\log_{10}$ CFU/g; total aerobic bacteria 8.30 vs 8.90 $\log_{10}$ CFU/g (control)	Carramiñana et al., 2008
Thyme (*Thymus vulgaris*) EO, 2.5 µg/g of minced pork	Minced pork	After 7 d at 4 °C: *L. monocytogenes* 4.49 $\log_{10}$ vs 5.16 (control) $\log_{10}$ CFU/g; total aerobic bacteria 6.86 vs 8.90 $\log_{10}$ CFU/g (control)	Carramiñana et al., 2008
Oregano and cinnamon EOs, 0.5% (w/w)	Italian salami	After 10 d at 4 °C: reduced *L. monocytogenes* from ≈10^6 CFU/g to below the detection limit	Gottardo et al., 2022
Basil oil, 0.075 % (w/w)	Italian salami	Slowed down lipid oxidation at the processing stage	Cichoski et al., 2021
Thyme *(Thymus vulgaris)* and rosemary (*Rosmarinus officinalis*)	Italian mortadella	Effectively inhibited *L. monocytogenes* growth during 30 days of storage at 4 °C	Giarratana et al., 2016
Juniperus communis EO, 0.01 (v/w)	Cooked pork sausages	Reduced TAMB count to 36.7 CFU/g compared with 137 CFU/g in the control	Šojić et al., 2017
Coriander (*Coriandrum sativum*) EO, 0.15 %	Cake	Inhibit the growth of fungal in the cake packed in polypropylene film and stored at 25 °C for 60 days, but had small negative effect on overall acceptability	Darughe et al., 2012
Ginger (*Zingiber officinale*) EO, or thyme EO (*Thymus vulgaris*), 0.1 mg/mL	Soft cheese	Reduced *Pseudomonas aeruginosa* by 44.1% and 52.5% (after 4 weeks storage at 4 °C) and completely inhibited *Staphylococcus aureus* after 1 and 2 weeks, respectively	Ahmed et al., 2021
Nigella sativa oil, 0.2% (w/w)	Domiati cheese	Suppress the growth of *S. aureus, S. enteritidis, E. coli, L. monocytogenes*	Mahgoub et al., 2013
Oregano (*Origanum vulgare*), 0.02% (v/v)	Minas cheese	Decreased undesirable bacteria and filamentous fungi; well accepted by sensory panel	De Campos et al., 2022
Lemongrass (*Cymbopogon citratus*) EO, 1 µl/g of cake	Cream-filled cakes	After 72 h at 4 °C: cakes contaminated with *E. coli*, *C. albicans, B. cereus*, or *S.* Typhimurium, $1.5 \cdot 10^5$ CFU/10 g, showed the absence of detectable microorganisms	Vazirian et al., 2012
Cinnamon EO (CEO)	Milk	Addition of CEO-loaded lipid NPs (0.15% chitosan) enhanced oxidative stability of milk	Bashiri et al., 2019
Cinnamon EO,2.0%	Tahini sauce	Addition of 2.0% EO to tahini reduced *E. coli* O157:H7 by 1.38, 1.79, and 2.20 $\log_{10}$ CFU/ml at 10, 25, and 37 °C, respectively, after 28 days	Al-Nabulsi et al., 2020
Thyme EO, 0.5 g/25 g of vegetables	Fresh-cut vegetables	Spraying EO on vegetables contaminated with *Listeria* (10^5–10^6 CFU/g) and stored in a sealed polypropylene bag at 8 °C reduced the *Listeria* counts by 6 $\log_{10}$ units, with no viable cells detected from day 0 to day 6	Scollard et al., 2013

Note: TVC - total viable bacterial count; TAMB - total aerobic mesophilic bacteria.

Basil leaf (*Ocimum basilicum*) essential oil (0.075%) has been reported to effectively inhibit lipid oxidation in Italian salami over 28 days of processing, resulting in lower TBARS values at the end compared with the synthetic antioxidant sodium erythorbate (0.25%). These findings confirm the potential of basil essential oil as a natural antioxidant for enhancing the oxidative stability of meat products (Cichoski et al., 2021). Addition of thyme (*Thymus vulgaris* L.) and rosemary (*Rosmarinus officinalis* L.) essential oils at 0.05% to Italian mortadella showed a pronounced antimicrobial effect. After cooking, samples were inoculated with a three-strain mixture of *Listeria monocytogenes*, packaged under modified atmosphere, and stored at 4 °C for 30 days. In treated samples, no growth was observed, with *L. monocytogenes* counts remaining stable from 2.47 $\log_{10}$ CFU/g at day 0 to 2.52 $\log_{10}$ CFU/g after 30 days. In contrast, the concentration of *L. monocytogenes* in control samples rose from 2.57 to 5.31 $\log_{10}$ CFU/g during storage (Giarratana et al., 2016).

Incorporation of *Juniperus communis* essential oil (0.1%, v/w) to sausage batter reduced the total aerobic mesophilic bacterial count in cooked pork sausages by 3.7-fold and decreased radical formation, as indicated by a lower IC_{50} DPPH value (87.8 μg/mL) compared with the control (95.3 μg/mL). The additive also improved sausage color, while only slightly affecting the original taste of the product (Šojić et al., 2017). The addition of lemongrass essential oil (1 μl/g) to cream-filled cakes (9 g of paste and 1 g of cream) inoculated with foodborne pathogens such as *E. coli, C. albicans, B. cereus*, or *S.* Typhimurium ($1.5 \cdot 10^5$ CFU per 10 g cake) resulted in the complete absence of detectable microorganisms in the entire mixture, which was heated to 120 °C for 10 minutes and then stored in the refrigerator for 72 hours, whereas in the control samples, the counts of each pathogen were approximately $1.5 \cdot 10^3$ CFU per cupcake (Vazirian et al., 2012).

Addition of cold-pressed black cumin (*Nigella sativa*) seed oil at 0.2% (w/w) to soft Domiati cheese artificially contaminated with foodborne pathogens significantly reduced bacterial counts after 42 days of storage at 4 °C compared with the control ($\log_{10}$ CFU/g): *S. aureus* ≈ 2.1 vs 3.0; *S. enteritidis* ≈ 2.0 vs 2.9; *L. monocytogenes* ≈ 1.9 vs 3.8, and E. coli ≈ 2.0 vs 3.2. In addition, the physicochemical and sensory properties of the cheese were improved (Mahgoub et al., 2013).

The addition of oregano essential oil (0.02%, v/v) to artificially contaminated Minas cheese resulted in a 7-log reduction of multidrug-resistant *Staphylococcus aureus* within 1 h of ripening and complete elimination of the pathogenic strain *Escherichia coli* EPEC O127:HNT (initial level: 10^5 CFU/g) after 3 days. In addition, spores of *Aspergillus flavus* CMT 00335 and *Penicillium citrinum* ATCC 28752 were inhibited for up to 15 days, while *Fusarium oxysporum* ATCC 48112 did not germinate throughout 30 days of cheese ripening (De Campos et al., 2022). Importantly, the minimum inhibitory concentration (MIC) of oregano essential oil against *E. coli* (0.06% v/v) and *S. aureus* (0.31% v/v) was lower than that for the starter culture R704 (0.15% v/v), composed of *Lactococcus lactis* subsp. *lactis* and *Lactococcus lactis* subsp. *cremoris* used in cheese production. This allows cheese processing without undesirable changes in its characteristic properties.

Numerous studies have indicated the potential for contamination of fresh vegetables and fruits with *L. monocytogenes*, a bacterium that is widespread in soil and agricultural environments. Thyme, oregano, and rosemary essential oils (0.5 g per 25 g of product) were sprayed on vegetable samples inoculated with *Listeria* (10^5–10^6 CFU/g), which were then sealed in packages and stored at 8 °C. Thyme EO significantly reduced *Listeria* populations (by 6 $\log_{10}$ counts, with no viable cells detected from day 0 to day 6), whereas the effect of oregano EO was less pronounced, and rosemary EO showed virtually no anti-listerial activity (Scollard et al., 2013).

Essential oils can be incorporated into foods in their natural form; however, encapsulation is often employed to enhance their effectiveness and reduce undesirable interactions with food matrix components (Noshirvani, 2024). This approach provides protection against environmental factors and enables controlled release over time. Microencapsulated oregano and cinnamon

essential oils, applied as a 1:1 mixture at 0.25% (w/w) each, reduced *L. monocytogenes* counts in Italian salami from approximately 10^6 CFU/g to below the detection limit after 10 days of storage at 4 °C (Gottardo et al., 2022).

Recent research has increasingly focused on nanotechnology-based delivery approaches for essential oils, which offer improved stability, greater surface area, and enhanced bioavailability of active compounds. In particular, chitosan-based nanoparticles (NPs) have attracted considerable attention as effective carriers for the encapsulation of bioactive compounds, including essential oils (Karam and Yammine, 2023). For example, cinnamon essential oil (CEO) was incorporated into nanostructured lipid carriers composed of cocoa butter, sweet almond oil, and Tween 80, which were subsequently coated with 0.15% chitosan. This process yielded CEO-loaded nanoparticles with a mean size of 119.4 nm and a zeta potential of +21.4 mV, indicating high stability and resistance to aggregation. The incorporation of these nanoparticles into cow milk significantly reduced thiobarbituric acid (TBA) values compared to the control over 21 days of storage, confirming their antioxidant activity. Specifically, the TBA absorbance of the control sample increased from 0.048 on day 1 to 0.668 on day 21, whereas in milk samples containing nanoparticles, TBA values remained relatively stable (0.11–0.172) throughout the storage period (Bashiri et al., 2019).

EOs, particularly those rich in phenolic compounds such as carvacrol, thymol, and eugenol, are highly effective in delaying lipid degradation by acting as chain-breaking antioxidants. They prevent lipid oxidation through multiple mechanisms, including blocking the initiation stage, scavenging free radicals, acting as reducing agents, decomposing peroxides, interrupting hydrogen abstraction, and inhibiting both singlet oxygen formation and the catalytic activity of transition metal ions. In addition, they can enhance termination reactions and act as physical quenchers of singlet oxygen.

The practical relevance of these mechanisms has been demonstrated in various food systems. For example, the addition of 0.5% lemongrass essential oil to lean pork mince stored at 4 °C for 12 days reduced lipid oxidation compared to a sample treated with 0.01% butylated hydroxytoluene (BHT): 2-TBARS values (mg malondialdehyde/kg) were 6.19 vs 6.29, and peroxide values (mEq/kg) were 4.25 vs 5.67 at the end of storage (Reddy et al., 2023).

The incorporation of essential oils into food products can enhance their antioxidant activity, which depends on the form in which the oils are applied, following the trend: nanoencapsulated > microencapsulated > free essential oil (Table 4).

Table 4

Effect of essential oil addition in food product on its antioxidant activity

Essential oil, dosage	Food product	Effect of EO application	Reference
Clove, g/100 g wheat flour: 1.0 (EO), 5.0 (microencapsulated); 5.0 (nanoencapsulated)	Biscuits	DPPH (IC_{50}), µg/ml, on 60 day of storage: 5.66 (control); 40.35 (with EO); 48.22 (with microencapsulated EO); 51.04 (with nanoencapsulated EO)	Hussein et al., 2022
Cumin, g/100 g wheat flour: 1.0 (EO), 5.0 (microencapsulated); 5.0 (nanoencapsulated)	Biscuits	DPPH (IC_{50}), µg/ml, on 60 day of storage: 4.25 (control); 26.52 (with EO); 28.54 (with microencapsulated EO); 31.48 (with nanoencapsulated EO)	Hussein et al., 2022

It has been widely reported the potential of using essential oils as natural alternatives to synthetic antioxidants in vegetable oils (Amariei et al., 2016; Taghvaei and Jafari, 2015). A comparative study assessed citron peel essential oil (800 mg/L) and butylated hydroxytoluene (BHT) (200 mg/L, the legally permitted level) addition on sunflower oil stored at 65 °C for 5

days. On day five, TOTOX values (a measure of fat oxidation, where higher values indicate greater degradation) were 66.47 for BHT and 73.47 for essential oil, while Oxidative Stability Index (OSI) decreased from initial 4.00 h to 3.00 h and 3.39 h, respectively. These results indicate that BHT limited oxidation slightly more effectively, but essential oil provided greater thermal stability, highlighting its potential as a natural alternative to synthetic antioxidants (Okhli et al., 2020).

It should be noted that the direct incorporation of essential oils into food products, even at low concentrations, may adversely affect their sensory properties; therefore, the use of essential oils in edible coatings represents a promising alternative.

Essential oils in edible coating for food products

Edible food coatings are typically composed of biopolymers such as proteins, lipids, polysaccharides, or their combinations and are applied as a thin, consumable layer on the surface of food products (Karnwal et al., 2025; Stabnikov et al., 2025). These coatings serve as barriers against water vapor, gases, and other environmental factors, extending the shelf life of food by reducing moisture loss, regulating respiration, and preventing oxidation. The most common methods for applying edible coatings to fresh product include dipping, spraying, and hand-coating (De Oliveira Filho et al., 2021). The incorporation of essential oils into such coatings enhances their antimicrobial properties, further improving food safety and prolonging shelf life. The incorporation of Shirazi thyme (*Zataria multiflora*) essential oil (main component: carvacrol, 36.62%) at 1% (w/v) into a 3.4% (w/v) corn starch coating applied to chicken meat enhanced its antimicrobial properties. After 20 days of storage at 4 °C, microbial loads (log_{10} CFU/g) in EO-coated samples were substantially lower than in the control without EO: total viable count, 9.77 vs. 12.58; psychrotrophic bacteria, 8.67 vs. 11.61; lactic acid bacteria, 6.51 vs. 11.03; Enterobacteriaceae, 8.11 vs. 10.94; and molds and yeasts, 6.31 vs. 10.26. The initial count of *Listeria monocytogenes* in artificial contaminated meat was 4.16 log_{10} CFU/g, increasing to 11.42 log_{10} CFU/g in control samples by day 20, whereas in EO-coated samples it remained around 7.8 log_{10} CFU/g (Abbasi et al., 2021) (Table 5).

Incorporation of shirazi thyme (*Zataria multiflora*) essential oil (1% w/v) into a chitosan (2% w/v) loaded nanoemulsion coating applied to turkey meat enhanced its antimicrobial properties. After 18 days of storage at 4 °C, the chitosan-loaded nanoemulsion containing 1% Shirazi thyme EO exhibited the greatest reductions in microbial counts (log_{10} CFU/g), including total viable bacteria (2.06), total psychrophilic bacteria (2.59), *Pseudomonas* spp. (2.07), *Enterobacteriaceae* (2.51), lactic acid bacteria (2.51), and yeasts and molds (2.10), compared with the control samples. The initial count of *L. monocytogenes* in artificially contaminated meat was 5.38 log_{10} CFU/g in the control samples, which increased to 7 log_{10} CFU/g after 18 days of storage. In contrast, in the EO-coated samples, the bacterial count remained around 2.2 log_{10} CFU/g (Keykhosravy et al., 2020) (Table 5). Finally, the shelf life of turkey meat was significantly extended to 15–18 days with the application of chitosan-loaded nanoemulsion containing essential oil, compared with 6 days for the control samples.

Addition of fennel (*Foeniculum vulgare*) (1%, v/v) to chitosan nanoparticles (1%, w/v) solution (CNP) using for coating of fish fillet stored 0–4 °C for 18 days decreased number of mesophilic and psychrotrophic bacteria from 7.17 log_{10} CFU/g in samples covered only with CNP (control) to 6.17 log_{10} CFU/g, and slowed down lipid peroxidation, measured by a decrease in malondialdehyde (MDA) content: after 27 days of experimental fish storage the content of MDA was 0.45 mg/kg compared with 0.88 mg/kg in control samples (Maghami et al., 2019).

Table 5

Effect of essential oil added into edible coating of food product on spoilage and pathogenic microorganisms

Essential oil in edible coating, dosage	Food product	Effect of EO inclusive in edible coating	Reference
Shirazi thyme (*Zataria multiflora*) EO, 1% (w/v), in corn starch coating	Chicken meat	Inhibited the growth of psychrotrophic and lactic acid bacteria, *Enterobacteriaceae,* molds and yeasts, and artificially inoculated *Listeria monocytogenes*	Abbasi et al., 2021
Shirazi thyme (*Zataria multiflora*) EO, 1% (w/v), in chitosan containing	Turkey meat	Inhibited the growth of psychrotrophic and lactic acid bacteria, *Enterobacteriaceae*, molds and yeasts, and artificially inoculated *Listeria monocytogenes*	Keykhosravy et al., 2020
Cinnamon EO (*Cinnamomum zeylanicum*), 1% in marinade	Pork filet, chicken filet, salmon	Products were immersed in marinade solution for 2 min and stored at 4 °C for 6 days. Addition of EO inhibited fungal growth on meat and fish	Van Haute et al., 2016
Fennel (*Foeniculum vulgare*), 1% (v/v) in chitosan nanoparticles	Fish *Huso huso*	Inhibited the growth of mesophilic and psychrotrophic bacteria; reduced lipid peroxidation	Maghami et al., 2019
Chavir (*Ferulago angulata),* 3%, into chitosan (1.0% w/v) coating	Fresh rainbow trout fillets	Reduced microbial growth and lipid oxidation	Shokri et al., 2020
Oregano EO (0.15%v/v) or cinnamon leaf EO (0.6% v/v) into chitosan (1.5% w/v) coating	Apple slices	Totally inhibited the growth of aerobic bacteria on apple slices stored for 9 days at 4 °C	Ali et al., 2025
Cinnamon EO (0.5% v/v) into chitosan (2% w/v) coating	Pineapple pieces	Decreased weight loss, higher firmness, lower microbial count, and higher overall evaluation of pineapple pieces stored for 15 days at 5 °C	Basaglia et al., 2021
Muña (*Minthostachys mollis*) EO, (0.2% v/v) into purple corn flour coating (3-4% w/v)	Strawberries	Reduced weight loss, maintained color and appearance, decreased mold and yeast counts by 1.24 $\log_{10}$ CFU/g compared to control strawberries stored for 12 days at 4 °C	Pacco-Huamani et al., 2025
Wild basil (*Ocimum gratissimum*) 1.5% (w/w) in K-P-OG	Mandarin oranges	Effectively delayed fungal spoilage, extending shelf life by at least 8 days	Yu et al., 2025
Cinnamon EO (20%) in zein-based coatings	Cherry tomatoes	Spraying reduced Salmonella Typhimurium counts by 4.6 $\log_{10}$ CFU/g on the smooth skin surface of inoculated tomatoes after 5 h, and reduced them to <1.0 $\log_{10}$ CFU/g on the stem scar after 7 d of storage at 10 °C	Yun et al., 2015
Moringa EO (*Moringa oleifera*)	Cheese slices	Spraying of EO onto cheese inoculated with *L. monocytogenes* significantly slowed bacterial growth	Cui et al., 2020

Oregano EO (0.5% v/v) in Na-alginate (2% w/v) edible film	Feta cheese	Mild inhibition, stronger for *L. monocytogenes* and weaker for *E. coli*; lactic cocci/streptococci remained relatively stable during storage	Doukaki et al., 2026
Thyme EO encapsulated in lecithin liposomes into a 2% (w/v) chitosan coating	Karish cheese (soft white cow's milk cheese)	The shelf life of the product was extended by two weeks compared to cheese coated with chitosan alone	Al-Moghazy et al., 2021

K-P-OG - konjac glucomannan- pectin-*Ocimum gratissimum.*

The incorporation of 3% *Ferulago angulata* (chavir) essential oil significantly enhanced the antimicrobial and antioxidant properties of a 1% chitosan emulsion, and these effects were further improved after ultrasound nanoemulsification. Chitosan (CH) with 3% essential oil (CH-3% EO), and nanoemulsified chitosan with 3% essential oil (CH-3%EO-NE) showed MIC values against *Pseudomonas fluorescens* and *Shewanella putrefaciens* of 20, 10, and 5%, respectively, while DPPH radical scavenging activity increased from 6.15% to 22.0% and 30.2%. The improved performance of the nanoemulsified coating is attributed to a more uniform distribution of the essential oil and greater stability of the chitosan–EO system. When applied to fresh rainbow trout fillets stored at 4 °C for 16 days, the coatings reduced microbial growth and lipid oxidation. At the end of storage, total viable counts (log_{10} CFU/g) were 7.5, 7.0, and 4.3; psychrotrophic counts were 7.0, 5.2, and 4.0; TBARS values (mg MDA/kg) were 0.25, 0.21, and 0.15; and overall acceptability scores were 3.1, 3.8, and 4.3 for CH, CH-3%EO, and CH-3%EO-NE coatings, respectively (Shokri et al., 2020).

According to the FAO & WHO report (2023), fresh and minimally processed fruits and vegetables are a major source of foodborne diseases. *Escherichia coli* O157:H7, *Salmonella*, and *Listeria monocytogenes* are among the most common foodborne pathogens, with documented outbreaks linked to the consumption of fresh vegetables and fruits (Alegbeleye et al., 2018; Dyda et al., 2020; Gaul et al., 2013; Lee et al., 2022). An analysis of 945 fruit and vegetable samples collected from street markets in Alexandria (Egypt) revealed that aerobic mesophilic counts (AMC) ranged from <0.69 to 5.92 log_{10} CFU/g in fruits and from <0.56 to 4.98 log_{10} CFU/g in vegetables, and *E. coli* was detected in 80% of the samples (Khalil and Gomma, 2016). Shiga toxin–producing *E. coli* O157:H7 was identified in 40 samples, including one sample each of blueberries, cantaloupe, and dates; three strawberry samples; ten carrot samples; eight green pepper samples; and five samples each of tomatoes and zucchini. Overall, 7.9% of vegetable samples were positive for *E. coli* O157:H7, with the highest contamination levels observed in carrots (4.96 log_{10} CFU/g) and green peppers (4.57 log_{10} CFU/g). Thus, research into natural antimicrobial compounds to enhance the safety of fresh produce during or after minimal processing is an urgent task, and edible coatings containing essential oils represent one promising approach to addressing this issue. Addition of oregano EO (0.15%) or cinnamon leaf EO (0.6%) into chitosan (1.5% w/v)-based edible coating of Braeburn apple (*Malus domestica*) slices stored for 9 days at 4 °C completely inhibited the growth of aerobic bacteria, while, total viable counts for uncoated apple slices and covered only with chitosan-based film increased, log_{10} CFU/g, to 3.9 and 0.7 on 2 day and 5.3 and 2.0 on 9 day, respectively (Ali et al., 2025).

The pineapple pieces, coated by immersion for 5 min in a chitosan-based edible solution (2% w/v) containing cinnamon essential oil (0.5%), packed in a PET (polyethylene terephthalate) container with a lid and stored at 5 °C, showed on day 15 compared to the uncoated control pieces lower weight loss (14.6% vs. 23.42%), higher firmness (0.30 N vs. 0.15 N), lower microbial counts (molds and yeasts: approximately 3.7 vs. 5.3 log_{10} CFU/g), and a higher overall evaluation score (3.5 vs. 2.8) (Basaglia et al., 2021). A coating based on *Konjac glucomannan* 1% (w/w) and

high-methoxyl pectin 2% (w/w), enriched with 1.5% (w/w) wild basil (*Ocimum gratissimum*) essential oil emulsion and applied to mandarin oranges, effectively delayed fruit fungal spoilage. While uncoated samples began to decay on day 2 (reaching 38% by day 18), the coated fruits showed no fungal growth for 10 days and only 7.1% decay on day 18 (≈30% lower than the control), resulting in a shelf-life extension of at least 8 days (Yu et al., 2025).

Spraying *Moringa* essential oil (MO) (10.0 mg/mL) onto cheese pieces (20×20×10 mm) inoculated with *L. monocytogenes* followed by storage at 4 °C for 14 days, significantly slowed bacterial growth. The population of *L. monocytogenes* on the surface of MO-treated cheeses increased only slightly (1.35–1.51 $\log_{10}$ CFU/g), whereas control samples showed an increase of approximately 4.5 $\log_{10}$ CFU/g (Cui et al., 2020). The incorporation of encapsulated thyme essential oil (TEO, 2% v/v) in lecithin-based liposomes into a 2% (w/v) chitosan coating applied to Karish cheese stored at 4 °C for 4 weeks resulted in a reduction of total mesophilic bacterial counts from 4.5 to 3.3 $\log_{10}$ CFU/g. The mean yeast and mould count decreased by 0.4 $\log_{10}$ CFU/g to 3.6 $\log_{10}$ CFU/g, with no visible microbial growth. Psychrotrophic bacteria were not detected. This treatment extended the shelf life of the product by two weeks compared to cheese coated with plain chitosan (Al-Moghazy et al., 2021).

Several studies have reported synergistic antimicrobial effects when essential oils are used in combination (Huang et al., 2021; Kim et al., 2021; Soulaimani et al., 2021). For example, a combination of peppermint (A) and thyme (B) essential oils demonstrated strong synergistic antimicrobial activity against *E. coli* ATCC 25922. Individually, peppermint and thyme had minimum bactericidal concentrations (MBCs) of 6.25 and 12.5 mg/mL, respectively, but in combination, the MBC of peppermint dropped to 0.20 mg/mL and that of thyme to 3.125 mg/mL, resulting in a fractional bactericidal concentration (FBC) index of 0.28, indicating synergistic activity (<0.5). A similar effect was observed against *Listeria monocytogenes* CDC H2446: both oils had individual MBCs of 25 mg/mL, which decreased to 3.125 mg/mL in combination, giving an FBC index of 0.25 (Angane et al., 2023). These results demonstrate that specific combinations of essential oils can markedly enhance antimicrobial efficacy compared to individual oils, allowing the use of lower concentrations while still achieving effective microbial inhibition.

It should be noted that chitosan, a natural biopolymer, is often proposed for edible product coatings. However, it is mainly produced by the deacetylation of chitin, which is abundant in the exoskeletons of crustaceans and other arthropods, as well as in mollusks, limiting its suitability for vegetarian, halal, and kosher applications. Nevertheless, it can also be obtained from alternative sources such as mushroom stems (Motelica et al., 2020).

Essential oil nanoemulsions as edible coatings for food products

Despite their bioactivity, the poor aqueous stability and high volatility of essential oils significantly constrain their direct application. To overcome these limitations, nanoemulsions have gained increasing attention as effective delivery systems. These systems typically consist of an oil phase, an aqueous phase (mainly water), and an emulsifier, with surfactants such as Tween 80 commonly used to stabilize the dispersion (McClements et al., 2021).

Nanoemulsions are stable colloidal systems in which oil droplets are dispersed within a continuous liquid phase, with droplet sizes generally ranging from 20 to 200 nm, which are substantially smaller than those in conventional emulsions (1–50 μm). This reduced size provides a larger surface area, improving solubility, stability, and controlled release of bioactive compounds. As a result, such formulations enhance biological activity while minimizing undesirable effects on sensory properties, such as taste and aroma. Improved dispersion and interfacial contact also facilitate more efficient interaction with target microorganisms, thereby strengthening antimicrobial and antioxidant efficacy. Furthermore, better distribution within the

food matrix allows for a reduction in the required dosage. Common methods for producing plant oil-based nanoemulsions include ultrasonication, which uses acoustic energy to reduce droplet size, and high-pressure homogenization, which applies intense mechanical shear to form fine dispersions (De Oliveira Filho et al., 2021; Hasan et al., 2020; Kumar et al., 2025) (Figure 2).

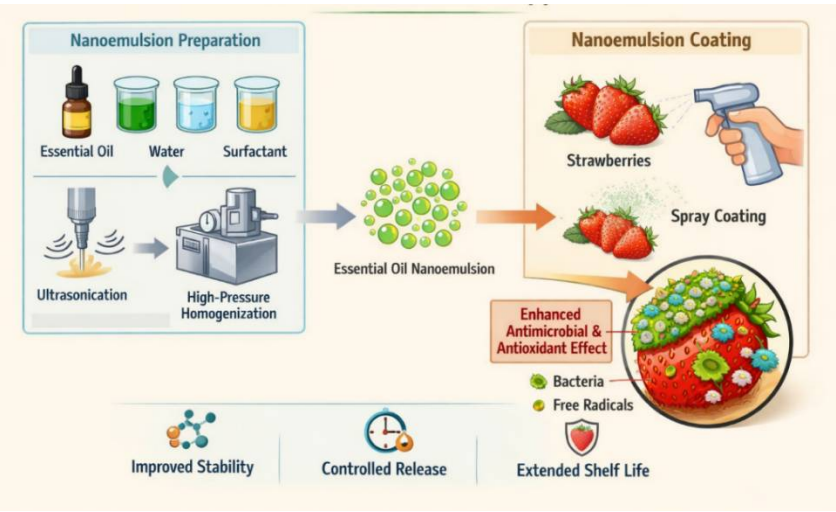

Figure 2. Example of essential oil nanoemulsion application (created by the authors)

Essential oil nanoemulsions, specifically cumin (*Cuminum cyminum*) and black pepper (*Piper nigrum*), prepared by ultrasonic emulsification, have been shown to be effective against foodborne pathogens *E. coli* and *S. enterica* isolated from fresh fruits and vegetables (Amrutha et al., 2017). These essential oil nanoemulsions significantly reduced biofilm formation by the pathogenic strains and exhibited potent anti-quorum sensing activity, as evidenced by inhibition of violacein production in *Chromobacterium violaceum* CV026, along with a reduction in exopolysaccharide synthesis. Furthermore, virulence-associated traits, including auto-aggregation and crystal violet binding, were markedly reduced by both nanoemulsions.

Essential oil nanoemulsions have been proposed as edible coatings to improve quality and prolong the shelf life of various fresh and fresh-like products. Recently, increasing attention has been directed toward their application in fruits and vegetables, aiming to extend shelf life through the antibacterial, antifungal, and antioxidant properties of essential oils (De Oliveira Filho et al., 2021; Hasan et al., 2020; Sharma et al., 2024). It should be mentioned that essential oil nanoemulsions can be used separately to treat the surface of the food product or as a component of edible coating covered food product. Numerous studies have demonstrated the antibacterial effectiveness of essential oil-based nanoemulsions in preserving different fresh fruits and vegetables (Chu et al., 2020; Gundewadi et al., 2018; Paudel et al., 2019; Pirozzi et al., 2020; Rude et al., 2018; Salvia-Trujillo et al., 2015; Sessa et al., 2015), as summarized in Table 6.

Application of pectin-based edible coatings containing 1.0% of orange peel EO nanoemulsion, on orange slices inhibited the growth of mesophilic aerobic bacteria (3.40 and 5.83 $\log_{10}$ CFU/g at 0 and 17 days of storage, respectively) compared with the control (3.29 and 6.73 $\log_{10}$ CFU/g at 0 and 17 days of storage, respectively) and fungi counts (2.78 and 6.93 $\log_{10}$ CFU/g at 0 and 17 days of storage, respectively) compared with the control (2.57 and 7.66 $\log_{10}$ CFU/g at 0 and 17 days of storage, respectively) (Radi et al., 2018) (Table 6).

Table 6

Effect of essential oil in form of nanoemulsion addition into edible coating of food product on spoilage and pathogenic microorganisms

Nanoemulsion with essential oil, dosage	Food product	Effect of EO nanoemulsion application	Reference
Cinnamon EO, 0.5% (v/v)	Dried honeydew melon cuts	After immersion in the nanoemulsion treatment (1 min dip), followed by storage for 72 h, reductions of 3.5 $\log_{10}$ CFU/g for *Salmonella* spp. and 3.0 $\log_{10}$ CFU/g for *L. monocytogenes* were observed on artificially contaminated melon, compared with initial counts of 5.5 and 5.6 $\log_{10}$ CFU/g, respectively.	Paudel et al., 2019
Lemongrass EO, 0.5% (v/v)	Fresh-cut Fuji apples	Nanoemulsion treatment (2 min dip, storage at 23 °C for 2 weeks) completely inhibited the natural microflora of fresh-cut Fuji apples	Salvia-Trujillo et al., 2015
Cinnamon EO nanoemulsion in pullulan (2%)-based coating, 0.16% (v/v)	Straw-berries	Treatment (1 min dip, storage at 20 °C for 6 days) showed, $\log_{10}$ CFU/g: molds and yeasts 1.96 (control without EO 4.78); total aerobic bacteria counts 2.54 (control 3.70)	Chu et al., 2020
Basil EO nanoemulsion in 2% (w/v) sodium alginate, 0.5% (v/v)	Okra fruits	Treatment (3-min dip, storage at 25 °C for 15 days) of okra fruits inoculated with *P. chrysogenum* and *A. flavus* reduced the infected area on day 15 from 22.4% to 12.6% and from 26.4% to 9.0%, respectively	Gundewadi et al., 2018
Orange peel EO nanoemulsion, 1.0%, in pectin 2%-based coating	Orange slices	Treatment (1 min dip, storage at 4 °C for 17 days) reduced the growth of mesophilic aerobic bacteria and fungi	Radi et al., 2018
Oregano EO nanoemulsion, 0.17% (w/w), in alginate 0.5%-based coating,	Tomatoes	Treatment (2 min dip, storage at 24 °C for 14 days) inhibited the growth of bacteria, yeasts, and molds on tomato surfaces, thereby prolonging their shelf life	Pirozzi et al., 2020
Lemon EO nanoemulsion, 0.1% (w/v) in 0.05% (w/v) modified chitosan	Rucola leaves	Treatment (3 min dip) reduced a microbial load, not significantly affect color, improved firmness retention, and prolonged shelf life by 3-7 days	Sessa et al., 2015
Cinnamon EO nanoemulsion, 2% (w/v)	Chicken breast fillets	Nanoemulsion treatment (3 min dip, 4 °C storage) reduced TVC and content of *P. deceptionensis*	Wang et al., 2021
Ajowan EO nanoemulsion, 0.5%, in 3% alginate coating	Turkey fillets	Treatment repeated three times (dipping into the coating solution for 1 min and immersing for 30 s in a 2% calcium chloride solution) suppressed the growth of *L. monocytogenes* ATCC 13311	Kazemeini et al., 2021

Dipping rucola leaves in a nanoemulsion of lemon essential oil combined with modified chitosan demonstrated a synergistic effect, reducing the microbial load by approximately 4 $\log_{10}$ units compared with the untreated sample (≈6 $\log_{10}$ CFU/g). In contrast, application of the essential oil nanoemulsion alone resulted in a reduction of about 2 $\log_{10}$ units, while modified chitosan alone achieved a reduction of approximately 3 $\log_{10}$ units (Sessa et al., 2015). During storage at 4 °C for 3 days, the total microbial count in untreated samples increased by approximately 1 $\log_{10}$ unit, whereas it remained essentially constant in samples treated with the edible coating. Subsequently, during storage at 8 °C for an additional 11 days, the microbial load

of treated samples was consistently about 1 $\log_{10}$ unit lower than that of the control. The treatment did not significantly affect color, while improved firmness retention was observed, allowing an extension of shelf life by approximately 3–7 days compared with untreated samples (Sessa et al., 2015).

EO nanoemulsions could be also applied to treat meat products. It was shown that treatment of chicken breast fillets by dipping in a nanoemulsion containing 2% (w/w) cinnamon EO for 3 min, followed by draining for 1 h, packaging in polyethylene bags, and storage at 4 °C, resulted in a decrease in comparison with untreated samples of total viable bacterial count (TVC) (3.95 $\log_{10}$ CFU/g vs 8.50 $\log_{10}$ CFU/g) on day 15 and in *Pseudomonas deceptionensis* CM2 cells (3.30 $\log_{10}$ CFU/g vs 8.78 $\log_{10}$ CFU/g) on day 10 (Wang et al., 2021)

It was shown that the nanoemulsion of essential oil exhibited higher antimicrobial activity than the emulsion itself. The ajowan (*Trachyspermum ammi*) nanoemulsion had a MIC of 2 mg/mL, whereas the ajowan emulsion had a MIC of 8 mg/mL. The edible coating consisted of 3% alginate, 5% glycerol (v/v) as a plasticizer, 0.2% Tween 80 as an emulsifier, and 0.5% ajowan essential oil in the form of an emulsion or nanoemulsion. Incorporation of the EO nanoemulsion into the coating of turkey fillets artificially inoculated with *L. monocytogenes* ATCC 13311 decreased the bacterial count on day 12 of storage at 4 °C to 5.53 $\log_{10}$ CFU/g, compared with 8.71 $\log_{10}$ CFU/g in control fillets without coating, 7.79 $\log_{10}$ CFU/g in fillets coated with alginate without essential oil, and 7.12 $\log_{10}$ CFU/g in fillets coated with alginate containing ajowan EO emulsion (Kazemeini et al., 2021).

Overall, these findings demonstrate that essential oil nanoemulsions incorporated into edible coatings represent a versatile and effective strategy for enhancing microbial safety, maintaining quality attributes, and extending the shelf life of a wide range of food products, particularly fresh and minimally processed fruits and vegetables.

In this context, it is appropriate to mention an original method for preserving fruits and vegetables against spoilage proposed by Pirog et al. (2019, 2022a, b), which involves the treatment of cucumbers, green and red tomatoes, peppers, and highly perishable sweet cherries with solutions of natural surfactants produced by bacterial cultures. This approach has been shown to significantly extend the shelf life of these products.

Essential oils in active packaging films for food products

Recently, considerable attention has been given to “active packaging” as a food storage approach, in which the packaging actively interacts with the product and its environment to extend shelf life, enhance safety, and maintain quality, in contrast to conventional passive packaging. Unlike edible coatings applied directly to food surfaces, active packaging systems utilize independent materials, such as polymeric or biopolymer films, engineered to interact intentionally with the food or the package headspace.

Within these systems, essential oils have emerged as particularly effective natural agents due to their antimicrobial and antioxidant properties, and they are incorporated into the packaging matrix to enable controlled release and prolonged activity at the food–package interface. Biodegradable packaging films containing essential oils (EOs) therefore represent a promising strategy for active food packaging (Atarés and Chiralt, 2016; Sharma et al., 2020). Their effectiveness depends on the compatibility between the essential oils and the polymer matrix, as well as on achieving controlled release that preserves antimicrobial efficacy while minimizing undesirable sensory effects. To address challenges related to EO volatility, stability, and potential impacts on mechanical properties, microencapsulation techniques are frequently employed to enhance stability and modulate release, thereby contributing to effective and sustainable food preservation solutions.

Plant essential oils are increasingly used as natural alternatives to conventional chemical preservatives to extend the shelf life of food products (Gubsky et al., 2025; Stabnikova et al., 2021). Their antioxidant and antimicrobial properties make them promising additives for food packaging films aimed at preventing microbial spoilage (Sharma et al., 2021). The use of natural antibacterial compounds instead of synthetic chemicals also meets consumer demand for safer and healthier foods. Moreover, essential oils applied in food packaging are classified as GRAS (Generally Recognized as Safe) by the U.S. Food and Drug Administration (Smaoui et al., 2022).

Although numerous studies have investigated the use of essential oils in conventional synthetic films (Otero et al, 2014; Takma and Korel, 2019), biodegradable packaging materials incorporating essential oils represents a more promising and environmentally friendly solution (Tanasă et al., 2024). However, the volatile components of essential oils can rapidly degrade in food systems under the influence of light, temperature, and oxidation (Gil and Rudy, 2023). Therefore, their incorporation into active packaging systems has been proposed as an effective strategy to protect these compounds and ensure their controlled release. In such systems, essential oils may be applied through several approaches: (a) release into the package headspace from a carrier, providing antimicrobial activity in the vapor phase; (b) placement of sachets or pads containing essential oils inside the package for gradual volatilization; and (c) direct incorporation into packaging films, where they are entrapped within the polymer matrix and released during storage. Among these strategies, direct incorporation is most widely used for producing active films that function as wrappers, lids, interlayers, or packaging materials for food products (Figure 3).

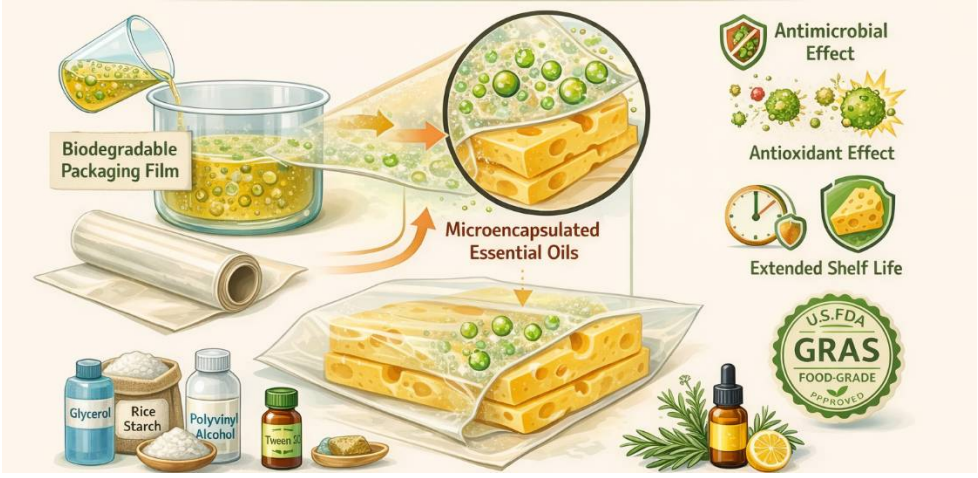

Figure 3. Essential oil in active packing films for food product (cheese) (created by the authors)

These films are often made from natural biopolymers such as chitosan, seaweed, rice starch, alginate, curdlan, or biodegradable synthetic polymer polyvinyl alcohol (Zubair et al., 2022). In addition, the composition of biodegradable films includes plasticizers (more often glycerol), which improve film flexibility and prevent brittleness, and Tween 80, which acts as a non-ionic emulsifier ensuring uniform dispersion and stability of hydrophobic essential oils within the biopolymer matrix. Incorporation of essential oils, 1-10% (w/w) into biodegradable films gives possibility to enhance preservation and prolong time of food product storage. Such films are extremely important for use in packaging meat products and fish. Examples of some films with EOs and the effect of their application on food products are presented in Table 8.

Table 8

Examples and effect of essential oil incorporation in packing film on food products during storage

Food product	Essential oil (EO)	Composition of film	Positive effects obtained	Reference
Sliced sausage	*Eucalyptus globulus* EO	0.7% (v/v) acetic acid; chitosan, 1.5% (w/v); EO, 1.5% (v/v); glycerol, 0.225% (w/v); Tween 80, 0.2% (v/v)	Wrapping in film inhibits the growth of the *Listeria monocytogenes* during the storage for 3 days at 23 °C	Azadbakht et al., 2018
Chilled meat	*Thyme* EO	PVA, 4 %; curdlan, 1 %; EO, 2% (w/w); Tween 80, 1% (w/w); glycerol, 1% (w/w)	Improved antioxidant property of film; the shelf life of chilled meat packed in the film was extended to10 days during storage at 4 °C	Zhang et al., 2020
Sliced ham	Oregano EO	Na-alginate, 2% (w/v); glycerol, 1% (v/v); EO, 1% (v/v); $CaCl_2$, 0.4 % (w/w)	Wrapping in film caused approximately 1.5 log_{10} reduction in *Listeria* living cells at 70 day of storage at 12 °C, and almost 2.5 log_{10} at 4 °C	Pavli et al., 2019
Beef loins	Cinnamon EO nanoemulsion	Chitosan in 1% (v/v), glycerol, 0.25 g/g chitosan; EO, 1% (v/v)	Wrapping beef pieces (2–3 cm thick) in a film slowed down or inhibited the growth of pathogens and allowed to extend the product's shelf life	Dini et al., 2020
Poultry meat	Thyme EO	Silk fibroin nanofibers	Reduced the number of *Salmonella Typhimurium* from 6.64 to 2.24 log_{10} CFU/g after storage for 7 days at 4 °C	Lin et al., 2019
Chicken breast fillets	*Laurus nobilis* or *Rosmarinus officinalis* EO	Cross-linked electrospun film PVA, 14 % (w/v), citric acid, 5% (w/w), EO, 10% (w/w)	Prolonged the shelf-life of chicken breast fillets, reducing the lipid oxidation process and reducing *Listeria* counts during cold storage	Göksen et al., 2021
Fish fillets	Oregano EO	Rice starch, 3% (w/v), glycerol, 0.9% (v/v), EO, 4.5% (w/w)	Decreased oxidation from 1.88 to 1.65 mg malonaldehyde/kg of sample; slowed down microbial growth from 10^8 to 10^7 CFU/g in 6 days of storage at 4 °C	Martins et al., 2021
Cheese slices	*Laurus nobilis* or *Rosmarinus officinalis*	Electrospun zein-based edible film loaded with 10% (w/v) EO in 25% (w/v) zein solution in glacial acetic acid: ethanol (30: 70)	Reductions (2 log_{10} CFU/g) in the populations of *L. monocytogenes* and *S. aureus* compared with the control after 28 days of storage at 4 °C.	Göksen et al., 2020
White bread	Thyme EO	P(3HB-co-4HB) film with 30% EO used to seal white bread	Extended shelf life to ≥5 days (vs. 1–4 days in control) due to mold suppression	Sharma et al., 2022

Thus, the incorporation of *Eucalyptus globulus* essential oil at 1.5% (v/v) into a chitosan-based biodegradable film effectively inhibited the growth of *Listeria monocytogenes* during 3 days of storage at 23 °C of sliced sausage individually wrapped with this film (Azadbakht et al., 2018) (Table 8). Addition of *Thyme* essential oil (TEO) in silk fibroin nanofibers reduced the number of *Salmonella Typhimurium* from 6.64 to 2.24 log_{10} CFU/g after storage of poultry meat

for 7 days at 4ºC (Lin et al., 2019a) and addition TEO, 2% (w/w), in polyvinyl alcohol film used for packing of chilled meat allowed to extend the shelf life of product to10 days during storage at 4 °C (Zhang et al., 2020). Application of *Laurus nobilis* or *Rosmarinus officinalis* essential oils, 10% (w/w), in polyvinyl alcohol film resulted in prolongation cold storage of chicken breast fillets shelf-life, reducing the lipid oxidation process and *Listeria* counts (Göksen et al., 2021). Incorporation of essential oils are extremely important to combat *Listeria* in meat products and fish. The addition of 1% (v/v) oregano essential oil in alginate film caused approximately a 1.5 $\log_{10}$ reduction in *Listeria* viable cells on sliced ham with the film placed onto/around it after 70 days of storage at 12 °C, and nearly a 2.5 $\log_{10}$ reduction after 70 days at 4 °C (Pavli et al., 2019). Addition of *Oregano* essential oil, 4.5% (w/w) in rice starch film protect stored for 6 days fish fillets at 4ºC from oxidation and slowed down microbial growth (Martins et al., 2021).

The incorporation of essential oils as nanoemulsions enhances their stability and antimicrobial effectiveness while ensuring homogeneous distribution within the biopolymer matrix. Addition of a cinnamon EO nanoemulsion to the chitosan film used to wrap beef loins inoculated with pathogenic bacteria reduced their counts after 21 days of chilled storage ($\log_{10}$ CFU/g): *Listeria monocytogenes* decreased to 3.57 compared with 8.95 in the control (chitosan film only); *Escherichia coli* O157:H7 was not detected versus 2.04 in the control; and *Salmonella* Typhimurium was not detected compared with 2.38 in the control (Dini et al., 2020). Based on sensory analysis, the shelf life of beef loins was 12 days for samples coated with chitosan alone and 15 days for those coated with chitosan containing the cinnamon EO nanoemulsion.

Another way to increase the effectiveness of essential oils in active packaging systems is their use in encapsulated form, which is more suitable for long-term storage, ensuring slow and controlled release while minimizing undesirable taste and odor.

Promising materials for the development of active food packaging are electrospun nanofibers produced by applying a high-voltage electric field to polymer solutions or melts, forming ultrafine fibers with diameters in the nanometer range. Commonly used polymers include polyvinyl alcohol (PVA), polylactic acid (PLA), polyethylene oxide (PEO), polycaprolactone (PCL), as well as natural biopolymers such as chitosan, gelatin, starch, cellulose derivatives, and zein (Munteanu and Vasile, 2021). Due to their high surface area and porous structure, electrospun nanofibers can encapsulate bioactive compounds, including essential oils, and provide their controlled release. This allows inhibition of spoilage and pathogenic microorganisms and slows oxidative degradation of food products. As a result, such nanofiber-based coatings and packaging materials can improve food safety and extend the shelf life of fruits, vegetables, meat, and dairy products while remaining environmentally friendly when biodegradable polymers are used.

Electrospun zein-based edible films loaded with essential oils of bay laurel (*Laurus nobilis*) or rosemary (*Rosmarinus officinalis*) exhibited a strong antibacterial effect against *Listeria monocytogenes* and *Staphylococcus aureus* when the active films were placed on the inoculated cheese slices. At the highest essential oil concentration (10% w/v), the active films achieved approximately 2 $\log_{10}$ CFU/g reductions in the populations of *Listeria monocytogenes* and *Staphylococcus aureus* compared with the control after 28 days of storage at 4 °C (Göksen et al., 2020). This significant microbial reduction demonstrates that essential oil-loaded electrospun nanofibrous films are effective in suppressing pathogenic microorganisms and can contribute to enhanced microbial safety and extended shelf life of cheese products (Table 8).

Cross-linked electrospun polyvinyl alcohol (PVOH) films loaded with bay laurel and rosemary essential oils demonstrated significant antimicrobial activity on chicken breast fillets under refrigerated storage, preserving meat quality parameters (pH, color) and inhibiting microbial growth compared with controls. The active films also reduced lipid oxidation by up to 68%, highlighting their potential to improve both microbial stability and oxidative stability in meat products (Göksen et al., 2021).

Electrospun poly(vinyl alcohol) nanofibrous film containing 2% (w/w) β-cyclodextrin-encapsulated cinnamon essential oil effectively prolonged the shelf life of strawberries, with unpacked fruits decaying by day 4 and those in conventional fresh-keeping film spoiling by day 6, while fruits packaged with the nanofibrous film showed no decay even after 6 days at 4 °C (Wen et al., 2016).

Therefore, essential oils can be effectively utilized in active packaging systems through their incorporation into electrospun polymer matrices, which improves their stability and functional performance. Encapsulation of essential oils within fibrous structures reduces their volatility and susceptibility to oxidative degradation, while enabling controlled and sustained release of bioactive compounds. This approach enhances the antimicrobial and antioxidant activity of essential oils even at low concentrations. Consequently, essential oil-based active packaging materials contribute to improved food safety and extended product shelf life. It should be noted that incorporation of essential oils resulted also in enhanced properties of packing films reducing their permeability and solubility of the material (Pires et al. 2011).

Since essential oils possess not only antimicrobial properties but also antioxidant activity, their incorporation into packaging films can protect stored products from oxidative processes (Tomić et al., 2023). Accordingly, the incorporation of 5% (w/w) grapeseed, bergamot, or ginger essential oil into biodegradable poly(3-hydroxybutyrate) (PHB) films significantly enhanced their antioxidant capacity. The DPPH radical scavenging activity of the films reached 53.17%, 50.70%, and 86.38%, respectively, whereas the control film without additives exhibited negligible radical scavenging activity (Kumari et al., 2023). Chitosan films containing 1.5% summer savory (*Satureja hortensis* L.) essential oil exhibited strong antioxidant activity (~66% DPPH scavenging), while control films showed negligible activity (Atlar et al., 2024).

It should be noted that not only essential oils themselves, but also their individual bioactive components with antimicrobial and antioxidant properties can be utilized in the development of active packaging systems. For instance, a low-density polyethylene film incorporating 10% (w/w) carvacrol has been shown to effectively inhibit fungal growth in white bread for up to six months, owing to its strong antioxidant and antifungal activities (Safakas et al., 2025). Similar results for bread preservation have been reported for active packaging systems containing thymol (Suwanamornlert et al., 2020). It was shown that carvacrol induced oxidative stress in *Aspergillus niger* by stimulating excessive reactive oxygen species (ROS) and H_2O_2 production, which caused lipid peroxidation, altered membrane lipid composition, and disrupted cell membrane integrity (Gao et al., 2025).

In addition, sodium alginate films enriched with β-cyclodextrin–microencapsulated carvacrol improved film properties, enabled controlled release of the active compound, and effectively inhibited *Trichoderma* sp., thereby reducing oxidative damage and delaying postharvest senescence of white mushrooms (Cheng et al., 2019). Thus, the incorporation of essential oils or their individual components into packaging materials represents a promising strategy to extend the shelf life of various food products by protecting them against microbial spoilage and oxidative deterioration during storage.

It is well established that interactions between food and packaging materials involve complex migration processes that can lead to the transfer of potentially harmful compounds from packaging into food (Gupta et al., 2025). In active packaging systems, antibacterial and antioxidant agents, including essential oils, are incorporated to enhance functionality. During prolonged contact, these substances may migrate into the food matrix, potentially posing risks to sensitive population groups and exceeding regulatory limits. In addition, uncontrolled release may negatively affect food quality and shelf life. Therefore, biopolymer films and coating-based packaging systems are increasingly designed to enable controlled release of active compounds, ensuring improved food safety and quality during storage (Zhang et al., 2025).

Despite their natural origin and widespread use in food preservation systems, essential oils are not inherently safe and require comprehensive toxicological evaluation. Their complex chemical composition may include constituents with potential genotoxic, neurotoxic, hepatotoxic, and endocrine-disrupting effects. Therefore, safety assessment should be performed on a case-by-case basis, taking into account individual components, particularly in applications such as active food packaging, where consumer exposure may occur through migration (Tamburlin et al., 2021).

Currently, essential oils have gained considerable attention as natural bio-preservatives due to their broad-spectrum antimicrobial and antioxidant properties. More recent approaches emphasise their application in vapour-based delivery systems, where volatile compounds are released through evaporation or controlled-release mechanisms. In active packaging, essential oil volatiles are emitted into the headspace, where they exert antimicrobial activity without direct contact with the food, enabling sustained release, improved microbial safety, reduced sensory impact, and extended shelf life of fresh products (Hoca et al., 2026). For example, vapour-phase application of sage essential oil has been shown to maintain tomato fruit quality at the red ripening stage by inhibiting microbial growth and modulating respiration and ripening processes (Chrysargyris et al., 2021). Essential oils have demonstrated strong antifungal activity, effectively inhibiting *Botrytis cinerea* in cherry tomatoes in vapour-phase applications and thereby extending shelf life of packaged foods; however, their practical use requires balancing antimicrobial efficacy with potential impacts on sensory quality (Petrović et al., 2025). Advanced technologies further allow the gradual and targeted release of bioactive volatiles, ensuring consistent antimicrobial performance and improving overall product acceptability.

Conclusions

Essential oils are natural biopreservatives with significant potential for application in the food industry. Their antimicrobial and antioxidant properties effectively inhibit spoilage microorganisms, retard oxidative processes, and extend the shelf life of a wide range of food products, including fresh fruits and vegetables, bread and other bakery products, as well as meat and dairy products.

Modern approaches, such as incorporation into edible coatings, nanoemulsions, and active packaging materials, as well as vapour-phase application in the package headspace, enable the controlled release of bioactive compounds. This improves their stability, enhances efficacy, and increases compatibility with food matrices while minimizing undesirable sensory effects.

At the same time, the practical application of essential oils requires careful control of concentrations, delivery systems, and formulation strategies to achieve a balance between antimicrobial efficacy and product quality. Furthermore, safety considerations, including potential toxicity and migration from packaging materials, necessitate thorough toxicological evaluation and compliance with regulatory requirements.

Overall, essential oils and their bioactive components represent an effective and environmentally friendly alternative to synthetic preservatives. However, further research is needed to improve their application technologies and ensure safe, stable, and consistent performance in food preservation systems.

Acknowledgments. The work was carried out with the financial support of a grant from the National Research Foundation of Ukraine "Development of packaging materials based on biopolymers with antimicrobial components of natural origin for long-term storage of food products" (Application ID 2025.07/0333).

References

Abbasi Z., Aminzare M., Hassanzad Azar H., Rostamizadeh K. (2021), Effect of corn starch coating incorporated with nanoemulsion of *Zataria multiflora* essential oil fortified with cinnamaldehyde on microbial quality of fresh chicken meat and fate of inoculated *Listeria monocytogenes*, *Journal of Food Science and Technology*, 58(7), pp. 2677-2687, https://doi.org/10.1007/s13197-020-04774-y.

Aburigal Y., Hamza N., Hussein I., Elmogtaba E., Osman T., Ali F., Siribel A. (2016), Variability in content and chemical constituents of essential oil of sweet basil (*Ocimum basilicum* L.) obtained from aerial plant parts, *Advances in Bioscience and Biotechnology*, 7(3), pp. 183-187, https://doi.org/10.4236/abb.2016.73016

Ahmed A.F., Shi M., Liu C., Kang W. (2019), Comparative analysis of antioxidant activities of essential oils and extracts of fennel (*Foeniculum vulgare* Mill.) seeds from Egypt and China, *Food Science and Human Wellness*, 1, pp. 67-72, https://doi.org/10.10.1016/j.fshw.2019.03.004

Ahmed L.I., Ibrahim N., Abdel-Salam A.B., Fahim K.M. (2021), Potential application of ginger, clove and thyme essential oils to improve soft cheese microbial safety and sensory characteristics, *Food Bioscience*, 42, 101177, https://doi.org/10.1016/j.fbio.2021.101177

Akarca G. (2019), Composition and antibacterial effect on food borne pathogens of *Hibiscus surrattensis* L. calyces essential oil, *Industrial Crops and Products*, 137, pp. 285–289, https://doi.org/10.1016/j.indcrop.2019.05.043

Alegbeleye O.O., Singleton I., Sant'Ana A.S. (2018), Sources and contamination routes of microbial pathogens to fresh produce during field cultivation: A review, *Food Microbiology*, 73, pp. 177-208, https://doi.org/10.1016/j.fm.2018.01.003

Alfikri D.N., Pujiarti R., Wibisono M.G., Hardiyanto E.B. (2020), Yield, quality, and antioxidant activity of clove (*Syzygium aromaticum* L.) bud oil at the different phenological stages in young and mature trees, *Scientifica*, 2020, 9701701, https://doi.org/10.1155/2020/9701701

Ali N., Dina E., Tas A.A. (2025), Bioactive edible coatings for fresh-cut apples: A study on chitosan-based coatings infused with essential oils, *Foods*, 14(13), 2362, https://doi.org/10.3390/foods14132362

Al-Moghazy M., El-Sayed H.S., Salama H.H., Nada A.A. (2021), Edible packaging coating of encapsulated thyme essential oil in liposomal chitosan emulsions to improve the shelf life of Karish cheese, *Food Bioscience*, 43, 101230, https://doi.org/10.1016/j.fbio.2021.101230

Al-Nabulsi A., Osaili T., Olaimat A., Almasri W., Al-Holy M., Jaradat Z., Ayyash M., Awaisheh S., Holley R. (2020), Inhibitory effect of thyme and cinnamon essential oils against *E. coli* O157:H7 in Tahini, *Food Science and Technology*, 40, pp. 885–893, https://doi.org/10.1590/fst.21619

Alirezalu K., Pateiro M., Yaghoubi M., Alirezalu A., Peighambardoust S.H., Lorenzo J.M. (2020), Phytochemical constituents, advanced extraction technologies and techno-functional properties of selected Mediterranean plants for use in meat products. A comprehensive review, *Trends in Food Science & Technology,* 100, pp. 292–306, https://doi.org/10.1016/j.tifs.2020.04.010

Amariei S., Gutt G., Hretcanu C.E., Leahu A., Oroian M.A., Poroch-Seriţan M., Roşu A.I. (2016), How properties of edible oils are improved by essential oils, *Scientific Study & Research Chemistry & Chemical Engineering, Biotechnology, Food Industry*, 17(3), pp. 227–238.

Amrutha B., Sundar K., Shetty P.H. (2017), Spice oil nanoemulsions: Potential natural inhibitors against pathogenic *E. coli* and *Salmonella* spp. from fresh fruits and vegetables, *LWT - Food Science and Technology*, 79, pp.152-159, https://doi.org/10.1016/j.lwt.2017.01.031

Angane M., Swift S., Huang K., Perera J., Chen X., Butts C.A., Quek S.Y. (2023), Synergistic antimicrobial interaction of plant essential oils and extracts against foodborne pathogens, *Food Science and Nutrition*,12(2), pp. 1189-1206, https://doi.org/10.1002/fsn3.3834

Ara K.M., Raofie F. (2016), Application of response surface methodology for the optimization of supercritical fluid extraction of essential oil from pomegranate (*Punica granatum* L.) peel, *Journal of Food Science and Technology*, 53(7), pp. 3113-3121, https://doi.org/10.10.1007/s13197-016-2284-y

Arasu M.V., Viayaraghavan P., Ilavenil S., Al-Dhabi N.A., Choi K.C. (2019), Essential oil of four medicinal plants and protective properties in plum fruits against the spoilage bacteria and fungi, *Industrial Crops and Products*, 133, 54–62, https://doi.org/10.1016/j.indcrop.2019.03.018

Ashrafi B., Ramak P., Ezatpour B., Talei G.R. (2019), Biological activity and chemical composition of the essential oil of *Nepeta cataria* L., *Journal of Research in Pharmacy*, 23, pp. 336-343, https://doi.org/10.12991/jrp.2019.141

Atarés L., Chiralt A. (2016), Essential oils as additives in biodegradable films and coatings for active food packaging, *Trends in Food Science & Technology*, 48, pp. 51–62, https://doi.org/10.1016/j.tifs.2015.12.001

Atlar G.C., Kutlu G., Tornuk F. (2024), Design and characterization of chitosan-based films incorporated with summer savory (*Satureja hortensis* L.) essential oil for active packaging, *International Journal of Biological Macromolecules*, 254, 127732, https://doi.org/10.1016/j.ijbiomac.2023.127732

Aumeeruddy-Elalfi Z., Gurib-Fakim A., Mahomoodally F. (2015), Antimicrobial, antibiotic potentiating activity and phytochemical profile of essential oils from exotic and endemic medicinal plants of Mauritius, *Industrial Crops and Products,* 71, pp. 197–204, https://doi.org/10.1016/j.indcrop.2015.03.058

Azadbakht E., Maghsoudlou Y., Khomiri M., Kashiri M. (2018), Development and structural characterization of chitosan films containing *Eucalyptus globulus* essential oil: Potential as an antimicrobial carrier for packaging of sliced sausage, *Food Packaging and Shelf Life*, 17, pp. 65–72, https://doi.org/10.1016/j.fpsl.2018.03.007

Bagheri H., Abdul Manap M.Y., Solati Z. (2014), Antioxidant activity of *Piper nigrum* L. essential oil extracted by supercritical CO_2 extraction and hydro-distillation, *Talanta*, 121, pp. 220-228, https://doi.org/10.1016/j.talanta.2014.01.007

Bajera T., Silha D., Ventura K., Bajerov P. (2017), Composition and antimicrobial activity of the essential oil, distilled aromatic water and herbal infusion from *Epilobium parviflorum* Schreb, *Industrial Crops and Products*, 100, pp. 95–105, https://doi.org/10.1016/j.indcrop.2017.02.016

Bakhshabadi H., Ganje M., Gharekhani M., Mohammadi-Moghaddam T., Aulestia C., Morshedi A. (2025), A review of new methods for extracting oil from plants to enhance the efficiency and physicochemical properties of the extracted oils, *Processes*, 13(4), 1124, https://doi.org/10.3390/pr13041124

Basaglia R.R., Pizato S., Santiago N.G., de Almeida M.M.M., Pinedo R.A., Cortez-Vega W.R. (2021), Effect of edible chitosan and cinnamon essential oil coatings on the shelf life of minimally processed pineapple (*Smooth cayenne*), *Food Bioscience*, 41, 100966, https://doi.org/10.1016/j.fbio.2021.100966

Bashiri S., Ghanbarzadeh B., Ayaseh A., Dehghannya J., Ehsani A. (2020), Preparation and characterization of chitosan-coated nanostructured lipid carriers (CH-NLC) containing cinnamon essential oil for enriching milk and anti-oxidant activity, *LWT - Food Science and Technology*, 119, 108836, https://doi.org/10.1016/j.lwt.2019.108836

Bolouri P., Salami R., Kouhi S., Kordi M., Asgari Lajayer B., Hadian J., Astatkie T. (2022), Applications of essential oils and plant extracts in different industries, *Molecules*, 27(24), 8999, https://doi.org/10.3390/molecules27248999

Bouhdid S., Abrini J., Amensour M., Zhiri A., Espuny M. J., Manresa A. (2010), Functional and ultrastructural changes in *Pseudomonas aeruginosa* and *Staphylococcus aureus* cells induced by *Cinnamomum verum* essential oil, *Journal of Applied Microbiology*, 109, pp. 1139–1149, https://doi.org/10.1111/j.1365-2672.2010.04740.x

Bozzini M.F., Pieracci Y., Ascrizzi R., Najar B., D'Antraccoli M., Ciampi L., Peruzzi L., Turchi B., Pedonese F., Alleva A., Flamini G., Fratini F. (2023), Chemical composition and antimicrobial activity against the *Listeria monocytogenes* of essential oils from seven salvia species, *Foods*, 12(23), 4235, https://doi.org/10.3390/foods12234235

Buonsenso F., Meloni G.R., Spadaro D. (2025), Detection of *Penicillium*-toxins in nuts commercialized in Italy through LC-MS/MS analyses, *Toxins*, 18(1), 12, https://doi.org/10.3390/toxins18010012

Çakaloğlu B., Özyurt V.H., Ötleş S. (2018), Cold press in oil extraction. A review, *Ukrainian Food Journal*, 7(4), pp. 640-654, https://doi.org/10.24263/2304-974X-2018-7-4-9

Carramiñana J.J., Rota C., Burillo J., Herrera A. (2008), Antibacterial efficiency of Spanish *Satureja montana* essential oil against *Listeria monocytogenes* among natural flora in minced pork, *Journal of Food Protection*, 71(3), pp. 502–508, https://doi.org/10.4315/0362-028x-71.3.502

Chaichi M., Mohammadi A., Badii F., Hashemi M. (2021), Triple synergistic essential oils prevent pathogenic and spoilage bacteria growth in the refrigerated chicken breast meat, *Biocatalysis and Agricultural Biotechnology*, 32, 101926, https://doi.org/10.1016/j.bcab.2021.101926

Chandrakala R., Venkatesan K., Senthamizh Selvi B., Senthil N., Karthikeyan G., VellaiKumar S. (2024), Variation in seed yield and essential oil composition of coriander (*Coriandrum sativum* L.), *Journal of Essential Oil Research*, 36(3), pp. 222–233, https://doi.org/10.1080/10412905.2024.2330915

Chen X., Shang S., Yan F., Jiang H., Zhao G., Tian S., Chen R., Chen D., Dang Y. (2023), Antioxidant activities of essential oils and their major components in scavenging free radicals, inhibiting lipid oxidation and reducing cellular oxidative stress, *Molecules*, 28(11), 4559, https://doi.org/10.3390/molecules28114559

Cheng M., Wang J., Zhang R., Kong R., Lu W., Wang X. (2019), Characterization and application of the microencapsulated carvacrol/sodium alginate films as food packaging materials, *International Journal of Biological Macromolecules*, 141, pp. 259-267, https://doi.org/10.1016/j.ijbiomac.2019.08.215

Chrysargyris A., Rousos C., Xylia P., Tzortzakis N. (2021), Vapour application of sage essential oil maintain tomato fruit quality in breaker and red ripening stages, *Plants*, 10, 2645, https://doi.org/10.3390/plants10122645

Chu Y., Gao C., Liu X., Zhang N., Xu T., Feng X., Yang Y., Shen X., Tang X. (2020), Improvement of storage quality of strawberries by pullulan coatings incorporated with cinnamon essential oil nanoemulsion, *LWT - Food Science and Technology*, 122, 109054, https://doi.org/10.1016/j.lwt.2020.109054

Cichoski A.J., Cansian R.L., de Oliveira D., Gaio I., Saggirato A.G. (2011), Lipid and protein oxidation in the internal part of Italian type salami containing basil essential oil (*Ocimum basilicum* L.), *Food Science and Technology (Campinas)*, 31(2), pp. 436-442, https://doi.org/10.1590/S0101-20612011000200024

Cui H., Li H., Li C., Abdel-Samie M.A., Lin L. (2020), Inhibition effect of moringa oil on the cheese preservation and its impact on the viability, virulence and genes expression of *Listeria monocytogenes*, *LWT - Food Science and Technology*, 134, 110163, https://doi.org/10.1016/j.lwt.2020.110163

Damyanova S., Mollova S., Stoyanova A., Gubenia O. (2016), Chemical composition of *Salvia officinalis* I. essential oil from Bulgaria, *Ukrainian Food Journal*, 5(4), pp. 695–700, https://10.24263/2304-974X-2016-5-4-8

Darughe F., Barzegar M., Sahari M. A. (2012), Antioxidant and antifungal activity of coriander (*Coriandrum sativum* L.) essential oil in cake, *International Food Research Journal*, 19(3), pp. 1253–1260.

De Campos A.C., Saldanha Nandi R.D., Scandorieiro S., Gonçalves M.C., Reis G.F., Dibo M., Medeiros L.P., Panagio L.A., Fagan E.P., Takayama Kobayashi R.K., Nakazato G. (2022), Antimicrobial effect of *Origanum vulgare* (L.) essential oil as an alternative for conventional additives in the Minas cheese manufacture, *LWT - Food Science and Technology*, 157, 113063, https://doi.org/10.1016/j.lwt.2021.113063A.C

De Oliveira Filho J.G., Miranda M., Ferreira M.D., Plotto A. (2021), Nanoemulsions as edible coatings: A potential strategy for fresh fruits and vegetables preservation, *Foods*, 10(10), 2438, https://doi.org/10.3390/foods10102438

Dini H., Fallah A.A., Bonyadian M., Abbasvali M., Soleimani M. (2020), Effect of edible composite film based on chitosan and cumin essential oil-loaded nanoemulsion combined with low-dose gamma irradiation on microbiological safety and quality of beef loins during refrigerated storage, *International Journal of Biological Macromolecules,* 164, pp. 1501–1509, https://doi.org/10.1016/j.ijbiomac.2020.07.215

Diowksz A., Kopeć P., Koziróg A. (2024), The inactivation of microscopic fungi in bakery products using hurdle technology - A case study, *Applied Sciences*, 14(22), 10648, https://doi.org/10.3390/app142210648

Do V.T.C., Nguyen T.Q., Pham Y.T.T., Do K.T. (2024), Study on the production and composition of essential oil from *Cinnamomum cassia* bark in Yen Bai Province of Vietnam, *Tropical Journal of Natural Product Research*, 8(4), pp. 6807-6813, https://doi.org/10.26538/tjnpr/v8i4.9

Dong Y., Wei Z., Yang R., Zhang Y., Sun M., Bai H., Mo M., Yao C., Li H., Shi L. (2023), Chemical compositions of essential oil extracted from eight thyme species and potential biological functions, *Plants*, 12(24), 4164, https://doi.org/10.3390/plants12244164

Doukaki A., Frantzi A., Xenou S., Schoina F., Katsimperi G., Nychas G.J., Chorianopoulos N. (2026), Antimicrobial effect of oregano essential oil in Na-alginate edible films for shelf-life extension and safety of feta cheese, *Pathogens*, 15(1), 65, https://doi.org/10.3390/pathogens15010065

Dyda A., Nguyen P.Y., Chughtai A.A., MacIntyre C.R. (2020), Changing epidemiology of Salmonella outbreaks associated with cucumbers and other fruits and vegetables, *Global Biosecurity*, 2(1), https://doi.org/10.31646/gbio.49

Damyanova S., Mollova S., Stoyanova A., Gubenia O. (2016), Chemical composition of *Salvia officinalis* L. essential oil from Bulgaria, *Ukrainian Food Journal*, 5(4), pp. 695–700, https://10.24263/2304-974X-2016-5-4-8

El Atki Y., Aouam I., El Kamari F., Taroq A., Nayme K., Timinouni M., Lyoussi B., Abdellaoui A. (2019), Antibacterial activity of cinnamon essential oils and their synergistic potential with antibiotics, *Journal of Advanced Pharmaceutical Technology & Research*, 10(2), pp. 63-67, https://doi.org/10.4103/japtr.JAPTR_366_18

El-Soud N.H., Deabes M., El-Kassem L.A., Khalil M. (2015), Chemical composition and antifungal activity of *Ocimum basilicum* L. essential oil, *Open Access Macedonian Journal of Medical Sciences*, 3(3), pp. 374-379, https://doi.org/10.3889/oamjms.2015.082

Falleh H. (2025), Demystifying the power of essential oils: A review of their antibacterial properties and potential as natural food preservatives, *EXCLI Journal: Experimental and Clinical Sciences*, 24, pp. 828-850, https://doi.org/10.17179/excli2025-8439

Gao Q., Feng Z., Wang Z., Zhao F., Ju J. (2025), Carvacrol induces apoptosis in *Aspergillus niger* through ROS burst, *World Journal of Microbiology and Biotechnology*, 41(7), 225, https://doi.org/10.1007/s11274-025-04437-0

Garnier L., Valence F., Mounier J. (2017), Diversity and control of spoilage fungi in dairy products: An update, *Microorganisms*, 5(3), 42, https://doi.org/10.3390/microorganisms5030042

Gaul L.K., Farag N.H., Shim T., Kingsley M.A., Silk B.J., Hyytia-Trees E. (2013), Hospital-acquired listeriosis outbreak caused by contaminated diced celery - Texas, 2010, *Clinical Infectious Diseases*, 56(1), pp. 20-26, https://doi.org/10.1093/cid/cis817

Gedikoğlu A., Sökmen M., Çivit A. (2019), Evaluation of *Thymus vulgaris* and *Thymbra spicata* essential oils and plant extracts for chemical composition, antioxidant, and antimicrobial properties, *Food Science and Nutrition*, 7(5), pp. 1704-1714, https://doi.org/10.1002/fsn3.1007

Gende L.B., Floris I., Fritz R., Eguaras M.J. (2008), Antimicrobial activity of cinnamon (*Cinnamomum zeylanicum*) essential oil and its main components against *Paenibacillus larvae* from Argentine, *Bulletin of Insectology*, 6(1), pp. 1-4.

Giarratana F., Muscolino D., Ragonese C., Beninati C., Sciarrone D., Ziino G., Mondello L., Giuffrida A., Panebianco A. (2016), Antimicrobial activity of combined essential oils of thyme and rosemary against *Listeria monocytogenes* in Italian mortadella packaged in a modified atmosphere, *Journal of Essential Oil Research*, 28, pp. 467–474, https://doi.org/10.1080/10412905.2016.1165744

Gil M., Rudy M. (2023), Innovations in the packaging of meat and meat products—A review, *Coatings,* 13(2), 333, https://doi.org/10.3390/coatings13020333

Göksen G., Fabra M.J., Pérez-Cataluña A., Ekiz H.I., Sanchez G., López-Rubio A. (2021), Biodegradable active food packaging structures based on hybrid cross-linked electrospun polyvinyl alcohol fibers containing essential oils and their application in the preservation of chicken breast fillets, *Food Packaging and Shelf Life,* 27, 100613, https://doi.org/10.1016/j.fpsl.2020.100613

Gottardo F.M., Biduski B., dos Santos L.F., dos Santos J.S., Rodrigues L.B., dos Santos L.R. (2022), Microencapsulated oregano and cinnamon essential oils as a natural alternative to reduce *Listeria monocytogenes* in Italian salami, *Food Bioscience*, 50(Part B), 102146, https://doi.org/10.1016/j.fbio.2022.102146

GRAS List FDA — 21 CFR 182.20. Available online at 04.09.2025. https://www.ecfr.gov/current/title-21/chapter-I/subchapter-B/part-182/subpart-A/section-182.20

Gubsky S., Stabnikova O., Stabnikov V., Paredes-López O. (Eds.), *Wild Edible Plants: Improving Foods Nutritional Value and Human Health through Biotechnology*, CRC Press, Boca Raton, London, New York, https://doi.org/10.1201/9781003486794

Gundewadi G., Rudra S.G., Sarkar D.J., Singh D. (2018), Nanoemulsion based alginate organic coating for shelf life extension of okra, *Food Packaging and Shelf Life*, 18, pp. 1–12, https://doi.org/10.1016/j.fpsl.2018.08.002

Guo J., Jiang X., Tian Y., Yan S., Liu J., Xie J., Zhang F., Yao C., Hao E. (2024), Therapeutic potential of cinnamon oil: Chemical composition, pharmacological actions, and applications, *Pharmaceuticals,* 17(12), 1700, https://doi.org/10.3390/ph17121700

Gupta R.K., Pipliya S., Karunanithi S., Eswaran U.G.M., Kumar S., Mandliya S., Srivastav P.P., Suthar T., Shaikh A.M., Harsányi E., Kovács B. (2024), Migration of chemical compounds from packaging

materials into packaged foods: Interaction, mechanism, assessment, and regulations, *Foods*, 13(19), 3125, https://doi.org/10.3390/foods13193125

György É., Laslo É. (2024), Microbiological quality assessment of some commercially available breads, *Foods*, 13(20), 3271, https://doi.org/10.3390/foods13203271

FAO & WHO. (2022), *Listeria monocytogenes* in ready-to-eat (RTE) foods: Attribution, characterization and monitoring, *Microbiological Risk Assessment Series 38*, FAO, Rome, Italy, https://iris.who.int/server/api/core/bitstreams/d635734b-264a-40b0-9304-69085a20ddeb/content

FAO & WHO. (2023), Prevention and control of microbiological hazards in fresh fruits and vegetables – Part 4: Specific commodities, *Meeting Report, Microbiological Risk Assessment Series No. 44*, Rome, https://doi.org/10.4060/cc7460en

Funk J.L., Frye J.B., Oyarzo J.N., Chen J., Zhang H., Timmermann B.N. (2016), Anti-inflammatory effects of the essential oils of ginger (*Zingiber officinale* Roscoe) in experimental

Han F., Ma G.Q., Yang M., Yan L., Xiong W., Shu J.C., Zhao Z.D., Xu H.L. (2017), Chemical composition and antioxidant activities of essential oils from different parts of the oregano, *Journal of Zhejiang University Science B*, 18(1), pp. 79-84, https://doi.org/10.1631/jzus.B1600377

Hasan S.M.K., Ferrentino G., Scampicchio M. (2020), Nanoemulsion as advanced edible coatings to preserve the quality of fresh-cut fruits and vegetables: A review, *International Journal of Food Science & Technology*, 55(1), pp. 1–10, https://doi.org/10.1111/ijfs.14273

Hoca G., Božík M., Bergo A.M., Bozikova K., Klouček P. (2026), Vapor-phase essential oils for postharvest vegetables: From laboratory to real-world use, *LWT - Food Science and Technology*, 239, 118900, https://doi.org/10.1016/j.lwt.2025.118900

Huang J., Xu X., Liu C., Liu L. (2025), Exploring the potential of lemon peel extracts in cosmetics: Chemical composition and bioactive properties, *Journal of Microbiology and Biotechnology*, 35, e2412042, https://doi.org/10.4014/jmb.2412.12042

Hudz N., Kobylinska L., Pokajewicz K., Horčinová Sedláčková V., Fedin R., Voloshyn M., Myskiv I., Brindza J., Wieczorek P.P., Lipok J. (2023), *Mentha piperita*: Essential oil and extracts, their biological activities, and perspectives on the development of new medicinal and cosmetic products, *Molecules*, 28(21), 7444, https://doi.org/10.3390/molecules28217444

Huang X., Lao Y., Pan Y., Chen Y., Zhao H., Gong L., Xie N., Mo C.H. (2021), Synergistic antimicrobial effectiveness of plant essential oil and its application in seafood preservation: A review, *Molecules*, 26(2), 307, https://doi.org/10.3390/molecules26020307

Hussein A., Mahmoud K.F., Kamil M.M., Hegazy N.A. (2022), Effect the addition of micro-and nano-capsule cumin and clove oils as antioxidants and anti-cancer on rancidity and shelf life in some biscuit products, *Egyptian Journal of Chemistry*, 65(1), pp. 593–606, https://doi.org/10.21608/EJCHEM.2021.83661.4105

Ibáñez M.D., Blázquez M.A. (2021), *Curcuma longa* L. rhizome essential oil from extraction to its agri-food applications. A review, *Plants*, 10(1), 44, https://doi.org/10.3390/plants10010044

Inobeme A., Adetunji C.O. (2024), Application of essential oils in the food industry, In: C.O. Adetunji, J.B.T. Sharifi-Rad, (Eds.), *Application of Essential Oils in the Food Industry*, pp. 1–8, Academic Press, Cambridge, MA, USA.

Ivanov V., Shevchenko O., Marynin A., Stabnikov V., Gubenia O., Stabnikova O., Shevchenko A., Gavva O., Saliuk A. (2021), Trends and expected benefits of the breaking edge food technologies in 2021–2030, *Ukrainian Food Journal*, 10(1), pp. 7-36, https://doi.org/10.24263/2304-974X-2021-10-1-3

Ji J., Shankar S., Royon F., Salmieri S., Lacroix M. (2023), Essential oils as natural antimicrobials applied in meat and meat products - A review, *Critical Reviews in Food Science and Nutrition*, 63(8), pp. 993-1009, https://doi.org/10.1080/10408398.2021

Jirovetz L., Buchbauer G., Stoyanova A.S., Georgiev E.V., Damianova S.T. (2005), Composition, quality control and antimicrobial activity of the essential oil of cumin (*Cuminum cyminum* L.) seeds from Bulgaria that had been stored for up to 36 years, *International Journal of Food Science and Technology*, 40(3), pp. 305–310, https://doi.org/10.1111/j.1365-2621.2004.00915.x

Ju J., Xie Y., Yu H., Guo Y., Cheng Y., Zhang R., Yao W. (2020), Synergistic inhibition effect of citral and eugenol against *Aspergillus niger* and their application in bread preservation, *Food Chemistry*, 310, 125974, https://doi.org/10.1016/j.foodchem.2019.125974

Kajjari S., Joshi R.S., Hugar S.M., Gokhale N., Meharwade P., Uppin C. (2022), The effects of lavender essential oil and its clinical implications in dentistry: A review, *International Journal of Clinical Pediatric Dentistry*, 15(3), pp. 385-388, https://doi.org/10.5005/jp-journals-10005-2378

Kačániová M., Čmiková N., Vukovic N.L., Verešová A., Bianchi A., Garzoli S., Ben Saad R., Ben Hsouna A., Ban Z., Vukic M.D. (2024), *Citrus limon* essential oil: Chemical composition and selected biological properties focusing on the antimicrobial (*in vitro, in situ*), antibiofilm, insecticidal activity and preservative effect against *Salmonella enterica* inoculated in carrot, *Plants*, 13(4), 524, https://doi.org/10.3390/plants13040524

Karam L., Yammine J. (2023), Chitosan nanoparticles with essential oils in food preservation, In: I.N. Savwaidis (Ed.), *Chitosan: Novel Applications in Food Systems*, Elsevier, pp. 115-153, https://doi.org/10.1016/B978-0-12-821663-7.00006-5

Karnwal A., Kumar G., Singh R., Selvaraj M., Malik T., Al Tawaha A.R.M. (2025), Natural biopolymers in edible coatings: Applications in food preservation, *Food Chemistry X*, 25, 102171, https://doi.org/10.1016/j.fochx.2025.102171

Kazemeini H., Azizian A., Adib H. (2021), Inhibition of *Listeria monocytogenes* growth in turkey fillets by alginate edible coating with *Trachyspermum ammi* essential oil nano-emulsion, *International Journal of Food Microbiology*, 344, 109104, https://doi.org/10.1016/j.ijfoodmicro.2021.109104

Keykhosravy K., Khanzadi S., Hashemi M., Azizzadeh M. (2020), Chitosan-loaded nanoemulsion containing *Zataria multiflora* Boiss and *Bunium persicum* Boiss essential oils as edible coatings: Its impact on microbial quality of turkey meat and fate of inoculated pathogens, *International Journal of Biological Macromolecules*, 150, pp. 904–913, https://doi.org/10.1016/j.ijbiomac.2020.02.09

Khalil R.K.S., Gomma M.A.E. (2016), Prevalence and characterization of Shiga toxin310 producing *Escherichia coli* (STEC) in fruits and vegetables sold at local street markets in Alexandria, Egypt, *LWT - Food Science and Technology*, 74, pp. 199-210, https://doi.org/10.1016/j.lwt.2016.07.041

Khammassi M., Loupassaki S., Tazarki H., Mezni F., Slama A., Tlili N., Zaouali Y., Mighri H., Jamoussi B., Khaldi A. (2018), Variation in essential oil composition and biological activities of *Foeniculum vulgare* Mill. populations growing widely in Tunisia, *Journal of Food Biochemistry*, 42, e12532, https://doi.org/10.1111/jfbc.12532

Kim J., Kim H., Beuchat L.R., Ryu J.H. (2021), Synergistic antimicrobial activities of plant essential oils against *Listeria monocytogenes* in organic tomato juice, *Food Control*, 125, https://doi.org/108000,10.1016/j.foodcont.2021.108000

Kostova I., Dimitrov D., Ivanova M., Vlaseva R., Damyanova S., Ivanova N., Stoyanova A., Gubenia O. (2014), The possibilities of using of essential oils in dairy products. 2. Dill (*Anethum graveolens*), *Ukrainian Food Journal*, 3(4), pp. 516–523.

Kostova I., Lasheva V., Georgieva D., Damyanova S., Stoyanova A., Stefanov S., Gubenia O. (2020), Antimicrobial active packaging paper based on dill weed essential oil, *Cellulose Chemistry and Technology*, 54(3-4), pp. 347-354, https://doi.org/10.35812/cellulosechemtechnol.2020.54.35

Kumar A., Kanwar R., Mehta S.K. (2025), Nanoemulsion as an effective delivery vehicle for essential oils: Properties, formulation methods, destabilizing mechanisms and applications in agri-food sector, *Next Nanotechnology*, 7, 100096, https://doi.org/10.1016/j.nxnano.2024.100096

Kumari S.V.G., Pakshirajan K., Pugazhenthi G. (2023), Facile fabrication and characterization of novel antimicrobial and antioxidant poly (3-hydroxybutyrate)/essential oil composites for potential use in active food packaging applications, *International Journal of Biological Macromolecules*, 252, 126566, https://doi.org/10.1016/j.ijbiomac.2023.126566

Lambrechts K., Rip D. (2024), *Listeria monocytogenes* in the seafood industry: Exploring contamination sources, outbreaks, antibiotic susceptibility and genetic diversity, *MicrobiologyOpen,* 13(5), e70003, https://doi.org/10.1002/mbo3.70003

Lee S., Han A., Yoon J.H., Lee S.Y. (2022), Growth evaluation of *Escherichia coli* O157:H7, *Salmonella typhimurium*, and *Listeria monocytogenes* in fresh fruit and vegetable juices via predictive modeling, *LWT - Food Science and Technology*, 162, 13485, https://doi.org/10.1016/j.lwt.2022.113485

Li Y.X., Zhang C., Pan S., Chen L., Liu M., Yang K., Zeng X., Tian J. (2020), Analysis of chemical components and biological activities of essential oils from black and white pepper (*Piper nigrum* L.) in five provinces of southern China, *LWT - Food Science and Technology*, 117, 108644, https://doi.org/10.1016/j.lwt.2019.108644

Lin L., Liao X., Cui H. (2019), Cold plasma treated thyme essential oil/silk fibroin nanofibers against *Salmonella* Typhimurium in poultry meat, *Food Packaging and Shelf Life,* 21, 100337, https://doi.org/10.1016/j.fpsl.2019.100337

Liñán-Atero R., Aghababaei F., García S.R., Hasiri Z., Ziogkas D., Moreno A., Hadidi M. (2024), Clove essential oil: Chemical profile, biological activities, encapsulation strategies, and food applications, *Antioxidants*, 13(4), 488, https://doi.org/10.3390/antiox13040488

Machado C.A., Oliveira F.O., de Andrade M.A., Hodel K.V.S., Lepikson H., Machado B.A.S. (2022), Steam distillation for essential oil extraction: An evaluation of technological advances based on an analysis of patent documents, *Sustainability*, 14(12), 7119, https://doi.org/10.3390/su14127119

Maghami M., Motalebi A.A., Anvar S.A.A. (2019), Influence of chitosan nanoparticles and fennel essential oils (*Foeniculum vulgare*) on the shelf life of *Huso huso* fish fillets during the storage, *Food Science & Nutrition*, 7(9), pp. 3030-3041, https://doi.org/10.1002/fsn3.1161

Mahgoub S.A., Ramadan M.F., El-Zahar K.M. (2013), Cold pressed *Nigella sativa* oil inhibits the growth of foodborne pathogens and improves the quality of Domiati cheese, *Journal of Food Safety*, 33(4), pp. 470-480, https://doi.org/10.1111/jfs.12078

Mahmoud E.A. (2017), Essential oils of citrus fruit peels antioxidant, antibacterial and additive value as food preservative, *Journal of Food and Dairy Sciences*, 8(2), pp. 111-116, https://doi.org/10.21608/jfds.2017.37135

Majewska E., Kozłowska M., Gruczyńska-Sękowska E., Kowalska D., Tarnowska K. (2019), Lemongrass (*Cymbopogon citratus*) essential oil: Extraction, composition, bioactivity and uses for food preservation – A review, *Polish Journal of Food and Nutrition Sciences*, 69(4), pp. 327-341, https://doi.org/10.31883/pjfns/113152

Martin M.E., Grao-Cruces E., Millan-Linares M.C., Montserrat-de la Paz S. (2020), Grape (*Vitis vinifera* L.) seed oil: A functional food from the winemaking industry, *Foods*, 9(10), 1360, https://doi.org/10.3390/foods9101360

Martins P.C., Bagatini D.C., Martins V.G. (2021), Oregano essential oil addition in rice starch films and its effects on the chilled fish storage, *Journal of Food Science and Technology*, 58(4), pp. 1562-1573, https://doi.org/10.1007/s13197-020-04668-z

Masyita A., Sari R.M., Astuti A.D., Yasir B., Rumata N.R., Emran T.B., Nainu F., Simal-Gandara J. (2022), Terpenes and terpenoids as main bioactive compounds of essential oils, their roles in human health and potential application as natural food preservatives, *Food Chemistry X,* 13, 100217, https://doi.org/10.1016/j.fochx.2022.100217

Matle I., Mbatha K.R., Madoroba E. (2020), A review of *Listeria monocytogenes* from meat and meat products: Epidemiology, virulence factors, antimicrobial resistance and diagnosis, *Onderstepoort Journal of Veterinary Research,* 87(1), pp. e1-e20, https://doi.org/10.4102/ojvr.v87i1.1869

McClements D.J., Das A.K., Dhar P., Nanda P.K., Chatterjee N. (2021), Nanoemulsion-based technologies for delivering natural plant-based antimicrobials in foods, *Frontiers in Sustainable Food Systems*, 5, 643208, https://doi.org/10.3389/fsufs.2021.643208

Miliordos D.E., Baliota G.V., Athanassiou C.G., Natskoulis P.I. (2025), Review on the occurrence of mycotoxigenic fungi in dried fruits and the role of stored-product insects, *Toxins*, 17(7), 313, https://doi.org/10.3390/toxins17070313

Mishra N., Gupta E., Singh P. (2022), Antibacterial and anti-biofilm activity of cinnamon and clove oils against uropathogens, *Ukrainian Journal of Food Science*, 10(1), pp. 74-83, https://doi.org/10.24263/2310-1008-2022-10-1-9

Moirangthem S., Patra G., Biswas S., Das A., Nath S., Verma A.K., Pal S., Chatterjee N., Bandyopadhyay S., Nanda P.K., Sharma G., Das A.K. (2024), Effect of nutmeg (*Myristica fragrans*) and tea tree (*Melaleuca alternifolia*) essential oils on the oxidative and microbial stability of chicken fillets during refrigerated storage, *Foods*, 13(24), 4139, https://doi.org/10.3390/foods13244139

Motelica L., Ficai D., Ficai A., Oprea O.C., Kaya D.A., Andronescu E. (2020), Biodegradable antimicrobial food packaging: Trends and perspectives, *Foods*, 9(10), 1438, https://doi.org/10.3390/foods9101438

Muhetaer H., Li H., Wang B., Cai X., Zhang Y., Li Y., Li C., Wu B. (2025), Exploring the effects and mechanisms of valerian volatile oil in treating insomnia using network pharmacology, molecular docking, and molecular dynamics simulation-based approaches, *International Journal of Molecular Sciences*, 26(4), 1726, https://doi.org/10.3390/ijms26041726

Munteanu B.S., Vasile C. (2021), Encapsulation of natural bioactive compounds by electrospinning - Applications in food storage and safety, *Polymers*, 13(21), 3771, https://doi.org/10.3390/polym13213771

Nascimento J.C., Gonçalves V.S.D.S., Souza B.R.S., Nascimento L.C., Carvalho B.M.R., Nogueira P.C.L., Santos J.P.S., Borges L.P., Goes T.C., Souza J.B., Coutinho H.D.M., Guimarães A.G. (2025), Effectiveness of aromatherapy with sweet orange oil (*Citrus sinensis* L.) in relieving pain and anxiety during labor, *Explore*, 21(1), 103081, https://doi.org/10.1016/j.explore.2024.103081

Nazzaro F., Fratianni F., De Martino L., Coppola R., De Feo V. (2013), Effect of essential oils on pathogenic bacteria, *Pharmaceuticals*, 6(12), pp. 1451-1474, https://doi.org/10.3390/ph6121451

Nikovska K., Stefanova G., Stefanov L., Damyanova S., Stoyanova A., Gubenia O. (2017), Influence of adding of laurel essential oil extracts on salad dressings properties, Ukrainian Food Journal, 6(3), pp. 433–442, https://doi.org/10.24263/2304-974X-2017-6-3-4

Noshad M., Behbahani B.A., Nikfarjam Z., Zargari F. (2023), Antimicrobial activity between *Coriandrum sativum* seed and *Cuminum cyminum* essential oils against foodborne pathogens: A multi-ligand molecular docking simulation, *LWT - Food Science and Technology*, 185, 115217, https://doi.org/10.1016/j.lwt.2023.115217

Noshad M., Behbahani B.A., Nikfarjam Z., Zargari F. (2023), Antimicrobial activity between *Coriandrum sativum* seed and *Cuminum cyminum* essential oils against foodborne pathogens: A multi-ligand molecular docking simulation, *LWT - Food Science and Technology*, 185, 115217, https://doi.org/10.1016/j.lwt.2023.115217

Noshirvani N. (2024), Essential oils as natural food preservatives: Special emphasis on antimicrobial and antioxidant activities, *Journal of Food Quality*, 2024, 5807281, https://doi.org/10.1155/jfq/5807281

Noumi E., Snoussi M., Alreshidi M.M., Rekha P.D., Saptami K., Caputo L., De Martino L., Souza L.F., Msaada K., Mancini E., Flamini G., Al-sieni, A., De Feo V. (2018), Chemical and biological evaluation of essential oils from cardamom species, *Molecules*, 23(11), 2818, https://doi.org/10.3390/molecules23112818

Okhli S., Mirzaei H., Hosseini S.E. (2020), Antioxidant activity of citron peel (*Citrus medica* L.) essential oil and extract on stabilization of sunflower oil, *OCL - Oilseeds and Fats, Crops and Lipids*, 27, 32, https://doi.org/10.1051/ocl/2020022

Orchard A., Sandasi M., Kamatou G., Viljoen A., van Vuuren S. (2017), The in vitro antimicrobial activity and chemometric modelling of 59 commercial essential oils against pathogens of dermatological relevance, *Chemistry & Biodiversity*, 14(1), e1600218, https://doi.org/10.1002/cbdv.201600218

Otero V., Becerril R., Santos J.A., Rodríguez-Calleja J.M., Nerín C., García-López M.L. (2014), Evaluation of two antimicrobial packaging films against *Escherichia coli* O157:H7 strains in vitro and during storage of a Spanish ripened sheep cheese (Zamorano), *Food Control*, 42, pp. 296-302, https://doi.org/10.1016/j.foodcont.2014.02.022

Pacco-Huamani M.C., Pacheco-Torreblanca N.X., Carlos-Tapia K.V., Pizato S., Cortez-Vega W.R., Choque-Delgado G.T. (2025), Influence of corn flour-based coating functionalized with muña essential oil for prolong storability of strawberries at refrigeration, *Plant Foods for Human Nutrition*, 80, 104, https://doi.org/10.1007/s11130-025-01350-7

Pandur E., Micalizzi G., Mondello L., Horváth A., Sipos K., Horváth G. (2022), Antioxidant and anti-inflammatory effects of thyme (*Thymus vulgaris* L.) essential oils prepared at different plant phenophases on *Pseudomonas aeruginosa* LPS-activated THP-1 macrophages, *Antioxidants*, 11, 1330, https://doi.org/10.3390/antiox11071330

Pavli F., Argyri A.A., Skandamis P., Nychas G.J., Tassou C., Chorianopoulos N. (2019), Antimicrobial activity of oregano essential oil incorporated in sodium alginate edible films: Control of *Listeria monocytogenes* and spoilage in ham slices treated with high pressure processing, *Materials,* 12(22), 3726, https://doi.org/10.3390/ma12223726

Paudel S.K., Bhargava K., Kotturi H. (2019), Antimicrobial activity of cinnamon oil nanoemulsion against *Listeria monocytogenes* and *Salmonella* spp. on melons, *LWT-Food Science and Technology*, 111, pp. 682-687, https://doi.org/10.1016/j.lwt.2019.05.087

Petrović E., T. Siber, Ćosić J., Vrandečić K. (2025), Natural preservation techniques: using essential oils to extend the shelf life of cherry tomatoes, *Journal of Central European Agriculture*, 26(3), pp. 680-693, https://doi.org/10.5513/JCEA01/26.3.4599

Pezantes-Orellana C., German Bermúdez F., Matías De la Cruz C., Montalvo J.L., Orellana-Manzano A. (2024), Essential oils: A systematic review on revolutionizing health, nutrition, and omics for optimal well-being, *Frontiers in Medicine*, 11, 1337785, https://doi.org/10.3389/fmed.2024.1337785

Pires C., Ramos C., Teixeira G., Batista I., Mendes R., Nunes L., Marques A. (2011), Characterization of biodegradable films prepared with hake proteins and thyme oil, *Journal of Food Engineering*, 105, pp. 422–428, https://doi.org/10.1016/j.jfoodeng.2011.02.036

Pirog T., Beregova K., Geichenko B., Stabnikov V. (2019), Application of surface-active substances produced by *Nocardia vaccinii* IMB B-7405 for the treatment of vegetables, *Ukrainian Food Journal*, 8(1), pp. 99-109, https://doi.org/10.24263/2304-974X-2019-8-1-

Pirog T., Stabnikov V., Antoniuk S. (2022a), Application of surface-active substances produced by *Rhodococcus erythropoli*s IMB Ac-5017 for post-harvest treatment of sweet cherry, *Ukrainian Food Journal*, 11(1), pp. 164–174, https://doi.org/10.24263/2304-974X-2022-11-1-15

Pirog T., Stabnikov V., Stabnikova O. (2022b), Bacterial microbial surface-active substances in food-processing industry, In: O. Paredes-Lopez, V. Stabnikov, O. Shevchenko, V. Ivanov (Eds.), *Bioenhancement and Fortification of Foods for a Healthy Diet*, pp. 271– 294, CRC Press, Boca Raton, London, https://doi.org/10.1201/9781003225287

Pirozzi A., Del Grosso V., Ferrari G., Donsì F. (2020), Edible coatings containing oregano essential oil nanoemulsion for improving postharvest quality and shelf life of tomatoes, *Foods*, 9(11), 1605, https://doi.org/10.3390/foods9111605

Priss O., Kolisnychenko T., Zahorko N. (2025), The catnip plant for beverage production, In: S. Gubsky, O. Stabnikova, V. Stabnikov, O. Paredes-López (Eds.),*Wild Edible Plants: Improving Foods Nutritional Value and Human Health through Biotechnology*, pp. 108-142, CRC Press, Boca Raton, London, New York, https://doi.org/10.1201/9781003486794-4

Raal A., Gontova T., Ivask A., Orav A., Koshovyi O. (2024), Yield, composition, and chemotypes of essential oils from *Origanum vulgare* L. aerial parts cultivated in different European countries, *Agronomy*, 14(12), 3046, https://doi.org/10.3390/agronomy14123046

Radi M., Akhavan-Darabi S., Akhavan H., Amiri S. (2018), The use of orange peel essential oil microemulsion and nanoemulsion in pectin-based coating to extend the shelf life of fresh-cut orange, *Journal of Food Processing and Preservation*, 42, e13441, https://doi.org/10.1111/jfpp.13441

Radivojac A., Bera O., Zeković Z., Teslić N., Mrkonjić Ž., Bursać Kovačević D., Putnik P., Pavlić B. (2021), Extraction of peppermint essential oils and lipophilic compounds: Assessment of process kinetics and environmental impacts with multiple techniques, *Molecules*, 26(10), 2879, https://doi.org/10.3390/molecules26102879

Rapper S., Kamatou G., Viljoen A., van Vuuren S. (2013), The in vitro antimicrobial activity of *Lavandula angustifolia* essential oil in combination with other aroma-therapeutic oils, *Evidence-Based Complementary and Alternative Medicine*, 2013, 852049, https://doi.org/10.1155/2013/852049

Razzouk S., Mazri M.A., Jeldi L., Mnasri B., Ouahmane L., Alfeddy M.N. (2022), Chemical composition and antimicrobial activity of essential oils from three Mediterranean plants against eighteen pathogenic bacteria and fungi, *Pharmaceutics*, 14(8), 1608, https://doi.org/10.3390/pharmaceutics14081608

Reddy B.V., Monish V., Mounika T., Reddy G.B., Mallika E.N., Mishra B.P. (2023), Oxidative and microbiological stability of ground pork incorporated with lemon grass essential oil, *Pharma Innovation Journal*, SP-12(7), pp. 1020–1024.

Sadgrove N.J., Padilla-González G.F., Phumthum M. (2022), Fundamental chemistry of essential oils and volatile organic compounds, methods of analysis and authentication, *Plants,* 11(6), 789, https://doi.org/10.3390/plants11060789

Saeed K., Pasha I., Jahangir Chughtai M. F., Ali Z., Bukhari H., Zuhair M. (2022), Application of essential oils in food industry: Challenges and innovation, *Journal of Essential Oil Research*, 34(2), pp. 97–110, https://doi.org/10.1080/10412905.2022.2029776

Safakas K., Lainioti G.C., Tsiamis G., Stathopoulou P., Ladavos A. (2025), Utilizing essential oil components as natural antifungal preservatives in the active packaging of bread, *Polymers*, 17(5), 697, https://doi.org/10.3390/polym17050697

Sahu V.K., Sahu P. (2024), A comprehensive study of rosemary (*Rosmarinus officinalis* L.) leaf: Its botanical properties, chemical composition, and potential applications, *International Journal of Research Publication and Reviews*, 5(12), pp. 634-639, https://ijrpr.com/uploads/v5issue12/ijrpr36093.pdf

Salvia-Trujillo L., Rojas-Graü M.A., Soliva-Fortuny R., Martín-Belloso O. (2015), Use of antimicrobial nanoemulsions as edible coatings: Impact on safety and quality attributes of fresh-cut Fuji apples, *Postharvest Biology and Technology*, 105, pp. 8–16, https://doi.org/10.1016/j.postharvbio.2015.03.009

Scherer R., Godoy H.T. (2009), Antioxidant activity index (AAI) by the 2,2-diphenyl1-picrylhydrazyl method, *Food Chemistry*, 112, pp. 654–658, https://doi.org/10.1016/j.foodchem.2008.06.026

Schneider G., Steinbach A., Putics Á., Solti-Hodován Á., Palkovics T. (2023), Potential of essential oils in the control of *Listeria monocytogenes*, *Microorganisms*, 11(6), 1364, https://doi.org/10.3390/microorganisms11061364

Scollard J., Francis G.A., O'Beirne D. (2013), Some conventional and latent anti-listerial effects of essential oils, herbs, carrot and cabbage in fresh-cut vegetable systems, *Postharvest Biology and Technology*, 77, pp. 87-93, https://doi.org/10.1016/j.postharvbio.2012.11.011

Sessa M., Ferrari G., Donsi F. (2015), Novel edible coating containing essential oil nanoemulsions to prolong the shelf life of vegetable products, *Chemical Engineering Transactions*, 43, pp. 55–60, https://doi.org/10.3303/CET1543010

Sharma R., Nath P.C., Das P., Rustagi S., Sharma M., Sridhar N., Hazarika T.K., Rana P., Nayak P.K., Sridhar K. (2024), Essential oil-nanoemulsion based edible coating: Innovative sustainable preservation method for fresh/fresh-cut fruits and vegetables, *Food Chemistry*, 1(460(Pt 1)), 140545, https://doi.org/10.1016/j.foodchem.2024.140545

Sharma S., Barkauskaite S., Jaiswal A.K., Jaiswal S. (2021), Essential oils as additives in active food packaging, *Food Chemistry,* 343, 128403, https://doi.org/10.1016/j.foodchem.2020.128403

Sharma P., Ahuja A., Izrayeel A.M.D., Samyn P., Rastogi V.K. (2022), Physicochemical and thermal characterization of poly (3-hydroxybutyrate-co-4-hydroxybutyrate) films incorporating thyme essential oil for active packaging of white bread, *Food Control*, 133, 108688, https://doi.org/10.1016/j.foodcont.2021.108688

Shevchenko A., Litvynchuk S., Zaporozhets Y., Drobot V., Galenko O., Shevchenko O. (2025), Wild edible plants in the manufacturing of bakery and meat products, In: S. Gubsky, O. Stabnikova, V. Stabnikov, O. Paredes-López (Eds.),*Wild Edible Plants*: *Improving Foods Nutritional Value and Human Health through Biotechnology,* pp. 84-107, CRC Press, Boca Raton, London, New York, https://doi.org/10.1201/9781003486794-3

Shokri S., Parastouei K., Taghdir M., Abbaszadeh S. (2020), Application an edible active coating based on chitosan-*Ferulago angulata* essential oil nanoemulsion to shelf life extension of rainbow trout fillets stored at 4 °C, *International Journal of Biological Macromolecules*, 153, pp. 846–854, https://doi.org/10.1016/j.ijbiomac.2020.03.080

Smaoui S., Hlima H.B., Tavares L., Ennouri K., Braiek O.B., Mellouli L., Abdelkafi S., Khaneghah A.M. (2022), Application of essential oils in meat packaging: A systemic review of recent literature, *Food Control,* 132, 108566, https://doi.org/10.1016/j.foodcont.2021.108566

Šojić B., Tomović V., Jokanović M., Ikonić P., Džinić N., Kocić-Tanackov S., Popović L., Tasić T., Savanović J., Živković Šojić N. (2017), Antioxidant activity of *Juniperus communis* L. essential oil in cooked pork sausages, *Czech Journal of Food Science*, 35(3), pp. 189-193, https://doi.org/10.17221/210/2016-CJFS

Soulaimani B., ElHidar N., Ben El Fakir S., Mezrioui N., Hassani L., Abbad A. (2021), Combined antibacterial activity of essential oils extracted from *Lavandula maroccana* (Murb.), *Thymus pallidus* Batt. and *Rosmarinus officinalis* L. against antibiotic-resistant gram-negative bacteria, *European Journal of Integrative Medicine*, 43, https://doi.org/101312. 10.1016/j.eujim.2021.101312

Stabnikov V., Kovshar I., Stabnikova O. (2025), Recent advances in the study of the properties and applications of lactic acid bacteria, *World Journal of Microbiology and Biotechnology*, 41, 287, https://doi.org/10.1007/S11274-025-04499-0

Stabnikova O., Marynin A., Stabnikov V. (2021), Main trends in application of novel natural additives for food production, *Ukrainian Food Journal,* 10(3), pp. 524–551, https://doi.org/10.24263/2304-974X-2021-10-3-8

Stabnikova O., Stabnikov V., Paredes-López O. (2026), Spices and essential oils in food preservation: From natural additives to active packaging systems, *Plant Foods for Human Nutrition*, 81, 69, https://doi.org/10.1007/s11130-026-01519-8

Stojanović N.M., Mladenović M.Z., Randjelović P.J., Radulović N.S. (2013), The potential of lemon balm (*Melissa officinalis* L.) essential oil as an anti-anxiety agent - is the citronellal the activity carrier? *Journal of Ethnopharmacology*, 314, 116661, https://doi.org/10.1016/j.jep.2023.116661

Šunić L., Ilić Z.S., Stanojević L., Milenković L., Stanojević J., Kovač R., Milenković A., Cvetković, D. (2023), Comparison of the essential oil content, constituents and antioxidant activity from different plant parts during development stages of wild fennel (*Foeniculum vulgare* Mill.), *Horticulturae*, 9(3), 364, https://doi.org/10.3390/horticulturae9030364

Suwanamornlert P., Kerddonfag N., Sane A., Chinsirikul W., Zhou W., Chonhenchob V. (2020), Poly(lactic acid)/poly(butylene-succinate-co-adipate) (PLA/PBSA) blend films containing thymol as alternative to synthetic preservatives for active packaging of bread, *Food Packaging and Shelf Life*, 25, 100515, https://doi.org/10.1016/j.fpsl.2020.100515

Taghvaei M., Jafari S.M. (2015), Application and stability of natural antioxidants in edible oils in order to substitute synthetic additives, *Journal of Food Science and Technology*, 52(3), pp. 1272–1282, https://doi.org/10.1007/s13197-013-1080-1

Takma D.K., Korel F. (2019), Active packaging films as a carrier of black cumin essential oil: Development and effect on quality and shelf-life of chicken breast meat, *Food Packaging and Shelf Life*, 19, pp. 210-217, https://doi.org/10.1016/j.fpsl.2018.11.002

Tamburlin I.S., Roux E., Feuillée M., Labbé J., Aussaguès Y., El Fadle F.E., Fraboul F., Bouvier G. (2021), Toxicological safety assessment of essential oils used as food supplements to establish safe oral recommended doses, *Food and Chemical Toxicology*, 157, 112603, https://doi.org/10.1016/j.fct.2021.112603

Tanasă F., Nechifor M., Teacă C.A. (2024), Essential oils as alternative green broad-spectrum biocides, *Plants*, 13(23), 3442, https://doi.org/10.3390/plants13233442

Teixeira B., Marques A., Ramos C., Neng N.R., Nogueira J.M.F., Saraiva J.A., Nunes M.L. (2013), Chemical composition and antibacterial and antioxidant properties of commercial essential oils, *Industrial Crops and Products,* 43, pp. 587–595, https://doi.org/10.1016/j.indcrop.2012.07.069

Tomić A., Šovljanski O., Erceg T. (2023), Insight on incorporation of essential oils as antimicrobial substances in biopolymer-based active packaging, *Antibiotics*, 12(9), 1473, https://doi.org/10.3390/antibiotics12091473

Van Haute S., Raes K., Van Der Meeren P., Sampers I. (2016), The effect of cinnamon, oregano and thyme essential oils in marinade on the microbial shelf life of fish and meat products, *Food Control*, 68, pp. 30–39, https://doi.org/10.1016/j.foodcont.2016.03.025, 2-s2.0-84962519021

Vassiliou E., Awoleye O., Davis A., Mishra S. (2023), Anti-inflammatory and antimicrobial properties of thyme oil and its main constituents, *International Journal of Molecular Sciences*, 24(8), 6936, https://doi.org/10.3390/ijms24086936

Vazirian M., Kashani S.T., Ardekani M.R.S., Khanavi M., Jamalifar H., Fazeli M.R., Toosi A.N. (2012), Antimicrobial activity of lemongrass (*Cymbopogon citratus* (DC) Stapf.) essential oil against food-borne pathogens added to cream-filled cakes and pastries, *Journal of Essential Oil Research*, 24(6), pp. 579–582, https://doi.org/10.1080/10412905.2012.729920

Verma T., Aggarwal A., Dey P., Chauhan A.K., Rashid S., Chen K.T., Sharma R. (2023), Medicinal and therapeutic properties of garlic, garlic essential oil, and garlic-based snack food: An updated review, *Frontiers in Nutrition*, 10, 1120377, https://doi.org/10.3389/fnut.2023.1120377

Viuda-Martos M., Ruiz-Navajas Y., Sánchez-Zapata E., Fernández-López J., Pérez-Álvarez J.A. (2010), Antioxidant activity of essential oils of five spice plants widely used in a Mediterranean diet, *Flavour and Fragrance Journal*, 25, pp. 13–19, https://doi.org/10.1002/ffj.1951

Walasek-Janusz M., Grzegorczyk A., Malm A., Nurzyńska-Wierdak R., Zalewski D. (2024), Chemical composition, and antioxidant and antimicrobial activity of oregano essential oil, *Molecules,* 29(2), 435, https://doi.org/10.3390/molecules29020435

Wang W., Zhao D., Xiang Q., Li K., Wang B., Bai Y. (2021), Effect of cinnamon essential oil nanoemulsions on microbiological safety and quality properties of chicken breast fillets during refrigerated storage, *LWT - Food Science and Technology*, 152, 112376, https://doi.org/10.1016/j.lwt.2021.112376

Wang Y., Yang Q., Zhao F., Li e M., Ju J. (2024), Synergistic antifungal mechanism of eugenol and citral against *Aspergillus niger*: Molecular level, *Industrial Crops and Products*, 213, 118435, https://doi.org/10.1016/j.indcrop.2024.118435

Wen P., Zhu D.H., Wu H., Zong M.H., Jing Y.R., Han S.Y. (2016), Encapsulation of cinnamon essential oil in electrospun nanofibrous film for active food packaging, *Food Control*, 59, pp. 366–376, https://doi.org/10.1016/j.foodcont.2015.06.00

WHO. (2024), World Health organization. Food safety, Available online https://www.who.int/news-room/fact-sheets/detail/food-safety

Yang J., Park M.J. (2025), Antioxidant effects of essential oils from the peels of citrus cultivars, *Molecules*, 30(4), 833, https://doi.org/10.3390/molecules30040833

Yang Y., Li Y., He H., Yang L., Zeng J., Bai M., Wu H. (2025), Comparison of essential oil components and in vitro antioxidant activity of *Zanthoxylum nitidum* from different parts, *Plants*, 14(8), 1194, https://doi.org/10.3390/plants14081194

Yu X., Zhu J., Wu J., Cheng Y., Gao Y., Liu Y., Jiang F. (2025), Edible coating based on *Konjac glucomannan* loading *Ocimum gratissimum* essential oil for postharvest preservation of orange, *Polymers*, 17(9), 1217, https://doi.org/10.3390/polym17091217

Yun J., Fan, X., Li X., Jin T.Z., Jia X., Mattheis J.P. (2015), Natural surface coating to inactivate *Salmonella enterica* serovar Typhimurium and maintain quality of cherry tomatoes, *International Journal of Food Microbiology*, 193, pp. 59–67, https://doi.org/10.1016/j.ijfoodmicro.2014.10.013

Zakaria L. (2024), An overview of *Aspergillus* species associated with plant diseases, *Pathogens*, 13(9), 813, https://doi.org/10.3390/pathogens13090813

Živković M., Stanisavljević I., Gajović N., Pavlović S., Simović Marković B., Jovanović I.P., Cupara S., Tadić V., Žugić A., Milenković M.T., Barjaktarević A. (2025), Comprehensive phytochemical analysis and evaluation of antioxidant, antimicrobial, cytotoxic, and immunomodulatory activities of commercial cinnamon bark essential oil (*Cinnamomum zeylanicum* L.), *International Journal of Molecular Sciences*, 26(13), 6482, https://doi.org/10.3390/ijms26136482

Zhang Y., Zhou L., Zhang C., Show P.L., Du A., Fu J.C., Ashokkumar V. (2020), Preparation and characterization of curdlan/polyvinyl alcohol/thyme essential oil blending film and its application to chilled meat preservation, *Carbohydrate Polymers*, 247, 116670, https://doi.org/10.1016/j.carbpol.2020.116670

Zhang Q., Huo Y., Yang Q., Zhao F., Li M., Ju J. (2025), Migration of chemical substances from packaging materials to food, *Food Chemistry*, 485, 144544, https://doi.org/10.1016/j.foodchem.2025.144544.

Zhao F., Huang J., Qi J., Li Q., Wu H., Ju J. (2022), Proteomic analysis of antifungal mechanism of star anise essential oil against Aspergillus niger and its application potential in prolonging bread shelf life, *LWT - Food Science and Technology*, 169, 114023, https://doi.org/10.1016/j.lwt.2022.114023

Zubair M., Shahzad S., Hussain A., Pradhan R.A., Arshad M., Ullah A. (2022), Current trends in the utilization of essential oils for polysaccharide- and protein-derived food packaging materials, *Polymers*, 14(6), 1146, https://doi.org/10.3390/polym14061146

Zuzarte M., Sousa C., Alves-Silva J., Salgueiro L. (2024), Plant monoterpenes and essential oils as potential anti-ageing agents: Insights from preclinical data, *Biomedicines*, 12(2), 365, https://doi.org/10.3390/biomedicines12020365

Cite:

Stabnikova, O., Marynin, A., Stabnikov, V., Svyatnenko, R., & Demchenko, V. (2026). Plant essential oils for food shelf-life extension and active packaging systems. *Ukrainian Food Journal, 15*(2), 323–360. https://doi.org/10.24263/2304-974X-2026-15-2-6

Polyphenolic phytochemical compounds from *Sambucus nigra* L. and *Rubus fruticosus* L. for food freshness indicators

Loredana-Mariana Huțuțui[1], Sonia Amariei[1], Dana Huțu[2]

1 – Ștefan cel Mare University of Suceava, Suceava, Romania
2 – Natanael High School Suceava, Suceava, Romania

Keywords:

Blackberry
Elderberry
Ultrasound extraction
Anthocyanins
Polyphenols
Freshness

Article history:

Received 21.01.2026
Received in revised form 12.04.2026
Accepted 30.06.2026

Corresponding author:

Loredana-Mariana Huțuțui
E-mail: loredana.hututui@student.usv.ro

DOI:
10.24263/2304-974X-2026-15-2-7

Abstract

Introduction. This study investigates extraction methods and the physicochemical and colorimetric properties of extracts obtained from fresh elderberries (*Sambucus nigra* L.) and blackberries (*Rubus fruticosus* L.) to evaluate their potential as natural food freshness indicators.

Materials and methods. Extraction was performed using ultrasound-assisted extraction (UAE) for 10, 15, and 20 min at ultrasonic powers of 80, 110, and 140 W, and by maceration (MAC) for 6, 12, and 24 h using water and aqueous ethanol solutions (20%, 50%, and 96%, v/v). The extracts were characterized by determining antioxidant activity (DPPH radical scavenging activity), total anthocyanin content (TAC), total polyphenol content (TPC), total flavonoid content (TFC), and pH-dependent colorimetric properties.

Results and discussion. Characterization of the raw materials revealed significant physicochemical differences between the two berry species. Blackberries contained 81.37% moisture, 1.77 g/100 g FW protein, 5.18 g/100 g FW fibre, and had a pH of 3.43, whereas elderberries exhibited a higher moisture content (85.18%), protein content (2.83 g/100 g FW), fibre content (6.68 g/100 g FW), and pH (4.43). Extraction efficiency depended on both the extraction method and solvent composition. Ultrasound-assisted extraction (UAE) provided the highest antioxidant activity, reaching 89.89% DPPH radical scavenging activity for blackberries and 72.20% for elderberries. In contrast, maceration (MAC) proved more effective for recovering phenolic compounds. Elderberry extracts showed substantially higher concentrations of bioactive compounds than blackberry extracts, with maximum values of 657.23 mg C3G/100 g FW for total anthocyanin content (TAC), 601.35 mg GAE/100 g FW for total polyphenol content (TPC), and 1140.59 mg QE/100 g FW for total flavonoid content (TFC), compared with 138.68 mg C3G/100 g FW, 287.90 mg GAE/100 g FW, and 491.93 mg QE/100 g FW, respectively, for blackberry extracts. In addition, both extracts exhibited distinct pH-dependent color changes over a wide pH range, demonstrating high sensitivity to changes in acidity. These findings confirm the potential of elderberry and blackberry extracts as natural colorimetric indicators for monitoring food freshness and spoilage.

Conclusion. Maceration was more effective for the extraction of anthocyanins, polyphenols, and flavonoids, whereas UAE resulted in the highest antioxidant activity. The pronounced pH-dependent color changes observed in the extracts support their potential use as natural food freshness indicators.

Introduction

Food loss and waste pose a major challenge to the sustainability of agri-food systems, occurring at every stage of the food supply chain, from production and processing to distribution and final consumption (Rahman et al., 2026). Globally, approximately one-third of the food produced annually is wasted, corresponding to an economic loss of about $1 trillion and involving the inefficient use of roughly 30% of agricultural resources (Rahman et al., 2026; Yu et al., 2023). The impact is significantly greater for perishable foods, such as meat, dairy products, and fresh produce, where inadequate storage conditions and the difficulty of accurately assessing freshness lead to significant losses, estimated at approximately 1.3 billion tons annually (Zhai et al., 2025).

Existing packaging and labelling systems do not provide real-time information on the condition of the product, and the use of pre-set expiration dates can lead to the premature disposal of food that is still safe to eat (Bhatlawande et al., 2024).

In this context, the growing demand for fresh and safe food products has led to the development of freshness indicators capable of monitoring critical parameters such as pH in real time (Almasi et al., 2022). This changes during spoilage processes as a result of microbiological activity and biochemical reactions that cause the degradation of compounds and the formation of biogenic amines, ammonia (NH_3), hydrogen sulfide (H_2S), and other alkaline or acidic metabolites (Dirpan et al., 2022; Jiao et al., 2023; Villarino et al., 2023). These changes are considered relevant indicators of freshness loss, particularly in the case of perishable products (Miller et al., 2023; Upadhyay et al., 2024; Wang et al., 2024).

Natural pigments, such as anthocyanins, react to changes in pH and change color depending on their environment, providing a clear and reproducible visual signal that allows for the differentiation between fresh, moderately fresh, and spoiled foods (Almasi et al., 2022; Kwak et al., 2024). The use of anthocyanin-based freshness indicators contributes to increased food safety, enabling more efficient management of food quality and shelf life (Kahyaoglu, 2024; Ma et al., 2021). Thus, without opening the packaging, consumers can quickly assess the freshness of food, contributing to increased food safety and reduced waste (Li et al., 2021; Nami et al., 2024).

The utilization of anthocyanins in such applications depends on the efficiency of the extraction process. The uneven distribution of pigments in plant tissues, high enzymatic activity, and the non-selective nature of extraction can lead to the degradation of bioactive compounds and low yields (Oladzadabbasabadi et al., 2022). For these reasons, optimizing extraction parameters is an essential step for maximizing the content of phenolic compounds as well as the antioxidant activity of the extracts (Airouyuwa et al., 2024; Barros et al., 2024).

In this context, the present study comparatively investigated two extraction methods: conventional solvent maceration (MAC), which involves immersing the raw material in a solvent for a specific period of time at a controlled temperature (Kunyk et al., 2025), and ultrasound-assisted extraction (UAE), an unconventional method that increases extraction yield through the mechanical action of ultrasonic energy on the plant matrix (Santos et al., 2021).

The study analysed extracts obtained from fresh elderberries (*Sambucus nigra* L.) and blackberries (*Rubus fruticosus* L.), species commonly found in wild flora, as natural sources of chromatic indicators (Stabnikov et al., 2025) (Figure 1).

By determining the content of total anthocyanins, polyphenols, and flavonoids, as well as by evaluating antioxidant activity and color behavior as a function of pH, this study aims to demonstrate whether these extracts meet the necessary criteria for use as colorimetric freshness indicators in smart packaging systems.



a b

Figure 1. Elderberries (*Sambucus nigra*) (a) and blackberries (*Rubus fruticosus*) (b)

Both species are characterized by intensely pigmented fruits rich in anthocyanins. The blackberry (*Rubus fruticosus* L.), of the *Rosaceae* family, native to Southwest Asia and widespread in Europe and South America, produces purple-black fruits (Mayuri et al., 2023; Rivero-Pérez et al., 2025), while the elderberry (*Sambucus nigra* L.), a deciduous shrub of the *Adoxaceae* family reaching heights of 4–12 m, grows abundantly in open fields and on forest edges, bearing small, spherical, dark purple fruits (Özgen and Özbaş, 2025; Stabnikova et al., 2024; Trojniak and Tabarkiewicz, 2023).

The aim of this study was to evaluate the influence of extraction parameters on the recovery, stability, and functional properties of phenolic compounds from fresh elderberries and blackberries. Furthermore, the pH-responsive color behavior of the extracted anthocyanins was investigated to determine their suitability for use as colorimetric freshness indicators.

Materials and methods

Raw materials

The elderberry (*Sambucus nigra*) samples were harvested at optimal maturity at the end of August 2025 from wild elderberry plants in the northeast region of Botoșani, Romania (48.15° N, 26.50° E). Blackberry fruits (*Rubus fruticosus*) were purchased from a local producer in Suceava, Romania (47.65° N, 26.26° E), harvested in September 2025 at their optimal maturity stage.

Sample preparation

Fresh fruit samples were homogenized by mechanical crushing and brought to a uniform mass. For the extraction of phenolic compounds, hydroalcoholic ethanol-water mixtures of 20% (v/v), 50% (1:1, v/v), 96% (v/v), as well as distilled water (0% v/v) were used. The extracts were prepared in a 1:10 (m/v) ratio, and the samples were brought to pH 3 with 0.1N HCl.

Extraction methods

Ultrasound-assisted extraction (UAE). UAE was performed using an ultrasonic bath (Elma Transsonic TI-H15, Singen, Germany) operating in normal mode at a constant frequency of 45 kHz. For each sample, 4 g of blackberry and elderberry puree were weighed, and 40 mL of ethanol–water solution (1:1, v/v) was added.

The resulting extracts were centrifuged (Ohaus Frontier 5718R, Parsippany, NJ, USA) at 5000 rpm for 20 min at a constant temperature of 25 °C. Filtration was performed in two successive stages using Whatman No. 1 filter paper, followed by filtration through Milli-pore syringe filters (Merck, Darmstadt, Germany) with a pore size of 0.45 μm.

Maceration extraction (MAC). MAC is a conventional method that involves immersing plant material in a solvent (Peron et al., 2024). It was used to extract phenolic compounds from blackberry and elderberry puree. The solid/solvent ratio used was 1:10 (m/v). The ethanol-based solvent was acidified to pH 3 with 0.1 N HCl. Maceration was performed at room temperature (20–25 °C), and the samples were stored in the dark. After extraction, the samples were centrifuged (Ohaus Frontier 5718R, Parsippany, NJ, USA) at 5000 rpm for 20 minutes at a constant temperature of 25 °C. The extracts were filtered to remove solid particles (Crişan et al., 2025; Plasencia et al., 2025; Varo et al., 2022).

Determination of the physicochemical and dimensional characteristics of the fruit

The weight was determined using a Partner AS 220.RS analytical balance (Radwag, Torunska, Poland, accuracy: ±0.1 mg). The length and diameter of the fruit were measured with a caliper (accuracy:±0.05 mm). The results for weight were expressed in grams (g), while those for length and width were expressed in millimeters (mm). For each sample, measurements were made in 3 replicates.

The physicochemical characterization of elderberry and blackberry samples included the determination of moisture, ash, crude fibre, and crude protein. Moisture content was determined gravimetrically by drying at 103±2 °C to constant weight (AOAC 925.10), and ash content by calcination at 550–600 °C in a muffle furnace (AOAC 940.26). Crude fibre was determined according to the standardized method (ISO 5498:1981) using a Fibretherm FT12 apparatus (Königswinter, Germany), while crude protein was determined by the Kjeldahl method using a conversion factor of N × 5.6.

The pH was determined using a Mettler Toledo pH meter (Seven Compact, Heusenstamm, Germany). Three measurements were taken for each of the two fruits (EL Cadi et al., 2020; Vujanović et al., 2020).

Influence of pH on chromatic behavior

The extracts were brought to pH values between 1 and 10 by titration with 0.1 N HCl and 0.1 N NaOH solutions, using a Mettler Toledo pH meter (Seven Compact, Heusenstamm, Germany). The color was determined using a Konica Minolta CM-700 colorimeter (Konica Minolta, Tokyo, Japan) in the CIELAB color system (Cuesta-Riaño et al., 2022; Sganzerla et al., 2021).

Determination of sample color parameters

The color of the samples was determined using a Konica Minolta CR 400 colorimeter (Konica Minolta, Tokyo, Japan) using the CIELAB laboratory method. The color parameters measured were L*, a*, b*, C*, H°. L* represents brightness, with values ranging from 0 (black) to 100 (white), a* represents the green (-) red (+) chromatic coordinate, and b* the blue (-) yellow (+) chromatic coordinate, C* represents chroma, which expresses color intensity, and the hue angle (H°), which describes color tone. Three measurements were taken for each sample (Zhou et al., 2020).

Total anthocyanin content (TAC)

The anthocyanin content of blackberry and elderberry extract was determined using the differential pH method. The total anthocyanin content was measured using the differential spectrophotometric pH method. The extract was adjusted with buffer solution (pH 1) based on potassium chloride (KCl) (0.025 mol L^{-1}) and buffer solution (pH 4.5) based on sodium acetate CH_3COOH (0.5 mol L^{-1}). The buffer solution was kept for 15 minutes in a dark place at room temperature. The reading was performed with a Shimadzu 300 UV-VIS-NIR spectrophotometer (Tokyo, Japan) at wavelengths of 510 nm and 700 nm (Česlová et al., 2023; Kim et al., 2023; Madrera and Bedriñana, 2023; Zubova et al., 2024). The total anthocyanin content (TAC) was calculated using equations (1) and equations (2). The results were expressed as cyanidin-3-glucoside equivalents (mg C3G/100 g FW) (Wu et al., 2022).

$$A = (A_{510} - A_{700})_{pH\,1} - (A_{510} - A_{700})_{pH\,4,5} \quad (1)$$

$$TAC = \frac{A \times mw \times DF \times V\,(ml)}{\varepsilon \times m(g) \times L} \quad (2)$$

where: A – (A_{520}nm − A_{700}nm) at pH 1.0 − (A_{520}nm − A_{700}nm) at pH 4.5; mw – molecular weight of cyanidin-3-glucoside (C3G) (449.2 g/mol); DF – sample dilution factor; V – sample volume (ml); ε – molar extinction coefficient of C3G (26,900 $L \cdot mol^{-1} \cdot cm^{-1}$); m – sample mass (g); L – cell length (1 cm).

Total polyphenol content (TPC)

The total polyphenol content of the blackberry and elderberry extract was determined using the Folin–Ciocalteu method. A volume of 0.25 ml of extract was taken, to which 1.25 ml of Folin–Ciocalteu reagent (reagent 1:10) was added and incubated for 5–7 min. 4 ml of 7.5% sodium carbonate was added. The color formation time was 2 hours. The analyses were performed in triplicate for each sample at λ = 765 nm using a Shimadzu 300 UV-VIS-NIR spectrophotometer (Tokyo, Japan), and the results were expressed in mg gallic acid equivalent (GAE)/100 g fresh weight (FW) using its calibration curve. The total polyphenolic compound content was calculated according to equation (3).

$$TPC = C \cdot (V/M) \cdot DF \cdot 100 \quad (3)$$

where: TPC – total polyphenol content, mg GAE/100g FW; C – concentration determined from the calibration curve, mg/ml; V – sample volume (l); DF – sample dilution factor; M – sample mass (g).

Total flavonoid content (TFC)

The total flavonoid content was determined using the spectrophotometric method. The extract, 1.5 ml, was mixed with 0.3 ml of 5% $NaNO_2$ and incubated for 5 minutes, then 0.3 ml of 10% $AlCl_3$ was added. The mixture was shaken for 1 min and then 3 ml of NaOH (1 mol/l) was added. The absorbance was measured using a Shimadzu 300 UV-VIS-NIR spectrophotometer (Tokyo, Japan) at 510 nm. For the calibration curve, different concentrations of quercetin (QE) standard solution were prepared. The analyses were performed in triplicate and only the average value, expressed in mg QE/100 g FW, was reported (Dos Santos et al., 2021; Kolarević et al., 2021; Nadeem et al., 2025). The total flavonoid content was calculated according to equation (4).

$$TFC = C \cdot (V/M) \cdot DF \cdot 100 \quad (4)$$

where: TFC – total flavonoid content, mg QE/100g FW; C – concentration determined from the calibration curve, mg/l; V – sample volume (l); DF = sample dilution factor; M – sample mass (g).

Antioxidant activity (DPPH)

The antioxidant activity of the extract was quantified using the DPPH (2,2-diphenyl-1-picrylhydrazyl) free radical scavenging activity method. Undiluted extract, 0.1 ml, was mixed with 3.9 ml of DPPH solution and incubated for 30 minutes in a dark place. After 30 minutes, the absorbance was measured at 517 nm using a spectrophotometer (Shimadzu 300 UV-VIS-NIR, Tokyo, Japan) (Deniz and Suna, 2025; Gil-Martínez et al., 2023; Golonka et al., 2024; Imenšek et al., 2021).

$$\text{Antioxidant activity}(\%) = \frac{\text{Ablank} - \text{Asample}}{\text{Asample}} \text{ x100} \quad (5)$$

FTIR-ATR (Fourier transform infrared spectroscopy with attenuated total reflectance)

A Thermo Scientific Nicolet iS20 spectrometer (Thermo Scientific, Karlsruhe, Germany) was used to record FTIR-ATR spectra in the region between 4000 and 650 cm^{-1}. The conditions used were: 32 scans and a resolution of 4 cm^{-1}. The spectra obtained were processed using the OMNIC program (version 9, Thermo Scientific, Waltham, MA, USA).

High-performance liquid chromatography

Individual polyphenols were determined using high-performance liquid chromatography (HPLC) (Shimadzu Corporation, Kyoto, Japan) equipped with a Kinetex Biphenyl HPLC column (150 × 4.6 mm, 2.6 µm, 100 Å, Kinetex 5 µm C18 100 Å (Phenomenex, California, USA), which was used for separation at 25 °C. The injection volume of the sample was 20 µL. Mobile phase A consisted of 0.1% acetic acid in water and mobile phase B consisted of acetonitrile. The solvent flow rate was 0.5 mL/min, and two injections were performed for each sample. The phenolic compounds were identified based on retention times, and quantification was obtained by the absorption recorded in chromatograms in relation to external standards, at 280 nm for gallic acid, protocatechuic acid, vanillic acid, p-hydroxybenzoic acid; and 320 nm for chlorogenic acid, caffeic acid, p-coumaric acid, rosmarinic acid, myricetin, and quercetin. All standard calibration curves showed high degrees of linearity (R2 > 0.99) (Česlová et al., 2023; Crăciun and Gutt, 2023).

Experimental design and statistical analysis

The extraction of phenolic compounds from fresh elderberries and blackberries was carried out using ultrasound-assisted extraction (UAE) and maceration (MAC). For UAE, the extraction conditions included different combinations of extraction time, temperature, and ultrasonic power. For MAC, different ethanol concentrations and extraction times were evaluated. All experiments were performed in triplicate under the conditions presented in Table 1.

Table 1

Extraction parameters applied in ultrasound-assisted extraction (UAE) and maceration (MAC)

Independent variable	Unit	Min	Max	Extraction method
Extraction time	min	10	20	UAE
Temperature	°C	30	50	
Ultrasonic power	W	80	140	
Concentration	%	0	96	MAC
Extraction time	h	6	24	

The experimental results were used to evaluate the effects of the extraction variables on total anthocyanin content (TAC), total phenolic content (TPC), total flavonoid content (TFC), and antioxidant activity (DPPH).

Statistical analysis

Statistical interpretation was performed using oneway ANOVA, with pH level as the independent factor, to evaluate its influence on the color parameters (L*, a*, b*) in blackberry and elderberry extracts. All results are presented as mean±standard deviation and were calculated using SPSS 25.0 statistical software (trial version) from IBM, New York, NY, USA. Letter distribution was performed automatically based on the groupings generted by the Tukey HSD (Honestly Significant Difference) test, with the significance level set at $p < 0.05$. Significant differences between mean values were noted with lowercase letters, indicating statistically significant differences between groups (Tukey HSD). Values followed by different letters (a, b, c, d, e, f, g, h, i, j, k) are statistically different at a 95% confidence level.

Data modeling were performed using Design-Expert 11 software (Stat-Ease Inc., USA). Statistical modeling was evaluated using ANOVA, and the quality and validity of the mathematical model were assessed based on specific statistical indicators: coefficient of determination (R^2), adjusted coefficient of determination (adjusted R^2), p-value, F-value, and lack of fit (LOF) test. The results are presented in Table 2, and the significance threshold was $p < 0.05$.

Table 2

Statistical coefficients (R^2, adjusted R^2, p-value, F-value, and Lack of Fit) for the TAC, TPC, TFC, and DPPH models

Sample	Extraction method	Model	R2	Adjusted R^2	Model p – value	Model F – value	Lack of Fit F – value
TAC	BB UAE	2FI	0.9801	0.9546	< 0.0001	0.5693	0.6643
	BB MAC	Quadratic	0.9825	0.9796	< 0.0001	2.37	0.0609
	EB UAE	2FI	0.9708	0.9333	0.0001	0.6550	0.6208
	EB MAC	Quadratic	0.9650	0.9592	< 0.0001	1.58	0.1962
TPC	BB UAE	2FI	0.9975	0.9943	< 0,0001	0.7284	0.5863
	BB MAC	Quadratic	0.9640	0.9580	< 0,0001	2.45	0.0543
	EB UAE	2FI	0.9852	0.9662	< 0.0001	4.05	0.1052
	EB MAC	Quadratic	0.9864	0.9842	< 0,0001	2.41	0.0575
TFC	BB UAE	2FI	0.9600	0.9086	0.0004	0.6309	0.6326
	BB MAC	Quadratic	0.9504	0.9421	< 0.0001	2.45	0.0543
	EB UAE	2FI	0.9990	0.9977	< 0.0001	2.58	0.1911
	EB MAC	Quadratic	0.9827	0.9798	< 0.0001	1.88	0.1266
DPPH	BB UAE	2FI	0.9883	0.9734	< 0.0001	1.50	0.3437
	BB MAC	Quadratic	0.9429	0.9334	< 0.0001	1.15	0.3631
	EB UAE	2FI	0.9875	0.9714	< 0.0001	1.05	0.4616
	EB MAC	Quadratic	0.9460	0.9370	< 0.0001	1.95	0.1135

Note: TAC – total anthocyanin content; TPC – total phenolic content; TFC – total flavonoid content; DPPH – antioxidant activity; EB – elderberry extract; BB – blackberry extract; UAE – ultrasound-assisted extraction; MAC – maceration.

Results and discussion

Physicochemical characterization

Table 3

Physicochemical parameters and color characteristics of fresh R. *fruticosus* and S. *nigra* fruits

Parameters		*Rubus fruticosus*	*Sambucus nigra*
Size (mm)	Length	4.67±0.42	28.67±2.52
	Width	4.47±0.21	17.67±1.53
Mass (g)		3.87±0.75	0.09±0.02
Moisture (%)		81.37±0.36	85.18±0.34
Protein (g/100 g FW)		1.77±0.15	2.83±0.08
Ash %		0.52±0.02	0.91±0.03
Fibre (g/100 g FW)		5.18±0.33	6.68±0.40
pH		3.43±0.02	4.43±0.01
Color	L*	10.03±0.02	5.94±0.25
	a*	21.38±0.02	5.26±0.02
	b*	6.69±0.09	0.98±0.17
	Chroma	22.40±0.02	5.32±0.02
	Hue(H°)	17.38±0.22	10.58±1.79

Data are presented as mean±standard deviation (n = 3). Differences between fresh elderberry and blackberry fruits were evaluated using an independent samples t-test, considering a significance level of $p < 0.05$.

The results presented in Table 3 show the characterization of fresh blackberries (*Rubus fruticosus*) and elderberries (*Sambucus nigra*), for which physical (mass, size, color) and physicochemical (moisture, protein, ash, fibre, and pH) parameters were determined. The values are specific to the batch analyzed, given that this composition may vary depending on the variety, origin, and ripeness (Mitroi et al., 2022).

Physical and dimensional characteristics of the fruit

The fruit mass and size (length and width) differed between the two species, with blackberry fruits being significantly larger than elderberry fruits ($p<0.01$). The literature reports significant differences in size between blackberries and elderberries (Dogan et al., 2025a; Martins et al., 2025b).

Moisture analysis of fresh fruit

The moisture content of blackberries was significantly lower ($p < 0.001$) than that of elderberries (81.37±0.36% and 85.18±0.34%, respectively). According to the literature, moisture content ranged from 64% to 83% in fresh blackberries and from 82% to 84% in fresh elderberries (Mattson et al., 2021; Memete et al., 2023).

Analysis of fruit nutritional composition

Fibre content showed a statistically significant difference between the two samples (5.18±0.33 and 6.68±0.405 g/100 g FW; $p < 0.05$), while the protein content (1,77±0,15and

2,83±0,08g/100 g FW) and ash content (0.52%±0.02 and 0.91%±0.03) showed very significant differences for blackberries and elderberries ($p < 0.001$). These values fall within the ranges reported in the literature, 5.3 g/100 g and 7 g/ 100 g for fibre, 1.28 g/100 g and 2.7–2.97 g/100 g for protein, and 0.42% and 0.75–1.02% for ash, respectively (Domínguez et al., 2021; Martins et al., 2023; Marțiș et al., 2021; Nawirska-Olszańska et al., 2022; Pascariu and Israel-Roming, 2022a; Vega-Castro et al., 2025).

pH values of fruits

Since pH is an important characteristic for defining the degree of ripeness (Costa et al., 2022) and fruit quality, pH measurements were taken for blackberries and elderberries. The results indicated significantly lower acidity in elderberries (pH 4.43±0.01) compared to blackberries (3.43±0.02), $p < 0.001$).

Determination of fruit color

The color parameters analyzed in the CIELAB space indicated significant differences between the blackberry and elderberry samples ($p < 0.05$). Low values were recorded for lightness (L*) (10.03±0.02 and 5.94±0.25), confirming the dark color of the fruits. Positive values for (a*) and (b*) indicate that the samples have a color represented by shades of red and yellow. In terms of Chroma (C*), which expresses the intensity and degree of color saturation, blackberries showed significantly higher values (22.40±0.02) compared to elderberries (5.32±0.02), highlighting a much more saturated and intense color in blackberries, and the hue angle (H°) had values between 17.38°±0.22 and 10.58°±1.79, being higher in elderberries, which indicates a color orientation towards reddish hues.

Influence of pH on the chromatic behavior of blackberry and elderberry extracts

The stability of anthocyanin pigments is mainly influenced by pH, as they are more stable in acidic environments (Ghareaghajlou et al., 2021). The analysis of color variation as a function of pH was performed for extracts obtained by conventional maceration (MAC) and ultrasound-assisted extraction (UAE) for both fruits analyzed. Since the chromatic behavior was similar for the two methods, a single representative graph was presented, corresponding to the extract obtained by conventional maceration, which, due to its higher anthocyanin content, allows for a clearer highlighting of color variations as a function of pH. According to Table 4, the anthocyanin rich extracts of both fruits (BB and EB) showed red coloration at acidic pH, the presence of flavylium cation (may be the cause of this color (Cuesta-Riaño et al., 2022). As the pH increases to 6.0, the structure of anthocyanins transforms into a neutral quinonoid base (Enaru et al., 2021). When the pH rises to 7-8, the anthocyanin solution turns blue due to the presence of neutral and anionic quinonoid bases (Rosales-Murillo et al., 2024). By increasing the pH above 8, chalcone structures appear, the color turning green, although the quinonoid base remains the major anthocyanin structure (Huang et al., 2023; Roy and Rhim, 2021; Zhang K. et al., 2025). The result is consistent with studies by Sganzerla et al. (2021), Guo et al. (2023), Lv et al. (2023), Zhu et al. (2023), and Cvetković et al. (2025), who reported color variations from intense red in acidic conditions to shades of purple and blue at neutral pH, becoming unstable in alkaline environments.

Table 4

Variation in color parameters (L*, a*, b*) of blackberry (*R. fruticosus*) and elderberry (*S. nigra*) extracts at different pH values

pH	L* Blackberries	L* Elderberries	a* Blackberries	a* Elderberries	b* Blackberries	b* Elderberries
pH 1	38.29±0.15^{d}	38.14±0.13^{d}	38.15±0.05^{k}	37.00±0.13^{k}	26.28±0.14^{e}	22.86±0.09^{e}
pH 2	35.78±0.12^{c}	35.74±0.52^{c}	37.60±0.87^{k}	33.18±0.28^{j}	23.10±0.21^{e}	20.10±0.09^{e}
pH 3	35.31±0.07^{c}	34.99±0.14^{c}	36.81±0.18^{k}	31.50±0.19^{i}	20.94±0.13^{e}	15.87±0.54^{c}
pH 4	37.17±0.15^{d}	46.67±0.91^{g}	37.43±0.17^{k}	23.27±0.19^{g}	19.47±0.22^{c}	6.22±1.16^{b}
pH 5	39.40±0.14^{e}	45.45±0.11^{g}	25.38±0.59^{h}	22.47±0.08^{g}	7.24±0.08^{b}	4.58±0.21^{b}
pH 6	40.49±0.34^{e}	47.49±0.09^{g}	19.18±0.70^{f}	19.68±0.09^{f}	4.71±0.14^{b}	4.62±0.09^{b}
pH 7	40.01±0.18^{e}	45.93±0.63^{g}	12.08±0.79^{d}	13.80±0.19^{e}	10.63±0.23^{b}	6.39±0.98^{b}
pH 8	35.98±0.30^{e}	44.98±0.41^{g}	7.87±0.14^{b}	7.61±0.27^{b}	10.00±0.07^{b}	6.12±0.28^{b}
pH 9	32.58±0.08^{b}	42.01±0.20^{f}	7.47±0.31^{b}	2.13±0.32^{a}	7.89±0.15^{b}	6.01±1.19^{b}
pH 10	28.32±0.21^{a}	49.17±0.00^{h}	10.30±0.15^{c}	1.85±0.15^{a}	4.43±0.21^{b}	−4.86±6.82^{a}

Data expressed as mean±standard deviation (n = 3). Different letters indicate significant differences according to Tukey's test ($p \leq 0.05$).

The change in pH caused significant variations in color parameters (L*, a*, b*) in both blackberry and elderberry extracts (Table 4), highlighting the sensitivity of anthocyanins in acidic and alkaline environments. In general, L* values (40.49±0.34 and 47.49±0.09) were higher for elderberry extract, indicating a lighter color compared to blackberry extract, which has darker tones at the same pH values.

The a* parameter had high positive values at acidic pH (37.60±0.87 and 33.18±0.28), especially in the case of blackberry extract, indicating a predominant red hue. As the pH increased, the a* values decreased significantly in both extracts (10.30±0.15 and 1.85±0.15), indicating a color shift towards greenish shades. This behavior is typical of anthocyanins, which in an alkaline environment vary from red to blue-green (Huang et al., 2023; Sganzerla et al., 2021).

The b* parameter showed increases at acidic pH (26.28±0.14 and 22.86±0.09) and decreases at alkaline pH (4.43±0.21 and 4.86±6.82), especially in elderberry extract, suggesting a warmer hue at high acidity and a reduction in the yellow component as pH increases. For elderberry extract, the b* component reaches high values at acidic pH (reddish-purple hue), but decreases sharply in an alkaline environment, indicating a shift towards a bluish-green color.

In both extracts, the variations in L*, a*, and b* show the typical transition of anthocyanins from red-violet colors in an acidic environment to shades of blue, green, or yellow in an alkaline environment. This variation explains the obvious visual differences observed experimentally and confirms the sensitivity of pigments to changes in the reaction environment (Figure 2).

FTIR-ATR (Fourier Transform Infrared Spectroscopy with Attenuated Total Reflectance)

Attenuated total reflectance Fourier transform infrared spectroscopy (FTIR-ATR) is a technique used to identify functional groups characteristic of bioactive compounds and to highlight differences determined by the extraction method and the sample analyzed. A total of 106 samples were analyzed, including 17 extracts obtained with UAE and 36 extracts obtained by MAC for elderberries and blackberries, respectively.

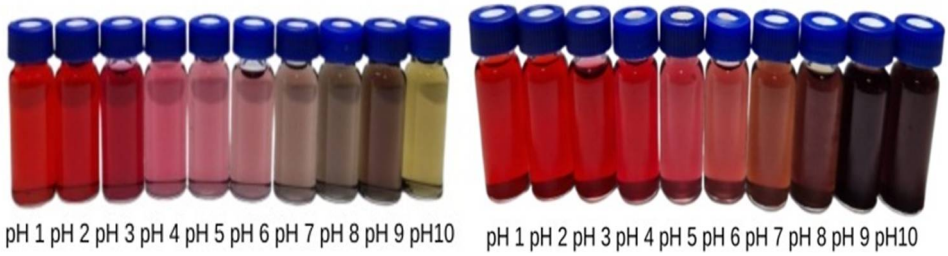

Figure 2. Color variation of elderberry (a) and blackberry (b) extracts depending on pH

The FTIR spectra for elderberry and blackberry extracts, both by UAE and MAC, showed seven wavenumbers in three different spectral regions, namely single bonds (4000–2500 cm^{-1}), double bonds (2000–1500 cm^{-1}), and fingerprint (1500–600 cm^{-1}) (Șuian et al., 2025).

The FTIR spectra of elderberry and blackberry extracts showed similar positions of the absorption bands, regardless of species, indicating the presence of common functional groups; however, the intensity of the bands varied depending on the type of solvent. In the case of extracts obtained with UAE and MAC using 50% and 96% ethanol, seven bands characteristic of both elderberry and blackberry were identified, suggesting a more efficient extraction of bioactive compounds. In contrast, for extracts obtained by MAC using water and 20% ethanol, the FTIR spectra showed only three main absorption bands.

In the first region, the band between 3332–3354 cm^{-1} corresponds to the stretching vibrations of the O–H group, originating from the alcoholic, phenolic, and carboxylic functional groups (Miljanić et al., 2024). The spectral bands between 2979–2974 cm^{-1} correspond to the stretching vibrations of C–H bonds associated with lignin and hemicellulose (Miljanić et al., 2024). A peak in the double bond region is characteristic of the stretching of amides I and II, namely 1644–1651 cm^{-1}, and are associated with the stretching vibrations of carbonyl (C=O) groups in the carboxylic groups of pectin and hemicellulose (Zannou et al., 2022).The 1454-1381 cm^{-1} band characteristic of phosphodiester groups is most likely attributed to carbohydrates, fatty acids, or the amino acid side chain (Hssaini et al. 2022). The band observed around 1085 cm^{-1} can be attributed to C–O and C–N stretching vibrations associated with carbohydrate structures, glycated phenolic compounds, and possibly some protein components present in elderberry and blackberry extracts (Pasieczna-Patkowska et al. 2025; Szaniawska et al. 2025). The bands at 1043 cm^{-1} and 951–877 cm^{-1} are characteristic of C–O and C–C stretching vibrations of flavonoids and phenolic compounds (Cvetković et al., 2025b; Marija et al., 2024).

Phenolic content of elderberry and blackberry extracts

Total anthocyanin content

Anthocyanins are natural pigments belonging to the flavonoid class, soluble in water, with antioxidant and antibacterial properties (Petruskevicius et al., 2023; Zhao et al., 2022). An essential aspect relevant to the present study is the sensitivity of anthocyanin color to pH variations, a characteristic that promotes their use in various applications, such as freshness

indicators for food monitoring (Barros et al., 2024; Cuesta-Riaño et al., 2022; Huang et al., 2025; Khezerlou et al., 2023; Sani et al., 2021). In this context, determining the anthocyanin content of elderberries and blackberries is necessary to assess the potential of these fruits for use in such systems.

The total anthocyanin content (TAC), expressed as mg C3G/100 g FW, varied significantly depending on the fruit source, extraction method, and solvent. Regarding the extraction method, the highest TAC values were obtained using maceration (MAC), with mean±SD concentrations (n = 36) of 138.67±32.23 mg C3G/100 g FW for blackberry and 657.23±51.61 mg C3G/100 g FW for elderberry. In contrast, ultrasound-assisted extraction (UAE) yielded mean±SD values (n = 17) of 107.79±8.15 mg C3G/100 g FW for blackberry and 576.73±28.39 mg C3G/100 g FW for elderberry.

Overall, elderberry consistently exhibited higher anthocyanin concentrations than blackberry regardless of the extraction method. This trend is consistent with previous studies, which reported TAC values ranging from 78 to 234 mg C3G/100 g for blackberries and from 220 to 1413 mg C3G/100 g for elderberries (Csorba et al., 2020; Dogan et al., 2025; Kolarov et al., 2021). Variations in TAC among studies can be attributed to differences in species and cultivar, geographical origin and environmental growing conditions, fruit ripeness, light exposure, postharvest handling, as well as extraction procedures and analytical methods (Mattioli et al., 2020).

Depending on the solvent and extraction time during maceration (MAC), the lowest TAC values were obtained with water (0% ethanol), ranging from 88.91 to 117.00 mg C3G/100 g FW for blackberries and from 565.63 to 606.24 mg C3G/100 g FW for elderberries. Hydroethanolic solvents (20%, 50%, and 96% ethanol) were more effective, with TAC increasing as the ethanol concentration increased. The highest values were achieved after 24 h of extraction with 96% ethanol, reaching 196.69 mg C3G/100 g FW for blackberries and 742.84 mg C3G/100 g FW for elderberries.

Under ultrasound-assisted extraction (UAE), the highest anthocyanin content in blackberries (118.61 mg C3G/100 g FW) was obtained after 15 min at 40 °C and 110 W, indicating that moderate temperature combined with high ultrasonic power promoted anthocyanin extraction. For elderberries, significantly higher values were observed, with a maximum TAC of 636.92 mg C3G/100 g FW after 20 min at 40 °C and 140 W.

These findings are consistent with previous studies demonstrating the superior efficiency of ethanol–water mixtures for anthocyanin extraction. Zhang et al. (2022) reported that increasing the ethanol concentration from 60% to 80% significantly enhanced anthocyanin recovery from blackberries, with a maximum value of 0.61±0.02 mg C3G/g, whereas a further increase to 100% did not improve extraction efficiency. Similarly, Marchenko et al. (2024) observed the highest anthocyanin concentration (0.29±0.02%, expressed as cyanidin-3-O-glucoside equivalents) when 96% ethanol was used as the extraction solvent.

The higher extraction efficiency of hydroethanolic solvents can be attributed to their optimal polarity, which improves anthocyanin solubility and enhances mass transfer from the plant matrix. Ethanol also facilitates cell wall disruption and increases solvent penetration into plant tissues, thereby promoting the release of anthocyanins (Pascariu and Israel-Roming, 2022).

The 2FI and Quadratic models were used to predict the total anthocyanin content. equations (6) and (7) describe the Quadratic model, while equations (8) and (9) correspond to the 2FI model for blackberries and elderberries, respectively.

$$TAC_{BB} = 116.43 + 1.77 \cdot X_1 + 4.48 \cdot X_2 + 3.18 \cdot X3 - 0.2502 \cdot X_1X_2 + 1.45 \cdot X_1X_3 + 3.58 \cdot X_2X_3 - 3.24 \cdot X_1^2 - 11.69 \cdot X_2^2 - 3.43 \cdot X_3^2 \quad (6)$$

$$TAC_{EB} = 573.49 + 2.15 \cdot X_1 + 10.44 \cdot X_2 + 12.37 \cdot X_3 - 0.6048 \cdot X_1 \cdot X_2 + 2.32 \cdot X_1 \cdot X_3 + 6.76 \cdot X_2 \cdot X_3 + 18.46 \cdot X_1^2 - 38.45 \cdot X_2^2 + 26.88 \cdot X_3^2 \quad (7)$$

$$TAC_{BB} = 149.64 + 40.78 \cdot Y_1 + 7.54 \cdot Y_2 - 2.51 \cdot Y_1Y_2 - 6.14 \cdot Y_1^2 - 1.39 \cdot Y_2^2 \quad (8)$$

$$TAC_{EB} = 704.28 + 56.30 \cdot Y_1 + 27.44 \cdot Y_2 + 12.47 \cdot Y_1Y_2 - 48.87 \cdot Y_1^2 - 11.28 \cdot Y_2^2 \quad (9)$$

where TAC_{BB} is total anthocyanin concentration in the blackberry extract; TAC_{EB} is total anthocyanin concentration in the elderberry extract; X_1 is coded factor representing extraction time (min); X_2 is coded factor representing extraction temperature (°C); X_3 is coded factor representing ultrasonic power (W); Y_1 is coded factor representing solvent concentration (%); Y_2 is coded factor representing extraction time (h); X_1X_2, X_1X_3, X_2X_3, Y_1Y_2 are interaction effects between factors.

According to equation (6), in the case of blackberry extract with UAE, the most pronounced positive effect on the total anthocyanin content is attributed to the linear factor X_2 (temperature), followed by the interaction between factors X_2 and X_3 (temperature and ultrasonic power), suggesting a favorable synergistic effect between these factors. On the other hand, the most significant negative influence is associated with the quadratic factor X_2 (temperature), followed by the quadratic factor X_3 (ultrasonic power), reflecting the sensitivity of anthocyanins to high temperatures, as well as the potential negative effect of ultrasonic power on their stability. In the case of blackberry extract extracted by MAC, according to equation (8), the term Y_1 (solvent concentration) has the greatest positive effect, followed by Y_2 (extraction time). At the same time, the quadratic factor Y_1 (solvent concentration) is responsible for the greatest negative effect.

Regarding the elderberry extract with UAE, equation (7), the strongest positive influence is given by the linear factor X_3 (ultrasonic power), followed by the quadratic factor X_3. On the other hand, the greatest negative influence is represented by the quadratic factor X_2 (temperature). The results confirm the instability of anthocyanins under high temperature conditions, as well as the positive influence of ultrasonic power. For the elderberry extract extracted by MAC, equation (9), the linear term Y_1 (concentration) has the greatest positive effect, followed by the linear factor Y_2 (time). The negative influences are given by the quadratic factor Y_1 (solvent concentration), followed by the quadratic factor Y_2 (time), indicating a high sensitivity of the compounds to these variables.

Total polyphenol content

Polyphenols are compounds that contribute to inhibiting oxidative reactions and extending the shelf life of foods when incorporated into smart packaging films. Increased levels of polyphenols suggest high efficiency for packaging (Dutta et al., 2025; Pan et al., 2024).

The total polyphenol content (TPC) was expressed as mg GAE/100 g FW. In terms of extraction method, the elderberry samples extracted by MAC showed the highest value, the mean±SD (n = 36) was 601.35±48.27 mg GAE/100 g FW, compared to extraction by UAE, where the mean±SD (n = 17) was 184.24±14.57 mg GAE/100 g FW. In the case of blackberry extract obtained by MAC, the mean±SD (n = 36) was 287.90±45.58 mg GAE/100 g FW, while UAE yielded a significantly higher mean±SD (n = 17) of 343.30±46.32 mg GAE/100 g FW.

Depending on the solvent used and the extraction time in the MAC, the lowest values were obtained using water (0%). The concentration ranged from 205.23 to 241.65 mg GAE/100 g FW for blackberries and 444.68 to 601.94 mg GAE/100 g FW for elderberries. Hydroalcoholic solvents (20%, 50%, and 96%) were more effective, with maximum polyphenol concentrations of 368.97 mg GAE/100 g FW and 682.21 mg GAE/100 g FW obtained with 50% ethanol (v/v) for 24 h, both for blackberries and elderberries.

Under UAE conditions, the highest TPC value for blackberry extract was 195.14 mg GAE/100 g FW, obtained at 15 min, 40 °C, and 110 W, indicating that a moderate temperature combined with high ultrasonic power favors polyphenol extraction. In the case of elderberry, significantly higher values were observed, reaching a maximum of 428.50 mg GAE/100 g FW at 20 min, 40 °C, and 140 W.

Compared with previously published data on elderberries, the total phenolic content (TPC) obtained in the present study falls within the broad range reported in the literature. For example, Papagrigoriou et al. (2023) reported TPC values ranging from 86.75 to 306.37 mg GAE/100 g FW, whereas Kan (2019) found values between 360 and 447 mg GAE/100 g FW. Considerably higher TPC values were reported by Rodríguez et al. (2023) (43.8 mg GAE/g DW) and Goud and Prasad (2020) (43.0±0.98 mg GAE/g DW).

According to the literature, the total phenolic content (TPC) of fresh blackberries is generally comparable to the values obtained in the present study. For example, Kukrić et al. (2020) reported TPC values ranging from 2.16 to 2.25 mg GAE/g FW (equivalent to approximately 216–225 mg GAE/100 g FW). In contrast, studies employing conventional maceration with prolonged extraction times have reported substantially higher TPC values. Qader and Yaman (2023) determined a TPC of 38.08 mg GAE/g in blackberry extracts, while Čechovičienė et al. (2024) reported 2380.60±15.10 mg GAE/100 g DW following 24 h maceration. Similarly, Demir (2023) found a TPC of 2132.66 mg GAE/100 g DW. These differences can be attributed to several factors, including the expression of results on a fresh- or dry-weight basis, as well as differences in blackberry species or cultivar, fruit maturity, climatic and growing conditions, extraction procedures, solvent composition, and analytical methodology.

The 2FI and Quadratic models were used to predict the total polyphenol content. equations (10) and (11) describe the Quadratic model, while equations (12) and (13) correspond to the 2FI model for blackberries and elderberries, respectively.

$$TPC_{BB} = 196.85 + 0.9897 \cdot X_1 - 15.45 \cdot X_2 + 1.21 \cdot X_3 + 2.01 \cdot X_1X_2 - 4.41 \cdot X_1X_3 + 0.0138 \cdot X_2X_3 - 4.50 \cdot X_1^2 - 15.06 \cdot X_2^2 - 7.24 \cdot X_3^2 \quad (12)$$

$$TPC_{EB} = 348.51 - 0.2822 \cdot X_1 + 34.92 \cdot X_2 + 37.59 \cdot X_3 - 2.65 \cdot X_1X_2 + 4.54 \cdot X_1X_3 - 13.48 \cdot X_2X_3 + 23.64 \cdot X_1^2 - 47.45 \cdot X_2^2 + 12.75 \cdot X_3^2 \quad (13)$$

$$TPC_{BB} = 347.17 + 37.81 \cdot Y_1 + 18.26 \cdot Y_2 + 7.14 \cdot Y_1Y_2 - 77.53 \cdot Y_1^2 - 9.71 \cdot Y_2^2 \quad (14)$$

$$TPC_{EB} = 665.38 - 12.75 \cdot Y_1 + 24.21 \cdot Y_2 - 6.63 \cdot Y_1Y_2 - 94.09 \cdot Y_1^2 - 11.19 \cdot Y_2^2 \quad (15),$$

where TPC_{BB} is total polyphenol concentration in the blackberry extract; TPC_{EB} is total polyphenol concentration in the elderberry extract; X_1 is coded factor representing extraction time (min); X_2 is coded factor representing extraction temperature (°C); X_3 is coded factor representing ultrasonic power (W); Y_1 is coded factor representing solvent concentration (%); Y_2 is coded factor representing extraction time (h); X_1X_2, X_1X_3, X_2X_3, Y_1Y_2 are interaction effects between factors.

For blackberry extract with UAE, equation (10), the interaction between factors X_1X_2 (extraction time and temperature) has the greatest positive effect, favoring polyphenol

extraction, while the quadratic factor X_2^2 (temperature) had a negative effect, highlighting the thermal sensitivity of the compound. In the case of the extract obtained by MAC, equation (12), the linear factor Y_1 (solvent concentration) has the greatest positive influence, and the negative effect is given by the quadratic factor Y_1^2 (solvent concentration). This indicates that there is an optimal solvent concentration above which the extraction efficiency decreases.

Regarding the elderberry extract with UAE, equation (11) the greatest positive effect is given by the linear factor X_3 (ultrasonic power), followed by X_2 (temperature), indicating increased UAE efficiency at higher temperatures; however, the quadratic term X_2^2 (extraction temperature) had a negative impact, indicating the existence of an optimal extraction temperature.

For the extract obtained by MAC, equation (13), the linear term Y_2 (temperature) exerted a positive effect on the extraction process, whereas the quadratic term Y_1^2 (extraction time) showed the strongest negative effect. These results indicate a favorable influence of temperature on the extraction efficiency and the existence of an optimal extraction time.

Total flavonoid content

Flavonoids are natural polyphenolic compounds with antimicrobial and antioxidant activity that provide hydrogen atoms that neutralize free radicals, reducing the occurrence of oxidation reactions. These characteristics confer a significant role as freshness indicators used for food monitoring. In addition, some flavonoids absorb UV radiation, contributing to the protection of photosensitive products and the stability of packaging films (Chandran et al., 2024; Liu et al., 2025; Zhang W. et al., 2025).

The total flavonoid content (TFC) was expressed in mg QE/100 g FW. Based on the extraction method, the highest values were obtained with MAC, where the total flavonoid concentration, mean±SD (n = 36) was 494.38±38.45 mg QE/100 g FW and 1140.59±31.26 mg QE/100 g FW, with a significantly higher value for elderberry extract compared to blackberries. Extraction by UAE had a lower efficiency, the mean±SD (n = 17) was 418.39±19.91 mg QE/100 g FW and 798.50±47.45 mg QE/100 g FW, the concentrations obtained for the elderberry extract also being higher.

Depending on the solvent and extraction time, the samples obtained by maceration showed different behaviors for the two matrices analyzed. In the case of elderberry, the highest flavonoid content values were obtained in water (0%), ranging from 1169.15 mg QE/100 g FW to 1191.96 mg QE/100 g FW, indicating a higher solubility of the compounds in an aqueous medium. For blackberries, the maximum extraction efficiency was recorded with the hydroalcoholic solvent of 50% ethanol, where the highest concentrations (548.50 mg QE/100 g FW) were observed. In both matrices, increasing the ethanol percentage above 50% led to a progressive decrease in extraction efficiency, with the lowest values obtained at a concentration of 96% ethanol at all three time intervals (6h, 12h, and 24h). At UAE, the highest flavonoid content for blackberries (458.39 mg QE/100 g FW) was obtained at 15 minutes, 50 °C, and 140 W. In the case of elderberries, the values were significantly higher, reaching a maximum of 850.90 mg QE/100 g FW at 15 minutes, 40 °C, and 110 W, indicating that maximum extraction can be achieved a moderate parameters. The literature indicates that both blackberries and elderberries are important sources of flavonoids, but the reported levels vary considerably depending on species, genotype, degree of ripeness, and extraction conditions. In the case of blackberries, Dogan et al. (2025) reported total flavonoid content values ranging from 158.40 to 868.13 mg QE/100 g FW, highlighting significant variability between genotypes (Dogan et al., 2025). The values are close to those reported in the present

study. Regarding studies based on the extraction method, Sik et al., in a recent study, showed that ultrasound-assisted extraction with hydroalcoholic solvent leads to a flavonoid content of approximately 5.78 mg QE/g DW in blackberry extracts, confirming the efficiency of the method in flavonoid extraction (Sik et al., 2024).

For elderberries, the TFC values reported in the literature are generally higher than those for blackberries. The values determined in this study fall within the ranges reported by previous studies for elderberries, indicating good agreement with scientific research and supporting the validity of the experimental approach used. Thus, Papagrigoriou et al. (2023) reported total flavonoid values that can exceed 189.34 mg QE/100 g FW for certain elderberry genotypes, while Kolarov et al. (2021) reported higher values, exceeding 8.09 mg QE/g FW, for wild elderberries. In addition, studies comparing extraction methods have shown that elderberry extracts obtained by maceration yielded higher values than those obtained by ultrasound-assisted extraction (Radojković et al., 2021).

The 2FI and Quadratic models were used to predict the total flavonoid content. equations (14) and (15) describe the 2FI model, while equations (16) and (17) correspond to the Quadratic model for blackberries and elderberries, respectively.

$$TFC_{BB} = 418.62 - 0.8022 \cdot X_1 + 19.95 \cdot X_2 + 16.55 \cdot X_3 - 0.2209 \cdot X_1X_2 - 3.87 \cdot X_1X_3 + 11.34 \cdot X_2X_3 + 4.54 \cdot X_1^2 - 2.41 \cdot X_2^2 - 2.62 \cdot X_3^2 \quad (14)$$

$$TFC_{EB} = 848.82 + 2.51 \cdot X_1 + 21.90 \cdot X_2 + 5.02 \cdot X_3 + 3.49 \cdot X_1X_2 - 0.3996 \cdot X_1X_3 + 2.75 \cdot X_2X_3 - 0.1617 \cdot X_1^2 - 81.52 \cdot X_2^2 - 25.24 \cdot X_3^2 \quad (15)$$

$$TFC_{BB} = 546.27 + 33.62 \cdot Y_1 + 20.87 \cdot Y_2 - 2.30 \cdot Y_1Y_2 - 60.78 \cdot Y_1^2 - 16.83 \cdot Y_2^2 \quad (16)$$

$$TFC_{EB} = 1127.88 - 34.32 \cdot Y_1 + 16.26 \cdot Y_2 + 6.94 \cdot Y_1Y_2 + 24.35 \cdot Y_1^2 - 6.38 \cdot Y_2^2 \quad (17),$$

where: TFC_{BB} is total flavonoid concentration in the blackberry extract; TFC_{EB} is total flavonoid concentration in the elderberry extract; X_1 is coded factor representing extraction time (min); X_2 is coded factor representing extraction temperature (°C); X_3 is coded factor representing ultrasonic power (W); Y_1 is coded factor representing solvent concentration (%); Y_2 is coded factor representing extraction time (h); X_1X_2, X_1X_3, X_2X_3, Y_1Y_2 are interaction effects between factors.

The flavonoid content in blackberry extract obtained by UAE equation (14), is positively influenced by the linear factor X_2 (temperature), followed by the linear factor X_3 (solvent concentration). Meanwhile, the strongest negative effect is associated with the interaction between factors X_1X_3 (time, solvent concentration), indicating a high sensitivity of flavonoid compounds to the combined effect of these variables. In the case of the extract obtained by MAC equation (16), the linear term Y_1 (solvent concentration) exhibits a strong positive effect, whereas the quadratic term Y_1^2 (solvent concentration) has a negative influence.

For the elderberry extract obtained by UAE equation (15), the linear factor X_2 (temperature) has the greatest positive influence, indicating a favorable effect on flavonoid content. Meanwhile, the quadratic factor X_2^2 (temperature) shows a negative effect, suggesting that there is an optimal extraction temperature. The elderberry extract obtained by MAC equation (17), shows that the quadratic term Y_1^2 (solvent concentration) has the strongest positive influence on extraction, whereas the linear term Y_1 (solvent concentration) has the greatest negative influence.

Antioxidant activity (DPPH)

The antioxidant capacity of the two fruits was determined using the DPPH method, based on spectrophotometric measurements of the ability of bioactive compounds

(anthocyanins, polyphenols, flavonoids) to eliminate DPPH (2,2-diphenyl-1-picrylhydrazyl) free radicals (Pusty et al., 2024).

In relation to the extraction method, the highest values for antioxidant activity were obtained at MAC, with a mean±SD (n = 36) of 87.12%±2.56 and 72.20%±1.47, and for UAE, the mean±SD (n = 17) was 89.89%±2.64 and 61.68%±4.52, with the concentrations obtained for blackberries being higher than those for elderberries in both extraction methods.

Depending on the solvent and extraction time at MAC, the lowest values for antioxidant activity were obtained in ethanol (50%) with values between 86.15% and 87.09% for blackberries and ethanol (20%) with values between 67.21% and 69.31% for elderberries. Under UAE, the highest antioxidant activity for blackberries (93.67%) was obtained at 15 minutes, 30 °C, and 140 W, which shows that a low temperature, medium extraction time, and high ultrasonic power favor extraction. In the case of elderberries, the values were significantly lower, reaching a maximum of 75.75% under the same conditions: 15 minutes, 30 °C, and 140 W. Comparatively, blackberry extracts showed much higher concentrations than elderberries under all extraction conditions, indicating higher antioxidant activity.

Antioxidant activity determined by the DPPH assay for blackberry and elderberry extracts was significantly influenced by both the extraction method and the solvent used. The results obtained in the present study are consistent with previous reports. For example, Marțiș et al. (2021), who evaluated the antioxidant capacity of different elderberry species, reported DPPH radical scavenging activity ranging from 30.58% to 89.04%. Similarly, Floares et al. (2013) found that hydroalcoholic extracts exhibited higher antioxidant activity (29.40–74.79% inhibition) than aqueous extracts (12.56–68.61%). The same study also demonstrated that ultrasound-assisted extraction yielded higher antioxidant activity (15.02–67.49% inhibition) than conventional extraction (12.56–66.29% inhibition). These findings are in agreement with the results of the present study, confirming the positive effect of hydroalcoholic solvents and ultrasound-assisted extraction on the recovery of antioxidant compounds.For blackberry extracts, Gil-Martínez et al. (2023) obtained a value of approximately 97.1±2.4% for the DPPH radical inhibition percentage, a result close to the values obtained in the present study. Values close to those in the present study were also reported in the research conducted by Pucel et al. (2021), who obtained an inhibition percentage between 41–82%.

The 2FI and Quadratic models were used to predict antioxidant activity. equations (18) and (19) describe the 2FI model, while equations (20) and (21) correspond to the Quadratic model for blackberries and elderberries, respectively.

$$DPPH_{BB} = 87.49 + 0.3160 \cdot X_1 - 3.40X_2 + 1.07 \cdot X_3 - 0.1243 \cdot X_1X_2 - 0.0444 \cdot X_1X_3 + 0.3293 \cdot X_2X_3 + 0.0425\ X_1^2 - 1.26 \cdot X_2^2 - 0.0611 \cdot X_2 \quad (18)$$

$$DPPH_{EB} = 72.01 + 0.2472 \cdot X_1 - 1.91 \cdot X_2 + 0.5238 \cdot X_3 - 0.1207 \cdot X_1X_2 - 0.0865\ X_1X_3 - 0.4161 \cdot X_2X_3 - 0.3150 \cdot X_1^2 + 0.7593 \cdot X_2^2 - 0.0354 \cdot X_3^2 \quad (19)$$

$$DPPH_{BB} = 82.90 + 4.88 \cdot Y_1 + 2.60 \cdot Y_2 + 0.7908 \cdot Y_1Y_2 - 12.59 \cdot Y_1^2 - 0.4082 \cdot Y_2^2 \quad (20)$$

$$DPPH_{EB} = 66.07 + 2.07 \cdot Y_1 + 2.65 \cdot Y_2 - 3.66 \cdot Y_1\ Y_2 - 5.07 \cdot Y_1^2 - 1.13 \cdot Y_2^2 \quad (21)$$

where $DPPH_{BB}$ is antioxidant activity of the blackberry extract; $DPPH_{EB}$ is antioxidant activity of the elderberry extract; X_1 is coded factor representing extraction time (min); X_2 is coded factor representing extraction temperature (°C); X_3 is coded factor representing ultrasonic power (W); Y_1 is coded factor representing solvent concentration (%); Y_2 is coded factor representing extraction time (h); X_1X_2, X_1X_3, X_2X_3, Y_1Y_2 are interaction effects between factors.

For blackberry extract with UAE, equation (18), linear factor X_3 (solvent concentration) has the greatest positive effect on antioxidant activity, and linear factor X_2 (temperature) has the greatest negative effect, which highlights reduced antioxidant activity at high temperatures. In the case of the extract obtained by MAC, equation (20), the linear factor Y_2 (solvent concentration) has the greatest positive influence, and the negative effect is given by the quadratic factor Y_2^2 (solvent concentration). This indicates that there is an optimal solvent concentration above which the extraction efficiency decreases.

Regarding the elderberry extract with UAE, equation (19), the greatest positive effect is given by the linear factor X_3 (ultrasonic power), indicating an increased efficiency of the ultrasonic power. Meanwhile, the linear term X_2 (extraction temperature) had a negative impact, indicating an influence of temperature on antioxidant activity.

For the extract obtained by MAC, equation (21), the linear term Y_2 (temperature) had a positive effect on the extraction process, while the quadratic factor Y_1^2 (time) had a negative effect. These results indicate a favorable effect of temperature on antioxidant activity and the existence of an optimal extraction time.

Individual polyphenol content by HPLC

The content of individual polyphenols in elderberry (EB) and blackberry (BB) extracts obtained using solvents with different polarities (water, 20%, 50%, and 96% ethanol) was determined by HPLC at wavelengths of 280 and 320 nm. The results are expressed in mg/100 g and show a clear influence of the solvent on the extraction efficiency of phenolic compounds (Table 5).

Table 5

Profile of individual polyphenols in elderberry (EB) extract (mg/100 g)

Compound	Extraction with			
	Water	Ethanol 20%	Ethanol 50%	Ethanol 96%
Elderberry extract				
Protocatechuic acid	2.64	4.71	n.d	n.d
p-Hydroxybenzoic acid	505.82	502.08	554.12	401.66
Vanillic acid	17.16	15.36	25.94	3.31
Caffeic acid	10.34	43.24	4.34	9.51
Quercetin	0.04	0.08	1.15	11.37
Blackberry extract				
Protocatechuic acid	1.38	1.98	n.d	n.d
p-Hydroxybenzoic acid	157.73	180.91	155.02	129.62
Vanillic acid	4.10	8.28	7.32	1.64
Caffeic acid	0.06	0.07	1.08	0.94
Quercetin	0.00	0.33	0.74	0.35

n.d – not detected

Protocatechuic acid was detected only in water and 20% ethanol extracts, reaching its highest level in 20% ethanol. p-Hydroxybenzoic acid was the dominant compound across all solvents, with maximum extraction in 50% ethanol. Vanillic and caffeic acids were present in moderate amounts, with 20–50% ethanol generally enhancing their extraction, whereas 96% ethanol reduced the levels of most phenolic compounds. In contrast, quercetin

was most abundant in 50% and 96% ethanol extracts, indicating higher affinity for lower-polarity solvents.

In the case of blackberry extracts, protocatechuic acid was also identified only in extracts obtained with water and 20% ethanol, with the maximum value recorded at 20% ethanol, being absent in extracts obtained with 50% and 96% ethanol. The polyphenolic profile was dominated by p-hydroxybenzoic acid, with higher values in extracts obtained with water and 20% ethanol. Vanillic and caffeic acids were present in lower concentrations, while quercetin was detected in small amounts in all samples, with the highest values observed in hydroalcoholic extracts.

Evaluation of the extraction process

The extraction of bioactive compounds was performed using the ultrasound-assisted extraction (UAE) and maceration (MAC) methods, and their efficiency was evaluated based on the DPPH, TAC, TPC, and TFC parameters (Table 6).

Table 6

Influence of extraction method on the antioxidant properties of elderberry and blackberry extracts (DPPH), total anthocyanin content, total polyphenol content, and total flavonoid content

Extraction methods	DPPH %		TAC mg C3G/100g FW		TPC mg GAE/100 g FW		TFC mg QE/100g FW	
	BB	EB	BB	EB	BB	EB	BB	EB
MAC	74.30 ±6.88	61.68 ±4.59	138.68 ±32.23	657.23 ±51.61	287.90 ±45.58	601.35 ±48.27	491.93 ±40.71	1140.59 ±31.26
UAE	89.89 ±2.63	72.20 ±1.49	107.79 ±8.15	576.73 ±28.39	184.24 ±14.57	343.30 ±46.32	418.39 ±19.91	798.50 ±47.45

Values are expressed as mean±standard deviation (SD), calculated based on experimental replicates generated using Design-Expert software, with the number of replicates varying according to the experimental conditions.

The highest antioxidant activity (DPPH) was obtained by UAE (72.20% for EB and 89.89% for BB), while the MAC method led to the highest values of total anthocyanin, polyphenol, and flavonoid content for both blackberries (TAC: 138.68 mg C3G/100 g FW; TPC: 287.90 mg GAE/100 g FW; TFC: 491.93 mg QE/100 g FW), and for elderberries (TAC: 657.23 mg C3G/100 g FW; TPC: 601.35 mg GAE/100 g FW; TFC: 1140.59 mg QE/100 g FW). These results indicate that the optimal method for compound extraction is MAC, and for antioxidant activity, UAE is more effective.

The influence of extraction time on antioxidant properties showed similar trends for both fruits analyzed, blackberries (BB) and elderberries (EB), in both UAE and MAC (Table 7).

For UAE, increasing the extraction time from 10 to 20 min led to maximum antioxidant activity (DPPH) values at 20 min for both extracts (90.19% for BB and 72.30% for EB) and the highest anthocyanin, polyphenols, and flavonoids contents (TAC: 107.40 mg C3G/100 g FW for BB and 588.31 mg C3G/100 g FW for EB; TPC: 182.19 mg GAE/100 g FW for BB and 354.52 mg GAE/100 g FW for EB; TFC: 419.85 mg QE/100 g FW for BB and 797.79 mg QE/100 g FW for EB). In the case of MAC, extending the extraction time from 6 h to 24 h resulted in a progressive increase in the phenolic compound content for both fruits, with

the highest values obtained at 24 h for blackberries (TAC: 147.02 mg C3G/100 g FW; TPC: 304.24 mg GAE/100 g FW; TFC: 510.48 mg QE/100 g FW) and for elderberries (TAC: 682.50 mg C3G/100 g FW; TPC: 625.94 mg GAE/100 g FW; TFC: 1155.73 mg QE/100 g FW), while DPPH antioxidant activity reached maximum values at 12 h for both extracts.

Table 7

Influence of extraction time on the antioxidant properties of elderberry and blackberry extracts (DPPH), total anthocyanin content, total polyphenol content, and total flavonoid content

Extraction time	DPPH %		TAC mg C3G/100g FW		TPC mg GAE/100 g FW		TFC mg QE/100g FW	
	BB	EB	BB	EB	BB	EB	BB	EB
10 min UAE	89.55 ±2.67	71.81 ±1.51	103.85 ±5.43	584.01 ±38.27	180.22 ±15.15	355.08 ±59.74	421.45 ±25.28	792.76 ±37.62
15 min UAE	89.90 ±2.83	72.33 ±1.55	109.71 ±9.41	568.35 ±16.25	186.94 ±16.29	333.09 ±38.52	416.39 ±19.31	801.37 ±58.55
20 min UAE	90.19 ±2.89	72.30 ±1.72	107.40 ±7.51	588.31 ±40.85	182.19 ±12.07	354.52 ±57.03	419.85 ±21.29	797.79 ±37.20
6 h MAC	71.96 ±6.19	58.55 ±5.10	131.26 ±34.29	631.00 ±43.32	269.65 ±41.07	575.72 ±39.20	468.12 ±38.70	1125.08 ±33.71
12 h MAC	73.99 ±6.64	61.66 ±3.33	137.75 ±32.67	658.20 ±41.49	289.81 ±43.05	602.40 ±45.97	497.20 ±35.48	1140.97 ±29.68
24 h MAC	76.29 ±7.84	64.84 ±2.87	147.02 ±30.43	682.50 ±58.56	304.24 ±49.10	625.93 ±48.86	510.48 ±38.64	1155.72 ±24.07

Values are expressed as mean±standard deviation (SD), calculated based on experimental replicates generated using Design-Expert software, with the number of replicates varying according to the experimental conditions.

The influence of the extraction solvent on antioxidant properties showed significant differences for both fruits analysed, blackberries (BB) and elderberries (EB) (Table 8).

Table 8

Influence of solvent concentration on the antioxidant properties of elderberry and blackberry extracts (DPPH), total anthocyanin content, total polyphenol content, and total flavonoid content

Solvent concentration	DPPH %		TAC mg C3G/100g FW		TPC mg GAE/100 g FW		TFC mg QE/100g FW	
	BB	EB	BB	EB	BB	EB	BB	EB
Water	65.41 ±1.86	57.24 ±5.25	99.24± 10.53	588.75 ±17.23	226.25 ±13.50	572.29 ±22.69	435.50 ±19.16	1181.78 ±10.02
Ethanol 20%	74.22 ±2.48	62.25 ±5.07	124.72 ±6.45	646.19 ±15.67	285.07 ±14.72	630.73 ±28.28	495.73 ±28.05	1148.74 ±8.42
Ethanol 50%	83.17 ±3.10	64.80 ±1.64	147.59 ±8.73	694.45 ±31.73	343.20 ±19.36	653.54 ±23.90	530.72 ±16.71	1121.22 ±16.30
Ethanol 96%	74.39 ±3.26	62.44 ±1.37	183.15 ±5.82	699.54 ±33.44	297.08 ±22.29	548.84 ±14.92	505.76 ±17.68	1110.63 ±20.54

Values are expressed as mean±standard deviation (SD), calculated based on experimental replicates generated using Design-Expert software, with the number of replicates varying according to the experimental conditions.

Compared with water, hydroethanolic solvents significantly enhanced the extraction of bioactive compounds and antioxidant activity. The highest DPPH radical scavenging activity, total phenolic content (TPC), and total flavonoid content (TFC) were generally obtained using 50% ethanol for both blackberries (DPPH: 83.17%; TPC: 343.20 mg GAE/100 g FW; TFC: 530.72 mg QE/100 g FW) and elderberries (TPC: 653.54 mg GAE/100 g FW; TFC: 1121.22 mg QE/100 g FW). In contrast, the maximum total anthocyanin content (TAC) was achieved with 96% ethanol, reaching 183.15 mg C3G/100 g FW for blackberries and 699.54 mg C3G/100 g FW for elderberries. These findings demonstrate that extraction efficiency depends on the chemical characteristics of the target compounds and the composition of the extraction solvent. Under the conditions evaluated, 50% ethanol was the most effective solvent for maximizing antioxidant activity, total phenolic content, and total flavonoid content, whereas 96% ethanol provided the highest recovery of anthocyanins.

Table 9 presents the influence of extraction temperature on the antioxidant properties of extracts obtained by UAE showed similar trends for blackberries (BB) and elderberries (EB).

Table 9

Influence of extraction temperature on the antioxidant properties of elderberry and blackberry extracts (DPPH), total anthocyanin content, total polyphenol content, and total flavonoid content

Temperature	DPPH %		TAC mg C3G/100g FW		TPC mg GAE/100 g FW		TFC mg QE/100g FW	
	BB	EB	BB	EB	BB	EB	BB	EB
30 °C	92.62 ±0.79	74.50 ±0.97	96.92 ± 1.25	547.26 ±4.50	191.37 ±2.00	284.33 ±37.82	397.22 ±4.23	732.69 ±14.93
40 °C	90.48 ±0.79	71.85 ±0.41	113.46 ±4.88	579.37 ±31.03	191.63 ±7.07	364.68 ±36.35	419.48 ±13.19	837.53 ±14.08
50 °C	85.82 ±1.29	70.69 ±0.27	105.88 ±5.50	568.15 ±17.85	160.48 ±3.23	354.18 ±17.98	437.13 ±23.74	776.50 ±16.40

Values are expressed as mean±standard deviation (SD), calculated based on experimental replicates generated using Design-Expert software, with the number of replicates varying according to the experimental conditions.

Increasing the temperature from 30 °C to 50 °C caused a progressive decrease in antioxidant activity (DPPH) for both extracts, with maximum values obtained at 30 °C (92.62% for BB and 74.50% for EB). Regarding phenolic compounds, the total anthocyanin (TAC) and flavonoid (TFC) content increased with temperature, reaching maximum values at 50 °C for both blackberries (TAC: 105.88 mg C3G/100 g FW; TFC: 437.13 mg QE/100 g FW), and for elderberries (TAC: 568.15 mg C3G/100 g FW; TFC: 776.50 mg QE/100 g FW), while the total polyphenol content (TPC) showed maximum values at 40 °C for both extracts (191.63 mg GAE/100 g FW for BB and 364.68 mg GAE/100 g FW for EB). These results indicate that the optimal extraction temperature by UAE depends on the target compound, with lower temperatures favoring antioxidant activity and higher temperatures improving the extraction of anthocyanins and flavonoids.

The variation in ultrasonic power significantly influenced the antioxidant properties of blackberry (BB) and elderberry (EB) extracts obtained by UAE as shown in Table 10.

Increasing ultrasonic power from 80 to 140 W led to a corresponding increase in antioxidant activity (DPPH) for both extracts, with the highest values recorded at 140 W (90.89% for blackberries and 72.72% for elderberries). A similar trend was observed for total anthocyanin content (TAC), total phenolic content (TPC), and total flavonoid content (TFC),

which increased with increasing ultrasonic power. The maximum values were obtained at 140 W for both blackberries (TAC: 108.71 mg C3G/100 g FW; TPC: 181.05 mg GAE/100 g FW; TFC: 433.62 mg QE/100 g FW) and elderberries (TAC: 602.74 mg C3G/100 g FW; TPC: 386.95 mg GAE/100 g FW; TFC: 787.75 mg QE/100 g FW). These findings suggest that, under the conditions investigated, 140 W provides the most effective ultrasonic power level for enhancing the extraction of phenolic compounds and improving the antioxidant properties of both berry extracts.

Table 10

Influence of ultrasound power on the antioxidant properties of elderberry and blackberry extracts (DPPH), total anthocyanin content, total polyphenol content, and total flavonoid content

Ultrasound power, W	DPPH %		TAC mg C3G/100g FW		TPC mg GAE/100 g FW		TFC mg QE/100g FW	
	BB	EB	BB	EB	BB	EB	BB	EB
80	88.75 ±3.39	71.67 ±1.37	102.35 ±4.98	578.00 ±32.88	178.62 ±15.21	311.76 ±51.59	400.52 ±6.17	777.72 ±48.76
110	89.95 ±2.34	72.21 ±1.36	109.79 ±8.52	560.83 ±12.18	188.16 ±14.91	337.93 ±29.79	419.57 ±16.78	812.52 ±45.84
140	90.89 ±2.80	72.72 ±2.09	108.71 ±9.13	602.74 ±37.82	181.05 ±14.37	386.95 ±49.61	433.62 ±24.20	787.75 ±52.05

Values are expressed as mean±standard deviation (SD), calculated based on experimental replicates generated using Design-Expert software, with the number of replicates varying according to the experimental conditions.

Conclusions

This study demonstrated that blackberry (*Rubus fruticosus* L.) and elderberry (*Sambucus nigra* L.) extracts are rich sources of phenolic compounds with significant antioxidant activity and pH-dependent color changes, supporting their potential use as natural freshness indicators in smart food packaging.

A comparison of ultrasound-assisted extraction (UAE) and conventional maceration (MAC) showed that extraction conditions strongly influence extract composition. MAC generally provided higher levels of total anthocyanins, total phenolics, and flavonoids, whereas UAE required shorter processing time and resulted in higher antioxidant activity. Among the tested parameters, solvent composition, extraction time, and ultrasonic power significantly affected extraction efficiency.

Both extracts exhibited pronounced pH-sensitive color changes due to anthocyanin structural transformations, confirming their suitability as visual spoilage indicators.

Overall, blackberry and elderberry extracts show strong potential for application in intelligent packaging systems as natural colorimetric sensors. Such systems could enable real-time monitoring of food quality and contribute to reducing food waste. However, further research is required to evaluate their performance when incorporated into polymeric matrices and under real storage conditions.

References

Airouyuwa J.O, Sivapragasam N., Ali Redha A., Maqsood S. (2024), Sustainable green extraction of anthocyanins and carotenoids using deep eutectic solvents (DES): a review of recent developments, *Food Chemistry*, 448, 139061, https://doi.org/10.1016/j.foodchem.2024.139061

Almasi H., Forghani S., Moradi M. (2022), Recent advances on intelligent food freshness indicators; an update on natural colorants and methods of preparation, *Food Packaging and Shelf Life*, 32, 100839, https://doi.org/10.1016/j.fpsl.2022.100839

Barros G.L., Silva F.T.S., Teixeira R.S., Wagner J.G., Rombaldi C.V., Vizzotto M., Ubeyitogullari A., Nora L. (2024), Anthocyanin extraction methods: synthesis of morpho-anatomical knowledge for decision-making based on decision-tree, *International Journal of Food Properties*, 27(1), pp. 1315–1346, https://doi.org/10.1080/10942912.2024.2409893

Bhatlawande A.R., Ghatge P.U., Shinde G.U., Anushree R.K., Patil S.D. (2024), Unlocking the future of smart food packaging: biosensors, IoT, and nano materials, *Food Science and Biotechnology*, 33(5), pp. 1075–1091, https://doi.org/10.1007/s10068-023-01486-9

Čechovičienė I., Viškelis J., Viškelis P., Hallman E., Kruk M., Tarasevičienė Ž. (2024), Potentially bioactive compounds and sensory compounds in by-products of several cultivars of blackberry (*Rubus fruticosus* L.), *Horticulturae*, 10(8), 862, https://doi.org/10.3390/horticulturae10080862

Česlová L., Kalendová P., Dubnová L., Pernica M., Fischer J. (2023), The effect of sample pretreatment on the anthocyanin content in Czech wild elderberry (*Sambucus nigra* L.), *Molecules*, 28(18), 6690, https://doi.org/10.3390/molecules28186690

Chandran G.U., Kumar A.A., Menon S.K., Sambhudevan S., Shankar B. (2024), The potential role of flavonoids in cellulose-based biopolymeric food packaging materials for UV radiation protection, *Cellulose*, 31(8), pp. 4733–4773, https://doi.org/10.1007/s10570-024-05838-4

Costa C.P., Patinha S., Rudnitskaya A., Santos S.A.O., Silvestre A.J.D., Rocha S.M. (2022), Sustainable valorization of *Sambucus nigra* L. berries: from crop biodiversity to nutritional value of juice and pomace, *Foods*, 11(1), 104, https://doi.org/10.3390/foods11010104

Crăciun A.L., Gutt G. (2023), Optimization of experimental parameters in the solvent extraction of trans-resveratrol from pruning waste of *Vitis vinifera*, Feteasc Neagră variety, *Applied Sciences*, 13(2), 823, https://doi.org/10.3390/app13020823

Crişan D., Frumuzachi O., Babotă M., Gavrilaş L., Ranga F., Mocan A., Vodnar D.C., Crişan G. (2025), Phytochemical variability and bioactive potential of *Sambucus nigra* L. flower extracts: a comparative study across four ecological regions from Romania, *Industrial Crops and Products*, 236, 121948, https://doi.org/10.1016/j.indcrop.2025.121948

Csorba V., Tóth M., László A.M., Kardos L., Kovács S. (2020), Cultivar and year effects on the chemical composition of elderberry (*Sambucus nigra* L.) fruits, *Notulae Botanicae Horti Agrobotanici Cluj-Napoca*, 48(2), pp. 770–782, https://doi.org/10.15835/nbha48211873

Cuesta-Riaño C.S., Castro-Guasca M.P., Tarazona-Díaz M.P. (2022), Anthocyanin extract from blackberry used as an indicator of hydrogen potential, *International Journal of Fruit Science*, 22(1), pp. 224–234, https://doi.org/10.1080/15538362.2022.2037036

Cvetković K., Lazarević A., Stamenković Stojanović S., Dordevic S., Dordevic D., Karabegović I., Danilović B. (2025), pH-sensitive starch-based packaging films enhanced with wild blackberry extract, *Processes*, 13(4), 1148, https://doi.org/10.3390/pr13041148

Demir N. (2023), Antioxidant activity and aroma profile of wild-type blackberry fruits grown in Arapgir, *Adıyaman Üniversitesi Mühendislik Bilimleri Dergisi*, 10(21), pp. 288–298, https://doi.org/10.54365/adyumbd.1378264

Deniz Z., Suna S. (2025), Unlocking the potential of elderberry (*Sambucus nigra* L.) fruit leather: optimization of production and evaluation of bioactive content and bioaccessibility using response surface methodology, *Food Chemistry*, 493, pp. 146046, https://doi.org/10.1016/j.foodchem.2025.146046

Dirpan A., Djalal M., Kamaruddin I. (2022), Application of an intelligent sensor and active packaging system based on the bacterial cellulose of *Acetobacter xylinum* to meat products, *Journal of*

Food and Packaging Science, Technique and Technologies, 22(2), 544, https://doi.org/10.3390/s22020544

Dogan H., Aglar E., Ozturk B., Tekin O., Alan D., Sumbul A. (2025), Pomological and biochemical properties of blackberry (*Rubus fruticocus*) genotypes, *Food Science and Nutrition*, 13(7), pp. 1–13, https://doi.org/10.1002/fsn3.70591

Domínguez R., Pateiro M., Munekata P.E.S., Santos López E.M., Rodríguez J.A., Barros L., Lorenzo J.M. (2021), Potential use of elderberry (*Sambucus nigra* L.) as natural colorant and antioxidant in the food industry. A review, *Foods*, 10(11), 2713, https://doi.org/10.3390/foods10112713

Dutta K., Förster C.Y., Orlova O.Yu., Dandekar T., Skorb E.V., Shityakov S. (2025), Natural polyphenols for sustainable active, smart, and intelligent food packaging: a structured narrative review, *Frontiers in Food Science and Technology*, 5, 1604816, https://doi.org/10.3389/frfst.2025.1604816

El Cadi H., El Cadi A., Ramdan B., Brigui J. (2020), Physicochemical study of *Rubus fruticosus* of the Mediterranean region of Morocco, *Mediterranean Journal of Chemistry*, 10(1), pp. 77–81, https://doi.org/10.13171/mjc10102001311086hec

Elisia I., Hu C., Popovich D.G., Kitts D.D. (2007), Antioxidant assessment of an anthocyanin-enriched blackberry extract, *Food Chemistry*, 101(3), pp. 1052–1058, https://doi.org/10.1016/j.foodchem.2006.02.060

Enaru B., Drețcanu G., Pop T.D., Stănilă A., Diaconeasa Z. (2021), Anthocyanins: factors affecting their stability and degradation, *Antioxidants*, 10(12), 1967, https://doi.org/10.3390/antiox10121967

Floares D., Cocan I., Alexa E., Poiana M.A., Berbecea A., Boldea M.V., Negrea M., Obistioiu D., Radulov I. (2023), Influence of extraction methods on the phytochemical profile of *Sambucus nigra* L., *Agronomy*, 13(12), 3061, https://doi.org/10.3390/agronomy13123061

Gil-Martínez L., Mut-Salud N., Ruiz-García J.A., Falcón-Piñeiro A., Maijó-Ferré M., Baños A., De la Torre-Ramírez J.M., Guillamón E., Verardo V., Gómez-Caravaca A.M. (2023), Phytochemicals determination, and antioxidant, antimicrobial, anti-inflammatory and anticancer activities of blackberry fruits, *Foods*, 12(7), pp. 1–18, https://doi.org/10.3390/foods12071505

Golonka I., Dryś A., Podgórska K., Polewska J., Musiał W. (2024), Evaluation of decay kinetics of black elderberry antioxidants from fruits and flowers, *Antioxidants*, 13(7), 804, https://doi.org/10.3390/antiox13070804

Goud N.S., Prasad G. (2020), Antioxidant, antimicrobial activity and total phenol and flavonoids analysis of *Sambucus nigra* (elderberry), *International Journal of Current Pharmaceutical Research*, 12(1), pp. 35–37, https://doi.org/10.22159/ijcpr.2020v12i1.36829

Guo N., Song M., Liu W., Zhang F., Zhu G. (2023), Preparation of an elderberry anthocyanin film and fresh-keeping effect of its application on fresh shrimps, *PLoS ONE*, 18(11), e0290650, https://doi.org/10.1371/journal.pone.0290650

Hssaini L., Razouk R., Bouslihim Y. (2022), Rapid prediction of fig phenolic acids and flavonoids using mid-infrared spectroscopy combined with partial least square regression, *Frontiers in Plant Science*, 13, pp. 1–16, https://doi.org/10.3389/fpls.2022.782159

Huang H.L., Tsai I.L., Lin C., Hang Y.H., Ho Y.C., Tsai M.L., Mi F.L. (2023), Intelligent films of marine polysaccharides and purple cauliflower extract for food packaging and spoilage monitoring, *Carbohydrate Polymers*, 299, pp. 120133, https://doi.org/10.1016/j.carbpol.2022.120133

Huang X., Zhang K., Li Z., Zhang J., Zhai X., Zhang N., Du L., Qin Z. (2025), Exploring the integration of anthocyanins with functional materials in smart food packaging: from stabilization to application, *Foods*, 14(16), 2896, https://doi.org/10.3390/foods14162896

Imenšek N., Kristl J., Kraner Šumenjak T., Ivančič A. (2021), Antioxidant activity of elderberry fruits during maturation, *Agriculture*, 11(6), 555, https://doi.org/10.3390/agriculture11060555

Jiao X., Xie J., Du H., Bian X., Wang C., Zhou L., Wen Y. (2023), Antibacterial smart absorbent pad with Janus structure for meat preservation, *Food Packaging and Shelf Life*, 37, 101066, https://doi.org/10.1016/j.fpsl.2023.101066

Kahyaoglu L.N. (2024), Intelligent packaging system: a promising approach to reduce food waste, *Current Food Science and Technology Reports*, 2(4), pp. 411–419, https://doi.org/10.1007/s43555-024-00044-6

Kan T. (2019), Some biochemical characteristics of fruit samples of Sambucus nigra genotypes from northeastern Turkey, *Notulae Botanicae Horti Agrobotanici Cluj-Napoca*, 47(3), pp. 553–557, https://doi.org/10.15835/nbha47311489

Khezerlou A., Tavassoli M., Alizadeh Sani M., Ehsani A., McClements D.J. (2023), Smart packaging for food spoilage assessment based on Hibiscus sabdariffa L. anthocyanin-loaded chitosan films, *Journal of Composites Science*, 7(10), 404, https://doi.org/10.3390/jcs7100404

Kim S., Son H., Pang S.Y., Yang J.J., Lee J., Lee K.H., Lee J.H., Park C., Yoo H.Y. (2023), Optimization of major extraction variables to improve recovery of anthocyanins from elderberry by response surface methodology, *Processes*, 11(1), 72, https://doi.org/10.3390/pr11010072

Kolarević T., Milinčić D.D., Vujović T., Gašić U.M., Prokić L., Kostić A., Cerović R., Stanojevic S.P., Tešić Ž.Lj., Pešić M.B. (2021), Phenolic compounds and antioxidant properties of field-grown and in vitro leaves, and calluses in blackberry and blueberry, *Horticulturae*, 7(11), 420, https://doi.org/10.3390/horticulturae7110420

Kolarov R., Peić Tukuljac M., Kolbas A., Kolbas N., Barać G., Ognjanov V., Ljubojević M., Prvulović D. (2021), Antioxidant capacity of wild-growing bilberry, elderberry, and strawberry fruits, *Acta Horticulturae et Regiotecturae*, 24(2), pp. 119–126, https://doi.org/10.2478/ahr-2021-0033

Kukrić Z., Vulić J., Jazić M. (2020), Polyphenol content and antioxidant activity of wild and cultivated blackberry (Rubus fruticosus L.) juices, *Glasnik Hemičara, Tehnologa i Ekologa Republike Srpske*, 1(1), pp. 21–27, https://doi.org/10.7251/jcte2001021k

Kunyk E., Leal E., Pasichniy V., Marynin A., Stabnikova O. (2025), Effect of tocopheryl and retinyl acetates on oxidative stability of *Hypericum perforatum* L. and *Matricaria recutita* L. macerates in corn oil during storage, *Ukrainian Food Journal*, 14(3), pp. 420–432, https://doi.org/10.24263/2304-974X-2025-14-3-5

Kwak M., Min S.C. (2024), Monitoring meat freshness with intelligent colorimetric labels containing red cabbage anthocyanins copigmented with gelatin and gallic acid, *Foods*, 13(21), pp. 3464, https://doi.org/10.3390/foods13213464

Li Y., Wu K., Wang B., Li X. (2021), Colorimetric indicator based on purple tomato anthocyanins and chitosan for application in intelligent packaging, *International Journal of Biological Macromolecules*, 174, pp. 370–376, https://doi.org/10.1016/j.ijbiomac.2021.01.182

Liu X., Xu F., Yong H., Chen D., Tang C., Kan J., Liu J. (2025), Recent advances in chitosan-based active and intelligent packaging films incorporated with flavonoids, *Food Chemistry: X*, 25, 102200, https://doi.org/10.1016/j.fochx.2025.102200

Lv Y., Ai Y., Fang F., Liao H. (2023), Development of active packaging films utilized natural colorants derived from plants and their diverse applications in protein-rich food products, *Food Innovation and Advances*, 2(3), pp. 203–216, https://doi.org/10.48130/FIA-2023-0022

Ma Q., Lu X., Wang W., Hubbe M.A., Liu Y., Mu J., Wang J., Sun J., Rojas O.J. (2021), Recent developments in colorimetric and optical indicators stimulated by volatile base nitrogen to monitor seafood freshness, *Food Packaging and Shelf Life*, 28, 100634, https://doi.org/10.1016/j.fpsl.2021.100634

Mæhre H.K., Dalheim L., Edvinsen G.K., Elvevoll E.O., Jensen I.J. (2018), Protein determination — method matters, *Foods*, 7(1), 5, https://doi.org/10.3390/foods7010005

Marchenko A., Maslov O., Komisarenko M., Ponomarenko S., Osolodchenko T., Kolisnyk S. (2024), Investigation relationship between antimicrobial, antioxidant activity and biologically active compounds of blackberry (*Rubus fruticosus* L.) fresh fruit liquid extracts, *Zenodo*, *Annals of Mechnikov Institute*, 4, https://doi.org/10.5281/zenodo.14275647

Martins M.S., Gonçalves A.C., Alves G., Silva L.R. (2023), Blackberries and mulberries: berries with significant health-promoting properties, *International Journal of Molecular Sciences*, 24(15), 12024, https://doi.org/10.3390/ijms241512024

Martins M.S., Azevedo R., Alves G., Almeida A., Guedes de Pinho P., Garcia-Viguera C., Moreno D.A., Silva L.R., Gonçalves A.C. (2025), Assessment of chemical composition of blackberries and mulberries from Covilhã region, Portugal, *Journal of Food Composition and Analysis*, 137, 106832, https://doi.org/10.1016/j.jfca.2024.106832

Marțiș G.S., Mureșan V., Marc R.M., Mureșan C.C., Pop C.R., Buzgău G., Mureșan A.E., Ungur R.A., Muste S. (2021), The physicochemical and antioxidant properties of Sambucus nigra L. and Sambucus nigra 'Haschberg' during growth phases: from buds to ripening, *Antioxidants*, 10(7), 1093, https://doi.org/10.3390/antiox10071093

Mattioli R., Francioso A., Mosca L., Silva P. (2020), Anthocyanins: a comprehensive review of their chemical properties and health effects on cardiovascular and neurodegenerative diseases, *Molecules*, 25(17), 3809, https://doi.org/10.3390/molecules25173809

Mattson M.L.G., Corfield R., Bajda L., Pérez O.E., Schebor C., Salvatori D. (2021), Potential bioactive ingredient from elderberry fruit: process optimization for a maximum phenolic recovery, physicochemical characterization, and bioaccessibility, *Journal of Berry Research*, 11(1), pp. 51–68, https://doi.org/10.3233/JBR-200629

Mayuri G., Rekha B., Priyanka T., Mohini U. (2023), A review on pharmacological properties of *Rubus fruticosus*, *International Journal of Ayurvedic Medicine*, 14(1), pp. 22–28, https://doi.org/10.47552/ijam.v14i1.3408

Memete A.R., Sărac I., Teusdea A.C., Budău R., Bei M., Vicas S.I. (2023), Bioactive compounds and antioxidant capacity of several blackberry (Rubus spp.) fruits cultivars grown in Romania, *Horticulturae*, 9(5), 556, https://doi.org/10.3390/horticulturae9050556

Miljanić J., Krstović S., Perović L., Kojić J., Travičić V., Bajac B. (2024), Assessment of the nutritional benefits and aflatoxin B1 adsorption properties of blackberry seed cold-pressed oil by-product, *Foods*, 13(19), pp. 3140, https://doi.org/10.3390/foods13193140

Miller K., Reichert C.L., Schmid M. (2023), Biogenic amine detection systems for intelligent packaging concepts: meat and meat products, *Food Reviews International*, 39(5), pp. 2543–2567, https://doi.org/10.1080/87559129.2021.1961270

Nadeem M., Leaks K.A., Abdullah A., Felix J.S.A., Shahid M.A. (2025), Enhancing postharvest quality of blackberries: impact of sonicated and microwave-assisted pasteurized edible coating gels at different storage temperatures, *Gels*, 11(4), 243, https://doi.org/10.3390/gels11040243

Nami M., Taheri M., Siddiqui J., Deen I.A., Packirisamy M., Deen M.J. (2024), Recent progress in intelligent packaging for seafood and meat quality monitoring, *Advanced Materials Technologies*, 9(12), pp. 2301347, https://doi.org/10.1002/admt.202301347

Nawirska-Olszańska A., Oziembłowski M., Brandova P., Czaplicka M. (2022), Comparison of the chemical composition of selected varieties of elderberry with wild growing elderberry, *Molecules*, 27(16), 5050, https://doi.org/10.3390/molecules27165050

Oladzadabbasabadi N., Mohammadi Nafchi A., Ghasemlou M., Ariffin F., Singh Z., Al-Hassan A.A. (2022), Natural anthocyanins: sources, extraction, characterization, and suitability for smart packaging, *Food Packaging and Shelf Life*, 33, 100872, https://doi.org/10.1016/j.fpsl.2022.100872

Özgen S., Özbaş Z. (2025), Multifunctional intelligent packaging films incorporated with elderberry anthocyanin for monitoring milk freshness, *Polymer Bulletin*, 82(3), pp. 837–859, https://doi.org/10.1007/s00289-024-05553-x

Pan J., Li C., Liu J., Jiao Z., Zhang Q., Lv Z., Yang W., Chen D., Liu H. (2024), Polysaccharide-based packaging coatings and films with phenolic compounds in preservation of fruits and vegetables — a review, *Foods*, 13(23), 3896, https://doi.org/10.3390/foods13233896

Papagrigoriou T., Iliadi P., Mitić M.N., Mrmošanin J.M., Papanastasi K., Karapatzak E., Maloupa E., Gkourogianni A.V., Badeka A.V., Krigas N., Lazari D. (2023), Wild-growing and conventionally or organically cultivated Sambucus nigra germplasm: fruit phytochemical profile, total phenolic content, antioxidant activity, and leaf elements, *Plants*, 12(8), 1701, https://doi.org/10.3390/plants12081701

Pascariu O.E., Dias L.G., Israel-Roming F. (2024), Optimization of extraction method of bioactive compounds from elderberries (Sambucus nigra L.) and testing extract stability, *Horticulturae*, 10(7), 743, https://doi.org/10.3390/horticulturae10070743

Pascariu O.E., Israel-Roming F. (2022), Bioactive compounds from elderberry: extraction, health benefits, and food applications, *Processes*, 10(11), 2288, https://doi.org/10.3390/pr10112288

Pasieczna-Patkowska S., Cichy M., Flieger J. (2025), Application of Fourier transform infrared (FTIR) spectroscopy in characterization of green synthesized nanoparticles, *Molecules*, 30(3), pp. 1–36, https://doi.org/10.3390/molecules30030684

Peron G., Ferrarese I., Dos Santos N.C., Rizzo F., Gargari G., Bertoli N., Gobbi E., Perosa A., Selva M., Dall'Acqua S. (2024), Sustainable extraction of bioactive compounds and nutrients from agri-food wastes: potential reutilization of berry, honey, and chicory byproducts, *Applied Sciences*, 14(23), 10785, https://doi.org/10.3390/app142310785

Petruskevicius A., Viskelis J., Urbonaviciene D., Viskelis P. (2023), Anthocyanin accumulation in berry fruits and their antimicrobial and antiviral properties: an overview, *Horticulturae*, 9(2), 288, https://doi.org/10.3390/horticulturae9020288

Plasencia P., Finimundy T.C., Carocho M., Calhelha R.C., Añibarro-Ortega M., Pires T.C.S.P., Barreiro F., Garcia P.A., Barros L., Heleno S.A. (2025), Extraction of bioactive compounds from Rubus idaeus bioresidues: a full screening on phenolic composition and bioactive potential, *Waste and Biomass Valorization*, 16(2), pp. 737–747, https://doi.org/10.1007/s12649-024-02696-w

Pucel N., Sarkar D., Labbe R.G., Khanongnuch C., Shetty K. (2021), Improving health targeted food quality of blackberry: pear fruit synergy using lactic acid bacterial fermentation, *Frontiers in Sustainable Food Systems*, 5, pp. 1–15, https://doi.org/10.3389/fsufs.2021.703672

Pusty K., Dash K.K., Giri S., Bhagya Raj G.V.S., Tiwari A., Shaikh A.M., Béla K. (2024), Ultrasound assisted phytochemical extraction of red cabbage by using deep eutectic solvent: modelling using ANFIS and optimization by genetic algorithms, *Ultrasonics Sonochemistry*, 102, 106762, https://doi.org/10.1016/j.ultsonch.2024.106762

Qader A.F., Yaman M. (2023), Blackberry (Rubus fruticosus L.) fruit extract phytochemical profile, antioxidant properties, column chromatographic fractionation, and high-performance liquid chromatography analysis of phenolic compounds, *ARO – The Scientific Journal of Koya University*, 11(2), pp. 43–50, https://doi.org/10.14500/aro.11189

Radojković M., Vujanović M., Majkić T., Zengin G., Beara I., Catauro M., Montesano D. (2021), Evaluation of Sambucus nigra L. biopotential as an unused natural resource, *Applied Sciences*, 11(23), pp. 11207, https://doi.org/10.3390/app112311207

Rahman M., Sobhan A., Sadak O. (2026), Emerging trends in intelligent packaging for tackling food waste in the modern food supply chain, *Trends in Food Science and Technology*, 167, 105436, https://doi.org/10.1016/j.tifs.2025.105436

Rivero-Pérez M.D., Gerardi G., Cavia-Saiz M., Ortega-Heras M., Muñiz P. (2025), The bioactivity of byproducts from the blackberry (*Rubus fruticosus*) juice industry, *Biology and Life Sciences Forum*, 40(1), p. 52, https://doi.org/10.3390/blsf2024040052

Rodríguez Madrera R., Pando Bedriñana R. (2023), The phenolic composition, antioxidant activity and microflora of wild elderberry in Asturias (Northern Spain): an untapped resource of great interest, *Antioxidants*, 12(11), 1986, https://doi.org/10.3390/antiox12111986

Rosales-Murillo S.S., Sánchez-Bodón J., Hernández Olmos S.L., Ibarra-Vázquez M.F., Guerrero-Ramírez L.G., Pérez-Álvarez L., Vilas-Vilela J.L. (2024), Anthocyanin-loaded polymers as promising nature-based, responsive, and bioactive materials, *Polymers*, 16(1), 163, https://doi.org/10.3390/polym16010163

Roy S., Rhim J.W. (2021), Anthocyanin food colorant and its application in pH-responsive color change indicator films, *Critical Reviews in Food Science and Nutrition*, 61(14), pp. 2297–2325, https://doi.org/10.1080/10408398.2020.1776211

Sani M.A., Tavassoli M., Hamishehkar H., McClements D.J. (2021), Carbohydrate-based films containing pH-sensitive red barberry anthocyanins: application as biodegradable smart food packaging materials, *Carbohydrate Polymers*, 255, pp. 117488, https://doi.org/10.1016/j.carbpol.2020.117488

Santos S.S., Paraíso C.M., Rodrigues L.M., Madrona G.S. (2021), Agro-industrial waste as a source of bioactive compounds: ultrasound-assisted extraction from blueberry (*Vaccinium myrtillus*) and raspberry (*Rubus idaeus*) pomace, *Acta Scientiarum – Technology*, 43, pp. 1–8, https://doi.org/10.4025/actascitechnol.v43i1.55567

Sganzerla W.G., Ribeiro C.P.P., Uliana N.R., Rodrigues M.B.C., da Rosa C.G., Ferrareze J.P., Veeck A.P.L., Nunes M.R. (2021), Bioactive and pH-sensitive films based on carboxymethyl cellulose and blackberry (*Morus nigra* L.) anthocyanin-rich extract: a perspective coating material to improve the shelf life of cherry tomato (*Solanum lycopersicum* L. var. *cerasiforme*), *Biocatalysis and Agricultural Biotechnology*, 33, 101989, https://doi.org/10.1016/j.bcab.2021.101989

Sharma P., Hamid A. (2025), Ultrasonication-assisted extraction of anthocyanins from fruit and vegetable waste, *Food and Humanity*, 5, https://doi.org/10.1016/j.foohum.2025.100713

Sik B., Ajtony Z., Lakatos E., Székelyhidi R. (2024), Wild blackberry fruit (Rubus fruticosus L.) as potential functional ingredient in food: ultrasound-assisted extraction optimization, ripening period evaluation, application in muffin, and consumer acceptance, *Foods*, 13(5), 666, https://doi.org/10.3390/foods13050666

Stabnikov V., Stabnikova O., Paredes-López O. (2025), Antioxidant compounds in wild edible berries, In: S. Gubsky, O. Stabnikova, V. Stabnikov, O. Paredes-López (Eds.), *Wild Edible Plants: Improving Foods Nutritional Value and Human Health through Biotechnology*, pp. 143-184, CRC Press, Boca Raton, https://doi.org/10.1201/9781003486794-5

Stabnikova O., Stabnikov V., Paredes-López O. (2024), Fruits of wild-grown shrubs for health nutrition, *Plant Foods for Human Nutrition*, 79(1), pp. 20-37, https://doi.org/10.1007/s11130-024-01144-3

Şuian B., Amariei S., Petraru A. (2025), Comprehensive characterization of Armoracia rusticana roots and leaves: physicochemical properties, functional potential, and nutritional composition, *International Journal of Molecular Sciences*, 26(19), 9462, https://doi.org/10.3390/ijms26199462

Szaniawska A., Grzeda J., Binder J., Kudelski A., Malek K., Wrobel T.P., Wysmolek A., Roguz K. (2025), Data-driven FTIR spectroscopy for the discrimination of nectars, *Molecules*, 30(20), pp. 1–19, https://doi.org/10.3390/molecules30204083

Tasić M.S., Zvezdanović J.B., Stanojević L.P., Stanojević J.S., Petrović S.M., Danilović B., Cvetković D.J. (2024), Synthesis, characterization and biological activity of gold nanoparticles stabilized by aqueous extracts of wild blackberry (Rubus spp.) leaves, *Colloid Journal*, 86(5), pp. 814–828, https://doi.org/10.1134/S1061933X24600398

Trojniak J., Tabarkiewicz J. (2023), Health-promoting properties: anti-inflammatory and anticancer properties of Sambucus nigra L. flowers and fruits, *Molecules*, 28(17), 6235, https://doi.org/10.3390/molecules28176235

Upadhyay A., Agbesi P., Arafat K.M.Y., Urdaneta F., Dey M., Basak M., Hong S., Umeileka C., Argyropoulos D. (2024), Bio-based smart packaging: fundamentals and functions in sustainable food systems, *Trends in Food Science and Technology*, 145, 104369, https://doi.org/10.1016/j.tifs.2024.104369

Varo M.A., Serratosa M.P., Martín-Gómez J., Moyano L., Mérida J. (2022), Influence of fermentation time on the phenolic compounds, vitamin C, color and antioxidant activity in the winemaking process of blueberry (Vaccinium corymbosum) wine obtained by maceration, *Molecules*, 27(22), 7744, https://doi.org/10.3390/molecules27227744

Vega-Castro O., Marulanda D.V., Tobón C.S., Marulanda V.L., Arboleda V.V., González D.H., Narváez F.G. (2025), Exploring the potential of spray-dried blackberry powder enriched with zinc and folic acid as a nutritional alternative for children and pregnant women, *Food Biophysics*, 20(1), pp. 23, https://doi.org/10.1007/s11483-024-09892-0

Villarino N., Lavilla I., Pena-Pereira F., Bendicho C. (2023), Droplet-based luminescent sensor supported onto hydrophobic cellulose substrate for assessing fish freshness following smartphone readout, *Food Chemistry*, 424, 136475, https://doi.org/10.1016/j.foodchem.2023.136475

Vujanović M., Majkić T., Zengin G., Beara I., Tomović V., Šojić B., Đurović S., Radojković M. (2020), Elderberry (Sambucus nigra L.) juice as a novel functional product rich in health-promoting compounds, *RSC Advances*, 10(73), pp. 44805–44814, https://doi.org/10.1039/d0ra09129d

Wang J., Wang H., Zhang H., Yang S., Lai K., Luan D., Yan J. (2024), Development of a novel colorimetric pH biosensor based on A-motif structures for rapid food freshness monitoring and spoilage detection, *Biosensors*, 14(12), pp. 605, https://doi.org/10.3390/bios14120605

Wu H., Di Q.R., Zhong L., Zhou J.Z., Shan C.J., Liu X.L., Ma A.M. (2022), Enhancement on antioxidant, anti-hyperglycemic and antibacterial activities of blackberry anthocyanins by processes optimization involving extraction and purification, *Frontiers in Nutrition*, 9, 1007691, https://doi.org/10.3389/fnut.2022.1007691

Yu Z., Boyarkina V., Liao Z., Lin M., Zeng W., Lu X. (2023), Boosting food system sustainability through intelligent packaging: application of biodegradable freshness indicators, *ACS Food Science and Technology*, 3(1), pp. 199–212, https://doi.org/10.1021/acsfoodscitech.2c00372

Zannou O., Koca I. (2022), Greener extraction of anthocyanins and antioxidant activity from blackberry (Rubus spp.) using natural deep eutectic solvents, *LWT – Food Science and Technology*, 158, 113184, https://doi.org/10.1016/j.lwt.2022.113184

Zhai X., Xue Y., Sun Y., Ma X., Ban W., Marappan G., Tahir H.E., Huang X., Wu K., Chen Z., Zou W., Liu B., Zhang L., Yang Z., Katona J. (2025), Colorimetric food freshness indicators for intelligent packaging: progress, shortcomings, and promising solutions, *Foods*, 14(16), pp. 1–34, https://doi.org/10.3390/foods14162813

Zhang K., Li Z., Khan S., Shishir M.R.I., Zheng H., Gao L., Shi J., Huang X., Zou X. (2025), An intelligent aerogel composed of anthocyanins, natural fiber, carboxymethyl cellulose, and sodium alginate for monitoring fish freshness, *International Journal of Biological Macromolecules*, 297, 138198, https://doi.org/10.1016/j.ijbiomac.2024.138198

Zhang W., Li Z., Jin W., Xu Y., Mei F., Cheng D., Cai G., Wang X. (2025), Biomass-based food packaging film of chitosan/flavonoids/silver nanoparticle for shelf life extension of food, *Colloids and Surfaces A: Physicochemical and Engineering Aspects*, 727, 138154, https://doi.org/10.1016/j.colsurfa.2025.138154

Zhao L., Liu Y., Zhao L., Wang Y. (2022), Anthocyanin-based pH-sensitive smart packaging films for monitoring food freshness, *Journal of Agriculture and Food Research*, 9, pp. 100340, https://doi.org/10.1016/j.jafr.2022.100340

Zhou Y., Gao Y.G., Giusti M.M. (2020), Accumulation of anthocyanins and other phytochemicals in American elderberry cultivars during fruit ripening and its impact on color expression, *Plants*, 9(12), pp. 1–14, https://doi.org/10.3390/plants9121721

Zhu B., Zhong Y., Wang D., Deng Y. (2023), Active and intelligent biodegradable packaging based on anthocyanins for preserving and monitoring protein-rich foods, *Foods*, 12(24), 4491, https://doi.org/10.3390/foods12244491

Zubova G., Melnyk H., Zaets I., Sergeyeva T., Havryliuk O., Rogalsky S., Khirunenko L., Zaika L., Ruban T., Antonenko S., Kozyrovska N. (2024), Halochromic bacterial cellulose/anthocyanins hybrid polymer film with wound-healing potential, *Polymers*, 16(16), 2327, https://doi.org/10.3390/polym16162327

Cite:

Huțuțui, L.-M., Amariei, S., & Huțu, D. (2026). Polyphenolic phytochemical compounds from *Sambucus nigra* L. and *Rubus fruticosus* L. for food freshness indicators. *Ukrainian Food Journal, 15*(2), 361–389. https://doi.org/10.24263/2304-974X-2026-15-2-7

Modification of potato starch by acylation with acetyllactic acid chloride for food and packaging applications

Sergij Shulga, Oksana Shulga

National University of Food Technologies, Kyiv, Ukraine

Keywords:

Starch
Acetyllactic acid
IR spectroscopy
X-ray
Thermogravimetric

Article history:

Received 24.01.2026
Received in revised form 10.04.2026
Accepted 30.06.2026

Corresponding author:

Oksana Shulga
E-mail:
shulgaos@ukr.net

DOI:
10.24263/2304-974X-2026-15-2-8

Abstract

Introduction. Starch is a natural polymer extensively used in the food industry and in related applications, such as biodegradable packaging materials. However, the inherent drawbacks of native starch limit its functionality and can be addressed through chemical modification.

Materials and methods. The substrate for modification was potato starch. Lactic acid and thionyl chloride were used as modifying agents. Dimethyl sulfoxide, N,N-dimethylformamide, methanol, and ethanol served as solvents. The modified starch was characterized using Fourier-transform infrared (FTIR) spectroscopy, X-ray diffraction (XRD) analysis, thermogravimetric analysis (TGA), and nuclear magnetic resonance (NMR) spectroscopy.

Results and discussion. The νOH stretching vibration band is narrower and more intense, appearing at 3409 cm^{-1} in the modified starch sample, whereas in the spectrum of native starch this band is broader, less intense, and located at 3389 cm^{-1}. The observed shift and change in band shape indicate a reduction in the number of hydrogen bonds in the modified starch. This can be explained by the lower content of free hydroxyl groups resulting from the acylation reaction. According to the modification conditions described in the experimental section, the degree of substitution corresponds to one substituent per glucopyranose unit. This assumption is supported by the elemental analysis data, which show good agreement between the experimental and calculated values. The starch esterification occurred at one hydroxyl group in the glucopyranose residues, since the experimentally determined carbon and hydrogen contents were 46.27% and 6.07%, respectively, while the calculated values were 46.15% and 5.98%, respectively. Although NMR spectroscopy confirmed the successful introduction of the acyl fragment, determination of the exact substitution position proved to be practically impossible due to the complexity and overlap of the starch signals. X-ray diffraction analysis showed that native potato starch possesses an amorphous-crystalline structure with a crystallinity degree of approximately 12%. After chemical modification, the crystallinity degree decreased significantly to about 3%, indicating substantial disruption of the ordered crystalline regions. The introduction of bulky substituents into the starch macromolecule likely interferes with intermolecular interactions and reduces the ability of polymer chains to form crystalline domains. As a result, the modified starch exhibits altered water-binding properties, which may be advantageous for specific food and packaging applications.

Conclusions. The success of the potato starch acylation reaction with acetyllactic acid chloride was confirmed by IR spectroscopy, NMR, X-ray analysis, thermogravimetric study and elemental analysis.

Introduction

Starch is environmentally friendly, easy to manufacture, common, non-toxic and biodegradable. However, natural starch cannot be used directly due to its rather low thermomechanical properties and water absorption capacity. Therefore, it is advisable to modify natural starch before using it (Amaraweera et al., 2021). The chemical properties of starch have been thoroughly studied, as it has been used in food production for a long time (Egharevba, 2020).

Starch modification can be carried out by physical (heat and moisture treatment, microwave method) (Mainardes et al., 2024), chemical (etherization, carboxymethylation, esterification, crosslinking and oxidation) and enzymatic processes or their combination (Kushwaha et al., 2018, Wurzburg, 2024). Acetylated starches have a low gelatinization temperature, high solubility, stability during freezing-thawing and stability during storage, which determines the scope of their application (for baking, canned and frozen foods; beverages; confectionery; baby food; gluten-free products and dairy) (Kaushik et al., 2024). Acetylated polysaccharides have significantly improved biological activity and have great potential in the food and pharmaceutical industries (Wang et al., 2024).

Starch modified with octenyl succinic anhydride is used to stabilize emulsions. However, the poor compatibility of starch with hydrophobic groups limits the effectiveness of modification with octenyl succinic anhydride. The researchers (Lim et al., 2023) treated potato starch one or two times (heated, acetylated, and acid treated) before modification with octenyl succinic anhydride. Pretreatment increased the degree of substitution, hydrophobicity/hydrophilicity, and emulsifying properties, and also reduced the amylose content, with double pretreatment having a more significant effect.

Martinez et al. (2021) proposed modifying pea starch, which allowed reducing syneresis and stiffness of its jellies. Subroto et al. (2023) claim that acetylation increases swelling capacity and retrograde stability. Double acetylation modification with crosslinking or hydrothermal treatment can improve the thermal starch stability. However, the modifications results depending on the type of starch, reagents, and processing methods. Acetylated starch can be used as an encapsulant for nanoparticles, biofilms, adhesives, fat substitutes, and other products with better stability and transparency.

Starch is a biodegradable natural polymer and is considered the most promising for replacing petroleum-based materials. It can be used as a fat substitute, emulsifier, etc. in the food industry (Wang et al., 2020). Acetic anhydride or acetyl chloride as reagents for starch modification, leading to acetylation of hydroxyl groups (Kaushik et al., 2024). The modification is possible due to the presence of three active hydroxyl groups on glucose molecules (C2, C3 and C6), which allows to increase its hydrophobicity (Jamzad et al., 2005). Starch copolymers modified with polylactic acid were obtained by Gong et al. (2006) through the in situ reaction of corn starch with lactic acid in an aqueous medium in the presence of tin 2-ethylhexanoate.

According to EU Regulation (EC) No. 1333/2008, acetylated starch is a food additive (E1420) and may contain a maximum level of acetyl groups of 2.5% according to Commission Regulation (EC) No. 231/2012 and the US Food and Drug Administration (FDA), which corresponds to the substitution degree.

The environmental aspect of starch modification should also be considered, since starch acetylation results in the generation of significant amounts of wastewater and sodium acetate (Ragavan et al., 2022). The aim of this work was to propose a simpler starch modification scheme using readily available reagents that are safe for food industry applications.

Materials and methods

Materials

The substrate for modification was potato starch (State Standard of Ukraine 4286:2004). Lactic acid (E270) and thionyl chloride were used as modifying agents, while dimethyl sulfoxide (DMSO), dimethylformamide (DMF), methanol, ethanol, calcium oxide (CaO), acetic anhydride, and sulfuric acid were used as reagents and solvents.

A starch modification method employing DMSO as a solvent was developed. Due to its complete miscibility with water, DMSO can be effectively removed from the reaction product during washing. In addition, DMSO is characterized by relatively low toxicity. Lactic acid (E270) is an approved food additive, making it a potentially safe reagent for applications in the food industry.

Starch preparation for the acylation reaction

100 g of potato starch was added to a 500 mL flask, connected to a water jet pump and heated in a boiling water bath for 8 hours. Product yield: 87.40 g (moisture loss due to drying – 12.60%).

Dimethyl sulfoxide preparation

Dimethyl sulfoxide (DMSO) (300 mL) was kept over calcined CaO at 400 °C for 2 days. DMSO was transferred to the flask (500 mL) and added dry benzene (35 mL). The remaining water was distilled off at atmospheric pressure as an azeotrope with benzene, then DMSO was distilled off in the vacuum by water jet pump.

Acetylation of lactic acid with acetic anhydride

$$CH_3\text{-}CHOH\text{-}COOH + (CH_3\text{-}COO)_2O = CH_3\text{-}CH(OCOCH_3)\text{-}COOH + CH_3COOH$$

In a 100 mL reactor with a magnetic stirrer and heating, a thermometer and a reflux condenser, 18 g (0.2 M) of lactic acid were introduced, 25.5 g (0.25 M) of acetic anhydride and 3 drops of sulfuric acid were added. The mixture was kept for 1.5 hours at 50-60 °C under stirring. Then the temperature was increased to 90 °C and stirred for another 0.5 h. Excess acetic anhydride and acetic acid were distilled off in the vacuum of a water jet pump. 25.7 g (97.3%) of product was obtained was used without further purification.

Synthesis of acetyllactic acid chloride

$$CH_3\text{-}CH(OCOCH_3)\text{-}COOH + SOCl_2 \rightarrow CH_3\text{-}CH(OCOCH_3)\,COCl + SO_2 + HCl$$

39.6 g (0.3 M) of acetyllactic acid was introduced in a 150 mL reactor with a magnetic stirrer with heating and a thermometer and a reflux condenser by a dropping funnel. 47.6 g (0.4 M) of thionyl chloride was added in small portions through a dropping funnel while stirring. The reaction mixture was gradually heated. Three drops of DMF were added after 1 h and the temperature was maintained at 55-65 °C for another 5 h. Excess thionyl chloride was removed in a water jet vacuum to give 40.7 g (90.4%) of product, which was used without further purification.

The starch esterification with acetyllactic acid chloride occurred according to the following reaction equation:

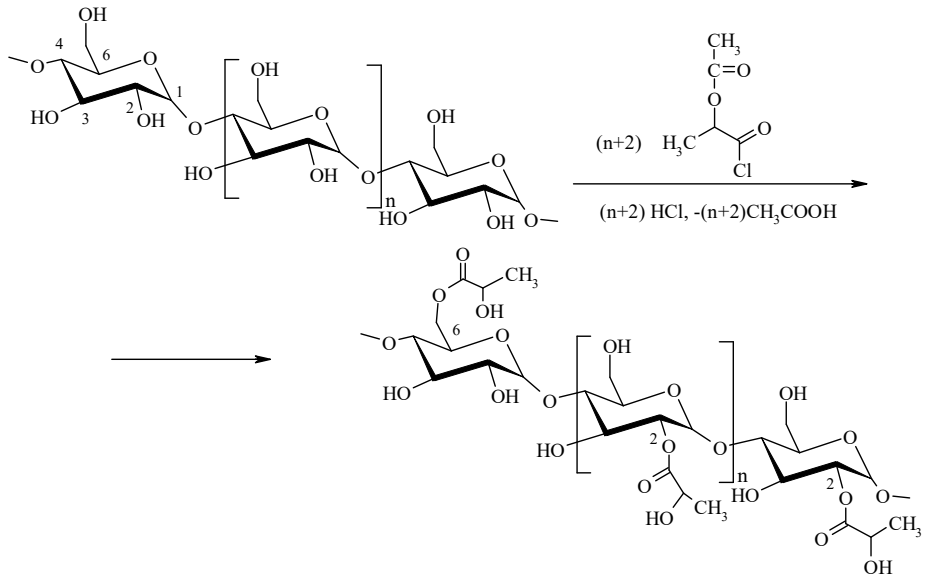

5.58 g (0.03 M, based on glucose) of dried starch and 75 mL of anhydrous DMSO were placed in a 150 mL three-neck reactor equipped with a magnetic stirrer with heating, a funnel, a thermometer and a reflux condenser. Stirred for 3 h at 70 °C until a transparent colorless jelly was formed. The heating was stopped and 0.12 g of K_2CO_3 (approximately 2% of the starch mass) was added. 6.02 g (0.04 M) of acetyllactic acid chloride was added in small portions while stirring. The reaction mass became thicker and the temperature rose to 75 °C. The reaction mixture turned into a thick light-yellow gel, and the temperature decreased to room temperature after 1 h. Then, 120 cm³ of ethanol was added, and the mixture was stirred intensively for 1 h. The precipitate was filtered using a water-jet vacuum pump and washed with ethanol (4 × 20 cm³). The product was air-dried at room temperature. A yield of 6.37 g (82.3%) was obtained.

Research methods

IR were carried out on a Nicolet Nexus-475 device, using KBr tablets.

X-ray was performed on a DRON-3M device in CuKα radiation with a Ni filter; U = 35 kV, I = 20 mA; counter movement angle $\Delta 2\Theta = 0.04°$; intensity counting time 3 s.

Thermogravimetric reaserch were carried out on a Q-1500V instrument in an air atmosphere, 10 ºC/min.

NMR were recorded on a MERCURY NMR, manufactured by VARIAN, 400 MHz in a DMSO–d_6 solution.

Results and discussion

IR-reaserch

The result of the starch acylation reaction were studied by IR (Sherban-Kline, 1999).

The samples of the original native potato starch and the esterified derivative have different spectra in the IR uncharacteristic region (400-1000 cm^{-1}) of native and esterified starch (Figure 1).

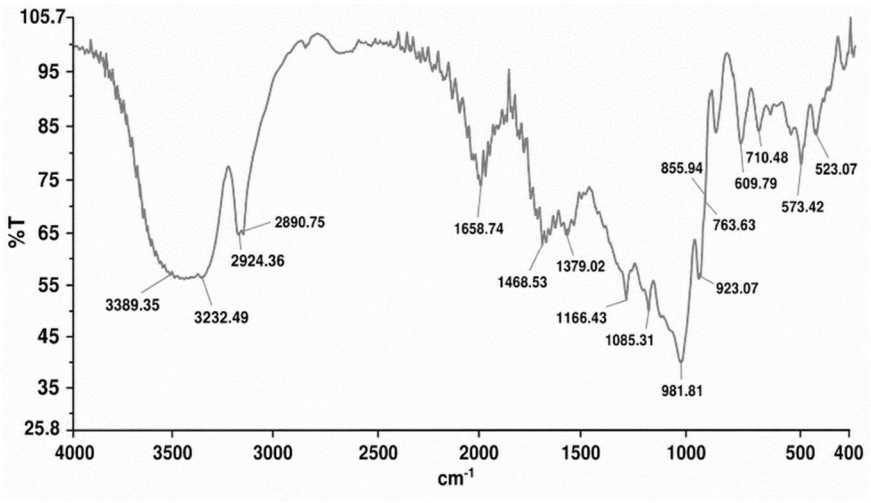

a

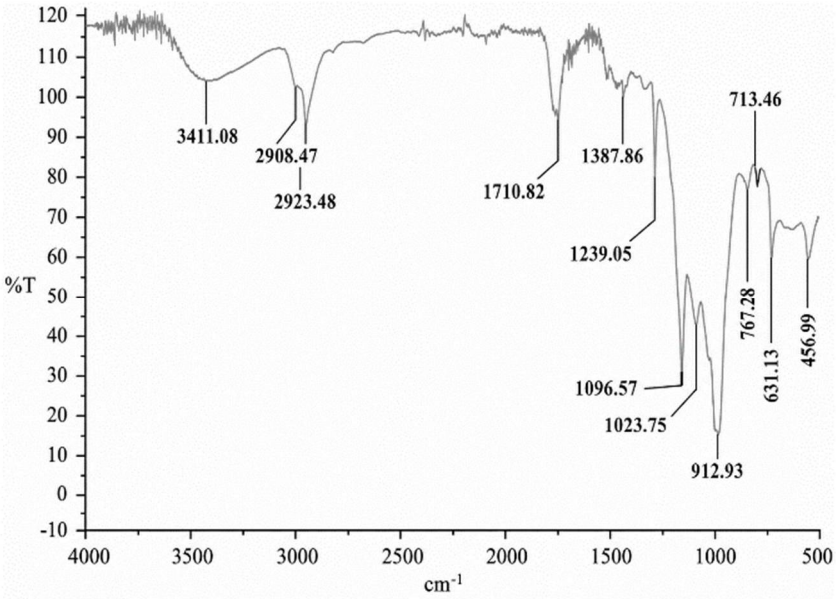

b

Figure 1. IR of native poptato starch (a) and the esterified derivative (b)

The original native potato starch sample (Figure 1a) contains fluctuations in the uncharacteristic region, in particular 981.81 cm^{-1}, 928.03 cm^{-1}, 603.58 cm^{-1}, and in the esterified derivative spectrum (Figure 1b) – 1024.65 cm^{-1}, 868.3 cm^{-1}, 678.23 cm^{-1}. Therefore the vibration frequency at 980.81 cm^{-1} shifted to 1024.65 cm^{-1}, the band with a frequency of 928.03 cm^{-1} shifted to 863.3 cm^{-1}, and the band with a vibration frequency of 603.58 cm^{-1} shifted to 678.23 cm^{-1}, which indicates uncharacteristic region change of the native starch spectrum after acylation. Therefore, the original native potato starch samples and the

esterified derivative have different chemical compositions due to the chemical potato starch modification (de Macêdo et al., 2023).

The maximum appeared at 1710.82 cm^{-1} in the characteristic region of the esterified derivative spectrum (Figure 1b), which is characteristic of C=O in the ester group. Confirmation of the potato starch acylation reaction is also based on the νOH stretching vibration band. There is a fairly broad intense band located at 3389 cm^{-1}, and in the esterified derivative spectrum, this band is more intense and less broad and is located at 3409 cm^{-1} in the spectrum of the original native potato starch sample.

It is known (Suart, 2004) the position and nature of the νOH band depend on the degree of hydroxyl group participation the in hydrogen bonds. Hydrogen bonds change the force constant of the O-H bond, which reduces the vibrational frequency. The hydroxyl group, which participates in intermolecular hydrogen bonding, is characterized by a broad, intense absorption maximum in the region 3200-3600 $см^{-1}$ (Azeez et al., 2025).

The νOH stretching vibration band is narrower and more intense, lying at 3409 cm^{-1} in the modified starch spectrum, while in the native starch spectrum this band is broader and less intense, lying at 3389 cm^{-1}. There are fewer hydrogen bonds in the modified starch, because the smaller hydroxyl groups number, which affected the nature and frequency of νOH oscillations of acylated potato starch (Coates, 2000).

Elemental analysis

The elemental analysis results indicate the potato starch esterification with acetyl lactic acid chloride occurred at one hydroxyl group in the residues of the glucopyranose rings, since 46.27% of Carbon was found, and 46.15% was calculated. Hydrogen was found 6.07%, and was calculated 5.98%. According to (Hong et al., 2015) the primary alcohol group and the hydroxyl group at C2 are most easily acylated.

Nuclear magnetic resonance study

It is known (Martins et al., 2018) that starch acetates contain an ester moiety predominantly at position 2 of the anhydroglucose unit and can be synthesized by converting starch with acetic anhydride in DMSO.

Since starch modified with acetyl lactic acid chloride is poorly soluble in DMSO, it is not possible to determine the substitution degree of hydroxyl groups from its spectrum, i.e., the quantitative determination of 2-hydroxypropionyl groups per monomer unit. It was found that the starch substitution degree, under the modification conditions specified in the experimental part, is 1:1, which is in good agreement with the data of elemental analysis. Determining the position of the substituent from the NMR proved to be practically impossible.

During the starch modification reaction with acetaminolactic acid chloride, deacylation of lactic acid occurred, since the NMR spectrum lacks the signal of the second methyl group, which is part of the acyl.

The influence of esterification degree on the crystallinity of the esterified potato starch structure was determined using X-ray analysis (Taguchi et al., 2023; Vermeylen et al., 2006). The diffraction patterns are shown in Figure 3.

The starch before esterification has an amorphous-crystalline structure with a relative crystallinity degree of 12% according to the potato starch diffractogram (Figure 3), while modified potato starch has a relative crystallinity degree of 3%.

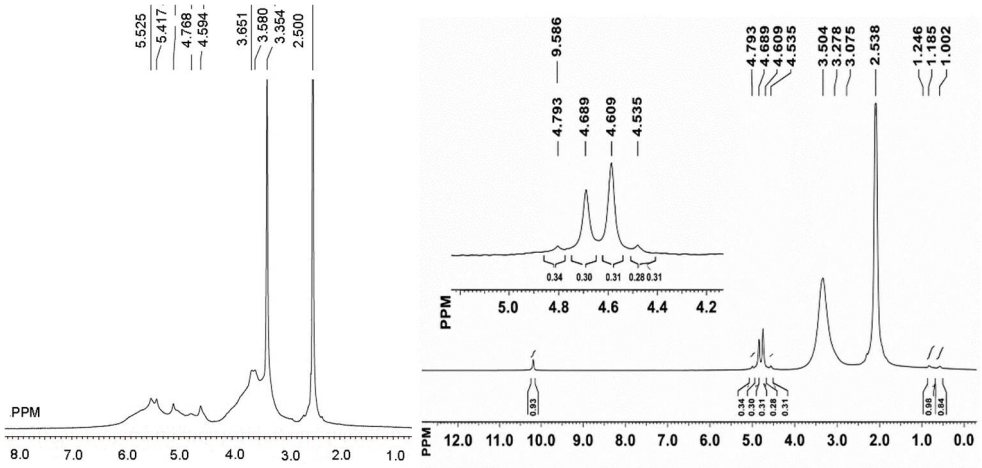

a **b**

Figure 2. NMR of the native potato starch (a) and the esterified derivative (b) *X-ray*

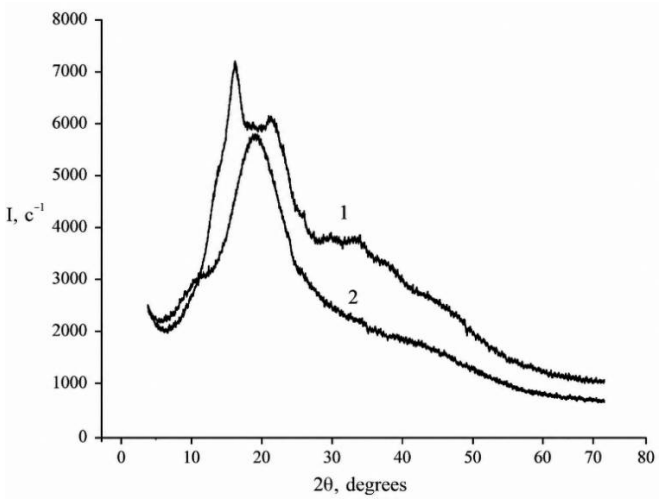

Figure 3. X-ray of the native potato starch (1) and the esterified derivative (2)

Therefore, the X-ray show the starch chemical modification to the destruction of its crystalline structure, which was also observed by the authors (Nep et al., 2016) during the study of the rheological and structural properties of modified starches from young shoots of *Borassus aethiopium*. Pourtakalo (2018) established using differential scanning calorimetry to confirmed the removal of the crystalline structure during acetylation and the reduction of the glass transition.

TGA/DTG-DTA analysis

Thermogravimetry is a method that allows you to confirm the effectiveness of the modification (Elomaa et al., 2004; Kaczmarska et al., 2019).

It was found that chemically modified starch differs in water retention characteristics from the native potato starch. There are four segments of mass loss (Figure 4a): the 1st at 63-140 °C is

3.7% on the TG curve of native potato starch. The mass loss is caused by the elimination of adsorbed water (up to 100 °C) and water of crystallization (100-135 °C). The given loss corresponds to a blurred effect of mass loss with a minimum at 110 °C on the DTG curve of a native potato starch sample (Figure 4a), which should be considered as the superposition of two separate effects associated with moisture removal. The second segment of mass loss corresponds to the temperature interval 300-380 °C and is 57.3%. This process corresponds to a sharp and profound effect of mass loss with a minimum at 330 °C on the DTG curve, which is caused by the thermal decomposition of the polysaccharide.

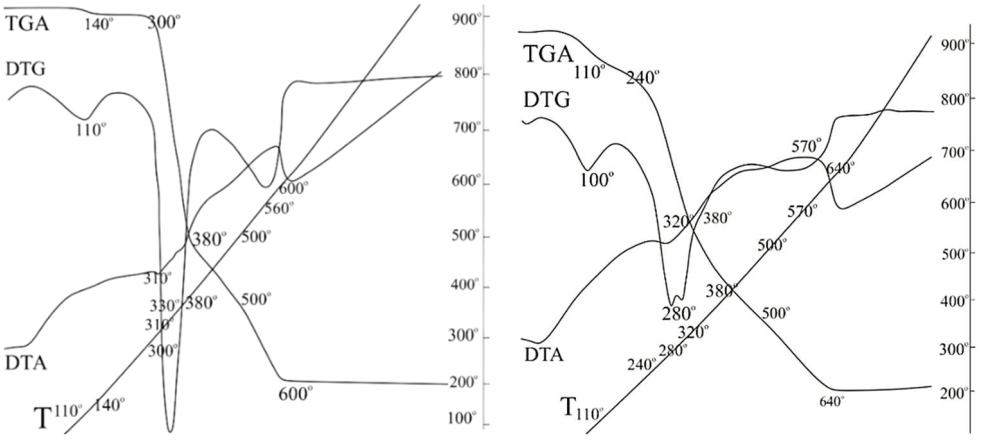

a **b**

Figure 4. TGA/DTG-DTA of native potato starch (a) and esterified potato starch (b)

In the third section, mass losses occur at 380-500 °C and 14.5% of the initial mass. In this temperature range, carbonization of previously formed intermediate thermolysis products up to 380 °C occurs. The mass loss Δm_4=17.5% on the 4th segment of the TG curve. This stage is caused by the complete thermal decomposition and charring of starch at 600 °C. The coke residue of this sample is 5.7% after heating to 950 °C.

The six segments can be distinguished on the TG curve of the esterified potato starch sample (Figure 4b): the 1st – 30-100 °C, associated with the release of adsorbed water Δm_1<7.5%. The mass loss at 110-240 °C is Δm_2=6.23%, because of the water crystallization separation. The process of anhydrous substance occurs thermal decomposition in the 3rd temperature interval 240-280 °C and the 4th – 280-320 °C ΔM_3=36.20%, which depends on the chemical composition. The 5th temperature interval 380-500 °C with Δm_5=13.75% is a consequence of charring. The 6th temperature interval of 500-640 °C corresponds to the further decomposition of previously formed charred products. The mass of the modified starch sample does not change above 640 °C. The coke residue is 6.25%. after heating to 900 °C.

The results obtained are consistent with the authors (Gunaratne et al., 2007; Ferreira-Villadiego et al., 2018) in acetylation reduced the temperature and enthalpy of gelatinization, but increased the swelling coefficient, amylose leaching.

Mitran et al. (2025) found acetylation increases the thermal stability of starch. It has been reported (Singh et al., 2004) that acetylation of corn and potato starches reduces the gelatinization transition temperature and enthalpy, while increasing swelling capacity and light transmittance. However, these changes are more pronounced in potato starch, which contains a higher proportion of fine granules. Overall, the modification of starch functional properties during acetylation

depends strongly on both the botanical source and the morphology of the native starch granules. Therefore, the thermogravimetric reaserch confirm the difference in the chemical structure and properties of the native starch and its esterified derivative.

The results showed that acetylated starch had a resistant starch 11.12%, an oxalate 7.20%, and a swelling capacity of 68.40%, but the water absorption and oil absorption of acetylated starch were similar to native starch (Pourtakalo, 2018; Sisilia et al., 2018).

Acetylation can increase swelling capacity, swelling volume, water/oil absorption capacity, and retrograde stability. The double acetylation modification with crosslinking or hydrothermal treatment can improve the thermal stability of starch/flour. However, the results of the modifications may vary depending on the type of starch, reagents and processing methods. Acetylated starch can be used as an encapsulant for nanoparticles, biofilms, adhesives, fat substitutes, and other products with better paste stability and transparency. The comparison of different characteristics of acetylated starches and their dual modifications should serve as a guideline for the development and application of acetylated starches/flours in various industries and products (Subroto et al., 2023).

Modified starches can be used in environmentally friendly materials. In particular, Koch et al. (2014) proposed films based on starch triacetate derived from various botanical sources. The barrier properties of these films, especially oxygen permeability, decrease with increasing degree of acetylation. Films have also been developed from cassava starch incorporating acetylated starch nanoparticles as reinforcing agents (Zhang et al., 2014). In addition, acetylated starches can serve as nanocarriers for curcumin due to the formation of branched starch micelles (Liu et al., 2021). Polymer blends of polylactic acid and starch are widely used in food packaging applications (Silva et al., 2023). Another important application of modified starches is in adhesive formulations (Watcharakitti et al., 2022).

Conclusions

The acylation reaction of potato starch with acetyllactic acid chloride was carried out and the new modified starch was reaserced by physicochemical methods. The IR spectra have various uncharacteristic regions: the vibration frequency at 980.81 cm^{-1} has increased and in the spectrum of modified starch lies at 1024.65 cm^{-1}, and the band with a vibration frequency of 928.03 cm^{-1} has shifted to 863.3 cm^{-1}, indicating a change in the spectrum. The esterified starch IR spectrum contains a band at 1710.82 cm^{-1} after acylation, which is characteristic of C=O in the ester group formed as a result of the starch acylation reaction with acetyl lactic acid chloride.

X-ray analysis of native and modified starches showed acylation leads to a decrease in the crystalline phase from 12 to 3%.

It has been established that acylation of potato starch with acetyl lactic acid chloride causes a change in the forms of moisture in starch.

References

Amaraweera S.M., Gunathilake C., Gunawardene O., Fernando N.M., Wanninayaka D.B., Dassanayake R.S., Manipura A. (2021), Development of starch-based materials using current modification techniques and their applications: A review, *Molecules*, 26(22), 6880, https://doi.org/10.3390/molecules26226880

Coates J. (2000), Interpretation of infrared spectra, a practical approach, *Encyclopedia of Analytical Chemistry*, 12, pp. 10815-10837, https://doi.org/10.1002/9780470027318.a5606

Debeuckelaere W. (2015), Legislation on food additives, food enzymes and flavourings in the European Union, *Current Opinion in Food Science*, 6, pp. 49-52, https://doi.org/10.1016/j.cofs.2015.12.001

de Macêdo I.Y.L., Dupuy N., Brito V.H.D.S., Gil E.D. S., Silva G.N.D.M.E., Moreno E.K., Cereda M.P. (2023), Modified cassava starches' identification through mid-infrared spectroscopy and exploratory analysis, *Analytica*, 4(2), pp. 126-140, https://doi.org/10.3390/analytica4020011

Egharevba H.O. (2020), Chemical properties of starch and its application in the food, In: M. Emeje (Ed.), *Chemical Properties of Starch*, IntechOpen, https://www.intechopen.com/books/8170

Elomaa M., Asplund T., Soininen P., Laatikainen R., Peltonen S., Hyvärinen S., Urtti A. (2004), Determination of the degree of substitution of acetylated starch by hydrolysis, 1H NMR and TGA/IR, *Carbohydrate Polymers*, 57(3), pp. 261-267, https://doi.org/10.1016/j.carbpol.2004.05.003

Ferreira-Villadiego J., García-Echeverri, J., Vidal, M. V., Pasqualino, J., Meza-Castellar P., Lambis-Miranda H.A. (2018), Chemical modification and characterization of starch derived from plantain (*Musa paradisiaca*) peel waste, as a source of biodegradable material, *Chemical Engineering Transactions*, 65, pp. 763-768, https://doi.org/10.3303/CET1865128

Gong Q., Wang L. Q., Tu K. (2006), In situ polymerization of starch with lactic acid in aqueous solution and the microstructure characterization, *Carbohydrate Polymers*, 64(4), pp. 501-509, https://doi.org/10.1016/j.carbpol.2005.09.005

Gunaratne A., Corke H. (2007), Influence of prior acid treatment on acetylation of wheat, potato and maize starches, *Food Chemistry*, 105(3), pp. 917-925, https://doi.org/10.1016/j.foodchem.2007.04.042

Hong L.F., Cheng L.H., Lee C.Y., Peh K.K. (2015), Characterisation of physicochemical properties of propionylated corn starch and its application as stabiliser, *Food Technology and Biotechnology*, 53(3), pp. 278-285, https://doi: 10.17113/ft b.53.03.15.3907

Jamzad S., Tutunji L., Fassihi R. (2005), Analysis of macromolecular changes and drug release from hydrophilic matrix systems, *International Journal of Pharmaceutics*, 292(1-2), pp. 75-85, https://doi.org/10.1016/j.ijpharm.2004.11.011

Kaczmarska K., Zymankowska-Kumon S., Byczynski L., Grabowska B., Bobrowski A., Cukrowicz S. (2019), Thermoanalytical studies (TG–DTG–DSC, Py–GC/MS) of sodium carboxymethyl starch with different degrees of substitution, *Journal of Thermal Analysis and Calorimetry*, 138(6), pp. 4417-4425, https://doi.org/10.1007/s10973-019-08892-4

Kaushik R., Kumar A., Rani N., Phogat R., Gehlot R. (2024), Acetylation/esterification of starch. In: S.P. Bangar, K.V. Sunooj, A.K. Siroha (Eds.), *Starch: Structure, Properties, and Modifications for Food Applications*, CRC Press, https://doi.org/10.1201/9781032655598-12

Koch K., Johansson D., Johansson K., Svegmark K. (2014), Material properties and molecular aspects of highly acetylated starch-based films, *Journal of Renewable Materials*, 2(2), pp. 134-144, https://doi.org/10.7569/JRM.2014.634110

Kushwaha R., Kaur D. (2018), Recent techniques used in modification of starches: A review, In: *Food Technology from Health to Wealth & Future Challenges*, pp. 1-15, Bharti Publication.

Lim X.X., Zulkurnain M., Yussof N.S., Utra U. (2023), Effects of dry heating, acetylation, and acid pre-treatments on modification of potato starch with octenyl succinic anhydride (OSA), *e-Polymers*, 23(1), 20228090, https://doi.org/10.1515/epoly-2022-8090

Liu Q., Li F., Ji N., Dai L., Xiong L., Sun, Q. (2021), Acetylated debranched starch micelles as a promising nanocarrier for curcumin, *Food Hydrocolloids*, 111, 106253, https://doi.org/10.1016/j.foodhyd.2020.106253

Mainardes B., Mikota L.M., Bet C.D., Marinho M.T., Bisinella R.Z.B., Romko S., Schnitzler E. (2024), Extraction and physical modification of Mango palmer kernel starch and its application in cookies, *Ukrainian Food Journal*, 13(2), pp. 231-246, https://doi.org/10.24263/2304-974X-2024-13-2- 3

Martinez M. M., Boukid F. (2021), Future-proofing dietary pea starch, *ACS Food Science & Technology*, 1(8), pp. 1371-1372, https://doi.org/10.1021/acsfoodscitech.1c00219

Martins P.C., Gutkoski L.C., Martins V.G. (2018), Impact of acid hydrolysis and esterification process in rice and potato starch properties. *International Journal of Biological Macromolecules*, 120, pp. 959-965, https://doi.org/10.1016/j.ijbiomac.2018.08.170

Mitran G., Pavel O. D., Hanganu A. (2025), Acylation of starch in the presence of carboxylic acids and amides as organocatalysts and as hydrogen bond donors in deep eutectic solvents, *International Journal of Biological Macromolecules*, 148696, https://doi.org/10.1016/j.ijbiomac.2025.148696

Nep E. I., Ngwuluka N. C., Kemas C. U., & Ochekpe N. A. (2016), Rheological and structural properties of modified starches from the young shoots of Borassus aethiopium. *Food Hydrocolloids*, 60, pp. 265-270, https://doi.org/10.1016/j.foodhyd.2016.02.037

Pourtakalo R.N. (2018), Development and characterization of poly (lactic acid)/acetylated starch blends (Doctoral dissertation, University of Waterloo.

Ragavan K.V., Hernandez-Hernandez O., Martinez M.M., Gutiérrez T.J. (2022), Organocatalytic esterification of polysaccharides for food applications: A review, *Trends in Food Science & Technology*, 119, pp. 45-56, https://doi.org/10.1016/j.tifs.2021.11.028

Sherban-Kline M. (1999), Infrared spectroscopy: A key to organic structure, *Teachers Institute, Yale University*, https://teachersinstitute.yale.edu/curriculum/units/1999/5/99.05.07.x.html

Silva L.R.C, Rios A.D.O., Santana R.M.C. (2023), Polymer blends of poly (lactic acid) and starch for the production of films applied in food packaging: A brief review, *Polymers from Renewable Resources*, 14(2), pp. 108-153, https://doi.org/10.1177/20412479231154924

Singh J., Kaur L., Singh N. (2004), Effect of acetylation on some properties of corn and potato starches, *Starch-Stärke*, 56(12), pp. 586-601, https://doi.org/10.1002/star.200400293

Sisilia F.Y., Herla R., Elisa J., Tampubolon S.D.R., Restuana S.D. (2018), Physicochemical characteristics of tuber modified by acetylation method and its application in dry noodle product, *IOP Conference Series: Earth and Environmental Science*, 205(1), 012044, https://doi.org/10.1088/1755-1315/205/1/012044

Subroto E., Cahyana Y., Indiarto R., Rahmah T.A. (2023), Modification of starches and flours by acetylation and its dual modifications: A review of impact on physicochemical properties and their applications, *Polymers*, 15(14), 2990, https://doi.org/10.3390/polym15142990

Suart B. (2004), *Infrared Spectroscopy: Fundamental and Applications*, John Wiley & Sons, Ltd.

Taguchi T. Onishi M., Katsuno N., Miwa N., Oomoto C., Sato M., Nishizu T. (2023), Evaluation of starch retrogradation by X-ray diffraction using a water-addition method. *LWT*, 173, 114341, https://doi.org/10.1016/j.lwt.2022.114341

Vermeylen R., Goderis B., Delcour J.A. (2006), An X-ray study of hydrothermally treated potato starch, *Carbohydrate Polymers*, 64(2), pp. 364-375, https://doi.org/10.1016/j.carbpol.2005.12.024

Wang X., Wang Z., Shen M., Yi C., Yu Q., Chen X., Xie M. (2024), Acetylated polysaccharides: Synthesis, physicochemical properties, bioactivities, and food applications, *Critical Reviews in Food Science and Nutrition*, 64(15), pp. 4849-4864, https://doi.org/10.1080/10408398.2022.2146046

Wang X., Huang L., Zhang C., Deng Y., Xie P., Liu, L., Cheng J. (2020), Research advances in chemical modifications of starch for hydrophobicity and its applications: A review, *Carbohydrate Polymers*, 240, 116292, https://doi.org/10.1016/j.carbpol.2020.116292

Watcharakitti J., Win E.E., Nimnuan J., Smith S.M. (2022), Modified starch-based adhesives: A review, *Polymers*, 14(10), 2023, https://doi.org/10.3390/polym14102023

Wurzburg O. B. (2024), *Modified food starches*, In Food Additive Toxicology, CRC Press.

Zhang Q., Wei S., Huang J., Feng J., Chang P.R. (2014), Effect of surface acetylated-chitin nanocrystals on structure and mechanical properties of poly (lactic acid), *Journal of Applied Polymer Science*, 131(2), 39809, https://doi.org/10.1002/app.39809

Cite:

Shulga, S., & Shulga, O. (2026). Modification of potato starch by acylation with acetyllactic acid chloride for food and packaging applications. *Ukrainian Food Journal, 15*(2), 390–400. https://doi.org/10.24263/2304-974X-2026-15-2-8

Active coating based on longan seed starch and pomelo peel pectin for extending shelf life of tomatoes

Sutapa Laha, Annalakshmi Chatterjee

University of Calcutta, Kolkata, India

Keywords:

Active coating
Tomato
Pomelo
Pectin
Longan
Starch
Shelf life

Article history:

Received 12.02.2026
Received in revised form 30.03.2026
Accepted 30.06.2026

Corresponding author:

Sutapa Laha
E-mail: sutapalaha15@gmail.com

DOI:
10.24263/2304-974X-2026-15-2-9

Abstract

Introduction. Biopolymer-based edible coatings derived from agro-industrial by-products represent a promising alternative to conventional synthetic packaging materials. They can reduce postharvest losses, preserve fruit quality, and contribute to a circular bioeconomy through the valorization of food-processing wastes.

Materials and methods. Polysaccharide-based edible coatings were prepared using starch extracted from longan seeds and pectin isolated from pomelo peels, with selected formulations supplemented with sodium benzoate as a preservative. The chemical interactions within the coating matrices were characterized by Fourier-transform infrared spectroscopy. Fresh tomatoes were coated, stored at 25 °C and 4 °C, and evaluated on days 0, 3, 7, and 11. Changes in weight loss, pH, total soluble solids (TSS), titratable acidity, antioxidant activity, and the activities of polyphenol oxidase (PPO) and peroxidase (POD) were determined.

Results and discussion. FTIR analysis revealed differences in intermolecular interactions among the coating components, including variations in hydrogen bonding as well as ester and amide linkages, indicating the successful formation of composite coating matrices. Application of the polysaccharide-based coatings effectively delayed ripening and quality deterioration of tomatoes under both storage conditions. Compared with the uncoated control, coated fruits exhibited significantly lower weight loss and slower increases in pH, TSS, and PPO activity throughout storage. The coatings also reduced the decline in titratable acidity, antioxidant capacity, and POD activity, demonstrating their ability to preserve biochemical stability. The formulation containing sodium benzoate provided the greatest protective effect. At 25 °C, uncoated tomatoes showed a 159.42% reduction in antioxidant activity, whereas coated fruits without preservative exhibited a decrease of 132.50%, and those coated with preservative showed only a 47.54% reduction. Similar preservation trends were observed during refrigerated storage, confirming the effectiveness of the coating system in maintaining fruit quality under different environmental conditions.

Conclusions. Polysaccharide-based active coatings produced from longan seed starch and pomelo peel pectin effectively enhanced the shelf life and quality retention of tomatoes during storage. The incorporation of sodium benzoate further improved preservation efficiency.

Introduction

Food preservation aims to maintain the sensory quality, safety, and nutritional value of food products while minimizing spoilage during storage. In recent decades, changes in consumer lifestyles have increased the demand for fresh, minimally processed, and convenient foods with extended shelf life (Pech-Canul et al., 2020). Consequently, food packaging has evolved from a passive barrier to an active preservation system (Pasichnyi et al., 2022). Packaging plays a crucial role in protecting food against physical, chemical, and biological deterioration by incorporating bioactive compounds that help maintain product quality and and preserve product quality during storage (Hasan et al., 2025; Kostova et al., 2020a, b; Maftoonazad and Ramaswamy, 2019).

Growing environmental concerns regarding conventional petroleum-based plastics have accelerated the development of sustainable and biodegradable packaging alternatives, including active packaging systems, edible coatings, dipping treatments, and modified atmosphere packaging (Sapper and Chiralt, 2018). Among these technologies, polymer-based active packaging has attracted considerable attention because it can be functionalized with antimicrobial agents, chemical preservatives, nanoparticles, essential oils, and plant-derived bioactive extracts to enhance food preservation (Valdés et al., 2015). Depending on their mode of action, active packaging systems are generally classified as chemo-active or bioactive. Chemo-active packaging regulates the gaseous environment or chemical composition surrounding the food, whereas bioactive packaging incorporates antimicrobial or preservative agents that directly interact with biological targets to inhibit microbial growth and delay quality deterioration (Sayed et al., 2023; Stabnikov et al., 2025).

Perishable fruits and vegetables are highly susceptible to postharvest physiological and biochemical changes, resulting in weight loss, tissue softening, surface shrinkage, cell wall degradation, and reduced marketability (Ballesteros et al., 2017; Pirog et al., 2022a). Tomato (*Solanum lycopersicum* L.), a climacteric fruit, is characterized by a high respiration rate and increased ethylene production during ripening, handling, and storage, which accelerate quality deterioration and limit its shelf life. Conventional postharvest preservation methods, including the application of synthetic waxes, chemical preservatives, and microbial polysaccharides have raised growing environmental and public health concerns (Das et al., 2022; Pirog et al., 2022b). Consequently, increasing attention has been directed toward the development of sustainable packaging technologies incorporating active ingredients, such as antimicrobial and preservative agents, to protect fresh produce by forming a functional barrier on the fruit surface (Tafa et al., 2023; Stabnikova et al., 2026a, b). Biodegradable edible films and coatings derived from natural biopolymers are considered safe for human consumption and offer several advantages, including reduced gas and water vapor exchange, improved firmness retention, decreased moisture loss, enhanced surface gloss, and improved mechanical properties, thereby extending the shelf life and maintaining the quality of fresh fruits and vegetables (Behere et al., 2022). Growing environmental pollution and the depletion of fossil fuel resources associated with the production and disposal of petroleum-based food packaging materials have accelerated the development of sustainable bio-based packaging technologies (Thakur et al., 2019). Simultaneously, the large quantities of food waste and agro-industrial by-products generated throughout agricultural production and food supply chains pose significant environmental, economic, and social challenges. These organic residues are rich sources of renewable biopolymers that can be valorized into biodegradable plastics and active edible coatings without competing with food resources. Among the various natural biopolymers investigated for food packaging applications, starch and pectin have attracted considerable attention because of their low cost, wide availability,

biodegradability, excellent film-forming ability, and physicochemical properties comparable to those of conventional synthetic polymers (Kharb and Saharan, 2024).

Longan (*Dimocarpus longan* Lour.) is a commercially important tropical fruit cultivated throughout Asia, particularly in India, China, Taiwan, Thailand, and Myanmar. During industrial processing, longan seeds constitute a major by-product and are commonly discarded despite their high starch content (Manzoor and Ahmad, 2024). Currently, the issue of utilizing by-products from fruit and vegetable processing is receiving special attention as a strategy for reducing environmental pollution and promoting sustainable resource management. These agro-industrial residues are increasingly recognized as valuable sources of biopolymers and bioactive compounds that can be converted into functional materials, including biodegradable packaging, edible coatings, and other value-added products. Such approaches contribute to waste minimization, resource efficiency, and the development of circular economy-based food systems (Stabnikova et al., 2023a, b).

According to Hu et al. (2018), longan seeds contain up to 49.5% (w/w) starch, including approximately 25.1% amylose. The relatively high amylose content makes longan seed starch an attractive biopolymer for the production of edible films and coatings because of its excellent film-forming properties. Pomelo (*Citrus maxima*), the largest citrus fruit, is another abundant source of agro-industrial waste. Its peel accounts for nearly 40% of the fruit mass and is rich in valuable biopolymers and bioactive compounds, including pectin, cellulose, flavonoids, and essential oils. Previous studies have demonstrated the successful application of polysaccharide-based coatings derived from agricultural by-products, such as tamarind seeds, teff, pea starch, banana peel, and mango kernel, for extending the shelf life of fresh fruits including grapes, avocados, strawberries, and guava (Quoc et al., 2015). Nevertheless, despite the increasing interest in sustainable edible coatings, limited information is available regarding the formulation, characterization, and optimization of biodegradable coatings based on longan seed starch and pomelo peel pectin, either individually or in combination. This knowledge gap highlights the need for further investigation into their potential application as sustainable active coatings for postharvest preservation.

The present study hypothesized that longan seed starch and pomelo peel pectin can be valorized into biodegradable polysaccharide-based active coatings to extend the shelf life of tomato (*Solanum lycopersicum*). This approach aims to improve postharvest preservation while promoting the sustainable utilization of food-processing by-products within a circular bioeconomy framework.

Materials and methods

Materials

Fresh tomato fruits (*Solanum lycopersicum*) at the harvest stage (approximately 80 days after full bloom) were purchased from a local market in Behala, South Kolkata, West Bengal, India. Fruits exhibiting an appropriate total soluble solids/titratable acidity (TSS/TA) ratio indicative of optimal maturity were selected for the study. Tomatoes showing any physiological, mechanical damage, or visible pathological symptoms were excluded.

Experimental design and conduction

Uniform-sized tomato fruits (*Solanum lycopersicum*) with similar shape and optimal ripening stage were selected for the study. Prior to treatment, the samples were sanitized using 100 ppm sodium chlorite solution for 30 s and subsequently air-dried at ambient

temperature for 30 min. The experiment was arranged in a completely randomized design, comprising three treatment conditions with five replicates per treatment, each consisting of 150 g of samples. Untreated fruits served as the control. The same experimental setup was applied under both ambient and refrigerated storage conditions.

Methods

Extraction of starch. Starch was extracted using a wet milling technique combined with acidic and alkaline steeping. Longan seeds were washed, disinfected with 2% sodium hypochlorite, and dried overnight in a hot air oven (Meta Lab Scientific Industries, Mumbai, India) at 40–60 °C. The dried seeds were separately treated with 2% NaOH and 1% citric acid at 60 °C for 10 min, blended with distilled water (1:2, w/v) for 5 min, and filtered through muslin cloth. The filtrate was repeatedly washed and allowed to settle until a white starch fraction was obtained. The recovered starch was dried at 50 °C for 24 h (Maniglia and Tapia-Blácido, 2015).

Extraction of pectin. Pectin extraction was carried out using a conventional acid extraction method as described by Kumar et al. (2021), with minor modifications. Pomelo peels were first dried in a hot air oven at 50 °C for 24 h and subsequently milled into a fine powder (250–500 μm) using a laboratory mixer grinder. For extraction, 10 g of peel powder was suspended in 250 mL of deionized water, acidified with 5 M H_2SO_4 to adjust the pH to 1.5–2. The mixture was heated at 80 °C for 1 h in a thermostatic water bath under intermittent stirring. After extraction, the suspension was filtered through 400-mesh muslin cloth and centrifuged at 5000 × g for 40 min. The supernatant was then precipitated by adding 96% ethanol at a 2:1 (v/v) ratio and incubated for 12 h. The resulting pectin was recovered by centrifugation at 6000 × g for 40 min and washed three times with 75% ethanol (solid-to-solvent ratio 3:1) to remove residual impurities and solvents. Finally, the purified pectin was lyophilized at −40 °C and stored in an airtight container for further use.

Preparation of coating solution and coating process

Preparation of coating solution. The coating solutions were prepared by dissolved all ingredients in distilled water. Sodium benzoate (C_6H_5COONa) was used as a preservative. Two separate coating formulations were developed for different storage conditions (25 °C and refrigerated storage), along with an untreated control, as summarized in Table 1.

Table 1

Treatments and their codes

Treatment	Codes		Content, % (w/v)					
	25 °C	4 °C	Starch	Pectin	Sorbitol	PVA	Citric acid	Sodium benzoate
Control	C	C1	0	0	0	0	0	0
Without preservative	A	A1	2	0.2	2.5	1.6	1.0	0
With preservative	B	B1	2	0.2	2.5	1,6	1.0	0.2

Note: PVA - polyvinyl alcohol.

All coating components were thoroughly homogenized until complete dissolution was achieved, resulting in uniform and stable coating solutions.

Coating application and storage conditions. Tomato samples were immersed in the coating solutions for 40 s and subsequently air-dried for 60 min at ambient temperature. After drying, properly labeled samples were placed on trays and stored for 14 days under two different storage conditions. Quality and safety parameters were evaluated at 0, 3, 7, and 11 days of storage to monitor postharvest changes over time.

Characterization of the coating solutions

FTIR analysis

Fourier transform infrared spectroscopy (FTIR) analysis was performed using a Bruker FTIR-ATR spectrometer (CSIR–IICB, Kolkata, India) to investigate potential interactions among the coating components. The infrared spectra were recorded over the range of 4000–400 cm^{-1}. Functional groups and molecular interactions within the coating matrices were identified based on characteristic absorption bands in the IR region (Bai et al., 2023).

Quality and safety criteria analysis

Visual quality rating and shelf life. Visual quality was assessed using a visual quality rating (VQR) scale. The postharvest shelf life of tomatoes under different storage conditions was determined based on the number of days required to reach a VQR score of 5 (Gonzales et al., 2019).

Table 2

VQR Coding for determining the shelf life of foods

VQR	Descriptions
9	Field fresh, no defects, excellent
7	Good, minor defects
5	Moderate defects, limit of marketability, fair
3	Limit of edibility, poor, serious defects
0	Lack of edibility under usual condition

Determination of weight loss. Weight loss of tomatoes was determined using a high-precision analytical balance (Wensar, India). Sample weight was recorded at each sampling interval. Weight loss percentage was calculated using the following equation:

$$\text{Weight loss (\%)} = [(W_0 - W_t)/W_0] \times 100, \quad (1)$$

where W_0 is the initial weight of the sample and W_t is the weight at a given storage time.

pH determination. Tomato samples were homogenized to a semi-liquid consistency using a mortar and pestle. The pH was measured using a digital pH meter (Hexane, China). Prior to analysis, the instrument was calibrated with standard buffer solutions at pH 4.0 and 7.0 (Suhaimi et al., 2021).

Titratable acidity (TA) determination. Titratable acidity was determined according to the method (Hernández-Guerrero et al., 2020). Briefly, 5 g of tomato sample was homogenized with 25 mL of distilled water under heated conditions. The homogenate was transferred to a volumetric flask, diluted to 50 mL with distilled water, and filtered through Whatman filter paper. An aliquot of 5–10 mL of the filtrate was pipetted into a 250 mL

conical flask and further diluted with 50 mL of distilled water. The solution was titrated against 0.1 N NaOH using phenolphthalein as an indicator until a persistent light pink endpoint was reached. Titratable acidity was expressed as malic acid equivalents per 100 g of fresh weight. The percentage of acidity was calculated using the standard titration equation:

$$\% \text{ acidity} = (V \times Eq.Wt \times N \times d \times 100)/(W \times V_1) \quad (2)$$

where V is the volume of NaOH solution used for titration (mL); Eq.Wt is the equivalent weight of the acid, g/mol, N is the normality of the titrant (0.1 N), d is the dilution factor, W is the weight of the sample, g, and V_1 is the volume of aliquot taken for titration, mL.

Total soluble solids (TSS) measurement. Total soluble solids were determined using a digital refractometer (Erma, China) following the method of Hernández-Guerrero et al. (2020). Approximately 1–2 drops of filtered tomato extract were placed onto the prism surface of the refractometer, and the TSS value was recorded and expressed as °Brix.

Determination of peroxidase (POD) and polyphenol oxidase (PPO) activity. Crude enzyme extracts were prepared by homogenizing 1 g of tomato tissue in 3 mL of 0.1 M phosphate buffer under ice-cold conditions. The homogenate was centrifuged under refrigeration, and the supernatant was used as the crude enzyme extract.

Peroxidase activity was assayed in a reaction mixture containing 0.1 M phosphate buffer (pH 6.0–7.0), guaiacol, H_2O_2, and crude enzyme extract. Enzyme activity was determined by monitoring the increase in absorbance due to tetraguaiacol formation at 470 nm and expressed as μmol tetraguaiacol/min/g fresh weight (FW).

Polyphenol oxidase activity was measured by recording the increase in absorbance at 420 nm over 90 s in a reaction mixture containing 0.1 M phosphate buffer, L-tyrosine, and crude enzyme extract. PPO activity was expressed as μmol quinone/min/g FW (Panahirad et al., 2020).

Antioxidant activity (DPPH assay). Antioxidant activity was determined using the DPPH free radical scavenging method. 2 mL of ethanolic sample extract was mixed with 1 mL of DPPH solution (40 μg/mL), vortexed thoroughly, and incubated in the dark for 30 min. Absorbance was then measured at 517 nm using a UV–visible spectrophotometer (Analytic Jena Specord 200, Germany). Different extract concentrations ranging from 250 to 5000 μg/mL were used to evaluate antioxidant activity, with ethanol serving as the blank control (Medina-Jaramillo et al., 2015). The percentage of radical scavenging activity was calculated using the following equation:

$$\% \text{ inhibition} = [(A_0 - A_1)/A_0] \times 100 \quad (3),$$

where A_0 is absorbance of sample extract, A_1 is absorbance of control against ethanol.

Statistical analysis

Statistical analysis of the data was performed using IBM SPSS software. Results were expressed as mean values ± standard deviation. One-way analysis of variance (ANOVA) was applied to determine significant differences among treatments, with significance set at $p < 0.05$. All experiments were conducted in triplicate, and the mean values were used for statistical evaluation.

Results and discussion

FTIR spectroscopy

The FTIR spectra of the coating solutions are presented in Figure 1.

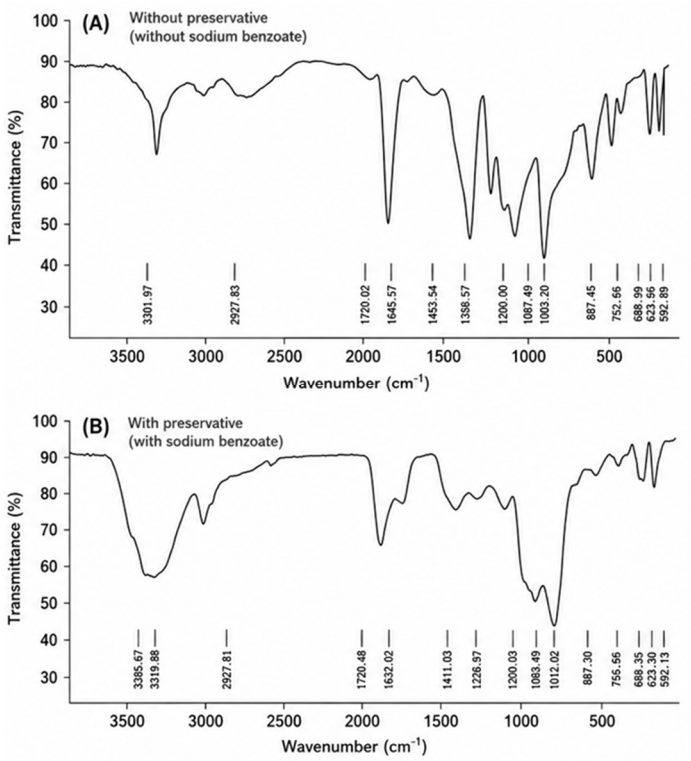

Figure 1. FTIR spectra of the longan seed starch-pomelo peel pectin coating formulations: (A) coating without sodium benzoate and (B) coating supplemented with sodium benzoate

The FTIR analysis revealed the presence of characteristic functional groups and intermolecular interactions among the coating components. The observed absorption bands confirmed the contribution of both starch (homopolysaccharide) and pectin (heteropolysaccharide) to the coating formulations.

A broad absorption band in the region of 3100–3700 cm^{-1} was assigned to O–H stretching vibrations of hydroxyl groups from polysaccharides, water molecules, and plasticizers. A weaker band near 2928 cm^{-1} corresponded to C–H stretching vibrations. The absorption band at approximately 1720–1723 cm^{-1} was attributed to ester carbonyl (C=O) stretching of esterified carboxyl groups characteristic of pectin. Another band in the range of 1630–1650 cm^{-1} was associated with COO^- asymmetric stretching and/or H–O–H bending of absorbed water.

Bands between 1455 and 1360 cm^{-1} were assigned to CH_2 bending and CH deformation vibrations, while the region of 1240–1200 cm^{-1} corresponded to C–O stretching. Strong absorptions in the range of 1150–1000 cm^{-1} were attributed to C–O–C and C–O stretching

vibrations of the polysaccharide backbone. In addition, the band near 887 cm^{-1} was associated with glycosidic linkages.

These observations are consistent with previous reports on starch–pectin-based biopolymer films, where similar ester and polysaccharide-related bands were detected (Arooj et al., 2023). The FTIR spectra of coating formulation A (without preservative) and formulation B (with preservative) showed similar band positions and profiles, indicating that the incorporation of sodium benzoate did not cause substantial chemical modifications in the polymer matrix. Comparable findings were reported by Rego et al. (2020) for cassava starch-based biofilms plasticized with different polyols. The major functional groups identified in the coating formulations are summarized in Table 3.

Table 3

Characteristic FTIR absorption bands of starch, pectin, and the developed coating formulations

Characteristic band (cm^{-1})	Assignment	Starch	Pectin	Coating A without	Coating B with
				sodium benzoate	
3700-3100	O–H stretching	✓	✓	3301.97	3385.67, 3319.88
2927-2880	C–H stretching	✓	✓	2927.83	2927.81
1745–1720	Ester C=O stretching	-	✓	1720.02	1723.48
1650–1600	COO^- asymmetric stretching / H–O–H bending	✓	✓	1645.57	1632.02
1455–1360	CH_2 bending / CH deformation	✓	✓	1453.54, 1368.57	1411.03, 1326.99
1240–1200	C–O stretching	–	✓	1200.00	1209.63
1150–1000	C–O–C and C–O stretching	✓	✓	1087.49, 1003.20	1083.99, 1012.02
900-850	Glycosidic linkage	✓	✓	887.45	887.30

Note: ✓ indicates that the absorption band is characteristic of the corresponding biopolymer; "-" indicates that the band is not considered characteristic of that biopolymer.

Overall, the FTIR results confirmed the successful formation of the starch–pectin coating matrix. The presence of characteristic absorption bands of both polysaccharides demonstrated their incorporation into the formulation, while the similar spectral profiles of coatings with and without sodium benzoate indicated that the preservative was physically entrapped within the polymer network without altering its chemical structure. These findings support the structural stability of the developed coating system.

Overall acceptability

Changes in visual quality, including loss of bright red colour, development of yellow discoloration, and appearance of brown or black spoilage spots, were used to evaluate consumer acceptability of tomato samples. The effect of different coatings on the visual quality rating (VQR) of tomatoes is presented in Figure 2.

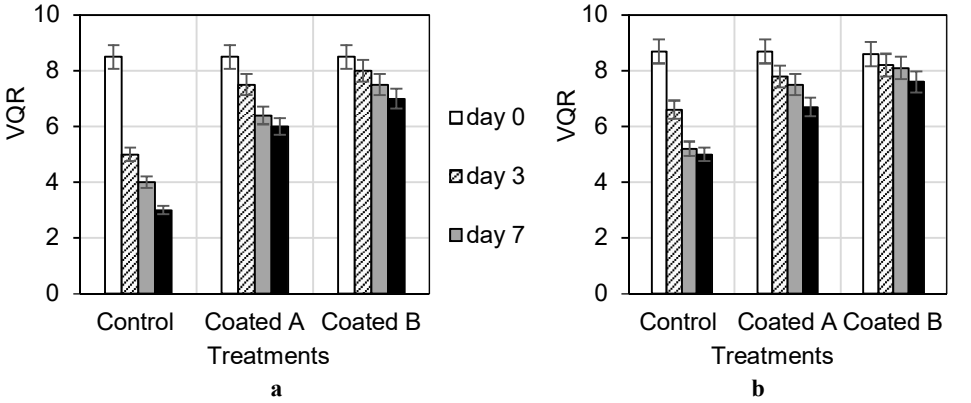

Figure 2. Changes in the visual quality rating (VQR) of tomatoes during storage at 25 °C (a) and 4 °C (b)

For the uncoated control samples, the acceptable shelf life was 3 and 5 days at 25 °C and 4 °C, respectively. In coated treatment A, the shelf life increased to 11 and 14 days at 25 °C and 4 °C, respectively. The best performance was observed for coating treatment B, which extended shelf life to 15 and 21 days under ambient and refrigerated conditions, respectively. The improved shelf life in treatment B may be attributed to the presence of preservatives combined with refrigeration, which likely created a modified atmosphere around the fruit surface, thereby reducing respiration rate, ethylene production, and oxygen availability, and consequently delaying ripening processes.

Similar findings were reported by Maftoonazad and Ramaswamy (2019), who observed that pectin-based edible coatings extended the shelf life of sweet lime to 25 days at 15 °C by slowing metabolic activity. Likewise, Kittur et al. (2001) reported that polysaccharide-based coatings under refrigerated conditions prolonged the shelf life of bananas and mangoes by delaying enzyme-mediated quality deterioration.

Weight loss

The effect of storage duration under different conditions on weight loss in coated and uncoated tomatoes is presented in Figure 3. Weight loss ranged between 11 and 21% during 0 to 11 days of storage under both ambient and refrigerated conditions.

At 25 °C, higher weight loss led to visible shriveling and reduced the shelf life of uncoated tomatoes to less than 7 days. The maximum weight loss (21.02%) was recorded in the control samples. In contrast, coated treatment B exhibited a lower weight loss (15.07%) over the same storage period, while coated treatment A showed a weight loss of 19.45%.

The reduced weight loss in coated samples may be attributed to the formation of a semi-permeable barrier that limited moisture transfer and respiration rate. In addition, the presence of preservatives in coating B likely further slowed biochemical changes, contributing to improved water retention. Similar observations were reported by Shiekh et al. (2021), who found that pectin-based coatings incorporated with thymol essential oil reduced weight loss in lime by delaying respiration, ripening, and spoilage processes.

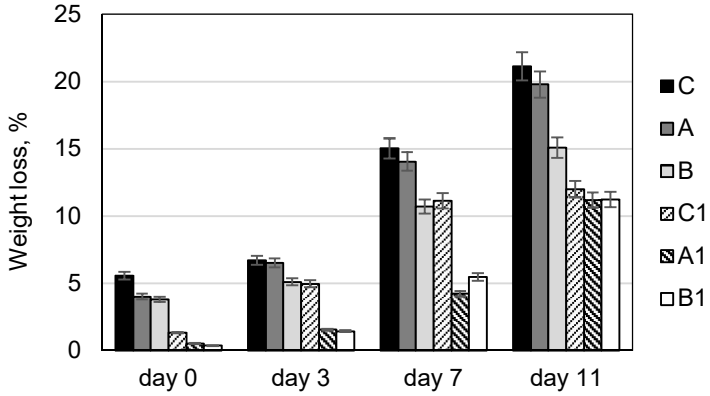

Figure 3. Weight loss of tomatoes with different treatment during storage at 25 °C (C, A, and B) and 4 °C (C1, A1, and B1)
C, C1 – control without coating; A, A1 – tomatoes coated without sodium benzoate;
B, B1 – tomatoes coated with sodium benzoate

A similar trend was observed under refrigerated conditions, although with lower overall weight loss compared to ambient storage. In this case, coated samples (A1 and B1) showed reduced weight loss compared to uncoated control (C1), indicating that combined coating and low-temperature storage further inhibited moisture loss and metabolic activity. Comparable results were reported by Shiekh et al. (2021), who demonstrated that carboxymethyl cellulose (CMC) coatings reduced weight loss, decay, and chilling injury in mandarin fruits during cold storage. Overall, the coating layer acted as a protective barrier against moisture loss as well as mechanical and microbial deterioration.

Titratable acidity and pH

Eventually, organic acid remains dissolved in cell vacuoles, either in free or combined form as salts, glycosides, ester in most of the fruits and vegetables. These organic acids which are available freely and measured by neutralizing cellular extract and juices with strong base are exemplified as titratable acidity. Eventually, the post-harvest increase in pH is due to the process of senescence which fruit undergoes when stored for longer period. Furthermost, the increase in pH is related with decrease in titratable acidity. The difference in pH and titratable acidity values of coated and non-coated tomatoes at variable storage conditions are provided in Figure 4 given below. At 25 °C the pH value for the control increased from 4.5 to 5.5 between 0 to 11 days. Meanwhile, the pH readings of coated A and coated B decreased from 4 to 3.8 and 4.1 to 3 respectively.

A similar trend was also observed at refrigerated condition where increase in pH value from 4.5 to 5 was noted in case of control C1 but in coated A1 and B1 the pH value decreased from 5 to 4 and 4.8 to 3.7 respectively. An inverse relationship trend was observed between pH and titratable acidity content. The maximum increase in titratable acidity was observed in coated B and B1, while a decrease of titratable acidity was reported in case on uncoated control both at 25 °C and refrigerated condition. In general, coated tomatoes exhibited lower pH value and high titratable acidity than non-coated control. This might be due to the ability of coating treatment in presence or absence of preservatives in decreasing the uptake of organic acids by reducing the rate of respiration, ethylene production and other metabolic process.

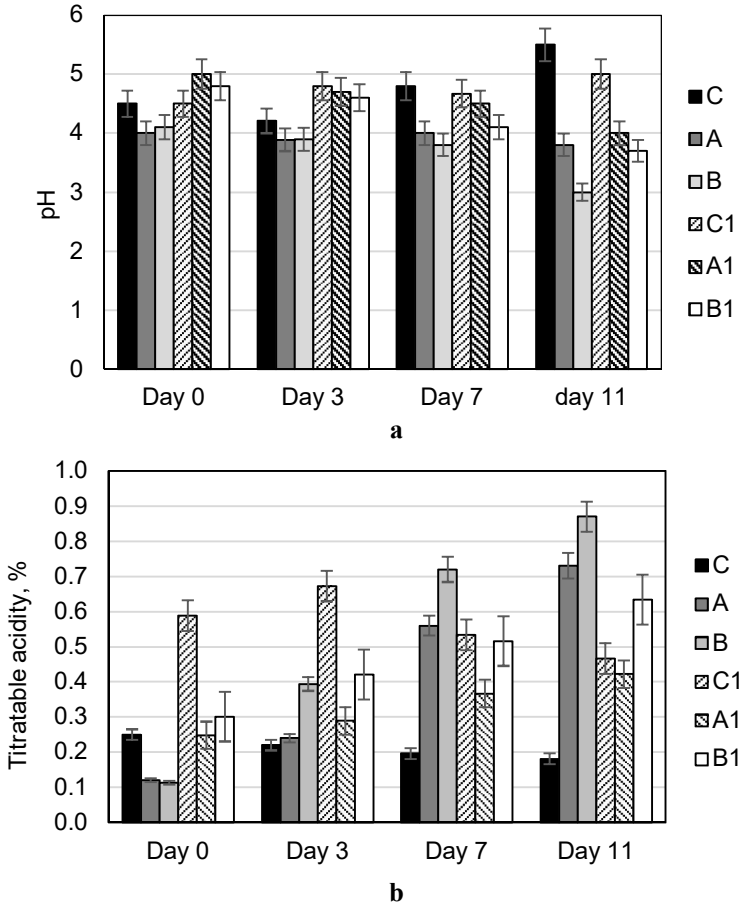

Figure 4. pH change (a) and titratable acidity (b) in coated and uncoated tomatoes at different storage conditions

Thus, the application of coating was successful in retention of acidity by delaying the senescence in post-harvest period. According to the studies conducted by Suhaimi et al. (2021), the pH of star fruits and mangoes coated with pectin and sorbitol was lower than the control fruits.

Total soluble solids (TSS)

Total soluble solids in fruits and vegetables represent the collective concentration of dissolved compounds, including sugars, organic acids, amino acids, ascorbic acid, and minerals. The increase in TSS during postharvest storage is mainly associated with metabolic processes such as the degradation of carbohydrates (particularly pectin), conversion of starch into sugars, partial protein hydrolysis, and breakdown of glycosides.

At 25 °C, the highest increase in TSS (7.2 °Brix) was observed in uncoated control samples (C) during the 0–11 day storage period. In contrast, coated samples (A and B) showed comparatively lower TSS values over the same storage duration, as presented in Figure 5.

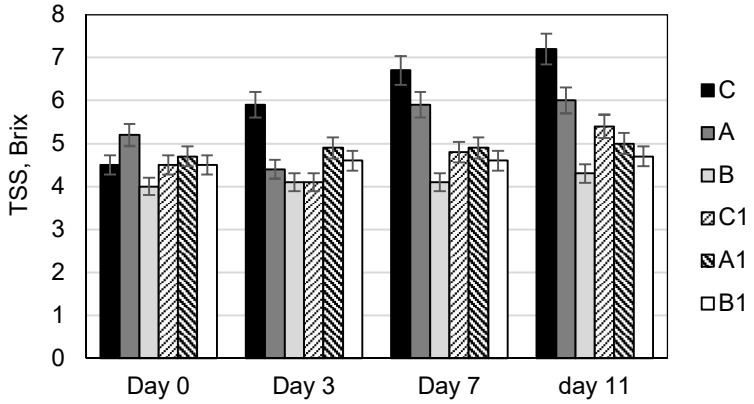

Figure 5. Effect of coating on TSS value of tomatoes at different storage conditions

A similar trend was observed under refrigerated storage conditions, where the increase in TSS was minimal in coated sample B1, indicating a reduced rate of metabolic degradation. The treatment means under both refrigerated and 25 °C storage conditions differed significantly from the control at $p < 0.05$. The coating treatments likely reduced respiration rate and ethylene production during postharvest storage, thereby slowing the increase in TSS values.

Several studies have reported similar effects of edible coatings on TSS in fruits and vegetables. The higher increase in TSS observed in uncoated tomatoes may be attributed to progressive moisture loss combined with accelerated metabolic activity. Panahirad et al. (2020) reported that polysaccharide-based coatings such as carboxymethyl cellulose (CMC) and guar gum reduced TSS accumulation in mangoes compared to controls. Similarly, CMC- and pectin-based edible coatings have been shown to improve postharvest quality of plums by limiting changes in TSS.

Peroxidase (POD) and polyphenolic oxidase (PPO) activity

The effect of coating treatments on peroxidase and polyphenolic oxidase activity of tomatoes at different storage conditions are presented in Figure 6.

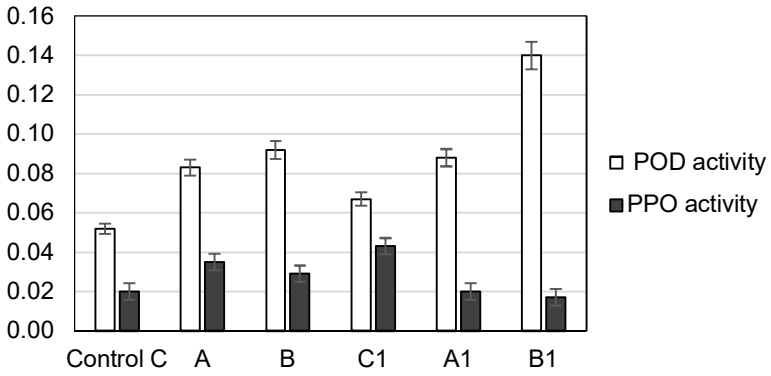

Figure 6. Peroxidase (POD) and polyphenolic oxidase (PPO) activity in coated and uncoated tomatoes

All the coating combinations both at 25 °C and 4 °C exhibited higher POD activity with highest activities of 0.140 μmol tetraguaiacol/min·g at coated B1 tomatoes than non-coated control (C1= 0.067 μmol tetraguaiacol/min·g). But on a contrary, the coating treatments significantly reduced the PPO activity in coated tomatoes. Maximum PPO activity was observed in case of control C while lowest enzyme activity was achieved in B1. The enhancement in POD activity after application of the coating treatment might be due to decrease in harmful peroxide, free radical content with improvement in antioxidant activity. This finding was also reported by Panahirad et al. (2020) in plum coated with sodium alginate/pectin, gum arabic and carboxymethylcellulose coating. Again, the increase in PPO activity and phenolic oxidation in unwrapped tomatoes might be due to senescence related disruption in the natural barrier between PPO and polyphenols. The decline in PPO activity in CMC and pectin coatings were also reported by Sanchís et al. (2017), due to post harvest storage improvement, preservation of membrane structure by slowing down senescence and softening process.

DPPH radical scavenging activity

The DPPH radical scavenging activity of the coated and non-coated tomatoes at different storage conditions are represented in Table 4.

The analysis of variance reveals that there is significant difference in the mean value of antioxidant activity for both treated and non-treated tomatoes at different storage conditions. However, both at 25 °C and refrigerated condition a gradual loss in potential anti-oxidant activity was reported for all the combinations. At 25 °C maximum retentions of antioxidant activity was exhibited by coated B between 0 to 11 days of storage, while maximum loss in antioxidant potential was recorded in non-coated control set. Similarly, between 0 to 11 days of storage the IC50 value of coated B1 increased from 6728 μg/ml to 7247 μg/ml which implies minimum loss in antioxidant activity of 7.71% rather than coated A1 (24.49% loss) and non-coated C1 (173.95% loss) at refrigerated condition.

Table 4

DPPH activity of coated and uncoated tomatoes at different storage condition

Treat-ment	IC_{50} value (μg/ml) on day of storage				
	0	3	7	11	Decrease in antioxidant activity (%)
20–5 °C					
C	3847±0.002^{a}	4751±0.014^{b}	7519±0.008^{a}	9980±0.023^{d}	159.42±0.007^{a}
A	3920±0.030^{b}	5536±0.017^{c}	5979±0.009^{b}	8484±0.006^{b}	132.5±0.004^{d}
B	2873±0.001^{c}	2936±0.012^{d}	3228±0.011^{c}	4239±0.015^{c}	47.54±0.006^{b}
4 °C					
C1	3004±0.001^{a}	7481±0.001^{a}	6312±0.003^{b}	8229±0.023^{d}	173.93±0.021^{c}
A1	5645±0.003^{b}	6287±0.014^{c}	4495±0.001^{a}	7028±0.007^{b}	24.49±0.005^{d}
B1	6728±0.005^{d}	7052±0.005^{b}	3387±0.004^{c}	7247±0.019^{d}	7.71±0.001^{a}

Note: different lowercase letters (a–d) within the same column indicate significant differences ($p<0.05$)

This might be due the protective action of the coating treatments against the loss of bioactive compounds including phenolic compounds, flavonoids anthocyanin, and vitamin C, which promoted better retention of antioxidant activity at post-harvest storage. However,

refrigerated storage combined with preservative-containing coating formulations resulted in improved retention of polyphenolic compounds by suppressing metabolic redox reactions and limiting oxygen permeation. Similar observations were reported by Gao et al. (2018), who found that oranges coated with a cinnamaldehyde–chitosan formulation retained higher levels of vitamin C and polyphenols after 120 days of storage. Likewise, Ebrahimi and Rastegar (2020) demonstrated that a guar gum-based edible coating enriched with *Spirulina platensis* effectively preserved vitamin C in mangoes throughout three weeks of storage. Comparable effects have also been reported for strawberries and blackberries, where polysaccharide-based coatings enhanced the retention of bioactive compounds, including anthocyanins and flavonoids. Accumulating evidence further suggests that edible coatings preserve, or even enhance, the activity of endogenous antioxidant enzymes in fruits and vegetables, thereby strengthening their defense against oxidative damage and lipid peroxidation. In agreement with these findings, Ali et al. (2019) reported that the activities of the antioxidant enzymes catalase and superoxide dismutase were better preserved in aloe vera gel-coated lychee fruit during storage, which may have contributed to the maintenance of antioxidant activity.

Conclusions

The physicochemical characteristics of coated and uncoated tomatoes confirmed the effectiveness of the edible coating based on longan seed starch and pomelo peel pectin in delaying postharvest deterioration and extending shelf life. FTIR analysis verified the successful formation of the starch–pectin coating matrix and showed that the incorporation of sodium benzoate did not induce significant chemical modifications, indicating its physical entrapment within the polymer network. The formulation, particularly when supplemented with sodium benzoate and combined with refrigerated storage, effectively maintained tomato quality for up to 21 days. Under ambient conditions (25 °C), the coating extended shelf life to approximately 11 days by slowing ripening and mitigating undesirable physicochemical changes, including weight loss, increases in pH and total soluble solids, and alterations in antioxidant enzyme activity.

These findings highlight the potential of fruit-processing by-products as sustainable sources of functional biopolymers for active edible coatings. The developed formulation offers an effective postharvest preservation strategy that improves product quality and safety while reducing postharvest losses. Moreover, the valorization of longan seeds and pomelo peels supports circular bioeconomy principles by converting agricultural waste into value-added biodegradable packaging materials, providing an environmentally friendly alternative to conventional plastic-based packaging.

Acknowledgement. The authors gratefully acknowledge the Department of Home Science, University of Calcutta, for providing the facilities and research environment that made this study possible.

References

Adjouman Y.D., Nindjin C., Kouassi K.N., Tetchi F.A., N'Guessan G.A., Sindic M. (2018), Effect of edible coating based on improved cassava starch on post-harvest quality of fresh tomatoes (*Solanum lycopersicum* L.), *International Journal of Nutritional Science and Food Technology*, 4(1), 1-10.

Ali S., Khan A.S., Nawaz A., Anjum M.A., Naz S., Ejaz S., Hussain S. (2019), *Aloe vera* gel coating delays postharvest browning and maintains quality of harvested litchi fruit, *Postharvest Biology and Technology*, 157, 110960, https://doi.org/10.1016/j.postharvbio.2019.110960

Arooj A., Khan M., Munawar K.S. (2023), Preparation and physicochemical characterization of starch/pectin and chitosan blend bioplastic films as future food packaging materials, *Journal of Environmental Chemical Engineering*, 12(18), 111825, https://doi.org/10.1016/j.jece.2023.111825

Bai W., Vidal N.P., Roman L., Portillo-Perez G., Martinez M.M. (2023), Preparation and characterization of self-standing biofilms from compatible pectin/starch blends: Effect of pectin structure, *International Journal of Biological Macromolecules*, 251, 126383, https://doi.org/10.1016/j.ijbiomac.2023.126383

Ballesteros L.F., Cerqueira M.A., Teixeira J.A., Mussatto S.I. (2018), Production and physicochemical properties of carboxymethyl cellulose films enriched with spent coffee grounds polysaccharides, *International Journal of Biological Macromolecules*, 106, pp. 647-655, https://doi.org/10.1016/j.ijbiomac.2017.08.060

Das S.K., Vishakha K., Das S., Chakraborty D., Ganguli A. (2022), Carboxymethyl cellulose and cardamom oil in a nanoemulsion edible coating inhibit the growth of foodborne pathogens and extend the shelf life of tomatoes, *Biocatalysis and Agricultural Biotechnology*, 42, 102369, https://doi.org/10.1016/j.bcab.2022.102369

Ebrahimi F., Rastegar S. (2020), Preservation of mango fruit with guar-based edible coatings enriched with *Spirulina platensis* and *Aloe vera* extract during storage at ambient temperature, *Scientia Horticulturae*, 265, 109258, https://doi.org/10.1016/j.scienta.2020.109258

Gao Y., Kan C., Wan C., Chen C., Chen M., Chen J. (2018), Quality and biochemical changes of navel orange fruits during storage as affected by cinnamaldehyde-chitosan coating, *Scientia Horticulturae*, 239, pp. 80-86, https://doi.org/10.1016/j.scienta.2018.05.012

Gonzales K.N., Torres F.G., Carsí M., Sanchis M.J. (2025), Effects of morphology and extraction procedures on the chemical, thermal and dielectric properties of ulvan polysaccharides, *International Journal of Biological Macromolecules,* 321(Pt 2), 146121, https://doi.org/ 10.1016/j.ijbiomac.2025.146121

Hasan M., Tasya G., Khaldun I., Rusman R., Hasanah U. (2025), Eco-friendly bio-nanocomposite films for sustainable packaging, *Journal of Ecological Engineering*, 26(4), pp. 301–312, https://doi.org/10.12911/22998993/200335

Hernández-Guerrero S.E., Balois-Morales R., Palomino-Hermosillo Y.A., López-Guzmán G.G., Berumen-Varela G., Bautista-Rosales P.U., Alejo-Santiago G. (2020), Novel edible coating of starch-based stenospermocarpic mango prolongs the shelf life of mango "ataulfo" fruit, *Journal of Food Quality*, 2020(1), 1320357, https://doi.org/10.1155/2020/1320357

Hu Z., Zhao L., Hu Z., Wang K. (2018), Hierarchical structure, gelatinization, and digestion characteristics of starch from longan (*Dimocarpus longan* Lour.) seeds, *Molecules*, 23(12), 3262, https://doi.org/10.3390/molecules23123262

Kharb J., Saharan R. (2025), Developing antimicrobial, biodegradable, sustainable, and eco-friendly biofilms: harnessing tea waste for a greener future, *Iranian Polymer Journal*, 34(10), pp.1577-1588, https://doi.org/10.1007/s13726-025-01451-9

Kittur F., Saroja N., Habibunnisa, Tharanathan R. (2001), Polysaccharide-based composite coating formulations for shelf-life extension of fresh banana and mango, *European Food Research and Technology*, 213, pp. 306-311, https://doi.org/10.1007/s002170100363

Kostova I., Lasheva V., Georgieva D., Damyanova S., Stoyanova A., Stefanov S., Gubenia O. (2020a), Antimicrobial active packaging paper based on dill weed essential oil, *Cellulose Chemistry and Technology*, 54(3-4), pp. 347-354, https://doi.org/10.35812/cellulosechemtechnol.2020.54.35

Kostova I., Lasheva V., Georgieva D., Damyanova S., Fidan H., Stoyanova A., Gubenia O. (2020b), Characterization of active paper packaging materials with coriander essential oil (*Coriandrum sativum* L.), *Journal of Chemical Technology and Metallurgy*, 55(6), pp. 2085–2093.

Kumar M., Potkule J., Tomar M., Punia S., Singh S., Patil S., Singh S., Ilakiya T., Kaur C., Kennedy J.F. (2021), Jackfruit seed slimy sheath, a novel source of pectin: Studies on antioxidant

activity, functional group, and structural morphology, *Carbohydrate Polymer Technologies and Applications*, 2, 100054, https://doi.org/10.1016/j.carpta.2021.100054

Maftoonazad N., Ramaswamy H.S. (2019), Application and evaluation of a pectin-based edible coating process for quality change kinetics and shelf-life extension of lime fruit (*Citrus aurantifolium*), *Coatings*, 9(5), 285, https://doi.org/10.3390/coatings9050285

Maniglia B.C., Tapia-Blácido D.R. (2016), Isolation and characterization of starch from babassu mesocarp, *Food Hydrocolloids*, 55, pp. 47-55, https://doi.org/10.1016/j.foodhyd.2015.11.001

Manzoor A., Ahmad S. (2024), Longan seed starch: structure, functionality and applications, In: Lorenzo J.M., Bangar S.P. (Eds.), *Non-Conventional Starch Sources,* pp. 103-121, Academic Press.

Medina-Jaramillo C., Gonzalez-Seligra P., Goyanes S., Bernal C., Famá L. (2015), Biofilms based on cassava starch containing extract of yerba mate as antioxidant and plasticizer, *Starch-Stärke*, 67(9-10), pp. 780-789, https://doi.org/10.1002/star.201500033

Moalemiyan M., Ramaswamy H.S., Maftoonazad N. (2012), Pectin-based edible coating for shelf-life extension of ataulfo mango, *Journal of Food Process Engineering*, 35(4), pp. 572-600, https://doi.org/10.1111/j.1745-4530.2010.00609.x

Panahirad S., Naghshiband-Hassani R., Bergin S., Katam R., Mahna N. (2020), Improvement of postharvest quality of plum (*Prunus domestica* L.) using polysaccharide-based edible coatings, *Plants*, 9(9), 1148, https://doi.org/10.3390/plants9091148

Pasichnyi V., Marynin A., Khrapachov O., Shvediuk D. (2022), Modern packaging systems application to extend meat products shelf life, In: O. Paredes-López, O. Shevchenko, V. Stabnikov, V. Ivanov. (Eds.), *Bioenhancement and Fortification of Foods for a Healthy Diet*, pp. 295-323, CRC Press, Boca Raton, London, https://doi.org/ 10.1201/9781003225287-19

Pech-Canul A.d.L.C., Ortega D., García-Triana A., González-Silva N., Solis-Oviedo R.L. (2020), A brief review of edible coating materials for the microencapsulation of probiotics, *Coatings*, 10(3), 197, https://doi.org/10.3390/coatings10030197

Pirog T., Stabnikov V., Antoniuk S. (2022a), Application of surface-active substances produced by *Rhodococcus erythropolis* IMB Ac-5017 for post-harvest treatment of sweet cherry, *Ukrainian Food Journal*, 11(1), pp. 164–174, https://doi.org/10.24263/2304-974X-2022-11-1-15

Pirog T., Stabnikov V., Stabnikova, O. (2022b), Bacterial microbial surface-active substances in food-processing industry, In: O. Paredes-López, O. Shevchenko, V. Stabnikov, V. Ivanov, (Eds.), *Bioenhancement and Fortification of Foods for a Healthy Diet*, pp. 271-294, CRC Press, Boca Raton, London, https://doi.org/10.1201/9781003225287-18

Quoc L.P.T., Huyen V.T.N., Hue L.T.N., Hue N.T.H., Thuan N.H.D., Tam N.T.T., Duy T.H. (2015), Extraction of pectin from pomelo (*Citrus maxima*) peels with the assistance of microwave and tartaric acid, *International Food Research Journal*, 22(4), pp. 16-37.

Rego J.D.A., da Costa M.L., Brasil D.D.S. B., Cruz J.N., Costa C.M.L. (2020), Characterization and evaluation of filmogenic, polymeric, and biofilm suspension properties of cassava starch base (*Manihot esculenta* Crantz) plasticized with polyols, *Brazilian Journal of Development*, 6(7), pp. 50417-50442, https://doi.org/10.34117/ bjdv6n7-62

Sanchís E., Gonzalez S., Ghidelli C., Sheth C.C., Mateos M., Palou L., Pérez-Gago M.B. (2016), Browning inhibition and microbial control in fresh-cut persimmon (*Diospyros kaki* Thunb. cv. Rojo Brillante) by apple pectin-based edible coatings, *Postharvest Biology and Technology*, 112, pp. 186-193, https://doi.org/10.1016/j.postharvbio.2015.09.024

Sapper M., Chiralt A. (2018), Starch-based coatings for preservation of fruits and vegetables, *Coatings*, 8(5), 152, https://doi.org/10.3390/coatings8050152

Sayed A., Safwat G., Abdel-raouf M., Mahmoud G.A. (2023), Alkali-cellulose/polyvinyl alcohol biofilms fabricated with essential clove oil as a novel scented antimicrobial packaging material, *Carbohydrate Polymer Technologies and Applications*, 5, 100273, https://doi.org/10.1016/j.carpta.2022.100273

Shiekh K.A., Ngiwngam K., Tongdeesoontorn W. (2021), Polysaccharide-based active coatings incorporated with bioactive compounds for reducing postharvest losses of fresh fruits, *Coatings*, 12(1), 8, https://doi.org/10.3390/coatings12010008

Stabnikov V., Kovshar I., Stabnikova O. (2025), Recent advances in the study of the properties and applications of lactic acid bacteria, *World Journal of Microbiology and Biotechnology*, 41, 287, https://doi.org/10.1007/S11274-025-04499-0

Stabnikova O., Shevchenko O., Stabnikov V., Paredes-López O. (Eds), (2023a), *Bioconversion of Waste to Value-Added Products*, CRC Press, Boca Raton, London, New York, https://doi.org/10.1201/9781003329671

Stabnikova O., Shevchenko A., Stabnikov V., Paredes-López O. (2023b), Utilization of plant processing wastes for enrichment of bakery and confectionery products, *Ukrainian Food Journal*, 12(2), pp. 299-308, https://doi.org/10.24263/2304-974X-2023-12-2-11

Stabnikova O., Stabnikov V., Paredes-López O. (2026a), Spices and essential oils in food preservation: from natural additives to active packaging systems, *Plant Food for Human Nutrition*, 81, 69, https://doi.org/10.1007/s11130-026-01519-8

Stabnikova O., Stabnikov V., Paredes-López O. (2026), Cacti as novel edible resources for human nutrition, *Food Science and Technology International*, 10820132261461422, https://doi.org/10.1177/10820132261461422. Epub ahead of print.

Suhaimi N.I.M., Ropi A.A.M., Shaharuddin S. (2021), Safety and quality preservation of starfruit (*Averrhoa carambola*) at ambient shelf life using synergistic pectin-maltodextrin-sodium chloride edible coating, *Heliyon*, 7(2), e06279, https://doi.org/10.1016/j.heliyon.2021.e06279

Tafa K.D., Satheesh N., Abera W. (2023), Mechanical properties of tef starch based edible films: Development and process optimization, *Heliyon*, 9(2), e13160, https://doi.org/10.1016/j.heliyon.2023.e13160

Thakur R., Pristijono P., Scarlett C.J., Bowyer M., Singh S.P., Vuong Q.V. (2019), Starch-based films: Major factors affecting their properties, *International Journal of Biological Macromolecules*, 132, pp. 1079-1089, https://doi.org/10.1016/j.ijbiomac.2019.03.190

Valdés A., Burgos N., Jiménez A., Garrigós M.C. (2015), Natural pectin polysaccharides as edible coatings, *Coatings*, 5(4), pp. 865-886, https://doi.org/10.3390/coatings5040865

Cite:

Laha, S., & Chatterjee, A. (2026). Active coating based on longan seed starch and pomelo peel pectin for extending shelf life of tomatoes. *Ukrainian Food Journal, 15*(2), 401–417. https://doi.org/10.24263/2304-974X-2026-15-2-9

Energy-efficient saturation and drying of pumpkin pieces

Iryna Huzova[1], Diana Kindzera[1], Oleksandr Shevchenko[2], Oleksandr Bessarab[2]

1 – Lviv Polytechnic National University, Lviv, Ukraine
2 – National University of Food Technologies, Kyiv, Ukraine

Keywords:

Pumpkin
Candy
Drying
Saturation
Energy efficiency

Article history:

Received 17.01.2026
Received in revised form 18.04.2026
Accepted 30.06.2026

Corresponding author:

Iryna Huzova
E-mail: iryna.o.huzova@lpnu.ua

DOI:
10.24263/2304-974X-2026-15-2-10

Abstract

Introduction. The aim of this study was to evaluate energy-efficient methods for the saturation and drying of pumpkin pieces, investigate the influence of saturation medium properties on process intensification, and determine the optimal processing conditions.

Materials and methods. Pumpkin pieces were used as the experimental material. The saturation process was investigated by periodically sampling the pieces from the sugar syrup and determining their soluble solids content using a refractometer. Drying was performed in a fixed bed by filtering drying air at alternating temperatures through the bed of saturated pumpkin pieces.

Results and discussion. Energy analysis demonstrated that the bubbling process at a saturation temperature of 80 °C and an air flow rate of 0.125 L/s represented the most energy-efficient operating conditions, with a thermal energy consumption of 0.73 MJ/kg of syrup. Compared with the static infusion process, gas bubbling enhanced mass transfer and reduced the energy required to achieve the desired saturation level.

A drying method based on filtration of drying air with alternating temperatures through a fixed bed of saturated pumpkin pieces was developed. This approach utilizes the residual heat accumulated in the upper layers of the bed to complete moisture removal from the lower layers, thereby improving heat utilization throughout the drying process. The proposed technology shortened the drying time and reduced overall energy consumption. In particular, using the residual heat of the upper layers during the final drying stage decreased the specific energy consumption by 31.26 MJ/kg of removed moisture. These results demonstrate that combining gas bubbling during saturation with the proposed drying strategy improves the overall energy efficiency of candied pumpkin production while maintaining effective heat and mass transfer throughout processing.

Conclusions. The proposed bubbling saturation method and the fixed-bed drying method with alternating-temperature drying air improved the energy efficiency of candied pumpkin production by reducing the energy required for both saturation and drying.

Introduction

Plant-based products are well recognized for their beneficial effects on human health; however, fresh fruits and vegetables have a limited shelf life due to their high moisture content and susceptibility to microbial and biochemical spoilage (Sniezhkin et al., 2025). The development of innovative processing methods and advanced equipment for sustainable food technologies remains highly relevant for reducing post-harvest losses (Petrova et al., 2025). Among preservation methods, candied fruit production converts perishable raw materials into shelf-stable confectionery products through impregnation of plant tissues with concentrated sugar syrup, followed by drying (Muccilli et al., 2020). The syrup impregnation stage is a critical unit operation, as its kinetics directly determine the final product's texture, sweetness, stability, and overall quality.

The most common saturation method is osmotic dehydration, which is driven by concentration gradients and promotes water removal and solute uptake, leading to reduced water activity and structural stabilization of tissues (González-Pérez et al., 2023; Vinod et al., 2024). To enhance mass transfer, steam blanching is often applied prior to dehydration; it preserves nutrients and pigments more effectively than hot-water blanching and demonstrates higher energy efficiency (Cherif et al., 2024). During saturation, the process may proceed via static infusion or active gas bubbling. Infusion is governed primarily by diffusion and requires mainly thermal energy, whereas gas bubbling intensifies mass transfer and reduces processing time but increases electrical energy consumption due to compressor operation. Convective drying remains the final and most energy-intensive stage of candied fruit production (Huzova and Atamanyuk, 2022). Consequently, modern production faces a multi-objective challenge of balancing technological efficiency and product quality with environmental sustainability and reduced energy consumption (Chinchkar et al., 2025).

Pumpkin (*Cucurbita pepo* L.) is an economically attractive raw material for candied fruit production due to its high yield, low cost, and robust cellular structure, which effectively maintains structural integrity during processing (Abraão et al., 2013). Despite extensive research, comparative data on the energy and technological optimization of combined saturation–drying cycles remain limited. In particular, the energetic feasibility of utilizing residual heat in pumpkin pieces immediately after hot syrup saturation has not been sufficiently investigated.

This study aimed to investigate energy-efficient approaches to the saturation and drying of pumpkin pieces by evaluating the influence of saturation medium properties on process intensification and identifying the optimal operating conditions.

Materials and methods

Material

Pumpkin of the variety "Stofuntovka Vassma" was used for candied fruit production. The raw material was washed and peeled, and the membranes, seeds, and seed cavity were removed. Samples were prepared from the outer part of the pumpkin (closer to the peel). Cubic pumpkin pieces with uniform dimensions (edge length 10 mm) and a mass of 5 g were used in the experiments (Figure 1).



Figure 1. Pumpkin pieces used in the study

Methods

Methodology for the blanching and saturation stages (infusion and bubbling modes) of pumpkin pieces

The experimental setup shown in Figure 2 was used to conduct two processes: blanching and saturation. The saturation process was studied under two operating modes: infusion and bubbling.

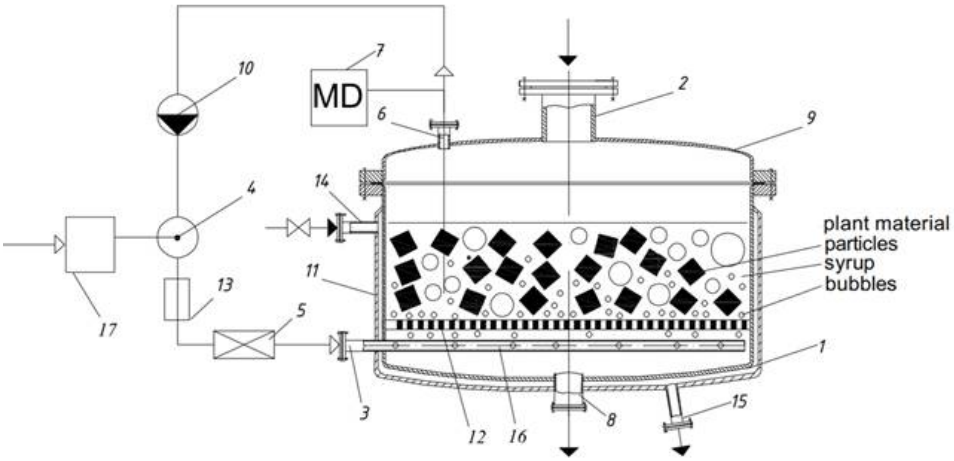

Figure 2. Schematic diagram of the experimental setup for saturation of pumpkin fruit pieces with soluble substances:
1 – food-grade stainless steel housing (diameter 200 mm, height 140 mm); 2 – inlet fitting pipe for supplying water, sugar syrup, and food plant raw material pieces; 3 – compressed air supply pipe; 4 – fan; 5 – air heater with temperature controller; 6 – air outlet pipe; 7 – temperature measuring device; 8 – outlet pipe for water and syrup; 9 –cover; 10 – droplet separator; 11 – jacket; 12 – grate; 13 – flow meter; 14 – inlet pipe for supplying saturated steam to the jacket; 15 – condensate outlet pipe; 16 – air bubbling plate; 17 – air preparation system

Blanching stage. Water was poured into the middle of the housing 1 through inlet fitting 2 up to the lower level of grate 12. Saturated steam was supplied to jacket 11 through inlet pipe 14 to heat the water in unit body 1 to the boiling state. When the saturated steam

generated by water evaporation completely filled the volume of housing 1, pumpkin fruit pieces (40–45 pieces) were loaded into it. In this way, they were subjected to blanching.

The blanching duration was 5 min. In the present study, blanching with saturated steam was selected as the thermal pretreatment method due to its uniform heat transfer characteristics and reduced leaching of vitamin complex compared to water blanching.

After blanching, the water was drained through outlet pipe 8, while the blanched pumpkin fruit pieces remained on grate 12. Three pumpkin fruit pieces were removed from the experimental setup to determine their soluble solids content.

Saturation stage (infusion mode). A pre-prepared sugar syrup of the required temperature and concentration was poured into the middle of the housing 1 containing the blanched pumpkin fruit pieces through inlet fitting 2. The mass and volume of the syrup were adjusted so that grate 12 was completely immersed. The saturation process then occurred, i.e., a diffusion-driven transfer of soluble substances from the syrup into the interior of the blanched pumpkin fruit pieces.

Saturated steam supplied through inlet pipe 14 into jacket 11 was used to maintain the constant syrup temperature, which was monitored using measuring device 7. At 30 s intervals, pieces were sequentially removed from the middle of the housing 1 to determine their soluble solids content by removing cover 9. Saturation was considered complete when the concentration of soluble substances in the last 3–5 samples remained constant. After completion of the process, the syrup was drained through outlet pipe 8.

Saturation stage (bubbling mode). The middle of the housing 1 containing the blanched pumpkin fruit pieces was filled with sugar syrup as described above. Subsequently, air was supplied by fan 4 into the syrup volume beneath grate 12 through supply pipe 3, where it bubbled through the syrup using the air bubbling plate 16. The air bubbling plate ensured uniform air distribution and bubbling, while the air flow rate was monitored using flow meter 13. The air was heated to the syrup temperature by air heater 5.

During bubbling, the gas exited unit body 1 through air outlet pipe 6, passed through droplet separator 10, and mixed with a fresh air stream supplied for bubbling from the air preparation system 17 by fan 4. The saturation process and determination of soluble solids content in the samples were carried out in the same manner as in the soaking mode.

The ratio of the total volume of pumpkin fruit pieces to the volume of sugar syrup was maintained at 1:5. This proportion was selected to ensure effective and uniform saturation of the pumpkin fruit pieces with soluble solids, while maintaining a constant sugar syrup concentration throughout the process.

Kinetics investigation of soluble solids uptake during saturation of pumpkin pieces

To investigate the saturation kinetics, it was necessary to determine the change in the concentration of soluble substances in pumpkin fruit pieces over time. The experiments were conducted as follows. From washed and peeled plant raw material, 40–45 pieces of identical mass, shape, and size were prepared. One pumpkin fruit particle was selected, and its soluble solids content was determined using a refractometer. The remaining pieces were loaded through inlet fitting 2 onto grate 12 located inside housing 1 and subjected to blanching in the experimental setup shown in Figure 2.

After blanching, one blanched pumpkin fruit particle was removed through inlet fitting 2, weighed, and its soluble solids content was determined. Subsequently, the pre-prepared sugar syrup of a specified temperature was poured into housing 1 through inlet fitting 2. Every 30 s, one pumpkin fruit particle was removed from the setup, weighed, and the soluble

solids content was determined. The experiment was continued until the concentration of soluble substances in the last 3–5 samples remained constant.

The experiments were carried out at temperatures ranging from 30 to 80 °C. At temperatures above 80 °C, water evaporation from the syrup occurs, leading to non-uniform saturation and therefore such conditions were not considered.

The investigation of saturation kinetics during air bubbling of the sugar syrup was performed in a similar manner. The only difference was that, at a fixed temperature, the air flow rate used for bubbling was varied and the change in soluble solids concentration over time was determined. In addition, at a fixed air flow rate, the sugar syrup temperature was varied and the corresponding changes in concentration over time were recorded. The air flow rate ranged from 0.03 to 0.156 L/s, which corresponds to an air velocity in supply pipe 3 (Figure 2) of 1.5–8 m/s. Air velocities below 1.5 m/s did not intensify the saturation process compared to the mode without bubbling, while velocities above 8 m/s led to entrainment of sugar syrup droplets from the saturation zone.

Changes in mass and soluble solids concentration of the samples over time were determined as follows. The particle was removed from the saturation zone, and excess sugar syrup was removed from its surface using filter paper, after which the particle was weighed. The mass was measured at the sugar syrup temperature. Subsequently, the pumpkin fruit particle was cooled to room temperature, one drop of juice was expressed from it and placed on the prism of the refractometer. The prism was covered with the transparent lid of the refractometer, oriented toward a bright light source, and the reading was taken through the eyepiece using the Brix scale. The obtained value was corrected depending on the temperature of the syrup in which the particle was kept, according to the tables provided in the operating manual of the NT118 refractometer (0–80% Brix). In this manner, the temporal changes in sample mass and soluble solids concentration were determined.

Investigation drying kinetics and temperature variation within layer of pumpkin fruit pieces

The schematic diagram of the experimental setup used to investigate the drying kinetics and temperature changes within the layer of pumpkin fruit pieces saturated with soluble substances is shown in Figure 3.

The experimental setup shown in Figure 3 consists of a container 1 mounted on a receiver 2, which is connected via a pipeline system, an electronic rotameter 3, a shut-off valve 4, and a control valve 5 to a water-ring vacuum pump 6. An air heater 7 diffuser is installed above the container 1 and connected to a fan 8.

To measure the temperature of the thermal agent above the material layer, thermocouple 9 is installed, while thermocouple 10 is positioned at the outlet. Additional thermocouples are installed inside the container. All thermocouples are connected to an electronic temperature controller (11). The vacuum level beneath the material layer is measured using a vacuum gauge (12) (Huzova, 2020).

The investigation of temperature variation within the layer during drying of the saturated pumpkin fruit pieces was carried out using the experimental setup shown in Figure 3, in a container whose schematic diagram is presented in Figure 4. The container housing 1 shown in Figure 4, with a diameter of 0.1 m, consists of four identical sections. Thermocouples 4 and 5 are installed at the inlet and outlet of the container 1, respectively. In addition, thermocouples I–IV are installed in each of the four container sections.

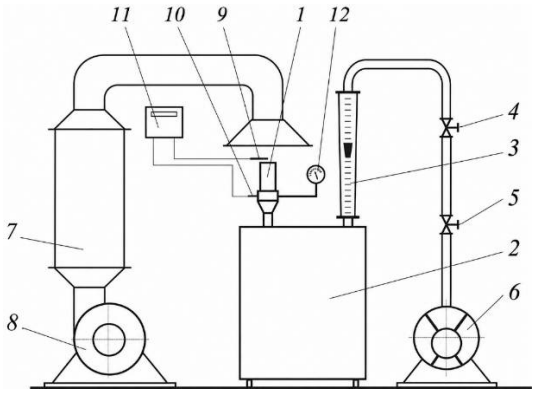

Figure 3. Schematic diagram of the experimental setup for studying drying kinetics:
1 – container; 2 – receiver; 3 – electronic rotameter; 4, 5 – shut-off and control valves; 6 – water-ring vacuum pump; 7 – air heater; 8 – fan; 9, 10 – thermocouples; 11 – SESTOS D1S electronic temperature controller; 12 – DV250A electronic vacuum gauge

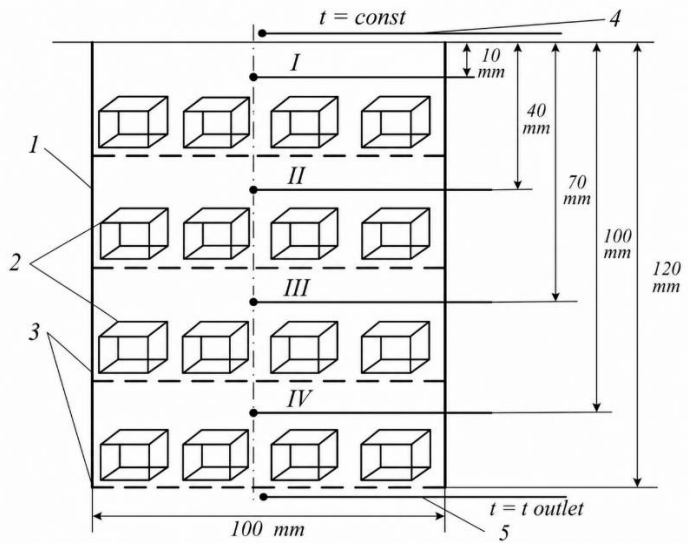

Figure 4. Schematic diagram of the container used to study temperature variation within the layer during drying of pumpkin fruit pieces saturated with soluble substances:
1 – housing; 2 – layers of the pumpkin fruit pieces; 3 – grates; 4 – thermocouple at the container inlet; 5 – thermocouple at the container outlet;
I – thermocouple above the first layer; II – thermocouple above the second layer;
III – thermocouple above the third layer; IV – thermocouple above the fourth layer

Saturated pumpkin fruit pieces were uniformly arranged in a single layer on each of the four grates (Figure 4). This arrangement was selected based on the results of hydrodynamic studies, as it ensures a uniform distribution of the thermal agent and minimizes the hydraulic resistance of the layer (Atamanyuk et al., 2016). Thermocouples were installed above each layer and positioned at the center of the container at the following distances from the upper edge of the container: thermocouple I – 10 mm, thermocouple II – 40 mm, thermocouple III – 70 mm, and thermocouple IV – 100 mm (Figure 4).

Thermocouple 4, located above the container, recorded the constant temperature of the thermal agent supplied to the system, while thermocouple 5, located below the container, recorded the temperature of the thermal agent at the container outlet.

The experiment was conducted as follows. Container 1 was mounted on the receiver 2 (Figure 3). The vacuum pump 6 was switched on, and the flow rate of the thermal agent was adjusted using the control valve 5. The thermal agent, with a constant temperature and flow rate, was filtered through four layers of candied pumpkin pieces. The flow rate of the thermal agent was selected based on an analysis of the scientific literature (Huzova, 2020). The flow rate was determined by rotameter 3, while pressure losses were measured using the electronic vacuum gauge 12. Temperatures over the entire height of the layer, as well as at the inlet and outlet, were recorded using an eight-channel thermoelectric converter PT-108, which enables data acquisition and transfer to a personal computer at intervals of 1.8 s (Huzova, 2020).

Drying of pumpkin fruit pieces saturated with soluble substances was carried out after saturation had been achieved under rational established conditions. The drying process was performed using a filtration method in the experimental setup shown in Figure 3, within a container whose schematic is presented in Figure 4.

The fan 8 and the air heater 7 were switched on, and after the preset temperature was reached, the vacuum pump 6 was activated. The container containing layers of moist material was then placed on the receiver 2. At specified time intervals, changes in the container mass were recorded using an AXIS-3000 electronic balance with an accuracy of 0.01 g. If the container mass remained unchanged for 120–180 s, the experiment was stopped (Huzova, 2020).

Results and discussion

Blanching of pumpkin fruit pieces

Blanching of pumpkin pieces was realized at the experimental setup shown in Figure 1. Images of pumpkin fruit tissue cross-sections (50× magnification) are presented in Figure 5. As can be seen from Figure 5a, the cells of raw pumpkin are almost square in shape, and the pores are clearly defined. After blanching (Figure 5b), the pumpkin cells are partially destroyed, and the pores become significantly wider.

The sample images were analyzed using the Aperio ImageScope software (v12.4.3.5008). This program makes it possible to determine the surface area of a cell fragment S_{total} (the square cross-section shown in Figure 4) as well as the average cell surface area S_{cell} within the selected fragment. All dimensions were recorded in micrometers. The measured values are presented in Table 1.

The porosity of raw and blanched pumpkin fruit was determined according to the following procedure. For analysis and measurements, different fragments of the main tissue were selected under various magnification. From each particle of the studied object, both longitudinal and transverse sections were taken to determine porosity (m, m^2/m^2).

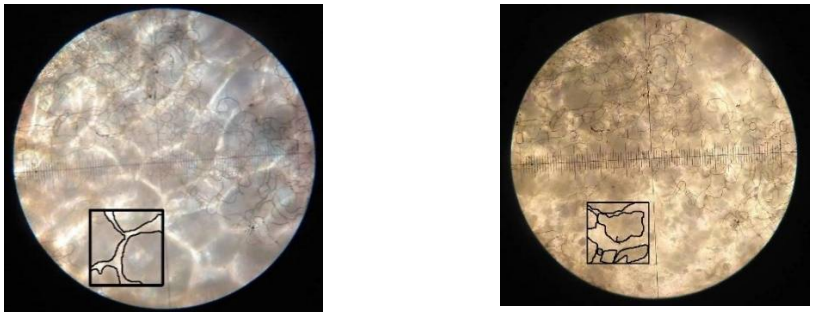

a b

Figure 5. Cross-sectional images of the main pumpkin tissue: (a) raw; (b) blanched

Table 1

Total area of pumpkin fruit fragment and cells within it

Raw pumpkin fruit		Blanched pumpkin fruit	
Fragment	**Surface area, μm²**	**Fragment**	**Surface area, μm²**
S_{total}	2720.21	S_{total}	3216.78
	S_{cell}:		S_{cell}:
1	795.97	1	367.16
2	425.43	2	47.38
3	551.4	3	962.71
4	250.23	4	204.52
ΣS_{cell}	**2023.03**	5	249.47
		6	230.73
		ΣS_{cell}	**2061.97**

Using the software, the total area of the fragment and the total area of each cell within the fragment were measured. The porosity value (m) of the studied samples was calculated according to the following equation:

$$m = \frac{S_{voids}}{S_{total}} = \frac{S_{total} - \sum S_{cells}}{S_{total}} \quad (1)$$

where ΣS_{cells} – total area of all cells within the selected fragment, m²; S_{total} – total area of the selected fragment, m²; S_{voids} – total area of all voids between cells within the selected fragment, m².

The following results were obtained: m_{raw} = 0.25 m²/m²; $m_{blanched}$ = 0.35 m²/m².

Kinetics investigation of soluble solids uptake during saturation of pumpkin fruit pieces

The kinetics of soluble solids uptake during saturation of pumpkin fruit pieces under infusion and bubbling modes were investigated according the appropriate methodology at the experimental setup shown in Figure 2. Figure 6 presents the kinetic curves of the saturation process of blanched pumpkin fruit pieces under infusion conditions.

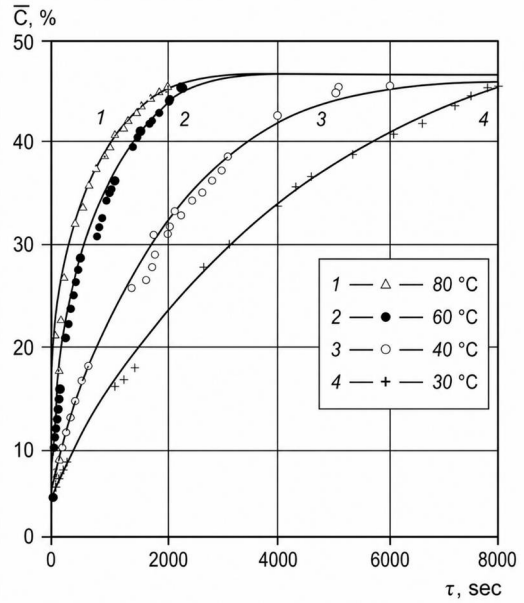

Figure 6. Influence of temperature on the kinetics of soluble solids uptake in pumpkin fruit pieces under infusion conditions

As shown in Figure 6, at a sugar syrup temperature of 80 °C, saturation occurs within the shortest period of time.

The saturation of pumpkin fruit pieces under bubbling mode with varying air flow rates was also examined. Figure 7 illustrates the kinetic curves of the saturation process of blanched pumpkin fruit pieces with soluble solids at 80 °C under sugar syrup bubbling with air flow rates (L/s) of 0.062, 0.08, 0.104, 0.125, and 0.156. These flow rates were selected to ensure intensive mixing of the syrup while preventing the entrainment of syrup droplets from the saturation zone.

Under syrup bubbling with an air flow rate of 0.156 L/s, the saturation of pumpkin fruit pieces proceeded most intensively (Figure 7). However, this flow rate resulted in the entrainment of syrup droplets from the saturation zone. Therefore, under the experimental conditions, an air flow rate of 0.125 L/s can be considered rational for syrup bubbling.

The saturation processes under both infusion and bubbling conditions occur within the internal diffusion-controlled regime.

The experimental results presented in Figures 6–7 were generalized using the following functional relationship (Huzova, 2023):

$$\frac{c^* - c}{c^* - c_0} = f\left(Fo_{d_\text{int}}\right) \tag{2}$$

where c* – equilibrium concentration of soluble substances in pumpkin pieces, m³ soluble substances/m³ solution; c – instantaneous concentration of soluble substances in pumpkin pieces, m³ soluble substances/m³ solution; c_0 – initial concentration of soluble substances in pumpkin pieces, m³ soluble substances/m³ solution; Fo_{d_int} – Fourier diffusion number for the internal diffusion region.

The plots of the function (Eq. 2) are presented in Figure 8.

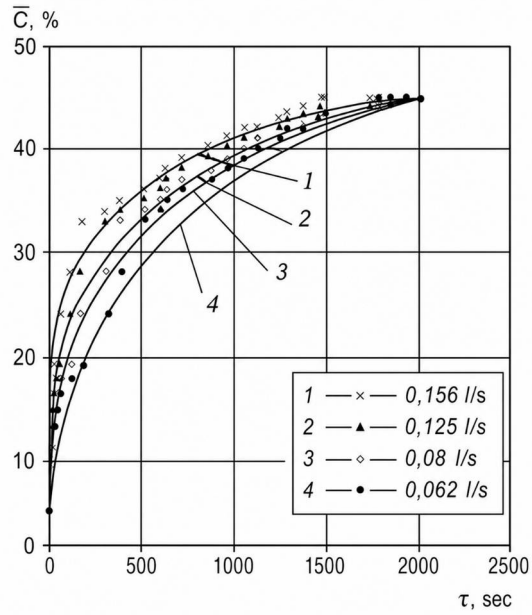

Figure 7. Influence of air flow rate on the kinetics of soluble solids uptake in pumpkin fruit pieces during sugar syrup bubbling at 80 °C

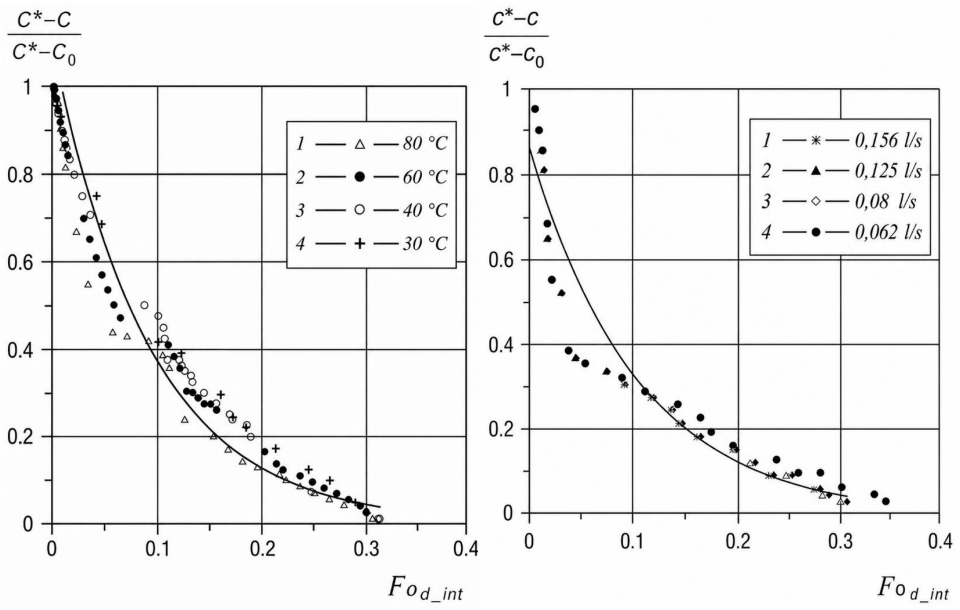

a **b**

Figure 8. Generalized saturation curves for pumpkin pieces:
a – at temperatures of 30–80 °C;
b – at air flow rates of 0.062–0.156 L/s

As shown in Figure 8, the generalized saturation curves in the internal diffusion-controlled regime can be approximated by a single exponential relationship over the temperature range of 30–80 °C (Figure 8a) and the air flow rate range of 0.062–0.156 L/s (Figure 8b). The analytical expression describing the change in soluble substance concentration within the pieces over time for the temperature range of 30–80 °C is as follows:

$$\frac{c^* - c}{c^* - c_0} = 1{,}1 \cdot e^{-10{,}77 \cdot Fo_{d_int}} \quad (3)$$

The analytical expression describing the change in soluble substance concentration within the pieces over time for the air flow rate range of 0.062–0.156 L/s is as follows:

$$\frac{c^* - c}{c^* - c_0} = 1{,}05 \cdot e^{-9{,}7 \cdot Fo_{d_int}} \quad (4)$$

The theoretical relationships (Eqs. 3–4) show good agreement with the experimental results (Figs. 6–7) and enable the prediction of soluble solids concentration changes in pumpkin pieces as a function of time. The deviation between the calculated and experimental values does not exceed 10%.

The comparison of the energy consumption during the saturation of pumpkin fruit pieces under infusion and bubbling modes was performed.

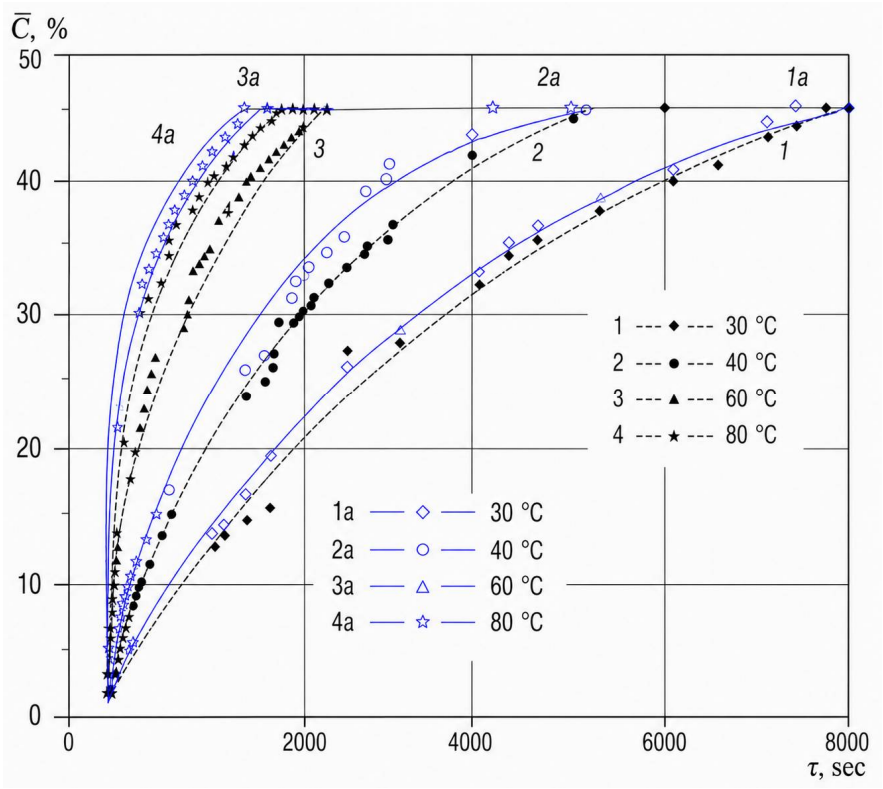

Figure 9. Change in soluble solids concentration in pumpkin fruit pieces over time during saturation under infusion conditions (curves 1–4) and under air bubbling at a flow rate of 0.125 L/s (curves 1a–4a)

As shown in Figure 9, conducting the saturation process under bubbling conditions intensifies the process. For example, saturation under bubbling at 60 °C (curve 3a) proceeds more intensively than under soaking at 80 °C (curve 4a).

To determine the most energy-efficient saturation mode for pumpkin fruit pieces, the specific heat consumption (MJ/kg of syrup) was calculated.

The specific heat consumption required for heating the sugar syrup to the set temperature and for maintaining the saturation process until equilibrium is reached (Q) was calculated according to Eq. 5 (Huzova and Atamanyuk, 2024). The energy consumption of the fan supplying air for bubbling (Q_{fan}) was calculated using Eq. 6. The heat consumption of the air heater (Q_{heater}) was determined according to Eq. 7. The total heat consumption (ΣQ) was calculated using Eq. 8 (Huzova, 2023):

$$Q = c_s \cdot (t_2 - t_1) \cdot \frac{\tau_2}{\tau_1} \cdot 10^{-6} \quad (5)$$

$$Q_{fan} = V_{air} \cdot \Delta p \cdot \tau_2 \cdot 10^{-6} / m_s \quad (6)$$

$$Q_{heater} = V_{air} \cdot c_{air} \cdot (t_2 - t_1) \cdot \tau_2 \cdot 10^{-6} \quad (7)$$

$$\sum Q = Q + Q_{fan} + Q_{heater} \quad (8)$$

where t_2 – saturation temperature, °C; t_1 – initial sugar syrup temperature, 20 °C; τ_2 – time required to saturate pumpkin fruit pieces to equilibrium concentration, s; τ_1 – time required to heat the sugar syrup to the saturation temperature, s; V_{air} – volumetric air flow rate for bubbling, m³/s; c_{air} – specific heat capacity of air, J/kg· °C; Δp – air pressure for bubbling, Pa; m_s – mass of sugar syrup, kg; c_s – specific heat capacity of sugar syrup, J/kg· °C.

The calculation results are presented in Table 2.

Table 2

Specific heat consumption of the investigated saturation modes of pumpkin fruits pieces in sugar syrup

Mode	t_2,°C	τ_1, s	τ_2, s	Q, MJ/kg	Q_{fan}, MJ/kg	Q_{heater}, MJ/kg	Σ Q, MJ/kg
Bubbling	80	450	1490	0.63	0.095	0.011	0.73
Infusion	80	450	1850	0.777	0	0	0.777
Bubbling	60	310	1570	0.638	0.1	0.0078	0.746
Infusion	60	310	2210	0.898	0	0	0.898
Bubbling	40	80	4200	3.3	0.268	0.0105	3.586
Infusion	40	80	5090	4.0	0	0	4.0
Bubbling	30	25	7400	9.32	0.472	0.0092	9.8
Infusion	30	25	7800	9.828	0	0	9.828

As shown in Table 2, the lowest total heat consumption is observed under the sugar syrup bubbling regime at the temperature of 80 °C.

Drying kinetics and temperature variation within layer of pumpkin fruit pieces

To evaluate the energy consumption of the candied fruit drying process and to substantiate the proposed drying method, the kinetic drying curves of pumpkin candied fruits (Figure 10a) and the profiles of thermal agent temperature variation over time along the height of the candied fruit layer (Figure 10b) are presented.

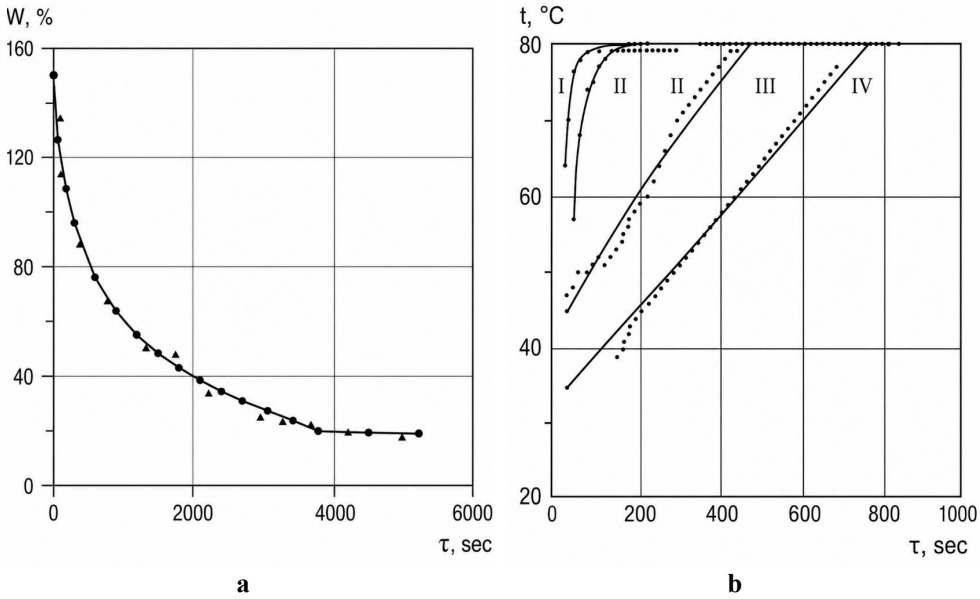

Figure 10. Kinetic curves (candied fruit temperature 80 °C, thermal agent velocity 2 m/s):
a – drying of candied fruits:
● – thermal agent temperature 80 °C; ▲ – thermal agent temperature 80 °C for 525 s;
b – variation of thermal agent temperature along the height of the candied fruit layer during drying

Filtration drying is known to exhibit a zonal character: the layers that first come into contact with the thermal agent dry earlier than the downstream layers. When the thermal agent interacts with the moist material, its temperature decreases to the wet-bulb temperature at the outlet of the container (Figure 4). Consequently, upon passing through the first (I) layer in the direction of flow, the thermal agent becomes only partially saturated with moisture. As it moves through subsequent layers, the saturation with moisture increases, and at the exit from the last layer the thermal agent is completely saturated. At the container outlet the thermal agent temperature is equal to the wet-bulb temperature under the specified drying conditions.

This phenomenon can be proven experimentally. Figure 10b illustrates the temporal variation of thermal agent temperature during filtration drying along the layer height. At the initial moment, the thermal agent temperature at the outlet of the first (I) layer is 64 °C; at the outlet of the second (II) layer – 47 °C; the third (III) – 45 °C; and the fourth (IV) – 35 °C. The curves in Figure 10b indicate that the upper layers dry more rapidly than the lower ones. This is evidenced by the specific time points at which the outlet temperature from each layer stabilizes and becomes equal to the inlet thermal agent temperature (80 °C). The first (I) layer reaches its final moisture content after 170 s; the second (II) layer after 340 s; the third (III) layer after 510 s; and the fourth

(IV) layer after 680 s. From the 680 s, only a negligible amount of moisture is removed from the entire layer, which does not influence the outlet temperature of the thermal agent.

Since the first layer reaches its final moisture content at 170 s and the fourth layer at 680 s, the fourth layer does not participate in mass transfer for 510 s, but only conserves energy of a dry layer (at temperature of 80 °C). A similar situation is observed for the second (II) and third (III) layers. Thus, it can be assumed that the thermal energy of the upper layers can be used to dry the lower layers.

As follows from Figure 10 and from the established drying mechanism, the temperature of the material and the thermal agent, as well as the moisture content vary both spatially and temporally. Therefore, the energy consumption was evaluated using the heat balance equation in the form of a differential equation describing an unsteady drying process (Huzova, 2020):

$$S \cdot dH \cdot \rho_{cand} \cdot \frac{\partial W}{\partial \tau} \cdot r \cdot d\tau = S \cdot dH \cdot \rho_{cand} \cdot \frac{\partial t_{cand}}{\partial \tau} \cdot c_{cand} \cdot d\tau + S \cdot dH \cdot \rho_{t.a.} \cdot \frac{\partial t_{t.a.}}{\partial \tau} \cdot c_{t.a.} \cdot d\tau \,, \quad (9)$$

or in general form:

$$Q_{evap} = Q_{w.layer} + Q_{t.a.} \,, \quad (10)$$

$$Q_{w.layer} = Q_{moist} + Q_{dry\,layer} \,, \quad (11)$$

where S – cross-sectional area of the layer, m²; dH – height of an elementary layer section, m; ρ_{cand} – density of candied fruits, kg/m³; $\partial W/\partial\tau$ – thermal agent moisture content change over time during time $d\tau$; r – specific heat of vaporization, J/kg; $\partial t_{cand}/\partial\tau$ – temperature change of wet candied fruit over time during time $d\tau$; c_{cand} – specific heat capacity of candied fruits, J/(kg·K); $\rho_{t.a.}$ – thermal agent density, kg/m³; $\partial t_{t.a}/\partial\tau$ – thermal agent temperature change over time during time $d\tau$; $c_{t.a}$ – specific heat capacity of the thermal agent, J/(kg·K); Q_{evap} – heat consumed for moisture evaporation, J; $Q_{t.a.}$ – heat supplied by the thermal agent, J; $Q_{w.layer}$ – heat accumulated by the wet material layer, J; Q_{moist} – heat accumulated by the material moisture, J; $Q_{dry.layer}$ – heat accumulated by the dry material layer, J.

Analysis of Eqs. 9–11 and the drying mechanism demonstrates that the heat content accumulated in the dry candied fruit layer remains constant during the drying process. Both the thermal agent and the saturated pieces enter the drying zone at 80 °C.

Therefore, the heat of the thermal agent is not spent on heating the material. Moreover, under laboratory conditions, heat losses associated with heating the drying container and losses to the environment are negligible. Thus, the energy required for moisture evaporation is supplied by both the thermal agent and the thermal energy stored in the dry material layer. This additional energy reserve may therefore be utilized to reduce the consumption of the 80 °C thermal agent and to shorten the drying time.

Furthermore, Figure 9b shows that the temperature of the thermal agent at the outlet of the material layer remains constant after 680 s, whereas the final moisture content of 20% of the candied pumpkin is reached only after 5220 s (Figure 10b). This phenomenon is attributed to the low degree of thermal agent saturation during the removal of osmotic intracellular and intercellular moisture, as well as to the hygroscopic properties of sugar, which binds water molecules. The hygroscopicity of sugar further contributes to reducing the required thermal agent consumption.

Using Eqs. 9–11, the heat quantities Q_{evap}, $Q_{t.a.}$, Q_{moist}, and $Q_{dry.layer}$ were calculated on an elementary section dH over the time $d\tau$. The summarized results are presented in Table 3.

Table 3

Heat quantities Q_{evap}, $Q_{t.a.}$, Q_{moist}, and $Q_{dry.layer}$ on an elementary section dH over the time dτ

dH, mm	dτ, s	$Q_{evap.}$, kJ	$Q_{t.a.}$, kJ	Q_{moist}, kJ	$Q_{dry.cand.}$, kJ
10	170	152.19	40.72	7.92	14.37
40	340	46.80	88.24	2.43	14.37
70	510	22.11	74.66	1.15	14.37
100	680	18.43	142.54	0.96	14.37
In total		239.54	169.80	12.47	57.48

As shown in Table 3, the energy required to evaporate moisture from the lowest (IV) layer of pumpkin fruit pieces is 18.43 kJ, whereas the thermal energy stored in the dry pumpkin layer amounts to 57.48 kJ. Therefore, the stored energy in the dry layers is sufficient to ensure drying of the final (IV) wet layer. Based on this finding, it is proposed to terminate the supply of the 80 °C thermal agent at 510 s and to complete the drying of the lower layer using the thermal agent at 18 °C. Under these conditions, the drying kinetic curve of candied pumpkin pieces using an 80 °C thermal agent over 5220 s will coincide with the kinetic curve obtained when drying is carried out at 80 °C for the first 510 s, followed by further drying with the thermal agent at 18 °C (Figure 10b).

The amount of thermal energy supplied by the thermal agent at 80 °C and consumed for drying the entire layer of candied fruits until the time the candied fruits reach the final moisture content of 20% ($Q^{I}_{t.a.}$, kJ) was calculated as well as the thermal energy provided by the 80 °C thermal agent consumed on drying candied pumpkin during the time period of 510 s ($Q^{II}_{t.a.}$, kJ) was determined. Furthermore, the energy consumption per unit mass of evaporated moisture (q, kJ/kg$_{moist.}$) was calculated, which allows to show energy savings in the proposed method of drying the stationary layer of candied fruits:

$$q = \frac{Q^{I}_{t.a.} - Q^{II}_{t.a.}}{m_{moist}} \quad (12)$$

Thus, terminating the supply of the 80 °C thermal agent at the time point of 510 s, and supplying of the 18 °C thermal agent for the next 4710 s reduces the energy consumption of the process by 31263.76 kJ/kg$_{moist.}$ (Table 4).

Table 4

Energy consumption of the drying process for candied pumpkin

$Q^{I}_{t.a.}$, kJ	$Q^{II}_{t.a.}$, kJ	q, kJ/kg$_{moist}$
6965.85	636.66	31263.76

Methods of dehydration are widely used worldwide during the saturation stage, which is often carried out in several steps with a gradual increase in syrup concentration to ensure uniform solute penetration and prevent excessive tissue shrinkage (González-Pérez et al., 2023). However, this approach requires complex technological procedures and sophisticated equipment design.

Vacuum impregnation is another widely applied technique in food processing (Gautam et al., 2024). This mechanism enables targeted modification of product composition while largely preserving the structural integrity of the food matrix (Saleena et al., 2024). As a result,

products with enhanced nutritional value, improved sensory properties, and extended shelf life can be obtained (Panayampadan et al., 2022). However, under various saturation conditions, these methods are highly energy-intensive (Gao et al., 2023; Vinod et al., 2024).

In contrast, the saturation of pumpkin pieces in a syrup of constant concentration demonstrated significantly greater benefits in terms of both reduced energy consumption and simplified equipment design. Such equipment can be used to perform both blanching and saturation processes under conditions of air-assisted syrup bubbling.

The filtration drying technique has been widely applied for dehydrating dispersed materials arranged in stationary layer, including various lignocellulosic biomasses. Among the studied materials are wild carrot pomace, a pharmaceutical industry by-product (Denysiuk et al., 2025); post-extraction pelargonium root residues (Kindzera et al., 2025); grain-based distillery stillage from food processing industry (Ivashchuk et al., 2021); brewer's spent grain derived from barley (Ivashchuk et al., 2024); ground sunflower stalk fibers (Kindzera et al., 2021; Kindzera and Kochubei, 2025) and crushed cotton stems representing agricultural residues (Kobeyeva et al., 2022). Drying kinetics for these materials were studied under different operating parameters, including variations in layer thickness, as well as the temperature and flow velocity of the thermal agent. The findings consistently demonstrated that filtration drying shortened the overall drying period and lowered energy demand compared with conventional convective drying systems, which are still predominantly used in industry. However, in the case of using the filtration method for drying pumpkin fruit pieces, the significantly greater effect was obtained in terms of reducing energy consumption – by using the thermal energy accumulated in the upper layers of pumpkin fruit pieces to complete the drying of the lower layers.

Conclusions

A method for saturating pumpkin pieces with soluble solids was developed, integrating blanching and saturation processes conducted under both infusion and bubbling conditions. A drying method for saturated pumpkin pieces in a fixed bed, based on the filtration of a variable-temperature drying agent, was also developed.

Energy consumption during saturation under different operating conditions was evaluated, and the following energy-efficient parameters were identified: bubbling mode, saturation temperature of 80 °C, air flow rate of 0.125 L/s, and total heat consumption of ΣQ = 0.73 MJ/kg syrup.

A novel drying approach for candied pumpkin pieces was developed, based on the utilization of thermal energy accumulated in the upper layers of the bed to complete drying of the lower layers. This approach reduced drying energy consumption by 31263.76 kJ/kg moisture removed.

References

Abraão A., Lemos A., Vilela A., Sousa J., Nunes F. (2013), Influence of osmotic dehydration process parameters on the quality of candied pumpkins, *Food and Bioproducts Processing,* 91(4), pp. 481-494, http://dx.doi.org/10.1016/j.fbp.2013.04.006

Atamanyuk V., Huzova I., Gnativ Z., Mykychak B. (2016), Selection of optimal method of forming a layer of candied fruits during filtration drying, *Eastern-European Journal of*

Enterprise Technologies, 5(11(83)), pp. 10–15, https://doi.org/10.15587/1729-4061.2016.81409

Cherif S., Leca A., Bureau S., Jameleddine Ben Abda J.B., Le Bourvellec L. (2024), Does hydration of 'Deglet Nour' date palm fruits improve their quality and help to reduce waste, *Food Chemistry,* 458, 140323, https://doi.org/10.1016/j.foodchem.2024.140323

Chinchkar A.V., Singh A., Singh S.V., Mazumder K., Bishnoi M., Kamble M.G. (2025), Application and toxicological study of polyvinyl acetate (PVAc) coating on lemon (*Citrus limon* L.) fruit to extend the shelf life, *Journal of Future Foods*, 5(2), pp. 145–152, https://doi.org/10.1016/j.jfutfo.2024.05.003

Denysiuk A., Atamanyuk V., Hnativ Z., Boldyryev S. (2025), Hydrodynamics of filtration drying of wild carrot pomace, *Journal of Environmental Problems*, 10(1), pp. 79–87, https://doi.org/10.23939/ep2025.01.079

Gao M., Nomura K., Ando Y., Nakaura Y., Zhang Z., Yamamoto K. (2023), Vacuum impregnation of liquid into carrot assisted by high hydrostatic pressure, *High Pressure Research*, 43, pp. 142–155, https://doi.org/10.1080/08957959.2023.2195109

Gautam S., Kathuria D., Hamid Dobhal A., Singh N. (2024), Vacuum impregnation: Effect on food quality, application and use of novel techniques for improving its efficiency, *Food Chemistry*, 460, 140729, https://doi.org/10.1016/j.foodchem.2024.140729

González-Pérez J.E., Romo-Hernández A., López-Malo A., Ramírez-Corona N. (2023), Evaluation of osmodehydration and vacuum-assisted osmodehydration as pre-treatments during fruit drying process: the effect on drying rates, effective water diffusion and changes in product quality, *Journal of Engineering Research*, 11(4), pp. 275–282, https://doi.org/10.1016/j.jer.2023.100153

Huzova I. (2020), Investigation of the energy-saving method during candied fruits filtration drying, *Periodica Polytechnica Chemical Engineering*, 64(4), pp. 555–561, https://doi.org/10.3311/PPch.15107

Huzova I., Atamanyuk V. (2022), Dynamics of drying processes of plant raw material in the period of decreasing speed, *Journal of Chemistry and Technologies,* 30(3), pp. 419–430, https://doi.org/10.15421/jchemtech.v30i3.259694

Huzova I.O., Atamanyuk V.M. (2024), Study of mass transfer and diffusion processes of sucrose into apple fruit pieces, *Journal of Chemistry and Technologies*, 32(3), pp. 649–661, https://doi.org/10.15421/jchemtech.v32i3.303315

Huzova I.O. (2023), Study on the diffusion process of zucchini fruits saturation with sucrose from an aqueous solution, *Journal of Chemistry and Technologies*, 31(3), pp. 552–562, https://doi.org/10.15421/jchemtech.v31i3.280561

Ivashchuk O.S., Atamanyuk V.M., Gnativ Z.Y., Chyzhovych R.A., Zherebetskyi R.R. (2021), Research into kinetics of filtration drying of alcohol distillery stillage, *Voprosy Khimii i Khimicheskoi Tekhnologii*, 4, pp. 58–65, https://doi.org/10.32434/0321-4095-2021-137-4-58-65

Ivashchuk O., Atamanyuk V., Chyzhovych R., Manastyrska V.A., Barabakh S.A., Hnativ Z. (2024), Kinetic regularities of the filtration drying of barley brewer's spent grain, *Chemistry & Chemical Technology*, 18(1), pp. 66–75, https://doi.org/10.23939/chcht18.01.066

Kindzera D., Hosovskyi R., Atamanyuk V., Simak D. (2021), Heat transfer process during drying of grinded biomass in a fixed bed dryer, *Chemistry & Chemical Technology*, 15(1), pp. 118–124, https://doi.org/10.23939/chcht15.01.118

Kindzera D., Kochubei V. (2025), Comparison of the energy properties of sunflower stalk fibers for solid biofuel production, *Journal of Chemistry*, 7990012, https://doi.org/10.1155/joch/7990012

Kindzera D., Kochubei V., Hosovskyi R. (2025), Sustainable utilization of post-extraction residual biomass for solid biofuel production, *South African Journal of Chemical Engineering*, 54, pp. 70–78, https://doi.org/10.1016/j.sajce.2025.07.008

Kobeyeva Z., Khussanov A., Atamanyuk V., Hnativ Z., Kaldybayeva B., Janabayev D., Gnylianska L. (2022), Analyzing the kinetics in the filtration drying of crushed cotton stalks, *Eastern-European Journal of Enterprise Technologies*, 1(8(115)), pp. 55–66, https://doi.org/10.15587/1729-4061.2022.252352

Muccilli V., Vitale A., Sheng L., Gentile A., Cardullo N., Tringali C., Distefano G. (2020), Substantial equivalence of a transgenic lemon fruit showing postharvest fungal pathogens resistance, *Journal of Agricultural and Food Chemistry*, 68(12), pp. 3806–3816, https://doi.org/10.1021/acs.jafc.9b07925

Panayampadan A.S., Alam M.S., Aslam R., Kaur J. (2022), Vacuum impregnation process and its potential in modifying sensory, physicochemical and nutritive characteristics of food products, *Food Engineering Reviews*, 14, pp. 229–256, https://doi.org/10.1007/s12393-022-09312-4

Petrova Z.O., Paziuk VM., Samoilenko K. M., Slobodianiuk K.S., Petrov P.I. (2025), Drying of protein-carotine-containing raw materials based on carrot and fabaceae, *Journal of Chemistry and Technologies*, 33(2), pp. 401–417, https://doi.org/10.15421/jchemtech.v33i2.320931

Saleena P., Jayashree E., Anees K.A. (2024), Comprehensive review on vacuum impregnation: mechanism, applications and prospects, *Food and Bioprocess Technology*, 17, pp. 1434–1447, https://doi.org/10.1007/s11947-023-03185-z

Sniezhkin Y., Petrova Z., Samoilenko K., Novikova Y., Vyshnievska T. (2025), Research of sorption of composites based on municipal solid waste and biomass, *Vidnovluvana Energetika*, 80(1), pp. 159–167, https://doi.org/10.36296/1819-8058.2025.1(80)

Sniezhkin Y.F., Paziuk V.M., Petrova Z.O., Petrov A.I., Biriukov S.O. (2025), Energy-efficient low-temperature unit of condensation type for drying seed grain, *Energy Technologies & Resource Saving*, 82(1), pp. 127–137, https://doi.org/10.33070/etars.1.2025.09

Vinod B.R., Asrey R., Sethi S., Menaka M., Meena N.K., Shivaswamy G. (2024), Recent advances in vacuum impregnation of fruits and vegetables processing: a concise review, *Heliyon*, 10(7), e28023, https://doi.org/10.1016/j.heliyon.2024.e28023

Cite:

Huzova, I., Kindzera, D., Shevchenko, O., & Bessarab, O. (2026). Energy-efficient saturation and drying of pumpkin pieces. *Ukrainian Food Journal, 15*(2), 418–435. https://doi.org/10.24263/2304-974X-2026-15-2-10

Enhancement of bakery product quality using chokeberry processing by-products

Galyna Khomych[1], Tetiana Lebedenko[2], Galina Krusir[3], Lali Elanidze[4]

1 – Poltava University of Economics and Trade, Poltava, Ukraine
2 – Odesa National Technological University, Odesa, Ukraine
3 – University of Applied Sciences and Arts Northwestern Switzerland, Switzerland
4 – Iakob Gogebashvili Telavi State University, Telavi, Georgia

Keywords:

Wheat bread
Chokeberry
Pomace
Extracts
Quality
Waste-free

Article history:

Received 10.12.2026
Received in revised form 22.04.2026
Accepted 30.06.2026

Corresponding author:

Tetiana Lebedenko
E-mail: tatyanalebedenko27@gmail.com

DOI:
10.24263/2304-974X-2026-15-2-11

Abstract

Introduction. The aim of the study was to evaluate the physicochemical characteristics and biological activity of chokeberry (*Aronia melanocarpa*) fruits and their processing by-products, and to identify the most promising forms for application as functional ingredients in bread production.

Materials and methods. Chokeberry fruits and pomace obtained after juice extraction were analyzed for titratable acidity, dry matter content, L-ascorbic acid, pigments, phenolic compounds, and biological activity. Chokeberry dry pomace and water- and whey-based extracts prepared from it were used to enrich wheat bread formulations.

Results and discussion. Chokeberry fruits and their pomace were found to contain L-ascorbic acid (13.0–35.8 mg/100 g), pigments (640.5–810.0 mg/100 g), phenolic compounds (900–1050 mg/100 g), and exhibited biological activity ranging from 5170 to 7710 activity units. The phenolic fraction comprised hydroxycinnamic acids and their derivatives (179.42–181.0 mg/100 g), flavones and their derivatives (29.3–43.1 mg/100 g), and anthocyanins (690.0–858.0 mg/100 g). Pigments were the predominant phenolic constituents in chokeberry pomace, accounting for 78.55% of the total phenolic content. The use of water- and whey-based extracts from chokeberry pomace powder was proposed for application in bread production. For the preparation of the extracts, dried pomace was pre-soaked for 60 min at 18 ± 2 °C. The optimal extraction conditions were a solid-to-liquid ratio of 1:10, an extraction temperature of 90 °C, and an extraction time of 60 min for water extraction, and a solid-to-liquid ratio of 1:10, an extraction temperature of 100 °C, and an extraction time of 90 min for whey-based extraction. In wheat bread formulations (from first-grade wheat flour), chokeberry pomace extract prepared with whey was added at 15% relative to flour weight, whereas water-based chokeberry pomace extract was added at 30%. The incorporation of the extracts at these levels positively affected the specific volume (increase of 7.2–7.5% compared to the control), porosity (by 6.0–6.2%), and titratable acidity (by 9.0–9.1%) of the wheat bread. In the case of water-based extract addition, changes in crumb colour were observed, along with the development of a sweet-sour taste. The extracts were also found to be effective in preventing potato disease (rope spoilage) and mold growth within 120 h of storage.

Conclusions. Chokeberry pomace is a valuable functional ingredient with high bioactive potential. Its extracts can be effectively used in bakery products to improve technological quality and shelf-life.

Introduction

Chokeberry (*Aronia melanocarpa*) is widely cultivated as a fruit, medicinal, and ornamental plant due to its high nutritional value and diverse biological activities. Its ripe fruits are widely consumed fresh or dried and are used for nutritional, therapeutic, and preventive purposes, while the leaves are also employed in traditional medicine (Kuru and Kılınç, 2026). Chokeberry fruits are rich in sugars (fructose, glucose, and sorbitol), organic acids (malic, citric, quinic, and succinic acids), pectin, tannins, and dietary fiber. They also contain a wide range of vitamins including vitamin C, tocopherols, riboflavin (B2), niacin (B3), pantothenic acid (B5), pyridoxine (B6), biotin (B7), folates (B9), vitamin K, vitamin A (retinol) and β-carotene, as well as nutritionally important macro- and microelements such as sodium, potassium, calcium, magnesium, iodine, iron, manganese, copper, molybdenum, boron, fluorine, and selenium (Artamonova et al., 2025; Bakhshaliyeva et al., 2023; Stabnikov et al., 2025).

Black chokeberry is recognized as one of the richest fruit sources of polyphenolic compounds, including rutin, quercetin, anthocyanins, catechins, flavones, and chlorogenic acid, which are largely responsible for its high antioxidant capacity (Aksoy, 2023; Cacak-Pietrzak et al., 2023; Khomych et al., 2024). Due to its rich phytochemical profile, chokeberry has attracted considerable attention for its wide range of biological activities, including antioxidant, antimicrobial, anti-inflammatory, anticarcinogenic, antimutagenic, radioprotective, and hepatoprotective properties. Available evidence indicates that regular consumption of chokeberry-derived products may be associated with a reduced risk of influenza, cardiovascular diseases, diabetes, and circulatory disorders. In addition, chokeberry has been shown to positively modulate gut microbiota composition, highlighting its potential as a functional food ingredient for supporting human health (Duman et al., 2025; Ren et al., 2022).

The global chokeberry market was valued at USD 876.11 million in 2024 and is projected to reach USD 1,461.81 million by 2031, reflecting a compound annual growth rate (CAGR) of 7.5% (ReportID: 244771, 2025). Poland remains the world's leading producer of chokeberry, accounting for approximately 60–70% of global production. A substantial proportion of the harvested fruits is processed into juices and juice-based beverages, the consumption of which continues to grow worldwide (Zbikowska et al., 2024). This increasing demand is largely attributed to growing consumer awareness of the health benefits associated with chokeberry and its derived products. Traditionally, the largest markets for chokeberry products have been located in North America and Europe; however, demand is also expanding rapidly in the Asia–Pacific region. This trend reflects the rising global interest in functional foods and natural sources of bioactive compounds (ReportID: 244771, 2025).

In recent years, growing interest in chokeberry has stimulated extensive research on its cultivation, processing, and application in functional foods (Andreica et al., 2025; Demir et al., 2025; Gurčík et al., 2023; Sharma et al., 2025). Chokeberry fruits and their derivatives are widely utilized in the pharmaceutical, cosmetic, and food industries. They are incorporated into a broad range of products, including juices, ciders, kombucha, and other beverages, as well as jams, teas, dairy products, meat products, confectionery, and natural food colorants intended to replace synthetic additives (Artamonova et al., 2025).

Chokeberry in the form of powders, purees, or extracts has also been successfully incorporated into flour-based confectionery and bakery products (Ghendov-Mosanu et al., 2022; Khomych et al., 2024; Koshak and Pokrasinskaya, 2020; Sady and Sielicka-Różyńska, 2019). For example, the addition of freeze-dried chokeberry fruits to cookies increased their antioxidant activity while causing only minor changes in sensory characteristics,

demonstrating the potential of chokeberry as a functional food ingredient (Sady and Sielicka-Różyńska, 2019).

Considerable attention has recently been directed toward the valorization of fruit and berry processing by-products, particularly pomace generated during juice and puree production. The incorporation of such by-products into food formulations can enhance nutritional quality and biological value while promoting sustainable resource utilization and supporting the development of waste-free technologies (Stabnikova et al., 2023a, b).

To improve the efficiency and sustainability of chokeberry processing, various approaches have been proposed for the utilization of pomace, which is produced in large quantities during juice manufacture and remains rich in bioactive compounds (Saracila et al., 2024). Notably, chokeberry pomace has been reported to exhibit higher antioxidant activity than either juice or fruit powder, highlighting its potential as a valuable source of functional ingredients for food applications (Mayer-Miebach et al., 2012). The incorporation of freeze-dried chokeberry pomace at levels up to 3% of flour weight increases the water absorption capacity of flour but reduces dough stability and weakens the gluten network. Consequently, bread volume decreases and crumb hardness increases. At the same time, the bread acquires a characteristic red-violet crumb color, while the dietary fiber, ash, and total phenolic contents increase by 80.9%, 2.6%, and 272%, respectively (Cacak-Pietrzak et al., 2023).

Due to its weakening effect on gluten network formation, chokeberry pomace has been proposed for use in confectionery products, particularly shortbread cookies and muffins (Raczkowska et al., 2022). Similar studies have demonstrated that chokeberry powder and aqueous extracts interfere with gluten development in wheat flour, supporting their application in shortcrust pastry technology (Korenets et al., 2017). Given the valuable chemical composition of chokeberry pomace and the widespread consumption of bakery products, its incorporation into bakery formulations offers a promising strategy for enhancing nutritional and biological value while preserving technological and sensory quality.

The aim of this study was to evaluate the quality and biological activity of chokeberry fruits and pomace, examine potential processing approaches, and identify the most promising chokeberry-derived ingredients for improving the organoleptic and physicochemical properties of bakery products, as well as their storage stability.

Materials and methods

Materials

Chokeberry fruits (cultivar ‘Vseslava’, Ukraine) and their pomace were used in this study. Chokeberry pomace was used in dried form. Drying was performed at 60 °C in a drying cabinet. The dried material was subsequently ground using laboratory mills LZM-1 and LMT-2. Extracts from chokeberry pomace powder were obtained by varying the extraction conditions, including temperature (80, 90, and 100 °C), extraction time (0, 15, 30, 45, 60, and 90 min), solid-to-liquid ratio (1:10), and type of extractant (water or milk whey).

Dough samples were prepared according to the following formulation (% flour basis): wheat flour, 100.0%; compressed baker's yeast (*Saccharomyces cerevisiae*, 70% moisture content), 3.0%; and salt, 1.5%.

Preparation of dough enriched with chokeberry processing by-products

Chokeberry pomace was incorporated into experimental dough formulations in

powdered form at levels of 1.0%, 3.0%, and 5.0% (flour basis). Water extracts prepared from chokeberry pomace powder were added at levels of 15.0%, 30.0%, and 45.0% of flour weight, with the highest level corresponding to complete replacement of the added water. Whey-based extracts of chokeberry pomace were incorporated at levels of 5.0%, 10.0%, and 15.0% (flour basis).

Dough samples with a moisture content of 44.0% were prepared using the straight-dough method. Fermentation was carried out for 60–90 min. Mixing was performed using a two-speed Kenwood KVC 5100T dough mixer. Dough pieces were proofed in a thermostatically controlled chamber at 38 ± 2 °C and a relative humidity of 78 ± 2% until optimum proofing was achieved. Baking was carried out in a Sveba-Dahlen deck oven at 200–220 °C with steam injection for 30 min.

Methods

Characteristics of raw materials

Moisture content in raw materials was determined by an accelerated gravimetric method using a KVARTS-21M content in chokeberry fruits and pomace was calculated using the equation:-33 analyser, based on drying samples to constant mass.

Dry matter content in chokeberry fruits and pomace was calculated using the equation:

$$S = 100 – W,$$

where S is the dry matter content, %, and W is the moisture content, %.

Dry matter content in whey and extract samples was determined by refractometric analysis (Chubenko et al., 2025).

Titratable acidity was measured by volumetric titration (Jamale and Vedpathak, 2025).

Total content of coloring compounds was expressed as mass concentration in fruits and pomace (Grek et al., 2026).

Ash content was determined by incineration of samples in a muffle furnace (Blazhenko et al., 2024; Harris, 2024).

Sensory properties of whey and extracts were evaluated according to ISO 22935-3:2009, based on individual sensory attributes (Grek et al., 2026).

Total phenolic compounds in fruits were determined by high-performance liquid chromatography (HPLC) using an Agilent Technologies 1100 system (Khomych et al., 2024).

The biological activity index in raw materials and pomace was determined by monitoring electron transport activity in a NADH–potassium ferricyanide system in phosphate buffer (pH 7.5) (Khomych et al., 2024).

Microscopic observations of chokeberry fruit surface sections were performed using scanning electron microscopy (SEM). Images were acquired at an accelerating voltage of 30 kV and magnifications of ×500 and ×5000.

The wet gluten content in flour was determined as the ratio of the mass of washed raw gluten to the mass of flour, expressed as a percentage. The gluten deformation index was measured based on the residual deformation of a gluten sample after the application of a standard load for 30 s (Shevchenko et al., 2023).

Characteristics of dry chokeberry pomace powder and its extracts

Particle size, bulk density, and swelling capacity were determined for dried and milled chokeberry pomace (Brubaker and Moghtadernejad, 2024; Chubenko et al., 2025).

T*he efficiency of the extraction process* was evaluated using the exhaustion coefficient, which characterizes the yield of dry matter in the extract relative to the initial dry matter content in the raw material–solvent system.

Total solids content (%) was determined by drying a weighed sample to constant mass (Grek et al., 2026).

Titratable acidity (°T) was measured by titration of the extract with 0.1 N sodium hydroxide solution (Jamale and Vedpathak, 2025).

Characteristics of bread quality

Sensory evaluation of bread was performed using sensory parameters, including appearance, surface condition, crust color, crumb porosity, taste, and odor (Galenko et al., 2024). The evaluation was conducted by a panel of 20 trained assessors using a 5-point scale for individual attributes (Sammalisto et al., 2021).

Moisture content of the bread crumb was determined by drying weighed samples to constant mass in a SESH-3M drying cabinet (Ukraine) at 130 °C for 40 min.

Acidity of the bread crumb was determined by titration of an aqueous extract of the crumb using sodium hydroxide solution in the presence of phenolphthalein as an indicator.

Crumb porosity was determined as the ratio of pore volume to total crumb volume and expressed as a percentage.

Specific volume of bread was measured using a volumetric displacement method. The volume of displaced grain (mL), measured in a graduated cylinder, corresponded to bread volume. Specific volume was calculated as the ratio of bread volume to mass and expressed as mL/g (Zhu et al., 2016).

Dimensional stability of bread was evaluated by measuring bread height and diameter (mm) and calculating their ratio.

Mold growth and potato disease of bread were assessed by placing bread samples on agar medium and examining them for mold colonies (culture-based analysis) (Garcia and Copetti, 2019). Potato disease was evaluated after baking and during 2 days of storage by visual observation of mold development (Uazhanova, 2014).

Statistical analysis

All analyses were performed in triplicate. Results are presented as mean values ± standard deviations.

Results and discussions

Physicochemical characteristics of chokeberry fruits and their pomace

During juice production from chokeberries, pomace accounts for more than 40% of the original fruit weight. The pomace consists of fruit peel, seed tissue fragments containing seeds, and residual pulp enriched with carbohydrates, minerals, and other biologically active compounds. The results of studies on the key physicochemical properties of chokeberry fruits and pomace are presented in Table 1.

Table 1

Physicochemical characteristics of chokeberry fruits and their pomace

Characteristic	Fruits	Pomace
Dry matter, %	20.80±0.12	32.00±0.14
Titratable acidity, %	0.92±0.10	0.84±0.11
Ash content, %	0.80±0.11	0.91±0.12
L-ascorbic acid, mg/100 g	35.80±0.70	13.00±0.15
Color compounds, mg/100 g	640.50±7.80	810.00±8.50
Total phenolic compounds, mg/100 g, including	900.0±13.5	1080.0±16.4
hydroxycinnamic acids and their derivatives	181.00	179.50
flavones and their derivatives	29.30	43.10
anthocyanins	690.00	858.00
Biological activity, activity units	7710.00	5170.00

The obtained results demonstrate significant differences in the physicochemical composition of chokeberry fruits and their pomace, reflecting the redistribution of bioactive compounds during juice processing. The dry matter content in pomace (32.00%) was considerably higher than in fruits (20.80%), which can be attributed to the removal of a substantial portion of water-soluble components during juice extraction, resulting in a more concentrated solid matrix.

A slight decrease in titratable acidity was observed in pomace (0.84%) compared to fruits (0.92%), which may be explained by the partial transfer of organic acids into the juice fraction. In contrast, ash content increased from 0.80% in fruits to 0.91% in pomace, indicating the relative concentration of mineral substances in the remaining solid residue. A pronounced reduction in L-ascorbic acid content was observed after processing, decreasing from 35.80 mg/100 g in fruits to 13.00 mg/100 g in pomace. This substantial loss can be associated with the high sensitivity of vitamin C to oxidation and thermal/mechanical degradation during juice extraction and subsequent handling.

Interestingly, pomace demonstrated higher levels of color compounds (810.00 mg/100 g) and total phenolic compounds (1080.00 mg/100 g) compared to fruits (640.50 mg/100 g and 900.00 mg/100 g, respectively). In particular, anthocyanins showed a marked increase in pomace (858.00 mg/100 g vs. 690.00 mg/100 g), suggesting their retention in the solid fraction bound to cell wall structures. A similar trend was observed for flavones and their derivatives, which increased from 29.30 to 43.10 mg/100 g. However, hydroxycinnamic acids remained relatively stable between fruits (181.00 mg/100 g) and pomace (179.50 mg/100 g), indicating minimal loss during processing.

Despite the higher concentration of phenolic compounds and pigments, the biological activity index was lower in pomace (5170.00 activity units) compared to fruits (7710.00 activity units). This may be attributed to differences in the chemical composition and matrix structure of the material, including a reduced level of ascorbic acid and possible changes in the interactions between low-molecular-weight antioxidants and phenolic compounds, which can influence the overall biological activity.

Overall, the results indicate that chokeberry pomace is a concentrated source of mineral and phenolic compounds, particularly anthocyanins and flavones, whereas fruits are characterized by higher levels of L-ascorbic acid and greater overall biological activity. These findings suggest the potential of pomace as a valuable raw material for functional food applications, particularly in bakery products, where enrichment with bioactive compounds is desirable.

Anthocyanins, the major pigments responsible for the characteristic dark purple color of black chokeberry and its high antioxidant activity, represent the predominant group of phenolic compounds in both fruits and pomace. The characteristics and content of anthocyanins are presented in Table 2 and Figure 1.

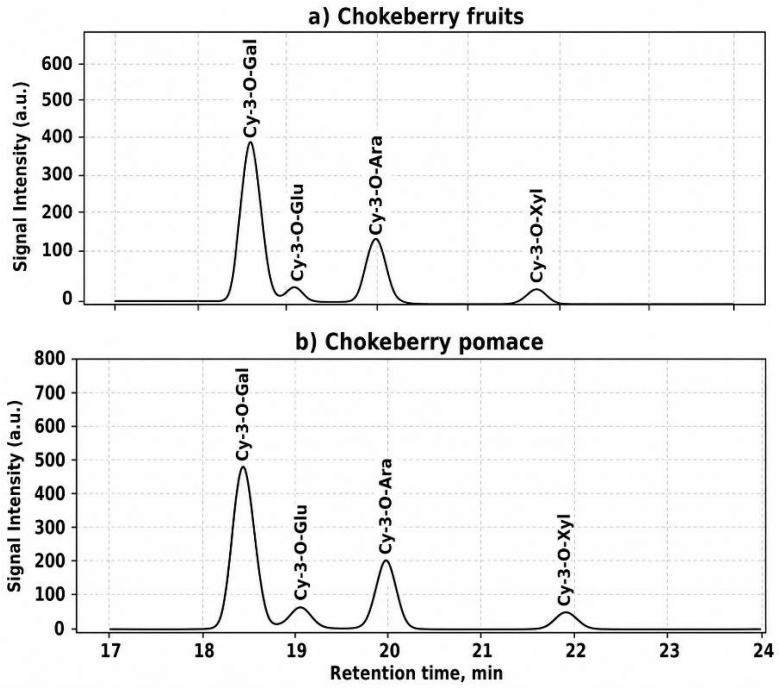

Figure 1. Chromatograms of anthocyanins in the fruits (a) and pomace (b) of chokeberry

Table 2

Anthocyanin composition and content in chokeberry fruits and pomace

Compounds	Content, mg/100 g	
	Fruits	Pomace
Cyanidin-3-O-galactoside	442.43	522.88
Cyanidin-3-O-glucoside	31.72	36.36
Cyanidin-3-O-arabinoside	185.36	221.58
Cyanidin-3-O-xyloside	30.04	33.70
Total	689.55	814.52

Research consistently confirms that the anthocyanin profile of black chokeberry (*Aronia melanocarpa*) is composed almost exclusively of cyanidin glycosides, which typically account for 90–100% of the total anthocyanins (Bushmeleva et al., 2022; Chen et al., 2026; Stabnikov et al., 2025).

The results (Table 2) indicate that cyanidin-3-O-galactoside accounts for the largest proportion (64.2%) of total anthocyanins among the coloring compounds. So, it has been shown that the majority of biologically active compounds in chokeberry fruits are localized in the peel and are therefore transferred to the pomace fraction during juice extraction.

Microscopic examination of chokeberry fruit surface sections was performed using thin cross-sections (Figure 2).

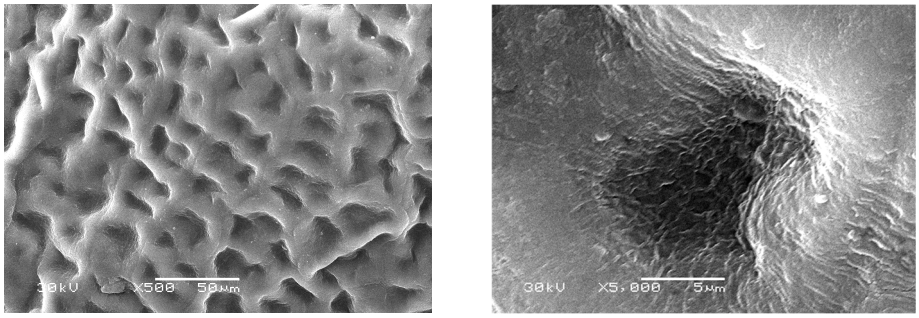

a **b**

Figure 2. SEM micrograph of the chokeberry fruit surface: a – 500 times magnification, b – 5000 times magnification

The surface of chokeberry fruit (Figure 2) is covered by a thick cuticle with pronounced surface invaginations; however, no distinct cell boundaries are visible. The pores are 8–10 µm in length and 1–2 µm in width. The outer epidermal layer (top view) consists of uniformly polygonal cells measuring 30–45 µm. Each cell (a) is covered by a ridge up to 10 µm in height. The ridge appears continuous on the external surface (b), while its internal structure is differentiated.

Thus, the microstructural analysis showed that chokeberry fruits possess a complex surface architecture characterized by a thick cuticle and dense cell walls. In addition to the well-developed peel, the fruits contain a considerable proportion of seeds. These anatomical components represent important reservoirs of nutrients and bioactive compounds. Although the pulp constitutes the largest fraction of the fruit (72.6%), followed by the peel (19.1%) and seeds (8.3%), the highest concentrations of coloring and phenolic compounds are localized in the peel. The content of coloring substances in the peel reached 1399.0 mg/100 g, which was 4.1-fold higher than in the pulp (343.0 mg/100 g). Similarly, the concentration of phenolic compounds in the peel (2000.0 mg/100 g) exceeded that in the pulp by approximately 3.3-fold. These findings explain the retention of a substantial proportion of bioactive compounds in pomace after juice extraction and confirm its potential as a valuable functional food ingredient.

Effect of chokeberry pomace powder on bread characteristics

The pomace obtained after juice extraction was dried and milled into a fine powder for subsequent use in bread production. Particle size distribution in chokeberry pomace powder is shown in Figure 3.

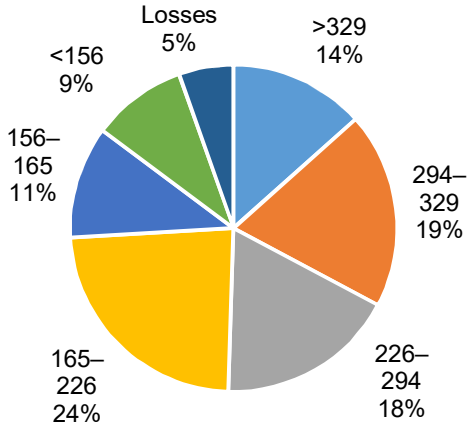

Figure 3. Fractional composition of powder particles from chokeberry pomace (size, µm)

The chokeberry pomace powder consisted of particles of various sizes and shapes, reflecting the heterogeneous morphological composition of the raw material. The particle size ranged from less than 156 µm to more than 329 µm. The largest fraction was represented by fragments of seed chambers. For particle size of premium- and first-grade wheat flour typically ranges from 1 to 240 µm. The comparison, the relatively large particle size of the pomace powder may adversely affect the texture and sensory characteristics of bread. Therefore, baking experiments were conducted using different levels of chokeberry pomace powder incorporation to evaluate its effect on the quality of the bread (Figure 4, Table 3).



a **b** **c** **d**

Figure 4. Control bread (a) and bread supplemented with chokeberry pomace powder at 1.0% (b), 3.0% (c), and 5.0% (d) of flour weight

Table 3

Characteristics of wheat bread with chokeberry pomace powder

Characteristics of bread	Chokeberry pomace powder, % of flour weight			
	0 (control)	1.0	3.0	5.0
Specific volume, cm^3/g	3.06	3.10	3.16	2.81
Dimension stability, H/D	0.64	0.68	0.64	0.58
Porosity, %	69	70	73	67
Moisture, %	40.60	41.40	42.60	43.00
Acidity, °T	2.20	2.40	2.90	3.00

The incorporation of 1.0% dried chokeberry pomace (flour weight basis) resulted in a darker crumb colour compared to the control sample. No noticeable changes in bread aroma were observed; however, coarse pomace particles were perceptible during chewing. Samples containing 3.0% and 5.0% pomace exhibited reduced dimensional stability. The specific volume increased at pomace levels of 1.0% and 3.0%, whereas a further increase to 5.0% led to a decrease in this parameter.

Considering the adverse effects of dried ground chokeberry pomace on bread quality parameters, the subsequent stage of the study involved the preparation of extracts from the pomace and the evaluation of their suitability for bread production.

Effect of extraction parameters on the properties of chokeberry pomace extracts

The effects of extraction parameters, including temperature, extraction time, and extractant type, on dry matter yield and titratable acidity were investigated at a hydromodule of 1:10. To improve extraction efficiency, the pomace was pre-soaked for 60 min at 18±2 °C. Such pretreatment promotes solvent penetration into the plant material, swelling of biopolymers, and intensification of mass transfer processes, thereby facilitating the release of soluble compounds into the extract (Brubaker and Moghtadernejad, 2024; Iorgachova and Lebedenko, 2015). The quality of the extracts was evaluated based on dry matter content and titratable acidity (Figures 5 and 6).

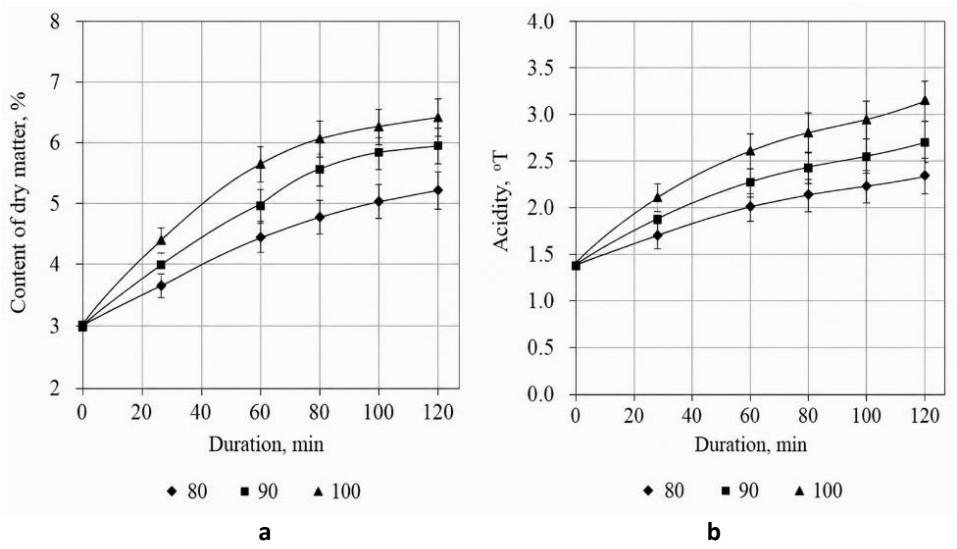

Figure 5. Changes in dry matter content (a) and acidity (b) in water extracts of chokeberry pomace under different extraction parameters (duration and temperature)

The transfer of soluble solids into the extract occurred most intensively during soaking and within the first 60 min of extraction. Based on the obtained results, the optimal extraction conditions were established as 90 °C for 60 min when water was used as the extractant and 100 °C for 90 min when whey was used.

During water extraction at 100 °C, the rate of dry matter transfer decreased during the first 30 min, which may be attributed to the dissolution of pectins and other polysaccharides and the formation of more viscous systems that hinder diffusion. At the same time, titratable acidity increased more rapidly under these conditions.

Whey was selected as an alternative extractant due to its content of valuable nutrients and biologically active compounds (Kochubei-Lytvynenko et al., 2022). As a by-product of cheese manufacture, whey represents a promising raw material for the production of functional ingredients. Its use in extraction processes not only improves the nutritional value of the obtained extracts but also promotes the efficient utilization of secondary dairy resources and supports the development of sustainable waste-free technologies (Fluerasu et al., 2025).

The use of whey as an extractant improved dry matter recovery and the degree of raw material exhaustion, particularly at 100 °C (Figure 6).

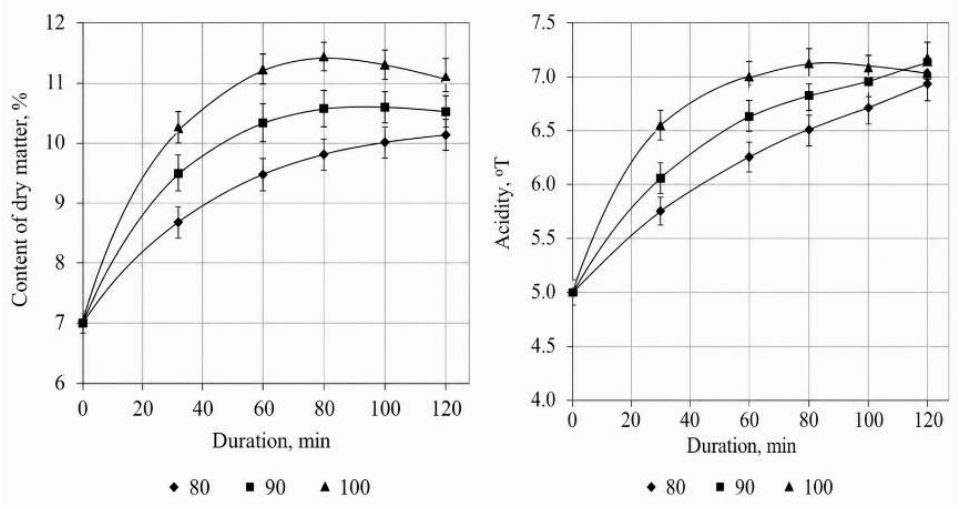

a **b**

Figure 6. Changes in dry matter content (a) and acidity (b) in whey extracts of chokeberry pomace under different extraction parameters (duration and temperature)

This effect may be attributed to enhanced swelling of plant tissues and accelerated diffusion processes in the presence of whey components, which facilitate the transfer of soluble compounds, including pectins and other polysaccharides, into the extract. However, further increases in extraction severity may not be advisable, since elevated temperatures can promote the degradation of heat-sensitive compounds.

Effect of chokeberry pomace extracts on the properties of wheat flour gluten and activity of baker's yeast

Since the technological properties of bread are largely determined by the quantity and quality of wheat flour gluten, the next stage of research was to study the effect of the obtained extracts from chokeberry pomace on its properties. Establishing the nature of the interaction of the components of the extracts with gluten proteins allows to predict their effect on the rheological properties of the dough and the quality of finished products.

The effect of selected extractants and extraction duration on the quantity and quality of gluten was investigated. Gluten washing was carried out in a flour-water system with partial replacement of water with extracts from chokeberry pomace powder. The water extract was added in an amount of 30% by weight of flour, and the whey extract was added in an amount of 15% by weight of flour. Gluten deformation index (GDI) was determined using an IDK apparatus based on the residual deformation of a wet gluten sample subjected to a standard load for 30 s. Lower GDI values indicate stronger and more elastic gluten (Table 4).

Table 4

The effect of extracts from chokeberry pomace on gluten content and quality

Parameters	Water (control)	With water extracts					With whey extract				
		Time of extraction, min					Time of extraction, min				
		0	30	60	90	120	0	30	60	90	120
Gluten content,%	25.9	26.4	26.1	25.3	24.6	24.2	25.4	24.7	23.7	23.3	21.6
GDI, IDK units	72	74	67	62	64	66	73	65	52	58	60
Extensibility, cm	16	15	16	16	14	13	14	15	14	14	15
Moisture, %	58.3	64.3	64.8	65.0	63.0	65.5	66.0	64.8	64.3	64.5	63.8

Note: GDI, Gluten Deformation Index.

The use of chokeberry pomace extracts affected the quantity and quality of wet gluten in wheat flour (Table 4). The addition of water- or whey-based extracts resulted in a decrease in the gluten deformation index (GDI), indicating strengthening of the gluten network and increased resistance to deformation. The most pronounced effect was observed for extracts obtained after soaking (60 min) and 60 min of extraction.

This effect may be related to the higher content of pectic substances, other polysaccharides, polyphenolic compounds, and organic acids in these extracts. These components can interact with wheat gluten proteins and affect the formation of hydrogen, disulfide, and ionic bonds, the ratio of high- and low-molecular-weight protein fractions, and the packing density of protein structures (Koh et al., 2021; Qi et al., 2024).

At the same time, the use of whey-based extracts resulted in a reduction in wet gluten content compared with the control. This effect may be associated with interactions between whey components and gluten proteins, which affect its hydration and recovery during the washing procedure used for wet gluten determination (Macedo et al., 2020; Zhou et al., 2017).

The simultaneous evaluation of yeast fermentation activity and gluten elasticity was performed because these parameters represent two complementary aspects of dough leavening. Yeast activity determines the rate of CO_2 production, while gluten elasticity defines the ability of the dough matrix to retain the produced gas. Therefore, any modification of either parameter by chokeberry extracts may directly affect the overall gas-holding capacity and final quality of wheat dough.

The effect of extracts from chokeberry pomace powder obtained by 60 min infusion and by extraction with water at 90 °C or whey at 100 °C, with different extraction durations (30, 60, 90, and 120 min), on yeast fermentation activity was studied using dough rising power (Figure 7a) and gluten elasticity (Figure 7b).

Changes in the rising power of compressed yeast indicate a positive effect of water and whey extracts at an extraction time of 30 min. Dough samples containing these extracts floated 12–28% faster compared to the control samples. However, an increase in extraction time led to a decrease in yeast fermentation activity.

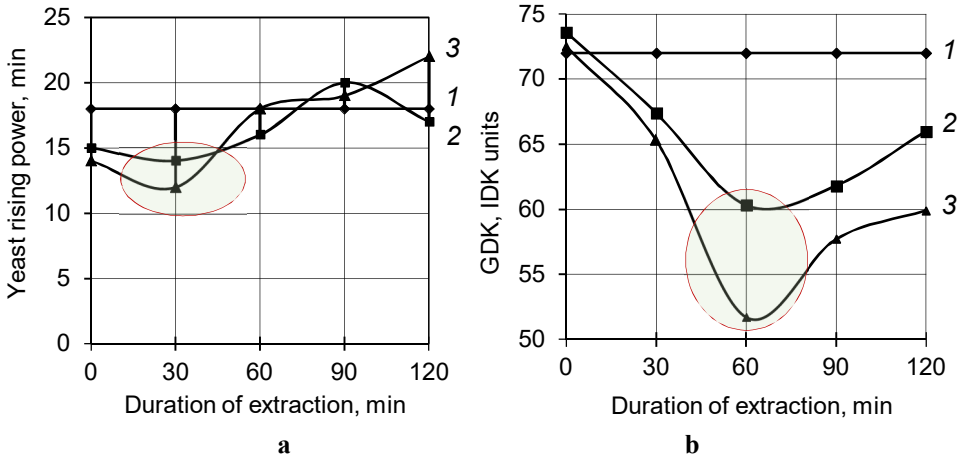

Figure 7. Effect of chokeberry pomace extracts on rising power of baker's yeast (a) and gluten quality (b):
1 – control with water; 2 – experiment with water extract; 3 –experiment with whey extract

It is likely that during infusion and short-term extraction (30 min), mainly water-soluble compounds are transferred into the aqueous phase, including sugars, amino acids, vitamins, organic acids, macro- and microelements, as well as partially tannins, pectins, and phenolic compounds. These substances enrich flour-based intermediates with

nutrients essential for the yeasts. Their incorporation into dough creates more favorable conditions in terms of nutrient composition and acidity, thereby stimulating yeast metabolism and increasing fermentative activity. This, in turn, positively affects the intensity of fermentation during bread-making processes.

In the case of longer extraction and increased medium acidity, a greater amount of phenolic and high-molecular compounds is transferred into the solution, the viscosity of the extracts changes, and some bioactive substances may partially degrade. This worsens the conditions for the viability of yeasts and hinders nutrient transport, leading to a decrease in its fermentative activity.

The incorporation of chokeberry extracts during dough mixing for gluten isolation resulted in increased gluten elasticity (Figure 7b). The highest strengthening effect (27.8%) was observed in samples containing 15.0% chokeberry extract based on whey and obtained after 60 min of extraction. However, gluten yield decreased by 8.5%, accompanied by a reduction in its extensibility and elasticity.

In samples prepared with 30% water-based chokeberry extracts (relative to flour mass), an increase in gluten elasticity was also observed. Water extracts obtained after 60 min of extraction demonstrated the most pronounced effect in improving gluten quality. Similar results have been reported for fruit-based phytocomponents of rosehip and hawthorn, as well as their extracts (Chochkov et al., 2024; Lebedenko et al., 2018; Oliinyk and Samokhvalova, 2025).

Effect of chokeberry pomace powder on bread characteristics

A test baking procedure was carried out. The dosage of water extracts ranged from 15% to 60%, while whey extracts were applied at 5% to 20% relative to flour weight. The results (Table 5) showed significant changes in the quality of the bread under the influence of chokeberry pomace extracts.

Table 5

Effect of water chokeberry extract on the quality parameters of bread

Parameters	Control	Extracts, % of flour weight			
		15	30	45	60
Moisture, %	42.8	43.0	42.8	43.2	43.6
Specific volume, mL/g	2.93	3.13	3.09	2.92	2.90
Dimensional stability, H/D	0.59	0.63	0.61	0.65	0.57
Porosity, %	69.8	73.6	74.1	70.1	69.7
Acidity, °T	2.2	2.2	2.4	2.6	2.8
Signs of mold	After 96 h	Not detected			
Signs of potato disease	After 48 h	Not detected			

According to the data presented in Table 7, the best quality characteristics of bread were obtained when using aqueous extracts of chokeberry pomace at a level of 30% relative to flour weight. All samples exhibited a uniform crumb structure without voids or surface ruptures, a uniformly coloured light-brown crust, and an elastic, well-chewable crumb. However, bread samples containing chokeberry extracts acquired a light pink coloration and a sweet-and-sour taste, which is not typical for conventional wheat bread. Therefore, their application is most appropriate for the development of a new range of bakery products, primarily bakery items with slightly unconventional sensory characteristics for consumers, as well as rye and wheat breads, particularly custard-type formulations.

Whey extracts were added in an amount of no more than 15% of the flour mass (Figure 8, Table 6).



a **b** **c** **d** **e**

Figure 8. Bread samples: control containing 15% whey (a); water-based control (b); and experimental samples supplemented with whey extracts of chokeberry pomace at levels of 5.0 (c), 10.0% (d), and 15.0% (e) of flour weight

Table 6

Effect of whey chokeberry extract on the quality parameters of bread

Parameters	Water	Extracts, % of flour weight			C1*
		5	10	15	
Moisture, %	42.8	42.0	42.8	42.6	42.7
Specific volume, cm^3/g	2.93	3.12	3.29	3.35	3.22
Dimensional stability, H/D	0.59	0.60	0.62	0.66	0.50
Porosity, %	69.8	74.8	75.0	75.2	74.5
Acidity, (°T)	2.2	3.1	3.3	3.6	3.4
Signs of mold	After 96 h	Not detected			
Signs of potato disease	After 48 h	Not detected			

Note: *C1 – whey, 15% of flour weight.

Bread samples containing chokeberry extracts based on whey exhibited a higher specific volume compared to the control samples with water extracts, as well as improved shape stability. The crumb color did not change with the addition of the extracts; however, acidity increased with higher dosage levels. The samples containing the extracts also showed higher resistance to mold growth and potato disease.

The dosage of whey-based chokeberry pomace extracts, which contain organic acids, denatured milk proteins, polysaccharides, phenolic compounds, and other phytochemical components, should not exceed 15.0% relative to flour weight.

Therefore, for wheat bread made from premium and first-grade flour, the use of chokeberry extracts based on whey is considered appropriate, provided that traditional sensory characteristics are preserved. For enhancing the biological value of bakery products, water-based chokeberry pomace extracts are more effective; however, they are better suited for enrichment of rye custard bread, bakery products with distinctive color and taste, and bread made from whole-grain flour.

The issues that remain relevant include a range of tasks: (a) the development of efficient technologies for the integrated processing of chokeberry fruits (Shi et al., 2024); (b) the search for rational approaches to the use of chokeberry fruits in terms of balancing technological properties, nutritional value, sensory perception of food products, and economic criteria.

These include their use in the form of puree from fresh or freeze-dried chokeberry fruits, as well as products of their processing (fresh pomace, freeze-dried pomace, pomace powder), and in the form of extracts obtained under different conditions, including the application of green extraction technologies (Kaloudi et al., 2022; Oszmiański and Lachowicz, 2016; Wieloc and Konopacka, 2025); (b) substantiation of the range of bakery products enriched with chokeberry processing products, selection of dough preparation parameters to maximize the preservation of chokeberry's biological value, and the formation of quality indicators characteristic of traditional products or the development of an expanded product range with specific quality attributes; (c) improvement of bakery technologies with the maximum possible incorporation of chokeberry pomace or its components and whey, which increase the value of by-products, enrich mass-market products with biologically active substances, and support producers in the context of a circular economy.

Conclusions

The results of the conducted research confirm that chokeberry (*Aronia melanocarpa*) is an accessible and promising raw material for the food industry. Its pomace, generated as a by-product of juice production and characterized by a high content of biologically active substances, can be effectively used to enhance the nutritional and biological value of food, particularly bakery products.

The valuable chemical composition and high biological activity of chokeberry fruits and pomace were confirmed. The technological properties of dried chokeberry pomace powder and its effect on the quality of wheat bread were determined. The use of pomace in the form of aqueous and whey-based extracts was proposed. For bread made from first-grade wheat flour, while maintaining traditional sensory characteristics, the recommended application is a whey-based chokeberry extract at a level of 15% relative to flour weight. For catering establishments, where product uniqueness and health-promoting properties are of greater importance, the use of an aqueous pomace extract at 30% of flour weight is recommended. At these dosages, the physicochemical parameters of bread improve, including increased resistance to mold growth and potato disease.

References

Aksoy A.S. (2023), A review of the nutritional profile, chemical composition and potential health benefits of *Aronia melanocarpa* (chokeberry) berries and products, *Turkish Journal of Agriculture - Food Science and Technology*, 11(10), pp. 2027–2043, https://doi.org/10.24925/turjaf.v11i10.2027-2043.6305

Andreica I., Gocan T.M., Rózsa S., Borsai O. (2025), Production costs and financial feasibility of black chokeberry cultivation in Romania, *Ingineria Mediului*, 30(66), 28, https://doi.org/10.52846/bihpt.v30i66.203

Artamonova M., Piliugina I., Aksonova O., Stabnikova O. (2025), Chokeberry and hibiscus as natural food additives in confectionery, In: S. Gubsky, O. Stabnikova, V. Stabnikov, O. Paredes-López (Eds.), *Wild Edible Plants: Improving Foods Nutritional Value and Human Health through Biotechnology*, pp. 201-219, CRC Press, Boca Raton, https://doi.org/10.1201/9781003486794-7

Bakhshaliyeva N., Aliyeva K., Mammadov J., Hummatov A. (2023), The content of microelements in fruits of the oriental persimmon (*Diospyros kaki*) and its dietary role in remedying micronutrient deficiency in the region, *Regulatory Mechanisms in Biosystems*, 14(3), pp. 444-450, https://doi.org/10.15421/10.15421/022365

Blazhenko M., Falendysh N., Shpak V. (2024), Effect of hemp seed by-products on wheat dough fermentation, *Ukrainian Food Journal*, 13(4), pp. 737–752, https://doi.org/10.24263/2304-974X-2024-13-4-8

Brubaker J., Moghtadernejad S. (2024), A comprehensive review of the rheological properties of powders in pharmaceuticals, *Powders*, *3*(2), pp. 233-254, https://doi.org/10.3390/powders3020015

Bushmeleva K., Vyshtakalyuk A., Terenzhev D., Belov T., Nikitin E., Zobov V. (2022), Antioxidative and immunomodulating properties of *Aronia melanocarpa* extract rich in anthocyanins, *Plants*, 11(23), 3333, https://doi.org/10.3390/plants11233333

Cacak-Pietrzak G., Dziki D., Gawlik-Dziki U., Parol-Nadłonek N., Kalisz S., Krajewska A., Stępniewska S. (2023), Wheat bread enriched with black chokeberry (*Aronia melanocarpa* L.) pomace: Physicochemical properties and sensory evaluation, *Applied Sciences*, *13*(12), 6936, https://doi.org/10.3390/app13126936

Chen J., Hu Z., Chen S., Yao Y., Wang X., Zou W., Shao X. (2026), A review of *Aronia*

melanocarpa's phytochemical profile, health benefits, and applications in agri-food systems, *Foods*, 15(10), 1627, https://doi.org/10.3390/foods15101627

Chochkov R., Zlateva D., Stefanova D., Ivanova P. (2024), Effect of pumpkin seed flour, chestnut flour, and rosehip flour on wheat bread staling rate, *Ukrainian Food Journal*, 13(1), pp. 76-90, https://doi.org/10.24263/2304-974X-2024-13-1-6

Chubenko L., Grek V., Tymchuk A., Solovyov N. (2025), Effect of ground psyllium on the quality characteristics of dairy-plant concentrates, *Ukrainian Food Journal*, 14(1), pp. 36–53, https://doi.org/10.24263/2304-974X-2025-14-1-6

Demir F.H., Acik G., Gul D. S. (2025), The boactive potential of fruit juice of black chokeberry (*Aronia melanocarpa*) produced in Edirne province - Türkiye: Phenolic profile, elemental composition, and in vitro antioxidant and antibacterial activities, *Food Science & Nutrition*, 13(9), e70784, https://doi.org/10.1002/fsn3.70784

DumanH., ÜnerB., SarıtaşS., BolatE., YalçıntaşY.M., KalkanA., Kalkan A.E., Eker F., Akdağ İ.Ş., Varol C.C., Özbilen A., Sezer F., Metin Ö.K., Taşkın K.M., Karav S., Proestos C., Babagil G.E., Oz E., Brennan C., Zeng M., Kumar M., Elobeid T., Oz F. (2025), Exploring the potential of black chokeberry (*Aronia melanocarpa*) as a health-enhancing agent: A comprehensive overview, *Journal of Food Biochemistry*, 2025(1), 8899523, https://doi.org/10.1155/jfbc/8899523

Fluerasu D., Neagu C., Dossa S., Negrea M., Jianu C., Berbecea A., Stoin D., Lalescu D., Brezovan D., Cseh L., Suba M., Ianasi C., Alexa E. (2025), The use of whey powder to improve bread quality: A sustainable solution for utilizing dairy by-products, *Foods*, 14(16), 2911, https://doi.org/10.3390/foods14162911

Galenko O., Shevchenko A., Ceccanti C., Mignani C., Litvynchuk S. (2024), Transformative shifts in dough and bread structure with pumpkin seed protein concentrate enrichment, *European Food Research and Technology*, 250, pp. 1177–1188,https://doi.org/10.1007/s00217-023-04454-z

Garcia M.V., Copetti M. (2019), Alternative methods for mold spoilage control in bread and bakery products, *International Food Research Journal,* 26(3), pp. 737–749.

Ghendov-Mosanu A., Ungureanu-Iuga M., Mironeasa S., Sturza R. (2022), Aronia extracts in the production of confectionery masses, *Applied Sciences*, 12(15), 7664, https://doi.org/10.3390/app12157664

Grek V., Tymchuk A., Chubenko L., Lisnyuk V. (2026), Milk protein concentrate and *Aronia melanocarpa*: Effects on coagulation of goat milk proteins, *Ukrainian Food Journal*, 15(1), pp. 60–78, https://doi.org/10.24263/2304-974X-2026-15-1-7

Gurčík Ľ., Bajusová Z., Ladvenicová J., Palkovič J., Novotná K. (2023), Cultivation and processing of modern superfood – *Aronia melanocarpa* (black chokeberry) in Slovak Republic, *Agriculture*, *13*(3), 604, https://doi.org/10.3390/agriculture13030604

Harris G.K. (2024), Ash analysis, In: B.P. Ismail, S.S. Nielsen (Eds.), Nielsen's Food Analysis, Food Science, Springer, Cham, https://doi.org/10.1007/978-3-031-50643-7_16

Iorgachova K.G., Lebedenko T.E. (2015), *Bakery Products for Health Purposes using Phytoextracts*, Kyiv, K-Press.

Jamale S.E., Vedpathak S.G. (2025), A comprehensive review of volumetric analysis: From classical titrations to modern cross-disciplinary applications, *International Journal of Advanced Chemistry Research*, 7(11), pp. 84-89, https://www.doi.org/10.33545/26646781.2025.v7.i11b.335

Kaloudi T., Tsimogiannis D., Oreopoulou V. (2022), *Aronia melanocarpa*: Identification and exploitation of its phenolic components, *Molecules*, 27(14), 4375, https://doi.org/10.3390/molecules27144375

Khomych G., Lebedenko T., Krusir G. (2024), Use of chokeberry in the preparation of bakery products, *Ukrainian Food Journal*, 13(2), pp. 303–315, https://doi.org/10.24263/2304-974x-2024-13-2-8

Kochubei-Lytvynenko O., Bilyk O., Bondarenko Y., Stabnikov V. (2022), Whey proteins in bakery products, In: O. Paredes-López, O. Shevchenko, V. Stabnikov, V. Ivanov (Eds.), *Bioenhancement and Fortification of Foods for a Healthy Diet*, pp. 67-88, CRC Press, Boca

Raton, London, https://doi.org/ 10.1201/9781003225287-5
Koh B.K., Kongraksawech T., Ross A.S. (2022), Effect of polyphenols on mixing properties and solvent retention of wheat flour doughs, *Journal of the Science of Food and Agriculture*, 102(6), pp. 2432–2436, https://doi.org/10.1002/jsfa.11582
KorenetsY., GoriainovaI., NykyforovR. (2017), The study of influence of aronia additives on functional-technological properties of wheat flour, *EUREKA*: *Life Sciences,* 1, pp. 27-34, https://pdfs.semanticscholar.org/76f6/10b47584b54276241f313f27db827e5b1d78.pdf
Koshak Z., Pokrashinskaya A. (2020), Chokeberry powder as an improver for pasta, *Food Science and Technology,* 14(1), https://doi.org/10.15673/fst.v14i1.1649
Kuru Y.A., Kılınç G.E. (2026), *Aronia melanocarpa* as a multifunctional superberry: From antioxidant potential to therapeutic and nanotechnological applications, *Current Nutrition Reports*, 15(1), 9, https://doi.org/10.1007/s13668-026-00736-6
Lebedenko T., Korkach H., Kozhevnikova V., NovichkovaT. (2018), Methods of regulating physical properties of dough using phytoextracts, *Food Science and Technology*, 12(4), pp. 52-62, https://doi.org/10.15673/fst.v12i4.1182
Macedo C., Nunes M. C., Sousa I., Raymundo A. (2020), Rheology methods as a tool to study the impact of whey powder on the dough and breadmaking performance of wheat flour, *Fluids*, 5(2), 50, https://doi.org/10.3390/fluids5020050
Mayer-Miebach E., Adamiuk M., Behsnilian D. (2012), Stability of chokeberry bioactive polyphenols during juice processing and stabilization of a polyphenol-rich material from the by-product, *Agriculture*, *2*(3), pp. 244-258, https://doi.org/10.3390/agriculture2030244
Oliinyk S., Samokhvalova O. (2025), Wild edible plants used in bakery production. Application of by-products from rose hip (*Rosa canina* L.) processing. In: S. Gubsky, O. Stabnikova, V. Stabnikov, O. Paredes-López. (Eds.), *Wild Edible Plants: Improving Foods Nutritional Value and Human Health through Biotechnology*, pp. 268-293, CRC Press, Boca Raton, https://doi.org/10.1201/9781003486794-10
Oszmiański J., Lachowicz S. (2016), Effect of the production of dried fruits and juice from chokeberry (*Aronia melanocarpa* L.) on the content and antioxidative activity of bioactive compounds, *Molecules*, 21(8), 1098, https://doi.org/10.3390/molecules21081098
Raczkowska E., Nowicka P., Wojdyło A., Styczyńska M., Lazar Z. (2022), Chokeberry pomace as a component shaping the content of bioactive compounds and nutritional, health-promoting (anti-diabetic and antioxidant) and sensory properties of shortcrust pastries sweetened with sucrose and erythritol, *Antioxidants*, *11*(2), 190, https://doi.org/10.3390/antiox11020190
Ren Y., Frank T., Meyer G., Lei J., Grebenc J.R., Slaughter R., Gao Y.G., Kinghorn A.D. (2022), Potential benefits of black chokeberry (*Aronia melanocarpa*) fruits and their constituents in improving human health, *Molecules*, *27*(22), 7823, https://doi.org/10.3390/molecules27227823
ReportID: 244771. (2025),*Global Aronia Berries Market Size by Product Type, by Distribution Channels, by Geographic Scope and Forecast*, Verified Market Research, Available at: Verified Market Research report page (Accessed: 10 July 2026).
Qi K., Cao S., Li C. (2024), Possible interaction between pectin and gluten alters the starch digestibility and texture of wheat bread, *International Journal of Biological Macromolecules*, 269(1), 131907, https://doi.org/10.1016/j.ijbiomac.2024.131907
Sady S., Sielicka-Różyńska M. (2019), Quality assessment of experimental cookies enriched with freeze-dried black chokeberry, *Acta Scientiarum Polonorum. Technologia Alimentaria*, 18(4), pp. 463–471, https://doi.org/10.17306/J.AFS.0686
Saracila M., Untea A.E., Oancea A.G., Varzaru I., Vlaicu P.A. (2024), Comparative analysis of black chokeberry (*Aronia melanocarpa* L.) fruit, leaves, and pomace for their phytochemical composition, antioxidant potential, and polyphenol bioaccessibility, *Foods*, *13*(12), 1856, https://doi.org/10.3390/foods13121856
Sharma P., Bratley K., Ford T., Ristvey A.G., Volkis V.V. (2025), *Aronia mitschurinii* – New generation of super fruits with multiple health benefits, *Journal of Berry Research*, 15(1), pp. 12-25, https://doi.org/10.1177/18785093241308676
Shevchenko A., Fursik O., Drobot V., Shevchenko O. (2023), The use of wastes from the flour mills and vegetable processing for the enrichment of food products, In: O. Stabnikova, O.

Shevchenko, V. Stabnikov, O. Paredes-López (Eds.), *Bioconversion of Wastes to Value-added Products*, pp. 1-35, CRC Press, Boca Raton, London, https://doi.org/10.1201/9781003329671

Stabnikov V., Stabnikova O., Paredes-López O. (2025), Antioxidant compounds in wild edible berries, In: S. Gubsky, O. Stabnikova, V. Stabnikov, O. Paredes-López (Eds.), *Wild Edible Plants: Improving Foods Nutritional Value and Human Health through Biotechnology*, pp. 143-184, CRC Press, Boca Raton, https://doi.org/10.1201/9781003486794-5

Stabnikova O., Shevchenko O., Stabnikov V., Paredes-López O. (Eds), (2023a). *Bioconversion of Waste to Value-Added Products*, CRC Press, Boca Raton, London, New York, https://doi.org/10.1201/9781003329671

Stabnikova O., Shevchenko A., Stabnikov V., Paredes-López O. (2023b), Utilization of plant processing wastes for enrichment of bakery and confectionery products, *Ukrainian Food Journal*, 12(2), pp. 299-308, https://doi.org/10.24263/2304-974X-2023-12-2-11

Shi D., Xu J., Sheng L., Song K. (2024), Comprehensive utilization technology of *Aronia melanocarpa*, *Molecules*, 29(6), 1388, https://doi.org/10.3390/molecules29061388

Uazhanova R.U. (2014), The research of the microbiological stability during storage of bread affected by potato disease, *World Applied Sciences Journal*, 30(10), pp. 1394–1396, https://www.idosi.org/wasj/wasj30(10)14/34.pdf

Wieloch D., Konopacka D. (2025), Black chokeberry extracts (*Aronia melanocarpa*) as an ingredient of functional food – potential, challenges and directions of development, *Molecules*, 30(21), 4237, https://doi.org/10.3390/molecules30214237

Zbikowska A., Lukasiak P., Kowalska M., Lukasiak A., Kozłowska M., Marciniak-Lukasiak K. (2024), Incorporation of chokeberry pomace into baked products: Influence on the quality of the dough and the muffins, *Applied Sciences*, *14*(21), 9675, https://doi.org/10.3390/app14219675

Zhou J., Liu J., Tang X. (2017), Effects of whey and soy protein addition on bread rheological property of wheat flour, *Journal of Texture Studies*, 49(1), pp. 38-46, https://doi.org/10.1111/jtxs.12275

Zhu F., Sakulnak R., Wang S. (2016), Effect of black tea on antioxidant, textural, and sensory properties of Chinese steamed bread, *Food Chemistry*, 194, pp. 1217–1223, https://doi.org/10.1016/j.foodchem.2015.08.110

Cite:

Khomych, G., Lebedenko, T., Krusir, G., & Elanidze, L. (2026). Enhancement of bakery product quality using chokeberry processing by-products. *Ukrainian Food Journal, 15*(2), 436–454. https://doi.org/10.24263/2304-974X-2026-15-2-11

Biological synthesis of copper nanoparticles using plants, microorganisms and other natural resources

Oksana Skrotska, Pavlo Holubiev

National University of Food Technologies, Kyiv, Ukraine

Keywords:

Copper
Nanoparticle
Biosynthesis
Biological systems
Microorganism
Plants
Mushrooms
Food product

Article history:

Received 30.11.2025
Received in revised form 24.03.2025
Accepted 30.06.2026

Corresponding author:

Oksana Skrotska
E-mail: skrotskaoi@nuft.edu.ua

DOI:
10.24263/2304-974X-2026-15-2-12

Abstract

Introduction. This article summarizes current approaches to the biosynthesis of copper nanoparticles using various biological systems.

Materials and methods. The study materials consisted of scientific publications indexed in international scientometric databases. The methodology was based on the systematization, comparative analysis, and generalization of research findings related to the biosynthesis of copper nanoparticles. Articles published between 2020 and 2025 were used for the preparation of this review.

Results and discussion. It was established that various biological systems (extracts of plants, food products and food waste, algae, mushrooms, microorganisms, and their metabolic products) contain a wide range of biologically active compounds, including polyphenols, proteins, polysaccharides, enzymes, and organic acids, which can simultaneously act as reducing and stabilizing agents during the formation of copper nanoparticles. It was shown that the choice of biological system and biosynthesis parameters, including medium pH, temperature, concentration and chemical nature of the precursor, biosynthesis duration, and component ratio, significantly affect the size, morphology, degree of aggregation, colloidal stability, and properties of the synthesized copper nanoparticles. Particular attention was paid to the mechanisms of copper ion bioreduction, as well as the formation and stabilization of nanoparticles when different biological systems are used for their biosynthesis. The analyzed data indicate that aqueous extracts of plants, food products, and food waste are promising materials for the biosynthesis of copper nanoparticles due to their availability, low cost, and high content of natural reducing compounds. The use of microorganisms (bacteria, fungi, and yeast) for nanoparticle biosynthesis provides better control over the formation of nanostructures with desired sizes and properties. The generalization of current research results confirms the significant potential of biosynthesized copper nanoparticles for the development of functional nanomaterials that can be applied in the food industry, agriculture, and environmental technologies. At the same time, despite significant advances in the biosynthesis of copper nanoparticles, further studies are required to facilitate the transition of these technologies from laboratory-scale investigations to industrial applications.

Conclusions. The results of this review can be used for the further development of effective biotechnological approaches to nanomaterial synthesis in the context of sustainable development.

Introduction

In modern biotechnology and nanoscience, there is a rapidly growing interest in the development of environmentally friendly and cost-effective methods for the synthesis of nanomaterials, particularly nanoparticles. Due to their unique physicochemical properties, including a high surface area-to-volume ratio, quantum confinement effect, enhanced reactivity, and the possibility of surface functionalization, nanoparticles are widely used in various fields (Antonio-Perez et al., 2023; Luque-Jacobo et al., 2023). Particular attention is being paid to copper nanoparticles (CuNPs), which exhibit antimicrobial, antioxidant, catalytic, and photocatalytic properties (Chaerun et al., 2022; Naikoo et al., 2021). Consequently, CuNPs are considered promising materials for applications in the food industry, agriculture, as well as resource-saving and environmentally sustainable technologies (Rautela et al., 2025; Vincent et al., 2022).

Physical methods (inert gas condensation, laser ablation, physical vapor deposition, laser pyrolysis, high-energy ball milling) and chemical methods (chemical vapor synthesis, hydrothermal synthesis, microwave-assisted synthesis, sol-gel method, plasma-assisted chemical vapor deposition, solvothermal synthesis, polyol synthesis, and microemulsion technique) are commonly applied for nanoparticle synthesis (Kumari et al., 2023). However, these methods have several significant limitations, including the use of toxic reagents, high energy consumption, and the generation of hazardous by-products (Chakraborty et al., 2022; Pathak et al., 2024).

In the context of global challenges related to environmental pollution, antimicrobial resistance, and the transition to sustainable technologies, green methods for nanoparticle synthesis are becoming increasingly relevant (Antonio-Perez et al., 2023). The biosynthesis of CuNPs using microorganisms, algae, fungi, plant extracts, and food waste represents a promising direction in modern biotechnology, as it enables the integration of metal ion bioreduction processes with their stabilization through natural biomolecules. Microbial systems play a particularly important role in these processes due to their ability to perform complex metabolic and enzymatic mechanisms of copper ion reduction. This opens up opportunities for integrating nanoparticle biosynthesis with bioremediation, biosorption, and waste valorization processes (Akintelu et al., 2021; Saleem et al., 2025).

Given the substantial number of studies in this field, contemporary scientific data require systematization. At the same time, many review papers focus on summarizing data related to the biosynthesis of CuNPs using specific biological systems or on narrow aspects of the biosynthesis process, which complicates the formation of a comprehensive understanding of the underlying patterns of CuNP biosynthesis. In addition, data on the molecular mechanisms of bioreduction, the role of different classes of biomolecules, and their influence on nanoparticle nucleation, growth, and stabilization remain insufficiently systematized. Another important scientific challenge is the lack of a systematic analysis of the influence of synthesis conditions on the physicochemical characteristics of nanoparticles, including their size, morphology, stability, and functional properties. This significantly limits the possibilities for the controlled synthesis of nanomaterials with tailored characteristics for specific practical applications (Banger et al., 2025; Siddiqi and Husen, 2020).

Thus, there is an urgent need for a comprehensive synthesis of current knowledge on the biosynthesis of copper nanoparticles, taking into account the diversity of biological systems, the mechanisms of CuNP biosynthesis, and the factors determining the properties of biosynthesized nanoparticles, as well as their role in addressing current challenges in applied microbiology and biotechnology.

Materials and methods

The search and analysis of scientific sources were conducted using the international scientometric databases Scopus, Web of Science, ScienceDirect, PubMed, and Google Scholar.

Scientific articles published between 2020 and 2025 were used for the preparation of this review, focusing on the biosynthesis of copper nanoparticles using various biological sources, including plants, algae, mushrooms, spices and herbs, food products and food waste, bacteria, fungi, and yeast. Full texts of relevant articles were obtained for further assessment. The selected publications were analyzed according to the following criteria: type of biological material, conditions of nanoparticle biosynthesis, nanoparticle size and morphology, nanoparticle properties, and their potential practical applications. The obtained experimental data were systematized and summarized in order to identify different strategies for the biosynthesis of copper nanoparticles and the prospects for their practical application in food technology and agriculture.

Results and discussion

Plants for the biosynthesis of copper nanoparticles

Leaf extracts

A considerable number of publications in the scientific literature address the use of leaf extracts from various plants for the biosynthesis of CuNPs. The extraction method and solvent selection are among the key factors determining the efficiency of biosynthesis and the properties of CuNPs. Aqueous plant extracts are the most commonly used for the biosynthesis of CuNPs. Typically, the preparation of an aqueous extract involves washing the plant material, drying and grinding it, followed by extraction of the plant biomass in distilled water. Extraction is most often carried out at temperatures of 60–100 °C for 10–60 minutes, followed by filtration of the resulting solution. Aqueous extracts contain a significant amount of hydrophilic compounds capable of effectively reducing copper ions and stabilizing the synthesized nanoparticles (Abdelhai et al., 2024; Al Musayeib et al., 2024; Joshi et al., 2025). Methanolic and ethanolic extracts provide isolation of less polar or specific biologically active compounds. Such solvents provide more efficient extraction of phenolic compounds, flavonoids, and other nonpolar substances (Kimta et al., 2025; Labaran et al., 2024).

Agricultural and cultivated plants represent an accessible and renewable source of biomass for the synthesis of CuNPs with high biological activity. In particular, leaf extract of *Mangifera indica* is used to obtain predominantly spherical nanoparticles with sizes ranging from 30 to 90 nm, which exhibit pronounced antioxidant and antimicrobial properties (Shah et al., 2024). Extracts of *Daucus carota* (both wild and cultivated forms) were employed for the synthesis of crystalline CuNPs with an average size of about 42.6 nm, which demonstrate cytotoxic activity against hepatocellular carcinoma cells (Abbas et al., 2025). Mint leaf extracts, due to the high content of flavonoids and terpenoids, facilitate the biosynthesis of copper oxide nanoparticles (CuONPs) with sizes around 19 nm. These nanoparticles have been shown to be effective against both Gram-positive and Gram-negative bacteria, including *Staphylococcus aureus* and *Escherichia coli* (Baral et al., 2025). Basil extracts (*Ocimum basilicum*, *Ocimum sanctum*) provided formation of nanoparticles with sizes ranging from 13 to 18 nm, with broad potential applications across various fields (Wang et al., 2024; Ullah et al., 2024). An aqueous extract of *Stevia rebaudiana* was applied to synthesize CuNPs with sizes ranging from 51 to 53 nm and moderate colloidal stability (zeta potential of approximately +10.8 mV) (Abdelhai et al., 2024). Leaf extract of *Azadirachta indica* enables the production of spherical CuONPs with sizes around 50 nm. These nanoparticles have been shown to possess antifungal activity against *Colletotrichum gloeosporioides*, a fungus responsible for anthracnose, the main cause of mango crop spoilage (Joshi et al., 2025).

Wild and invasive plants are also of significant interest as raw materials for the biosynthesis of nanomaterials, as their use allows the utilization of biomass that is often considered waste, as well as the control of the spread of undesirable plant species. In particular, invasive species such as *Lantana camara* and *Senna spectabilis* can be used for the production of CuONPs with antifungal properties against *Corynespora cassiicola*. These fungi infect plants, including forest stands (Yadava et al., 2025). An aqueous extract of dandelion leaves (*Taraxacum officinale*) enables the synthesis of CuONPs with sizes of about 26.7 nm with high antibacterial and photocatalytic activity (Kasthuri et al., 2024). Leaf extract of *Jatropha curcas* contains flavonoids, tannins, and alkaloids, which act as reducing and stabilizing agents during the biosynthesis of CuNPs with sizes of 10–12 nm (Ghosh et al., 2020). Desert plants, particularly *Citrullus colocynthis* (Nazir et al., 2023) and *Ephedra alata* (Atri et al., 2023), were applied for the synthesis of nanoparticles with sizes ranging from 15 to 17 nm, which possess high potential in photocatalytic processes, particularly in the removal of organic dyes from water. Using an aqueous extract of *Hyptis suaveolens*, spherical CuNPs with an average size of 7.2 nm have been obtained (Shubhashree et al., 2022). The aqueous leaf extract of *Avicennia marina* contains carbohydrates (D-mannose, D-fructose) and phenolic compounds, which enable the biosynthesis of CuNPs. Depending on concentration, these nanoparticles can be used either as plant growth stimulators or as herbicides (Essa et al., 2021). *Cissus vitiginea*, a wild perennial plant common in tropical regions of India, contains antioxidants in its leaf extract that participate in the synthesis of spherical CuNPs with sizes ranging from 5 to 20 nm (Wu et al., 2020). Special attention has been given to ferns, particularly *Adiantum venustum*, whose extracts contain biologically active compounds such as quercetin and kaempferol, capable of effectively reducing copper ions to the nanoscale and stabilizing the resulting CuONPs (Kimta et al., 2025). There are reports on the use of extracts from the inedible fruits of the evergreen shrub *Ligustrum lucidum* for the biosynthesis of spherical CuONPs with sizes of about 22 nm (Ogwuegbu et al., 2024).

Among trees of importance for the food industry and medicine, *Moringa oleifera* attracts considerable attention. Moringa leaves contain flavonoids and phenolic compounds, which ensure the efficient reduction of copper ions and the formation of stable nanoparticles with pronounced antioxidant and antimicrobial properties (Das et al., 2020). Leaves of *Alstonia scholaris* are rich in alkaloids and flavonoids. The use of *Alstonia scholaris* leaf extract enables the synthesis of CuNPs with various morphologies, including triangular and cylindrical shapes (Labaran et al., 2024). *Hagenia abyssinica* is a traditional medicinal plant of Ethiopia. Its' leaves contain compounds (polyphenols, tannins) capable of acting as ligands that bind copper ions and promote the formation of crystalline nanostructures (Murthy et al., 2020). Leaf extracts of *Cassia fistula* provide the synthesis of spherical CuONPs with sizes ranging from 15 to 25 nm and pronounced antibacterial and cytotoxic activity (Tyagi et al., 2024).

Among herbs and shrubs of importance for the food industry and medicine, thyme should be noted. In particular, CuNPs with an average size of about 60 nm were obtained using an aqueous extract of *Thymus fedtschenkoi* leaves (Dehnoee et al., 2024). Extracts of *Euphorbia serpens* (Idrees et al., 2025) and *Heliotropium bacciferum* (Hamdy et al., 2024) contain specific phytochemical components, such as terpenoids and tannins, which prevent the oxidation and aggregation of CuONPs.

Depending on the selected plant source and biosynthesis conditions, the characteristics of nanoparticles obtained using leaf extracts of different plants may vary significantly (Table 1).

Various copper salts are used as sources of copper ions, serving as precursors during nanoparticle biosynthesis. The choice of a specific precursor has a substantial impact on the reduction kinetics, morphology, size, and stability of the resulting CuNPs. Copper sulfate is most commonly applied as a precursor, typically in the form of pentahydrate ($CuSO_4 \times 5H_2O$). Its popularity is due to its high solubility in water, availability, and stability (Alshammari, 2023; Philip, 2025). Copper nitrate is also a widely used precursor, more often applied in the form of trihydrate ($Cu(NO_3)_2 \times 3H_2O$) (Abbas et al., 2025).

Table 1

Biosynthesis of copper nanoparticles using plant leaves

Plant	Nanoparticles biosynthesis parameters	Characteristics of nanoparticles	Reference
Acacia cornigera	Aqueous extract, 10 mM $CuSO_4$, 50 °C, pH 7, 0.5 h	CuNPs, non-spherical 63–153 nm, zeta potential +9.6 mV	Solorzano Toala et al., 2024
Aegle marmelos	Aqueous extract, 1 mM CH_3COOCu, 80 °C, 2 h	CuONPs, almost spherical ~200 nm, PDI 0.09	Tarangini et al., 2024
Alstonia scholaris	Methanol extract, 0,1 M $CuSO_4$, 1:9 ratio	CuNPs, triangular, cylindrical, polygonal, spherical	Labaran et al., 2024
Cassia fistula	Aqueous extract, $CuCl_2 \times 2H_2O$ (1.34 g in 100 mL), mixing, 1 h	CuONPs, mostly spherical 15–25 nm, PDI 0.712	Tyagi et al., 2024
Ziziphus spina-christi	Aqueous extract, 10 mM $CuSO_4 \times 5H_2O$, 80 °C,1 h	CuONPs, spherical 13.4–30.9 nm	El-Abeid et al., 2024
Lupinus arcticus	Aqueous extract, 1 mM $CuSO_4$, 25 °C, 12 h	CuNPs, spherical 10–85 nm (mostly 30–50 nm)	Saeedi et al., 2025
Crossandra infundibuliformis	Aqueous extract, $CuSO_4 \times 5H_2O$, 18-20 °C, pH 7	CuNPs, spherical 2–20 nm, zeta potential –17.9 mV	Philip et al., 2025
Daucus carota	Aqueous extract, 4 mM $Cu(NO_3)_2 \times 3H_2O$, 60 °C, pH 7, 3-4 h	CuNPs, mostly spherical and oval, mean size 58.3 nm	Abbas et al., 2025
Euphorbia serpens	Aqueous extract, $Cu(CH_3COO)_2$ (2 g in 100 mL), 60 °C, 2 h	CuONPs, mean size 20,39 nm, zeta potential +32.1 mV, PDI 1	Idrees et al., 2025
Ocimum basilicum	Aqueous extract, 0,25 M $Cu(NO_3)_2 \times 3H_2O$, 25 °C, 3 h	CuNPs/CuONPs, spherical, mean size 20–30 nm, zeta potential –5 mV	Wang et al., 2024
Ocimum sanctum	Ethanol extract, 1 mM $CuSO_4 \times 5H_2O$, direct sunlight, 1 h	CuNPs, quasispherical ~60,3 nm, zeta potential –17.3 mV, PDI 0.26	Ashokkumar et al., 2024
Opuntia ficus indica	Aqueous extract, 0,1 M $Cu(CH_3COO)_2$, 60 °C	CuONPs, spherical 65 nm	Soliman et al., 2025
Pterocarpus santalinus	Aqueous extract, 10 mM $CuSO_4$, 60 °C, 0,5 h	CuONPs, mean size 10.62 nm	Babulla et al., 2024
Rhus microphylla	Aqueous extract, 0,1 mM $CuSO_4 \times 5H_2O$, 60 °C, 3 h	CuONPs, spherical, mean size 32.45 nm	Al Musayeib et al., 2024
Thymus fedtschenkoi	Methanol-aqueous extract (70:30), 40 mM $CuSO_4$, pH 12, 0.5 h	CuNPs, Spherical-elliptical 50–75 nm, zeta potential 15.5 mV	Dehnoee et al., 2024

Copper (II) acetate – $Cu(CH_3COO)_2$ – is another common precursor (Idrees et al., 2025). There are also reports on the use of copper(I) acetate – CH_3COOCu; however, in most cases this precursor leads to CuONPs formation (Tarangini et al., 2024). Copper chloride is used less frequently, typically in the form of dihydrate ($CuCl_2 \times 2H_2O$) (Tyagi et al., 2024).

Plant roots

Extracts from the roots of various plants are also used for the biosynthesis of CuNPs (Table 2), although the number of recent studies in this area remains limited.

Table 2

Biosynthesis of copper nanoparticles using plant roots

Plant	Nanoparticles biosynthesis parameters	Characteristics of nanoparticles	Reference
Biebersteinia multifida	Ethanol extract, 50 mM $CuSO_4$, 60 °C, 2 h	CuNPs, semi-spherical, mean size 29 nm	Issa et al., 2025
Krameria sp.	Aqueous extract, 0.3 M $CuSO_4 \times 5H_2O$, 70 °C, pH 11, 3 h	CuNPs, spherical 5.2–7.7 nm	Alshammari et al., 2023
Lannea discolor	Aqueous, methanol or acetone extract, 1 mM $CuSO_4$, 25 °C and 80 °C, 24 h	CuNPs, spherical 20–104 nm; zeta potential from –43.3 to –13.4 mV	Rambau et al., 2024
Senna didymobotrya	Methanol extract, 12.5 mM $CuSO_4 \times 5H_2O$, 80 °C, pH 3.0, 4 h	CuNPs, spherical 5.55–63.60 nm, zeta potential –69.4 mV	Sadia et al., 2021

Analysis of scientific sources indicates the successful use of root extracts from different plants for the synthesis of CuNPs with controlled morphological characteristics. In particular, the use of methanol, acetone, and aqueous root extracts of Lannea discolor results in the formation of predominantly spherical nanoparticles with sizes ranging from 20 to 104 nm (Rambau et al., 2024). When Senna didymobotrya root extract is used, CuNPs are synthesized within a size range from 5.55 to 63.60 nm (Sadia et al., 2021). In the case of Biebersteinia multifida, the application of an ethanol root extract promotes the formation of hemispherical nanoparticles with an average size of about 29 nm (Issa et al., 2025). Aqueous root extracts of Krameria sp. are rich in tannins and enable the formation of highly dispersed spherical CuNPs with an average size of approximately 6.16 nm (Alshammari et al., 2023).

Flowers

In recent years, the scientific literature has also reported isolated studies on the use of flower extracts for the biosynthesis of CuNPs and CuONPs (Table 3).

Table 3

Biosynthesis of copper nanoparticles using plant flowers

Plant	Nanoparticles biosynthesis parameters	Characteristics of nanoparticles	Reference
Acacia saligna	Aqueous extract, 0.1 mM $CuSO_4 \times 5H_2O$, 65–70 °C, pH 7, 4 h	CuONPs, spherical, mean diameter 8.488 nm	Abdullah, 2025
Bauhinia variegata	Aqueous extract, 50 mM $CuSO_4$, 80 °C	CuNPs, polydisperse with rough surface 8.721 nm	Kumar et al., 2024
Lonicera japonica	Aqueous extract, 0,1 M $CuCl_2$, 80 °C, 8 h	CuNPs, 2–4 nm, zeta potential –0.087 mV	Yu et al., 2025
Passiflora	Aqueous extract, 0.1 M $Cu(NO_3)_2$, 20 °C, pH 9, 24 h	CuNPs/CuONPs, spherical 10–20 nm	Sahib et al., 2025

Available data indicate that the use of flower extracts enables the production of nanoparticles with small sizes, typically in the range of 2–20 nm, which is important in terms of their physicochemical and biological properties. It was shown that the use of extracts from certain flower species (*Bauhinia variegata*, *Lonicera japonica*, *Passiflora*, *Saussurea lappa*) promotes the formation of CuNPs (Kumar et al., 2024; Yu et al., 2025; Sahib et al., 2025), whereas the use of others (*Acacia saligna*) results in the formation of CuONPs (Abdullah, 2025). This is likely due to differences in the chemical composition of the phytoextracts.

Seeds

The number of studies on the biosynthesis of CuNPs using plant seed extracts (Table 4) remains limited. In most cases, seeds are previously being grounded to obtain biologically active compounds, after which extraction is carried out using water or organic solvents, particularly ethanol.

Table 4

Biosynthesis of copper nanoparticles using plant seeds

Plant	Nanoparticles biosynthesis parameters	Characteristics of nanoparticles	Reference
Chenopodium quinoa	Aqueous extract, $CuSO_4 \times 5H_2O$ (3.5% m/w), 80 °C, 3 h	CuNPs, cubical 8.41 nm	Hassan et al., 2023
Foeniculum vulgare	Ethanol extract, $CuSO_4 \times 5H_2O$, 60 °C, pH 7, 3 h	CuNPs, spherical 20–40 nm, zeta potential –32.1 mV, PDI 0.25	Huang et al., 2025
Nigella sativa	Aqueous extract, 0.05 M $CuSO_4 \times 5H_2O$, 80 °C, 150 rpm	CuNPs, 98.23 nm	Kumar et al., 2023
Silybum marianum	Aqueous extract, $Cu(CH_3COO)_2 \times H_2O$ (10 g in 100 mL of extract), 50 °C, 2 h	CuONPs, spherical 15 nm, zeta potential –16.9 mV, PDI 0.136	Iqbal et al., 2022

It has been shown that the use of seed extracts from plants such as *Nigella sativa*, *Chenopodium quinoa*, and *Foeniculum vulgare* promotes the formation of CuNPs (Kumar et al., 2023; Hassan et al., 2023; Huang et al., 2025). At the same time, the use of Silybum marianum seed extract leads to the formation of CuONPs (Iqbal et al., 2022). Such differences in biosynthesis products are likely result from the specific chemical composition of the respective phytoextracts and their redox properties. In particular, Silybum marianum seed extracts are characterized by a high content of the silymarin complex, which includes silybin A – a compound with a pronounced reducing potential (Iqbal et al., 2022). In turn, Chenopodium quinoa seeds contain significant amounts of phenolic compounds, such as quercetin, ferulic acid, and gallic acid, which also play an important role in the reduction of copper ions and the stabilization of the formed nanoparticles (Hassan et al., 2023).

A comprehensive scheme of biosynthesis of CuNPs using plant-derived materials provided in Figure 1.

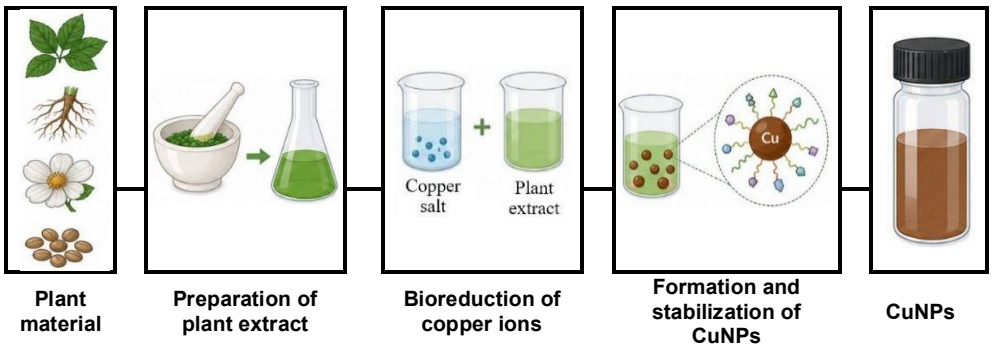

Figure 1. Biosynthesis of CuNPs using plant-derived materials

Mechanisms of copper nanoparticle biosynthesis using plants

The biosynthesis of copper nanoparticles using plant extracts is based on the ability of biologically active compounds to reduce copper ions (Cu^{2+}) to the metallic state (Cu^0) or to oxide forms (CuO, Cu_2O), as well as to stabilize the formed nanostructures.

Various classes of phytochemical compounds are involved in this process, acting both as reducing agents and as capping agents, which determines the efficiency of nucleation and the subsequent growth of nanoparticles (Soliman et al., 2025).

An important role in bioreduction is played by polyphenols and phenolic compounds, which act as electron donors. Their activity is provided by the presence of hydroxyl (–OH) and carbonyl (C=O) groups capable of participating in redox reactions (Dehnoee et al., 2024). This group includes phenolic acids (gallic, ellagic, chlorogenic, *p*-coumaric), flavonoids (quercetin, kaempferol, epicatechin, luteolin, flavanol glycosides), and tannins (Al Musayeib et al., 2024). Polyphenols reduce copper ions and stabilize the surface of nanoparticles. They adsorb onto the nanoparticle surface through π-electron interactions of aromatic rings or hydrogen bonding of hydroxyl groups. This organic shell creates repulsive forces (electrostatic or steric), which prevent nanoparticle aggregation and ensure their stability in solution (Philip et al., 2025).

Nitrogen-containing compounds, in particular alkaloids, proteins, amino acids, and amides present in plant extracts, also play an important role in the biosynthesis of CuNPs and CuONPs. Alkaloids are capable of interacting with copper ions through amino groups, ensuring both their reduction and the subsequent stabilization of nanoparticles. They participate in nucleation processes, promoting the formation of primary nuclei of the metallic or oxide phase (Yu et al., 2025). Proteins and amino acids perform a dual function: they can reduce metal ions while simultaneously capping the particle surface, forming a stable organic layer (Sazak et al., 2023).

Terpenoids and steroidal compounds also participate in the processes of bioreduction and stabilization of nanoparticles. Compounds such as phytol, carotol, β-bisabolene, limonene, α- and β-pinene, as well as saponins, can act as auxiliary reducing agents and stabilizers. They impart specific biological properties to the nanoparticles, which is important for their further practical applications (Abbas et al., 2025).

In addition, carbohydrates present in plant extracts play a significant role in the biosynthesis of copper nanoparticles. Due to the presence of hydroxyl and carbonyl groups, mono- and polysaccharides can act as natural reducing agents, converting Cu^{2+} ions into Cu^0 or oxide forms. At the same time, they are capable of stabilizing the formed nanoparticles by creating a protective layer on their surface (Ashokkumar et al., 2024).

In the case of using plant root extracts, phenolic compounds and flavonoids play a key role in the biosynthesis of CuNPs. For example, quercetin facilitates the reduction of copper ions through π-electron interactions (Sadia et al., 2021). Tannins, particularly catechins and proanthocyanidins, as well as rhataniatannic acid, effectively reduce copper ions and contribute to the stabilization of the formed nanoparticles by creating an organic layer on their surface (Alshammari et al., 2023). Root extracts may also contain terpenoids and alkaloids that participate in reduction-stabilization processes, including citraconic anhydride and γ-sitosterol (Issa et al., 2025).

Algae for the biosynthesis of copper nanoparticles

Marine algae

Species of marine algae from different taxonomic groups are employed in CuONPs and CuNPs biosynthesis. The most studied are brown algae, particularly *Cystoseira myrica* (Soureshjani et al., 2021), *Macrocystis pyrifera* (Araya-Castro et al., 2020), *Sargassum vulgare* (Marzban et al., 2022), *Sargassum cervicorne* (Anwar et al., 2024) and species of *Turbinaria*

genera (Anbalagan et al., 2024). Brown algae aside, CuONPs biosynthesis research also involve green (*Ulva lactuca*) (Hamouda et al., 2023) and red (*Pterocladia capillacea*) (Aboeita et al., 2022) algae (Table 5).

Table 5

Biosynthesis of copper nanoparticles using marine algae

Plant	Nanoparticles biosynthesis parameters	Characteristics of nanoparticles	Reference
Cystoseira myrica	Aqueous extract, $CuSO_4 \times 5H_2O$ (1 g / 200 mL), 100 °C, pH 12, 20 min	CuONPs, mean size 12–26 nm	Soureshjani et al., 2021
Macrocystis pyrifera	Purified protein fractions, 2 mM $CuSO_4$, 45 °C, 48 h	CuONPs , spherical, 2–50 nm	Araya-Castro et al., 2020
Pterocladia capillacea	Aqueous extract, $CuSO_4 \times 5H_2O$, 18–20 °C, pH 7	CuONPs, mean size 62 nm, zeta potential –16,8 mV	Aboeita et al., 2022
Sargassum cervicorne	Aqueous extract, 0.05 M $CuSO_4 \times 5H_2O$, 18–20 °C, 24 h	CuNPs, spherical, 2.6–3 nm	Anwar et al., 2024
Sargassum longifolium	Aqueous extract, 10 mM $CuSO_4$, 18–20 °C, 6 h	CuONPs, 40–60 nm	Rajeshkumar et al., 2021
Sargassum vulgare	Algae polysaccharides, 3 mM $CuSO_4 \times 5H_2O$, 70 °C, 24 h	CuONPs, spherical, 40–50 nm	Marzban et al., 2022
Turbinaria sp.	Aqueous extract, $Cu(NO_3)_2$, 60 °C, 24 h	CuNPs/CuONPs, almost rectangular, 18 nm	Anbalagan et al., 2024
Ulva lactuca	Aqueous extract, 9 mM $CuSO_4$, 18–20 °C, 2 h	CuONPs, rod-shaped (width 10–40 nm, length 46–65 nm), zeta potential –0.195 mV	Hamouda et al., 2023

In most cases, marine algae-mediated nanoparticles biosynthesis is performed using aqueous extracts of biomass. Such extracts are obtained by boiling or ultrasound treatment that results in extracting biomolecules that act as nanoparticles reducers and stabilizers (Soureshjani et al., 2021; Aboeita et al., 2022). There are reports on purified biomolecules fractions, particularly proteins or water-soluble polysaccharides, that play key role in nanostructures formation and stabilization (Araya-Castro et al., 2020; Marzban et al., 2022).

The use of different species of brown algae allows to obtain nanoparticles with different physicochemical properties. For example, synthesis of CuONPs with size range from 12 to 26 nm was provided with aqueous extracts of *Cystoseira myrica* and *Sargassum latifolium* (Soureshjani et al., 2021). The use of protein fractions from *Macrocystis pyrifera* provides formation of spherical CuONPs in size range 2–50 nm (Araya-Castro et al., 2020). At the same time *Sargassum cervicorne* extracts allow for thevsynthesis of amorphous, highly thermostable CuNPs with size around 3 nm (Anwar et al., 2024).

Green macroalgae, particularly species of *Ulva*, *Enteromorpha* and *Codium* genera, are characterized by complex and diverse biochemical composition. They contain considerable amounts of proteins, carbohydrates, lipids and pigments, particularly chlorophylls, as well as wide spectrum of secondary metabolites, such as phenolic compounds, flavonoids, terpenoids, amines and amides. These components provide metals ions reduction and further stabilization of nanoparticles formed. Different green algae species allow for the synthesis of copper nanoparticles with various morphology and sizes. The use of *Ulva lactuca* provides synthesis of rod-shaped CuONPs. Moreover, same specimen was used to obtain hexagonal silver-copper nanocomposites with size range 10–35 nm (Hamouda et al., 2023).

Red marine algae are characterized by a high content of specific bioactive compounds that play a key role in metal nanoparticles biosynthesis processes. One of the red algae notable features is a high content of polysaccharides, which can act as natural reducers turning metal ions into zero-valency state as well as stabilizing agents that prevent nanoparticles aggregation. Moreover, red algae contain broad spectrum of bioactive macromolecules, including proteins, amino acids, phenolic compounds and uronic acids. These components provide expressing antioxidant properties, which are important for running reduction reactions during nanoparticles synthesis (Aboeita et al., 2022).

Freshwater algae

Among freshwater algae applied for nanoparticles biosynthesis most notable are filamentous green macroalgae *Cladophora glomerata*. Using specifically its' extracts allows the obtaining of spherical CuONPs in size range 40–50 nm. Biochemical composition of *Cladophora glomerata*, particularly presence of fatty acids, phenolic compounds and proteins, provides effective copper ions reduction and obtained nanoparticles stabilization (Kumar et al., 2025).

Green filamentous algae *Oedogonium* sp. were used for synthesis of CuNPs with expressed antimicrobial activity, specifically against phytopathogenic bacteria, such as citrus cancer agent *Xanthomonas citri*. It opens a perspective of using biogenic CuNPs for plants protection against bacterial infections (Waqif et al., 2024).

The algae of *Zygnema* sp. genera are another source of biogenic CuONPs. Aqueous extracts from these filamentous algae contain phenolic compounds and flavonoids, which provide synthesis of predominantly spherical nanoparticles with mean diameter around 30 nm (Alsalamah et al., 2024).

Unicellular microalgae *Chlorella ellipsoidea* are often isolated from wastewater. They are used for the biosynthesis of copper sulfide nanoparticles (CuSNPs) with sizes in the range of 9–23 nm. These algae are capable of hyperaccumulating metal ions and can grow in both clean and polluted or wastewater environments. This makes them an accessible and renewable resource for nanoparticle biosynthesis, as well as opening up prospects for combining bioremediation processes with nanobiotechnology (Borah et al., 2022).

Unicellular microalgae *Chlamydomonas reinhardtii* are characterized by a unique ability to combine bioremediation processes with nanoparticle biosynthesis. They are capable of efficiently removing copper ions from wastewater while simultaneously synthesizing CuNPs with sizes below 10 nm. In this process, cell viability is a critical factor that determines the efficiency of both metal sorption and its subsequent reduction (Zvab et al., 2021).

Particular attention is drawn to unicellular algae such as *Asterarcys quadricellulare* and *Coelastrella terrestris*. It has been established that the use of aqueous extracts of these algae leads to the synthesis of CuONPs with variable morphology – ranging from rice-like structures to petal-like forms. This morphological diversity depends on the conditions of biosynthesis and opens up possibilities for the targeted control of nanomaterial properties (Khandelwal et al., 2023; Khandelwal et al., 2024).

The conditions of biosynthesis and the type of freshwater algae used significantly influence the characteristics of the resulting nanoparticles (Table 6).

Mechanisms of copper nanoparticle biosynthesis using algae

Specific biosynthesis mechanisms largely depend on the algal species and the composition of their metabolites. In the case of the marine alga *Cystoseira myrica*, the process occurs in two stages: first, stable complexes of copper ions with ligands (e.g., sodium citrate) are formed, followed by their reduction under the activity of biomolecules from the algal extract in an alkaline medium. The pigment fucoxanthin plays an important role in this process; due to the presence of electron-donating groups, it effectively interacts with copper ions, ensuring both their reduction and the stabilization of the resulting CuONPs (Soureshjani et al., 2021).

Table 6

Biosynthesis of copper nanoparticles using freshwater algae

Algae	Nanoparticles biosynthesis parameters	Characteristics of nanoparticles	Reference
Asterarcys quadricellulare	Aqueous extract, $CuSO_4 \times 5H_2O$, 60 °C, pH 11, 24–72 h	CuONPs, rice-like or petal-like structures, 4.76–13.70 nm	Khandelwal et al., 2023
Chlamydomonas reinhardtii	Living cells, TAP medium (wastewater simulation), 10 mg/L $CuCl_2 \times 2H_2O$, 26–28 °C, pH 7.7–8, 24–72 h	CuNPs, spherical, <10 nm	Zvab et al., 2021
Chlorella ellipsoidea	Aqueous extract, 2 mM $CuCl_2 \times 2H_2O$, 2 mM Na_2S, 40 °C, 4 h	CuSNPs, predominantly spherical, 9–23 nm	Borah et al., 2022
Cladophora glomerata	Aqueous extract, 1 M $Cu(NO_3)_2 \times 3H_2O$, 80 °C, pH 7–8, 24 h	CuONPs, spherical, 40–50 nm	Kumar et al., 2025
Coelastrella terrestris	Aqueous extract, $CuSO_4 \times 5H_2O$, 60 °C	CuONPs, rice-like or petal-like structures, 4.26–28.51 nm	Khandelwal et al., 2024
Oedogonium sp.	Aqueous extract, 1–10 mM $Cu(CH_3COO)_2$, 37 °C, pH 5–9, 24 h	CuNPs, spherical, 15–32 nm, zeta potential –30.172 mV	Waqif et al., 2024
Zygnema sp.	Aqueous extract, 1 mM $Cu(CH_3COO)_2$, 80 °C, 18 h	CuONPs, spherical, mean diameter 30.06 nm	Alsalamah et al., 2024

When using extracts of *Turbinaria* sp., the reduction of copper ions is driven by polyphenols and polysaccharides. The hydroxyl groups of biomolecules act as active centers that initiate nanoparticle nucleation and promote the subsequent stabilization of the colloidal system (Anbalagan et al., 2024). In the case of *Ulva lactuca*, the biosynthesis mechanism is associated with the presence of amines, amides, proteins, and pigments in the aqueous extract. It was established that N–H groups are directly involved in bioreduction processes, while alcohol and aldehyde groups initiate the nucleation stage of CuONPs (Hamouda et al., 2023).

During nanoparticle biosynthesis using *Pterocladia capillacea* extract, sulfated polysaccharides, particularly galactose sulfates, as well as uronic acids, play a leading role (Aboeita et al., 2022). The potential use of polysaccharides from *Sargassum vulgare* for CuONPs biosynthesis was also investigated. Their hydroxyl (–OH) and aliphatic (–CH) groups ensure efficient nanoparticle formation by creating a stable protective layer and preventing aggregation (Marzban et al., 2022). A protein-mediated mechanism of CuONPs synthesis was also identified when using purified protein fractions of *Macrocystis pyrifera*. The reduction of copper ions occurs with the participation of tyrosine residues in proteins, while the carboxyl groups of aspartic and glutamic acids regulate nanoparticle growth. Additional stabilization is provided by cysteine, which contains thiol groups capable of binding to the nanoparticle surface (Araya-Castro et al., 2020).

The mechanisms of nanoparticle biosynthesis exhibit pronounced species specificity and are determined by the characteristics of the metabolic profile, including in the case of freshwater algae. For example, when using an aqueous extract of *Asterarcys quadricellulare*, the synthesis of CuONPs occurs in two stages. At the first stage, biomolecules (proteins, carbohydrates, and lipids) reduce Cu^{2+} ions to the zero-valent state (Cu^0), after which, at the second stage, they are oxidized by dissolved oxygen in the medium to form CuO. Further stabilization is provided by proteins, polysaccharides, and long-chain fatty acids, which form a protective coating around the nanoparticles (Khandelwal et al., 2023).

When using an aqueous extract of *Chlorella ellipsoidea*, a single-stage mechanism of CuSNPs synthesis is observed. Phytochemical components of the extract (proteins, carbohydrates, exopolysaccharides, and phenolic compounds) bind copper ions and promote their interaction with sulfide ions, ensuring the simultaneous formation of the nanoparticle core and stabilizing shell (Borah et al., 2022). An important role of terpenoids and polyphenols was also demonstrated in the biosynthesis of nanoparticles using extracts of freshwater algae *Oedogonium* sp. and *Coelastrella terrestris* (Khandelwal et al., 2024; Waqif et al., 2024).

In the case of using living cells of *Chlamydomonas reinhardtii*, the mechanism of CuNPs biosynthesis is complex and involves several interrelated processes. A determining factor is cell viability, as efficient reduction of copper ions occurs only under conditions of active metabolism. Studies using damaged cells or photosensitive mutants have shown that in the absence of metabolic activity, only soluble copper complexes with cellular components are formed, while the formation of metallic nanoparticles does not occur.

The reduction of copper ions to metallic nanoparticles is associated with intracellular redox processes. An additional factor is the ability of this alga to photoproduce hydrogen, which can act as a reducing agent for Cu^{2+} ions to Cu^0. At the same time, polysaccharides, proteins, and alkaloids ensure the stabilization of the formed CuNPs (Zvab et al., 2021).

Mushrooms for the biosynthesis of copper nanoparticles

Mushrooms are considered promising biological systems for the biosynthesis of copper nanoparticles due to their unique combination of nutritional value and a high content of bioactive compounds. However, the number of contemporary studies in this area remains limited. An important prerequisite for the use of mushrooms in nanobiotechnology is their wide spectrum of secondary metabolites.

Mushrooms of the species *Agaricus bisporus* contain bioactive components with antimicrobial, antiviral, and antitumor properties, as well as polysaccharides with immunomodulatory activity (Sriramulu et al., 2020). Representatives of the genus *Ganoderma*, including *Ganoderma sessile*, are known as medicinal mushrooms with a high content of triterpenoids, sterols, and polysaccharides exhibiting antioxidant and anti-inflammatory activity (Flores-Rabago et al., 2023). Species of the genus *Pleurotus*, in particular *Pleurotus ostreatus* and *Pleurotus cystidiosus*, are characterized by the presence of phenolic compounds and flavonoids, which can act as reducing and stabilizing agents during nanoparticle formation (Kamakshi et al., 2024; Roslan et al., 2025).

The biosynthesis of CuNPs using mushrooms (Table 7) can be carried out either with the involvement of intracellular components or through extracellular metabolites. The preparation of biological material includes washing the mushrooms, drying them, and grinding them into a powder-like state, followed by mixing with distilled water. The resulting suspension is subjected to thermal treatment to extract bioactive compounds (Amirtham et al., 2023). In the case of *Ganoderma sessile*, submerged cultivation is performed, after which the supernatant and aqueous cell extracts are used for the biosynthesis of copper nanoparticles (Rivera-Mendoza et al., 2024).

Mechanisms of copper nanoparticle biosynthesis using mushrooms

The first key stage is the biochemical reduction of copper ions, which, under the action of fungal metabolites, are reduced to zero-valent copper (Cu^0) or transformed into oxide forms (CuO). A decisive role in this process is played by the functional groups of biomolecules, particularly hydroxyl (–OH) and amide groups present in phenolic compounds, proteins, and polysaccharides. These groups can act as electron donors, initiating the reduction of copper ions and the subsequent formation of nanoparticles (Sriramulu et al., 2020). Additionally, it was established that flavoproteins, particularly riboflavin derivatives, are involved in the nucleation

and growth of nanoparticles, promoting the aggregation of copper atoms into stable nanostructures. Enzymatic activity is also an important component: extracellular enzymes such as laccase, lignin peroxidase, and manganese peroxidase are involved in the biotransformation of copper ions and can catalyze redox reactions accompanying nanoparticle formation (Amirtham et al., 2023).

Table 7

Biosynthesis of copper nanoparticles using mushrooms

Mushrooms	Nanoparticles biosynthesis parameters	Characteristics of nanoparticles	Reference
Agaricus bisporus	Aqueous extract, 1 mM $Cu(NO_3)_2$, 18–20 °C, 300 rpm, 24 h	CuNPs, spherical, 10–60 nm, zeta potential –40 mV	Sriramulu et al., 2020
Ganoderma sessile	Aqueous extract of mycelium cells, 5 mM $CuSO_4 \times 5H_2O$, 60 °C, pH 10, 24 h	CuONPs, spherical, 5.2 nm, zeta potential –28.7 mV, PDI 0.67	Flores-Rabago et al., 2023
Ganoderma sessile	Aqueous extract of mycelium cells, 10 mM $CuSO_4 \times 5H_2O$, 60 °C, pH 8, 72 h	CuONPs, spherical, 2.9 nm, zeta potential –21.0 mV	Rivera-Mendoza et al., 2024
Lentinus squarrosulus	Aqueous extract, 5 mM $CuSO_4$	CuNPs, spherical, 200–300 nm	Amirtham et al., 2023
Pleurotus cystidiosus	Aqueous extract, 5 mM $CuSO_4$, 60 °C, 10–20 min	CuONPs, spherical and oval-shaped, 80–110 nm	Kamakshi et al., 2024
Pleurotus ostreatus	Aqueous extract, $CuSO_4 \times 5H_2O$ (1 g in 10 mL of extract), autoclaving (121 °C, 15 min)	CuNPs, irregular shape, 41.56–131.9 nm	Roslan et al., 2025

The second stage involves the stabilization of the formed nanoparticles. Proteins, amino acids, and polysaccharides adsorb onto their surface, acting as stabilizers and preventing aggregation. In addition, the stability of the colloidal system is maintained through electrostatic effects: nanoparticles acquire a negative surface charge, which ensures effective electrostatic repulsion between them and prevents their agglomeration (Flores-Rabago et al., 2023).

Spices and herbs for the biosynthesis of copper nanoparticles

Extracts of various spices and herbs can be applied for the biosynthesis of CuNPs and CuONPs, as they contain phytochemical compounds (phenolic compounds, flavonoids, terpenoids, alkaloids, and tannins) that act as natural reducing and stabilizing agents (Amaliyah et al., 2020) (Table 8).

Aqueous extracts of cinnamon bark and leaves (*Cinnamomum zeylanicum*) contain a wide range of biologically active compounds, including flavonoids, tannins, glycosides, and alkaloids, which enable efficient reduction of copper ions, resulting predominantly in spherical nanoparticles. A key role in this process is played by antioxidant components such as cinnamic acid, eugenol, and cinnamaldehyde, which participate in redox reactions and stabilize the surface of CuNPs (Kothari, 2023; Liu, 2021c).

Seeds of star anise (*Illicium verum*) are rich in anethole and D-limonene – compounds with pronounced antioxidant properties that promote reduction processes. Extracts of nutmeg seeds and mace (*Myristica fragrans*) contain myristic acid, methyleugenol, and other phenolic compounds involved in the reduction and stabilization of nanoparticles (Vijayakumar et al., 2021). Due to the high content of essential oils, as well as mono- and sesquiterpenes, aqueous extracts of caraway seeds (*Carum carvi*) are also used for the biosynthesis of CuONPs (Oraibi et al., 2023).

Table 8

Biosynthesis of copper nanoparticles using spices and herbs

Spices and herbs	Nanoparticles biosynthesis parameters	Characteristics of nanoparticles	Reference
Allium sativum (garlic)	Aqueous extract, 10 mM $CuSO_4 \times 5H_2O$, 18–20 °C, 24 h	CuNPs	Amatya et al., 2020
Carum carvi (caraway)	Aqueous extract seeds, 1 mM $Cu(NO_3)_2 \times 2H_2O$, 45 °C, 12 h	CuNPs, spherical, ~12.4 nm	Oraibi et al., 2023
Cinnamomum zeylanicum (cinnamon)	Aqueous extract of bark, 3 mM $CuSO_4$, 18–20 °C, 24 h	CuNPs, oval-shaped / spherical, mean size ~66.16 nm	Kothari, 2023
Cinnamomum zeylanicum (cinnamon)	Aqueous extract of leaves, 0.3 M $Cu(NO_3)_2 \times 2H_2O$, 65 °C, 24 h	CuONPs, spherical, 19.55–69.70 nm	Liu et al., 2021c
Illicium verum (star anise)	Aqueous extract seeds, 0.5 M $CuSO_4$, 37 °C, 24 h	CuONPs, spherical, 210–270 nm	Vijayakumar et al., 2021
Myristica fragrans (nutmeg)	Aqueous extract seeds, 0.5 M $CuSO_4$, 37 °C, 24 h	CuONPs, spherical, 170–210 nm	Vijayakumar et al., 2021
Myristica fragrans (nutmeg)	Aqueous extract of seed shell, 0.5 M $CuSO_4$, 37 °C, 24 h	CuONPs, spherical, 150–220 nm	Vijayakumar et al., 2021
Piper longum (long pepper)	Aqueous and ethanol extracts of fruit, 0.1 M $CuSO_4 \times 5H_2O$, 35 °C, 24 h	CuNPs, spherical, 35–320 nm	Mahal et al., 2024
Piper retrofractum (Jawan pepper)	Aqueous extract of fruits, 0.1 M $CuSO_4$, 80 °C, pH 8, 1 h	CuNPs, spherical, 2–10 nm	Amaliyah et al., 2020
Zingiber officinale (ginger)	Aqueous extract of root, $CuSO_4$, 90 °C, 12 h	CuNPs, spherical, 60 nm	Abbas et al., 2022
Zingiber officinale (ginger)	Aqueous extract of root, 1 mM $CuSO_4$, L-ascorbic acid, microwaves (700 W), 17 min	CuNPs, spherical and oval-shaped, 11.32–33.70 nm, zeta potential –24.4 mV	Jahan et al., 2020

Extracts of the fruits of *Piper retrofractum* and *Piper longum* contain flavonoids, tannins, steroids, and alkaloids, including piperidine derivatives. These compounds ensure both the reduction of metal ions and the stabilization of the resulting CuNPs (Amaliyah et al., 2020; Mahal et al., 2024).

Mechanisms of copper nanoparticle biosynthesis using spices and herbs

Phytochemical compounds present in spices and herbs play a key role in the biosynthesis of CuNPs and CuONPs. These include a wide range of compounds such as flavonoids, polyphenols, tannins, alkaloids, terpenoids, and saponins. During nanoparticle biosynthesis, they perform a dual function, acting both as reducing agents and stabilizers (Mahal et al., 2024; Kothari, 2023). As bioreducing agents, polyphenols, flavonoids, and ascorbic acid present in ginger are capable of donating electrons or hydrogen atoms, thereby enabling the conversion of copper ions into metallic copper or its oxide forms (Abbas et al., 2022). At the same time, the oxidized forms of these compounds, as well as alkaloids and amides, adsorb onto the surface of nanoparticles, forming a protective layer that prevents their aggregation and uncontrolled oxidation under the influence of atmospheric oxygen (Amatya et al., 2020).

The mechanism of nanoparticle formation has been described for extracts of jawan pepper and nutmeg. At the initial stage, complex formation occurs, during which phytochemical components of the extract interact with copper ions, forming intermediate coordination complexes. The next stage is reduction, which is often accompanied by tautomeric transformations of flavonoids: the transition from the enol to the keto form is associated with the release of hydrogen atoms that participate in the reduction of Cu^{2+} to Cu^0. This stage is typically accompanied by a characteristic color change of the reaction medium from blue to green, brown, or black, serving as a visual indicator of nanoparticle formation. Following reduction, nucleation and growth of nanoparticles occur. Stabilization of the nanoparticle surface is achieved through the adsorption of biomolecules containing functional groups such as carbonyl, phenolic, and amide groups (Amaliyah et al., 2020; Vijayakumar et al., 2021).

Food products and food wastes for the biosynthesis of copper nanoparticles

Analysis of the literature indicates usage of various categories of food products and food waste for the biosynthesis of CuNPs and CuONPs (Table 9).

Table 9

Biosynthesis of copper nanoparticles using food products and food wastes

Food products or food wastes	Nanoparticles biosynthesis parameters	Characteristics of nanoparticles	Reference
Actinidia deliciosa (kiwi)	Aqueous extract of fruit peel, 0.1 M $Cu(CH_3COO)_2$, 18–20 °C, ultrasound, 24–48 h	CuONPs, spherical / cubical, 51–62 nm	Ahmed et al., 2025
Allium sativum (garlic)	Aqueous extract of husk, 0.1 M $CuSO_4$, 60 °C, pH 9, 2 h	CuNPs, ellipsoid / spherical, 14 nm, zeta potential –19.3 mV	Senthilkumar et al., 2024
Ananas comosus (pineapple)	Aqueous extract of fruit peel, 20 mM $CuSO_4 \times 5H_2O$, PEG 6000, 80 °C, pH 11, 1 h	CuNPs, spherical, 53–70 nm	Ali et al., 2020
Ananas comosus (pineapple)	Aqueous extract of fruit peel, 25 mM $CuSO_4 \times 5H_2O$, 60 °C, 2 h	CuNPs, spherical, 100–730 nm (mean size 290.5 nm), zeta potential –12.3 mV	Mitra et al., 2024
Citrus limon (lemon)	Aqueous extract of fruit, $CuSO_4$, 18–20 °C, 4 h	CuNPs, spherical, 20–30 nm	Amer et al., 2021
Citrus sinensis (orange)	Aqueous extract of fruit peel, 0.5 M $Cu(NO_3)_2$, 90 °C, pH 12, 10 h	CuONPs, spherical, 14.32–40.77 nm	Albrahim et al., 2025
Citrus sinensis (orange)	Fruit juice, 1 mM $CuSO_4$, 80 °C, microwaves 700 W, 15 min	CuNPs, spherical, 7–21 nm, zeta potential –25.6 mV	Jahan et al., 2021
Juglans regia (walnut)	Aqueous extract of green husk, 1 mM $Cu(CH_3COO)_2$, 18–20 °C, 24 h	CuNPs, spherical, mean size 28 nm	Ahmadi et al., 2023
Malpighia glabra (Barbados cherry)	Fruit juice, 21.9 mM $Cu(CH_3COO)_2$, starch, 40 °C, ultrasound, 2 h	CuNPs, spherical, 22.5 nm, zeta potential –11.8 mV	Nguyen et al., 2024
Mangifera indica (mango)	Aqueous extract of seed kernel, 150 mM $CuSO_4$, 60 °C, 400 rpm, 2 h	CuONPs, spherical or irregular shape, mean size 211 nm, zeta potential –14 mV	Pramanik et al., 2025
Persea americana (avocado)	Aqueous extract of seed kernel, 1 M $CuSO_4$, 25 °C, 2 h	CuNPs, spherical, mean size 21.289 nm	Ibrahim et al., 2023
Salvadora persica (toothbrush tree)	Fruit extract, 10 mM $CuSO_4$, 70 °C, 15 h	CuNPs, spherical, 90–139 nm, zeta potential –25.2 mV	Elhabal et al., 2022

Among these, a distinct group is represented by fruits, from which fruit juice is obtained for CuNPs biosynthesis. All insoluble residues are removed from the juice by centrifugation followed by filtration. For example, orange juice facilitated the rapid synthesis of CuNPs under microwave irradiation (700 W) for 15 minutes (Jahan et al., 2021). The juice of Barbados cherry (*Malpighia glabra*) contains a high amount of ascorbic acid, which ensures efficient reduction of copper ions (Nguyen et al., 2024). Fruit extracts are also utilized. To obtain an extract of *Salvadora persica*, the fruits are crushed and then mixed with an ethanol-water solution (50/50 v/v). After centrifugation, the supernatant is evaporated under vacuum, and for CuNPs biosynthesis, the resulting dry residue is dissolved in water (Elhabal et al., 2022). An aqueous fruit extract of *Citrus limon* provided the synthesis of CuNPs (Amer et al., 2021).

The second group includes food waste, such as mango seed kernels (Pramanik et al., 2025) and avocado seeds (Ibrahim et al., 2023), as well as fruit peels (Mitra et al., 2024) and other secondary plant materials (Ahmadi et al., 2023), the use of which aligns with the principles of the circular economy and green chemistry.

Mechanisms of copper nanoparticle biosynthesis using food products and food waste

The key stage of the process is the bioreduction of copper ions (Cu^{2+}) to atomic copper (Cu^0) under the action of phytochemical compounds present in the extracts. Sources of electrons include polyphenols, flavonoids, tannins, vitamins, and reducing sugars found in extracts of food products and food waste. An important role in this process is played by functional groups of biomolecules – carbonyl, hydroxyl, amino, and methoxy groups – which are capable of binding copper ions through electrostatic interactions and facilitating their reduction (Elhabal et al., 2022).

Flavonoids can undergo transformation from the enol to the keto form, releasing a reactive hydrogen atom that enables the reduction of Cu^{2+} to Cu^0 (Mitra et al., 2024). Ascorbic acid, in turn, is oxidized to ascorbate radicals, which actively interact with copper ions, promoting nanoparticle formation while simultaneously preventing their undesired oxidation, which is critically important for the stability of CuNPs (Nguyen et al., 2024).

Nanoparticle formation proceeds through a sequence of physicochemical stages. During nucleation, primary crystallization centers are formed. The subsequent stage involves particle growth and aggregation, during which their final size and morphology are established. In the case of CuONPs biosynthesis, after the reduction stage, atomic copper may undergo further oxidation to form copper oxide, often induced by thermal treatment, particularly calcination, or by specifically controlled reaction conditions (Albrahim et al., 2025).

The final stage is stabilization and the formation of a surface coating on the nanoparticles. Biomolecules such as proteins, lignins, and saponins adsorb onto the surface of the formed nanoparticles, creating a protective layer. This results in electrostatic repulsion between CuNPs, preventing their aggregation and ensuring high colloidal stability of the system (Pramanik et al., 2025).

Bacteria for the biosynthesis of copper nanoparticles

Thermophiles

Non-pathogenic strain of the thermophilic bacteria *Bacillus anthracis* PFAB2 was isolated from the Panifala hot spring (India). For the biosynthesis of CuONPs, cell wall polysaccharides are used, which are characterized by high thermal stability and have a degradation temperature of about 283.10 °C. These polysaccharides are rich in carboxyl and phosphate functional groups. The presence of these groups gives the polysaccharides a negative charge, creating favorable conditions for effective electrostatic interaction with positively charged copper ions (Banerjee et al., 2024). A strain of *Anoxybacillus rupiensis* BS1 was isolated from the Pasinler hot spring

(Erzurum, Turkey). These bacteria are capable of forming endospores and synthesizing lignin peroxidase, which is active at 60 °C. The biosynthesis of CuNPs involving this enzyme has been studied (Sus et al., 2024).

Psychrophiles

Bacterial consortia including representatives of psychrophilic microorganisms were isolated from Antarctic marine ecosystems. Such microbial communities include representatives of the genera *Marinomonas*, *Rhodococcus*, *Pseudomonas*, *Brevundimonas*, and *Bacillus*. These bacteria can be applied for the biosynthesis of nanoparticles at relatively low temperatures, which opens up prospects for the development of energy-efficient biotechnological processes for the production of CuNPs (John et al., 2021). A psychrotolerant strain *Stenotrophomonas* sp. BS95 was isolated from alpine soil in Iran. For the biosynthesis of CuONPs, the supernatant of cell lysate is used, which contains a large number of enzymes and proteins (Talebian et al., 2023).

Marine bacteria

The use of marine bacteria for the biosynthesis of copper nanoparticles is possible due to the unique adaptive properties of these microorganisms. Marine bacteria have evolved under conditions of high salinity, elevated hydrostatic pressure, limited nutrient availability, and often low temperatures. Such extreme conditions have led to the development of specific metabolic pathways and biomolecules that can effectively participate in the reduction of metal ions and the stabilization of nanoparticles. The bacterium *Pseudomonas aeruginosa* MO1 was isolated directly from seawater. These bacteria are characterized by high metabolic flexibility and the ability to synthesize various secondary metabolites and biopolymers that function as natural reducing agents and stabilizers during nanoparticle formation. With the involvement of such biomolecules, copper ions can be reduced to copper oxide under neutral pH conditions, and the resulting nanoparticles exhibit antimicrobial activity (Tejaswi et al., 2025). *Stenotrophomonas rhizophila* BGNAK1 was isolated from coastal marine sediments of the western coast of India. This species is adapted to marine soil conditions and is characterized by increased resistance to pollutants and heavy metals. The BGNAK1 strain synthesizes various biomolecules, including phenolic compounds and other metabolites, which are involved in the reduction of copper ions and the stabilization of the formed nanoparticles (Karthikeyan et al., 2024).

The actinobacterial strain *Streptomyces* sp. MHM38 was isolated from marine sediments of the Gulf of Suez. These Gram-positive bacteria are known for their high metabolic activity and ability to synthesize a wide range of extracellular enzymes and proteins that can act as reducing and stabilizing agents during nanoparticle formation. In particular, proteins with molecular weight of approximately 10–80 kDa contribute to the formation of stable nanostructures (Bukhari et al., 2021). *Enterococcus thailandicus* E12 was isolated from seawater samples of the Gulf of Suez (Red Sea, Egypt). These bacteria are characterized by an enhanced ability to synthesize nitrate reductase, which plays a key role in the bioreduction of metal ions. This enzyme acts as the main catalyst for the reduction of Cu^{2+} ions to their elemental form, leading to the intracellular formation of nanoparticles (Zaki et al., 2021).

Endophytes

Endophytic bacteria colonize the internal tissues of plants without causing harm and exist in close metabolic interaction with their host plants. During this interaction, endophytic bacteria produce a wide range of secondary metabolites that can act as natural reducing agents and stabilizers in the biosynthesis of nanoparticles. Due to this, endophytic bacteria are capable of effectively catalyzing the reduction of copper ions and ensuring the stabilization of the formed

nanostructures. For example, *Brevibacillus brevis* PI-5 was isolated from the leaves of the medicinal plant *Pulicaria incisa*, which grows in arid regions of the Sinai Peninsula. The PI-5 strain is used for the synthesis of spherical, well-dispersed CuONPs with sizes ranging from 2 to 28 nm (Fouda et al., 2022).

The strain *Bacillus licheniformis* CPJN13S was identified as a plant growth-promoting endophyte. The biosynthesis of CuNPs in a cell-free system using the supernatant of the CPJN13S strain has been studied (Rani et al., 2025a).

Endophytic bacteria *Pantoea agglomerans* CPHN2 belong to the group of plant growth-promoting bacteria. The CPHN2 strain was isolated from the roots and nodules of leguminous plants. When these bacteria were used, hexagonal CuNPs or CuONPs with sizes of 5–35 nm are formed. The nanoparticles biosynthesized using these bacteria exhibit antimicrobial activity and are more effective against *Staphylococcus aureus* and *Bacillus subtilis* compared to nanoparticles obtained using traditional chemical methods (Rani et al., 2025b).

Bacteria from polluted ecosystems

The strain *Serratia* sp. ZTB29 was isolated from zinc-lead ore enrichment sites (India). These bacteria demonstrate resistance to copper ions (up to 22.5 mM) and can be used for the biosynthesis of CuONPs with their subsequent application as nanofertilizers (Singh et al., 2023). *Ralstonia* sp. KF264453 bacterial strain was isolated from soils near a copper deposit (Iran). With the involvement of extracellular metabolites of *Ralstonia* sp. KF264453, the bioreduction of Cu^{2+} ions to metallic copper (Cu^0) occurs, forming nanoparticles with an average size of about 70 nm (Vakili et al., 2025).

Microorganisms inhabiting industrial and municipal wastewater are typically adapted to elevated concentrations of toxic compounds, including heavy metal ions. As a result of this adaptation, they possess well-developed detoxification mechanisms, including metal-binding proteins, transport systems, and reductase enzymes capable of reducing metal ions to their elemental form. *Escherichia* sp. SINT7 bacterial strain was isolated from wastewater (Pakistan). With their involvement, CuNPs were biosynthesized that exhibit photocatalytic activity and can be used for the degradation of organic dyes (Noman et al., 2020a). *Bacillus flexus* FB-1 bacterial strain was isolated from textile industry wastewater in Faisalabad (Pakistan). The biosynthesis of CuNPs using the culture supernatant of the FB-1 strain and their potential application for wastewater treatment have been investigated (Batool et al., 2024).

Proteus mirabilis AB 932526.1 was isolated from activated sludge of wastewater treatment plants. For the biosynthesis of CuNPs, a bioflocculant produced by *Proteus mirabilis* AB 932526.1 is used, which performs a dual function during synthesis: acting both as a reducing agent and as a stabilizer for the formed nanoparticles. The use of biogenic CuNPs for water purification from dyes and excess nutrients has been studied (Nkosi et al., 2025).

Bacillus cereus FM1 and *Bacillus thuringiensis* FM2, isolated from electronic waste landfills (Iran), are characterized by a high level of metal resistance. The FM1 strain tolerates high concentrations of copper ions (MIC = 333 mM when using copper sulfate). Both strains are capable of biosorbing copper ions up to 79.8%. Such properties make these bacteria particularly promising for applications under conditions of high anthropogenic load (Moeini et al., 2024).

Bacteria capable of being used for the biosynthesis of copper oxide nanoparticles were isolated from formation water of the Al-Halfaya oil fields (Iraq). In the course of the study, nine bacterial strains were isolated, including *Klebsiella quasipneumoniae* KP18-31, *Klebsiella pneumoniae* IOB-L, *Klebsiella quasipneumoniae* subsp. *similipneumoniae* 2437, *Bacillus cereus* DBA1, *Bacillus thuringiensis* MSP51 (later identified as a new strain AMHWRB3), *Neobacillus drentensis* ROA042, *Enterococcus faecalis* 2674, *Exiguobacterium mexicanum* AB201, and *Acinetobacter lwoffii* K34. Among the studied microorganisms, the most effective was *Bacillus*

thuringiensis AMHWRB3. Notably, this study represents one of the first examples of using bacteria isolated from oil reservoirs for the biosynthesis of CuONPs (Alshami et al., 2023).

Other polluted environments, including soils near metallurgical enterprises or agricultural lands irrigated with wastewater, are also sources of metal-resistant bacteria. *Klebsiella pneumoniae* NST2 was isolated from the rhizosphere of maize grown on lands irrigated with textile wastewater (Noman et al., 2021). The strain *Klebsiella pneumoniae* SN35 was isolated from agricultural lands polluted with wastewater. Using these bacteria, CuNPs were obtained that can reduce the toxic effects of heavy metals on plants, particularly by increasing wheat resistance to chromium stress (Noman et al., 2020b). *Pseudomonas fluorescens* MAL2 bacterial strain was isolated from soils polluted with heavy metals near metallurgical plants in Egypt. Unlike chemically synthesized analogues, CuNPs biosynthesized using the MAL2 strain demonstrated significant toxicity to the insect *Tribolium castaneum* (a pest of grain and grain products) even at low concentrations (El-Saadony et al., 2020).

Particular attention has been paid to the use of lactic acid bacteria as biologically safe microorganisms with the "Generally Recognized as Safe" (GRAS) status assigned by the U.S. Food and Drug Administration (FDA) (Stabnikova et al., 2023) for the synthesis of metal nanoparticles (Gregirchak et al., 2023; Stabnikov et al., 2025). It has been shown that the probiotic bacterium *Lactobacillus casei* subsp. *casei* can synthesize CuONPs exhibiting high antimicrobial activity and cytotoxic effects against cancer cell lines (Kouhkan et al., 2020).

Mechanisms of copper nanoparticle biosynthesis using bacteria

In bacterial-mediated biosynthesis of CuNPs, both intracellular and extracellular synthesis mechanisms can occur. For this purpose, liquid culture, supernatant, cell-free extracts, specific bacterial metabolites, and other bacterial-derived products may be utilized (Figure 2).

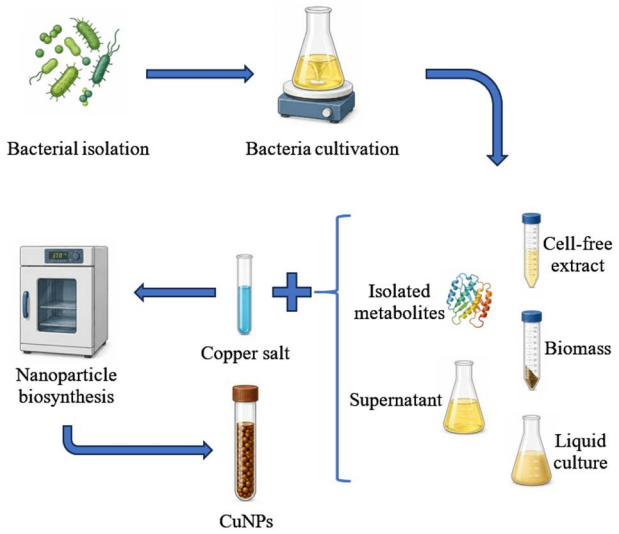

Figure 2. Biosynthesis of CuNPs using bacteria

Intracellular biosynthesis of CuNPs (Table 10) is a component of the bacterial detoxification system that ensures their survival in environments with high concentrations of heavy metals. This process involves the uptake of copper ions from the external environment, their transport into the cell, and subsequent enzymatic reduction to elemental or oxide forms directly within cellular structures.

Table 10

Biosynthesis of copper nanoparticles using liquid bacterial culture

Bacteria	Nanoparticles biosynthesis parameters	Characteristics of nanoparticles	Reference
Desulfamplus magnetovallimortis BW-1	13.9 μM $CuSO_4$ × $5H_2O$, 28 °C, 20 h	CuSNPs, spherical, 69 nm	Park et al., 2022
Enterococcus thailandicus (E12)	5 mM $Cu(NO_3)_2$ × $3H_2O$, 30 °C, 120 h	CuNPs, spherical, 8–18 nm	Zaki et al., 2021
Klebsiella pneumoniae NST2	5 mM $CuSO_4$, 28 °C, 150 rpm, pH 7, 48 h	CuNPs, spherical, 22.44–44.26 nm	Noman et al., 2021
Klebsiella pneumoniae SN35	5 mM $CuSO_4$, 30 °C, 150 rpm, 24 h	CuNPs, spherical, 19.01–47.47 nm	Noman et al., 2020b
Lactobacillus casei subsp. *casei* ATCC 39392	1 mM $CuSO_4$, 37 °C, pH 6.0, 200 rpm, 48 h	CuONPs, spherical, average size 200 nm	Kouhkan et al., 2020
Priestia megaterium AMD 2024	1 мМ $CuSO_4$ × $5H_2O$, 30 °C, 150 rpm, 48 h	CuNPs, 57.73 nm, zeta potential –20.1 mV	Mohamed et al., 2024
Pseudomonas putida	1 mM $CuSO_4$, 30 °C, 150 rpm, 24 h	CuNPs, semispherical, 18.6–43.9 nm, zeta potential –23.4 mV	El-Sayed et al., 2025
Serratia sp. ZTB29	5 mM $CuSO_4$ × $5H_2O$, 28 °C, 150 rpm, 48 h	CuONPs, spherical 20–40 nm, zeta potential –15.4 mV	Singh et al., 2023

The first stage of intracellular biosynthesis is the interaction of Cu^{2+} ions with components of the cell envelope. Positively charged copper ions electrostatically bind to negatively charged groups of the cell wall or are transported into the cell via specialized transport systems (Kashyap et al., 2023).

A key role in the bioreduction process is played by intracellular enzymes. In particular, NADH-dependent reductases facilitate the transfer of electrons from the cofactor NADH to metal ions. As a result, copper ions are reduced to the zero-valent state, followed by a nucleation stage and subsequent nanoparticle formation. The membrane-bound enzyme NADH dehydrogenase-2 can catalyze the reduction of Cu(II) to Cu(I) under aerobic conditions. After reduction, copper atoms begin to aggregate, forming primary nanoclusters. Further growth of nanoparticles occurs through nucleation and coalescence of metal atoms, and their size and morphology largely depend on intracellular conditions such as pH, temperature, and metal ion concentration (Aziz et al., 2024).

Hypothetical models of intracellular nanoparticle formation are based on natural detoxification mechanisms that allow bacteria to survive in environments with high metal concentrations by converting toxic ions into inert nanostructures. In the cytoplasmic reduction model, characteristic of *Enterococcus thailandicus*, copper ions are reduced by nitrate reductase enzymes localized on the periplasmic or cytoplasmic bacterial membrane. This is followed by the nucleation stage and the formation of CuNPs, which typically aggregate in the central part of the cell and are stabilized by cytoplasmic proteins, preventing their uncontrolled release outside the cell (Zaki et al., 2021).

In the periplasmic space, a biomineralization model is realized, which was described in detail for magnetotactic sulfate-reducing bacteria *Desulfamplus magnetovallimortis* BW-1. In this case, copper ions accumulate in the periplasm and interact with sulfide ions (S^{2-}) formed as a result of sulfate reduction. This leads to the formation of CuSNPs. The process occurs under the control of specific proteins, including DegP-like proteins that regulate nucleation and nanoparticle formation (Park et al., 2022).

In the case of intracellular biosynthesis, nanoparticles are localized inside the cell. Therefore, their extraction requires a cell disruption step, for example, using ultrasonic treatment, mechanical disruption, or detergents (Karthikeyan et al., 2024).

The biosynthesis of CuNPs and CuONPs in cell-free systems was studied, particularly using liquid culture supernatants (Table 11).

Table 11

Biosynthesis of copper nanoparticles using cell-free supernatant

Bacteria	Nanoparticles biosynthesis parameters	Characteristics of nanoparticles	Reference
Bacillus licheniformis CPJN13S	5 mM $CuSO_4$, 37 °C, pH 7, 18 h	CuNPs, hexagonal, mean size 12.4 nm, zeta potential –24.7 mV, PDI 0.386	Rani et al., 2025a
Bacillus subtilis MTCC 441	3 mM $CuCl_2$, 18–20 °C, pH 8, 12 h	CuONPs, spherical, 11.47 nm, zeta potential –26.9 mV, PDI 0.43	Kataria et al., 2025
Lactobacillus sp.	1 mM $CuSO_4$, pH 7, 35 min	CuNPs / CuONPs, spherical, 40–110 nm	Hamood et al., 2025
Niallia circulans G9	100 mM $CuSO_4$, 37 °C, pH 7, 120 rpm, 24 h	CuONPs, spherical / hexagonal, 13–100 nm	Aziz et al., 2024
Paenibacillus sp. S4c	100 mM $CuSO_4$, 45°C, pH 7, 120 rpm, 48 h	CuONPs, spherical, 5–40 nm	Aziz et al., 2024
Pantoea agglomerans CPHN2	5 mM $CuSO_4$, 23°C, 6 h	CuNPs / CuONPs, hexagonal 5–35 nm, zeta potential –21 mV	Rani et al., 2025b
Proteus mirabilis	$Cu(CH_3COO)_2 \times H_2O$ (20 g in 200 mL), 37 °C, 24 h	CuONPs, spherical / hexagonal, 13–19 nm	Faiq et al., 2024
Pseudomonas aeruginosa	1 mM $CuSO_4$	CuNPs, spherical, 56.40 nm	Hamady et al., 2024
Pseudomonas aeruginosa MO1	1 mM $CuSO_4$, 18–20 °C, pH 7, 24 h	CuONPs, cubical, 108–252 nm, zeta potential –23 mV	Tejaswi et al., 2025
Ralstonia sp. KF264453	3 mM $Cu(NO_3)_2 \times 3H_2O$, 18–20 °C, 150 rpm, 24 h	CuNPs, spherical, mean size 69.7 nm, zeta potential –5.1 mV, PDI 0.38	Vakili et al., 2025
Staphylococcus haemolyticus	1 mM $Cu(CH_3COO)_2$, 30–35 °C, 72 h	CuONPs, spherical, mean diameter 35 nm	Romi et al., 2024
Stenotrophomonas maltophilia SCS1.1	4 mM $CuSO_4$, 30 °C, pH 8, 48 h	CuONPs, spherical, rectangular, 18.4–31.7 nm	Kashyap et al., 2023
Streptomyces sp. S29	5 mM $CuSO_4$, 28–30 °C, pH 8, 48 h	CuNPs, spherical, square, hexagonal, 25–35 nm, zeta potential –33.7 mV, PDI 0.1–0.546	Elshaer et al., 2023
Streptomyces sp. MHM38	5 mM $CuSO_4$, 30–32 °C, pH 8, 1 h	CuONPs, spherical 1.72–13.49 nm	Bukhari et al., 2021
Streptomyces rochei	1 mM $CuSO_4$, 28 °C	CuONPs, spherical, mean size 10.7 nm, zeta potential –1.3 mV	El-Sherbiny et al., 2022
Xenorhabdus sp. NP2	5 mM $CuSO_4$, 30 °C, 150 rpm, 24 h	CuNPs, spherical 5–20 nm, PDI 0.312	Bharathi et al., 2022

In this case, the main role in nanoparticle biosynthesis is played by cellular metabolites, enzymes, and other biomolecules secreted by bacteria during cultivation. These compounds can simultaneously act as both reducing agents and stabilizers during nanoparticle formation. The extracellular biosynthesis process typically proceeds in several sequential phases. At the initial stage, which can be referred to as the activation or reduction phase, Cu^{2+} ions are reduced to atomic copper (Cu^0). This is followed by the growth phase, during which individual copper atoms combine into small clusters or nuclei. At the final stage, bioactive molecules adsorb onto the surface of the formed nanoparticles, limiting their further growth and preventing aggregation (El-Sherbiny et al., 2025).

In cell-free systems, the reduction of copper ions is provided by various compounds. One of the key mechanisms is the enzymatic reduction of copper ions involving extracellular reductases, which initiate the reduction process (Elshaer et al., 2023). When thermophilic bacteria *Anoxybacillus rupiensis* BS1 are used for the biosynthesis of CuNPs, lignin peroxidase can act as a reducing agent; this enzyme belongs to the class of oxidoreductases and is also capable of catalyzing electron transfer reactions (Sus et al., 2024).

In addition to enzymes, various bacterial metabolites present in cell-free systems (Table 12) play a significant role in the reduction of copper ions. Proteins and amino acids, due to the presence of amino, hydroxyl, and carboxyl groups, are capable of donating electrons, thereby promoting the formation of elemental copper (Rani et al., 2025b). Moreover, secondary metabolites such as polysaccharides, alcohols, and phenolic compounds actively participate in the nucleation and formation of nanostructures (Hamood et al., 2025).

Table 12

Cell-free biosynthesis of copper nanoparticles using bacterial metabolites

Bacteria	Nanoparticles biosynthesis parameters	Characteristics of nanoparticles	Reference
Anoxybacillus rupiensis BS1	Bacterial lignin peroxidase, 100 mM $CuCl_2$, 60 °C, 350 rpm, pH 8, 4 h	CuNPs, spherical and cubical	Sus et al., 2024
Bacillus anthracis PFAB2	Cell wall polysaccharides, 1 mM $CuSO_4$, 45 °C, 12 h	CuONPs, spherical, mean size 702 nm, zeta potential –3.84 mV, PDI 0.437	Banerjee et al., 2024
Brevibacillus brevis PI-5	Aqueous cell-free extract, 5 mM $Cu(CH_3COO)_2 \times H_2O$, 100 rpm, pH 8, 1 h	CuONPs, spherical 2–28 nm	Fouda et al., 2022
Proteus mirabilis AB 932526.1	Purified carbohydrate bioflocculant, 3 mM $CuSO_4$, 18–20 °C, 24 h	CuNPs, spherical, mean size 20 nm	Nkosi et al., 2025
Spirulina platensis	Supernatant of cell lysate, 5 mM $Cu_2(CH_3COO)_4$, 100 °C, 1 h	CuONPs, spherical, 3.75–12.4 нм, zeta potential –21.63 mV	Doman et al., 2024
Stenotrophomonas sp. BS95	Supernatant of cell lysate, 10 mM $CuSO_4 \times 5\ H_2O$, 121°C, pH 7.0, 20 min	CuONPs, spherical, mean size 35.24 nm, zeta potential –28.57 mV, PDI 0.26	Talebian et al., 2023

After the reduction stage, nanoparticle stabilization occurs, which is ensured by biomolecules present in the reaction medium. These compounds adsorb onto the surface of newly formed CuNPs, acting as so-called capping agents. Protein and carbonyl groups form a protective layer that creates a negative zeta potential and, consequently, electrostatic repulsion between particles, preventing their aggregation and ensuring the colloidal stability of the system (Alshami et al., 2023; Kataria et al., 2025).

Fungi for the biosynthesis of copper nanoparticles

Fungi from soil and plants

Soil is one of the most common sources for the isolation of micromycetes that can be used for the biosynthesis of copper nanoparticles (Table 13). *Aspergillus versicolor* EM-CN2 was isolated from agricultural land samples in Sharkia Governorate, Egypt (Ammar et al., 2019). The strain *Aspergillus terreus* AH20 was isolated from soil samples collected in the garden of the Faculty of Science, Al-Azhar University (Egypt) (El-Naggar et al., 2022). Of particular interest is rhizospheric soil – the zone of direct interaction between plant root systems and microorganisms. Recently, the biosynthesis of multimetallic Se-BiO-CuO nanoparticles (selenium - bismuth oxide - copper oxide) using a cell-free aqueous extract of the fungus *Talaromyces haitouensis*, isolated from the rhizosphere, was reported for the first time (Rasheed et al., 2024).

Table 13

Biosynthesis of copper nanoparticles using micromycetes

Fungi	Nanoparticles biosynthesis parameters	Characteristics of nanoparticles	Reference
Biomass			
Shizophyllum commune KF954705	1 mM $CuCl_2 \times 2\ H_2O$	CuNPs, spherical, 40–65 nm	Fatima et al., 2022
Trichoderma harzianum	2 mM $CuSO_4$, 25 °C, 180 rpm, 36 h	CuSNPs, spherical, rod-like, 40–90 nm	Abishad et al., 2022
Cell-free aqueous extract			
Aspergillus flavus	100 mM $CuSO_4 \times 5\ H_2O$, 1% ascorbic acid, heating, stirring, 12 min	CuNPs, spherical, 5–12 nm, zeta potential –26.4 mV	Shende et al., 2021
Aspergillus niger SBA3	15 mM $CuSO_4$, 37 °C, 24 h	CuNPs, spherical, 260 nm, zeta potential +18.8 mV	Noor et al., 2025
Aspergillus terreus BR.1	5 mM $Cu(CH_3COO)_2 \times H_2O$, 100 rpm, pH 8, 1 h	CuONPs, spherical, 15–55 nm, zeta potential –26.6 mV, PDI 0.362	Nassar et al., 2023
Aspergillus versicolor EM-CN2	3 mM $CuSO_4 \times 5\ H_2O$, 30 °C, 72–96 h	CuNPs, round, polygonal, 23–82 nm, zeta potential –10.2 mV, PDI 0.447	Ammar et al., 2019
Phoma glomerata MTCC-2210	100 mM $CuSO_4 \times 5\ H_2O$	CuONPs, spherical, mean size 119 nm, zeta potential –23.5 mV	Ingle et al., 2024
Trichoderma sp.	$CuSO_4 \times 5\ H_2O$, 24–25 °C, 24 h	CuONPs, quasi-spherical, 1.3–30 nm, zeta potential –32.6 mV	Garcia-Marin et al., 2022
Fungal biomass filtrate			
Aspergillus carbonarius	150 mM $CuCl_2$, 18–20 °C, 24 h	CuNPs, cubical, pyramidal, prismatic, 15–84.29 nm	Al-Qaissi et al., 2024
Aspergillus fumigatus SM4	5 mM $Cu(CH_3COO)_2 \times H_2O$, 100 rpm, pH 8, 1 h	CuONPs, spherical, 20–150 nm	Hassan et al., 2025
Aspergillus niger AH1	1 mM $Cu(CH_3COO)_2$, 1 mM Na_2SeO_3, 30 °C, 150 rpm, 24 h	CuSeNPs (bimetallic), spherical, mean size 15 nm, zeta potential –31 mV, PDI 0.18	Attia et al., 2025

Aspergillus niger KY 401431	10 mM $CuSO_4$, 80 °C, 4 h	CuNPs / CuONPs, spherical, 4–10 nm, PDI 0.403	Abd El Rahman et al., 2025
Aspergillus niger	5 mM $Cu(NO_3)_2$, 30 °C, 150 rpm, 96 h	CuNPs, spherical, oval, 3–70 nm	Suood et al., 2021
Aspergillus sydowii FCSRL3	0.1 mM $CuSO_4$, 27 °C, 96–168 h	CuONPs, spherical, mean size 86 nm	Radhakrishnan et al., 2025
Aspergillus terreus AH20	2 mM$Cu(CH_3COO)_2$, 30 °C, 150 rpm, 24 h	CuNPs / CuONPs, spherical, mean size 20 nm, zeta potential –33.7 mV	El-Naggar et al., 2022
Aspergillus terreus	10 mM $CuSO_4$, 30 °C, 180 rpm, pH 6, 48 год	CuONPs, spherical, mean size 15.75 nm	Mousa et al., 2020
Chaetomium globosum	1 mM $CuSO_4$, 96–168 h	CuNPs, spherical, 10–120 nm	Dorjee et al., 2024
Fusarium solani KJ 623702	1 mM $CuSO_4$, 28 °C, 120 rpm, pH 5, 24 h	CuNPs, spherical, 9.97–19.49 nm, zeta potential –34.8 mV	El Sayed et al., 2019
Neurospora crassa	20 mM $CuCl_2$, 25 °C, 60 rpm, pH 7.5, 12 h	CuNPs, spherical, 20–40 nm	Liu et al., 2021a
Penicillium chrysogenum ATCC 48271	2 mM $Cu(CH_3COO)_2 \times 2$ H_2O, 65 °C, 200 rpm, 4 h	CuONPs, spherical (4–15 nm), rod-like (11–53.8 nm)	Shehabeldine et al., 2023
Penicillium pimiteouiense	5 mM $CuSO_4$, 18–20 °C, 6 h	CuONPs, sphrical, 50–60 nm	Zhou et al., 2024
Trichoderma virens	1 mM $CuSO_4$, 96–168 h	CuNPs, spherical, 7–90 nm	Dorjee et al., 2024

In addition to soils, plants are an important source of fungi for the biosynthesis of CuNPs, particularly endophytic fungi that colonize internal plant tissues without causing pathogenic effects. Due to their close interaction with plant metabolism, such microorganisms are capable of producing a wide range of biologically active compounds involved in the reduction of metal ions and the stabilization of nanoparticles. For example, the strain *Aspergillus terreus* BR.1 was isolated from garlic roots (*Allium sativum*) (Nassar et al., 2023). The endophytes strains *Aspergillus sydowii* FCSRL3 and *Aspergillus versicolor* FCPRS11 were isolated from the tissues of the neem tree (*Azadirachta indica*) (Radhakrishnan et al., 2025).

An additional, yet equally important, source for the isolation of micromycetes is organic waste, particularly decaying fruits and vegetables. Such substrates harbor microbial communities with high adaptive potential, capable of active metabolism and the biosynthesis of secondary metabolites. It is from similar organic residues that *Aspergillus niger* STA9 was isolated, whose cell-free filtrate can be used for the biosynthesis of CuNPs (Noor et al., 2020).

Fungi from polluted ecosystems

Polluted ecosystems are an important source for the isolation of micromycetes that can be used for the biosynthesis of CuNPs. Such fungi are adapted to adverse environmental conditions and are characterized by increased tolerance to heavy metals, the ability to bioaccumulate them, and effective participation in bioreduction processes. *Penicillium pimiteouiense* fungus was isolated from soils of the Sossego copper mine in Brazil (Zhou et al., 2024). Another important source is industrial effluents and wastes. The strain *Fusarium solani* KJ 623702 was isolated from soils that had long been irrigated with industrial wastewater (El Sayed et al., 2019). In addition, micromycetes are isolated from coal mines, municipal and industrial waste landfills, as well as sewage systems. Based on the screening of 21 micromycete representatives isolated from polluted

areas of Uzbekistan, the most promising fungi for the biosynthesis of CuNPs were selected: *Fusarium oxysporum*, *Penicillium* sp., *Trichoderma harzianum*, *Alternaria pluriseptata*, *Aspergillus terreus*, *Aspergillus versicolor*, and *Aspergillus oryzae* (Zaynitdinova et al., 2025).

Mechanisms of copper nanoparticle biosynthesis using fungi

From a biological perspective, the ability of micromycetes to synthesize CuNPs should be considered an evolutionarily developed adaptive mechanism aimed at environmental detoxification. Copper ions at high concentrations are toxic to cells. The conversion of soluble Cu^{2+} ions into insoluble zero-valent forms (Cu^0) reduces their toxicity. The activation of nanoparticle biosynthesis processes is often associated with the fungal response to stress caused by the presence of heavy metals in the cultivation medium. Under such conditions, biosorption processes are intensified, during which metal ions are adsorbed onto the cell surface. This is followed by their intracellular or extracellular transformation involving enzymatic and non-enzymatic mechanisms (Abishad et al., 2022). Fungi, particularly representatives of the genera *Aspergillus* and *Penicillium*, are characterized by high tolerance to heavy metals. This ensures their ability to survive and maintain metabolic activity under extreme conditions, including anthropogenically polluted ecosystems (Zaynitdinova et al., 2025).

A key role in the enzymatic reduction of copper ions is played by NADH- or NADPH-dependent nitrate reductases. The mechanism of action of these enzymes is based on the transfer of electrons from reduced cofactors (NADH or NADPH) to copper ions. As a result, copper ions are reduced to the zero-valent state, which is a prerequisite for the formation of metallic nanoparticles, or to oxide forms of copper as a result of subsequent redox transformations (Noor et al., 2020). NADPH plays a particularly important role in this process, often acting as the main electron donor in the extracellular environment, ensuring efficient reduction of copper ions and stabilization of intermediate forms (Zhou et al., 2024).

In addition to nitrate reductase, other fungal enzymes are also involved in the biosynthesis of CuNPs. In particular, it has been established that laccases and NADPH-dependent sulfite reductases can directly or indirectly catalyze the reduction of copper ions (Nassar et al., 2023). Oxidoreductases with broad activity spectra, secreted by fungi such as *Aspergillus* and *Fusarium*, also play an important role. These enzymes not only participate in redox transformations but also contribute to the binding, transport, and detoxification of copper ions, which is critical for microbial survival in metal-rich environments (Noor et al., 2020).

A separate mechanism is associated with the activity of the enzyme urease, particularly in fungi such as *Neurospora crassa*. Urease catalyzes the hydrolysis of urea to form ammonium and carbonate ions, leading to an increase in environmental pH. Under alkaline conditions, carbonate ions interact with copper ions, promoting the formation of copper carbonate nanoparticles. Thus, in this case, biosynthesis occurs not only through direct enzymatic reduction but also via indirect biochemical changes in the environment that initiate nucleation and nanoparticle growth (Liu et al., 2021a).

Phenolic compounds and polyphenols play a particularly important role in the reduction of copper ions, as they are among the most active reducing agents of fungal origin. Due to the presence of multiple hydroxyl groups, especially in ortho- and para-positions, these compounds can efficiently donate electrons, facilitating copper ion reduction. The high reducing potential of phenolic metabolites leads to rapid reaction rates, in some cases allowing nanoparticle synthesis to be completed within minutes. In addition, phenolic compounds exhibit strong chelating ability, promoting copper ion binding, initiating nucleation processes, and forming more ordered and stable nanostructures (Zhou et al., 2024).

Organic acids and carbohydrates also play an important role in the biosynthesis of CuNPs and CuONPs. Organic acids such as citric, oxalic, oleic, and palmitic acids can perform a dual function: they participate in the reduction of metal ions and stabilize the formed nanoparticles by

adsorbing onto their surface and forming a protective layer. Carbohydrates (glucose, fructose) can also act as mild reducing agents, participating in redox processes and promoting gradual nanoparticle formation (Nassar et al., 2023).

Other fungal secondary metabolites are also involved in CuNP biosynthesis. Alkaloids and terpenoids can act as reducing or capping agents, stabilizing the nanoparticle surface and preventing aggregation. Fungal pigments such as naphthoquinones and anthraquinones can function as electron carriers, accelerating electron transfer to copper ions and intensifying the reduction process. Vitamins, including folic acid, may also participate in redox transformations, further contributing to the formation of CuNPs or CuONPs (El Sayed et al., 2019).

Capping and stabilization processes are critical stages in the formation of functionally stable CuNPs or CuONPs. The main capping agents include secreted proteins, peptides, polysaccharides, glycoproteins, and low-molecular-weight secondary metabolites, particularly phenolic compounds and organic acids. Among proteins, special attention is given to enzymes such as triosephosphate isomerase, which may be involved not only in metabolic processes but also in nanoparticle stabilization (Liu et al., 2021b). The attachment of biomolecules to the copper surface occurs through various interactions, including coordination bonds involving amino groups, thiol groups of cysteine residues, hydroxyl groups of phenols, as well as electrostatic interactions with carboxylate groups of cell wall components (Zhou et al., 2024).

Yeast for the biosynthesis of copper nanoparticles

It is important to note that a limited number of studies on the biosynthesis of CuNPs using yeasts were reported in the scientific literature in recent years. Considering this, in order to obtain a more comprehensive overview of the current state of research in this field, the time frame for source analysis was extended back to 2014. Despite this approach, the overall number of relevant publications remained relatively limited. (Table 14). This indicates both the novelty of this research area and its significant potential for further investigation.

Table 14

Biosynthesis of copper nanoparticles using yeast

Yeast	Nanoparticles biosynthesis parameters	Characteristics of nanoparticles	Reference
Biomass (living cells)			
Filobasidium stepposum	2 mM $CuSO_4$, 8 mM $InCl_3$, 20 °C, pH 9, 14–30 days	CuInSNPs (copper-indium-sulphur), various shapes, 3.4–4.9 nm	Arriaza-Echanes et al., 2024
Komagataella phaffii X-33-Cyb5R	$CuSO_4$ (12 mM), 30 °C, pH 4, 36 h	CuNPs, spherical, 40–80 nm	Dong et al., 2025
Rhodotorula mucilaginosa	2.5 mM $CuSO_4$, 30 °C, 230 rpm, pH 7, 24 h	CuONPs, spherical, 51.6–111.4 nm, zeta potential –2.9 mV, PDI 0.43	Hassabo et al., 2022
Biomass (autoclaved)			
Rhodotorula mucilaginosa	$CuCl_2 \times 2\ H_2O$ (100 mg/L), 30 °C, pH 5, 1 h	CuNPs, spherical, mean size 10.5 nm	Salvadori et al., 2014
Yarrowia lipolytica AUMC 9256	$CuSO_4 \times 4\ H_2O$ (450 mg/L), 30 °C, 120 rpm, pH 6, 1.5 h	CuNPs, spherical, 22.34 nm	El-Sayed et al., 2018
Polysaccharides			
Pichia kudriavzevii MH545928.1	3 mM $CuSO_4$, 18–20 °C, 24 h	CuNPs, spherical, polygonal, mean size 20 nm	Tsilo et al., 2023

One of the sources for yeast isolation is marine ecosystems. Twenty yeast isolates were obtained from seawater, beach sand, and coastal areas of the Red Sea shoreline (Giftun Island, Egypt). Among them, *Rhodotorula mucilaginosa* showed the highest efficiency for the biosynthesis of CuONPs (Hassabo et al., 2022).

Psychrophilic yeasts are of particular interest. From soil samples collected in the Ellsworth Mountains near Union Glacier (Antarctica), *Filobasidium stepposum*, *Naganishia uzbekistanensis*, and *Naganishia vishniacii* were isolated. Notably, the use of *Filobasidium stepposum* biomass enabled the synthesis of complex semiconductor nanoparticles of the Cu-In-S (copper - indium - sulphur) type (Arriaza-Echanes et al., 2024).

Yeasts isolated from food and fermented products also represent a promising group for nanoparticle biosynthesis. In particular, the strain *Pichia kudriavzevii* MH545928.1 was isolated from a symbiotic culture of bacteria and yeast used for kombucha production (Kombucha tea SCOBY). The polysaccharides of these yeasts act as natural reducing and capping agents, ensuring the formation of stable CuNPs (Tsilo et al., 2023).

Another important reservoir of metal-resistant yeasts is industrial wastewater and polluted environments. Prolonged exposure to toxic metals promotes the development of efficient detoxification and metal biotransformation mechanisms in these microorganisms. *Rhodotorula mucilaginosa* was isolated from wastewater of the Sossego copper mine (Pará State, Brazil). These yeasts have adapted to extremely high concentrations of copper ions (up to 2000 mg/L) (Salvadori et al., 2014).

Genetically modified yeasts are also of considerable interest, particularly the strain *Komagataella phaffii* (formerly *Pichia pastoris*) X-33-Cyb5R, into which the cytochrome b5 reductase (Cyb5R) gene from *Aspergillus oryzae* has been integrated. The expression of Cyb5R increases yeast tolerance to high concentrations of copper ions (up to 12–14 mM), as this enzyme facilitates electron transfer from NADH to metal ions, promoting their reduction and decreasing toxicity. As a result of this genetic modification, the cells' ability to reduce copper ions and accumulate them intracellularly is enhanced, thereby increasing the efficiency of CuNP biosynthesis (Dong et al., 2025).

Mechanisms of copper nanoparticle biosynthesis using yeasts

The mechanisms of CuNP biosynthesis involving yeasts result from a complex interplay of physicochemical and biological processes occurring at different levels of cellular organization. The initial stage is the biosorption and binding of copper ions by yeast cell structures. The cell wall of *Komagataella phaffii* contains mannoproteins and polysaccharides with various functional groups: carboxyl, hydroxyl, amino, sulfhydryl, and phosphate. These groups act as active binding sites for Cu^{2+} cations through electrostatic interactions and complex formation. A key stage is the bioreduction of copper ions to the zero-valent state. This process can occur via both enzymatic and non-enzymatic pathways. Enzymatic reduction is associated with the activity of oxidoreductases, which facilitate electron transfer from intracellular donors such as NADH to copper ions. Cytochrome b5 reductase plays a particularly important role, catalyzing electron transport and contributing to copper detoxification while simultaneously initiating nanoparticle formation (Dong et al., 2025). Non-enzymatic reduction may occur with the participation of low-molecular-weight compounds. For example, phenolic compounds characteristic of marine yeasts such as *Rhodotorula mucilaginosa* act as effective electron donors (Hassabo et al., 2022). In addition, hydrogen sulfide (H_2S), produced by *Filobasidium stepposum* during the metabolism of sulphur-containing amino acids, can react with metal ions, promoting nanoparticle formation (Arriaza-Echanes et al., 2024).

The localization of nanoparticle biosynthesis depends on yeast species and cultivation parameters. Extracellular synthesis involves the adsorption of copper ions onto the cell wall surface, followed by their reduction and nanoparticle formation. This mechanism has been

described for *Yarrowia lipolytica* and genetically modified yeasts *Komagataella phaffii* (El-Sayed, 2018; Dong et al., 2025). Intracellular synthesis occurs via the transport of copper ions into the cell, where they are reduced by cytoplasmic enzymatic systems. The formed CuNPs may accumulate in the cytoplasm or be deposited in vacuoles, which is considered a cellular defense mechanism against metal toxicity. In this case, nanostructures of various morphologies may form, including needle-like or rod-shaped aggregates (Salvadori et al., 2014).

The final stage is nanoparticle stabilization (capping), which prevents aggregation and ensures colloidal stability. Yeasts produce a variety of biomolecules, including proteins, peptides, exopolysaccharides, and low-molecular-weight thiols (e.g., glutathione), which adsorb onto the nanoparticle surface and form a protective layer. Glutathione performs a dual function, acting both as a stabilizer and as a heavy metal detoxification agent. This biogenic coating creates steric hindrance that prevents CuNPs from approaching each other, ensuring their kinetic stability and preventing precipitation (Arriaza-Echanes et al., 2024).

A distinctive feature of copper nanoparticle biosynthesis using yeasts is also the formation of copper oxide forms. In many cases, metallic copper (Cu^0) is initially formed, which, due to its high reactivity, is rapidly oxidized by atmospheric oxygen to form Cu_2O or CuO. When marine yeasts such as *Rhodotorula mucilaginosa* are used, the process may involve preliminary hydrolysis of copper salts ($CuSO_4$) to form $Cu(OH)_2$, which is subsequently reduced by phenolic compounds to Cu_2O (Hassabo et al., 2022).

Use of biogenic copper nanoparticles for wastewater purification

Dye removal

Biogenic CuNPs demonstrate high efficiency in removing a wide range of synthetic dyes (Table 15) which are widely used in the textile, paper, and other industries. In particular, for the dye Congo red, a removal efficiency of up to 99.2% has been reported when using CuONPs (Kamakshi et al., 2024). CuNPs synthesized using bacteria provide approximately 97% degradation of Congo red (Noman et al., 2020a). Biogenic CuONPs show over 94% degradation efficiency for Amido black 10B (Khandelwal et al., 2024). High performance has also been observed for brilliant green and malachite green, where the removal efficiency using biogenic CuONPs can exceed 98% (Khandelwal et al., 2023). Methylene blue is effectively degraded both by CuSNPs synthesized using unicellular algae (Borah et al., 2022) and by CuNPs synthesized with the involvement of bacterial polysaccharides (Nkosi et al., 2025) and plant extracts (Nazir et al., 2023; Yu et al., 2025).

The high efficiency of biogenic copper nanoparticles in water purification processes is due to the combination of several mechanisms of action. One of the key mechanisms is the photocatalytic process, in which, under the influence of light radiation, reactive oxygen species such as hydroxyl and superoxide radicals are generated on the surface of the nanoparticles. These active species are capable of oxidizing complex organic dye molecules into simpler and less toxic compounds, including carbon dioxide and water (Khandelwal et al., 2023). Another important mechanism is catalytic reduction, which occurs in the presence of electron donors, where nanoparticles act as effective electron carriers and promote the breakdown of chromophoric groups in dyes, particularly azo bonds (Yu et al., 2025). Additionally, adsorption and flocculation processes play a significant role: functional groups (hydroxyl, carboxyl) on the surface of biogenic nanoparticles enable the binding of dye molecules and their subsequent removal from the aqueous environment through sedimentation (Nkosi et al., 2025).

Table 15

Use of biogenic copper nanoparticles for wastewater purification

Biological object for nanoparticles synthesis	Pollutant	Nanoparticles-mediated degradation	Reference
Acer palmatum (leaves)	Amido black 10B	86 % in 1.5 h	Sazak et al., 2023
Asterarcys quadricellulare (unicellular algae)	Brilliant green; Malachite green	98.02 % in 1 h; 96.04 % in 1 h	Khandelwal et al., 2023
Bacillus flexus FB-1 (bacteria)	Reactive black 5; phosphates; sulphates	88.16 % in 4 h; 49.49 %; 43.16 %	Batool et al., 2024
Celastrus paniculatus (leaves)	Methylene blue	90 % in 2 h	Mali et al., 2020
Chlorella ellipsoidea (unicellular algae)	Methylene blue	88.5 % in 1 h	Borah et al., 2022
Citrullus colocynthis (leaves)	Methylene blue	65 % in 2.6 h	Nazir et al., 2023
Coelastrella terrestris (unicellular algae)	Amido black 10B	94.19 % in 1.5 h	Khandelwal et al., 2024
Escherichia sp. SINT7 (bacteria)	Congo red	97.07 % in 5 h	Noman et al., 2020a
Malpighia glabra (fruit)	Phenol red	97 % in 9 min	Nguyen et al., 2024
Neurospora crassa (fungi)	Methyl red; Chrome (VI)	Over 90 % in 6 h; ~75 % in 5 h	Liu et al., 2021a
Pleurotus cystidiosus (mushroom)	Congo red; Malachite green; Remazole blue	99 %, 71.3 % and 49.2 % in 1.5 h	Kamakshi et al., 2024
Proteus mirabilis (bacteria)	Methyl orange; sulphates; phosphates; nitrates	93 %; 93 %; 88 %; 82 %	Nkosi et al., 2025
Chenopodium quinoa (seeds)	Cefixime	122.9 mg/g (absorption capacity)	Hassan et al., 2023
Sargassum cervicorne (brown algae)	Methyl orange	98.58 % in 8–10 h	Anwar et al., 2024
Stenotrophomonas maltophilia SCS1.1 (bacteria)	Chlorpyrifos, profenofos, imidacloprid	90.35 %; 87.24 %; 51.29 %	Kashyap et al., 2023
Zygnema sp. (filamentous green algae)	Reactive red	84.66 % in 1.25 h	Alsalamah et al., 2024

Removal of metal ions, pesticides, antibiotics, and other compounds

One of the key applications of biogenic CuNPs is the removal of metal ions (Table 15) from wastewater. Copper nanoparticles synthesized using the fungus *Neurospora crassa* are capable of removing up to 75% of toxic chromium (VI). The mechanism of this process includes both physical adsorption of chromium ions onto the nanoparticle surface and their chemical reduction to the less toxic chromium (III) form due to the action of active copper species on the nanoparticle surface (Liu et al., 2021a). Bacteria of the genus *Bacillus*, isolated from technogenically polluted environments, demonstrate the ability for complex wastewater purfication from metal ions. In particular, *Bacillus cereus* provides removal of up to 79.81% of copper, *Bacillus paramycoides* up to 86.74% of nickel, and *Bacillus wiedmannii* up to 91.96% of manganese, with simultaneous nanoparticle formation (Moeini et al., 2024). An important example of bioremediation is also the yeast *Yarrowia lipolytica*,

which is capable of extracellular synthesis of CuNPs directly during the treatment of ceramic industry wastewater, where copper ions accumulate both on the cell wall surface and within cellular vacuoles (El-Sayed, 2018).

CuONPs synthesized using the culture supernatant of *Stenotrophomonas maltophilia* SCS1.1 exhibit catalytic activity toward the degradation of common insecticides – chlorpyrifos, profenofos, and imidacloprid. The main mechanism in this case is the generation of reactive oxygen species on the nanoparticle surface, which induce oxidative degradation of pesticide molecules into less toxic compounds (Kashyap et al., 2023).

A promising direction is the use of CuNPs as nano-adsorbents for the removal of pharmaceutical pollutants from industrial wastewater. In particular, copper nanoparticles synthesized using an aqueous extract of quinoa seeds effectively adsorb antibiotics. For cefixime, the maximum adsorption capacity reaches 122.9 mg/g at pH 4, allowing nearly complete removal of this drug from real samples of pharmaceutical wastewater (Hassan et al., 2023).

The use of biogenic CuNPs leads to a significant reduction in the concentration of inorganic anions in water. Copper nanoparticles synthesized using bacteria reduce the concentration of sulfates and phosphates in textile industry wastewater (Batool et al., 2024). CuNPs enable the removal of up to 88% of phosphates, 80% of nitrates, and 63% of sulfates from coal mine effluents. In domestic wastewater, nitrate removal efficiency reaches 82% and total nitrogen removal 97%, indicating the significant potential of biogenic CuNPs in preventing eutrophication of aquatic ecosystems (Nkosi et al., 2025).

Improvement of general wastewater quality indicators

The application of CuNPs and CuONPs significantly affects key physicochemical parameters of wastewater quality. In particular, chemical oxygen demand (COD), which is an indicator of the level of organic pollution, is substantially reduced when biogenic nanoparticles are used. It has been established that CuONPs synthesized using an aqueous extract of freshwater unicellular algae *Coelastrella terrestris* are capable of reducing COD levels by more than 80% (Khandelwal et al., 2024). CuNPs obtained using the bacteria *Bacillus flexus* FB-1 and *Escherichia* sp. SINT7 ensure a reduction of this parameter within the range of 40–70% (Batool et al., 2024; Noman et al., 2020a). In the case of CuNPs synthesized using bacterial polysaccharides, the efficiency of COD reduction can exceed 90%. A similar trend is observed for biological oxygen demand (BOD), where the use of biogenic CuNPs leads to a reduction of 75–91% (Nkosi et al., 2025).

An important effect is also the normalization of the acid-base balance of wastewater. Treatment with biosynthesized nanoparticles contributes to reducing alkalinity and bringing pH values closer to neutral, which is critically important for the subsequent discharge of water into natural reservoirs. At the same time, a significant increase in dissolved oxygen levels is observed, associated with the degradation of organic pollutants and improved aeration properties of water. This creates favorable conditions for the restoration of aquatic ecosystems (Khandelwal et al., 2024).

In addition, the use of biogenic CuNPs leads to a reduction in both dissolved and suspended impurities in wastewater. The level of total dissolved solids (TDS) decreases by 57–89%, while total suspended solids (TSS) are reduced by 55–78%. A decrease in electrical conductivity by 55–81% confirms the effective removal of dissolved salt ions. A reduction in total water hardness by 45–61% and a decrease in chloride concentration by 44–61% are also observed, indicating reduced mineralization and improved overall wastewater quality (Noman et al., 2020a).

Use of biogenic copper nanoparticles for agriculture

Impact on bacterial and fungal infections agents

Copper nanoparticles perform broad spectrum of antimicrobial activity against numerous phytopathogens (Table 16).

Table 16

Copper nanoparticles activity against phytopathogens

Copper nanoparticles synthesis platform	Pathogen test culture	Nanoparticles antimicrobial activity indicator	Reference
Aspergillus carbonarius (fungi)	*Fusarium oxysporum*	Growth reduction zone 16 mm at 150 mM CuNPs	Al-Qaissi et al., 2024
Aspergillus niger AH1 (fungi)	*Ralstonia solanacearum*	Growth reduction zone 30 mm at 200 µg/mL CuSeNPs; MIC 12.5 µg/mL	Attia et al., 2025
Azadirachta indica, *Lantana camara*, *Senna spectabilis*, *Tectona grandis* (leaves)	*Corynespora cassiicola*	Mycelium growth reduction 75 % at 1000 ppm CuONPs	Yadava et al., 2025
Chaetomium globosum; *Trichoderma virens* (гриби)	*Xanthomonas euvesicatoria*	Growth reduction zone at 50 µg/mL CuNPs 22–22.6 mm	Dorjee et al., 2024
Citrus aurantium (fruit peel)	*Alternaria alternata*	Radial growth reduction 73,7 % at 2.5 mg/mL CuONPs	Albrahim et al., 2025
Heliotropium bacciferum (leaves)	*Rhizoctonia solani*; *Fusarium oxysporum*	Mycelium growth reduction at 100 µg/mL CuONPs 81.48 % for *R. solani* and 71.11 % for *F. oxysporum*	Hamdy et al., 2024
Mangifera indica (leaves)	*Rhizopus oryzae*	Mycelium growth reduction at 100 µg/mL CuONPs	Shah et al., 2024
Oedogonium sp. (freshwater algae)	*Xanthomonas citri*	Growth reduction zone 35.2 mm at 1200 ppm CuNPs; MIC 2000 µg/mL	Waqif et al., 2024
Phoma glomerata MTCC-2210 (fungi)	*Aspergillus niger*; *Aspergillus flavus*	Growth reduction zone at 1 mg/mL CuONPs: 19 mm for *A. niger*, 23 mm for *A. flavus*; MIC: 180–220 µg/mL	Ingle et al., 2024
Pseudomonas aeruginosa MO1 (bacteria)	*Colletotrichum capsici*; *Rhizoctonia solani*	At 30 µg/mL CuONPs growth reduction zone 25.16 mm for *C. capsici* and 16.1 mm for *R. solani*	Tejaswi et al., 2025
Pterocarpus santalinus (leaves)	*Aspergillus niger*	Mycelium growth reduction zone 23 mm at 120 µg/mL CuONPs	Babulla et al., 2024
Serratia sp. ZTB29 (bacteria)	*Alternaria* sp.	Mycelium growth reduction 91 % at 200 µg/mL CuONPs	Singh et al., 2023
Stenotrophomonas maltophilia SCS1.1 (bacteria)	*Penicillium digitatum*; *Fusarium oxysporum*	Mycelium growth reduction zone at 100 ppm CuONPs 100% for *P. digitatum*, 95.19 % for *F. oxysporum*	Kashyap et al., 2023
Xenorhabdus sp. NP2 (bacteria)	*Fusarium* sp.	Growth reduction zone 19 mm at 100 µg/mL CuNPs	Bharathi et al., 2022
Ziziphus spina-christi (leaves)	*Fusarium solani*	Mycelium growth reduction zone 91.17 % at 250 µg/mL CuONPs	El-Abeid et al., 2024

Biosynthesized CuNPs exhibit complex multimodal antimicrobial mechanisms, which significantly reduce the likelihood of development of the resistance in microorganisms. One of the initial stages of antimicrobial action is their interaction with the cell wall of phytopathogens.

Due to electrostatic attraction between positively charged nanoparticles and negatively charged components of the cell wall, adsorption onto the cell surface occurs. Their small size and high surface-area-to-volume ratio facilitate the penetration of CuNPs through cellular barriers, leading to mechanical damage of membrane structures. As nanoparticles accumulate, defects such as pores and localized disruptions are formed, accompanied by loss of membrane selective permeability, decreased membrane potential, and loss of intracellular contents, ultimately resulting in microbial cell death (Shah et al., 2024).

A key mechanism of CuNP cytotoxicity is the induction of oxidative stress. Biosynthesized nanoparticles are capable of catalyzing the formation of reactive oxygen species (ROS), including hydrogen peroxide and hydroxyl radicals. Excessive ROS accumulation disrupts the cellular antioxidant system and causes lipid peroxidation of membranes. This leads to further damage to cellular structures and enhances the overall cytotoxic effect (Tejaswi et al., 2025).

An important component of antimicrobial action is the gradual release of copper ions (Cu^{+} and Cu^{2+}) from the nanoparticle surface. These ions penetrate the cell and disrupt ionic homeostasis by interacting with key biomolecules and interfering with metabolic processes. In particular, they can replace other metal ions in the active sites of enzymes, leading to their functional inactivation. At the intracellular level, CuNPs and copper ions cause significant damage to genetic material and proteins. Interaction with DNA and RNA disrupts their spatial organization, induces strand breaks, and causes mutational changes, thereby blocking replication and transcription processes (Dorjee et al., 2024).

In addition to general mechanisms, CuNPs demonstrate specific activity against fungal pathogens. They are capable of inhibiting chitin synthase activity – a key enzyme in fungal cell wall chitin biosynthesis – leading to cell wall weakening and increased sensitivity to external factors (Hamdy et al., 2024). Interaction of nanoparticles with membrane ergosterol has also been established, resulting in pore formation and disruption of osmotic balance (Tahir et al., 2022). Furthermore, CuNPs affect fungal morphogenesis by causing hyphal deformation and suppressing sporulation processes, thereby limiting their reproduction and spread (Ammar et al., 2019).

Insecticidal activity

Biogenic CuNPs demonstrate pronounced insecticidal activity against various groups of insects, including storage pests, lepidopterans, as well as representatives of social insects and dipterans. For example, CuNPs synthesized using aqueous leaf extracts of *Acacia cornigera* and *Annona purpurea* ensure high mortality of *Tribolium castaneum* (red flour beetle), reaching levels of 90% and 76.6%, respectively (Solorzano Toala et al., 2024). CuNPs obtained using the bacterium *Pseudomonas fluorescens* MAL2 also exhibit significant toxicity toward *Tribolium castaneum* (LC50 = 36.89 ppm) (El-Saadony et al., 2020).

High efficacy of CuNPs has also been established against lepidopteran pests. Nanoparticles synthesized using the liquid culture supernatant of *Xenorhabdus* sp. NP2 cause up to 80% mortality in larvae of *Spodoptera litura* (cotton leafworm) (Bharathi et al., 2022).

There are also reports on the effectiveness of CuNPs against termites and mosquitoes. For instance, nanoparticles synthesized using leaf extract of *Grewia asiatica* cause high mortality of *Heterotermes indicola* (termites) at a concentration of 100 ppm and also exhibit pronounced toxicity toward larvae of *Aedes aegypti* (mosquitoes), highlighting their potential use as biodegradable insecticides (Tahir et al., 2022).

Remediation and enhancement of plant resistance to abiotic stress

Biosynthesized CuNPs are considered an effective tool for mitigating abiotic stress in plants, particularly under conditions of soil salinity and heavy metal pollution. One of the key applications of biogenic CuNPs is reducing the negative impact of salt stress. In particular,

nanoparticles synthesized using the liquid culture of *Klebsiella pneumoniae* NST2 have demonstrated the ability to significantly improve the physiological state of maize plants under saline conditions. The protective mechanism is based on the ability of nanoparticles to interact with sodium and chloride ions in the external environment, thereby limiting their uptake and accumulation in plant tissues (Noman et al., 2021).

Equally important is the use of biogenic CuNPs to reduce the toxic effects of heavy metals, particularly chromium. It has been shown that nanoparticle treatment increases wheat tolerance to high concentrations of chromium in soil. This is attributed to the ability of CuNPs to immobilize chromium ions by converting them into forms less available for uptake. As a result, the translocation of chromium ions from the root system to aboveground organs and grains is reduced, thereby limiting their toxic effects on cellular structures and metabolic processes (Noman et al., 2020b).

Nanofertilizers

The application of biogenic copper nanoparticles has a positive effect on the morphological parameters of plant development. In particular, treatment of tomatoes with CuONPs synthesized using an aqueous leaf extract of *Ziziphus spina-christi* leads to an increase in the seedling vigor index, higher fresh and dry biomass, and a significant increase in plant height – up to 65.33 cm compared to 37 cm in the control. Stimulation of tomato root system development also was observed, promoting more efficient uptake of water and mineral nutrients (El-Abeid et al., 2024).

Biosynthesized CuNPs stimulate growth processes in maize under saline soil conditions. Specifically, root length increases by 43.5% and shoot length by 44%, along with enhanced fresh and dry biomass compared to untreated plants (Noman et al., 2021). Low doses of CuNPs (0.06 mg/mL) stimulate wheat root growth by 173% and shoot growth by 216% (Essa et al., 2021). Treatment of eggplant with CuSeNPs leads to increased levels of photosynthetic pigments and activation of systemic resistance mechanisms, positively affecting plant growth and development (Attia et al., 2025).

At the physiological and biochemical levels, biosynthesized CuNPs activate key processes that determine plant growth and stress tolerance. Their application is associated with increased levels of photosynthetic pigments (chlorophyll a, chlorophyll b) and carotenoids, linked to the activation of photosystems I and II, as well as regulation of gene expression encoding enzymes of the photosynthetic apparatus (El-Abeid et al., 2024; Oraibi et al., 2023). Biogenic CuNPs also stimulate the antioxidant system by increasing the activity of enzymes such as peroxidase, polyphenol oxidase, and catalase, thereby reducing oxidative stress and enhancing plant resistance to both biotic and abiotic factors (Attia et al., 2025; Noman et al., 2021).

The effectiveness of CuNP application shows a pronounced dose-dependent pattern. The use of nanoparticles at concentrations of 25–50 mg/kg of soil provides a stimulatory effect, ensuring optimal copper supply as an essential micronutrient and improving plant nutrition. However, exceeding optimal doses above 100 mg/kg of soil may lead to phytotoxic effects, manifested by growth inhibition, reduced levels of photosynthetic pigments, and the development of oxidative cellular damage (Essa et al., 2021).

Application of biosynthesized copper nanoparticles in the food industry

Active antimicrobial packaging

Active antimicrobial packaging based on biosynthesized CuNPs is considered one of the most promising innovations in the modern food industry, aimed at enhancing microbiological safety and extending the shelf life of food products. To create such packaging materials, nanoparticles are incorporated into various polymer matrices, primarily biodegradable and environmentally friendly ones. Among the most commonly used biopolymers are chitosan and agarose, which, due to their inherent antimicrobial properties and high biocompatibility, form

effective composite systems. For example, films based on chitosan, agarose, CuNPs, and CuONPs are effective against a wide range of pathogenic microorganisms, including *Escherichia coli*, *Pseudomonas aeruginosa*, *Bacillus cereus*, *Staphylococcus aureus*, and *Staphylococcus epidermidis* (Abd El Rahman et al., 2025).

Polylactic acid (PLA) is also an important carrier for CuNPs due to its biodegradability and good mechanical properties. Copper nanoparticle-modified PLA composite films effectively inhibit microbial growth in fresh food products, particularly poultry meat, fish, and dairy products (Santos et al., 2024). Similarly, hypromellose is used to create flexible packaging materials embedded with copper nanowires, characterized by controlled release of Cu^{2+} ions and consequently reduced cytotoxicity (Bagchi et al., 2022).

The combination of cellulose acetate with polycaprolactone in the presence of CuNPs enables the production of superhydrophobic films with improved moisture barrier properties and high mechanical strength. Such materials are especially promising for packaging high-moisture products, where the risk of microbial spoilage is particularly significant (El-Naggar et al., 2022).

Biogenic CuNPs can also be applied to the surface of cellulose paper, cardboard, or textile materials used for packaging fruits, vegetables, and other food products. Antimicrobial activity of such packaging has been demonstrated against bacteria such as *Escherichia coli*, *Staphylococcus aureus*, *Klebsiella pneumoniae*, as well as the yeast *Candida albicans* (Aziz et al., 2024).

The antimicrobial mechanism of biosynthesized CuNPs is multifactorial and operates through several interconnected pathways. The first stage involves interaction of nanoparticles with the bacterial cell surface, leading to its deformation (Rajamma et al., 2020). Subsequently, CuNPs penetrate the cell and release Cu^{+}/Cu^{2+} ions, which interact with biomolecules. Copper ions bind to specific sites of nucleic acids, causing their denaturation (Baral et al., 2025). Copper also interacts with thiol, carboxyl, and amino groups of amino acids, leading to protein denaturation and enzyme inactivation (Shah et al., 2024).

A crucial role is played by the induction of oxidative stress through the generation of reactive oxygen species, including superoxide anions, hydrogen peroxide, and hydroxyl radicals. These compounds initiate lipid peroxidation, damage proteins and nucleic acids, and disrupt cellular functions (Idrees et al., 2025). Copper additionally catalyzes Fenton-like reactions, enhancing the formation of highly reactive radicals (Yu et al., 2025). Moreover, biosynthesized CuNPs and CuONPs affect key metabolic processes in microbial cells. In particular, they can inhibit the enzyme dihydrofolate reductase (DHFR), which is essential for nucleotide synthesis and cell proliferation. CuONPs also exhibit high affinity for DNA gyrase (GyrB), blocking its ATPase activity and thereby halting DNA replication and bacterial growth (Sazak et al., 2023).

An important aspect of implementing active antimicrobial packaging is its safety and environmental friendliness. Studies on the migration of copper ions from polymer matrices into model food media have shown that the level of copper release remains below the permissible limits (5 mg/kg) established by regulatory standards. This indicates that such materials comply with food safety requirements (Santos et al., 2024; Scattareggia Marchese et al., 2022). The integration of CuNPs does not hinder the biodegradation of polymer matrices. PLA-based biocomposites demonstrate a high degree of degradation under composting conditions, reaching near-complete degradation within 14–30 days. This highlights the suitability of such materials in the context of sustainable packaging solutions and the circular economy (Santos et al., 2024).

Preservation of freshness and quality of fruits and vegetables

Postharvest losses of fruits and vegetables can reach 20–50%, which requires the implementation of innovative technologies capable of effectively suppressing pathogen development while maintaining the physiological and biochemical characteristics of products. Postharvest treatment of mango fruits by immersion in a CuONP solution extends their shelf life from 10 to 18 days. Such treatment helps preserve pulp firmness, reduces weight loss, and maintains higher levels of ascorbic acid and titratable acidity, indicating a slowdown in ripening and senescence processes (Joshi et al., 2025).

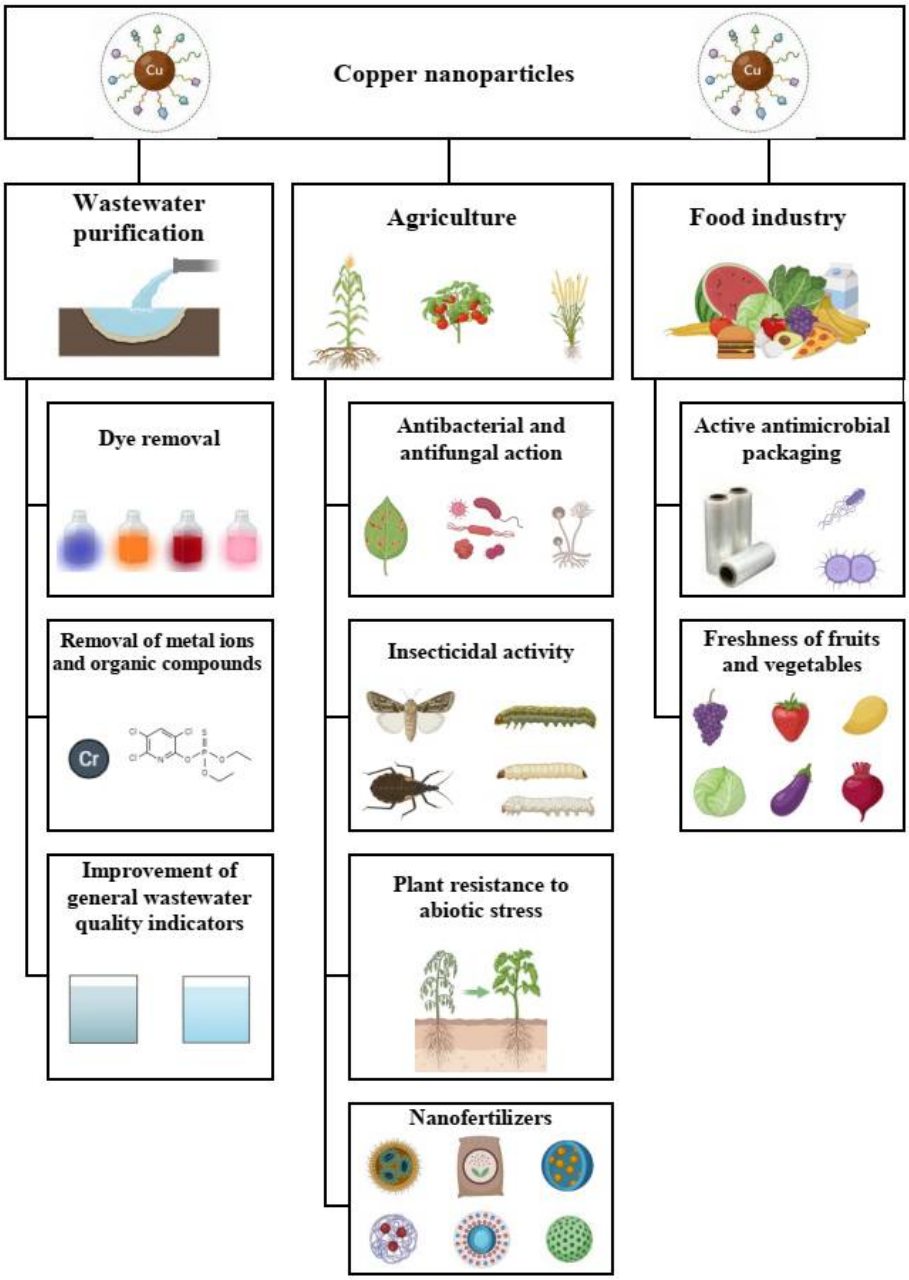

Figure 3. Practical application of CuNPs
(elements from BioRender.com have been used for scheme)

Conclusions

An important advantage of biosynthesized CuNPs is their pronounced antimicrobial activity against a wide range of pathogens. In the case of persimmon, CuONPs demonstrated strong antifungal activity against *Rhizopus oryzae*. The use of nanoparticles at a concentration of 100 μg/mL leads to inhibition of mycelial growth on the fruit surface and a reduction in infection levels compared to untreated fruits (Shah et al., 2024). It was shown that CuONPs inhibit the development of *Fusarium solani* – the pathogen of Fusarium root rot in tomatoes (El-Abeid et al., 2024) – and *Aspergillus niger*, responsible for black rot in onions (Babulla et al., 2024). Biosynthesized CuNPs completely inhibit the growth of *Phytophthora parasitica* and *Fusarium oxysporum*, pathogens that cause vegetable spoilage (Ammar et al., 2019).

Among the key advantages of biosynthesized CuNPs is their environmental friendliness, as plant-based waste materials, such as pineapple peels, can be used for their synthesis, contributing to reduced environmental impact (Mitra et al., 2024). In addition, studies indicate a low level of copper ion migration into fruit pulp, which does not exceed established food safety limits (Joshi et al., 2025; Santos et al., 2024). At the same time, copper nanoparticles exhibit antioxidant properties, providing additional protection of bioactive compounds in fruits against oxidative degradation (Abd El Rahman et al., 2025; Shah et al., 2024).

Considering all the data, biosynthesized CuNPs can be applied for wastewater treatment, as antimicrobial and insecticidal agents in agriculture, as a part of nanoferilizers, for the soil remediation and as a part of active antimicrobial package materials. Moreover, CuNPs are potential solution for fruits and vegetables treatment for the extension of shelf-life (Figure 3).

At the same time, despite significant advances in the biosynthesis of copper nanoparticles, further studies are required to facilitate the transition of these technologies from laboratory-scale investigations to industrial applications. Particular attention should be given to improving the reproducibility and scalability of biosynthesis processes, as well as to the standardization of synthesis conditions and the long-term stability of the obtained nanoparticles.

The biosynthesis of copper nanoparticles using biological systems represents a promising direction in modern nanobiotechnology, consistent with the principles of sustainable development and green chemistry. A generalization of current scientific data indicates that a wide range of biological systems (plants, spices, condiments, food products and food waste, algae, fungi, and microorganisms) can be employed for the reduction of copper ions and the stabilization of the resulting nanoparticles.

It was demonstrated that biologically active compounds (polyphenols, flavonoids, proteins, amino acids, polysaccharides, and enzymes) play a key role in biosynthesis processes, functioning both as reducing and stabilizing agents. The mechanisms of nanoparticle formation are complex and multistage, involving processes of complexation, bioreduction, nucleation, growth, and stabilization. At the same time, the path of these processes largely depends on the nature of the biological system and its metabolic profile.

It has been established that the type of biological system and synthesis conditions (the nature and concentration of the precursor, pH of the medium, temperature, and process duration) determine the morphology, size, colloidal stability, and functional properties of the nanoparticles. This creates opportunities for the controlled synthesis of nanomaterials with tailored characteristics. However, unified approaches for predicting these parameters are currently lacking.

Despite significant progress in the field of nanoparticle biosynthesis, a number of unresolved challenges remain. In particular, the systematization of data regarding the comparative efficiency of different biological systems remains limited; the molecular and enzymatic mechanisms of copper ion bioreduction are insufficiently understood; and standardized approaches to scaling up biosynthesis processes are lacking. Additionally, the relationship between synthesis conditions and the functional properties of nanoparticles in the context of their practical applications requires

further in-depth investigation. It should also be noted that studies on the biosynthesis of copper nanoparticles using yeasts remain limited, highlighting the perspectives of this research direction.

The practical significance of biogenic copper nanoparticles lies in their broad potential applications as antimicrobial agents, catalysts, and photocatalysts, as well as in water purification and bioremediation processes. Particularly promising is the integration of nanoparticle biosynthesis with waste treatment and the remediation of polluted environments, in line with the concept of a circular bioeconomy. Further development of this field requires the integration of approaches from microbiology, biotechnology, biochemistry, materials science, and engineering in order to develop efficient, controllable, and scalable technologies for the biosynthesis of copper nanoparticles. Special attention should be given to the development of standardized synthesis methods, a deeper understanding of the underlying mechanisms, and the expansion of their practical applications across various areas of biotechnology.

References

Abbas A.H., Fairouz N.Y. (2022), Characterization, biosynthesis of copper nanoparticles using ginger roots extract and investigation of its antibacterial activity, *Materials Today: Proceedings*, 61, pp. 908–913, https://doi.org/10.1016/j.matpr.2021.09.551

Abbas J.M., Tawfeeq T.A., Al-hussaniy H.A., Altimari U.S. (2025), Green synthesis of copper nanoparticles using *Daucus carota* leaf extract and their anticancer activity against Hep3B liver cancer cells, *Pharmacia*, 72, pp. 1–11, https://doi.org/10.3897/pharmacia.72.e164282

Abd El Rahman H.A., El-Sharif A.A., Youssef A.M., Gomaa S.K., Mohamed S. S., El Refai H.A. (2025), A novel chitosan agarose nanocopper composite film (Cs/Agr/Cu-Cu_2O NPs) using *Aspergillus niger* KY 401431: Preparation, characterization and evaluation of their antibacterial activity, *3 Biotech*, 15(9), 306, https://doi.org/10.1007/s13205-025-04471-7

Abdelhai M.F., Shabaan R.H., Kamal N.M., Elemary E.A., Abd-Elhalim B.T., Hassan E. A. (2024), Copper nanoparticles biosynthesis by *Stevia rebaudiana* extract: Biocompatibility and antimicrobial application, *AMB Express*, 14(1), 59, https://doi.org/10.1186/s13568-024-01707-2

Abdullah F.O. (2025), Phytoextract-mediated cupper nanoparticles via *Acacia saligna*: Synthesis, characterization and in vitro anticancer and apoptosis inducing effects, *Bioresources and Bioprocessing*, 12(1), 85, https://doi.org/10.1186/s40643-025-00918-0

Abishad P., Namratha K., Nayan M.B., Jayashankar M., Srinath B.S., Jess V., Byrappa K. (2022), Facile synthesis of copper sulphide nanoparticles using *Trichoderma harzianum* and antibacterial efficiency enhancement by gentamicin sulfate, *Pharmaceutical Research*, 6(2), 000268, https://doi.org/10.23880/oajpr-16000268

Aboeita N.M., Fahmy S.A., El-Sayed M.M., Azzazy H.M.E.S., Shoeib T. (2022), Enhanced anticancer activity of nedaplatin loaded onto copper nanoparticles synthesized using red algae, *Pharmaceutics*, 14(2), 418, https://doi.org/10.3390/pharmaceutics14020418

Ahmadi M., Elikaei A., Ghadam P. (2023), Antiviral activity of biosynthesized copper nanoparticle by *Juglans regia* green husk aqueous extract and iron nanoparticle: molecular docking and in-vitro studies, *Iranian Journal of Microbiology*, 15(1), 138, https://doi.org/10.18502/ijm.v15i1.11930

Ahmed M.E., Saleh I.A., Al-Masri H.A., Hamoud Y.A., Okla M.K., Shaghaleh H. (2025), Green synthesis of copper nanoparticles from kiwi peel: antibacterial properties and the role of MexY gene expression in *Pseudomonas aeruginosa* efflux pumps, *Applied Biochemistry and Biotechnology*, 197(10), pp. 6741–6764, https://doi.org/10.1007/s12010-025-05354-6

Akintelu S.A., Oyebamiji A.K., Olugbeko S.C., Latona D.F. (2021), Green chemistry approach towards the synthesis of copper nanoparticles and its potential applications as therapeutic agents and environmental control, *Current Research in Green and Sustainable Chemistry*, 4, 100176, https://doi.org/10.1016/j.crgsc.2021.100176

Al Musayeib N.M., Amina M., Al-Yousef H.M., Haq M.U., Al-Daihan S., Bhat R.S. (2024), *Rhus microphylla*-mediated biosynthesis of copper oxide nanoparticles for enhanced antibacterial and antibiofilm efficacy, *Green Processing and Synthesis*, 13(1), 20240102, https://doi.org/10.1515/gps-2024-0102

Albrahim J.S., Saleh A.K., Abdalla O.A., El-Gendi H. (2025), *Citrus aurantium* peel extract mediated green synthesis of copper oxide and zinc oxide nanoparticles: characterization and antifungal efficacy against post-harvest spoilage of tomato fruits by locally isolated *Alternaria alternata*, *Journal of Cluster Science*, 36(4), 151, https://doi.org/10.1007/s10876-025-02874-3

Ali B.M.H. (2020), Green synthesis of copper nanoparticles by using fresh aqueous *Ananas comosus* L. (pineapple) peels extract, *Biochemical & Cellular Archives*, 20(2), 5965, https://connectjournals.com/03896.2020.20.5965

Al-Qaissi A.R., Fouzi S.H., AL-Baytay A.J. (2024), Characterization of biologically synthesized copper nanoparticles by *Aspergillus carbonarius* and evaluation of their activity in reducing the pathogenic stress of tomatoes infected with *Fusarium oxysporum*, *Tikrit Journal for Agricultural Sciences*, 24(2), pp. 161–177. https://doi.org/10.25130/tjas.24.2.12

Alsalamah S.A., Alghonaim M.I., Bakri M.M., Abdelghany T.M. (2024), *Zygnema* sp. as creator of copper oxide nanoparticles and their application in controlling of microbial growth and photo-catalytic degradation of dyes, *Applied Biological Chemistry*, 67(1), 47, https://doi.org/10.1186/s13765-024-00891-w

Alshami H.G.A., Al-Tamimi W.H., Hateet R.R. (2023), The antioxidant potential of copper oxide nanoparticles synthesized from a new bacterial strain, *Biodiversitas: Journal of Biological Diversity*, 24(5), https://doi.org/10.13057/biodiv/d240519

Alshammari S.O., Mahmoud S.Y., Farrag E.S. (2023), Synthesis of green copper nanoparticles using medicinal plant *Krameria* sp. root extract and its applications, *Molecules*, 28(12), 4629, https://doi.org/10.3390/molecules28124629

Amaliyah S., Pangesti D.P., Masruri M., Sabarudin A. Sumitro S.B. (2020), Green synthesis and characterization of copper nanoparticles using *Piper retrofractum Vahl* extract as bioreductor and capping agent, *Heliyon*, 6(8), https://doi.org/10.1016/j.heliyon.2020.e04636

Amatya S.P., Joshi L.P. (2020), Bio-synthesis of copper nanoparticles (CuNPs) using garlic extract to investigate antibacterial activity, *Bibechana*, 17, pp. 13–19, https://doi.org/10.3126/bibechana.v17i0.23485

Amer M.W., Awwad A.M. (2021), Green synthesis of copper nanoparticles by *Citrus limon* fruits extract, characterization and antibacterial activity, *Chemistry International*, 7(1), 1, https://doi.org/10.5281/zenodo.4017993

Amirtham P.J.M., Shenbhagaraman R., Siva R. (2023), Photocatalytic dye degradation and bacteriostatic efficacy of myco synthesized copper nanoparticles by new isolate *Lentinus squarrosulus* (Mont.) from dead trunk of *Nerium odourum*, *Indian Journal of Science and Technology*, 16, pp. 1802–1809, https://doi.org/10.17485/IJST/v16i24.252

Ammar H.A., Rabie G.H., Mohamed E. (2019), Novel fabrication of gelatin-encapsulated copper nanoparticles using *Aspergillus versicolor* and their application in controlling of rotting plant pathogens, *Bioprocess and Biosystems Engineering*, 42(12), pp. 1947–1961, https://doi.org/10.1007/s00449-019-02188-5

Anbalagan G., Subramanian B., Suresh V., Sivaperumal P. (2024), Green synthesis of copper and copper oxide nanoparticles from brown algae *Turbinaria* species' aqueous extract and its antibacterial properties, *Cureus*, 16(4). https://doi.org/10.7759/cureus.57366

Antonio-Perez A., Duran-Armenta L.F., Perez-Loredo M.G., Torres-Huerta A.L. (2023), Biosynthesis of copper nanoparticles with medicinal plants extracts: From extraction methods to applications, *Micromachines*, 14(10), 1882, https://doi.org/10.3390/mi14101882

Anwar S.J., Yusoff H.M., Bhat I.U.H., Ern L.K. (2024), Remediation of dye-contaminated water using brown algae seaweed supported copper nanoparticles, *Arabian Journal for Science and Engineering*, 49(1), pp. 475–496, https://doi.org/10.1007/s13369-023-08199-5

Araya-Castro K., Chao T.C., Duran-Vinet B., Cisternas C., Ciudad G., Rubilar O. (2020), Green synthesis of copper oxide nanoparticles using protein fractions from an aqueous extract of brown algae *Macrocystis pyrifera*, *Processes*, 9(1), 78, https://doi.org/10.3390/pr9010078

Arriaza-Echanes C., Campo-Giraldo J.L., Valenzuela-Ibaceta F., Ramos-Zuniga J., Perez-Donoso J.M. (2024), Biosynthesis of Cu-In-S nanoparticles by a yeast isolated from Union Glacier, Antarctica: a platform for enhanced quantum dot-sensitized solar cells, *Nanomaterials*, 14(6), 552, https://doi.org/10.3390/nano14060552

Ashokkumar M., Palanisamy K., Ganesh Kumar A., Muthusamy C., Senthil Kumar K.J. (2024), Green synthesis of silver and copper nanoparticles and their composites using *Ocimum sanctum* leaf extract displayed

enhanced antibacterial, antioxidant and anticancer potentials, *Artificial Cells, Nanomedicine, and Biotechnology*, 52(1), pp. 438–448, https://doi.org/10.1080/21691401.2024.2399938

Atri A., Echabaane M., Bouzidi A., Harabi I., Soucase B.M., Chaabane R.B. (2023), Green synthesis of copper oxide nanoparticles using *Ephedra alata* plant extract and a study of their antifungal, antibacterial activity and photocatalytic performance under sunlight, *Heliyon*, 9(2), https://doi.org/10.1016/j.heliyon.2023.e13484

Attia M.S., Hasanin M.S., Hashem A.H., Abdel-Kader S.A., Aloufi A.S., Baazeem, A., Abdelaziz A.M. (2025), *Aspergillus niger* mediated biosynthesis of bimetallic copper–selenium nanoparticles and their roles in enhancing resistance to *Ralstonia solanacearum*, *Biotechnology Journal*, 20(9), e70123, https://doi.org/10.1002/biot.70123

Aziz N.M.A., Goda D.A., Abdel-Meguid D.I., El-Sharouny E.E., Soliman N.A. (2024), A comparative study of the biosynthesis of CuNPs by *Niallia circulans* G9 and *Paenibacillus* sp. S4c strains: characterization and application as antimicrobial agents, *Microbial Cell Factories*, 23(1), 156, https://doi.org/10.1186/s12934-024-02422-0

Babulla S., Kumari A.M. (2024), Green synthesis of CuO and ZnO nanoparticles using *Pterocarpus santalinus* leaf extract and their role in inhibiting the growth of *Aspergillus niger* isolated from infected onions, *Journal of Pure and Applied Microbiology*, 18(3), pp. 1838–1847, https://doi.org/10.22207/JPAM.18.3.31

Bagchi B., Fernandez C.S., Bhatti M., Ciric L., Lovat L., Tiwari M.K. (2022), Copper nanowire embedded hypromellose: an antibacterial nanocomposite film, *Journal of Colloid and Interface Science*, 608, pp. 30–39, https://doi.org/10.1016/j.jcis.2021.09.130

Banerjee A., Roy R.K., Sarkar S., Lopez J.L., Vuree S., Bandopadhyay R. (2024), Synthesis of hot spring origin bacterial cell wall polysaccharide-based copper nanoparticles with antibacterial property, *Electronic Journal of Biotechnology*, 68, pp. 11–19, https://doi.org/10.1016/j.ejbt.2023.11.005

Banger A., Kumari A., Jangid N.K., Jadoun S., Srivastava A., Srivastava M. (2025), A review on green synthesis and characterisation of copper nanoparticles using plant extracts for biological applications, *Environmental Technology Reviews*, 14(1), pp. 94–126, https://doi.org/10.1080/21622515.2025.2453950

Baral J., Pokharel N., Dhungana S., Tiwari L., Khadka D., Pokhrel M.R., Poudel B.R. (2025), Green synthesis of copper oxide nanoparticles using *Mentha* (mint) leaves characterization and its antimicrobial properties with phytochemicals screening, *Journal of Nepal Chemical Society*, 45(1), pp. 111–121, https://doi.org/10.3126/jncs.v45i1.74491

Batool F., Shahid M., Mahmood F., Shahzad T., Azeem F., Hussain S., Tahani S., Mohamed S., Wed A., Mustafa S. (2024), Biosynthesis of copper nanoparticles using *Bacillus flexus* and estimation of their potential for decolorization of azo dyes and textile wastewater treatment, *Journal of King Saud University-Science*, 36(8), 103309, https://doi.org/10.1016/j.jksus.2024.103309

Bharathi B.G., Lalitha K., Shivakumar M.S. (2022), Biosynthesis of copper nanoparticles using symbiotic bacterium *Xenorhabdus* sp, isolated from entomopathogenic nematode and its antimicrobial and insecticidal activity against *Spodoptera litura, Inorganic and Nano-Metal Chemistry*, 54(9), pp. 858–870, https://doi.org/10.1080/24701556.2022.2078359

Borah D., Saikia P., Sarmah P., Gogoi D., Rout J., Ghosh N.N., Bhattacharjee C.R. (2022), Composition controllable alga-mediated green synthesis of covellite CuS nanostructure: An efficient photocatalyst for degradation of toxic dye, *Inorganic Chemistry Communications*, 142, 109608, https://doi.org/10.1016/j.inoche.2022.109608

Bukhari S.I., Hamed M.M., Al-Agamy M.H., Gazwi H.S., Radwan H.H., Youssif A.M. (2021), Biosynthesis of copper oxide nanoparticles using *Streptomyces* MHM38 and its biological applications, *Journal of Nanomaterials*, 2021(1), 6693302, https://doi.org/10.1155/2021/6693302

Chaerun S.K., Prabowo B.A., Winarko, R. (2022), Bionanotechnology: the formation of copper nanoparticles assisted by biological agents and their applications as antimicrobial and antiviral agents, *Environmental Nanotechnology, Monitoring & Management*, 18, 100703, https://doi.org/10.1016/j.enmm.2022.100703

Chakraborty N., Banerjee J., Chakraborty P., Banerjee A., Chanda S., Ray K., Acharya K., Sarkar J. (2022), Green synthesis of copper/copper oxide nanoparticles and their applications: a review, *Green Chemistry Letters and Reviews*, 15(1), pp. 187-215, https://doi.org/10.1080/17518253.2022.2025916

Das P.E., Abu-Yousef I.A., Majdalawieh A.F., Narasimhan S., Poltronieri P. (2020), Green synthesis of encapsulated copper nanoparticles using a hydroalcoholic extract of *Moringa oleifera* leaves and

assessment of their antioxidant and antimicrobial activities, *Molecules*, 25(3), 555, https://doi.org/10.3390/molecules25030555

Dehnoee A., Javad Kalbasi R., Zangeneh M.M., Delnavazi M.R., Zangeneh A. (2024), Characterization, anti-lung cancer activity, and cytotoxicity of bio-synthesized copper nanoparticles by *Thymus fedtschenkoi* leaf extract, *Journal of Cluster Science*, 35(3), pp. 863–874, https://doi.org/10.1007/s10876-023-02512-w

Doman K.M., Gharieb M.M., Abd El-Monem A.M., Morsi H.H. (2024), Synthesis of silver and copper nanoparticle using *Spirulina platensis* and evaluation of their anticancer activity, *International Journal of Environmental Health Research*, 34(2), pp. 661–673, https://doi.org/10.1080/09603123.2022.2163987

Dong C., Wu F., Liu S., Rong Y., Hong K., Li Y., Meng J., Wu X. (2025), Production of copper nanoparticles using genetically engineered *Komagataella phaffii*, *Bioprocess and Biosystems Engineering*, 48(9), pp. 1495–1508, https://doi.org/10.1007/s00449-025-03191-9

Dorjee L., Kamil D., Kumar R., Khokhar M.K., Aggarwal R., Gogoi R. (2024), Synthesis of promising copper nanoparticles utilizing biocontrol agents, *Trichoderma virens* and *Chaetomium globosum*, *The Indian Journal of Agricultural Sciences*, 94(1), pp. 061–067, https://doi.org/10.56093/ijas.v94i1.142836

El-Abeid S.E., Mosa M.A., El-Tabakh M.A., Saleh A.M., El-Khateeb M.A., Haridy M.S. (2024), Antifungal activity of copper oxide nanoparticles derived from *Zizyphus spina* leaf extract against *Fusarium* root rot disease in tomato plants, *Journal of nanobiotechnology*, 22(1), 28, https://doi.org/10.1186/s12951-023-02281-8

Elhabal S.F., Elwy H.M., Hassanin S., El-Rashedy A.A., Hamza A.A., Khasawneh M.A. (2022), Biosynthesis and characterization of gold and copper nanoparticles from *Salvadora persica* fruit extracts and their biological properties, *International Journal of Nanomedicine*, 17, pp. 6095–6112, https://doi.org/10.2147/IJN.S385543

El-Naggar M. E., Hasanin M., Hashem, A.H. (2022), Eco-friendly synthesis of superhydrophobic antimicrobial film based on cellulose acetate/polycaprolactone loaded with the green biosynthesized copper nanoparticles for food packaging application, *Journal of Polymers and the Environment*, 30(5), pp. 1820–1832, https://doi.org/10.1007/s10924-021-02318-9

El-Saadony M.T., Abd El-Hack M.E., Taha A.E., Fouda M.M., Ajarem J.S., Maodaa S.N., Allam A.A., Elshaer N. (2020), Ecofriendly synthesis and insecticidal application of copper nanoparticles against the storage pest *Tribolium castaneum*, *Nanomaterials*, 10(3), 587, https://doi.org/10.3390/nano10030587

El-Sayed M.T. (2018), Bioremediation and extracellular synthesis of copper nanoparticles from wastewater using *Yarrowia lipolytica* AUMC 9256, *Egyptian Journal of Botany*, *58*(3), pp. 563–579, https://doi.org/10.21608/ejbo.2018.3047.1157

El Sayed M.T., El-Sayed A.S. (2019), Biocidal activity of metal nanoparticles synthesized by *Fusarium solani* against multidrug-resistant bacteria and mycotoxigenic fungi, *Journal of Microbiology and Biotechnology*, 30(2), 226, https://doi.org/10.4014/jmb.1906.06070

El-Sayed O., Abd-Elhalim B.T., Mosa M.A., Hassan E.A. (2025), Characterization and optimization of biogenic copper nanoparticles synthesized by *Pseudomonas putida* with cytocompatibility investigation, *Scientific Reports*, 15(1), 32504, https://doi.org/10.1038/s41598-025-17705-8

Elshaer S., Shaaban M.I. (2023), Antibiofilm activity of biosynthesized silver and copper nanoparticles using *Streptomyces* S29, *AMB Express*, 13(1), 139, https://doi.org/10.1186/s13568-023-01647-3

El-Sherbiny G.M., Kalaba M.H., Sharaf M.H., Moghannem S.A., Radwan A.A., Askar A.A., Ismail M.K.A., El-Hawary A.S., Abushiba M.A. (2022), Biogenic synthesis of CuO-NPs as nanotherapeutics approaches to overcome multidrug-resistant *Staphylococcus aureus* (MDRSA), *Artificial Cells, Nanomedicine, and Biotechnology*, 50(1), pp. 260–274, https://doi.org/10.1080/21691401.2022.2126492

El-Sherbiny G.M., Shehata M.E., Kalaba M.H. (2025), Biogenic copper and copper oxide nanoparticles to combat multidrug-resistant *Staphylococcus aureus*: green synthesis, mechanisms, resistance, and future perspectives, *Biotechnology Reports*, 46, e00896, https://doi.org/10.1016/j.btre.2025.e00896

Essa H.L., Abdelfattah M.S., Marzouk A.S., Shedeed Z., Guirguis H.A., El-Sayed M.M. (2021), Biogenic copper nanoparticles from *Avicennia marina* leaves: Impact on seed germination, detoxification enzymes, chlorophyll content and uptake by wheat seedlings, *PLoS One*, 16(4), e0249764, https://doi.org/10.1371/journal.pone.0249764

Faiq N.H., Ahmed M.E. (2024), Inhibitory effects of biosynthesized copper nanoparticles on biofilm formation of *Proteus mirabilis*, *Iraqi Journal of Science*, pp. 65–78, https://doi.org/10.24996/ijs.2024.64.1.7

Fatima F., Wahid I. (2022), Eco-friendly synthesis of silver and copper nanoparticles by *Shizophyllum commune* fungus and its biomedical applications, *International Journal of Environmental Science and Technology*, 19(8), pp. 7915–7926, https://doi.org/10.1007/s13762-021-03517-6

Flores-Rabago K.M., Rivera-Mendoza D., Vilchis-Nestor A.R., Juarez-Moreno K., Castro-Longoria E. (2023), Antibacterial activity of biosynthesized copper oxide nanoparticles (CuONPs) using *Ganoderma sessile*, *Antibiotics*, 12(8), 1251, https://doi.org/10.3390/antibiotics12081251

Fouda A., Hassan S.E.D., Eid A.M., Awad M.A., Althumayri K., Badr N.F., Hamza M.F. (2022), Endophytic bacterial strain, *Brevibacillus brevis*-mediated green synthesis of copper oxide nanoparticles, characterization, antifungal, in vitro cytotoxicity, and larvicidal activity, *Green Processing and Synthesis*, 11(1), pp. 931–950, https://doi.org/10.1515/gps-2022-0080

Garcia-Marin L.E., Juarez-Moreno K., Vilchis-Nestor A.R., Castro-Longoria E. (2022), Highly antifungal activity of biosynthesized copper oxide nanoparticles against *Candida albicans*, *Nanomaterials*, 12(21), 3856, https://doi.org/10.3390/nano12213856

Ghosh M.K., Sahu S., Gupta I., Ghorai T.K. (2020), Green synthesis of copper nanoparticles from an extract of *Jatropha curcas* leaves: Characterization, optical properties, CT-DNA binding and photocatalytic activity, *RSC advances*, 10(37), pp. 22027–22035, https://doi.org/10.1039/d0ra03186k

Gregirchak N., Sinyavskaya D., Khonkiv M., Stabnikov V. (2023), Lactic acid bacteria for the synthesis of metals nanoparticles, *Ukrainian Food Journal*, 12(4), pp. 599–626, http://doi.org/10.24263/2304-974X-2023-12-4-8

Hamady S.R., Abbass I.J., Kadhim K.F. (2024), Detection of biosynthesis of CuNPs using *P. aeruginosa* isolated from soil, *International Journal of Biotech Trends and Technology-IJBTT*, 14, https://doi.org/10.14445/22490183/IJBTT-V14I1P101

Hamdy E., El-Gendi H., Al-Askar A., El-Far A., Kowalczewski P., Behiry S., Abdelkhalek A. (2024), Copper oxide nanoparticles-mediated *Heliotropium bacciferum* leaf extract: antifungal activity and molecular docking assays against strawberry pathogens, *Open Chemistry*, 22(1), 20240028, https://doi.org/10.1515/chem-2024-0028

Hamood I.A., Hamad S.A., Salman W.L. (2025), Evaluation of the inhibitory effect of copper nanoparticles synthesized by *Lactobacillus* sp. on pathogenic bacterial strains, *Indonesian Journal on Health Science and Medicine*, 2(1), https://doi.org/10.21070/ijhsm.v2i1.164

Hamouda R.A., Alharthi M.A., Alotaibi A.S., Alenzi A.M., Albalawi D.A., Makharita R.R. (2023), Biogenic nanoparticles silver and copper and their composites derived from marine alga *Ulva lactuca*: Insight into the characterizations, antibacterial activity, and anti-biofilm formation, *Molecules*, 28(17), 6324, https://doi.org/10.3390/molecules28176324

Hassabo A.A., Ibrahim E.I., Ali B.A., Emam H.E. (2022), Anticancer effects of biosynthesized Cu_2O nanoparticles using marine yeast, *Biocatalysis and Agricultural Biotechnology*, 39, 102261, https://doi.org/10.1016/j.bcab.2021.102261

Hassan E., Gahlan A.A., Gouda G.A. (2023), Biosynthesis approach of copper nanoparticles, physicochemical characterization, cefixime wastewater treatment, and antibacterial activities, *BMC chemistry*, 17(1), 71, https://doi.org/10.1186/s13065-023-00982-7

Hassan M.G., Shahin M.S., Shafie F.A., Baraka D.M., Hamed A.A. (2025), Myco-fabricated CuONPs and Ch-CuONPs conjugate mediated by the endophytic fungus *Aspergillus fumigatus* SM4 with in vitro antimicrobial, antibiofilm, antioxidant and anticancer activity, *Inorganic Chemistry Communications*, 176, 114216, https://doi.org/10.1016/j.inoche.2025.114216

Huang T., Ma K., Wang Y. (2025), Characterization and evaluation of the cytotoxic, antioxidant, and anti-human lung cancer properties of copper nanoparticles green-synthesized by fennel extract following the PI3K/AKT/Mtor signaling pathway, *PloS one*, 20(1), e0309207, https://doi.org/10.1371/journal.pone.0309207

Ibrahim F.M., Najeeb D.A., ThamerSadeq H. (2023), Green preparation of Cu nanoparticles of the avocado seed extract as an adsorbent surface, *Materials Science for Energy Technologies*, 6, pp. 130–136, https://doi.org/10.1016/j.mset.2022.12.006

Idrees S., Abbasi B.A., Iqbal J., Kazi M. (2025), *Euphorbia serpens* extracts mediated synthesis of copper oxide nanoparticles and their biological applications, *Heliyon*, 11(1), https://doi.org/10.1016/j.heliyon.2024.e41397

Ingle P.U., Shende S.S., Hande D., Rai M., Golinska P., Gade A.K. (2024), Mycogenic copper oxide nanoparticles for fungal infection management in agricultural crop plants, *Bionanoscience*, 14(1), pp. 359–367, https://doi.org/10.1007/s12668-023-01255-2

Iqbal J., Andleeb A., Ashraf H., Meer B., Mehmood A., Jan H., Zaman G., Nadeem M., Drouet S., Fazal H., Giglioli-Guivarc'h N., Hano C., Abbasi B.H. (2022), Potential antimicrobial, antidiabetic, catalytic, antioxidant and ROS/RNS inhibitory activities of *Silybum marianum* mediated biosynthesized copper oxide nanoparticles, *RSC advances*, 12(22), pp. 14069–14083, https://doi.org/10.1039/d2ra01929a

Issa K.D., Othman H.O., Amin H.I.M., Omar S.E., Jihad S.S., Rasool D.D., Ahmed A.S., Ghazali M.F., Hussain F.H. (2025), Sustainable antimicrobial and anticancer agents: eco-friendly synthesis of copper nanoparticles using *Biebersteinia multifida* DC, *Chemistry & Biodiversity*, 22(9), e202402612, https://doi.org/10.1002/cbdv.202402612

Jahan I., Erci F., Cakir-Koc R., Isildak I. (2020), Microwave-irradiated green synthesis of metallic silver and copper nanoparticles using fresh ginger (*Zingiber officinale*) rhizome extract and evaluation of their antibacterial potentials and cytotoxicity, *Inorganic and Nano-Metal Chemistry*, 51(5), pp. 722–732, https://doi.org/10.1080/24701556.2020.1808017

Jahan I., Erci F., Isildak I. (2021), Facile microwave-mediated green synthesis of non-toxic copper nanoparticles using *Citrus sinensis* aqueous fruit extract and their antibacterial potentials, *Journal of Drug Delivery Science and Technology*, 61, 102172, https://doi.org/10.1016/j.jddst.2020.102172

John M.S., Nagoth J.A., Zannotti M., Giovannetti R., Mancini A., Ramasamy K.P., Miceli C., Pucciarelli S. (2021), Biogenic synthesis of copper nanoparticles using bacterial strains isolated from an antarctic consortium associated to a psychrophilic marine ciliate: characterization and potential application as antimicrobial agents, *Marine drugs*, 19(5), 263, https://doi.org/10.3390/md19050263

Joshi R.L., Sharma H., Mehta V.N., Patel S.K., Bambharoliya K. (2025), *Azadirachta indica* derived copper oxide nanoparticles: a sustainable approach for reducing post-harvest losses and enhancing mango quality, *Food Chemistry*, 480, 143625, https://doi.org/10.1016/j.foodchem.2025.143625

Kamakshi S., Shenbhagaraman R., Jenavio Maria Amirtham P., Siva R., Lakshmanan G., Selvakumari J. (2024), Antibacterial and photo dye degradative ability of copper oxide nanoparticles from *Pleurotus cystidiosus*, *Nano Express*, 5(2), 025029, https://doi.org/10.1088/2632-959X/ad560f

Karthikeyan A., Gopinath N., Nair B.G. (2024), Ecofriendly biosynthesis of copper nanoparticles from novel marine *S. rhizophila* species for enhanced antibiofilm, antimicrobial and antioxidant potential, *Microbial Pathogenesis*, 194, 106836, https://doi.org/10.1016/j.micpath.2024.106836

Kashyap P., Shirkot P., Das R., Pandey H., Singh D. (2023), Biosynthesis and characterization of copper nanoparticles from *Stenotrophomonas maltophilia* and its effect on plant pathogens and pesticide degradation, *Journal of Agriculture and Food Research*, 13, 100654, https://doi.org/10.1016/j.jafr.2023.100654

Kasthuri K., Kumar J.K., Rajkumar P., Kalpana S., Balasubramani V. (2024), Feasible antibacterial nanomaterials: copper oxide nanoparticles synthesized using dandelion leaf extract, *Inorganic Chemistry Communications*, 167, 112804, https://doi.org/10.1016/j.inoche.2024.112804

Kataria M., Lal S., Dilbaghi N. (2025), Bacteriologically derived copper nanoparticles as novel arsenal against multidrug-resistant pathogens, *Indian Journal of Microbiology*, 65(3), pp. 1725–1733, https://doi.org/10.1007/s12088-024-01281-y

Khandelwal M., Choudhary S., Harish, Kumawat A., Misra K.P., Vyas Y., Singh B., Rathore D.S., Soni K., Bagaria A., Khangarot R.K. (2024), An eco-friendly synthesis approach for enhanced photocatalytic and antibacterial properties of copper oxide nanoparticles using *Coelastrella terrestris* algal extract, *International Journal of Nanomedicine*, pp. 4137–4162, https://doi.org/10.2147/IJN.S452889

Khandelwal M., Choudhary S., Kumawat A., Misra K.P., Rathore D.S., Khangarot, R.K. (2023), *Asterarcys quadricellulare* algae-mediated copper oxide nanoparticles as a robust and recyclable catalyst for the degradation of noxious dyes from wastewater, *RSC advances*, 13(40), pp. 28179–28196, https://doi.org/10.1039/d3ra05254k

Kimta N., Chauhan A., Puri S., Kumari A., Sharma R., Kumar A., Kapoor D. (2025), Phytomediated copper oxide nanoparticles derived from the fronds of *Adiantum venustum* D. Don: evaluation of their biomedical potential, *Applied Biochemistry and Biotechnology*, 197(1), pp. 398–426, https://doi.org/10.1007/s12010-024-05031-0

Kothari R. (2023), Green synthesis of copper nanoparticles from an extract of cinnamon bark: spectroscopic characterization, optical properties, antimicrobial, and antioxidant activities, *RASAYAN Journal of Chemistry*, 16(03), pp. 1298–1308, http://doi.org/10.31788/RJC.2023.1638274

Kouhkan M., Ahangar P., Babaganjeh L. A., Allahyari-Devin M. (2020), Biosynthesis of copper oxide nanoparticles using *Lactobacillus casei* subsp. *casei* and its anticancer and antibacterial activities, *Current Nanoscience*, 16(1), pp. 101–111, https://doi.org/10.2174/1573413715666190318l5.

Kumar M., Kaushik D., Kumar A., Gupta, P., Proestos, C., Oz, E., Orhan E., Kaur J., Khan M.R., Elobeid T., Bordiga M., Oz F. (2023), Green synthesis of copper nanoparticles from *Nigella sativa* seed extract and evaluation of their antibacterial and antiobesity activity, *International Journal of Food Science and Technology*, 58(6), pp. 2883–2892, https://doi.org/10.1111/ijfs.16359

Kumar M., Kaushik D., Kumar A., Krishnan H., Oz F., Proestos C., Hashem A., Abd Allah, E.F. (2024), A sustainable approach to prepare green synthesis of copper nanoparticles of *Bauhinia variegata* & *Saussurea lappa*: Unveiling in-vitro anti-obesity applications, *Heliyon*, 10(8), https://doi.org/10.1016/j.heliyon.2024.e29433

Kumar V., Singh Y., Kaushal S., Kumar R. (2025), Bioinspired synthesis of copper oxide nanoparticles using aqueous extracts of *Cladophora glomerata* (L.) Kuetz and their potential biomedical applications, *Bioprocess and Biosystems Engineering*, 48(4), pp. 633–646, https://doi.org/10.1007/s00449-025-03133-5

Kumari S., Raturi S., Kulshrestha S., Chauhan K., Dhingra S., Andras K., Thu K., Khargotra R., Singh, T. (2023), A comprehensive review on various techniques used for synthesizing nanoparticles, *Journal of Materials Research and Technology*, 27, pp. 1739–1763, https://doi.org/10.1016/j.jmrt.2023.09.29

Labaran A.N., Zango Z.U., Tailor G., Alsadig A., Usman F., Mukhtar M.T., Garba A.M., Alhathlool R., Ibnaouf K.H., Aldaghri O.A. (2024), Biosynthesis of copper nanoparticles using *Alstonia scholaris* leaves and its antimicrobial studies, *Scientific reports*, 14(1), 5589, https://doi.org/10.1038/s41598-024-56052-y

Liu F., Shah D.S., Csetenyi L., Gadd G.M. (2021a), Application of fungal copper carbonate nanoparticles as environmental catalysts: organic dye degradation and chromate removal, *Microbiology*, 167(12), 001116, https://doi.org/10.1099/mic.0.001116

Liu F., Shah D.S., Gadd G.M. (2021b), Role of protein in fungal biomineralization of copper carbonate nanoparticles, *Current Biology*, 31(2), pp. 358–368, https://doi.org/10.1016/j.cub.2020.10.044

Liu H., Wang G., Liu J., Nan K., Zhang J., Guo L., Liu Y. (2021c), Green synthesis of copper nanoparticles using *Cinnamomum zelanicum* extract and its applications as a highly efficient antioxidant and anti-human lung carcinoma, *Journal of Experimental Nanoscience*, 16(1), pp. 410–423, https://doi.org/10.1080/17458080.2021.1991577

Luque-Jacobo C.M., Cespedes-Loayza A.L., Echegaray-Ugarte T.S., Cruz-Loayza J.L., Cruz I., de Carvalho J.C., Goyzueta-Mamani L.D. (2023), Biogenic synthesis of copper nanoparticles: A systematic review of their features and main applications, *Molecules*, 28(12), 4838, https://doi.org/10.3390/molecules28124838

Mahal A., Mahal E., Al-Mutlaq S., Daham A.H., Sadiq J.Z., Zinad D.S., Alotaibi H.F., Mohapatra, R.K. (2024), Green synthesis and antimicrobial activity of copper nanoparticles (Cu-NPS) by *Piper longum* fruit extract, *Bulletin of the Chemical Society of Ethiopia*, 38(6), pp. 1653–1666, https://doi.org/10.4314/bcse.v38i6.12

Mali S.C., Dhaka A., Githala C.K. Trivedi R. (2020), Green synthesis of copper nanoparticles using *Celastrus paniculatus* Willd. leaf extract and their photocatalytic and antifungal properties, *Biotechnology Reports*, 27, e00518, https://doi.org/10.1016/j.btre.2020.e00518

Marzban A., Mirzaei S.Z., Karkhane M., Ghotekar S.K., Danesh A. (2022), Biogenesis of copper nanoparticles assisted with seaweed polysaccharide with antibacterial and antibiofilm properties against methicillin-resistant *Staphylococcus aureus*, *Journal of Drug Delivery Science and Technology*, 74, 103499, https://doi.org/10.1016/j.jddst.2022.103499

Mitra S., Dua T.K., Easmin S., Sarkar S., Roy A.P., Sahu R., Nandi G., Haydar S., Roy S., Paul P. (2024), Green synthesis of copper nanoparticles by using pineapple peel waste: *in vitro* characterizations and antibacterial potential, *Bioprocess and Biosystems Engineering*, 47(8), pp. 1151–1161, https://doi.org/10.1007/s00449-024-02982-w

Moeini F., Doudi M., Karvani Z.E., Fouladgar M. (2024), Biosorption of copper, nickel, and manganese as well as the production of metal nanoparticles by *Bacillus species* isolated from soils contaminated with

electronic wastes, *Brazilian Journal of Microbiology*, 55(3), pp. 2131–2147, https://doi.org/10.1007/s42770-024-01369-z

Mohamed S.H., Othman B.A., Abd-Elhalim B.T., Seada M.N.A. (2024), Copper nanoparticles biosynthesis by *Priestia megaterium* and its application as antibacterial and antitumor agents, *Scientific Reports*, 14(1), 23615, https://doi.org/10.1038/s41598-024-72598-3

Mousa A.M., Aziz O.A.A., Al-Hagar O.E., Gizawy M.A., Allan K.F., Attallah M.F. (2020), Biosynthetic new composite material containing CuO nanoparticles produced by *Aspergillus terreus* for ^{47}Sc separation of cancer theranostics application from irradiated Ca target, *Applied Radiation and Isotopes*, 166, 109389, https://doi.org/10.1016/j.apradiso.2020.109389

Murthy H.A., Desalegn T., Kassa M., Abebe B., Assefa T. (2020), Synthesis of green copper nanoparticles using medicinal plant *Hagenia abyssinica (Brace) JF. Gmel.* leaf extract: Antimicrobial properties, *Journal of Nanomaterials*, 2020(1), 3924081, https://doi.org/10.1155/2020/3924081

Naikoo G., Al-Mashali F., Arshad F., Al-Maashani N., Hassan I.U., Al-Baraami Z., Faruck L.H., Qurashi A., Ahmed W., Asiri A.M., Aljabali A.A., Bakshi H.A., Tambuwala M.M. (2021), An overview of copper nanoparticles: synthesis, characterisation and anticancer activity, *Current Pharmaceutical Design*, 27(43), pp. 4416–4432, https://doi.org/10.2174/1381612827666210804100303

Nassar A.R.A., Atta H.M., Abdel-Rahman M.A., El Naghy W.S., Fouda A. (2023), Myco-synthesized copper oxide nanoparticles using harnessing metabolites of endophytic fungal strain *Aspergillus terreus*: an insight into antibacterial, anti-*Candida*, biocompatibility, anticancer, and antioxidant activities, *BMC Complementary Medicine and Therapies*, 23(1), 261, https://doi.org/10.1186/s12906-023-04056-y

Nazir A., Alam S., Alwadai N., Abbas M., Bibi I., Ali A., Ahmad N., Huwayz M., Iqbal M. (2023), Green synthesis of copper nanoparticles using *Citrullus colocynthis* leaves extract: photocatalytic, antimicrobial and antioxidant studies, *Zeitschrift für Physikalische Chemie*, 237(11), pp. 1733–1751, https://doi.org/10.1515/zpch-2023-0331

Nguyen T.D., Hoang Y.H., Thai N.T.T., Trinh G.T.N. (2024), Synthesis of copper nanoparticles by a sonication-mediated method using *Malpighia glabra* fruit extract and their applications, *RSC Advances*, 14(46), pp. 34119–34134, https://doi.org/10.1039/d4ra06087c

Nkosi N.C., Basson A.K., Ntombela Z.G., Dlamini N.G., Pullabhotla R.V. (2025), Green synthesis of copper nanoparticles using a bioflocculant from *Proteus mirabilis* AB 932526.1 for wastewater treatment and antimicrobial applications, *Applied Nano*, 6(1), 5, https://doi.org/10.3390/applnano6010005

Noman M., Ahmed T., Shahid M., Niazi M.B.K., Qasim M., Kouadri F., Abdulmajeed A.M., Alghanem S.M., Ahmad N., Zafar M., Ali S. (2021), Biogenic copper nanoparticles produced by using the *Klebsiella pneumoniae* strain NST2 curtailed salt stress effects in maize by modulating the cellular oxidative repair mechanisms, *Ecotoxicology and Environmental Safety*, 217, 112264, https://doi.org/10.1016/j.ecoenv.2021.112264

Noman M., Shahid M., Ahmed T., Niazi M.B.K., Hussain S., Song F., Manzoor I. (2020a), Use of biogenic copper nanoparticles synthesized from a native *Escherichia* sp. as photocatalysts for azo dye degradation and treatment of textile effluents, *Environmental Pollution*, 257, 113514, https://doi.org/10.1016/j.envpol.2019.113514

Noman M., Shahid M., Ahmed T., Tahir M., Naqqash T., Muhammad S., Song F., Abid H.M.A, Aslam Z. (2020b), Green copper nanoparticles from a native *Klebsiella pneumoniae* strain alleviated oxidative stress impairment of wheat plants by reducing the chromium bioavailability and increasing the growth, *Ecotoxicology and Environmental Safety*, 192, 110303, https://doi.org/10.1016/j.ecoenv.2020.110303

Noor S., Hassan M.A., Aslam M.A., Muhammad S.A., Quosain Naqvi T., Batool Alvi G., Nagaraj H., Hussain S.B., Rotello V.M. (2025), Fungal biosystems for the fabrication of copper nanoparticles: an effective approach for the treatment of bacterial biofilms, *ACS Applied Materials & Interfaces*, 17(30), pp. 42706–42716, https://doi.org/10.1021/acsami.5c07764

Noor S., Shah Z., Javed A., Ali A., Hussain S.B., Zafar S., Ali H., Muhammad S.A. (2020), A fungal based synthesis method for copper nanoparticles with the determination of anticancer, antidiabetic and antibacterial activities, *Journal of Microbiological Methods*, 174, 105966, https://doi.org/10.1016/j.mimet.2020.105966

Ogwuegbu M.C., Ayangbenro A.S., Mthiyane D.M., Babalola O.O., Onwudiwe D.C. (2024), Green synthesis of CuO nanoparticles using *Ligustrum lucidum* extract, and the antioxidant and antifungal evaluation, *Materials Research Express*, 11(5), 055010, https://doi.org/10.1088/2053-1591/ad4e9d

Oraibi A.G., Rashad A.A., Ahmed M.H. (2023), *Carum carvi* mediated green synthesis of copper nanoparticles and its effect on *Solanum lycopersicum* seedlings, *Journal of Aridland Agriculture*, 9, pp. 9–15, https://doi.org/10.25081/jaa.2023.v9.8191

Park Y., Eyal Z., Pekker P., Chevrier D.M., Lefèvre C.T., Arnoux P., Armengaud J., Monteil C.L., Gal A., Posfai M., Faivre D. (2022), Periplasmic bacterial biomineralization of copper sulfide nanoparticles, *Advanced Science*, 9(28), 2203444, https://doi.org/10.1002/advs.202203444

Pathak R., Punetha V.D., Bhatt S., Punetha M. (2024), A review on copper-based nanoparticles as a catalyst: synthesis and applications in coupling reactions, *Journal of Materials Science*, 59(15), pp. 6169–6205, https://doi.org/10.1007/s10853-024-09546-z

Philip R.R., Seetharaman J., Priya R.A., Vedakumari S.W., Sankari D. (2025), Biogenic synthesis and characterization of copper nanoparticles using *Crossandra infundibuliformis* leaves and evaluation of antimicrobial, antioxidant, cytotoxic analysis and wound healing activity on HaCaT cells, *3 Biotech*, 15(6), 194, https://doi.org/10.1007/s13205-025-04360-z

Pramanik P., Dakua K., Kar T., Sahu R., Dua T. K., Nandi G., Dey S., Kumar A., Khanra R., Paul P. (2025), Biosynthesis and in-vitro characterizations of copper oxide nanoparticle using *Mangifera indica* seed kernel extract and assessment of pharmacological properties, *Hybrid Advances*, 8, 100375, https://doi.org/10.1016/j.hybadv.2024.100375

Radhakrishnan S., Balasubramanian B., Kavibharath S., Thangaraj N., Paramasivam D., Kamyab H., Manon Mani V., Chelliapan S., Khalili E. (2025), Synthesis and therapeutic potential of copper oxide nanoparticles from endophytic fungi: anti-cancer activities and mechanisms, *Bioorganic Chemistry*, 163, 108679, https://doi.org/10.1016/j.bioorg.2025.108679

Rajamma R., Gopalakrishnan Nair S., Abdul Khadar F., Baskaran B. (2020), Antibacterial and anticancer activity of biosynthesised CuO nanoparticles, *IET Nanobiotechnology*, 14(9), pp. 833–838, https://doi.org/10.1049/iet-nbt.2020.0088

Rajeshkumar S., Nandhini N.T., Manjunath K., Sivaperumal P., Prasad G.K., Alotaibi S.S., Roopan S.M. (2021), Environment friendly synthesis copper oxide nanoparticles and its antioxidant, antibacterial activities using seaweed (*Sargassum longifolium*) extract, *Journal of Molecular Structure*, 1242, 130724,https://doi.org/10.1016/j.molstruc.2021.130724

Rambau U., Masevhe N. A., Samie A. (2024), Green synthesis of gold and copper nanoparticles by *Lannea discolor*: characterization and antibacterial activity, *Inorganics*, 12(2), 36, https://doi.org/10.3390/inorganics12020036

Rani S., Dhankher S., Kumar P., Dahiya P., Arora K., Dang A.S., Suneja P. (2025a), Biosynthesis, optimization, and characterization of CuNPs using *Bacillus licheniformis* CPJN13S and their antibacterial activity, *Frontiers in Nanotechnology*, 7, 1663115, https://doi.org/10.3389/fnano.2025.1663115

Rani S., Kumar P., Dahiya P., Mehta A., Dang A.S., Suneja P. (2025b), Optimization, characterization and antibacterial activity of copper nanoparticles biosynthesized using *Pantoea agglomerans* CPHN2, *Indian Journal of Microbiology*, 65(2), pp. 1345–1356, https://doi.org/10.1007/s12088-025-01455-2

Rasheed R., Uzair B., Raza A., Binsuwaidan R., Alshammari N. (2024), Fungus-mediated synthesis of Se-BiO-CuO multimetallic nanoparticles as a potential alternative antimicrobial against ESBL-producing *Escherichia coli* of veterinary origin, *Frontiers in Cellular and Infection Microbiology*, 14, 1301351, https://doi.org/10.3389/fcimb.2024.1301351

Rautela G., Rizvi R., Ansari S. (2025), Role of biosynthesized copper nanoparticles in agriculture and other fields, *Journal of Nanoscience and Technology*, 10(1), pp. 990–994, https://doi.org/10.30799/jnst.351.25100102

Rivera-Mendoza D., Quiñones B., Huerta-Saquero A., Castro-Longoria E. (2024), Antimicrobial activity of green synthesized silver and copper oxide nanoparticles against the foodborne pathogen *Campylobacter jejuni*, *Antibiotics*, 13(7), 650, https://doi.org/10.3390/antibiotics13070650

Romi Z.M., Ahmed M.E. (2024), The influence of biologically synthesized copper nanoparticles on the biofilm produced by *Staphylococcus haemolyticus* isolated from seminal fluid, *Iraqi Journal of Science*, pp. 1948-1968, https://doi.org/10.24996/ijs.2024.65.4.15

Roslan R.A., Zakaria N.A., Mohamad S.A.S., Yunus N.M., Ahmad L.W.Z. (2025), Autoclave-assisted mycosynthesis of copper nanoparticles from *Pleurotus ostreatus* extract: characterisation and toxicity analysis, *Sarhad Journal of Agriculture*, 41(5), https://doi.org/10.17582/journal.sja/2025/41.5.34.47

Sadia B.O., Cherutoi J.K., Achisa C.M. (2021), Optimization, characterization, and antibacterial activity of copper nanoparticles synthesized using *Senna didymobotrya* root extract, *Journal of Nanotechnology*, 2021(1), 5611434, https://doi.org/10.1155/2021/5611434

Saeedi N.H., Alanazi A.D., Alenazy R., Shater A.F. (2025), Antimicrobial, anti-inflammatory, angiogenesis, and wound healing activities of copper nanoparticles green synthesized by *Lupinus arcticus* extract, *Iranian journal of pharmaceutical research: IJPR*, 24(1), e147434, https://doi.org/10.5812/ijpr-147434

Sahib O.H., Mohammed L.Z., Mahdi M.A. (2025), Biosynthesis of copper nanoparticles using *Passiflora* flower extract and study their antimicrobial, antioxidant and anticancer activity, *Asian Pacific Journal of Cancer Prevention: APJCP*, 26(8), 2953, https://doi.org/10.31557/APJCP.2025.26.8.2953

Saleem M.H., Ejaz U., Vithanage M., Bolan N., Siddique K. H. (2025), Synthesis, characterization, and advanced sustainable applications of copper oxide nanoparticles: a review, *Clean Technologies and Environmental Policy*, 27(10), pp. 5719–5744, https://doi.org/10.1007/s10098-024-02774-6

Salvadori M.R., Ando R.A., Oller do Nascimento C.A., Correa B. (2014), Intracellular biosynthesis and removal of copper nanoparticles by dead biomass of yeast isolated from the wastewater of a mine in the Brazilian Amazonia, *PLoS One*, 9(1), e87968, https://doi.org/10.1371/journal.pone.0087968

Santos X., Dominguez G., Rodriguez J., Pozuelo J., Hernandez M., Martin O., Fajardo C. (2024), Evaluation of PLA-based composite films filled with $Cu_2(OH)_3NO_3$ nanoparticles as an active material for the food industry: biocidal properties and environmental sustainability, *Polymers*, 16(13), 1772, https://doi.org/10.3390/polym16131772

Sazak C., Attar A., Yilmaz A., Altikatoglu Yapaoz M. (2023), Biofabrication of *Acer palmatum*-mediated multifunctional CuO nanoparticles for dye removal, antibacterial – antifungal activity, and molecular docking, *ACS Omega*, 8(40), pp. 36835–36844, https://doi.org/10.1021/acsomega.3c03591

Scattareggia Marchese A., Destro E., Boselli C., Barbero F., Malandrino M., Cardeti G., Fenoglio I., Lanni L. (2022), Inhibitory effect against listeria monocytogenes of carbon nanoparticles loaded with copper as precursors of food active packaging, *Foods*, 11(19), 2941, https://doi.org/10.3390/foods11192941

Senthilkumar A., Muthuswamy R., Nallal U.M., Ramaiyan S., Kannan P., Muthupandi S., Lakshminarayanan S.P., Sambasivam S., Ayyar M. (2024), Green synthesis of copper nanoparticles from agro-waste garlic husk, *Zeitschrift für Physikalische Chemie*, 238(1), pp. 75–88, https://doi.org/10.1515/zpch-2023-0291

Shah I.H., Sabir I.A., Ashraf M., Rehman A., Ahmad Z., Azam M., Ashraf G.A., Rashid H., Li G., Mouna J., Faizan M., Altaf M.A., Shakoor A., Song C., Manzoor M.A. (2024), Phyto-fabrication of copper oxide nanoparticles (NPs) utilizing the green approach exhibits antioxidant, antimicrobial, and antifungal activity in *Diospyros kaki* fruit, *Fruit Research*, 4, e022, https://doi.org/10.48130/frures-0024-0015

Shehabeldine A.M., Amin B.H., Hagras F.A., Ramadan A.A., Kamel M.R., Ahmed M.A., Atia K.H., Salem S.S. (2023), Potential antimicrobial and antibiofilm properties of copper oxide nanoparticles: time-kill kinetic essay and ultrastructure of pathogenic bacterial cells, *Applied Biochemistry and Biotechnology*, 195(1), pp. 467–485, https://doi.org/10.1007/s12010-022-04120-2

Shende S., Bhagat R., Raut R., Rai M., Gade A. (2021), Myco-fabrication of copper nanoparticles and its effect on crop pathogenic fungi, *IEEE Transactions on NanoBioscience*, 20(2), pp. 146–153, https://doi.org/10.1109/TNB.2021.3056100

Shubhashree K.R., Reddy R., Gangula A.K., Nagananda G.S., Badiya P.K., Ramamurthy, S.S., Aramwit P., Reddy N. (2022), Green synthesis of copper nanoparticles using aqueous extracts from *Hyptis suaveolens* (L.), *Materials Chemistry and Physics*, 280, 125795, https://doi.org/10.1016/j.matchemphys.2022.125795

Siddiqi K.S., Husen A. (2020), Current status of plant metabolite-based fabrication of copper/copper oxide nanoparticles and their applications: a review, *Biomaterials Research*, 24(1), 11, https://doi.org/10.1186/s40824-020-00188-1

Singh D., Jain D., Rajpurohit D., Jat G., Kushwaha H.S., Singh A., Mohanty S.R., Al-Sadoon M.K., Zaman W., Upadhyay S.K. (2023), Bacteria assisted green synthesis of copper oxide nanoparticles and their potential applications as antimicrobial agents and plant growth stimulants, *Frontiers in Chemistry*, 11, 1154128, https://doi.org/10.3389/fchem.2023.1154128

Soliman M.K., Salem S.S. (2025), Comparative evaluation of antimicrobial, antibiofilm, antioxidant, antiviral, and antidiabetic activities of copper oxide nanoparticles biofabricated via *Opuntia ficus indica*, *Scientific Reports*, 15(1), 24823, https://doi.org/10.1038/s41598-025-08878-3

Solorzano Toala R., Gutierrez-Miceli F., Valdez-Salas B., Beltran-Partida E., Gonzalez-Mendoza D., Tzintzun-Camacho O., Grimaldo-Juarez O., Basilio-Cortes A. (2024), Biosynthesis of copper nanoparticles from *Acacia cornigera* and *Annona purpurea* and their insecticidal effect against *Tribolium castaneum*, *Reactions*, 5(2), pp. 274–284, https://doi.org/10.3390/reactions5020013

Soureshjani P.T., Shadi A., Mohammadsaleh F. (2021), Algae-mediated route to biogenic cuprous oxide nanoparticles and spindle-like $CaCO_3$: a comparative study, facile synthesis, and biological properties, *RSC Advances*, 11(18), pp. 10599–10609, https://doi.org/10.1039/d1ra00187f

Sriramulu M., Shanmugam S., Ponnusamy V.K. (2020), *Agaricus bisporus* mediated biosynthesis of copper nanoparticles and its biological effects: an in-vitro study, *Colloid and Interface Science Communications*, 35, 100254, https://doi.org/10.1016/j.colcom.2020.100254

Stabnikov V., Kovshar I., Stabnikova O. (2025), Recent advances in the study of the properties and applications of lactic acid bacteria, *World Journal of Microbiology and Biotechnology*, 41, 287, https://doi.org/10.1007/S11274-025-04499-0

Stabnikova O., Khonkiv M., Kovshar I., Stabnikov V. (2023), Biosynthesis of selenium nanoparticles by lactic acid bacteria and areas of their possible applications, *World Journal of Microbiology and Biotechnology*, 39, 230, https://doi.org/10.1007/s11274-023-03673-6

Suood A.M., Saleh M.K., Thalij K.M. (2021), Synthesis of copper nanoparticles using *Aspergillus niger* and their efficacy against pathogenic *Staphylococcus aureus*, *IOP conference series: Earth and environmental science* 910(1), 012083, https://doi.org/10.1088/1755-1315/910/1/012083

Sus B., Baltaci M.O., Nadaroglu H., Adiguzel A. (2024), From agro-food waste to nanoparticles: green synthesis of copper nanoparticles with lignin peroxidase enzyme produced by *Anoxybacillus rupiensis* using peanut shells, *Environmental Science and Pollution Research*, 31(39), pp. 52049–52059, https://doi.org/10.1007/s11356-024-34489-y

Tahir A., Quispe C., Herrera-Bravo J., Iqbal H., Anum F., Javed Z., Sehar A., Sharifi-Rad J. (2022), Green synthesis, characterization and antibacterial, antifungal, larvicidal and anti-termite activities of copper nanoparticles derived from *Grewia asiatica* L., *Bulletin of the National Research Centre*, 46(1), 188, https://doi.org/10.1186/s42269-022-00877-y

Talebian S., Shahnavaz B., Nejabat M., Abolhassani Y., Rassouli F.B. (2023), Bacterial-mediated synthesis and characterization of copper oxide nanoparticles with antibacterial, antioxidant, and anticancer potentials, *Frontiers in Bioengineering and Biotechnology*, 11, 1140010, https://doi.org/10.3389/fbioe.2023.1140010

Tarangini K., Sherlin S.N., Jakkala S., Borah P., Wacławek S., Sabarinath S., Rao K.J., Padil V.V. (2024), Optimising biosynthesis of antimicrobial copper nanoparticles using aqueous *Aegle marmelos* leaf extract-based medium, *Ecological Chemistry and Engineering S*, 31(1), pp. 7–17, https://doi.org/10.2478/eces-2024-0001

Tejaswi T.S., Devi P.S. (2025), Biogenesis of copper oxide nanoparticles using marine bacteria *Pseudomonas aeruginosa*: in vitro antimicrobial and photocatalytic activities, *Journal of Pure & Applied Microbiology*, 19(1), https://doi.org/10.22207/JPAM.19.1.12

Tsilo P.H., Basson A.K., Ntombela Z.G., Dlamini N.G., Pullabhotla R.V. (2023), Biosynthesis and characterization of copper nanoparticles using a bioflocculant produced by a yeast *Pichia kudriavzevii* isolated from Kombucha tea SCOBY, *Applied Nano*, 4(3), pp. 226–239, https://doi.org/10.3390/applnano4030013

Tyagi S., Kumar A., Tyagi P.K., Hatami M. (2024), Development and characterization of biogenic copper oxide nanoparticles, with an exploration of their antibacterial and antioxidant potential, *3 Biotech*, 14(1), 20, https://doi.org/10.1007/s13205-023-03869-5

Ullah I., Ullah A., Al-Qaaneh A.M., Aman K., Bekhit M.M., Ullah, I. Zengin G., Farid, A. (2024), Green synthesis of silver and copper nanoparticles using *Parthenium hysterophorus*: antibacterial, antioxidant, and anticancer properties, *ChemistrySelect*, 9(40), e202401573, https://doi.org/10.1002/slct.202401573

Vakili N., Ashengroph M., Sharifi A., Zorab M.M. (2025), Eco-friendly synthesis of copper nanoparticles by using *Ralstonia* sp. and their antibacterial, anti-biofilm, and antivirulence activities, *Biochemistry and Biophysics Reports*, 42, 101978, https://doi.org/10.1016/j.bbrep.2025.101978

Vijayakumar G., Kesavan H., Kannan A., Arulanandam D., Kim J.H., Kim K.J., Song H.J., Kim H.J., Rangarajulu S.K. (2021), Phytosynthesis of copper nanoparticles using extracts of spices and their antibacterial properties, *Processes*, 9(8), 1341, https://doi.org/10.3390/pr9081341

Vincent J., Lau K.S., Evyan Y.C.Y., Chin S.X., Sillanpää M., Chia C.H. (2022), Biogenic synthesis of copper-based nanomaterials using plant extracts and their applications: current and future directions, *Nanomaterials*, 12(19), 3312, https://doi.org/10.3390/nano12193312

Wang W., Liu L., Han, Z. (2024), Effect of copper nanoparticles green-synthesized using *Ocimum basilicum* against *Pseudomonas aeruginosa* in mice lung infection model, *Open Chemistry*, 22(1), 20240062, https://doi.org/10.1515/chem-2024-0062

Waqif H., Munir N., Farrukh M.A., Hasnain M., Sohail M., Abideen Z. (2024), Algal macromolecular mediated synthesis of nanoparticles for their application against citrus canker for food security, *International Journal of Biological Macromolecules*, 263, 130259, https://doi.org/10.1016/j.ijbiomac.2024.130259

Wu S., Rajeshkumar S., Madasamy M., Mahendran V. (2020), Green synthesis of copper nanoparticles using *Cissus vitiginea* and its antioxidant and antibacterial activity against urinary tract infection pathogens, *Artificial Cells, Nanomedicine, and Biotechnology*, 48(1), pp. 1153–1158, https://doi.org/10.1080/21691401.2020.1817053

Yadava Y.P., Raju V., Chathoth A.M., Vasu A.E., Vijayaraghavan R., Surendran A.K. (2025), Characterization and antifungal potential of green-synthesized copper nanoparticles using waste leaf biomass, *Chemical Papers*, 79(8), pp. 5261–5275, https://doi.org/10.1007/s11696-025-04124-2

Yu W., Tang J., Gao C., Zheng X., Zhu P. (2025), Green synthesis of copper nanoparticles from the aqueous extract of *Lonicera japonica* thunb and evaluation of its catalytic property and cytotoxicity and antimicrobial activity, *Nanomaterials*, 15(2), 91, https://doi.org/10.3390/nano15020091

Zaki S.A.E.F., Kamal A., Ashmawy N.A., Shoeib A.A. (2021), Nano-metals forming bacteria in Egypt. I. Synthesis, characterization and effect on some phytopathogenic bacteria in vitro, *Scientific Reports*, 11(1), 12876, https://doi.org/10.1038/s41598-021-92171-6

Zaynitdinova L.I., Tashpulatov J.J., Lazutin N.A., Juraeva R.N., Mavjudova A.M. (2025), Biosynthesis of copper nanoparticles by cultures from collection of microorganisms, *Proceedings of the Pakistan Academy of Sciences: B. Life and Environmental Sciences*, 62(1), pp. 19–24, https://doi.org/10.53560/PPASB(61-4)864

Zhou Y., Nguyen H.N., Peña-Bahamonde J., Robles-Hernandez F.C., Gimenes L.J., Rodrigues D.F. (2024), The role of secondary metabolites in the production of CuO nanoparticles by fungi: a physiological and metabolic approach, *Environmental Science: Nano*, 11(11), pp. 4487–4500, https://doi.org/10.1039/d4en00403e

Zvab U., Kukulin D.S., Fanetti M., Valant M. (2021), Bioremediation of copper polluted wastewater-like nutrient media and simultaneous synthesis of stable copper nanoparticles by a viable green alga, *Journal of Water Process Engineering*, 42, 102123, https://doi.org/10.1016/j.jwpe.2021.102123

Cite:

Skrotska, O., & Holubiev, P. (2026). Biological synthesis of copper nanoparticles using plants, microorganisms and other natural resources. *Ukrainian Food Journal, 15*(2), 455–502. https://doi.org/10.24263/2304-974X-2026-15-2-12

Utilization of plant biomass and agro-industrial waste for low-cost biocementation processes

Iryna Kovshar, Viktor Udymovych, Viktor Stabnikov

National University of Food Technologies, Kyiv, Ukraine

Keywords:

Biocementation
MICP
EICP
Urease
Waste
Soybean meal hydrolysate

Article history:

Received 29.10.2025
Received in revised form 01.03.2026
Accepted 30.06.2026

Corresponding author:

Iryna Kovshar
E-mail: irynakovshar @ukr.net

DOI:
10.24263/2304-974X-2026-15-2-13

Abstract

Introduction. Biocement is a promising alternative to conventional cement technologies, but its application is limited by high cost. This study evaluated plant materials and soybean-processing wastes as low-cost resources for biocementation.

Materials and methods. Urease activity was determined conductometrically in plant materials and soybean processing products. The effects of nickel salt supplementation to soil and urea concentration during seed germination on urease activity were evaluated using soybean as a model plant. Soybean meal hydrolysate was prepared by acid hydrolysis and used as a cultivation medium for *Bacillus* sp. VUK5. Bacterial growth, viable cell density, pH, and urease activity were compared with those obtained in tryptic soy broth (TSB) and yeast extract medium.

Results and discussion. The highest urease activity among the studied samples was observed in Hokkaido pumpkin seeds (167.83±2.55 μM urea/min/g), soy milk (123.17±1.65 μM urea/min/mL), soybean meal (97.00±1.06 μM urea/min/g), and okara (90.07±1.15 μM urea/min/g), indicating significant variability in enzymatic activity depending on the plant matrix and processing type. Dried soybean leaves, stems, and pods after long-term storage exhibited 1.2–3.1 times higher urease activity than fresh samples, which may be associated with structural degradation of tissues and improved enzyme accessibility or release during storage. Addition of $NiCl_2$ to soil exerted a stronger stimulatory effect than $NiSO_4$. Urease activity increased in soybean plants grown at low nickel concentrations, reaching a maximum at 50 mg/kg for both nickel salts. In contrast, germination of soybean seeds in the presence of urea resulted in a progressive decrease in urease activity with increasing urea concentration. Soybean meal hydrolysate proved to be the most favorable medium for *Bacillus* sp. VUK5 cultivation, providing the highest biomass accumulation (>5 g dry biomass/L), viable cell density (up to 8 $\log_{10}$ CFU/mL), and urease activity (423.44 μM urea/min after 72 h of cultivation), thereby demonstrating its suitability as a nutrient-rich alternative to conventional media. In comparison, TSB supported moderate biomass production (approximately 4.5 g/L) and urease activity (approximately 200 μM urea/min), whereas yeast extract medium showed the lowest biomass accumulation (approximately 2.2 g/L) and the weakest urease production, confirming its lower efficiency for this strain.

Conclusions. Soybean-based materials showed variable urease activity, with soybean meal, soy milk, and okara exhibiting the highest levels. Soybean meal hydrolysate was the effective medium for urease-producing bacteria cultivation.

Introduction

Cement production is a major source of anthropogenic carbon dioxide emissions. According to the International Energy Agency (IEA) and the Intergovernmental Panel on Climate Change (IPCC), the cement industry accounts for approximately 7–8% of global CO_2 emissions. These emissions arise both from the high energy demand of clinker production at temperatures of approximately 1400–1500 °C and from the decarbonation of carbonate raw materials during thermal processing (IEA, 2023; IPCC, 2022). Consequently, alternative low-carbon technologies are being actively developed, among which biocementation is considered a promising approach in sustainable construction materials science (Ivanov and Stabnikov, 2017).

Biocementation is a process of biologically induced calcium carbonate precipitation that fills the pore space of materials such as sand or soil, thereby increasing their strength and reducing water permeability. Biocementation comprises two main approaches: microbial-induced calcium carbonate precipitation (MICP), which relies on metabolically active urease-producing microorganisms, and enzyme-induced calcium carbonate precipitation (EICP), which uses free urease extracted from biological sources (Ivanov et al., 2019; Zhang et al., 2022). MICP is primarily based on the ureolytic pathway, in which urease catalyses urea hydrolysis, generating carbonate ions and increasing the pH, thereby creating favourable conditions for $CaCO_3$ precipitation (Carter et al., 2023; Chu et al., 2012). The most extensively studied microorganism is *Sporosarcina pasteurii* due to its high and stable urease activity (Lapierre and Huber, 2024; Stabnikov et al., 2025). Members of the genus *Bacillus* (particularly *Bacillus megaterium* and *Bacillus sphaericus*) are also considered promising urease-producing bacteria (Chu et al., 2012; Wani et al., 2024). Enzyme-induced calcium carbonate precipitation (EICP) employs urease derived from biological sources, particularly plant materials. Plant-derived urease is considered a potentially lower-cost alternative for biocementation because it eliminates the need for microbial cultivation while maintaining the catalytic function required for $CaCO_3$ precipitation (Ahenkorah et al., 2021; Dilrukshi et al., 2018; Stabnikov et al., 2022).

Despite the effectiveness of urease-producing microorganisms in MICP, their industrial cultivation is associated with several limitations. The main challenge is the high cost of nutrient media, particularly commercial complex media such as tryptic soy broth (TSB), which provide high urease activity but are economically unfavorable for large-scale applications. Less expensive yeast extract-based media may serve as alternatives; however, reduced urease activity and slower biocementation rates have been reported for certain strains compared with commercial media (Abharian et al., 2026; Erdmann et al., 2023).

In this context, plant materials and agro-industrial wastes can be considered multifunctional resources for biocementation processes. Waste products (e.g., soybean meal, oil cake, and texture) and plant materials (e.g., seeds) may serve as inexpensive urease sources for EICP processes (Khodadadi et al., 2020; Liu et al., 2024). After preliminary treatment (e.g., hydrolysis), such materials may also serve as a basis for the formulation of alternative nutrient media (Chaparro et al., 2021; Cuzman et al., 2015). This approach enables the partial or complete replacement of expensive commercial nutrient media while maintaining urease production for MICP applications.

Soybean is one of the most important agricultural crops worldwide, and Ukraine is among the leading soybean producers in Europe. According to Donau Soja (2024), total soybean production in Europe exceeds 13 million tons per year, with Ukraine accounting for the largest share among European countries (Table 1).

Table 1

Global soybean production

Country	Production, Mt/year	Note	Source
Brazil	152	Largest producer in the world	Stockholm Environment Institute, 2025
USA	115	Second-largest producer	Statista, 2026
Argentina	49	One of the leading global producers	UkrAgroConsult, 2026
Ukraine	>6	Largest producer in Europe	Donau Soja, 2024

This substantial production ensures a stable supply of raw materials and soybean processing by-products, highlighting soybean as a promising and sustainable substrate for urease activity assessment and biocementation applications.

The aim of this study was to evaluate plant materials and agro-industrial wastes as alternative urease sources and nutrient substrates for EICP- and MICP-based biocementation processes, and to investigate soybean (*Glycine max* L.) as a model biocementation material, focusing on its urease activity, the effect of material condition (fresh and frozen) on enzyme activity, and the use of soy processing waste as a nutrient medium for the cultivation of urease-producing bacteria.

Materials and methods

Microorganisms

Bacillus sp. VUK5 was isolated from Ukrainian soils and characterized as a urease-producing, halo- and alkali-tolerant Gram-positive bacterium. Phylogenetic analysis based on the 16S rRNA gene showed high similarity (≈99%) to members of the genus *Bacillus* originating from diverse ecological niches, including marine and soil environments (Stabnikov et al., 2013).

Materials

The plant materials used in this study included soybean (*Glycine max* L.), pea (*Pisum sativum* L.), common bean (*Phaseolus vulgaris* L.), chickpea (*Cicer arietinum* L.), mung bean (*Vigna radiata* L.), red and green lentils (*Lens culinaris* L.), and pumpkin seeds of the Butternut (*Cucurbita moschata* 'Butternut') and Hokkaido (*Cucurbita maxima* 'Red Kuri') varieties, purchased from retail stores in Kyiv, Ukraine.

Soybean agro-industrial by-products (soybean meal, soybean cake, soybean texturate, and soy protein isolate) were obtained from local online marketplaces (prom.ua). Vegetative plant materials, including soybean leaves, stems, and pods, as well as leaves of white mulberry (*Morus alba* L.) and black mulberry (*Morus nigra* L.), were collected in the Kyiv region.

Technical-grade urea (98% purity) and ammonium chloride (analytical grade, Himlaborreactiv, Ukraine) were used for urease activity assays in plant samples. Nickel salts, including nickel sulfate ($NiSO_4$) and nickel chloride ($NiCl_2$) (analytical grade,

Himlaborreactiv, Ukraine), were used to investigate the effect of nickel ions on soybean urease activity.

Preparation of plant raw material and agro-industrial waste samples for urease activity determination

To determine urease activity, 1 g of plant material was homogenized in a mortar with 10 mL of distilled water adjusted to the required pH value (7.0–8.0). The resulting suspension was transferred into a 50 mL beaker, followed by the addition of 40 mL of 1 M urea solution. Prepared samples were subsequently used for urease activity determination.

Preparation of plant milk and okara samples from legume seeds for urease activity determination

To obtain plant milk and okara, legume seeds (soybean, pea, bean, chickpea, mung bean, red lentil, and green lentil) were pre-soaked in distilled water at a 1:2 ratio (100 g seeds per 200 mL distilled water) for 12 h. After soaking, the seeds together with water were blended until a homogeneous suspension was formed. The suspension was filtered through a gauze filter to separate the liquid fraction (plant milk) from the solid residue (okara). Obtained samples were used for subsequent urease activity determination.

Drying of soybean leaves, stems, and pod samples

The study used fresh samples of soybean leaves, stems and pods, as well as samples of the same plant parts that were frozen (–18 °C) and stored frozen for a long time (1 year). To determine moisture content, plant material was dried in a drying oven at 105 °C until constant weight was achieved. Moisture values were considered when recalculating urease activity to constant dry weight.

Moisture content was determined using the equation:

$$W = \frac{m_1 - m_2}{m_1} \times 100\%$$

where: m_1 is sample mass before drying, g; m_2 is sample mass after drying (constant dry weight), g

Determination of urease activity

Urease activity (UA) was determined by the amount of ammonium released from 1 M urea solution per minute. The amount of ammonium formed from urea hydrolysis was measured using a conductivity meter (Bante901, Bante Instruments Limited, China), which demonstrated a linear correlation ($R^2 = 0.9966$) between molar NH_4^+ concentrations (Y) and changes in solution conductivity (ΔX) in μS/cm or mS/cm over 5 min (Stabnikov et al., 2013).

Urease activity recalculated to dry weight (DW) was determined according to the following equation:

$$UA_{DW} = \frac{UA}{100 - W} \times 100, \mu M\ urea/min/g,$$

where UA is the urease activity of the fresh sample, expressed as μM urea/min/g fresh weight (FW); W is the sample moisture content (%); and (100 − W) is the dry matter content (%).

Effect of nickel salts in soil on urease activity of soybean tissues

The effect of nickel salts on soybean urease activity was investigated under controlled laboratory conditions at room temperature (25 °C). Soybean plants (*Glycine max* L.) cultivated in soil supplemented with different concentrations of nickel salts were used as the experimental material. The experimental procedure was based on Zhou et al. (2023) with slight modifications.

Nickel sulfate ($NiSO_4$) and nickel chloride ($NiCl_2$) were added to the soil to final concentrations of 25, 50, 75, 100, and 150 mg/kg. The control treatment contained no added nickel salts. Each pot contained 60 g of prepared soil.

Prior to sowing, soybean seeds were surface-sterilized in a 5% sodium hypochlorite solution for 5 min and thoroughly rinsed with distilled water. Germination was carried out in Petri dishes at 25 °C in the dark for 7 days. Uniform seedlings were selected and transplanted into the prepared pots.

Plants were cultivated for 80 days, after which they were harvested. The harvested plants were separated into leaves, stems, and roots, washed to remove adhering soil particles, and used for urease activity determination.

Effect of urea concentration on urease activity in germinated soybean seeds

The effect of different urea concentrations on urease activity was investigated under controlled laboratory conditions at room temperature (25 °C). Germinated soybean seeds (*Glycine max* L.) served as the experimental material.

Prior to germination, seeds were surface-sterilized in a 5% sodium hypochlorite solution for 5 min, thoroughly rinsed with distilled water, and soaked for 24 h in the corresponding urea solutions to ensure uniform exposure. Germination was carried out in sterile Petri dishes on filter paper moistened with aqueous urea solutions at final concentrations of 0 M (control), 0.1 M, 0.25 M, 0.5 M, 0.75 M, and 1.0 M. The moisture content of the filter paper was maintained throughout the germination period by periodic addition of the respective urea solutions.

Germination proceeded at 25 °C in the dark for 7 days. After germination, the seedlings were harvested and used for urease activity determination.

Preparation of soybean meal hydrolysate as a nutrient medium for the cultivation of urease-producing bacteria

Soybean meal hydrolysate was prepared according to the method of Hunsu et al. (2017) with slight modifications. One hundred grams of soybean meal were suspended in 0.9 L of 1 N hydrochloric acid in a glass beaker. Hydrolysis was carried out on a heated magnetic stirrer (JOAN LAB Equipment Co., Ltd., China) at 50 °C and 400 rpm for 1 h. The suspension was then incubated at the same temperature without stirring for an additional 20 h.

After hydrolysis, the suspension was cooled to room temperature and filtered through filter paper using a vacuum filtration unit (Millipore, Merck KGaA, Germany) connected to a Value V-i115S-M vacuum pump (China). The filtrate was neutralized to pH 6.8 with 10 N sodium hydroxide.

The resulting soybean meal hydrolysate (SMH) was sterilized by autoclaving at 121 °C for 15 min and used as the basal medium for the cultivation of urease-producing bacteria.

Nutrient media and cultivation conditions for urease-producing bacteria

The urease-producing bacterium *Bacillus* sp. VUK5 (Stabnikov et al., 2013) was used in this study. The performance of soybean meal hydrolysate (SMH) as a nutrient medium was compared with that of commercial tryptic soy broth (TSB; Difco Laboratories, Detroit, MI, USA) and an alternative yeast extract (YE) medium containing 20 g/L yeast extract (CondaLab, Spain) and 10 g/L NaCl. All media were sterilized by autoclaving at 121 °C for 15 min.

A sterile stock solution of urea (100 g/L) was prepared by membrane filtration through a Whatman™ nitrocellulose membrane filter (0.2 μm pore size). Ten milliliters of the sterile urea solution were added to 90 mL of each sterile medium prior to inoculation with 10% (v/v) bacterial inoculum.

Cultivation was carried out on an orbital shaker (Biosan ES-20/60, Latvia) at 120 rpm and 25 °C for 72 h. Urease activity was determined by incubating bacterial cultures with 1 M urea for 5 min, followed by quantification of the hydrolysis products.

Determination of biomass concentration

Biomass concentration was determined gravimetrically. Culture samples were filtered, and the biomass retained on the filter was dried at 105 °C to constant weight. Biomass concentration was expressed as dry biomass (g/L).

The number of viable cells was determined by the serial tenfold dilution method followed by spread plating on solid nutrient medium. Plates containing TSB supplemented with 20 g/L agar were incubated at 30 °C for 5 days, after which colony-forming units (CFU) were counted

Statistical analysis

All experiments were performed in triplicate. Statistical analysis of the experimental data was carried out using Statistica 6.0 software and Microsoft Excel. Results are presented as the mean±standard deviation (SD).

Results and discussion

Urease activity of plant raw materials and agro-industrial waste samples

Table 2 presents the urease activity of plant raw materials and agro-industrial waste samples.

The obtained data indicate substantial variability in enzymatic activity depending on the type and processing of plant material. The highest urease activity values were observed in soybean-derived samples, particularly soybean meal, soy milk, and okara, as well as in Hokkaido pumpkin seeds. In contrast, bean, chickpea, mung bean, lentil, and white mulberry leaf samples exhibited low or negligible urease activity. Soy protein isolate showed reduced urease activity compared with other soybean-derived products, which may be associated with technological processing and denaturation of protein fractions containing enzymatic systems.

Given the high production of soybean in Ukraine and the resulting stable supply of raw materials and processing by-products, further investigation of soybean as a substrate for urease activity assessment and biocementation applications is justified.

Table 2

Urease activity of plant raw materials and agro-industrial waste

Plant material	UA, μM urea/ min/g(mL)	Plant material	UA, μM urea/ min/g(mL)
Soybean meal	97.00±1.06	Red lentil milk	0.73±0.12
Soybean cake	89.30±1.04	Red lentil okara	0.73±0.13
Soy texturate	46.17±0.87	Green lentil milk	0.00
Soy protein isolate	13.83±0.67	Green lentil okara	1.50±0.10
Soy milk	123.17±1.65	Mung bean milk	1.50±0.10
Soy okara	90.07±1.15	Mung bean okara	5.36±0.41
Pea milk	7.67±0.40	Butternut pumpkin seeds	31.53±0.60
Pea okara	4.60±0.26	Hokkaido pumpkin seeds	167.83±2.55
Bean milk	0.70±0.10	White mulberry leaves	0.00
Bean okara	3.80±0.17	Wild (black) mulberry leaves	30.70±0.56
Chickpea milk	0.73±0.12	Red lentil milk	0.73±0.12
Chickpea okara	3.83±0.21	Red lentil okara	0.73±0.13

Note: results are presented as mean values ± SD (n = 3). UA is urease activity.

Urease activity of soybean leaves, stems, and pods

Urease activity was evaluated in fresh soybean samples, samples stored frozen for 1 year, and frozen samples after drying. The results showed that urease activity in stored samples was higher than in fresh samples by 1.23–3.15 times, depending on tissue type and storage conditions. This effect may be attributed to partial disruption of cellular structures during storage, which facilitates the release of intracellular ureolytic enzymes and improves their accessibility to the substrate. The results are presented in more detail in Figure 1.

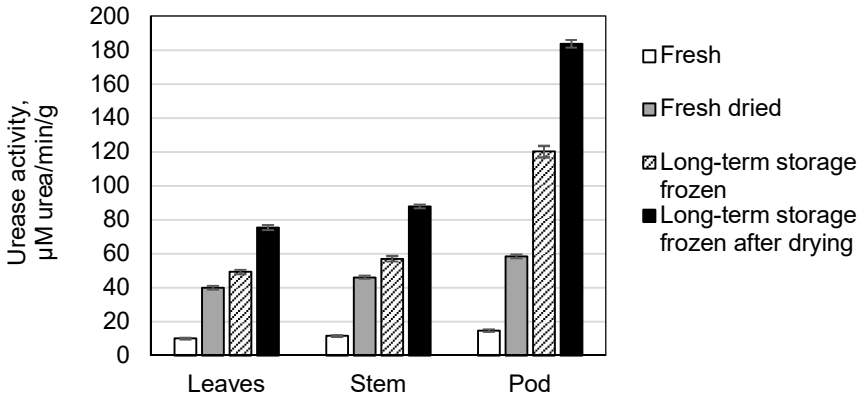

Figure 1. Urease activity of soybean leaf, stem and pod samples of different storage periods. Data are presented as mean ± SD (n = 3)

The obtained results are consistent with literature data reporting high urease activity in soybean tissues and its dependence on the structural state of the sample. In particular, for

crushed soybean samples with different particle sizes, urease activity ranged from 0.040 to 0.080 mM/min/g, depending on the degree of dispersion, with higher values observed in more finely ground (mechanically disrupted) samples (Chen and Hazarika, 2025).

Following the identification of soybean as one of the most promising plant sources of urease, the next objective of this study was to investigate factors affecting urease activity in soybean tissues. Since the efficiency of enzyme-induced calcium carbonate precipitation (EICP) strongly depends on urease activity, identifying conditions that enhance or suppress enzyme performance is important for optimizing the biocementation process. Therefore, the effects of nickel supplementation, as an essential urease cofactor (Zhou et al., 2023), and urea concentration, as the enzyme substrate (Stabnikov et al., 2013), were evaluated.

Effect of soil-applied nickel salts on urease activity in soybean tissues

The obtained data demonstrate a pronounced dose-dependent response of urease activity in different soybean organs under the influence of nickel ions. In all investigated tissues (leaves, stems, and roots), a characteristic hormetic response was observed, with an increase in urease activity at low concentrations (25–50 mg/kg of nickel salt to soil), followed by a gradual decrease at higher concentrations (100–150 mg/kg). The maximum urease activity was recorded at 50 mg/kg for both nickel salts, indicating an optimal stimulatory range for Ni^{2+}.

Comparative analysis (Figure 2) showed that $NiCl_2$ induced a more pronounced increase in urease activity than $NiSO_4$, which may be associated with differences in solubility and bioavailability of Ni^{2+} in the soil environment. The highest urease activity was observed in stems, which may reflect their active role in nitrogen transport and metabolic integration between root and photosynthetic tissues (Sirko and Brodzik, 2000).

The obtained results are consistent with the current understanding of the role of nickel in plant nitrogen metabolism, particularly as a cofactor of enzymes involved in nitrogen transformation processes (Maroney and Ciurli, 2014). In a study on the effects of nickel oxide nanoparticles (NiO-NPs) in soybean, a significant activation of key nitrogen metabolism enzymes was observed at a concentration of 50 mg/kg, including nitrate reductase, glutamine synthetase, glutamate synthase, and urease. Specifically, the activities of nitrate reductase, glutamate synthase, and urease in shoots increased by 138%, 25%, and 27%, respectively, indicating enhanced nitrate and ammonium assimilation pathways (Zhou et al., 2023). At the same time, in contrast to the nanoform NiO, which provides a more pronounced and multi-level enhancement of nitrogen assimilation, ionic forms of nickel ($NiSO_4$ and $NiCl_2$) exhibit a more narrowly specific effect, mainly limited to urease activation (Zhou et al., 2023). This may be explained by differences in the mechanisms of uptake and intracellular availability of nickel: nanoparticles are characterized by a sustained release and a broader influence on enzymatic systems, whereas salts provide a faster but less regulated effect.

Overall, the results indicate that moderate nickel supplementation can effectively enhance urease activity in soybean tissues. The optimal stimulatory effect was observed at 50 mg/kg soil for both nickel salts, with $NiCl_2$ producing a stronger response than $NiSO_4$. These findings suggest that controlled nickel supplementation may represent a practical approach for increasing plant-derived urease activity intended for EICP applications.

Effect of urea concentration on urease activity of germinated soybean seeds

The results showed that increasing urea concentration from 0 to 1 M led to a gradual decrease in urease activity of germinated soybean seeds (Table 3).

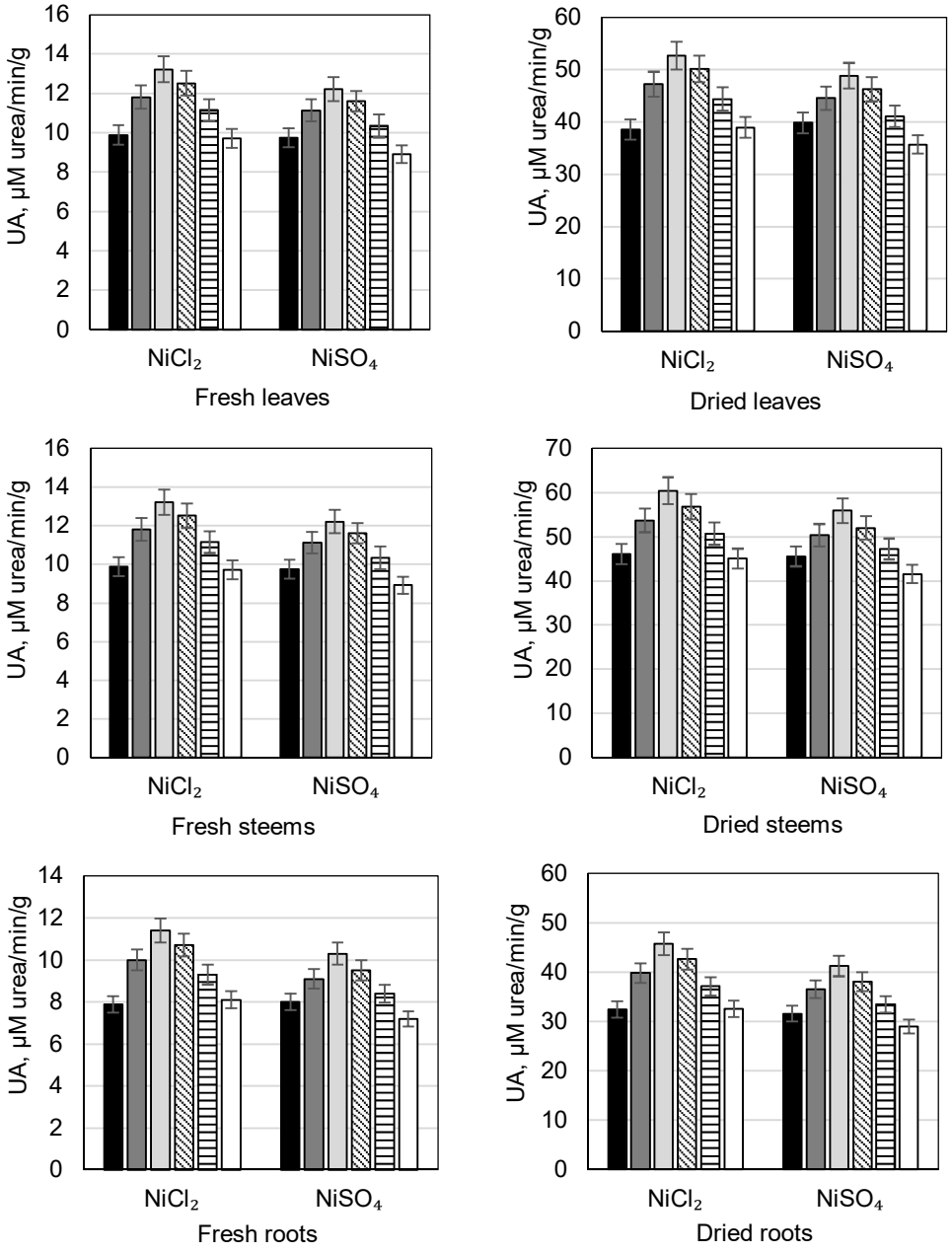

Figure 2. Effect of nickel salts on urease activity in different parts of soybean plants.
UA - urease activity, **UA_{CDW}** - urease activity of constant dry weight.
Data are presented as mean values ± SD (n = 3).

Table 3

Effect of urea concentration on urease activity of germinated soybean seeds

Concentrations of urea solutions, M	Urease activity, μM urea/min/g of seeds
0.00	79.67±0.72
0.10	39.63±0.39
0.25	41.94±0.12
0.50	26.54±0.22
0.75	26.15±0.34
1.00	16.91±0.77

Note: results are presented as mean values ± SD (n = 3).

The highest urease activity was observed in seeds germinated in water without added urea (79.67±0.72 μmol urea/min/g). At urea concentrations of 0.1–0.25 M, activity decreased approximately twofold (39.63–41.94 μmol/min/g), while at 0.5–0.75 M it further declined to about 26 μmol/min/g. The lowest activity was recorded at 1 M urea (16.91±0.77 μmol/min/g), corresponding to an approximately 4.7-fold reduction compared with the control.

According to Liu et al. (2026), high urea concentrations exert an inhibitory effect on soybean urease. The authors suggest that excess urea molecules may bind not only to the binuclear nickel-containing active site but also to peripheral regions of the enzyme, causing steric hindrance that reduces catalytic efficiency and product release. Singh and Nye (1984), who investigated urea hydrolysis by soil urease, reported that the reaction rate initially increases with increasing substrate concentration, reaches a maximum, and then decreases at higher substrate levels.

The observed decrease in urease activity with increasing urea concentration reflects a combined physiological and biochemical response of germinating soybean seeds. At low urea concentrations (0.1–0.25 M), a partial metabolic adaptation may occur, potentially involving induction of urease activity; however, this effect is likely masked by the inhibitory influence of urea on seed germination and overall metabolic activity. At higher concentrations (0.5–1.0 M), strong suppression of enzymatic activity is observed, which can be attributed to substrate inhibition and stress-induced reduction in metabolic processes.

Overall, increasing urea concentration during soybean seed germination resulted in a progressive reduction in urease activity. The highest activity was observed in seeds germinated in the absence of urea, indicating that exogenous urea does not stimulate enzyme activity under germination conditions. Therefore, germination without urea supplementation is more suitable for obtaining soybean material with high urease activity for subsequent EICP applications. These findings emphasize the importance of avoiding substrate exposure during germination to preserve enzymatic potential.

Soybean meal hydrolysate as a potential low-cost nutrient medium for cultivation of urease-producing bacteria

The accumulation of biomass, urease activity in the culture liquid, and pH changes during *Bacillus* sp. VUK5 cultivation in three nutrient media are presented in Figure 3.

Overall, all media supported the growth of *Bacillus* sp. VUK5; however, substantial differences were observed in biomass accumulation rate, pH evolution, cell viability, and urease activity. During the first 24 h of cultivation, a sharp increase in pH was recorded, from approximately 6.8 to 9.0-9.5. The highest pH values were observed in TSB and YE media (9.4±0.1), whereas SMH showed slightly lower values (approximately 9.2). This indicates

active urea hydrolysis with ammonium release, which is a typical characteristic of urease-producing *Bacillus* species. Similar pH shifts have been reported in the literature, where urease activity typically reaches its maximum under neutral to alkaline conditions (pH 7-9) (Yahya et al., 2021; Vitolo, 2022).

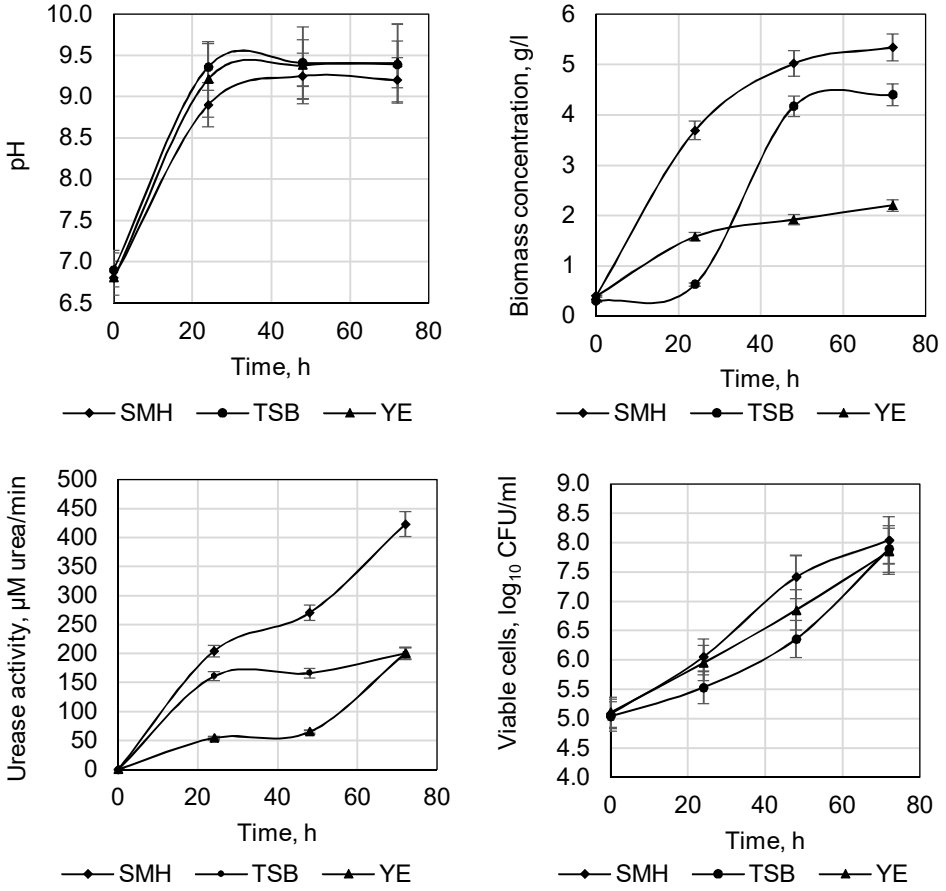

Figure 3. Growth parameters of *Bacillus* sp. VUK5 cultivated in different nutrient media: SMH (◆), TSB (●), and YE (▲).
Data are presented as mean ± standard deviation (n = 3).

Biomass accumulation was highest in SMH medium: after 24 h, the concentration reached approximately 3.5 g/L and exceeded 5 g/L at the end of cultivation. In TSB, growth was slower during the initial phase; however, a pronounced increase was observed after 24–48 h, reaching approximately 4.5 g/L. The lowest biomass levels were recorded in YE medium (approximately 2.2 g/L at 72 h). These results are consistent with literature data indicating that ureolytic *Bacillus* species often exhibit more intensive growth in TSB-type or protein-rich media (Mols and Abee, 2008; Stabnikov, 2016).

Urease activity strongly depended on medium composition. The highest activity was recorded in SMH (approximately 420 µM urea/min at 72 h). In TSB, activity was moderate (approximately 200 µM urea/min), while YE medium showed the lowest values, although a

gradual increase was observed after 48 h. The high urease activity in SMH may indicate an optimal balance of nitrogen sources and effective induction of urease synthesis. It is known that urea induces urease expression in *Bacillus* spp., whereas an excess of readily available nitrogen may suppress enzyme production (He et al., 2023).

The number of viable cells increased in all variants during cultivation; however, the highest values were again observed in SMH (up to 8 $\log_{10}$ CFU/mL). TSB and YE media showed slightly lower but steadily increasing counts. A similar trend between cell density and urease activity was observed, suggesting a relationship between metabolic activity and enzyme production. A similar association between biomass development and urease activity has been reported for soil ureolytic bacteria (Ma et al., 2020).

Among the tested media, SMH proved to be the most favorable for the growth of *Bacillus* sp. VUK5 and urease production. TSB supported good biomass accumulation but resulted in lower enzymatic activity, whereas YE medium was the least effective.

Overall, our findings demonstrate that soybean is a promising renewable resource for biocement production through two complementary approaches: (i) the use of soybean meal hydrolysate as an inexpensive nutrient medium for the cultivation of urease-producing bacteria, and (ii) the use of soybean plants as a natural source of urease, whose activity can be further enhanced by nickel supplementation during plant growth (Figure 4). Together, these approaches broaden the biotechnological applications of soybean and its processing products as sustainable resources for biocementation.

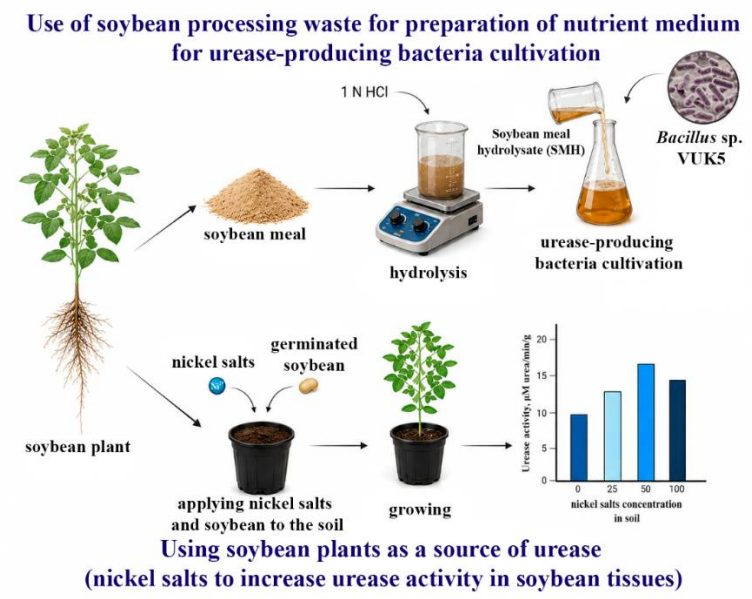

Figure 4. Soybean-based approaches for biocement production

Conclusions

The present study evaluated the potential of plant raw materials and agro-industrial by-products as low-cost resources for biocementation applications. Soybean-derived products (soy

milk, soybean meal, and okara) together with Hokkaido pumpkin seeds exhibited the highest urease activity, indicating their strong potential as enzyme sources for EICP systems.

Storage and drying of soybean tissues increased urease activity by 1.2–3.1 times, suggesting that disruption of plant cell structures improves enzyme release. Furthermore, urease activity was positively affected by nickel supplementation, with the strongest stimulatory effect observed at 50 mg/kg soil, while $NiCl_2$ was more effective than $NiSO_4$.

In contrast, increasing urea concentration during soybean seed germination caused a progressive decline in urease activity, demonstrating substrate inhibition at elevated substrate concentrations. These findings indicate that optimization of both nickel supplementation and urea concentration is essential for maximizing plant-derived urease activity.

Soybean meal hydrolysate proved to be the most effective low-cost cultivation medium for *Bacillus* sp. VUK5, supporting the highest biomass accumulation, viable cell density, and urease activity compared with TSB and yeast extract medium.

Overall, the obtained results demonstrate that soybean raw materials and agro-industrial by-products can serve as economical resources for both EICP and MICP technologies. Soybean can be exploited through two complementary approaches: soybean meal hydrolysate as a low-cost cultivation medium for urease-producing bacteria (MICP) and soybean tissues as a natural source of urease for EICP. In addition, appropriate regulation of factors affecting urease activity, particularly nickel availability, may further improve the efficiency and cost-effectiveness of biocementation processes.

References

Abharian S., Sadrekarimi A. (2026), Development of a low-cost MICP protocol for strengthening mine tailings, *Construction and Building Materials*, 518, 145828, https://doi.org/10.1016/j.conbuildmat.2026.145828

Ahenkorah I., Rahman M. M., Karim M. R., Beecham S., Saint C. (2021), A review of enzyme induced carbonate precipitation (EICP): the role of enzyme kinetics, *Sustainable Chemistry*, 2(1), pp. 92-114, https://doi.org/10.3390/suschem2010007

Ali I., Canpolat O., Doğruöz G. N., Yüzer N., Uysal M., Tanyıldızı H., Ziada M., Al Hayo B. (2025), Comparison of bacterial healing performances of cave bacteria and *Sporosarcina pasteurii* in cement-based mortar, *Processes*, 13(3), 673, https://doi.org/10.3390/pr13030673

Carter M.S., Tuttle M.J., Mancini J.A., Martineau R., Hung C.S., Gupta M.K. (2023), Microbially induced calcium carbonate precipitation by *Sporosarcina pasteurii*: a case study in optimizing biological $CaCO_3$ precipitation, *Applied and Environmental Microbiology*, 89(8), e01794-22, https://doi.org/10.1128/aem.01794-22

Chaparro S., Rojas H.A., Caicedo G., Romanelli G., Pineda A., Luque R., Martínez J.J. (2021), Whey as an alternative nutrient medium for growth of *Sporosarcina pasteurii* and its effect on $CaCO_3$ polymorphism and fly ash bioconsolidation, *Materials*, 14(10), 2470, https://doi.org/10.3390/ma14102470

Chen Y., Hazarika H. (2025), Extraction efficiency and activity determinants of soybean urease for sustainable biomineralization technology, *Smart Construction and Sustainable Cities*, 3(1), 11, https://doi.org/10.1007/s44268-025-00056-8

Chu J., Stabnikov V., Ivanov V. (2012), Microbially induced calcium carbonate precipitation on surface or in the bulk of soil, *Geomicrobiology Journal*, 29(6), pp. 544-549, https://doi.org/10.1080/01490451.2011.592929

Cuzman O.A., Richter K., Wittig L., Tiano P. (2015). Alternative nutrient sources for biotechnological use of *Sporosarcina pasteurii*, *World Journal of Microbiology and Biotechnology*, 31(6), pp. 897-906, https://doi.org/10.1007/s11274-015-1844-z

Donau Soja. (2024), Donau Soja expects record European soybean harvest of more than 13 million tonnes, https://www.donausoja.org/donau-soja-expects-record-european-soybean-harvest-of-more-than-13-million-tonnes/

Erdmann N., Strieth D. (2023), Influencing factors on ureolytic microbiologically induced calcium carbonate precipitation for biocementation, *World Journal of Microbiology and Biotechnology*, 39(2), 61, https://doi.org/10.1007/s11274-022-03499-8

He H., Li Y., Zhang L., Ding Z., Shi G. (2023), Understanding and application of *Bacillus* nitrogen regulation: A synthetic biology perspective, *Journal of Advanced Research*, 49, pp. 1-14, https://doi.org/10.1016/j.jare.2022.09.003

Hunsu V.O., Chikwem J., Chikwem U.J., Swinton D. (2017), Production of soy peptone by acid hydrolysis of soy flour, *Lincoln University Journal of Scie*nce, 6, pp. 25-31.

IEA (2023), *Cement – Analysis and Emissions*, International Energy Agency, https://www.iea.org/reports/cement

IPCC (2022), *AR6 WGIII – Mitigation of Climate Change*, https://www.ipcc.ch/report/ar6/wg3/

Ivanov V., Stabnikov V. (2017), *Construction Biotechnology: Biogeochemistry, Microbiology and Biotechnology of Construction Materials and Processes*, Springer, Singapore.

Khodadadi T.H., Javadi N., Krishnan V., Hamdan N., Kavazanjian Jr.E. (2020), Crude urease extract for biocementation, *Journal of Materials in Civil Engineering*, 32(12), 04020374, https://doi.org/10.1061/(asce)mt.1943-5533.0003466

Lapierre F.M., Huber R. (2024), Feeding strategies for *Sporosarcina pasteurii* cultivation unlock more efficient production of ureolytic biomass for MICP, *Biotechnology Journal*, 19(4), 2300466, https://doi.org/10.1002/biot.202300466

Liu J., Hu Y., Shen J., Liu W., Xu Y. (2026), A review of urease-based biomineralization: MICP and EICP, *Minerals*, 16(6), 588, https://doi.org/10.3390/min16060588

Liu L., Gao Y., Cao X., Meng H., Wang Z., Qi Y., Li R., He J. (2024), A comparative study of low-cost crude ureases extracted from multi-species of natural plant sources in enzyme-induced carbonate precipitation, *Journal of Environmental Chemical Engineering*, 12(6), 114824, https://doi.org/10.1016/j.jece.2024.114824

Ma L., Pang A. P., Luo Y., Lu X., Lin F. (2020), Beneficial factors for biomineralization by ureolytic bacterium *Sporosarcina pasteurii*, *Microbial Cell Factories*, 19(1), 12, https://doi.org/10.1186/s12934-020-1281-z

Maroney M.J., Ciurli S. (2014), Nonredox nickel enzymes, *Chemical Reviews*, 114(8), pp. 4206-4228, https://doi.org/10.1021/cr4004488

Mols M., Abee T. (2008), Role of ureolytic activity in *Bacillus cereus* nitrogen metabolism and acid survival, *Applied and Environmental Microbiology*, 74(8), 2370-2378, https://doi.org/10.1128/AEM.02737-07

Singh R., Nye P.H. (1984), The effect of soil pH and high urea concentrations on urease activity in soil, *Journal of Soil Science*, 35(4), pp. 519-527, https://doi.org/10.1111/j.1365-2389.1984.tb00609.x

Sirko A., Brodzik R. (2000), Plant ureases: roles and regulation, *Acta Biochimica Polonica*, 47(4), pp. 1189-1195, https://doi.org/10.18388/abp.2000 3972

Stabnikov V. (2016), Production of bioagent for calcium-based biocement, *International Journal of Biotechnology*, 5(2), 61, https://doi.org/10.6000/1927-3037.2016.05.02.5

Stabnikov V., Jian C., Ivanov V., Li Y. (2013), Halotolerant, alkaliphilic urease-producing bacteria from different climate zones and their application for biocementation of sand, *World Journal of Microbiology and Biotechnology*, 29(8), pp. 1453-1460, https://doi.org/10.1007/s11274-013-1309-1

Stabnikov V., Stabnikov D., Udymovych V. (2022), Increase the ecological safety of the soil biogrouting using plant urease, *Ukrainian Food Journal*, 11(2), pp. 302–314, https://doi.org/10.24263/2304-974X-2022-11-2-10

Stabnikov V., Kovshar I., Stabnikov D. (2025), Biotechnology approaches and improvement strategies in biocement production, *Ukrainian Food Journal*, 14(3), pp. 521-553, https://doi.org/10.24263/2304-974X-2025-14-3-11

Statista (2026), *Production of Soybeans for Beans in the United States since 2000*, https://www.statista.com/statistics/192058/production-of-soybeans-for-beans-in-the-us-since-2000/

Stockholm Environment Institute (2025), *Brazilian Soy Exports and Deforestation*, https://www.sei.org/features/brazilian-soy-exports-and-deforestation/

UkrAgroConsult (2026), Argentina's soybean production will increase to 49 mln tons, https://ukragroconsult.com/en/news/argentinas-soybean-production-will-increase-to-49-mln-tons/

Vitolo M. (2022), Notes on urea hydrolysis by urease, *Journal of Pharmacy & Pharmaceutical Sciences*, 11(3), pp. 96-135, https://doi.org/10.20959/wjpps20223-21380

Yahya M.N., Gökçekuş H., Orhon D., Keskinler B., Karagunduz A., Omwene P.I. (2021), A study on the hydrolysis of urea contained in wastewater and continuous recovery of ammonia by an enzymatic membrane reactor, *Processes*, 9(10), 1703, https://doi.org/10.3390/pr9101703

Zhang Q., Ye W.M., Liu Z.R., Wang Q., Chen Y.G. (2022), Advances in soil cementation by biologically induced calcium carbonate precipitation, *Rock and Soil Mechanics*, 43(2), pp. 345-357, https://doi.org/10.16285/j.rsm.2021.6249

Zhou P., Jiang Y., Adeel M., Shakoor N., Zhao W., Liu Y., Li Y., Li M., Azeem I., Rui Y., Tan Z., White J.C., Guo Z., Lynch I., Zhang P. (2023), Nickel oxide nanoparticles improve soybean yield and enhance nitrogen assimilation, *Environmental Science & Technology*, 57(19), pp. 7547-7558, https://doi.org/10.1021/acs.est.3c00959

Cite:

Kovshar, I., Udymovych, V., & Stabnikov, V. (2026). Utilization of plant biomass and agro-industrial waste for low-cost biocementation processes. *Ukrainian Food Journal, 15*(2), 503–517. https://doi.org/10.24263/2304-974X-2026-15-2-13

Iron accumulation in yeast under different cultivation conditions

Hanna Bondar, Viktoriia Krasinko

National University of Food Technologies, Kyiv, Ukraine

Keywords:

Saccharomyces cerevisiae
Iron
Cultivation
Aeration
Bioaccumulation

Article history:

Received 02.12.2025
Received in revised form 23.04.2026
Accepted 30.06.2026

Corresponding author:

Hanna Bondar
E-mail:
abn2292@gmail.com

DOI:
10.24263/2304-974X-2026-15-2-14

Abstract

Introduction. The aim of this study was to evaluate the effects of key cultivation parameters of *Saccharomyces cerevisiae* (iron source, aeration intensity, medium composition and pH, and timing of iron addition) on biomass concentration and intracellular iron bioaccumulation.

Materials and methods. *Saccharomyces cerevisiae* was cultivated in media of different compositions supplemented with iron salts ($FeSO_4$, $FeCl_3$, and Fe(III) citrate) to obtain iron-enriched biomass. Aeration intensity, medium pH, and the timing of iron addition were varied to achieve maximal intracellular iron accumulation without significant growth inhibition.

Results and discussion. Comparative analysis of the effect of different iron sources ($FeCl_3$, $FeSO_4$, and Fe (III) citrate) was performed separately for each agitation rate (120, 150, and 320 rpm). The type of iron compound was found to have a statistically significant effect on biomass accumulation and intracellular iron content (one-way ANOVA; pairwise comparisons by Welch t-test with Holm correction; $p < 0.05$). As the rotation speed increased from 120 to 320 rpm, biomass concentration rose from ~0.53–0.59 to ~1.20–2.60 g/L, depending on the iron source; the highest biomass values at 320 rpm were obtained for $FeCl_3$ (2.60±0.02 g/L) and $FeSO_4$ (2.10±0.12 g/L).

The highest intracellular iron content was recorded for Fe(III) citrate (2.02±0.30 mg/g DW), albeit at a lower biomass concentration (1.20±0.11 g/L). Medium composition substantially altered Fe bioavailability: the molasses-based medium provided stable biomass growth (6.31–6.43 g/L) with balanced Fe accumulation (1.28–1.45 mg/g DW). For the molasses-based medium, the optimum Fe uptake was observed at pH 5.0 (4.88±0.42 mg/g DW) compared to pH 4.5 (2.21±0.06 mg/g DW) and pH 5.5 (2.66±0.16 mg/g DW). The highest Fe accumulation level (5.09 mg/g DW) was achieved upon addition of $FeSO_4$ at 24 h after the onset of cultivation, corresponding to the phase of active cellular metabolism.

The results demonstrate the effectiveness of controlled optimization of *Saccharomyces cerevisiae* cultivation conditions for enhancing intracellular iron accumulation while maintaining high biomass yield. The findings indicate that selection of the iron source, aeration regime, nutrient medium composition and pH, as well as the timing of iron addition, enables targeted regulation of the balance between biomass production and intracellular iron enrichment.

Conclusions. The results establish a technological basis for the reproducible production of iron-enriched yeast biomass, highlighting its potential as a promising ingredient for food applications and dietary supplements.

Introduction

Iron is an essential trace element for eukaryotes and is involved in key biochemical processes. However, despite its abundance in the Earth's crust, the bioavailability of this element remains low because of the poor solubility and hydrolysis of Fe^{3+} ions at physiological pH values (Ramos-Alonso et al., 2020). Iron deficiency is one of the most widespread nutrient deficiencies worldwide (Pasricha et al., 2021). A lack of this micronutrient may impair immune response, physical performance, and cognitive function, and may also lead to iron deficiency anemia (Kolarš et al., 2025), thereby driving the search for iron forms with higher bioavailability and lower toxicity.

Conventional iron-based fortificants, such as iron salts (sulfate, chloride, and fumarate), although inexpensive, are characterized by limited absorption and frequently cause gastrointestinal discomfort, which reduces adherence to their use (Sun et al., 2022). Therefore, the use of microorganisms, particularly yeasts of the genus *Saccharomyces*, has emerged as a relevant area of research, as these organisms are capable of accumulating iron within the cell and converting it into biomolecule-bound forms with improved stability and safety (Oliveira et al., 2023). In addition, the yeast *Saccharomyces cerevisiae* M437 has been shown to be effective for the biosynthesis of silver (Skrotska et al., 2021) and selenium nanoparticles (Skrotska et al., 2025).

The efficiency of iron bioaccumulation by yeast is determined by the growth phase, aeration level, carbon source, and the composition and pH of the nutrient medium (Stehlik-Tomas et al., 2003; Wang et al., 2011). The effect of the chemical form of iron is also substantial and may vary depending on cultivation conditions and medium composition: inorganic and complexed forms (e.g., Fe-citrate and Fe-EDTA) differ in stability, transport rate, and cellular availability (Jach et al., 2022; Piskin et al., 2022). Maintenance of controlled pH, buffering capacity, and the presence of phosphates contributes to stable cellular metabolic activity and improved availability of metal ions, thereby promoting more efficient iron uptake and biomass growth (Tafazzoli et al., 2024). Thus, optimization of these parameters is key to achieving a balance between cellular growth processes, biomass production, and the efficiency of iron accumulation.

In addition to optimization of cultivation conditions, the literature describes methods for enhancing iron uptake by altering membrane permeability, including the application of pulsed electric fields (PEF) (Nowosad et al., 2021), as well as genetic modification approaches, for example, ferritin expression to regulate iron accumulation and reduce Fe toxicity (Llanos et al., 2016). However, for the practical production of iron-enriched yeast biomass, establishing reproducible relationships between cultivation parameters and the simultaneous indicators of growth and intracellular Fe content remains critically important.

Therefore, an important scientific objective is to establish the patterns of iron accumulation by *Saccharomyces cerevisiae* under different cultivation conditions, taking into account the effects of the type of iron salt, medium composition, and the duration of cell contact with iron salts. The aim of this study was to experimentally determine the optimal combination of cultivation parameters for maximizing intracellular iron content while maintaining technologically acceptable biomass growth.

Materials and methods

Materials

Saccharomyces cerevisiae M437 (Collection of Live Microbial Cultures, Department of Biotechnology and Microbiology, National University of Food Technologies) and a technically

pure dry yeast culture marketed as "Lvivski Drizhdzhi" and manufactured by PrJSC "Enzym Company" were used in the study.

The following reagents were used: iron (II) sulfate heptahydrate and iron (III) chloride hexahydrate (Carlo Erba), iron (III) citrate (Sigma-Aldrich), ammonium iron (II) sulfate hexahydrate (Sigma-Aldrich), Certipur® MS multi-element standard solution (Sigma-Aldrich) containing Fe at a concentration of 1000 ppm, and Milli-Q chromatography-grade water (Millipore).

Media for yeast cultivation

Medium 1. Rieder medium of the following composition (g/L): ammonium sulfate – 3.0; dipotassium hydrogen phosphate – 1.0; potassium dihydrogen phosphate – 0.1; sodium chloride – 0.7; magnesium sulfate – 0.5; glucose –10.0; yeast extract –1.0; pH 5.0.

***M*edium 2**. Glucose-phosphate-ammonium medium of the following composition (g/L): ammonium sulfate – 1.0; ammonium hydrogen phosphate – 5.5; potassium dihydrogen phosphate – 5.5; calcium chloride – 0.021; magnesium sulfate – 0.025; glucose – 15.0; yeast extract – 0.5; casein peptone – 1.5; pH 6.1.

Medium 3. Molasses-based medium of the following composition (g/L): molasses – 20.0; ammonium sulfate – 6.0; potassium dihydrogen phosphate – 10.0; potassium chloride – 0.1; pH 5.0.

Medium 4. Malt extract medium of the following composition (g/L): malt extract – 30.0; casein peptone – 3.0; pH 5.8.

Media 1-4 were used for the cultivation of iron-enriched S. cerevisiae.

Medium *5*. Peptone-yeast medium (YPD) of the following composition (g/L): dextrose – 20; peptone – 20; yeast extract – 10. Medium 5 was used for the maintenance of the *S. cerevisiae* culture and for inoculum preparation in test tubes.

All nutritional media were prepared and sterilized by autoclaving. Iron salt solutions were aseptically added to sterile cooled media.

Iron salt solutions. Stock solutions of iron salts were prepared in distilled water. To ensure sterility, the iron salt solutions were sterilized by filtration through a 0.22 μm membrane filter and added to sterile culture media to achieve the target final concentrations.

At the stage of studying the effect of the iron source, iron salt solutions were added to the nutrient medium, and the dosage was calculated to provide the same final molar concentration of elemental iron in the medium. The final iron concentration was 1 mM for iron (III) chloride ($FeCl_3 \cdot 6H_2O$), iron (II) sulfate ($FeSO_4 \cdot 7H_2O$), and ammonium iron (II) sulfate ($(NH_4)_2Fe(SO_4)_2 \cdot 6H_2O$). For iron (III) citrate ($C_6H_5FeO_7 \cdot H_2O$), an increased dosage of the compound equivalent to 100 mM Fe was initially applied because of its lower solubility and slower release/bioavailability of Fe^{3+} from the complex form. In subsequent experiments, the concentration of added iron was unified and set at 1 mM Fe for all iron sources.

The control variant consisted of the culture medium without the addition of iron compounds (i.e., without an exogenous Fe source).

Yeast cultivation

The inoculum for all cultivation variants was prepared by washing a 24 h seed culture with sterile physiological saline. For this purpose, sterile physiological saline was added to a test tube containing the seed culture, and the yeast cells were resuspended using a sterile inoculating loop.

An aliquot of the resulting inoculum was aseptically transferred with a sterile pipette into a flask containing 50 or 150 mL of sterile nutrient medium, with the inoculum volume corresponding to 10% (v/v) of the medium volume. All manipulations involving the yeast culture were performed under aseptic conditions.

Cultivation was carried out in smooth Erlenmeyer flasks with nominal volumes of 250 mL (working volume 50 mL) and 750 mL (working volume 150 mL) at 30±2 °C. Limited aeration (microaerobic conditions) was provided by static cultivation in an incubator without agitation; gas exchange occurred at the liquid-gas interface without intensified interphase contact, resulting in reduced oxygen supply compared with shaken cultures.

Aerobic conditions were established in a shaker incubator by agitation, and aeration intensity was controlled by the shaking speed at fixed cultivation geometry parameters (50 mL of medium in a 250 mL flask). The following agitation regimes were applied: 120 rpm (low aeration, limited O_2 transfer), 150 rpm (standard aeration, a typical operating regime for yeast), and 320 rpm (high aeration, enhanced O_2 transfer, which may affect the respiration/fermentation balance). The use of two flask sizes with proportional working volumes (50/250 mL and 150/750 mL; identical filling ratio of 20%) made it possible to evaluate the reproducibility of the results during scale-up of the culture liquid volume while maintaining comparable gas-exchange conditions at the larger scale.

Monitoring of yeast growth (OD_{600} determination)

At defined time intervals, 1 mL of culture was withdrawn from each flask and diluted to a final volume of 10 mL with distilled water. Optical density (OD) was measured at λ = 600 nm using a photoelectric colorimeter. Distilled water was used as the blank solution. Culture growth was monitored every 12 h over 72 h, and the late exponential phase characteristic of *Saccharomyces cerevisiae* was observed at approximately 48 h of cultivation. This time point was therefore used as the standard sampling point for the assessment of iron bioaccumulation in all subsequent experiments.

Determination of dry biomass of iron-enriched yeast

After 48 h of cultivation, the culture broth was centrifuged (10 min, 6000 rpm, 20 °C), and the cell pellet was washed three times with distilled water to remove weakly bound (surface-adsorbed) iron. Washing was performed by successive centrifugation cycles with complete removal of the supernatant after each cycle.

The completeness of washing was verified by determining the Fe content in the final supernatant using atomic absorption spectrometry; washing was considered sufficient when no detectable iron remained in the supernatant.

The washed biomass was transferred into pre-weighed weighing dishes and dried at 80 °C to constant weight. Dry biomass was quantified as dry cell weight (DW) and expressed in g/L of culture medium.

Determination of iron content

Intracellular iron content was determined using a Shimadzu AA-7000 atomic absorption spectrometer (Shimadzu Corporation) with flame atomization in an air-acetylene flame. The instrument was equipped with a hollow cathode lamp, and measurements were performed at 248.3 nm, corresponding to the maximum absorbance of iron. Calibration standards were prepared by serial dilution of the Certipur® MS multi-element standard solution containing

iron at a concentration of 1000 ppm in 3% (v/v) nitric acid. Sample preparation for the determination of intracellular iron content was performed according to the previously described method (Bondar and Krasinko, 2025).

Statistical analysis

Statistical processing of the results was performed using descriptive and inferential statistical methods. Calculation of mean values, graph construction, and assessment of data normality were carried out in Microsoft Excel 2016. To compare variants within a single regime (e.g., one agitation speed or one medium), one-way ANOVA was applied. When a significant result was obtained, pairwise comparisons were performed using Welch's *t*-test, given the possible inequality of variances between groups, with Holm correction to control for multiple-comparison error. In multifactorial analyses and in evaluating relationships between variables, regression analysis was used (Data Analysis ToolPak, Microsoft Excel 2016).

Each experiment was performed using three parallel flasks within a single experimental run, and the results are presented as mean±standard deviation (SD) of these triplicate measurements. These triplicate flasks were treated as parallel experimental replicates for statistical analysis. Mean values obtained for each condition were used for comparison, and statistical significance was accepted at $p < 0.05$.

Results and discussion

Selection of the optimal iron source and cultivation time

To determine the optimal source of iron ions in the yeast cultivation medium, a comparative study was conducted to evaluate the effects of different iron compounds on biomass growth and intracellular iron content in *Saccharomyces cerevisiae*. At this stage, all experiments were performed using Medium 1.

Figure 1 shows the change in optical density (OD_{600}) of the *Saccharomyces cerevisiae* M437 yeast suspension over 72 h of cultivation at an aeration intensity of 120 rpm, in the absence of added iron (control) and in the presence of different iron compounds, namely $FeCl_3$, $FeSO_4$, $(NH_4)_2Fe(SO_4)_2$, and iron (III) citrate.

Distinct growth dynamics of the *Saccharomyces cerevisiae* M437 strain were observed depending on the iron source. All variants were adjusted to the same final iron concentration (1 mM, calculated as Fe) (Figure 1).

At the end of the cultivation period, biomass accumulation in all experimental variants exceeded that of the control (without added iron), indicating a stimulatory effect of iron supplementation on yeast growth.

During the first 24 h of cultivation, an increase in optical density was observed in all variants, corresponding to the phase of active growth. However, the subsequent changes in OD_{600} depended strongly on the chemical form of the added iron (Table 1).

In the control variant (without added iron), *Saccharomyces cerevisiae* M437 exhibited growth dynamics during the first 24 h of cultivation, reaching maximum values, after which the parameter remained almost unchanged up to 72 h. This growth pattern indicates rapid depletion of available nutrient sources and accessible iron in the medium, followed by limitation of further biomass accumulation.

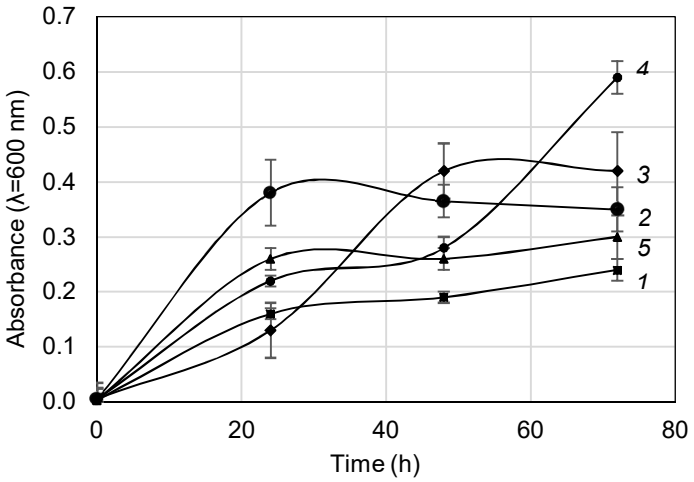

Figure 1. Growth of *Saccharomyces cerevisiae* M437 in medium without iron salts (1) and in the presence of iron (III) chloride (2), iron (II) sulfate (3), ammonium iron (II) sulfate (4), and iron (III) citrate (5).

The addition of iron(III) chloride resulted in the most intensive biomass increase at the early stage of cultivation; however, at later stages, growth stabilized with a tendency toward slight decline. This behavior may be explained by the initial activation of iron-dependent enzymatic systems, particularly components of the yeast respiratory chain, followed by the development of inhibitory or pro-oxidant effects characteristic of Fe^{3+} ions.

In contrast, media supplemented with $FeSO_4$ and $(NH_4)_2Fe(SO_4)_2$ showed a more gradual but stable increase in biomass, that continued until the end of the experiment. The most pronounced effect was observed for ammonium iron (II) sulfate, for which the highest OD_{600} values were recorded after 72 h of cultivation. This may indicate the higher bioavailability of Fe^{2+} and its more efficient incorporation into cellular metabolism without a pronounced toxic effect.

The addition of iron (III) citrate resulted in relatively stable growth dynamics without sharp fluctuations in optical density. This may be attributed to complexation of iron ions with an organic ligand, which reduces their reactivity and promotes moderate but sustained biomass accumulation.

The end of the exponential phase was estimated from growth curves as the point of deviation from linearity in $\ln(OD_{600})$ vs. time.

Table 1

Effect of different iron sources on the growth kinetic parameters of *Saccharomyces cerevisiae*

Iron source	t_{max}, h	OD_{max}	μ_{max}, 1/h	End of the exponential phase (estimated)
$FeCl_3$	24	0.380	0.1804	≤24 h
$FeSO_4$	48	0.420	0.1358	≈48 h
$(NH_4)_2Fe(SO_4)_2$	72	0.590	0.1577	>72 h
Fe (III) citrate	72	0.300	0.1739	≈24–48 h
Control	72	0.240	0.1537	>72 h

Note. t_{max} – time to maximum optical density; OD_{max} – maximum absorbance; μ_{max} – maximum biomass growth rate. The specific growth rate (μ) was calculated as follows: $\mu = \ln(OD_2/OD_1)/\Delta t$, where Δt = 24 h.

Thus, the obtained results confirm that not only iron concentration but also its chemical form is a determining factor affecting yeast growth and biomass accumulation dynamics.

To evaluate the effect of aeration intensity on yeast growth and iron accumulation, biomass production and cellular Fe content in *Saccharomyces cerevisiae* were compared under different aeration regimes, adjusted by shaker rotation speed (120–320 rpm), in the presence of different iron sources (Table 2).

Table 2

Intracellular iron content and biomass accumulation in *Saccharomyces cerevisiae* under different aeration conditions and with different iron sources

Agitation speed, rpm	Iron source	Iron content, mg/g DW	Biomass, g/L
120	Control	n.d.	0.56±0.03[a]
	Fe (III) citrate	0.81±0.11[a]	0.59± 0.13[a]
	$FeCl_3$	0.56±0.05[a]	0.55± 0.03[a]
	$FeSO_4$	0.51±0.13[a]	0.53± 0.13[a]
	$(NH_4)_2Fe(SO_4)_2$	0.19±0.05[b]	0.58± 0.13[a]
150	Control	n.d.	1.18±0.06[a]
	$FeCl_3$	1.71±0.25[a]	1.46±0.11[a]
	$FeSO_4$	1.21±0.13[ab]	0.58±0.05[c]
	Fe (III) citrate	0.75±0.18[b]	1.05±0.09[b]
320	Control	n.d.	2.20±0.04[b]
	$FeCl_3$	1.48±0.11[a]	2.60±0.02[a]
	$FeSO_4$	1.42±0.01[a]	2.10±0.12[b]
	Fe (III) citrate	2.02±0.30[a]	1.20±0.11[c]

Note. Data are presented as mean±SD ($n = 3$). Different superscript letters (a–c) within the same aeration level indicate statistically significant differences between iron-supplemented variants for the respective parameter ($p < 0.05$; ANOVA followed by pairwise Welch's t-tests with Holm correction). The control (Fe = 0) was not included in the letter grouping for Fe content.

n.d.– not detected.

An increase in aeration intensity (from 120 to 320 rpm) promoted biomass growth from 0.53–0.59 to 1.20–2.60 g/L, depending on the iron source, indicating enhanced cellular metabolic activity. The highest biomass values were observed in the variants containing $FeCl_3$ (2.60±0.02 g/L) and $FeSO_4$ (2.10±0.12 g/L). This effect is likely related to the fact that Fe^{2+} and Fe^{3+} ions participate in electron transport processes and are components of hemoproteins involved in respiratory metabolism (Holmes-Hampton et al., 2013). Iron serves as an active center in cytochromes and peroxidases; therefore, its availability in a biologically accessible form stimulates aerobic metabolism. The increased biomass growth rate and the high levels of iron accumulation (1.42–1.48 mg/g dry mass), which substantially exceeded the control, indicate that $FeCl_3$ and $FeSO_4$ may be considered optimal sources of this micronutrient for the production of iron-enriched yeast biomass.

In contrast, different patterns were observed in the medium supplemented with iron (III) citrate. At a concentration of 100 mM (in the experiments conducted at 120 rpm), its stimulatory effect on growth was negligible, and biomass remained at the control level (0.59±0.13 g/L). At the same time, the mean iron content in the biomass was 0.81±0.11 mg/g, which exceeded the value obtained with $FeSO_4$, mainly due to the higher initial concentration of the compound in the nutrient medium. This may be related to the high stability of citrate complexes, which can readily

penetrate the cell wall but, at elevated concentrations, may inhibit growth. A similar tendency was reported in previous studies (Paš et al., 2007), where Fe^{3+} citrate concentrations above 10 mM caused partial inhibition of yeast growth due to excessive phosphate binding and reduced metabolic activity.

In the present study, this was manifested as reduced biomass accumulation while maintaining a high level of Fe accumulation, which is characteristic of passive metal uptake mechanisms.

Among the studied compounds, ammonium iron (II) sulfate proved to be the least effective iron source for yeast cells, as reflected by the lowest iron accumulation levels. For this reason, this salt was excluded from further experiments. Presumably, its presence in the medium promoted the formation of stable complexes that limited the bioavailability of Fe^{3+} ions and reduced their uptake by the cells.

This interpretation is supported by the observation that, in one of the experimental variants, despite a noticeable increase in optical density, only minimal iron concentrations were detected in the biomass. This discrepancy between optical density and actual Fe content indicates that an increase in absorbance does not necessarily reflect a true increase in yeast biomass. Most likely, changes in optical properties were associated with complex formation processes in the medium, which affected absorbance measurements but were not accompanied by substantial cell growth.

Aeration conditions during yeast cultivation were controlled by varying the shaking (agitation) speed at 120, 150, and 320 rpm. Under moderate aeration conditions (150 rpm), statistically significant differences in both Fe content and biomass were observed depending on the iron source ($p < 0.05$). The highest Fe accumulation was achieved with $FeCl_3$ (1.71±0.25 mg/g), which was also associated with the highest biomass value (1.46±0.11 g/L), indicating the most balanced combination of growth and bioaccumulation under this regime. For $FeSO_4$, lower biomass accumulation values were recorded (1.21±0.13 mg/g; 0.58±0.05 g/L), which may indicate a toxic effect of excess ferrous iron. It is known that Fe^{2+} can initiate the formation of reactive oxygen species via the Fenton reaction, leading to oxidative stress in cells (Sorribes-Daudén et al., 2022).

Under intensive aeration conditions (320 rpm), an increased level of iron accumulation was observed in all experimental variants. The maximum Fe content (2.02±0.30 mg/g dry mass) was recorded in biomass grown in the presence of iron(III) citrate. At the same time, despite the relatively lower biomass yield (1.20±0.11 g/L), these data indicate intensive intracellular metal accumulation. A similar pattern was reported by Gaensly et al. (2011), who showed that increased iron availability may lead to enhanced accumulation even under conditions of partial inhibition of microbial growth. Thus, biomass growth and iron bioaccumulation appear to be inversely related: under intensive aeration, ion transport is enhanced, whereas excessive intracellular accumulation may limit further biomass increase (Table 2).

Selection of the optimal nutrient medium composition

The results of the preliminary experiments showed that the classical Rieder medium did not provide efficient *Saccharomyces cerevisiae* growth or a high level of iron accumulation. Despite its balanced composition in terms of major components, this medium exhibited a limited capacity to support intensive cellular metabolism and the uptake of Fe^{2+}/Fe^{3+} ions. The obtained iron content values in the biomass (1.21–2.02 mg/g) indicated the need to modify the nutrient medium in order to improve iron bioavailability and optimize yeast growth conditions.

Accordingly, the next stage of the study involved investigating the effect of alternative culture media on the process of iron bioaccumulation by *S. cerevisiae*. Media of different compositions were tested, including a glucose-phosphate-ammonium medium, a malt extract

medium, and a molasses-based medium, in order to identify the optimal combination of carbon, phosphorus, and nitrogen sources that would promote intensive cell growth and iron accumulation.

In view of the obtained results and to increase the practical relevance of the study, the source of yeast biomass was also changed at this stage of the experiments. The laboratory strain *Saccharomyces cerevisiae* M437 was replaced with a technically pure dry baker's yeast culture marketed as "Lvivski Drizhdzhi" (manufactured by PrJSC "Enzym Company") and enriched with iron. This substitution made it possible to evaluate the efficiency of the modified nutrient medium and the iron bioaccumulation process under conditions closer to industrial practice, as well as to verify the reproducibility of the observed effects using a commercially available culture with known technological properties.

Preliminary experiments involving variation of aeration intensity showed that excessive medium turbulence could negatively affect iron bioaccumulation due to intensified oxidative processes and Fe^{3+} precipitation. Therefore, the subsequent studies were carried out under limited aeration conditions (static cultivation) at 30 °C, making it possible to minimize the effect of oxygen and focus on evaluating the role of nutrient medium composition.

Comparative analysis of four culture media – Rieder medium, glucose-phosphate-ammonium medium, malt extract medium, and molasses-based medium – revealed substantial differences in iron content in the cells of the technically pure yeast culture marketed as "Lvivski Drizhdzhi" and in biomass increment (Figures 2 and 3).

The classical Rieder medium (Medium 1) supported moderate *Saccharomyces cerevisiae* growth (5.26–8.97 g/L), but the level of accumulated iron remained low (1.23–2.72 mg/g). At the same time, Fe content in the $FeCl_3$ variant (2.72±0.33 mg/g) was statistically higher than that in the $FeSO_4$ variant (1.23±0.07 mg/g; different superscript letters, $p < 0.05$). This may be related to the limited solubility of Fe compounds and the insufficient buffering capacity of the medium, which hampers iron ion transport into the cell under microaerophilic conditions. The iron(III) citrate variant in this medium was characterized by the greatest biomass increase (8.97±0.51 g/L); however, iron was not detected in the biomass, which may indicate the absence of intracellular Fe accumulation under these conditions.

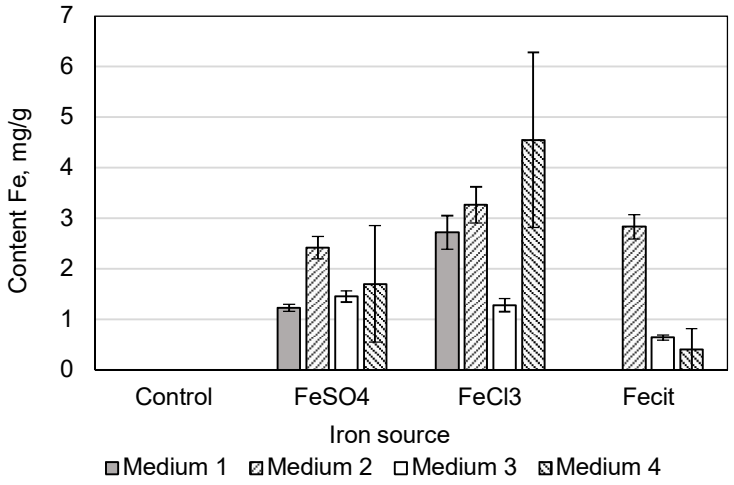

Figure 2. Iron concentration (mg/g dry biomass) in *Saccharomyces cerevisiae* biomass under different iron sources and nutrient medium compositions

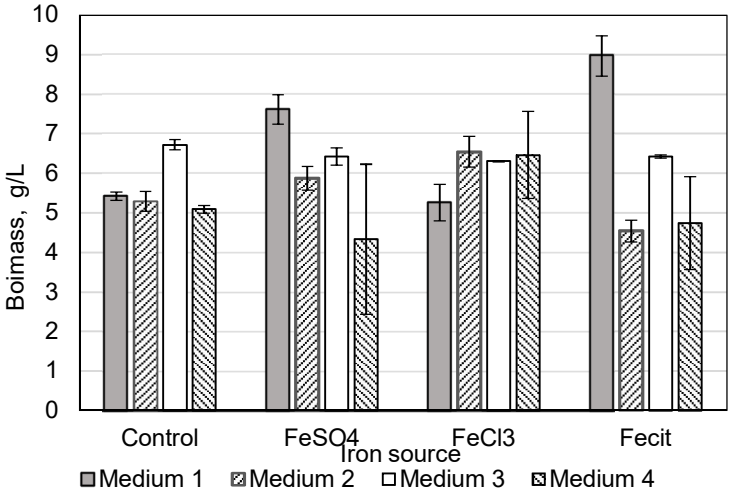

Figure 3. Yeast biomass accumulation depending on the iron source and nutrient medium composition

In the glucose-phosphate-ammonium medium (Medium 2), a marked increase in the iron accumulation capacity of the yeast was observed: Fe content reached 2.42±0.22 mg/g for $FeSO_4$ and 3.26±0.36 mg/g for $FeCl_3$, which was approximately 1.5-fold higher than the values obtained in the Rieder medium. Within Medium 2, no statistically significant differences between iron sources were found for Fe content (identical superscript letters, $p > 0.05$), indicating that the overall increase in Fe bioavailability was primarily attributable to the medium composition itself. This may be explained by the presence of phosphates and ammonium salts, which stabilize pH, reduce iron precipitation, and improve its bioavailability. In the glucose-phosphate-ammonium medium (Medium 2), yeast biomass ranged from 4.54 to 6.54 g/L and was characterized by relatively low variability (SD = 0.25–0.39 g/L). Although biomass values were somewhat lower than those observed in the Rieder medium, these conditions resulted in a substantial increase in iron bioaccumulation.

In the malt extract medium (Medium 4), considerable variability of the results was observed: in the $FeCl_3$-supplemented variant, biomass reached 6.46±1.10 g/L, whereas the content of accumulated iron varied within a broad range (for example, from 0.40±0.42 to 4.55±1.73 mg/g). No statistically significant differences between iron sources were detected within this medium ($p > 0.05$), which is consistent with the high SD values. Such instability may be attributed to the presence of polyphenols and other organic compounds capable of forming chelate complexes with Fe^{3+} and reducing its availability to cells (Piskin et al., 2022). Given the substantial variability in both accumulated iron content and biomass increment, the malt extract medium was excluded from further experiments as non-reproducible and unsuitable for a stable technological process of yeast iron enrichment.

The best results were obtained in the molasses-based medium (Medium 3), in which both a high level of biomass growth (6.31–6.43 g/L) and a balanced Fe content (1.28–1.45 mg/g) were recorded. Although iron accumulation was somewhat lower than in Medium 2, molasses provided stable culture growth without signs of inhibition. This can be explained by its rich composition, including carbohydrates, amino acids, nitrogen-containing compounds, trace elements, and a small amount of organically bound iron, all of which

support yeast metabolic activity even under limited aeration (Chen et al., 2024). In addition, molasses has a natural buffering capacity that stabilizes pH and helps maintain soluble iron in a form available for cellular uptake.

Thus, the obtained results indicate that a molasses-based medium provides an optimal balance between biomass growth and iron uptake under microaerophilic cultivation conditions. In addition to its favorable technological performance, this medium is economically advantageous and environmentally safe, as it is based on molasses, a by-product of sugar production, the utilization of which contributes to waste valorization and reduces the environmental burden associated with agro-industrial residues. Therefore, this approach aligns with the principles of sustainable resource use and makes the proposed medium a promising option for industrial yeast iron-enrichment technologies.

Selection of medium pH

The effect of pH on iron bioaccumulation by *Saccharomyces cerevisiae* was investigated using Medium 3 (molasses-based medium). For this purpose, a series of separate medium samples was prepared that differed only in pH (4.5, 5.0, and 5.5), whereas the medium composition and $FeSO_4$ concentration were kept constant. The obtained results showed that medium pH substantially affected both Fe^{2+} uptake and biomass growth intensity (Table 3).

At pH 4.5, moderate iron accumulation was observed, reaching 2.21±0.06 mg/g at a biomass concentration of 6.49±0.20 g/L, indicating stable metal uptake without noticeable inhibition of cell growth.

When the pH was increased to 5.0, the iron content in the biomass rose to 4.88±0.42 mg/g, indicating improved availability of iron ions for cellular transporters. However, a slight decrease in biomass was observed under these conditions (5.80±0.13 g/L), possibly due to partial precipitation of Fe^{2+} ions or changes in the activity of pH-sensitive enzymes.

A further increase in pH to 5.5 led to a decrease in iron accumulation (2.66±0.16 mg/g), although biomass concentration remained stable (6.24±0.14 g/L). This may be associated with the conversion of Fe^{2+} ions into poorly soluble forms such as $Fe(OH)_2$ and $Fe(OH)_3$, which reduces the efficiency of iron transport into the cell.

Thus, the most effective iron uptake was observed at pH 5.0, at which *S. cerevisiae* cells exhibited a balanced relationship between growth and intracellular iron accumulation. This result is consistent with reports by other researchers indicating that the optimal pH range for iron bioaccumulation by yeast is 4.8–5.2 (Gaensly et al., 2007; Pas et al., 2007).

Table 3

Intracellular iron content and biomass formation in *Saccharomyces cerevisiae* at different medium pH values

pH	Iron source	Iron content, mg/g DW	Biomass, g/L
4.5	Control	n.d.	6.07±0.11
4.5	$FeSO_4$	2.21±0.06	6.49±0.20
5.0	Control	n.d.	6.72±0.13
5.0	$FeSO_4$	4.88±0.42	5.80±0.13
5.5	Control	n.d.	6.32±0.21
5.5	$FeSO_4$	2.66±0.16	6.24±0.14

n.d.– not detected

Effect of culture growth stage on iron accumulation in yeast cells

To evaluate how the growth stage of the culture affects iron bioaccumulation, $FeSO_4$ was added to the medium at 0, 12, 24, and 48 h after the start of cultivation. Intracellular iron content (mg/g DW) and biomass concentration (g/L) were then determined (Figure 4). The aim of this experiment was to identify the optimal time of Fe addition that would ensure maximum iron uptake without inhibiting yeast growth.

The results demonstrated that the ability of the cells to accumulate iron was closely related to the growth phase of the culture (Figure 4). When iron was added at the beginning of cultivation (0 h), the level of iron accumulation reached 3.10 mg/g, while the biomass attained 6.45 g/L. This indicates active uptake of iron ions during the initial growth phase, when the cells are in a state of intensive metabolism and actively absorb nutrients.

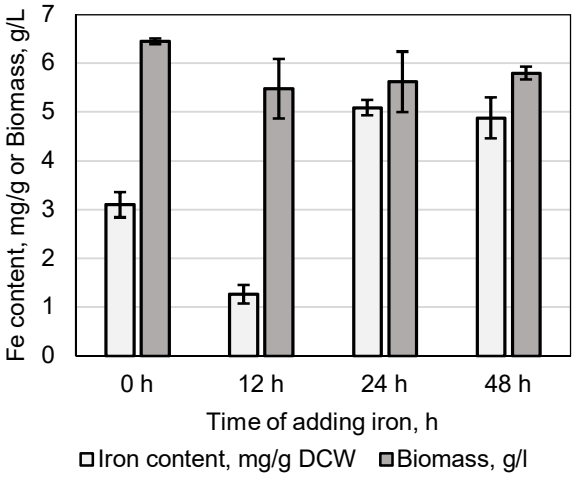

Figure 4. Effect of iron addition timing on iron accumulation and biomass production in *Saccharomyces cerevisiae*

Addition of iron during the exponential phase (12 h) was accompanied by a decrease in iron content to 1.26 mg/g, whereas biomass remained relatively stable (5.48 g/L). The lower level of iron accumulation at this stage may be associated with intensive cell division and redistribution of Fe^{2+} among intracellular structures, while the slight decrease in optical density suggests the onset of the transition out of the exponential growth phase.

The highest intracellular iron content was recorded when $FeSO_4$ was added at 24 h after the start of cultivation. The mean intracellular iron accumulation reached 5.09 mg/g, while the biomass was 5.62 g/L. These findings indicate that yeast accumulates iron most efficiently during the phase of active metabolism, possibly owing to enhanced expression of transport proteins responsible for Fe^{2+} binding and its transport across the cell membrane.

When iron was added after 48 h of cultivation, iron accumulation reached 4.88 mg/g, whereas biomass remained stable (5.80 g/L). This may be associated with the transition of the culture into the stationary phase, when part of the iron may become bound in insoluble forms or deposited in intracellular inclusions.

The obtained data indicate that iron addition after 24 h of cultivation provides the most favorable balance between biomass growth and Fe^{2+} uptake. At this time point, the culture is in a phase of active metabolism, during which yeast cells exhibit intensive growth and

efficient uptake of iron ions. Addition of $FeSO_4$ during the stationary phase of yeast development (48 h) also ensured a high level of intracellular iron accumulation, with only a slight reduction in biomass increase.

These patterns are consistent with reports from other researchers, who have shown that enhanced iron accumulation in *Saccharomyces cerevisiae* cells occurs during the period of active growth (exponential phase) and gradually stabilizes in the stationary phase, when enzymatic systems regulate intracellular Fe^{2+} concentration in order to prevent oxidative stress. Thus, the addition of ferrous sulfate to the cultivation medium promotes efficient bioaccumulation of this element by yeast cells without suppressing their growth processes. The optimal time interval for the addition of iron sources to obtain iron-enriched biomass may therefore be considered to be 24–48 h of cultivation, when a balance is achieved between biomass accumulation and maximum iron uptake.

Conclusions

An increase in aeration intensity promoted higher biomass concentration; however, the effect depended on the chemical form of iron, as not all iron sources equally supported culture growth and metal accumulation. The molasses-based medium was shown to provide a technologically acceptable balance between biomass growth and iron enrichment, thereby justifying its further use as a promising basis for the yeast iron-enrichment process. The effect of pH on Fe bioaccumulation was substantial, with the most efficient uptake observed at pH 5.0 (4.88±0.42 mg/g) compared with pH 4.5 and 5.5, confirming the importance of pH control as a key process parameter. The optimal timing of $FeSO_4$ addition depended on the stage of culture development: the maximum Fe content in the biomass was obtained when iron was added after 24 h of cultivation (5.09 mg/g), whereas addition at 0 and 12 h was less effective; addition after 48 h also provided high Fe accumulation.

References

Bondar H., Krasinko V. (2025), Rapid spectrophotometric method for the determination of iron content in yeast, *Ukrainian Journal of Food Science*, 13, pp. 80–90, https://doi.org/10.24263/2310-1008-2025-13-1-9

Chen Y., Pang Y., Wan H., Zhou X., Wan M., Li S., Liu X. (2024), Production of iron-enriched yeast and its application in the treatment of iron-deficiency anemia, *BioMetals*, 37, pp. 1–13, https://doi.org/10.1007/s10534-024-00592-3

Gaensly F., Picheth G., Brand D., Bonfim T.M. (2014), The uptake of different iron salts by the yeast *Saccharomyces cerevisiae*, *Brazilian Journal of Microbiology*, 45(2), pp. 491–494, https://doi.org/10.1590/S1517-83822014000200016

Jach M.E., Serefko A., Ziaja M., Kieliszek M. (2022), Yeast protein as an easily accessible food source, *Metabolites*, 12(1), 63, https://doi.org/10.3390/metabo12010063

Holmes-Hampton G.P., Jhurry N.D., McCormick S.P., Lindahl P.A. (2013), Iron content of *Saccharomyces cerevisiae* cells grown under iron-deficient and iron-overload conditions, *Biochemistry*, 52(1), pp. 105–114, https://doi.org/10.1021/bi3015339

Kolarš B., Mijatović Jovin V., Živanović N., Minaković I., Gvozdenović N., Dickov Kokeza I., Lesjak M. (2025), Iron deficiency and iron deficiency anemia: a comprehensive overview of established and emerging concepts, *Pharmaceuticals*, 18(8), 1104, https://doi.org/10.3390/ph18081104

de Llanos R., Martínez-Garay C.A., Fita-Torró J., Romero A.M., Martínez-Pastor M.T., Puig S. (2016), Soybean ferritin expression in *Saccharomyces cerevisiae* modulates iron accumulation and resistance to elevated iron concentrations, *Applied and Environmental Microbiology*, 82(10), pp. 3052–3060, https://doi.org/10.1128/AEM.00305-16

Nowosad K., Sujka M. (2021), The use of iron-enriched yeast for the production of flatbread, *Molecules*, 26(17), 5204, https://doi.org/10.3390/molecules26175204

Oliveira S., Ferreira C., Pereira J., Silva S., Costa E., Pereira A., Faustino M., Durão J., Pintado M., Carvalho A. (2023), Iron-peptide complexes from spent yeast: evaluation of iron absorption using a Caco-2 monolayer, *Food Bioscience*, 56, 103106, https://doi.org/10.1016/j.fbio.2023.103106

Pas M., Piskur B., Sustaric M., Raspor P. (2007), Iron enriched yeast biomass – a promising mineral feed supplement, *Bioresource Technology*, 98(8), pp. 1622–1628, https://doi.org/10.1016/j.biortech.2006.06.002

Pasricha S.R., Tye-Din J., Muckenthaler M.U., Swinkels D.W. (2021), Iron deficiency, *The Lancet*, 397(10270), pp. 233–248, https://doi.org/10.1016/S0140-6736(20)32594-0

Piskin E., Cianciosi D., Gulec S., Tomas M., Capanoglu E. (2022), Iron absorption: factors, limitations, and improvement methods, *ACS Omega*, 7(24), pp. 20441–20456, https://doi.org/10.1021/acsomega.2c01833

Ramos-Alonso L., Romero A.M., Martínez-Pastor M.T., Puig S. (2020), Iron regulatory mechanisms in *Saccharomyces cerevisiae*, *Frontiers in Microbiology*, 11, 582830, https://doi.org/10.3389/fmicb.2020.582830

Skrotska O., Kharchenko Y., Laziuka Y., Marynin A., Kharchuk M. (2021), Biosynthesis and characterictics of silver nanoparticles obtained using *Saccharomyces cerevisiae* M437, *Ukrainian Food Journal*, 10(3), pp. 615-631, https://doi.org/10.24263/2304-974X-2021-10-3-14

Skrotska O., Protsenko M., Zholobko M., Marynin M. (2025), Biosynthesis and characterization of selenium nanoparticles by *Saccharomyces cerevisiae* M437, *Ukrainian Journal of Food Science*, 13(1), pp. 91-110, https://doi.org/10.24263/2310-1008-2025-13-1-10

Sorribes-Dauden R., Jordá T., Peris D., Martínez-Pastor M.T., Puig S. (2022), Adaptation of *Saccharomyces* species to high-iron conditions, *International Journal of Molecular Sciences*, 23(22), 13965, https://doi.org/10.3390/ijms232213965

Stehlik-Tomas V., Grba S., Stanzer D., Vahčić N., Zetić V. (2003), Uptake of iron by yeast cells and its impact on biomass production, *Acta Alimentaria*, 32(3), pp. 279–287, https://doi.org/10.1556/AAlim.32.2003.3.7

Sun J., Xu S., Du Y., Yu K., Jiang Y., Weng H., Yuan W. (2022), Accumulation and enrichment of trace elements by yeast cells and their applications: a critical review, *Microorganisms*, 10(9), 1746, https://doi.org/10.3390/microorganisms10091746

Tafazzoli K., Ghavami M., Khosravi-Darani K. (2024), Production of iron enriched *Saccharomyces boulardii*: impact of process variables, *Scientific Reports*, 14(1), Article 4844, https://doi.org/10.1038/s41598-024-55433-7

Wang Z., Zhang J., Su T., Guan Z., Ji M. (2011), Screening of iron- and zinc-enriched yeast strain and optimization of cultivation conditions, *Preparative Biochemistry & Biotechnology*, 41(3), pp. 278–286, https://doi.org/10.1080/10826068.2010.539656

Cite:

Bondar, H., & Krasinko, V. (2026). Iron accumulation in yeast under different cultivation conditions. *Ukrainian Food Journal, 15*(2), 518–531. https://doi.org/10.24263/2304-974X-2026-15-2-14

Soil-derived *Bacillus* strains producing proteolytic enzymes for food industry applications

Olena Gudzenko[1], Liudmyla Varbanets[1], Liudmyla Butsenko[1,2], Lidiia Pasichnyk[1]

1 – D.K. Zabolotny Institute of Microbiology and Virology, National Academy of Sciences of Ukraine, Kyiv, Ukraine
2 – National University of Food Technologies, Kyiv, Ukraine

Keywords:

Protease
Elastase activity
Fibrinogenase activity
Bacillus

Article history:

Received 27.01.2026
Received in revised form 11.04.2026
Accepted 30.06.2026

Corresponding author:

Olena Gudzenko
E-mail: alena.gudzenko81@gmail.com

DOI:
10.24263/2304-974X-2026-15-2-15

Abstract

Introduction. The aim of the study was to screen soil isolates of the genus *Bacillus* for their ability to produce extracellular proteolytic enzymes exhibiting elastase, fibrinogenolytic, and caseinolytic activities, and to identify the most promising strains for potential applications in food biotechnology and related industries.

Materials and methods. Three soil isolates (A1, A2, A3) preliminarily assigned to the genus *Bacillus* were cultivated under submerged conditions in a gelatin-containing medium to induce protease synthesis. Proteolytic activities in culture supernatants were evaluated using casein, elastin Congo red and fibrinogen substrates. Phenotypic characteristics were assessed using conventional microbiological methods, API 20E, GC–MS fatty acid analysis, and MALDI-TOF MS.

Results and discussion. Strains A2 and A3 demonstrated pronounced extracellular proteolytic activity, whereas strain A1 showed no detectable activity. The investigated strains hydrolysed elastin, fibrinogen, and casein, indicating broad substrate specificity. The highest elastase activity was observed in *Bacillus amyloliquefaciens* A3 (12.0 U/mL), while fibrinogenolytic activity reached 7.0 U/mL. In contrast, caseinolytic activity remained comparatively low, resulting in high elastase/casein and fibrinogen/casein specificity coefficients. Morphological, biochemical, fatty acid, and MALDI-TOF analyses confirmed the affiliation of all isolates to *B. amyloliquefaciens*. The fatty acid profiles were characterized by a predominance of iso- and anteiso-branched fatty acids. These findings demonstrate that soil *Bacillus* strains, particularly *B. amyloliquefaciens* A3, are promising producers of extracellular proteases. Its high elastolytic and fibrinogenolytic activities combined with low nonspecific caseinolytic activity enable the selective hydrolysis of connective tissue proteins without excessive degradation of muscle proteins. Therefore, these proteases are promising for meat tenderization, fish ripening, production of bioactive protein hydrolysates, and bioconversion of collagen- and elastin-containing industrial waste. Additionally, the ability of the strain to synthesize proteases on inexpensive nutrient media increases its attractiveness for large-scale industrial production. The results highlight the potential of these enzymes for sustainable food industry applications.

Conclusions. Soil strains of *B. amyloliquefaciens* are promising producers of extracellular proteases with elastase and fibrinogenolytic activities. Strain A3 exhibited the highest activity and substrate specificity, indicating its potential for food biotechnology.

Introduction

The use of enzymes in various industries attracts researchers due to their environmental friendliness and especially in response to consumer demands for reduced use of chemicals in processed foods. Among the various sources of enzymes, microorganisms play a crucial role. This is because microorganisms are easily accessible, generate and multiply faster compared to animals and plants, and can be genetically modified to increase catalytic efficiency (Bilal and Iqbal, 2020).

Proteases are the most widely used among enzymes. They are used in pharmaceuticals, agriculture, textile, leather and food industries (Kumar et al., 2024; Rosazza et al., 2023; Song et al., 2023). In modern food biotechnology, microbial enzymes are increasingly applied for the valorisation of agro-industrial by-products and the development of functional food ingredients (Ivanov et al., 2021). In particular, plant-processing wastes can be successfully utilized for enrichment of bakery and confectionery products, improving their nutritional and technological properties (Stabnikova et al., 2023). An important source of industrially significant proteolytic enzymes are microorganisms isolated from various ecological niches, in particular from aquatic ecosystems, plant and animal substrates, extreme environments, and soil. However, it is soil microorganisms that are distinguished by their special biotechnological potential, which is due to their high level of metabolic diversity, ability to adapt to changing environmental conditions, and synthesize enzymes with broad substrate specificity and increased stability (Chen et al., 2024). Among such microorganisms, the leading place is occupied by representatives of the genus *Bacillus* (Blanco Crivelli et al., 2024; Dobrzyński et al., 2023; Gudzenko et al., 2025; Qian et al., 2023; Shakilanishi et al., 2024). They show significant potential in the use in food technologies, in particular in the production of protein hydrolysates, meat tenderization and lactic fermentation (Abril et al., 2023; Yousefi et al., 2025).

Soil microorganisms play a key role in the cycling of organic matter and maintaining soil fertility (Wang et al., 2024). Among them, representatives of the genus *Bacillus* are of particular importance, which, due to their ability to synthesize a wide range of extracellular enzymes, take an active part in the decomposition of polymeric, including protein, substrates in the soil (Sarwan et al., 2025). The proteolytic activity of bacilli determines the rate of mineralization of organic compounds, affects the formation of nitrogen forms available to plants (Radhakrishnan et al, 2025) and can be used in biotechnological processes – from the production of enzyme preparations to bioremediation. The study of the level and features of proteolysis in soil isolates of *Bacillus* allows not only to assess their ecological function, but also to identify promising strains for practical application.

In recent years, particular attention has been paid to the concept of sustainable food design, which involves the development of innovative food systems through biotechnological approaches, including microbial fermentation. Fermentation of plant-based matrices is considered a promising strategy for improving nutritional value, digestibility, and sensory characteristics of food products, while also contributing to resource efficiency and waste minimization (Covaliov et al., 2026). In this context, microbial enzymes, particularly proteases, play a key role in modifying protein structures and generating bioactive compounds.

Of particular interest for food technologies are proteolytic enzymes capable of hydrolysing a wide range of proteins, including casein, elastin, and fibrinogen. Caseinolytic enzymes are widely used in the production of milk and fermented dairy products, where they catalyze casein hydrolysis, resulting in milk coagulation and cheese curd formation. Controlled proteolysis of casein also plays an important role in the development of the texture

and sensory properties of dairy products. In addition, proteases can be applied in the processing of plant raw materials for the production of functional foods and beverages. Proteases capable of hydrolyzing connective tissue proteins, particularly elastin, are of considerable interest to the meat industry because they improve meat tenderness through the degradation of muscle and connective tissue proteins (Ivanov and Shutyuk, 2023; Kumar et al., 2024; Topchii et al., 2023; Yukalo et al., 2023). Such enzymes may also be used for the valorization of protein-rich waste and the production of protein hydrolysates with improved functional properties. Fibrinogenolytic proteases are considered promising for the generation of biologically active peptides and functional ingredients intended for specialized foods and nutraceutical applications.

Therefore, the search for new *Bacillus* strains producing proteases with different substrate specificities, particularly toward casein, elastin, and fibrinogen, remains an important task for both microbiology and modern food biotechnology, opening prospects for the development of effective enzyme preparations for the food industry.

The aim of this study was to screen soil isolates of the genus *Bacillus* for their ability to produce extracellular proteolytic enzymes with elastase, fibrinogenolytic and caseinolytic activities.

Materials and methods

Bacterial cultures

Three isolates (A1, A2, and A3), previously identified as representatives of the genus *Bacillus*, were used in this study. The strains were isolated from soil collected in August 2019 from a wheat field in the Fastiv District, Kyiv Region. For comparative studies, the strain *Bacillus subtilis* UCM B-5001 from the Ukrainian Collection of Microorganisms was used.

Medium and growth conditions

The strains were cultivated under submerged conditions in Erlenmeyer flasks containing 100 mL of medium for 72 h at 28 °C. The medium composition (g/L) was as follows: KH_2PO_4, 1.0; $MgSO_4 \cdot 7H_2O$, 0.75; $ZnSO_4 \cdot 7H_2O$, 0.25; $(NH_4)_2SO_4$, 0.5; maltose, 1.0; gelatin, 10.0; yeast autolysate, 0.15; pH 7.0. After fermentation, the cells were separated from the culture liquid supernatant (CLS) by centrifugation at 5000 × g for 30 min. Proteolytic (caseinolytic, elastolytic, and fibrinogenolytic) activities were determined in the CLS.

Enzyme Activity Assays

Total proteolytic (caseinolytic) activity

The total proteolytic (caseinolytic) activity was determined by the quantitative determination of tyrosine formed during the enzymatic hydrolysis of casein under the influence of enzymes of the studied supernatants. 0.5 mL of CLS and 0.5 mL of 1% casein were added to the test tube. The control tube contained 0.5 mL of CLS and 2 mL of 4% trichloroacetic acid (TCA). Incubation was carried out in a water bath at 37 °C for 30 min, after which 2 mL of 4% TCA was added to the test tube, kept for 20 min at room temperature and centrifuged at 10000g for 5 min. 2.5 mL of 0.5 M Na_2CO_3 and 0.5 mL of diluted Folin`s

reagent (1:3) were added to 0.5 mL of CLS and kept for 20 min at room temperature. The cleavage products were determined on a SF-26 spectrophotometer at a wavelength of 670 nm (cuvette of 10 mm). The activity was expressed in units corresponding to the number of micromoles of tyrosine released from casein during enzymatic hydrolysis for 1 min under the experimental conditions (Gudzenko, 2025).

Elastase activity

Elastase activity was determined colorimetrically by the intensity of the color of the solution upon enzymatic hydrolysis of elastin stained with Congo red. The incubation mixture contains 2.5 ml of 0.01 M Tris-HCl buffer (pH 7.5), 5 mg of elastin stained with 0.002% Congo red solution and 1 ml enzyme solution. The reaction mixture is incubated for 5 hours at a temperature of 37 °C. The reaction is stopped by keeping the test tubes with the reaction mixture in an ice bath for 30 minutes. Unhydrolyzed elastin is separated by centrifugation for 10 min at 10000 g. The color intensity was determined by colorimetrically at 515 nm. The amount of enzyme that catalyzes the hydrolysis of 1 mg of substrate per hour under standard conditions was taken as a unit of elastase activity.

Fibrinogenolytic activity

When studying fibrinogenolytic activity, 1 mg of fibrinogen, 1.8 ml of 0.01 M Tris-HCl buffer (pH 7.5) and 0.2 ml of CLS were added to the test tube. The reaction mixture was incubated for 30 min at 37 °C. The reaction was stopped by adding 2 ml of 10% trichloroacetic acid (TCA) solution. TCA was added immediately to the control sample. The samples were kept at room temperature for 20 min, and then centrifuged for 10 min at 10,000 g to remove precipitated protein. The optical density was measured on a spectrophotometer by absorption at 275 nm. The amount of enzyme that increases the optical density of the reaction mixture by 0.01 in 1 min was taken as a unit of fibrinogenolytic activity (Sharma et al., 2021 b).

Microbiological methods

The morphological and cultural properties of the selected isolates were studied by the standard microbiological methods.

The physiological and biochemical characteristics of the isolates were evaluated using the API 20E (Analytical Profile Index) test system (BioMerieux, France).

Transmission electron microscopy

The morphology and size of bacterial cells were determined using transmission electron microscopy (TEM) on a JEM-1400 electron microscope (Jeol, Japan) at the Center for Collective Use of the D.K. Zabolotny Institute of Microbiology and Virology.

Fatty acid composition

The fatty acid composition of total cellular lipids of soil bacteria was studied by the method of chromato-mass-spectrometry of methyl esters of fatty acids. To obtain methyl esters of fatty acids, raw biomass was suspended in a 1.5% solution of sulfuric acid in

methanol. Methanolysis was carried out at a temperature of 80 ºC for 1 h. Methyl esters of fatty acids were extracted with a mixture of ether-hexane (1:1). Separation of methyl esters was carried out on a chromato-mass spectrometric system Agilent 6890N/5973 inert at the Center for Collective Use of the D.K. Zabolotny Institute of Microbiology and Virology. The peaks were identified by comparison with standard samples of fatty acid methyl esters ("Serva"), as well as with the integrated NIST 02 mass spectral database. The content of individual fatty acids was determined as a percentage of the total peak areas.

MALDI-TOF assay

Confirmation of the taxonomic position of the obtained bacterial isolates was carried out using MALDI-TOF (Matrix Assisted Laser Desorption/Ionization) analysis on a VITEK MS mass spectrometer (Kačániová et al., 2019; Tsuchida et al., 2020). Identification of microorganisms is based on obtaining the total mass spectrum of proteins in the range of 1000-10000 daltons and bioinformatic comparison of the obtained spectrum with a database of reference spectra of known bacterial species on a VITEK MS mass spectrometer (Kačániová et al., 2019; Tsuchida et al., 2020).

Statistical analysis

All experiments were performed in 5 repetitions. The Student's t-test was used for statistical analysis. Data are presented as mean ± standard deviation error (M ± m). The results, presented in the form of graphs, were processed using Microsoft Excel 2007.

Results and discussion

Bacteria of the genus *Bacillus*, known as efficient producers of proteolytic enzymes, are common inhabitants of the plant rhizosphere, where they play an important role in enhancing plant resistance to biotic and abiotic stresses through induced systemic resistance, biofilm formation, and lipopeptide production (Hernández-Amador et al., 2026; Karačić et al., 2024; Mahapatra et al., 2022; Tsotetsi et al., 2025). At the same time, bacteria of the genus *Bacillus* are one of the most promising producers for the biotechnology industry among soil microorganisms (Lyng and Kovács, 2023; Yahya et al., 2021).

In recent years, particular attention has been paid to members of the *Bacillus subtilis* species complex, especially *Bacillus amyloliquefaciens*, due to their ability to synthesize a wide range of biologically active metabolites, including proteases, antimicrobial lipopeptides, polyketides, phytohormones, and volatile organic compounds. These metabolites confer competitive advantages in natural microbial communities and contribute to the high biotechnological potential of these bacteria in the food, agricultural, and pharmaceutical industries (Ngalimat et al., 2021, Shopinskyi and Butsenko, 2026).

Within the biotechnology field, the *Bacillu*s genus of bacteria presents extremely versatile microorganisms capable of producing a great variety of products with little to no dependency on petrochemicals. They are able to grow in different agro-industrial wastes and extreme conditions, resulting in healthy and environmentally friendly products, such as foods, feeds, probiotics, plant growth promoters, biocides, enzymes, and bioactive compounds (Herrmann et al., 2024). In addition, bacilli are capable of secreting extracellular enzymes directly into the culture medium, which considerably facilitates downstream

purification and reduces production costs compared to intracellular enzyme systems (Raman et al., 2025).

The biological activity of a culture is directly related to its physiological activity, including the synthesis of secondary metabolites. The latter include extracellular proteases. The extracellular proteolytic activity of soil bacteria is a component of their adaptation to the environment and an effective way to compete for sources of nutrition and energy.

Extracellular proteolytic activity of soil bacteria represents an important adaptive mechanism that enables microorganisms to hydrolyse complex protein substrates in the environment and utilize them as sources of carbon and nitrogen. Proteases also participate in antagonistic interactions with competing microorganisms and may contribute to the degradation of structural proteins of host tissues or microbial biofilms (Zhang et al., 2020).

Proteolytic activities of isolated *Bacillus* strains

In the CLS of the studied cultures, proteolytic activity was investigated. It was established that in the culture of *Bacillus* sp. A1 under the experimental conditions, proteolytic activity was not observed, while *Bacillus* sp. strains A2 and A3 showed high proteolytic activity during deep cultivation (Figure 1), and the activity was maximal on the third day.

The absence of detectable proteolytic activity in strain *Bacillus* sp. A1 may indicate differences in the regulation of extracellular enzyme synthesis, lower expression of protease genes, or dependence of enzyme production on specific cultivation conditions. In contrast, *Bacillus* sp. strains A2 and A3 demonstrated active secretion of extracellular proteases already during the exponential growth phase, suggesting an efficient adaptation to protein-containing substrates and a high metabolic potential for industrial enzyme production.

Of special attention is the fact that the cultures of *Bacillus* strains A2 and A3 showed broad substrate specificity, namely the ability to hydrolyze elastin, fibrinogen and casein. Thus, *Bacillus* sp. A2 and *Bacillus* sp. A3 showed elastase activity at the level of 8.1 and 12 U/ml, as well as fibrinogenolytic activity at the level of 2.33 and 7 U/ml, respectively. At the same time, the caseinolytic activity of the cultures was low. The ratio of fibrinogenolytic activity to caseinolytic (F/C) was 3.37 and 12.7 for *Bacillus* sp. A2 and A3, respectively; the ratio of elastase to caseinolytic (E/C) was 11.7 and 21.8 for *Bacillus* strains A2 and A3, respectively.

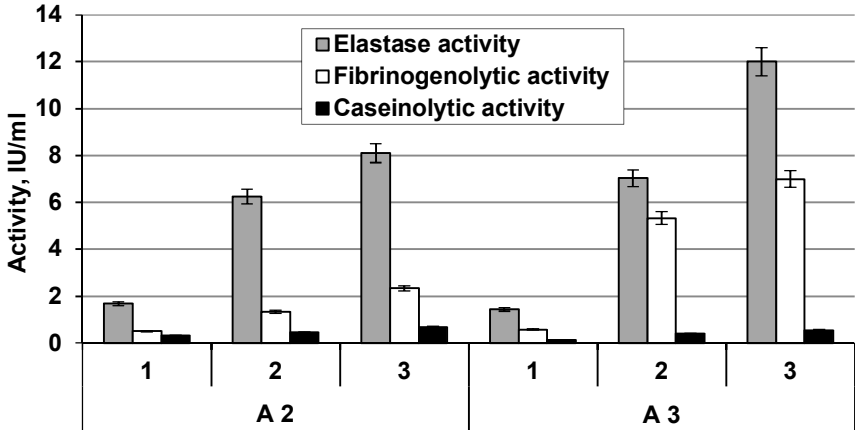

Figure 1. Proteolytic activity of cell-free culture supernatants of *Bacillus* strains A2 and A3 on day 1, 2, and 3 of cultivation

Such high specificity coefficients indicate that the synthesized proteases preferentially hydrolyze fibrillar and structural proteins rather than nonspecific globular substrates such as casein. This characteristic is particularly important for practical applications because highly specific elastases and fibrinogenases are considerably more valuable in biotechnology and medicine than nonspecific proteases with broad caseinolytic activity. High substrate specificity may also reduce undesirable side reactions during industrial processing of protein-containing raw materials.

Morphological features and cultivation properties of soil *Bacillus* isolates

Since three isolates previously identified as representatives of the genus *Bacillus* sp. were isolated from the same biotope - soil, which differed significantly in proteolytic activity, it was necessary to identify them to the species for comparison with other known producers.

Electron microscopy revealed that the isolated soil strains are rod-shaped bacteria measuring 2.0–3.0 μm × 0.7–0.8 μm, forming spores of elliptical shape that are positioned laterally within the cell and do not alter its morphology (Figure 2).

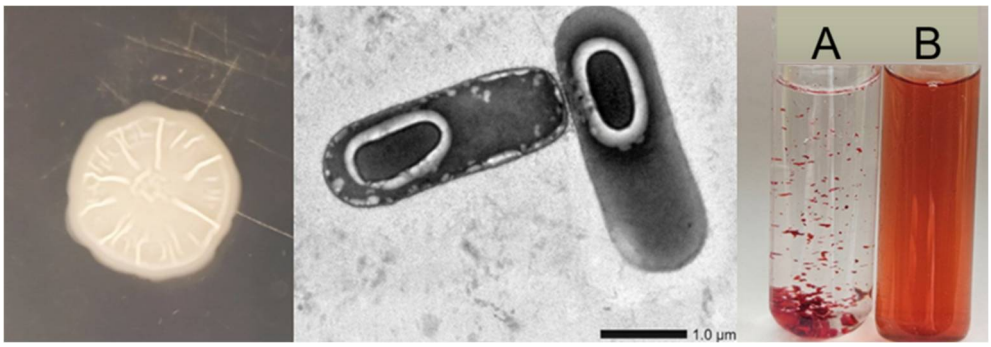

Figure 2. Colony and cell morphology of *Bacillus amyloliquefaciens* A3 and elastin fiber degradation induced by its elastase-active culture supernatant: A – untreated control; B – fibers after 3 h incubation

To identify strains of *Bacillus* strains A1, A2 and A3, their morphological and cultural properties were studied (Table 1, Figure 2), on the basis of which their belonging to the genus *Bacillus* was confirmed (Logan and Vos, 2015).

Aerobic Gram-positive spore-forming bacteria of the genus *Bacillus* are widely distributed in nature and are an important component of the soil microbial community (Poulaki et al., 2023; Saxena et al., 2020,). For example, the presence of up to 4.2×10^7 CFU/g of soil of spore-forming bacteria was found in the cultivation of certain wheat varieties (Honchar et al., 2021). Spore-forming bacteria of the genus *Bacillus* are characterized by high biological activity, in particular, they synthesize a variety of biologically active substances.

Based on studies of morphological-cultural and physiological-biochemical properties of the isolates (Table 2), they were assigned to *Bacillus amyloliquefaciens*. It should be noted that the species *B. amyloliquefaciens* and *Bacillus subtilis* are similar in properties (Logan and Vos, 2015) and belong to the "*subtilis* species complex". However, the strains A1, A2,

and A3 studied by us do not produce urease, which distinguishes representatives of the species *B. subtilis* from *B. amyloliquefaciens* (Table 2).

Table 1

Morphological and cultural characteristics of soil *Bacillus* strains

Characteristics	*Bacillus* strains			*Bacillus subtilis*[1]	*Bacillus amyloliquefaciens*[2]
	A1	A2	A3		
Colony morphology on solid media					
Colony color	Whitish-gray	White	Whitish-gray	Cream-colored	Cream-colored
Colony shape	Circular colonies with undulate margin	Circular colonies with undulate margin	Circular colonies with undulate margin	Circular or irregular-shaped colonies	Circular or irregular-shaped colonies
Colony surface	Rough colonies	Rough colonies	Rough colonies	Matte, later compact and opaque surface	
Cell shape	Rods	Rods	Rods	Rods	Rods
Gram staining	+	+	+	+	+
Spore formation	+	+	+	+	+
Cell morphology changes during sporulation	–	–	–	–	–
Cell size	2.0 μm × 0.8 μm	2.1 μm × 0.8 μm	2.6 μm × 0.9 μm	(2.0-3.0) μm × (0.7-0.8) μm	
Growth in nutrient broth	Pellicle formation	Pellicle formation	Pellicle formation	Pellicle formation	Pellicle formation
Growth in glucose medium					
aerobically	+	+	+	+	+
anaerobically	–	–	–	–	–
Growth in 7% NaCl broth	–	+	+	+	+
Gelatin hydrolysis	+	+	+	+	+
Starch hydrolysis	+	+	+	+	+
Esculin hydrolysis	+	+	+	+	+
Casein hydrolysis	+	+	+	+	+
H_2S production	–	–	–	–	–

Note: 1 - according to Priest et al., 1988; 2 - according to Priest et al., 1987.

Additional differential characteristics supporting the affiliation of the isolates to *B. amyloliquefaciens* include the ability to grow under elevated salt concentrations, active hydrolysis of gelatine and starch, and formation of stable pellicles in nutrient broth. These traits are characteristic of metabolically active *Bacillus* adapted to fluctuating environmental conditions.

Analysis of the fatty acid composition of total cellular lipids of strains A1, A2, and A3 (Table 3) confirmed the presence of iso- and antiiso-C15 fatty acids typical of the "*subtilis* species complex". Strains A1, A2, and A3 show close similarity to the reference strain *B. subtilis* UCM B-5001, confirming taxonomic placement.

Table 2

Physiological and biochemical characteristics of soil *Bacillus* strains
(determined using API 20 E test system)

Biochemical test (substrate/enzyme name)	A1[3]	A2[3]	A3[3]	*Bacillus subtilis*[1]	*Bacillus amyloliquefaciens*[1]
ß-D-galactopyranoside	+	–	+	100[2]	90[2]
L-arginine	–	–	–	–	–
L-lysine	–	–	–	–	–
L-ornithine	–	–	–	–	–
Trisodium citrate	+	+	+	100[2]	98[2]
Sodium thiosulfate	–	–	–	–	–
Urea	–	–	–	100[2]	–
L-tryptophan	–	–	–	–	–
L-tryptophan	–	–	–	–	–
Sodium pyruvate	+	+	+	100[2]	100[2]
Gelatin (bovine origin)	–\+	+	+	100[2]	100[2]
D-glucose	+	+	+	n.r.	n.r.
D-mannitol	+	+	+	n.r.	n.r.
Inositol	+	+	-	n.r.	n.r.
D-sorbitol	–	–	–	n.r.	n.r.
L-rhamnose	+	+	+	n.r.	n.r.
D-sucrose	+	+	+	n.r.	n.r.
D-melibiose	+	+	+	n.r.	n.r.
Amygdalin	+	+	+	n.r.	n.r.
L-arabinose	+	+	+	n.r.	n.r.

Note: 1 – according to Logan and Berkeley, 1984; 2 – values (100, 90) indicate the percentage of strains showing a positive reaction in the test. Negative results (i.e. 0% positive strains) have been omitted for clarity; n.r. – not reported; 3 – in our experimental results, positive reactions are indicated by "+", negative reactions by "–".

Table 3

Fatty acid composition of total cellular lipids of *Bacillus* strains A1, A2, and A3

Fatty acid		Fatty acid content, % in strains			
Systematic name	**Shorthand name**	**A1**	**A2**	**A3**	***B. subtilis* UCM B-5001**
12-Methyl tridecanoic acid	i-C14:0	1.1	1.3	1.9	2.6
Tetradecanoic acid	C14:0	1.5	3.1	1.2	0.7
13-Methyl tetradecanoic acid	i-C15:0	9.5	10.3	18.0	19.3
12-Methyl tetradecanoic acid	a-C15:0	48.0	33.0	52.3	50.4
Pentadecanoic acid	C15:0	1.2	1.8	1.2	1.1
14-Methyl pentadecanoic acid	i-C16:0	3.4	2.2	5.5	6.3
Hexadecanoic acid	C16:0	24.0	37.5	11.7	9.2
15-Methyl hexadecanoic acid	i-C17:0	1.5	1.3	1.9	2.9
14-Methyl hexadecanoic acid	a-C17:0	7.2	5.4	5.8	7.0
cis-9-Octadecenoic acid	C18:1cis	1.8	4.0	0.4	0.4

Identification by MALDI-TOF mass spectrometry

To confirm the belonging of the isolated bacterial strains to the species *Bacillus subtilis*/*B. amyloliquefaciens*, matrix-assisted laser desorption/ionization (MALDI-TOF) was used. It was shown that the mass spectra of isolates A1, A2 and A3 were identical to each other and corresponded to the profile of *Bacillus subtilis*/*B. amyloliquefaciens* (Table 4). The identification accuracy was 99.9%. Figure 4 shows the representative MALDI-TOF MS spectrum of *B. amyloliquefaciens* A3, illustrating characteristic cellular protein peaks confirming accurate identification within the *B. subtilis* species complex.

Table 4

Results of identification of *Bacillus* strains A1, A2, and A3 using MALDI-TOF

Isolate	Identified epiphytic bacteria	Identification accuracy, %
A1	*Bacillus subtilis/amyloliquefaciens*	99.9
A2	*Bacillus subtilis/amyloliquefaciens*	99.9
A3	*Bacillus subtilis/amyloliquefaciens*	99.9

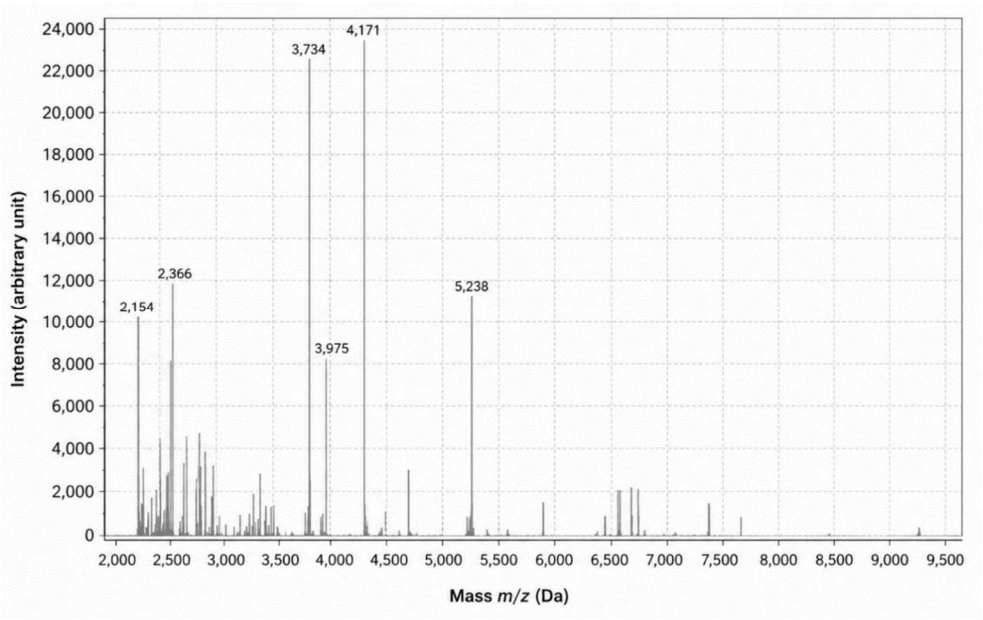

Figure 3. Mass spectrum of *B. amyloliquefaciens* A3

MALDI-TOF MS is currently considered one of the most rapid and reliable approaches for routine identification of bacteria because it is based on the analysis of ribosomal protein profiles characteristic for each microbial species. The high identification confidence obtained in this study confirms the quality of the acquired spectra and demonstrates the suitability of MALDI-TOF MS for differentiation of closely related representatives of the *B. subtilis* species complex. However, because of the high genetic similarity between *B. subtilis* and *B. amyloliquefaciens*, additional phenotypic and biochemical criteria remain necessary for final species identification.

Taking into account all the studied properties and the inability to form urease, we attributed strains A1, A2 and A3 to the species *B. amyloliquefaciens*.

The combination of morphological, biochemical, chemotaxonomic and MALDI-TOF analyses provided a comprehensive characterization of the isolates and significantly increased the reliability of identification. Such a polyphasic taxonomic approach is especially important for representatives of the *Bacillus subtilis* species complex because of the high phenotypic and genetic similarity among species included in this group.

The studied cultures are of particular interest because of their high specific proteolytic activity. In recent years, considerable attention has been focused on microbial fibrinolytic and fibrinogenolytic enzymes due to their potential application in thrombosis therapy (Farwa et al., 2021). These enzymes are capable of degrading fibrin and fibrinogen and may also exhibit nonspecific proteolytic activity toward substrates such as hemoglobin, casein, elastin, mucin, and gelatin. Fibrinolytic enzymes have been reported in various microorganisms, including *Fusarium* sp. (Peng et al., 2005; Wu et al., 2009), *Streptomyces* sp. (Silva et al., 2015), and *Penicillium chrysogenum* (El-Aassar et al., 1990). Particular attention has been paid to representatives of the genus *Bacillus*, including strains isolated from fermented foods (Yogesh and Halami, 2017), *Bacillus* sp. (Kim et al., 1996), *Bacillus subtilis* (Chen et al., 2013; Frias et al., 2021; Hu et al., 2019; Wang et al., 2006), and *Bacillus cereus* (Sharma et al., 2021).

Microbial fibrinogenolytic enzymes are of special biomedical interest because they may serve as alternatives to traditional thrombolytic agents such as streptokinase and urokinase. Compared with chemical thrombolytics, microbial enzymes often possess lower toxicity, higher substrate specificity and lower production costs. In addition, enzymes produced by non-pathogenic *Bacillus* strains are considered safer for industrial and pharmaceutical applications.

The range of producers of fibrinogenolytic enzymes among microorganisms is quite narrow. To date, only a few strains with fibrinogenolytic activity have been described in *Bacillus* sp. (Choi et al., 2004), *Bacillus cereus* (Majumdar et al., 2015), *Bacillus subtilis* (Frias et al., 2021), *Paenibacillus polymyxa* (Lu et al., 2010). The formation of fibrinogenolytic enzymes by microorganisms is not associated with their pathogenic properties, and the action of such enzymes on fibrinogen is due primarily to the features of the primary and secondary structure of fibrinogen sites as a substrate of the enzymatic reaction, which are complementary to the active center of the enzyme. The fibrinogenolytic activity of the cultures studied by us in terms of the specificity coefficient (the ratio of fibrinogenolytic to caseinolytic activity) is similar, or even prevails in comparison with the above-mentioned producers.

The studied strains are also promising in terms of their elastolytic activity. Elastases of non-pathogenic microorganisms can be used in industry for the hydrolysis of raw materials with a high content of elastin, in the processes of meat ripening and obtaining food additives (Zhang et al., 2023). Elastases are also used in the complex therapy of burns, inflammatory processes, and hematomas. As for elastase, to date, their producers have been described among representatives of characteristics of the most potent producer, *Priestia* (AlShaikh-Mubarak et al., 2023), *Pseudomonas* (Zupetic et al., 2021), *Bacillus*, *Vibrio* (AlShaikh-Mubarak et al., 2023), *Aspergillus* (Lee et al., 1995), *Streptomyces* (Fujii et. al., 2020), and *Chryseobacterium* (Lei et al., 2018).

Elastases are industrially important because elastin is highly resistant to hydrolysis due to its cross-linked structure and hydrophobicity. Therefore, microorganisms capable of producing efficient elastases are relatively rare. The elastolytic activity demonstrated by *B. amyloliquefaciens* A3 (12 U/ml) is comparable to or exceeds the activity levels reported for

many known microbial elastase producers, indicating the exceptional enzymatic potential of the isolate.

The bacteria isolated by us showed activity at the enzyme level with *Pseudomonas* (Yan et al., 1995), but the advantage of the cultures studied by us can be considered high substrate specificity, the E/C ratio was 11.7 and 21.8 for *Bacillus* sp. A2 and A3, respectively. Therefore, the isolated cultures of *Bacillus* sp. are promising strains for industry.

High elastase specificity combined with low nonspecific caseinolytic activity is particularly advantageous for food biotechnology because it allows selective hydrolysis of connective tissue proteins without excessive degradation of muscle proteins. This may improve texture characteristics of meat products and reduce losses of valuable proteins during technological processing.

Thus, of the three studied strains of *B. amyloliquefaciens*, two A2 and A3 were able to hydrolyse elastin, fibrin and casein. The caseinolytic activity of both cultures was insignificant, while the elastase activity was 8.1 and 12.0 U/ml, and the fibrinogenolytic activity was lower and was 2.33 and 7.0 U/ml, respectively, for *B. amyloliquefaciens* A2 and A3. For further studies, one strain of *B. amyloliquefaciens* A3 was selected, which was characterized by high both elastase and fibrinogenolytic activity in comparison not only with the two strains we studied, but also with known producers. This is evidenced by the fact that we received two patents for the invention for the strain *Bacillus* sp. A3, as a producer of elastase (Patent of Ukraine for utility model No. 145188) and fibrinogenase (Patent of Ukraine for utility model No. 145577).

The patented strain *B. amyloliquefaciens* A3 therefore represents a valuable biotechnological resource with significant industrial potential. Its ability to synthesize highly specific proteases on inexpensive nutrient media creates favorable conditions for scaling-up enzyme production and implementation in industrial biotechnology. The use of low-cost cultivation media is particularly important for commercial enzyme production because nutrient costs represent a substantial part of the total production expenses. Safety testing of the *B. amyloliquefaciens* A3 strain (former *Bacillus* sp. IMV B-78) demonstrated that it belongs to a group of avirulent microorganisms with no significant allergenic or general toxic effects that are approved by the Ministry of Health of Ukraine for industrial use (Gudzenko et al., 2020).

The potential applications of extracellular proteases produced by *B. amyloliquefaciens* A3 in food biotechnology are summarized schematically in Figure 4. The scheme illustrates the possible use of elastolytic and fibrinogenolytic enzymes in meat processing, fish industry, production of protein hydrolysates, functional ingredients and sustainable biotechnological processes.

Since the producer is grown on a very cheap medium, it can be promising for use in various branches of the food industry. Thus, in the meat processing industry, elastases are used in the process of ripening meat and to increase its yield by 40–43%. In the fish industry, the use of such enzymes accelerates the processes of salting and ripening of herring by 6–6.5 times, promotes a more uniform distribution of salt throughout the carcass. When treating fish liver with proteases, the yield of fat from it increases.

In addition to food biotechnology, proteases produced by *B. amyloliquefaciens* A3 may also be applicable in processing of collagen- and elastin-containing wastes generated by meat and fish industries. Bioconversion of such protein-rich wastes into valuable hydrolysates and feed additives corresponds to modern principles of sustainable biotechnology and circular bioeconomy.

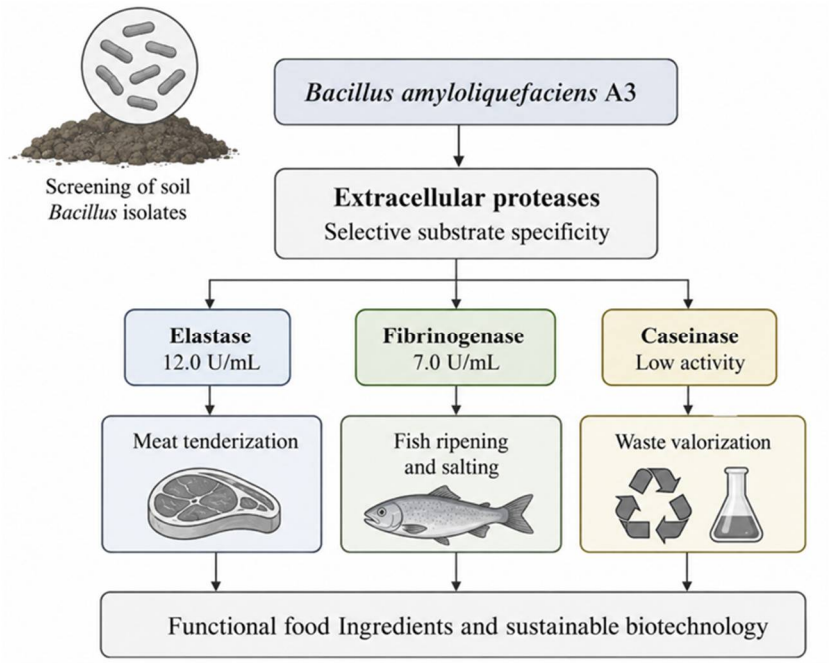

Figure 4. Extracellular proteases of soil *Bacillus amyloliquefaciens* A3: Functional applications in food biotechnology

Conclusions

The obtained results demonstrated that soil isolates of the genus *Bacillus*, identified as *Bacillus amyloliquefaciens*, possess significant biotechnological potential as producers of extracellular proteolytic enzymes with broad substrate specificity. Among the studied strains, *B. amyloliquefaciens* A2 and A3 exhibited pronounced proteolytic activity under submerged cultivation conditions, whereas strain A1 showed no detectable activity under the tested conditions.

Strains A2 and A3 were capable of hydrolysing structurally different protein substrates, including elastin, fibrinogen, and casein, indicating the production of proteases with elastase and fibrinogenolytic activities. The highest elastase activity was detected in strain A3 (12.0 U/mL), accompanied by considerable fibrinogenolytic activity (7.0 U/mL). In contrast, caseinolytic activity remained relatively low, resulting in high elastase/casein and fibrinogen/casein specificity coefficients. Such substrate specificity distinguishes the studied strains from many previously described *Bacillus* protease producers.

Comprehensive characterization of the isolates, including morphological, physiological, biochemical, fatty acid, and MALDI-TOF analyses, confirmed their affiliation with the species *B. amyloliquefaciens*. The fatty acid profiles were typical of representatives of the subtilis species complex and were characterized by high contents of iso- and anteiso-branched fatty acids.

Among the investigated isolates, *B. amyloliquefaciens* A3 was identified as the most promising producer due to its combination of high elastolytic and fibrinogenolytic activities.

The ability of this strain to synthesize proteases on inexpensive nutrient media indicates its potential for industrial applications, particularly in food biotechnology, including meat tenderization, acceleration of fish ripening, production of protein hydrolysates, and valorisation of protein-containing waste.

Overall, soil strains of *B. amyloliquefaciens* represent a valuable source of extracellular proteases with high substrate specificity and considerable potential for the development of enzyme preparations for food and biotechnological industries.

Acknowledgment. The authors would like to acknowledge the use of the equipment of the Center for Collective Use of NAS of Ukraine (Agilent 6890N/5973inert GCMS System), transmission electron microscope (TEM) on a JEM-1400 (Jeol, Japan).

References

AlShaikh-Mubarak G.A., Kotb E., Alabdalall A.H., Aldayel M.F. (2023), A survey of elastase-producing bacteria and characteristics of the most potent producer, *Priestia megaterium* GASM32, *PLoS One*, 18(3), e0282963, https://doi.org/10.1371/journal.pone.0282963

Blanco Crivelli X., Cundon C., Bonino M. P., Sanin M. S., Bentancor A. (2024), The complex and changing genus *Bacillus*: A diverse bacterial powerhouse for many applications, *Bacteria*, 3, pp. 256–270, https://doi.org/10.3390/bacteria3030017

Cascon A., Yugueros J., Temprano A., Sánchez M., Hernanz C. et al. (2000), A major secreted elastase is essential for pathogenicity of *Aeromonas hydrophila*, *Infection and Immunity*, 68(6), pp. 3233–3241, https://doi.org/10.1128/IAI.68.6.3233-3241.2000

Chen B., Huo J., He Z., He Q., Hao Y., Che Z. (2013), Isolation and identification of an effective fibrinolytic strain *Bacillus subtilis* FR-33 from the Chinese doufuru and primary analysis of its fibrinolytic enzyme, *African Journal of Agricultural Research*, 7, pp. 2001–2009.

Chen Q., Song Y., An Y., Lu Y., Zhong G. (2024), Soil microorganisms: Their role in enhancing crop nutrition and health, *Diversity,* 16(12), 734, https://doi.org/10.3390/d16120734

Choi N.S., Chang K.T., Maeng P.J., Kim S.H. (2004), Cloning, expression, and fibrin(ogen)olytic properties of a subtilisin DJ-4 gene from *Bacillus* sp. DJ-4, *FEMS Microbiology Letters*, 236(2), pp. 325–331, https://doi.org/10.1111/j.1574-6968.2004.tb09665.x

Covaliov E., Capcanari T., Popovici V., Radu O., Negoiță C. (2026), Sustainable food design via fermentation of plant-based matrices, *Ukrainian Food Journal*, 15(1), pp. 8–34, https://doi.org/10.24263/2304-974X-2026-15-1-4

Dobrzyński J., Wróbel B., Górska E.B. (2023), Taxonomy, ecology, and cellulolytic properties of the genus *Bacillus* and related genera, *Agriculture*, 13(10), 1979, https://doi.org/10.3390/agriculture13101979

El-Aassar S.A., El-Badry H.M., Abdel-Fattah A.F. (1990), The biosynthesis of proteases with fibrinolytic activity in immobilized cultures of *Penicillium chrysogenum* H9, *Applied Microbiology and Biotechnology*, 33(1), pp. 26–30, https://doi.org/10.1007/BF00170568

Farwa A., Shourong W., Vivi K. (2021), Role of fibrinolytic enzymes in anti-thrombosis therapy, *Frontiers in Molecular Biosciences*, 680397, https://doi.org/10.3389/fmolb.2021.680397

Frias J., Toubarro D., Fraga A., Botelho C., Teixeira J., Pedrosa J., Simoes N. (2021), Purification and characterization of a thrombolytic enzyme produced by a new strain of *Bacillus subtilis*, *Journal of Microbiology and Biotechnology*, 31(2), pp. 327–337, https://doi.org/10.4014/jmb.2008.08010

Fujii T., Fukano K., Hirano K., Mimura A., Terauchi M., Etoh S., Iida A. (2020), A new serine protease family with elastase activity is produced by *Streptomyces* bacteria, *Microbiology*, 166(3), https://doi.org/10.1099/mic.0.000880

Gudzenko O.V., Varbanets L.D., Butsenko L.M., Pasichnyk L.A., Chernyshenko V.O., Stogniy E.M. (2020), Strain *Bacillus* sp. IMV B-7883 – producer of extracellular proteinase with fibrinogenolytic activity, Utility model patent No. 145577, Bulletin No. 24, https://sis.nipo.gov.ua/uk/search/detail/1470142/

Gudzenko O.V., Avdiyuk K.V., Varbanets L.D., Pasichnyk L.A., Reshetnikov M.V. (2025), *Bacillus* strains isolated from soryz are producers of proteolytic enzymes, *Microbiological Journal*, 87(2), pp. 25–33, https://doi.org/10.15407/microbiolj87.02.025

Herrmann L.W., Letti L.A.J., Penha R.O., Soccol V.T., Rodrigues C., Soccol C.R. (2024), *Bacillus* genus industrial applications and innovation: First steps towards a circular bioeconomy, *Biotechnology Advances,* 70, 108300, doi:10.1016/j.biotechadv.2023.108300

Hernández-Amador E., Montesdeoca-Flores D.T., Luis-Jorge J.C. (2026), *Bacillus* as premier biocontrol agents: Mechanistic insights, strategic application, and future regulatory landscapes in sustainable agriculture, *Plants,* 15(3), 516, https://doi.org/10.3390/plants15030516

Honchar A., Tonkha O., Patyka M., Makarchuk O. S. (2021). Features of changes in the number and composition of the microbiome of the rhizosphere of winter wheat in the process of ontogeny, *Plant and Soil Science*, 12(3), pp. 56-65, https://doi.org/10.31548/agr2021.03.0056

Hu Y., Yu D., Wang Z., Hou J., Tyagi R., Liang Y., Hu Y. (2019), Purification and characterization of a novel, highly potent fibrinolytic enzyme from *Bacillus subtilis* DC27 screened from Douchi, a traditional Chinese fermented soybean food, *Scientific Reports*, 9(1), 9235, https://doi.org/10.1038/s41598-019-45686-y

Ivanov V., Shevchenko O., Marynin A., Stabnikov V., Gubenia O., Stabnikova O., Shevchenko A., Gavva O., Saliuk A. (2021), Trends and expected benefits of the breaking edge food technologies in 2021–2030, *Ukrainian Food Journal*, 10(1), pp. 7-36, https://doi.org/10.24263/2304-974X-2021-10-1-3

Ivanov Y., Shutyuk V. (2023), Effect of prolonged proteolisis on biochemical composition of the malt wort, *Ukrainian Food Journal*, 12(3), pp. 352-364, https://doi.org/10.24263/2304-974X-2023-12-3-4

Kačániová M., Klūga A., Kántor A., Medo J., Žiarovská J., Puchalski C., Terentjeva M. (2019), Comparison of MALDI-TOF MS Biotyper and 16S rDNA sequencing for the identification of *Pseudomonas* species isolated from fish, *Microbial Pathogenesis*, 132, pp. 313-318, https://doi.org/10.1016/j.micpath.2019.04.024

Karačić V., Miljaković D., Marinković J., Ignjatov M., Milošević D., Tamindžić G., Ivanović M. (2024), *Bacillus* species: Excellent biocontrol agents against tomato diseases, *Microorganisms*, 12(3), 457, https://doi.org/10.3390/microorganisms12030457

Kim W., Choi K., Kim Y., Park H., Choi J., Lee Y., Oh H., Kwon I., Lee S. (1996), Purification and characterization of a fibrinolytic enzyme produced from *Bacillus* sp. strain CK 11-4 screened from Chungkook-Jang, *Applied and Environmental Microbiology,* 62, pp. 2482–2488, https://doi.org/10.1128/AEM.62.7.2482-2488.1996

Kumar A., Dhiman S., Krishan B. Samtiya M., Kumari A., Pathak N., Kumari A., Aluko R.E., Dhewa T. (2024), Microbial enzymes and major applications in the food industry: A concise review, *Food Production*, *Processing and Nutrition,* 6, 85, https://doi.org/10.1186/s43014-024-00261-5

Lei Y., Zhao P., Li C., Zhao H., Shan Z., Wu Q. (2018), Isolation, identification and characterization of a novel elastase from *Chryseobacterium indologenes*, *Applied Biological Chemistry,* 61, pp. 365–372, https://doi.org/10.1007/s13765-018-0364-6

Lee J.D., Kolattukudy P.E. (1995), Molecular cloning of the cDNA and gene for an elastinolytic aspartic proteinase from *Aspergillus fumigatus* and evidence of its secretion by the fungus during invasion of the host lung, *Infection and Immunity*, 63, pp. 3796–3803, https://doi.org/10.1128/iai.63.10.3796-3803.1995

Logan N.A., Berkeley R.C. (1984), Identification of *Bacillus* strains using the API system, *Journal of General Microbiology*, 130(7), pp. 1871–1882, https://doi.org/10.1099/00221287-130-7-1871

Logan N.A., Vos P. (2015), *Bacillus*, In: Bergey's Manual of Systematics of Archaea and Bacteria, John Wiley & Sons, Ltd., https://doi.org/10.1002/9781118960608.gbm00530

Lu F., Lu Z., Bie X., Yao Z., Wang Y., Lu Y., Guo Y. (2010), Purification and characterization of a novel anticoagulant and fibrinolytic enzyme produced by endophytic bacterium *Paenibacillus polymyxa* EJS-3, *Thrombosis Research*, 126, pp. e349–e355, https://doi.org/10.1016/j.thromres.2010.08.001

Lyng M., Kovács Á.T. (2023), Frenemies of the soil: *Bacillus* and *Pseudomonas* interspecies interactions, *Trends in Microbiology*, 31(8), pp. 845–857, https://doi.org/10.1016/j.tim.2023.02.003

Mahapatra S., Yadav R., Ramakrishna W. (2022), *Bacillus subtilis* impact on plant growth, soil health and environment: Dr. Jekyll and Mr. Hyde, *Journal of Applied Microbiology*, 132(5), pp. 3543–3562, https://doi.org/10.1111/jam.15480

Majumdar S., Dutta S., Das T., Chattopadhyay P., Mukherjee A.K. (2015), Antiplatelet and antithrombotic activity of a fibrin(ogen)olytic protease from *Bacillus cereus* strain FF01, *International Journal of Biological Macromolecules*, 79, pp. 477–489, https://doi.org/10.1016/j.ijbiomac.2015.04.075

Ngalimat M.S., Yahaya R.S.R., Baharudin M.M.A., Yaminudin S.M., Karim M., Ahmad S.A., Sabri S. (2021), A review on the biotechnological applications of the operational group *Bacillus amyloliquefaciens*, *Microorganisms*, 9(3), 614, https://doi.org/10.3390/microorganisms9030614

Peng Y., Xiaojuan Y., Yizheng Z. (2005), Microbial fibrinolytic enzymes: An overview of source, production, properties, and thrombolytic activity in vivo, *Applied Microbiology and Biotechnology*, 69, pp. 126–132, https://doi.org/10.1007/s00253-005-0159-7

Poulaki E.G., Tjamos S.E. (2023), *Bacillus* species: Factories of plant protective volatile organic compounds, *Journal of Applied Microbiology*, 134(3), lxad037, https://doi.org/10.1093/jambio/lxad037

Priest F.G., Goodfellow M., Shute L.A., Berkeley R.C.W. (1987), *Bacillus amyloliquefaciens* sp. nov., nom. rev., *International Journal of Systematic Bacteriology*, 37(1), pp. 69–71, https://doi.org/10.1099/00207713-37-1-69

Priest F.G., Goodfellow M., Todd C. (1988), A numerical classification of the genus *Bacillus*, *Journal of General Microbiology*, 134(7), pp. 1847–1882, https://doi.org/10.1099/00221287-134-7-1847

Qian J., Wang Y., Hu Z., Shi T., Wang Y., Ye C., Huang H. (2023), *Bacillus* sp. as a microbial cell factory: Advancements and future prospects, *Biotechnology Advances*, 69, 108278, https://doi.org/10.1016/j.biotechadv.2023.108278

Raman J., Noh J.S., Kim J.S., Cho G., Kim D.H., Song J., Kim S.J. (2025), Role of *Bacillus* Species in food industry: Advantages and limitations, *Journal of Microbiology and Biotechnology*, 35, e2507043, https://doi.org/10.4014/jmb.2507.07043

Rosazza T., Eigentler L., Earl C., Davidson F.A., Stanley-Wall N.R. (2023), *Bacillus subtilis* extracellular protease production incurs a context-dependent cost, *Molecular Microbiology*, 120(2), pp. 105–121, https://doi.org/10.1111/mmi.15110

Sarwan J., Uddin N., Sahani S., Mittal K., Maurya D.D.K.P., Bose K.J.C. (2025), Isolation and characterization of novel *Bacillus* with dual enzymes, biodegradation potential: A special reference to cellulolytic and proteolytic activities, *Biomass Conversion and Biorefinery,* 15(3), pp. 4167–4183, https://doi.org/10.1007/s13399-024-05329-3

Saxena A. K., Kumar M., Chakdar H., Anuroopa N., Bagyaraj D.J. (2020), *Bacillus* species in soil as a natural resource for plant health and nutrition, *Journal of Applied Microbiology*, 128(6), pp. 1583–1594, https://doi.org/10.1111/jam.14506

Shakilanishi S., Mrudula P., Shanthi C. (2024), Production of dehairing protease by *Bacillus cereus* VITSN04: A model cradle-to-cradle approach for sustainable greener production of leathers, *Environmental Technology*, 45(1), pp. 180–191, https://doi.org/10.1080/09593330.2022.2102938

Sharma C., Nigam A., Singh R. (2021), Computational-approach understanding the structure-function prophecy of fibrinolytic protease RFEA1 from *Bacillus cereus* RSA1, *PeerJ*, 9, e11570, https://doi.org/10.7717/peerj.11570

Sharma C., Osmolovskiy A., Singh R. (2021), Microbial fibrinolytic enzymes as anti-thrombotics: Production, characterisation and prodigious biopharmaceutical applications, *Pharmaceutics,* 13(11), 1880, https://doi.org/10.3390/pharmaceutics13111880

Shopinskyi V., Butsenko L. (2026), Metabolic profile and biocontrol potential of endophytic bacteria *Bacillus amyloliquefaciens* E12, *Ukrainian Food Journal*, 15(1), pp. 176–194, https://doi.org/10.24263/2304-974X-2026-15-1-14

Silva G.M.M., Bezerra R.P., Teixeira J.A., Porto T.S., Lima-Filho J.L., Porto A.F. (2015), Fibrinolytic protease production by new *Streptomyces* sp. DPUA 1576 from Amazon lichens, *Electronic Journal of Biotechnology*, 18(1), pp. 16–19, https://doi.org/10.1016/j.ejbt.2014.11.001

Song P., Zhang X., Wang S., Xu W., Wang F., Fu R., Wei F. (2023), Microbial proteases and their applications, *Frontiers in Microbiology*, 14, 1236368, https://doi.org/10.3389/fmicb.2023.1236368

Stabnikova O., Shevchenko A., Stabnikov V., Paredes-López O. (2023), Utilization of plant processing wastes for enrichment of bakery and confectionery products, *Ukrainian Food Journal*, 12(2), pp. 299-308, https://doi.org/10.24263/2304-974X-2023-12-2-11

Topchii O., Pasichniy V., Marynin A., Stabnikova O. (2023), Biotransformation of collagen-containing meat materials into valuable product, In: O. Stabnikova, O. Shevchenko, V. Stabnikov, O. Paredes-López (Eds.), *Bioconversion of Waste to Value-added Products*, pp. 37-68, CRC Press, Boca Raton, London, New York, https://doi.org/10.1201/9781003329671-2

Tsotetsi T., Nephali L., Malebe M., Tugizimana F. (2022), *Bacillus* for plant growth promotion and stress resilience: What have we learned?, *Plants*, 11(19), 2482, https://doi.org/10.3390/plants11192482

Tsuchida S., Hiroshi U., Tomohiro N. (2020), Current status of matrix-assisted laser desorption/ionization-time-of-flight mass spectrometry (MALDI-TOF MS) in clinical diagnostic microbiology, *Molecules,* 25(20), 4775, https://doi.org/10.3390/molecules25204775

Wang C.T., Ji B.P., Li B., Rob N., Li P.L., Ji H., Chen L.F. (2006), Purification and characterization of a fibrinolytic enzyme of *Bacillus subtilis* DC33, isolated from Chinese traditional Douchi, *Journal of Industrial Microbiology and Biotechnology*, 33, pp. 750–758, https://doi.org/10.1007/s10295-006-0111-6

Wang X., Chi Y., Song S. (2024), Important soil microbiota's effects on plants and soils: a comprehensive 30-year systematic literature review, *Frontiers in Microbiology*, 15, 1347745, https://doi.org/10.3389/fmicb.2024.1347745

Wu B., Wu L., Chen D., Yang Z., Luo M. (2009), Purification and characterization of a novel fibrinolytic protease from *Fusarium* sp. CPCC 480097, *Journal of Industrial Microbiology and Biotechnology*, 36(3), pp. 451–459, https://doi.org/10.1007/s10295-008-0516-5

Yahya G., Ebada A., Khalaf E.M., Mansour B., Nouh N.A., Mosbah R.A., Saber S., Moustafa M., Negm S., El-Sokkary M.M.A., El-Baz A.M. (2021), Soil-associated *Bacillus* species: A reservoir of bioactive compounds with potential therapeutic activity against human pathogens, *Microorganisms*, 9(6), 1131, https://doi.org/10.3390/microorganisms9061131

Yan Z.Y., Guan G.X., Zhang W.Q., Lin Z.F. (1995), Extracellular elastase produced bacteria screening and enzyme purification, *Acta Microbiologica Sinica*, 35, pp. 50–55.

Yogesh D., Halami P.M. (2017), Fibrinolytic enzymes of *Bacillus* spp.: An overview, *International Food Research Journal*, 24(1), pp. 35–47.

Yousefi N., Shokrollahi Yancheshmeh B., Gernaey K.V. (2025), The potential of fermentation-based processing on protein modification: A review, *Foods*, *14*(20), 3461, https://doi.org/10.3390/foods14203461

Yukalo V., Krupa O., Datsyshyn K., Storozh L. (2023), Proteolytic activity of the Carpathian traditional liquid milk coagulant, *Ukrainian Food Journal*, 12(2), pp. 240-251, https://doi.org/10.24263/2304-974X-2023-12-2-7

Zhang Y.Z., Zhang W.X., Chen X.L. (2020), Mechanisms for induction of microbial extracellular proteases in response to exterior proteins, *Applied and Environmental Microbiology*, 86(19), pp. e01036-20, https://doi.org/10.1128/AEM.01036-20

Zhang J., Liu Y., Jiang L., Zhao T., Su G., Zhao M. (2023), Exploring the release of elastin peptides generated from enzymatic hydrolysis of bovine elastin via peptide mapping, *Molecules, 28,* 7534, https://doi.org/10.3390/molecules28227534

Zupetic J., Peñaloza H.F., Bain W., Hulver M., Mettus R., Jorth P., Doi Y., Bomberger J., Pilewski J., Nouraie M., Lee J.S. (2021), Elastase activity from *Pseudomonas aeruginosa* respiratory isolates and ICU mortality, *Chest*, 160(5), pp. 1624–1633, https://doi.org/10.1016/j.chest.2021.04.015

Cite:

Gudzenko, O., Varbanets, L., Butsenko, L., & Pasichnyk, L. (2026). Soil-derived Bacillus strains producing proteolytic enzymes for food industry applications. *Ukrainian Food Journal, 15*(2), 532–549. https://doi.org/10.24263/2304-974X-2026-15-2-15

Mathematical modeling of water-polymer jet cutting for frozen food products

Andriy Pogrebnyak[1], Iryna Perkun[2], Volodymyr Pogrebnyak[2], Maxim Korneyev[1], Svitlana Haponenko[1], Yehor Beliaiev[1], Olena Yudina[1]

1 – University of Customs and Finance, Dnipro, Ukraine
2 – Ivano-Frankivsk National Technical University of Oil and Gas, Ivano-Frankivsk, Ukraine

Keywords:

Hydro-cutting
Water-polymer jet
Polyethylene oxide
Ultimate strength
Frozen product

Article history:

Received 16.12.2025
Received in revised form 09.04.2026
Accepted 30.06.2026

Corresponding author:

Andriy Pogrebnyak
E-mail: pogrebnyak.av1985@gmail.com

DOI: 10.24263/2304-974X-2026-15-2-16

Abstract

Introduction. Hydro-cutting of frozen food products requires the optimization of jet structural and dynamic parameters through the incorporation of polymer additives. The objectives of this study are to establish cutting resistance criteria, investigate the characteristics of high-speed water–polymer jets, and develop a comprehensive mathematical model describing their interaction with frozen materials. These results serve as the scientific foundation for the design and development of innovative hydro-cutting equipment.

Materials and methods. Cutting pork, beef, broiler chicken fillet, and hake fish was investigated using aqueous solutions of polyethylene oxide $4 \cdot 10^6$ and $6 \cdot 10^6$ at pressures up to 100 MPa. Final cut depth and width were measured. Product hardness (ball indentation), ultimate shear stress (punch shear test), and ultimate uniaxial compressive strength (compression between flat plates) were determined at temperatures from -3 °C to -25 °C inside a cryogenic thermostatic chamber.

Results and discussion. Ultimate uniaxial compressive strength most accurately characterizes frozen food cutting resistance. Cut depth exhibits an inverse power-law dependence on tissue compressive strength and jet moving speed, while increasing linearly with fluid pressure and nozzle diameter. A self-similar flow regime initiates above a threshold pressure of 35–45 MPa. Adding 0.007% polyethylene oxide significantly expands the initial compact jet section, maintaining cutting ability over 0.1 m from the nozzle exit. The polymer stabilizes the jet core, restricting cut width to 0.36–0.48 mm, compared to 0.45–0.77 mm for pure water. Maximum dynamic impact force on a flat obstacle occurs within a dimensionless standoff distance of 30–300 nozzle diameters. A comprehensive model based on dimensional analysis demonstrated that practically viable cutting depths are achieved at nozzle moving speeds of 50–100 mm/s. The model showed good agreement with experimental data and can be used to predict cutting performance under various operating conditions. These findings provide a scientific basis for optimizing hydro-cutting processes and developing advanced industrial equipment for frozen food processing.

Conclusions. The developed multi-parameter mathematical model reliably simulates fluid-structure interactions during water–polymer jet cutting and serves as a theoretical tool for engineering calculations, optimization of operating parameters, and the design of advanced 3D hydro-cutting equipment.

Introduction

Developing innovative cutting equipment remains a critical challenge for the advancement of the food industry (Cui et al., 2022; Hu et al., 2015; Xu et al., 2022). Traditional cutting methods and equipment currently in use possess significant disadvantages: they pose safety hazards during maintenance, generate high levels of noise and vibration, and exhibit a low level of sanitary safety. Furthermore, the wear and degradation of traditional cutting tools can lead to the contamination of products with metal particles. Rapid blunting requires constant sharpening and replacement of the working elements, while the wide cutting kerf and chip formation result in additional product losses. These difficulties become particularly pronounced when cutting deep-frozen food products (Liu, 2019; Ranjan et al., 2022: Wang and Shanmugam, 2009;).

An alternative method for cutting food products, especially at low temperatures, is the hydro-cutting (waterjet) process, which effectively eliminates the aforementioned disadvantages (Gyliene et al., 2014; Duspara et al., 2018). The widespread adoption of waterjet technology across various industries is primarily driven by its high technological efficiency (Perec and Tavodova, 2016: Natarajan et al., 2020). A standout advantage of this technology is its compatibility with computer numerical control (CNC), enabling the precise 3D processing of food products. The jet-forming head can maneuver in three dimensions using servo drives, processing the product from multiple angles to create cuts of any complexity. This capability allows for the consolidation of a traditional robotic primary processing line into a single, universal processing station.

However, this method is still rarely implemented in the food industry. The main obstacle is the substantial capital and maintenance costs associated with expensive high-pressure equipment. Additionally, the use of abrasive waterjets, common in other industries–is strictly prohibited in food production due to inevitable product contamination. Conversely, using a pure water jet as a cutting tool presents limitations due to the rapid dissipation of its kinetic energy in the air.

Enhancing the food hydro-cutting process is directly linked to modifying the hydrodynamic characteristics of the high-speed thin jet to maximize productivity while minimizing energy consumption. This objective can be achieved by replacing the standard water jet with a water-polymer jet. The introduction of minor polymer additives, specifically polyethylene oxide (PEO), into the working fluid significantly alters the jet's dynamics, increasing its compactness, kinetic stability, and overall cutting ability. This innovation paves the way for a substantial reduction in operational pressures and the utilization of more cost-effective equipment.

While the addition of high-molecular-weight polymers (such as polyacrylamide) to jets has been studied globally to improve jet coherence and reduce energy loss when cutting industrial materials (Annoni et al., 2009; Klichova et al., 2015; Sreekumar et al., 2023), the specific application of polyethylene oxide (PEO) solutions for cutting frozen food products is a novel direction pioneered and systematically investigated by our research group (Pogrebnyak et al., 2020, 2025).

Despite the considerable potential of water-polymer cutting technology, the relationship between the physical and mechanical properties of frozen food raw materials and the hydrodynamic parameters of the modified jet remains insufficiently explored. The absence of clear criteria for material resistance to destruction and comprehensive mathematical models hinders the industrial implementation of this technology. Designing efficient industrial equipment requires a precise understanding of the jet's spatial structure and dynamics, as well as a robust mathematical model governing its interaction with food products.

The aim of this study is to determine the criteria for the resistance of frozen food products to cutting, to investigate the structural and dynamic characteristics of a high-speed water–polymer jet, and to establish a comprehensive mathematical model of their interaction as the scientific basis for designing innovative technological equipment.

Materials and methods

Materials

The investigated samples included pork, beef, poultry (broiler chicken fillet), and hake fish. Test samples were prepared by slicing sections from the back muscle of an adult pig and a cow of average fatness. Fish and poultry samples were formed by joining several layers to achieve the required dimensions. The working fluid utilized was an aqueous solution of polyethylene oxide (PEO) with molecular weights of 4·106 and 6·106 (Voloshyn, 2010).

Experimental methods

The investigations were carried out using a specially designed hydro-test bench with an operating pressure of up to 300 MPa and the ability to change and control both integral and differential parameters of the food products hydro-cutting process by a water-polymer jet. The evidence base for the practical feasibility of using the developed mathematical model was the experimental results obtained on a prototype of a universal hydro-cutting machine (Pogrebnyak et al., 2025) (Figure 1).

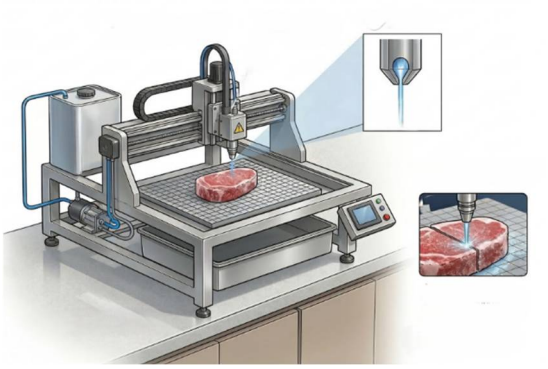

Figure 1. Prototype of a universal machine for cutting food products

The cutting machine is table-mounted and comprises a high-pressure pump, a receiver, and a reservoir for the working fluid. To achieve the necessary low temperatures (down to -40 °C), a specialized low-temperature thermostating system was employed (Pogrebnyak et al., 2023). Temperature was stabilized at the target level with an accuracy of ±0.1 °C.

The cut depth (h) in the food product was evaluated using a precision depth gauge with a measurement resolution of 0.01 mm. To determine *the cut width* (b), including micro-cuts smaller than $0.4 \cdot 10^{-3}$ m, a digital optical microscope equipped with a calibrated measuring scale (at 20×magnification) and a set of precision feeler gauges were utilized. The relative measurement error for both the cut depth and width did not exceed 2.5–3%. The application of optical microscopy and precision mechanical gauges for assessing kerf geometry is a standard and highly accurate approach in modern water jet cutting research (Cui et al., 2022; Xu et al., 2022).

Hardness (HB) were evaluated using testing machine equipped with a spherical indenter and a specialized cutting cylinder fixture (Warner-Bratzler type device), respectively (Sydor et al., 2020).

The ultimate shear stress (τ_{sh}) was determined using a texture analyzer equipped with a cylindrical penetration probe, performing a punch shear test. During the procedure, the probe penetrated the sample at a constant speed, and the ultimate shear stress was calculated from the

maximum force recorded prior to sample rupture, following the methodology described in recent literature (Yang et al., 2026).

The ultimate uniaxial compressive strength (σ_c) was measured using a universal electromechanical texture analyzer (testing machine) equipped with a load cell and a customized low-temperature thermostatic chamber. Cylindrical samples of frozen meat and fish were compressed between two parallel flat plates at a constant crosshead speed until macroscopic failure occurred. (Chen et al., 2024; Gemi et al., 2021; Kęska et al., 2021). This methodology is widely accepted in modern food science for determining the bulk mechanical properties, structural integrity, and internal resistance to applied stress of both native and engineered meat tissues (Bikos et al., 2021; Yuen et al., 2023).

A critical requirement for accurately determining these strength characteristics is the appropriate temperature control (thermostating) of the entire testing system at low temperatures. A specialized thermostatic chamber was used to cryostat the test samples and measuring devices (Pogrebnyak et al., 2023). The precooled objects were placed inside, and the target temperature was maintained using liquid nitrogen vapors managed by the thermostating system. The target temperatures during the tests were strictly maintained at levels from -3 °C to -25 °C using liquid nitrogen vapor circulation. The error in measuring the strength characteristics did not exceed 3%.

To visualize and analyze the structural characteristics of the high-speed jets, high-speed photography was employed. The images of the aqueous PEO solution and pure water jet outflows (Figures 2d and 2c, respectively) were captured using a high-speed digital camera. The camera was positioned perpendicularly to the jet axis and synchronized with a high-intensity pulsed light source to "freeze" the motion of the high-velocity flow and prevent motion blur. Figure 2a represents a theoretical schematic diagram of the hydro-jet structure, specifically illustrating the initial (l_i) and main (l_{main}) sections, which was developed based on the obtained visual and hydrodynamic data.

The energy capabilities of the water-polymer jet were evaluated by measuring the impact force of the jet on a steel obstacle on which strain gauges were mounted. The obstacle was made of a steel (St3) sheet with dimensions of $(220x220x3)\cdot10^{-3}$ m. There was a gap of $5\cdot10^{-2}$ m between the plane of the obstacle and the table of the hydro-cutting installation (Pogrebnyak et al., 2022).

Results and discussion

Criteria for the resistance of frozen food products to hydro-cutting

To substantiate and select an appropriate criterion for the resistance of frozen food products to high-speed water-polymer jet cutting, it is necessary to determine how various physical and mechanical properties affect the cut depth. This criterion serves as a refined metric (Cui et al., 2022) for evaluating a material's resistance specifically to thin, high-speed fluid jets.

The primary indicators evaluated were: hardness HB, ultimate shear stress τ_{sh} and ultimate uniaxial compressive strength σ_c (Table 1).

To establish the criterion of resistance of frozen food products to cutting by a water-polymer jet, the method of pairwise correlation analysis was used, which consists of finding the relationship between the cut depth and each of the selected physical and mechanical indicators at different temperatures based on experimental data. Five options of correlation relationship were considered:

$$y = A+Bx \quad (1);$$

$$y = A+Bx+Cx^2 \quad (2);$$

$$y = Ae^{Bx} \ (3); \quad y = Ax^B \quad (4);$$

$$y = A\sqrt{x} + B \quad (5).$$

Table 1

Hardness of pork, ultimate shear stress of pork and ultimate uniaxial compressive strength of broiler chicken fillet, hake fish, pork, and beef

Temperature, °C	Physical-mechanical properties					
	HB_c, H/mm² (pork)	τ_{sh}, KPa (pork)	σ_c, MPa (chicken fillet)	σ_c, MPa (hake fish)	σ_c, MPa (pork)	σ_c, MPa **(beef)**
-3	9.67	0.80	2.92	3.11	3.50	3.54
-5	11.03	0.91	3.47	3.54	3.99	4.03
-7	-	-	3.83	3.96	4.45	4.56
-10	13.69	1.12	4.23	4.41	4.95	5.13
-15	15.04	1.26	5.00	5.18	5.43	5.45
-20	16.73	1.40	5.63	5.79	6.05	6.24
-25	17.86	1.51	6.24	6.40	6.45	6.57

The results of calculations determining the relationship between the cut depth h and the three indicators of physical and mechanical properties of beef and pork, broiler chicken fillet, and hake fish in the temperature range from -3 to -25 °C for different options of correlation relationships showed that the highest values of the correlation indices $R^2 = 0.994$ were found when approximating the experimental data with a dependence of type (4). The highest value of the correlation index $R^2 = 0.994$ and the lowest coefficient of variation $K_{var} = 4.5$ % occurred when comparing the cut depth h with the ultimate uniaxial compressive strength σ_c.

The obtained empirical dependencies showing the relationship between the cut depth by the water-polymer jet and the ultimate uniaxial compressive strength for beef and pork, broiler chicken fillet, and hake fish have the following form:

for beef

$$h = 0.5597 \cdot \sigma_c^{-1} \quad (6);$$

for pork

$$h = 0.5915 \cdot \sigma_c^{-1} \quad (7);$$

for chicken fillet

$$h = 0.6162 \cdot \sigma_c^{-1} \quad (8);$$

for hake fillet

$$h = 0.6097 \cdot \sigma_c^{-1} \quad (9).$$

Thus, the criterion that most accurately characterizes the resistance of frozen food products to cutting is the ultimate uniaxial compressive strength σ_c. This finding aligns with recent fundamental studies on solid food processing (Xu et al., 2022) and agricultural material hydro-cutting (Cui et al., 2022), which emphasize that compressive strength is the primary macro-mechanical barrier to jet penetration. However, while previous authors focused primarily on cutting biological tissues with pure water (where kinetic energy dissipates rapidly) or abrasive jets (which cause unacceptable cross-contamination in food), our results demonstrate a unique interaction mechanism. Specifically, the high-speed water-polymer jet acts as a cohesive continuous kinetic indenter. Because the addition of PEO suppresses flow fragmentation and maintains a high dynamic pressure within the jet core, the penetration depth depends fundamentally on overcoming the ultimate compressive limit of the frozen biomatrix, rather than merely its surface hardness or shear resistance. This physical mechanism thoroughly explains the exceptionally high correlation ($R^2 = 0.994$) obtained for ultimate uniaxial compressive strength compared to other mechanical properties

Structural and dynamic characteristics of the water-polymer jet

Previous studies (Pogrebnyak et al., 2020, 2023) demonstrated that at pressures below a threshold of ΔP_{lim} = 35–45 MPa, the hydro-jet is incapable of cutting frozen food products (i.e., cut depth at temperatures of -18 to -25 °C is essentially zero). The optimal distance l_{opt} between the nozzle exit and the food surface corresponded to the maximum cut depth achieved at -18 °C under pressures exceeding 50 MPa. Comparing the threshold pressures required for the onset of a self-similar flow regime with the minimum pressure required to initiate cutting reveals a near-perfect correlation. This proves that the operational modes and cutting productivity are fundamentally dictated by the structural, hydrodynamic, and dynamic parameters of the jet (Cui et al., 2022; Ranjan et al., 2022; Xu et al., 2022).

The obtained results allow us to assert that the value of ΔP_{lim} is a limiting parameter in terms of the minimum working pressure, starting from which the process of hydro-jet water-polymer cutting of deep-frozen food products should occur. It is also important to know what determines the limiting parameter in terms of the maximum pressure. The maximum possible pressure is determined, first of all, by the thermal effects in the main units of the equipment, the consideration of which was carried out in (Pogrebnyak et al., 2023), and the limiting parameter in terms of high pressures ΔP_{max} was obtained there as well.

Experiments demonstrated that under the influence of pressure and turbulent disturbances, the jet inevitably expands, altering its diameter and internal structure (Figure 2). Beyond the initial section of the water-polymer jet, as a result of its expansion and decay, the axial longitudinal velocity and dynamic pressure gradually decrease according to a certain hyperbolic dependence, and the dynamic pressure and velocity in the cross-section of the jet sharply decrease from their maximum value to a minimum in the boundary region. This section of the jet l_{main} (beyond the initial section l_i), in which the jet retains high density and compactness, is called the main section of the jet (Liu et al., 2019; Xu et al., 2022). Within the main section, a high density of the jet is maintained at low values of the expansion angle of the jet boundaries (White, 2015). The initial and main sections together make up the working section of the water-polymer jet.

The main structural characteristic of a liquid jet is the length of the initial section l_i. Using the dimensionless value of the length of the initial section of the water $l_{i,w}/d_{noz}$ and water-polymer $l_{i,p}/d_{noz}$ jets, the quality of their formation can be integrally evaluated, which depends on the shape of the profile, and for the water-polymer jet, also on the molecular weight of PEO and its concentration (Figure 2). Photographs of jets of aqueous PEO solutions indicate that the use of PEO additives in water leads to a significant increase in the initial section $l_{i,p}$ of the water-polymer jet, which characterizes the quality of its formation and a significant increase in compactness due to a decrease in its diameter.

Comparison of the experimental and calculated values of the dimensionless magnitude of the initial sections of the water $l_{i,w}$ and water-polymer $l_{i,p}$ jets was performed using the experimentally obtained distribution of the impact force of the water and water-polymer jets on a metal obstacle along the flow axis (Figure 3). The experimental data are described with sufficient accuracy by the following equation:

$$\frac{l_{i,p}}{d_{noz}} = \frac{l_{i,w}}{d_{noz}} \cdot \dot{\varepsilon} \cdot \theta_c = 25\left(\frac{d_{noz}}{R_{az}}\right)^{1/6} \lg K \left(1 - 1.25\exp\left(-0.095 \cdot \frac{l_{ch}}{d_{ch}}\right)\right) \cdot \dot{\varepsilon} \cdot \theta_c . \qquad (10)$$

where K is the flow compression coefficient, equal to 10 at the ratio of the length to the diameter of the flow channel of the head $l_{ch}/d_{ch} > 10$; R_{az} is the roughness parameter of the inner surface of the jet-forming head.

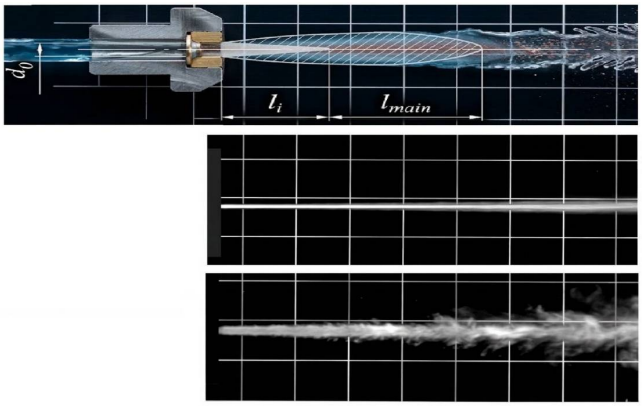

Figure 2. Diagram of the hydro-jet structure (a), photographs of jets: aqueous PEO solution $M_{PEO} = 4 \cdot 10^6$, $C_{PEO} = 0.007\%$ (b) and water (c), flowing out of a nozzle with a diameter of $0.35 \cdot 10^{-3}$ m at a pressure of 100 MPa

The influence of the PEO molecular weight and its concentration in the water-polymer jet in equation (10) is taken into account by the obtained analytical expressions (Pogrebnyak, 2025), which allow calculating the relaxation time of aqueous PEO solutions θ_c from the known molecular characteristics of PEO and the longitudinal velocity gradient on the flow axis in the inlet section of the nozzle $\dot{\varepsilon}$. When $\dot{\varepsilon} \cdot \theta_c < 1$, the initial section of the water-polymer jet $l_{i,p}$ is equal to the initial section of the water jet $l_{i,w}$. Formula (10) has the following limits of applicability: aqueous PEO solutions must satisfy the dilute solution concentration criterion $[\eta]_0 \cdot C < 1$ (Dinić and Sharma, 2019), and the value of the product of the longitudinal velocity gradient $\dot{\varepsilon}$ in the inlet section of the nozzle and the relaxation time θ_c of the aqueous PEO solution must satisfy the condition for the coil-stretch transition $1 \le \dot{\varepsilon} \cdot \theta_c < 10$ (Haward et al., 2023; Dinić and Sharma, 2019).

The coefficient of variation when using dependence (10) was K_{var} = 11%, which indicates a sufficient convergence of the calculated values of the dimensionless lengths of the initial section of water-polymer jets with the experimental ones.

The dimensions of $l_{i,p}$ are of great importance in the development of a mathematical model of the process of hydro-jet water-polymer cutting of food products under conditions of reducing the energy intensity of cutting and resource saving (due to an increase in the resource and a decrease in the kerf width). It turns out that when cutting food products, the most effective is the working section of the jet, which is equal to the sum of the initial and main sections. Beyond the working section, the hydro-jet loses stability and acquires a sinuous shape. This section in hydro-cutting technology is practically non-working. An experimental study of the width of cuts in a food product (Table 2) indicates that the water-polymer jet has better hydrodynamic properties than the water jet (Figure 2) (smaller diameter and, accordingly, smaller cut width), which provide high productivity with high quality of the lateral surface of the cuts (Pogrebnyak et al., 2020).

Table 2

Influence of distance between beef surface and nozzle exit on the cut width by water-polymer and water jets

(M_{PEO}= 4·10^6; C_{PEO}=0.007%; ΔP_o=100 MPa; d_{noz}=0.35·10^{-3} m; t = -25 °C)

Working fluid	Cut width b·10^3, m for different l_o·10^3, m				
	10	20	40	60	90
Aqueous PEO solution	0.36	0.37	0.38	0.42	0.48
Water	0.45	0.50	0.57	0.62	0.77

It has been experimentally proven that an increase in the PEO concentration in the water-polymer jet leads to an increase in the initial section of the jet $l_{i.p}$, which characterizes the quality of its formation and the compactness of the water-polymer jet due to a decrease in its diameter (Figure 2b).

Table 2 shows the cut width in beef at a temperature of -25 °C depending on the distance between the meat surface and the nozzle exit. The data in Table 2 indicate that the water-polymer jet has better hydrodynamic properties than the water jet (the cut width is significantly smaller than when using a water jet). This allows obtaining significant cut depths at a distance of more than 0.1 m, which is critically important for the technology of 3D cutting of bulky pieces of raw materials.

Interpretation of the obtained experimental data requires the study of not only the structural changes occurring in the water-polymer jet under different modes of its outflow from the nozzle, but also the degree of force impact of the water-polymer jet on an obstacle. Currently, the nature of the change in the impact force of a water-polymer jet depending on the distance of the obstacle from the nozzle is not fully understood.

Regarding this issue, there are contradictory points of view even for a pure water jet. Some researchers indicate (Natarajan et al., 2020; Ranjan et al., 2022) that the impact force and kinetic energy of a water jet significantly decrease with increasing standoff distance from the nozzle exit due to aerodynamic drag and flow fragmentation. Conversely, other studies on jet hydrodynamics (Liu et al., 2019; Xu et al., 2022) suggest that the total length of the water jet can be divided into distinct structural sections: an initial section where the effective impact pressure increases and reaches its maximum value at a certain optimal distance from the nozzle, and a subsequent main section during which the core cutting capability is temporarily maintained before ultimate decay.

Therefore, the experiments discussed below were set up with the aim of establishing the dynamics of water-polymer jets; by elucidating these, it is possible to obtain relationships between the parameters of the hydro-cutting process, without which it is impossible to establish rational parameters of equipment for hydro-jet water-polymer cutting of food products.

The results reflecting the development of the impact force of a hydro-jet with different PEO contents on the obstacle along the flow axis in dimensionless coordinates, with a measurement error of no more than 1%, are presented in Figure 3.

The obtained experimental data are described by at least two sections with a linear change in the impact force of the hydro-jet on the obstacle. It can be seen from Figure 3 that the maximum value of the impact force of the water-polymer jet on a flat obstacle depends on the PEO concentration in the water-polymer jet and is located in the range of dimensionless distances from the nozzle $30 < l_o/d_{noz} < 300$.

Comparison of the distribution of the impact force of the hydro-jet on the obstacle along the flow axis (Figure 3) with its structural features (Figure 2) shows that the region $l_o/d_{noz} < 100$ belongs to the initial section of the jet, and the region $30 < l_o/d_{noz} < 300$ belongs to the working section.

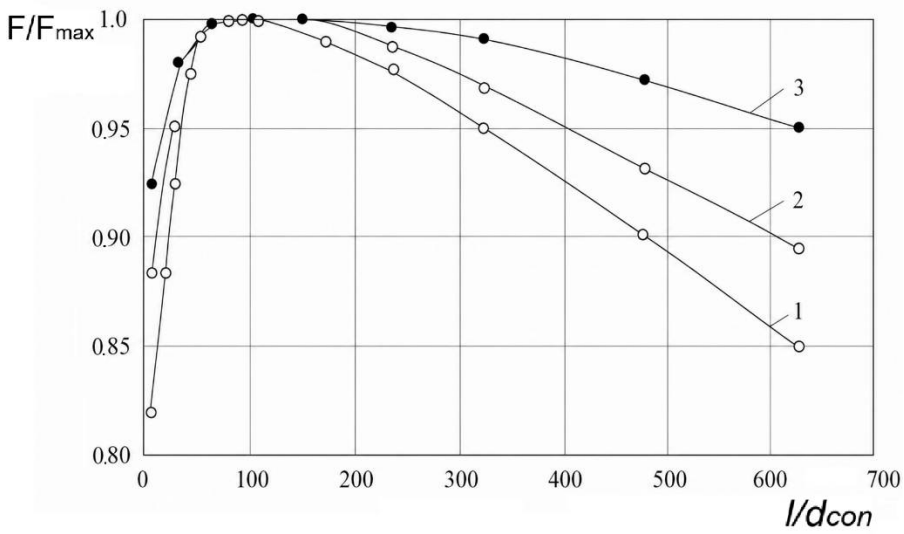

($M_{PEO} = 4 \cdot 10^6$)

Figure 3. Distribution of the impact force of the pure water jet (1), the 0.003% aqueous PEO solution jet (2), and the 0.007% aqueous PEO solution jet (3) on an obstacle along the flow axis

The experimental data on the dynamics of the water-polymer jet fully explain the nature of the change in the cutting properties of the jet depending on the distance between the surface of the food product being cut and the nozzle exit. It becomes clear why in some cases the cut depth increases with an increase in the nozzle diameter, and in others it decreases. Taking into account the data in Figure 3, we come to the conclusion: if the distance from the nozzle to the surface of the food product is less than the dimensions of the initial section of the water-polymer jet, then an increase in the diameter of the nozzle exit will lead to a decrease in the cut depth. If the distance from the nozzle to the surface of the food product approaches the dimensions of the main section of the water-polymer jet or exceeds it, then the cut depth will increase with an increase in the nozzle diameter at a constant pressure drop.

Thus, the structural and hydrodynamic parameters of the water-polymer jet make it possible to interpret the obtained experimental data on the effect of the concentration of polymer additives in the water jet, and the geometric and dynamic parameters of the water-polymer jet on the indicators of the hydro-jet water-polymer cutting process of food products. It becomes clear that the structural and dynamic parameters of the water-polymer jet are of primary importance, which must be taken into account when developing equipment for universal water-polymer cutting of food products in 3D mode under conditions of efficient use of energy resources.

Mathematical model of the water-polymer cutting process

The study of the process of water-polymer cutting of frozen food products allowed transitioning to complex modeling. The obtained experimental data for beef, pork, broiler chicken fillet, and hake fish made it possible to prove that the criterion of resistance of frozen food products to cutting by a water-polymer jet is the ultimate uniaxial compressive strength.

Typical data characterizing the process of hydro-jet water-polymer cutting of frozen food products are presented in (Pogrebnyak et al., 2020, 2025), as well as in Figures 4 and 5 and in Tables 3 and 4.

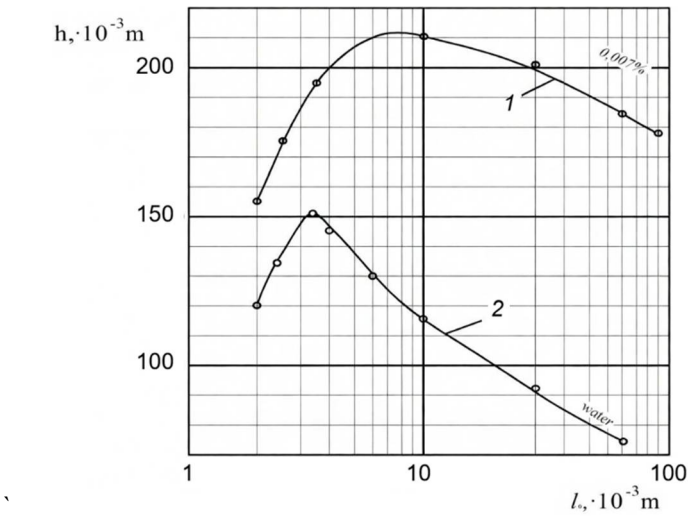

($V_{m,j}$=15·10^{-3} m/s)

Figure 4. Dependence of cut depth by a water-polymer jet in pork on distance to nozzle exit: t= -7 ºC, ΔP_o=100 PIIa, d_{noz}=0,35·10^{-3} m, C_{PEO}=0,007% (1), water (2)

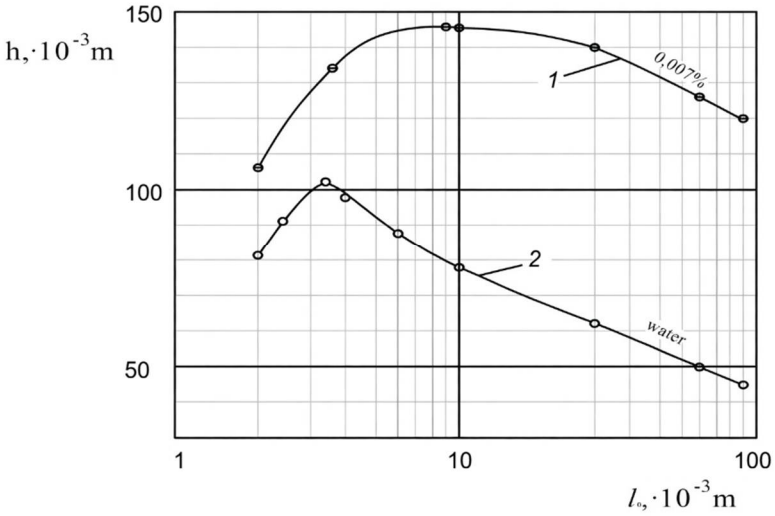

($V_{m,j}$=25·10^{-3} m/c)

Figure 5. Dependence of ut depth by water-polymer jet in pork on distance between its surface and nozzle exit: t = -7 ºC, ΔP_o=100 PIIa, d_{noz}=0,35·10^{-3} m, C_{PEO}=0,007% (1), water (2)

Table 3

Influence of distance from nozzle exit to surface of frozen beef being cut, moving speed of water jet, and nozzle diameter on cut depth for ΔP_o=100 MPa

t, °C beef	D_{noz} ·10³, m	$V_{m,j}$ ·10³, m/s	Cutting depth h·10³, m								
			l_o·10³, m								
			2	2.5	3.5	4	6	10	20	60	90
-7 °C	0.35	7,5						192	161	123	110
		15	120	134	151	143	130	114	96	73	66
		25	81	91	103	98	88	78	65	50	45
		50	50	54	61	58	53	46	39	30	27
		100	30	32	36	35	31	27	23	18	16
-7 °C	0.60	15							192	146	132
		25	135		151	157	176	155	130	99	90
		50	80		90	94	105	92	78	59	53
		100	45		53	56	62	55	46	35	32
-25 °C	0.35	7,5	131	150	175	166	150	152	111	85	76
		15	78	96	104	99	89	79	67	50	45
		25	53	62	71	67	61	54	45	34	31
		50	32	38	42	40	36	32	27	20	18
		100	19	22	25	24	22	19	13	12	11
-25°C	0.60	7,5								169	153
		15	125		148	156	178	157	132	111	91
		25	85		105	108	121	107	90	69	62
		50	50		61	65	72	64	54	41	37
		100	30		43	40	43	38	32	24	22

Table 4

Influence of the distance from the nozzle exit to the surface of the hake fish fillet cut by a water-polymer the jet, moving speed, and the nozzle diameteron the cut depth

($C_{ПЕО}$=0,007%, $M_{ПЕО}$=4·10⁶, ΔP_o=100 МПа)

t, °C hake fillet	d_{noz} ·10³, m	$V_{m,j}$ ·10³, m/s	Cutting depth h·10³, m						
			l_o·10³, m						
			2	4	6	10	20	60	90
-7°C	0,35	15	181	>200	>200	>200	>200	>200	>200
		25	122	159	166	168	163	146	141
		50	76	93	98	99	94	87	85
		100	45	56	57	58	56	51	50
	0,60	50	129	158	166	168	160	149	144
		100	77	95	96	99	95	87	85
-25°C	0,35	15	104	144	150	148	144	130	125
		25	71	97	102	103	97	89	86
		50	43	58	61	61	58	52	50
	0,60	25	115	165	174	176	165	151	146
		50	73	98	102	104	98	88	85

Analysis of these experimental data shows that the depth of cuts in frozen food products linearly increases with an increase in pressure over the entire range of its values and decreases with an increase in their strength (Table 1) under uniaxial compression. It is also evident from the obtained data that an increase in the nozzle exit diameter leads to an increase in the cut depth in the frozen food product.

Experimental results (Pogrebnyak et al., 2020) characterizing the effect of the high-speed hydro-jet moving speed on the cut depth in food products, as well as those presented in Tables 3 and 4, indicate a power-law dependence of the cut depth on the moving speed of the water-polymer jet. It can be seen that in the entire investigated pressure range, with an increase in the moving speed of the PEO solution jet, the cut depth rapidly decreases. Practically important cut depths on samples of frozen food products in the temperature range from -3 °C to -25 °C can be obtained at moving speeds of water-polymer jets from $50 \cdot 10^{-3}$ до $100 \cdot 10^{-3}$ m/s.

One of the main conditions for the successful application of high-speed water-polymer jets for cutting food products is obtaining a jet with good hydrodynamic properties that ensure sufficient efficiency of the hydro-jet water-polymer cutting process. The obtained equation (10) for determining the dimensionless length of the initial section of the water-polymer jet for different PEO molecular weights and concentrations must be necessarily taken into account when developing a mathematical model of the hydro-jet water-polymer cutting process of food products.

A comprehensive study of the features of the food products cutting process by a water-polymer jet and the analysis of the obtained experimental data characterizing the process of hydro-jet water-polymer cutting of beef, pork, broiler chicken fillet, and hake fish, using the methods of similarity and dimensional theory, as well as methods of mathematical statistics, made it possible to develop a mathematical model of the process of cutting food products by a water-polymer jet, which describes the influence of the food product strength σ_c and the distance l_o to its surface from the nozzle exit, hydraulic ΔP_o and dynamic $V_{m,j}$ parameters of the water-polymer jet, the moving speed of the jet $V_{o,p}$ and the concentration and molecular weight of the polymer on the cut depth h of the food product:

$$\frac{h}{d_{noz}} = \frac{\Delta P_o}{\sigma_c} \cdot \left(\frac{l_o}{5.4 \cdot l_{i,w} \cdot \dot{\varepsilon} \cdot \theta_c} \right)^{-0,25} \cdot \left(\frac{V_{o,p}}{V_{m,j}} \right)^{0,75} \cdot 10^{-2}, \qquad (11)$$

$$\text{where } \dot{\varepsilon} \cdot \theta_c = \theta_0 e^k \frac{2Q \cdot tg(\beta^\circ / 2)}{d_{noz}^3}, \quad \text{a } k = [\eta]_0 \cdot C_{PEO} \le 1.$$

The influence of the PEO molecular weight and its concentration in the water-polymer jet in equation (11) is taken into account by the dependence of the relaxation time $\theta_c = \theta_0 e^k$ of aqueous PEO solutions on M_{PEO} and C_{PEO} (Pogrebnyak, 2025). Provided that $\dot{\varepsilon} \cdot \theta_c < 1$, the initial section $l_{i,p}$ of the water-polymer jet is equal to the initial section $l_{i,w}$ of the water jet. Formula (11) has the following limits of applicability: aqueous PEO solutions must satisfy the Debye concentration criterion – $[\eta]_0 \cdot C_{PEO} < 1$ (Dinić and Sharma, 2019), and the value of the product of the longitudinal velocity gradient (extensional rate) in the converging inlet section of the nozzle $\dot{\varepsilon} = \frac{2 \cdot Q \cdot tg(\beta^\circ / 2)}{A \cdot d_{noz}}$ (Chaffin et al., 2022; Haward et al., 2023) and the relaxation time θ_c of the aqueous PEO solution must satisfy the condition – $1 \le \dot{\varepsilon} \cdot \theta_c < 10$. A feature of equation (11) is that it takes into account the quality of formation of the aqueous PEO solution jet when varying the concentration C_{PEO} and molecular weight M_{PEO} of the polymer.

Table 5

Ranges of change of the main parameters in formula (11) for calculating the depth of cuts in frozen food products

Parameter name	Range of parameter change
Set parameters	
Nozzle exit diameter – $d_{noz}\cdot10^3$, m	0.35–0,60
Nozzle entry angle – β°	$\left(\beta^0 \approx \pi/4\right)$
Molecular weight M_{PEO}	$10^6 \le M_{PEO} \le 8\cdot10^6$
Concentration of aqueous PEO solution C_{PEO}	$[\eta]_0 \cdot C_{PEO} < 1$
$\dot{\varepsilon}\cdot\theta_c$	$1 \le \dot{\varepsilon}\cdot\theta_c < 10$
Pressure of aqueous PEO – ΔP_o, PПa	50–150
Ultimate uniaxial compressive strength of a food product – σ_c, MPa	2.4–6.8
Distance between the nozzle exit and the food product surface – $l_o\cdot10^3$, m	$l_{opt} \le l_o < 400$
Surface roughness of the jet-forming head and the supply channel – R_{az}, mkm	2.5–1.25
Length of the channel supplying the aqueous PEO solution to the nozzle – $l_{ch}\cdot10^3$, m	45–100
Diameter of the supply channel $d_{ch}\cdot10^3$, m	4–6
Moving speed of the water-polymer jet relative to the food product sample – $V_{m,j}\cdot10^{-3}$, m/s	15–350
Calculated parameters	
Outflow velocity of the water-polymer jet from the nozzle – $V_{o,p}$, m/s	to 150
Length of the initial section of the aqueous PEO solution jet – $l_{i,p}\cdot10^3$, м	10–60
Optimal distance between the nozzle exit and the food product surface – $l_{opt}\cdot10^3$, m	3–100

Table 5 indicates the ranges of change of the main parameters in the experimental studies, the values of which were taken into account when developing the calculation method for the most efficient process of hydro-jet water-polymer cutting of food products and for which equation (11) is valid. The correlation coefficient for expression (11) is $R^2 = 0.860$, and the coefficient of variation of the experimental data relative to the calculated ones is not more than $K_{var} = 12.2\%$. This confirms the adequacy of the obtained mathematical model to the experimental data.

The obtained empirical power-law dependence of the cut depth on the ultimate compressive strength aligns with recent findings in the field of high-pressure abrasive waterjet cutting (Cui et al., 2022; Xu et al., 2022), which emphasize that the compressive strength of the target material is the primary factor resisting jet penetration. However, unlike traditional abrasive waterjets, which rely on particle kinetic energy for material removal (Natarajan et al., 2020), our results demonstrate that for frozen biomaterials, pure kinetic energy of a liquid jet is sufficient if polymer additives are used. Furthermore, the observed

stabilization of the jet core (initial section) due to the addition of PEO confirms the theoretical assumptions made by Annoni et al. (2009) and Klichova et al. (2015) regarding the role of high-molecular-weight polymers in reducing turbulent dissipation and aerodynamic drag. While previous studies primarily focused on polyacrylamide for cutting industrial materials (Sreekumar et al., 2023), our findings specifically validate the efficacy of PEO solutions in maintaining a coherent cutting tool for deep-frozen organic structures at significantly lower threshold pressures.

Conclusions

It was experimentally demonstrated and confirmed by pairwise correlation analysis that the ultimate uniaxial compressive strength is the criterion that most accurately characterizes the resistance of frozen food products to cutting by a high-speed water–polymer jet. The structural and dynamic characteristics of the high-speed water–polymer jet were established, showing that the addition of 0.007% and 0.01% polyethylene oxide with molecular weights of 6×10^6 and 4×10^6, respectively, significantly increases the length of the initial compact jet section. This effect preserves the jet's cutting ability at standoff distances exceeding 0.1 m, which is essential for the implementation of automated 3D hydro-cutting technologies for bulky food raw materials. Furthermore, a comprehensive multi-parameter mathematical model was developed based on similarity principles and dimensional analysis. The model successfully relates the ultimate uniaxial compressive strength of frozen products, the hydrodynamic parameters of the jet, and the rheophysical properties of the polymer solution to the resulting cut depth. Its adequacy was experimentally validated ($R^2 = 0.86$; coefficient of variation, $K_{var} = 12.2\%$), enabling its use as a robust theoretical framework for process parameter optimization and the design of innovative industrial hydro-cutting equipment.

References

Annoni M., Monno M., Bertola V., Goletti M. (2009), The role of polymeric additives in water jet cutting, *International Journal of Machining and Machinability of Materials*, 6(3/4), pp. 285–304, https://doi.org/10.1504/IJMMM.2009.027329

Bikos D., Samaras G., Cann P., Masen M., Hardalupas Y., Hartmann C., Vieira J., Charalambides M. N. (2021), Effect of micro-aeration on the mechanical behaviour of chocolates and implications for oral processing, *Food & Function*, 12(11), pp. 4864–4886, https://doi.org/10.1039/d1fo00045d

Chaffin W. B., Zimmerman J., Wagner N. J. (2022), Extensional flow affecting shear viscosity: Experimental evidence and comparison to models, *Journal of Rheology*, 66(4), pp. 793–808, https://doi.org/10.1122/8.0000380

Chen H., Wang Y., Zhang L. (2024), Uniaxial compression behavior and mechanical properties of composite biogels, Foods, 13(2), 245, https://doi.org/10.3390/foods13020245

Cui D., Li H., He J., Wang Q., Lu C., Hu H., Cheng X., Wang C. (2022), Applications of water jet cutting technology in agricultural engineering: A review, *Applied Sciences*, 12(18), 8988, https://doi.org/10.3390/app12188988

Dinić J., Sharma,V. (2019), Extensional relaxation times of dilute, aqueous polymer solutions, *Proceedings of the National Academy of Sciences*, 116(18), pp. 8766–8774, https://doi.org/10.1073/pnas.1820277116

Duspara M., Starcevic V., Samardzic I. (2018), Preliminary communication analysis of zones created with water jet cutting of AISI 316 L corrosion resistant steel, *Technical Gazette*, 25, pp. 2616–2621, https://doi.org/10.17559/TV-20170216095042

Gemi L., Mofidi A., Al-Jaberi Z. K., Fereidoon A. (2021), Uniaxial compressive testing of composites to determine mechanical properties: A review, *Materials*, 14(20), 6216, https://doi.org/10.3390/ma14206216

Gylienė V. (2014), Investigation of abrasive water-jet cutting parameters influence on 6082 aluminium alloy surface roughness, M*echanika*, 20(6), pp. 602–606, https://doi.org/10.5755/j01.mech.20.6.8865

Haward S. J., Hopkins C. C., Shen A. Q. (2023), Polymer and surfactant flows through a periodically constricted tube, *Journal of Fluid Mechanics*, 961, A17, https://doi.org/10.1017/jfm.2023.238

Hu D., Tang C.-L., Kang Y., Li X. (2015), Quality by adding polymer in abrasive water jet, *Particulate Science and Technology*, 34(3), pp. 270–276, https://doi.org/10.1080/02726351.2015.1082522

Kęska P., Stadnik J., Wójciak W. (2021), Texture profile analysis (TPA) and instrumental compression test of dry-cured meats, *Foods*, 10(11), 2883, https://doi.org/10.3390/foods10112883

Klichová D., Sitek L., Foldyna J. (2015), Effect of polymeric additives on water jet properties, *Advanced Materials Research*, 1115, pp. 411–414, https://doi.org/10.4028/www.scientific.net/AMR.1115.411

Liu X., Liang Z., Wen G., Yuan X. (2019), Water-jet machining and research developments: A review, *The International Journal of Advanced Manufacturing Technology*, 102, 1257–1335, https://doi.org/10.1007/s00170-018-3094-3

Natarajan Y., Murugesan P. K., Mohan M., Liyakath Ali Khan S. A. (2020), Abrasive water jet machining process: A state of art of review, *Journal of Manufacturing Processes*, 49, pp. 271–322, https://doi.org/10.1016/j.jmapro.2019.11.030

Perec A., Tavodova M. (2016), Abrasive water jet cutting depth optimization by Taguchi approach, *Manufacturing Technology*, 16(3), 585–590, https://doi.org/10.21062/ujep/x.2016/a/1213-2489/MT/16/3/585

Pogrebnyak A., Pogrebnyak V., Perkun I., Vasyliv N. (2020), Influence of geometric and dynamic parameters of a water-polymer jet on characteristics of food products hydrocutting process, *Ukrainian Food Journal*, 9(1), pp. 197–208, https://doi.org/10.24263/2304-974X-2020-9-1-17

Pogrebnyak A., Korneyev M., Pogrebnyak V., Yudina O., Nebaba N., Vishnikina O. (2023), Intensification of water jet cutting process in deep-frozen food products, *Ukrainian Food Journal*, 12(3), pp. 433–443, https://doi.org/10.24263/2304-974X-2023-12-3-9

Pogrebnyak A. V., Perkun I. V., Pogrebnyak V. G., Kucher M. M., Sabirov O. V., Saihak Y. I., Nebaba N. O. (2025), Cutting products with a water-polymer jet: Scientific and practical aspects, *Journal of Chemistry and Technologies*, 33(4), pp. 1118–1125, https://doi.org/10.15421/jchemtech.v33i4.325223

Pogrebnyak V. G., Chudyk I. I., Pogrebnyak A. V., Perkun I. V. (2022), Perforation of oil and gas wells by a high-velocity jet of polymer solution, *Nafta-Gaz*, 1, pp. 3–12, https://doi.org/10.18668/NG.2022.01.01

Ranjan P., Chaubey P., Suresh P., Vidya S. (2022), Current research aspects and trends in abrasive water jet machining: A review, *Advances in Mechanical Engineering and Technology*, pp. 193–198, Springer, https://doi.org/10.1007/978-981-16-9613-8_19

Sreekumar M., Purushothaman S., Srinivas M. S., Katiyar J. K., Sankar M. R. (2023), A review of additives in abrasive water jet machining and their performance, *Proceedings of the Institution of Mechanical Engineers, Part J: Journal of Engineering Tribology*, 237(4), pp. 844–862, https://doi.org/10.1177/13506501221144722

Sydor M., Pinkowski G., Jasińska A. (2020), The Brinell method for determining hardness of wood flooring materials, *Forests*, 11(8), 878, https://doi.org/10.3390/f11080878

Voloshyn V.S. (2010), *Ecological Technology of Creating Water-Protective Screens*, Knowledge.

Wang J., Shanmugam D.K. (2009), Cutting meat with bone using an ultrahigh pressure abrasive water jet, *Meat Science*, 81(4), pp. 671–677, https://doi.org/10.1016/j.meatsci.2008.11.010

White F.M. (2015), *Fluid Mechanics* (8th ed.), McGraw-Hill Education.

Xu W., Wang J., Deng Y., Li J., Yan T., Zhao S., Yang X., Xu E., Wang W., Liu D. (2022), Advanced cutting techniques for solid food: Mechanisms, applications, modeling approaches and future perspectives, *Comprehensive Reviews in Food Science and Food Safety*, 21(2), pp. 1568–1597, https://doi.org/10.1111/1541-4337.12896

Yang S., Gao G., Xu Z. (2026), In situ steel strength evaluation using Brinell hardness method: A case study on Q235 and Q345 steel, *Journal of Materials in Civil Engineering*, 38(5), https://doi.org/10.1061/jmcee7.mteng-22292

Yuen J.S.K. Jr, Saad M.K., Xiang N., Barrick B.M., DiCindio H., Li C., Zhang S.W., Rittenberg M., Lew E.T., Zhang K.L., Leung G., Pietropinto J.A., Kaplan D.L. (2023), Aggregating in vitro-grown adipocytes to produce macroscale cell-cultured fat tissue with tunable lipid compositions for food applications, *eLife*, 12, e82120, https://doi.org/10.7554/eLife.82120

Cite:

Pogrebnyak, A., Perkun, I., Pogrebnyak, V., Korneyev, M., Haponenko, S., Beliaiev, Y., & Yudina, O. (2026). Mathematical modeling of water-polymer jet cutting for frozen food products. *Ukrainian Food Journal, 15*(2), 550–565. https://doi.org/10.24263/2304-974X-2026-15-2-16

Bibliometric analysis of artificial intelligence applications in food quality control and safety

Ali Kılıç[1], Müge Hendek[2], Damla Uslu[3]

1 – Konya Food and Agriculture University, Konya, Turkiye
2 – Kastamonu University, Kastamonu, Turkiye
3 – Konya Technical University, Konya, Turkiye

Keywords:

Food
Safety
Quality
Artificial Intelligence
Bibliometric analysis

Article history:

Received 18.01.2026
Received in revised form 10.03.2026
Accepted 30.06.2026

Corresponding author:

Müge Hendek
E-mail: mugehendek@kastamonu.edu.tr

DOI:
10.24263/2304-974X-2026-15-2-17

Abstract

Introduction. Food safety remains a critical global challenge due to risks associated with food production, processing, packaging, and distribution. Artificial intelligence (AI) has emerged as a promising tool for improving food quality control and safety through intelligent monitoring, traceability, and decision-making across the food supply chain.

Materials and methods. A bibliometric analysis was conducted to evaluate AI applications in food quality control and safety. Data were collected from the Web of Science database using the query "Food*" AND "Safety" AND "Quality Control" AND "Artificial Intelligence", without restrictions on publication year, language, or document type. The retrieved records were analyzed to identify publication trends and key research themes.

Results and discussion. The results were organized into two sections: Descriptive Findings and Content Analysis. Data retrieved from the Web of Science (WoS) database were analyzed using the Bibliometrix software package. The publication period spanned 2008–2025 and showed a steady increase in research interest in the application of artificial intelligence (AI) to food quality control and safety, with the highest number of publications recorded in 2025. Following the screening process, 70 relevant studies were included in the analysis.

Keyword co-occurrence analysis identified the most frequent terms as “Artificial Intelligence,” “Food Safety,” “Machine Learning,” “Quality,” “Quality Control,” and “Computer Vision,” highlighting the growing role of AI technologies in food safety and quality assessment. The findings also indicate increasing adoption of machine learning, data analytics, and computer vision in food industry applications. Content analysis revealed five major research themes: food analysis, food supply chain management, food traceability, food quality monitoring and management, and food fraud prevention. These themes demonstrate the broad applicability of AI for improving food quality, safety, transparency, and sustainability throughout the food system.

Conclusions. The review demonstrates that AI is increasingly being integrated with technologies such as the Internet of Things (IoT) and blockchain to enable real-time monitoring and improve traceability. However, most current applications remain focused on analytical support rather than fully autonomous systems. Future research should prioritize multimodal data fusion and the implementation of explainable artificial intelligence (XAI) to enhance predictive performance, transparency, and user trust.

Introduction

Today, advanced artificial intelligence (AI) technologies, particularly machine learning (ML), are increasingly being integrated into a wide range of academic disciplines and industrial applications. Food science and technology also benefit greatly from these innovations. The use of AI contributes to advances in agriculture, supports more efficient crop identification, aids in designing new formulations and developing innovative food and nutraceutical products, and enhances the accuracy of sensory analysis. Moreover, AI enhances industrial processing, provides valuable tools for estimating nutritional and caloric content, supports supply chain monitoring and optimization, promotes waste valorization, and reduces both operational costs and processing time. AI-based systems also strengthen food quality and safety management, making them highly influential in modern food research and production.

Defined broadly, AI refers to the simulation of human intelligence processes by computational systems, utilizing algorithms to identify patterns, correlations, and anomalies within vast datasets (Jiménez-Carvelo et al., 2024). The integration of these computational capabilities into quality control (QC) systems marks a paradigm shift from reactive inspection to proactive, data-driven management, essential for ensuring the integrity of complex modern food supply chains (Liakos et al., 2025).

Building upon these technological capabilities, Food Quality Control (FQC) functions as the essential operational framework for ensuring that food products meet established standards of safety, nutritional value, and sensory attributes (Bhavna et al., 2024; Peres et al., 2025). While food quality traditionally refers to consumer expectations regarding taste, texture, and appearance, it is closely linked to food safety, which ensures protection against biological, chemical, and physical hazards (Bhavna et al., 2024). The effective implementation of FQC systems is vital for global public health; unsafe food containing harmful pathogens or chemical substances causes an estimated 600 million illnesses and 420,000 deaths annually, with children under five years of age bearing a disproportionate 30% to 40% of this mortality burden.

Beyond the human cost, the economic consequences of quality failures are staggering. In low- and middle-income countries alone, the aggregate loss in productivity and medical expenses resulting from unsafe food is estimated at US$ 110 billion per year (Aslam et al., 2025; Kumagai et al., 2015; WHO, 2026). Consequently, maintaining rigorous quality standards is not only a public health priority but a critical economic imperative to prevent trade disruptions, protect brand reputation, and sustain national economies (WHO, 2026).

To address these critical challenges, the agri-food sector is undergoing a digital transformation driven by artificial intelligence (AI) and machine learning (ML), enabling a shift from reactive inspection to proactive, data-driven quality management (Agrawal et al., 2025; Peres et al., 2025). In the domains of food analysis and quality monitoring, AI algorithms coupled with non-destructive sensing technologies, specifically Near-Infrared Spectroscopy (NIRS) and Hyperspectral Imaging (HSI), have revolutionized the assessment of internal quality attributes without damaging the product (Fodor et al., 2024; Liakos et al., 2025). Deep learning models, particularly Convolutional Neural Networks (CNNS), are extensively employed in Computer Vision systems to automate the visual inspection of production lines, detecting physical defects and foreign bodies with a consistency and speed that far exceed human capabilities (Agrawal et al., 2025; Wu et al., 2022).

Beyond the factory floor, the integration of AI significantly enhances the food supply chain and traceability. By converging with the Internet of Things (IoT) and Blockchain technology, AI models enable the real-time monitoring of critical logistical parameters, such as temperature and humidity, while creating immutable digital ledgers that ensure transparency from farm to fork (Agrawal et al., 2025). These systems support dynamic risk prediction, allowing stakeholders to

prevent spoilage and rapidly trace contamination sources during outbreaks. Furthermore, AI has emerged as a powerful tool for food fraud prevention. Advanced pattern recognition algorithms analyse complex multivariate data to detect sophisticated adulteration in high-value commodities, such as olive oil, honey, and meat, identifying fraudulent substitutions that often bypass traditional sensory and chemical analyses (Magdas et al., 2025; Njiru et al., 2025).

Although the integration of AI into food quality assurance is a relatively nascent domain compared to other mature disciplines, the volume of scholarly output has exhibited an exponential trajectory, particularly in the post-2019 period (Liu et al., 2023; Pennells et al., 2025). This rapid proliferation has led to a fragmented body of knowledge that is increasingly difficult to synthesize through traditional qualitative methods alone. While systematic reviews are effective for answering specific, narrow research questions, they often fall short in capturing the structural evolution and the "panoramic" breadth of a fast-growing interdisciplinary field (Liu et al., 2023; Pennells et al., 2025). To address this limitation and provide a holistic framework, this study employs a quantitative bibliometric analysis.

The primary justification for selecting this methodology lies in its capacity to handle large volumes of unstructured bibliographic data, thereby objectively mapping the field's intellectual, conceptual, and social structures (Radu et al., 2023; Zhu et al., 2024). Unlike manual reviews, bibliometric analysis enables the visualization of complex relationships, such as author collaborations, keyword co-occurrences, and thematic evolution, revealing hidden patterns and emerging "hotspots" that define the current state of the art (Radu et al., 2023). To execute this analysis, we utilized the Bibliometrix, a comprehensive tool specifically designed for rigorous science mapping. By leveraging this approach, this study aims to identify and analyse the current state of artificial intelligence techniques applied in food quality control and safety systems and provide a macro-level perspective on how AI technologies are reshaping food quality control and safety systems globally.

To systematically map this knowledge landscape, this study addresses three primary research questions:

- What is the temporal evolution and geographic distribution of scientific production regarding AI applications in food quality control and safety?
- What are the dominant intellectual structures, application domains, and thematic clusters characterizing the use of AI in food quality control and safety systems?
- What research gaps and emerging trends can be identified to guide future developments in AI-driven food quality and safety research?

After the Introduction, the remainder of this paper is organized as follows: Section 2 details the bibliometric methodology. Section 3 presents the quantitative results, visualizing the publication trends, citation metrics, and collaboration networks. Additionally, this section discusses the evolution of thematic hotspots, interpreting the shift from traditional machine learning to advanced deep learning applications in quality control. Finally, Section 4 concludes the study by outlining the limitations of current research and proposing a strategic agenda for future investigations into AI-driven food safety systems.

This review aims to critically evaluate current applications of artificial intelligence in food quality and safety monitoring, with particular emphasis on its integration with emerging digital technologies, existing limitations, and future research directions.

Materials and methods

A systematic literature review was conducted in this study regarding the applications of AI techniques applied to food quality and safety issues. A hybrid approach based on the reporting

items via systematic literature reviews and meta-analysis used by Armand et al. (2024) was used. The approach was structured into the following parts:

A. In the first section, the descriptive findings obtained from the selected studies were examined. (Defining research scope and meta-search query formulation; Literature selection and obtaining descriptive findings)
B. In the second section, the chosen study's content was reviewed and discussed in clusters.

Defining the research scope and question.

This study aimed to identify and analyze the current state of artificial intelligence techniques applied in food quality control and safety systems. A primary research question that guided our exploration was: How has AI been employed to impact and enhance our understanding, monitoring, and optimization of quality control or food safety system outcomes?

Literature selection process. By searching electronic databases that provide articles on AI and food safety and quality control issues, the authors decided that wos has most suitable scientific publications within their scope of study. "Food *" AND "Safety" AND "Quality Control" AND "Artificial Intelligence" meta-search query formulation was used to obtain the results.

Firstly, the authors identified the relevant literature through the formulation for artificial intelligence (machine learning, deep learning, etc.) And food quality control and safety), resulting in only 70 research items. A systematic review requires details of the publication period, search terms and criteria, inclusion and exclusion criteria, and databases used in the research selection process. Due to the limited number of studies conducted on the subject, no research selection criteria were applied.

In the second step of the selection process, the authors screened the titles and abstracts of articles based on this study's predefined aims, scopes, and keywords. This stage resulted in the inclusion of 65 publications.

Reviewing the study's content. The authors screened the titles and abstracts of articles based on this study's predefined aims, scopes, and keywords. This stage resulted in the inclusion of 67 publications. The chosen study's content was reviewed and discussed in clusters.

Results and discussion

This section examines the descriptive findings obtained from the selected studies. Additionally, the chosen study's content is analyzed and discussed in clusters.

Descriptive Analysis

Among the 70 papers finally included in this study, only one paper was published in 2008, one paper was published in 2021, 2 papers were published in 2022, 4 papers were published in 2023, 14 papers were published in 2024 and 48 papers published in 2025 as shown in Figure1. According to the publication period, the highest set of papers involved in this review was published in 2025 (especially in 2 years), thus signifying the recent interest in this research area.

According to bibliometric analysis, the leading academic journals for research on the use of artificial intelligence in food science and safety are mostly food science and technology publications with high impact factors (Figure 2).

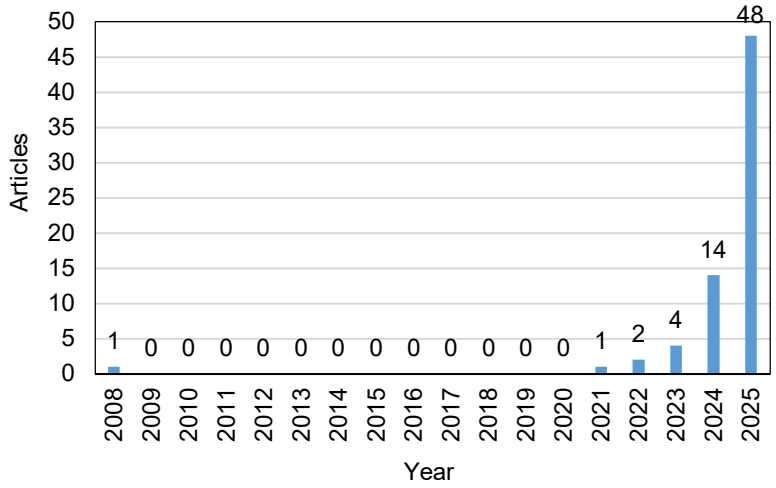

Figure 1. Evolution of relevant research studies according to years

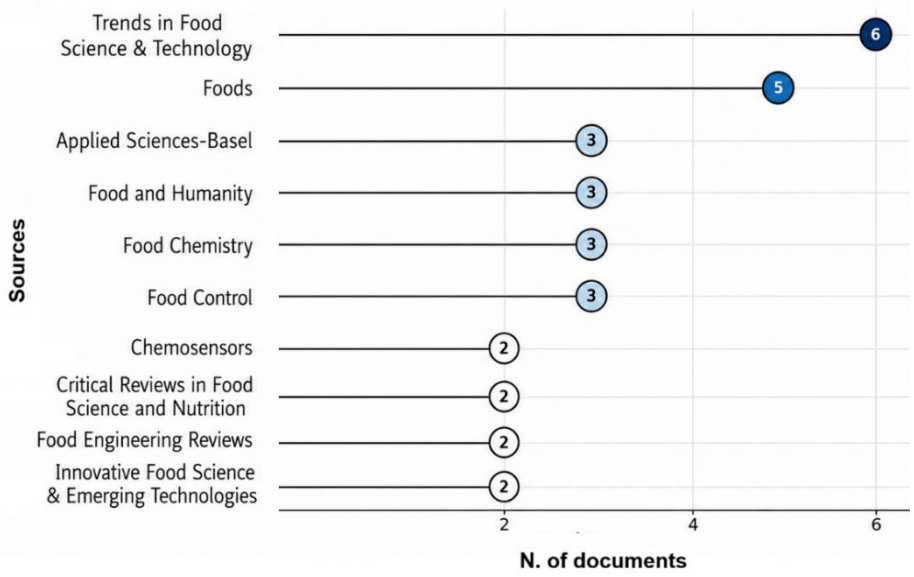

Figure 2. Most relevant sources

The most publications came from Trends in Food Science and Technology (6 documents) and Foods (5 documents), showing their main role in publishing research on AI innovations in the food industry. Other major sources like Applied Sciences-Basel, Food and Humanity, Food Chemistry, and Food Control (3 documents each) attest to the diverse nature of this research area, which includes topics like assessing food quality, detecting contamination, predictive modeling, and digital transformation of food systems. Journals

such as Chemosensors, Critical Reviews in Food Science and Nutrition, Food Engineering Reviews, and Innovative Food Science & Emerging Technologies are other examples that highlight the increasing popularity of incorporating advanced technologies such as AI, sensors, and data-driven methods for enhancing food safety, sustainability, and supply chain management.

Further, the most frequent words were extracted in the studies from the 70 papers used and performed a word analysis via Bibliometrics. The results are shown in Figure 3.

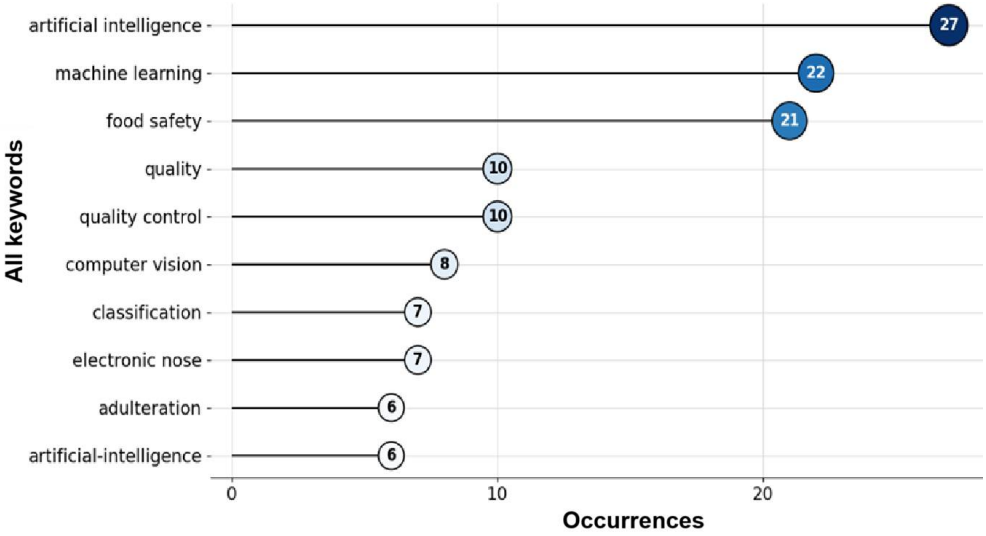

Figure 3. Most frequent words in studies

The conceptual mapping through factorial analysis (also known as the conceptual structure map) of a Multiple Correspondence Analysis (MCA) was used to explore the thematic focuses and their interconnection within the scientific domain of artificial intelligence (AI) in food safety and quality (Figure 4). This method displays the co-occurrence of keywords, with those collocated indicating concepts that are most frequently found together in research publications. The layout of keywords on two-dimensional axes that account for 17.52% (X axis) and 10.79% (Y axis) of the variance is indicative of the main research groups and the progression of AI-related topics in the food industry.

Results from the factorial analysis showed that research on the intersection of AI and food science is clustered around a few strong and interlinked topics. The largest thematic group deals with the use of AI in assessing food quality, verifying authenticity, ensuring safety, and rapid detection of contaminants, mainly through computer vision, spectroscopy, and hyperspectral imaging. Besides, a substantial part of research is devoted to synergizing AI with technologies like IoT, blockchain, and digital transformation to enhance food traceability, supply chain efficiency, and farm management through smart agricultural practices. The discovery through research of there being explainable AI, Industry 4.0, coming up with AI based prediction, and automated systems, opens the door to a future research landscape that centers on food production systems that are transparent, sustainable, and capable of smart ways of production at the same time.

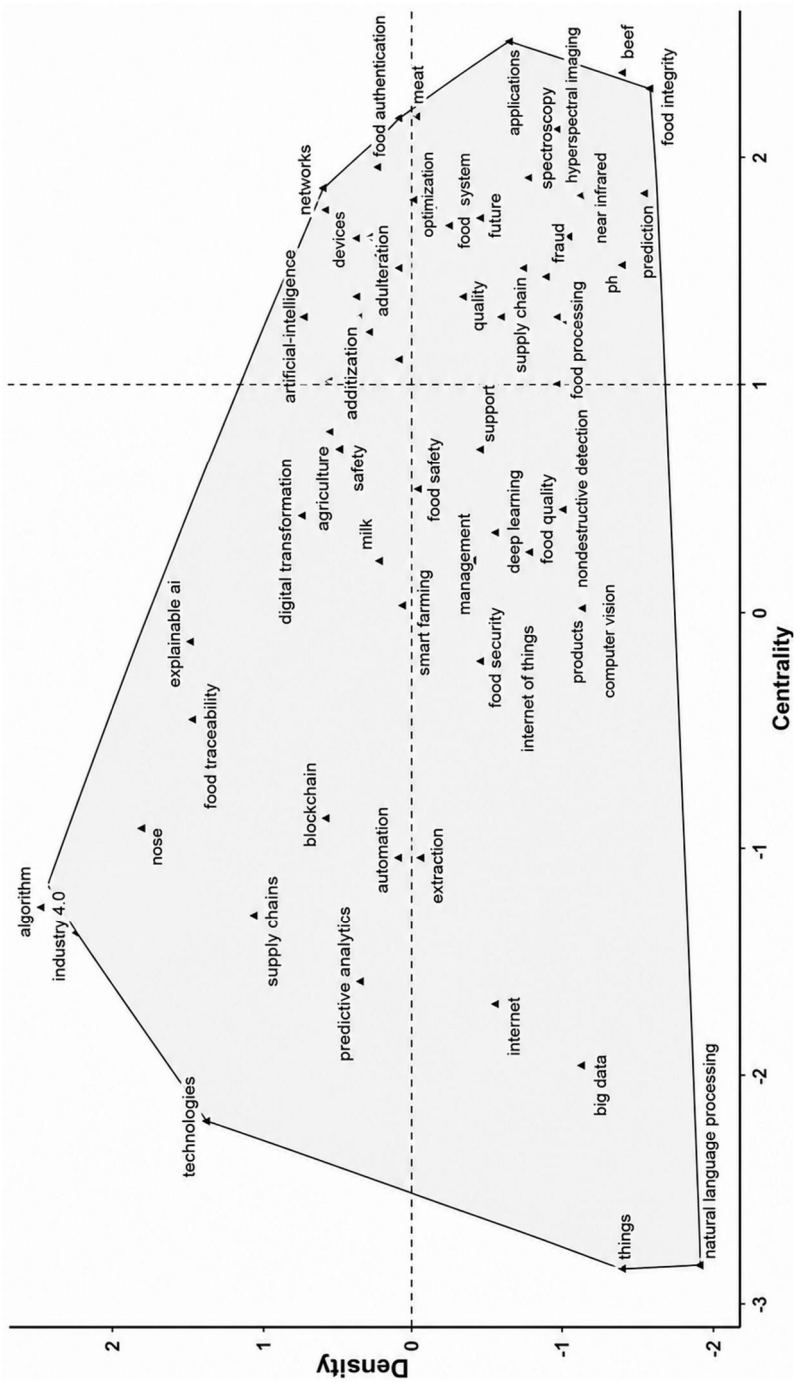

Figure 4. Thematic conceptual mapping of artificial intelligence research in food quality control and safety using Multiple Correspondence Analysis

The most frequent keywords were also extracted from the 70 papers used and performed a keyword analysis by Bibliometrics. The results were given in Figure 5. The size of the words and letters is directly proportional to the frequency of the word from the reviewed studies. As expected, the most important keywords are “Artificial intelligence”, “Machine learning”, “Food safety”, “Quality” and “Quality control”.



a

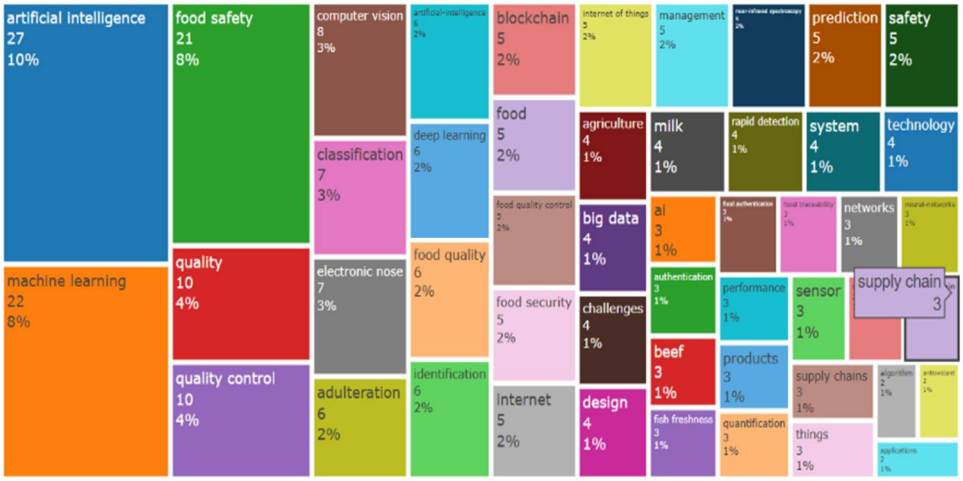

b

Figure 5. Word cloud (a) and Time tree (b) of the reviewed studies

The thematic map shows two dimensions (Figure 6). The x-axis (centrality or relevance degree) indicates the level of connection and influence a theme has within the general research area. The y-axis (density or development degree) shows the internal consistency, maturity, and development level of a theme. On the basis of these two measures, the thematic map is separated into four mains quadrants.

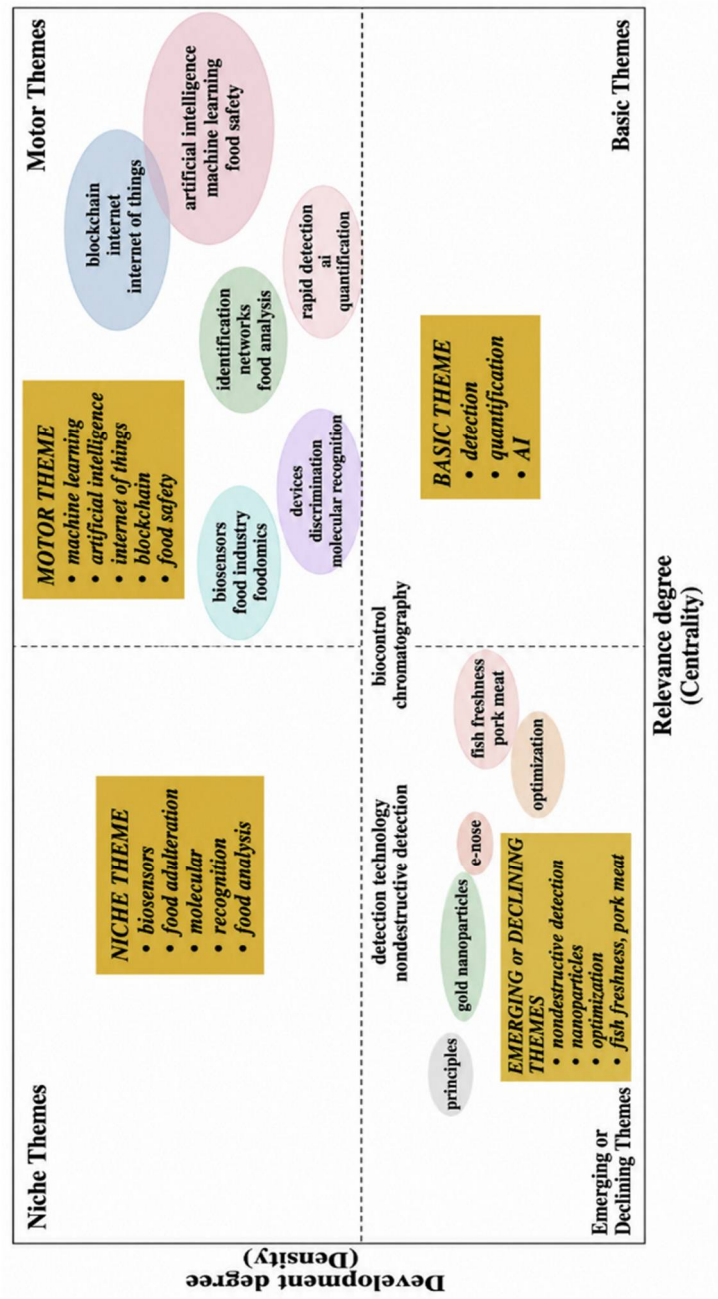

Figure 6. Thematic map of the studies

Motor Themes (Upper Right Quadrant). Motor themes represent the dominant research paradigm and constitute the primary driving forces shaping the future development of the field. Positioned in the upper right quadrant, these themes are both highly central and well developed, reflecting their mature status and strong influence within the scientific literature. The inclusion of artificial intelligence (AI), machine learning (ML), and the Internet of Things (IoT) indicates that these technologies have become established methodological tools for food safety and quality control. The presence of blockchain further highlights an integrated research direction focused on traceability, supply chain transparency, and secure data management. This convergence is exemplified by recent frameworks that combine AI models, IoT devices, and blockchain technology to establish decentralized, tamper-resistant traceability systems across the global agri-food supply chain (Liu et al., 2025).

Basic Themes (Lower Right Quadrant). The topics located in this quadrant are considered fundamental to the broader research field but remain insufficiently developed. AI-based approaches for the detection and quantification of chemical compounds and microbial contaminants are widely recognized as core research directions and form the basis for numerous practical applications. However, most existing studies focus on the implementation of established machine learning algorithms rather than on the development of novel computational methods or theoretical frameworks. A representative example is the extensive use of machine learning models for the rapid detection and quantification of chemical adulterants and microbial contamination based on data obtained from various sensing platforms (Wang et al., 2025). These findings also highlight substantial opportunities for future research, particularly in the development of novel AI methodologies, systematic comparisons of algorithm performance, and the establishment of standardized datasets and evaluation protocols to improve the reliability, reproducibility, and practical applicability of AI-based food safety systems.

Niche Themes (Upper Left Quadrant). Niche themes are characterized by high density but low centrality, indicating that they are well developed internally while remaining only weakly connected to the broader research landscape. These themes represent scientifically mature, specialized areas with strong methodological foundations but limited integration into mainstream AI-driven food safety research. Typical examples include AI-assisted biosensors, molecular recognition technologies, and advanced analytical techniques for food characterization.

Within this thematic cluster, AI has been increasingly integrated with spectroscopic methods, chromatography, mass spectrometry, and sensor technologies to improve the detection, identification, and quantification of food contaminants and quality-related compounds (Gu et al., 2025). Although these approaches are technologically advanced and inherently multidisciplinary, they remain confined to relatively small research communities, which limits their influence on the wider AI-based food safety domain. As these technologies become more accessible and increasingly incorporated into routine food safety monitoring, they are expected to establish stronger links with the core research field and contribute more substantially to mainstream AI-driven food safety applications.

Emerging or Declining Themes (Lower Left Quadrant). Themes located in this quadrant exhibit both low centrality and low density, indicating that they are weakly developed and have limited influence on the overall research field. These themes may represent either emerging research directions that are still in the early stages of development or declining topics that are gradually losing their relevance. Distinguishing between these two possibilities requires further analysis of their temporal evolution.

Examples within this cluster include non-destructive detection techniques and nanoparticle-assisted sensing. These topics may represent promising research directions that are only beginning to be integrated with AI technologies and therefore have not yet gained widespread attention. Conversely, some highly product-specific applications may gradually lose prominence as research shifts toward broader, more versatile AI-based solutions.

Overall, the thematic map identifies artificial intelligence as a central enabling technology in food safety and quality control research. Recent studies increasingly emphasize the integration of AI with complementary digital technologies, such as the Internet of Things (IoT), blockchain, cloud computing, and smart sensing systems, rather than focusing solely on the development of individual algorithms. Future research is expected to prioritize multimodal data fusion, explainable artificial intelligence (XAI), trustworthy and transparent decision-making, and real-time intelligent systems capable of meeting regulatory and industrial requirements.

Figure 7 presents the most cited countries based on publications retrieved from the Web of Science database using the keywords "Food" AND "Safety" AND "Quality Control" AND "Artificial Intelligence."* A total of 70 publications were identified, and the citation analysis indicates that China achieved the highest citation impact (363 citations), followed by India (194), USA (109), and United Kingdom (106). Although Turkey contributed fewer citations (27), the results demonstrate that research impact in this field is concentrated in a limited number of countries with strong scientific productivity and international visibility.

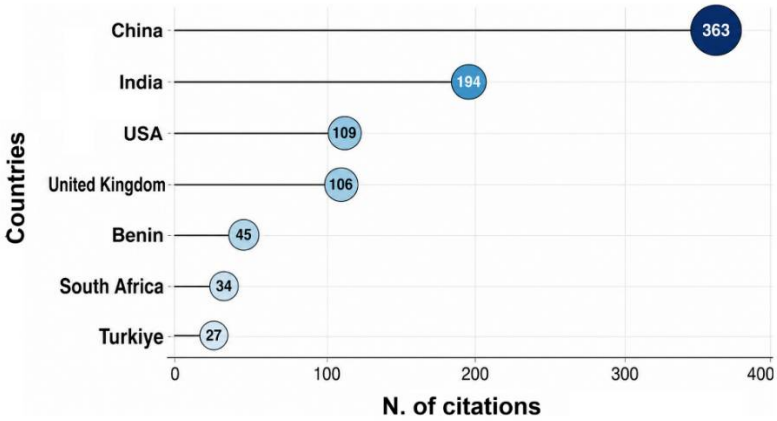

Figure 7. Most cited countries

The country-level bibliometric analysis also reveals several notable patterns. In this analysis, the distribution of publications by corresponding authors' countries is examined by distinguishing between single-country publications (SCP), which involve authors from a single country, and multi-country publications (MCP), which result from international collaboration. China and India emerge as the leading countries in terms of corresponding author output, with China showing a strong predominance of SCP, indicating mainly domestic-led research. In contrast, countries such as the USA, the United Kingdom, and Korea display a higher share of MCP, reflecting stronger international collaboration. Overall, the results highlight notable differences in corresponding author leadership and collaboration patterns across countries.

Content analysis

Initially, 70 papers related to the application of artificial intelligence in food quality and safety management were identified, and a subset of 67 papers was specially earmarked for the domain of artificial intelligence in food safety and quality. The authors deemed them appropriate for subsequent analysis in the present research study. In this section, the authors conducted an in-depth analysis of the full text of the selected papers (Table 1).

Table 1

Clusters of identified studies

Cluster	References	Records	Records (%)
Food analysis	(Moskvin and Spakovica, 2006; Wang et al., 2022; Liu et al., 2022; Feng et al., 2024; Beck et al., 2024; Shi et al., 2024; Liakos et al., 2025; Pereira et al., 2025; Ince et al., 2025; Ziani et al., 2025; Cao et al., 2025; Movahedi et al., 2025; Vanaraj et al., 2025; Mor et al., 2025; Ramachandran et al., 2025; Melendreras et al., 2025; Jayan et al., 2025; Kim et al., 2025; Pawde and Dave, 2025; Revelou et al., 2025; Zhang et al., 2025; Wang et al., 2025; Zong et al., 2025; Gu et al., 2026; Gerdan Koc et al., 2026; Alkanan et al., 2025)	26	38.8
Food supply chain	(Hassoun et al., 2023; Taneja et al., 2023; Konfo et al., 2023; Izquierdo-Bueno et al., 2024; Li et al., 2024; Koushki et al., 2024; Chhetri, 2024; Yu et al., 2024; Zatsu et al., 2024; Peres et al., 2025; Karchiyappan et al., 2025; Yin et al., 2025; Dhal and Kar, 2025; Mohammadi et al., 2025; Saha et al., 2025; Kilinc et al., 2025; Naseem and Rizwan, 2025; Semercioz-Oduncuoglu and Luning, 2025; Al-Thani et al., 2025; Ibarra-Muñoz et al., 2025; Parra-López et al., 2025; Luo et al., 2025; Saha et al, 2025; Kanicheril Ambikalekshmi et al., 2026; Hadi et al., 2024)	25	37.31
Food quality monitoring and management. Traceability focus	(Shi et al., 2021; Yasin et al., 2023; Alvarez-García et al., 2024; Stanescu et al., 2025; Nawaz et al., 2025; Liu et al., 2025; Nisenbaum et al., 2025; Femimol and Joseph, 2025; Singh, 2025; Kundu et al., 2025)	10	14.93
Food quality monitoring and management. Food fraud prevention	(Aqeel et al., 2024; Gbashi and Njobeh, 2024; Ahranjani et al., 2025; Li et al., 2025; L. Zhang et al., 2025; Lim et al., 2025)	6	8.96

Food analysis

A significant area of application for artificial intelligence in food quality is food analysis. The literature emphasizes integration (AI + analytical platforms) more than standalone algorithm comparisons-consistent with mapping "where AI is applied". AI is concentrated in instrument-supported food analysis (spectroscopy, chromatography, mass-spectrometry, NMR/MR, metabolomics, microfluidics) for faster interpretation of complex signals (Gu et al., 2026;

Movahedi et al., 2025). AI-based methods combined with leading food analysis techniques like spectroscopy, chromatography, mass spectrometry, and sensor-based systems have been documented to improve food quality monitoring, safety evaluation, authenticity check, and bioactive compound analysis. These AI-guided analytical methods are seen as effective means for swiftly understanding complex food chemistry information, allowing precise forecasting of food ingredients, discovering contaminants, estimating shelf-life, and creating new functional food items (Gu et al., 2026). Typical use is also pattern recognition + prediction to support contaminant/ biomarker detection and compositional or nutritional analysis (Wang et al., 2025). The role of artificial intelligence (AI) in MR-based food analysis is majorly to help decipher complex spectral and imaging data. This paves the way for quick assessment of food quality, confirming the authenticity of food items and uncovering food adulteration. When it comes to prediction, classification, and tracking food attributes like composition, safety, processing-induced changes, and shelf-life, AI-empowered MR-based techniques have really got the back of food quality control by enhancing its efficiency and reliability (Alkanan et al., 2025). Besides data analysis applications, artificial intelligence (AI) has become a potent instrument in the sphere of image processing-based approaches. Specifically, AI-based image analysis tools have brought a revolutionary change in the traditional methods of evaluation, which are usually time-consuming, labor-intensive, and heavily reliant on expert knowledge, by offering quick, unbiased, and highly accurate classification. Moreover, in these scenarios, deep learning and convolutional neural network (CNN)-based frameworks have been recognized for their ability to automatically learn representative features from pollen images, thereby facilitating effective pollen identification and classification and leading to superior results as compared to classical microscopic inspection methods (Koc et al., 2025). Moreover, it has been reported that artificial intelligence-based machine learning approaches have been applied in food microbiome analysis to monitor microbial community changes associated with food quality and safety. Using 16S rRNA sequencing data combined with machine learning algorithms, including Random Forest, XGBoost, Support Vector Machine (SVM), and LightGBM, AI models have been developed to classify normal and abnormal samples, detect microbial shifts associated with contamination or spoilage, and identify key microbial biomarkers responsible for quality deterioration. Explainable AI approaches, such as SHAP analysis, further enable the interpretation of model predictions by revealing which microbial taxa contribute to the detection of anomalies, providing a reliable tool for predictive food safety monitoring (Beck et al., 2024).

In addition to microbiome-based approaches, the integration of metabolomics with artificial intelligence (AI) and deep learning has emerged as a promising strategy for the rapid detection and prediction of microbial hazards in food systems. By analyzing metabolite fingerprints and microbial biomarkers, these AI-driven metabolomic approaches enable the early identification of foodborne pathogens, real-time risk monitoring, and improved safety management throughout food production and processing (Feng et al., 2024). Furthermore, AI-integrated microfluidic platforms have been developed for the rapid detection of foodborne pathogens, including *Salmonella*, *Escherichia coli*, and *Campylobacter*, as well as pesticide residues, biotoxins (e.g., aflatoxins), and food adulteration through advanced sensing technologies coupled with machine learning-based data analysis. These systems improve food analysis by delivering fast, sensitive, and highly accurate detection with only a very small volume of sample needed, less chemicals used, highly portable devices, and the ability to make decisions in real time as compared to the standard laboratory methods. The merging of AI and microfluidics is a good way to address food safety and quality control in the future as it will lead to more automated, reliable, and accessible analytical technologies (Movahedi et al., 2025).

Food supply chain

AI is frequently framed as a system component in digitalized supply chains, commonly alongside IoT, smart sensors, and blockchain-enabled architectures. Content patterns emphasize operational integration (data capture → secure storage → AI-based detection/alerts) rather than reporting performance leaderboards. It is thought that the integration of AI technologies can be significantly improved traceability, reduced post-harvest losses, and enhanced food safety in complex supply networks (Al-Thani et al., 2025; Naseem and Rizwan, 2025). Artificial intelligence can help food supply chains become more efficient by using data collected from various sources like IoT sensors, customer preferences, and transport management systems. This gathered information allows for better control over production levels, stock maintenance, and delivery timings. With the use of artificial intelligence, companies can smoothly align their inventory levels with actual consumer demand while at the same time identifying factors leading to product perishing and responding immediately to instances posing a threat to food safety. These measures not only help in reducing food wastage but also result in greater resource utilization throughout the supply chain. Furthermore, combining AI capabilities with those of IoT devices and blockchain offers new possibilities for food supply chains that are transparent, traceable, and sustainable. Continuous live feed monitoring coupled with instantaneous updating of databases through blockchains paves the way for decisions backed up by reliable and comprehensible data at any moment (Al-Thani et al., 2025). Artificial intelligence is not only helpful in general food supply chain optimization but also has led to a transformation of specific agricultural sectors by enhancing production processes, quality control, and sustainability. The wine industry, in particular, is a leading case of AI use throughout the whole process: from the grape production to the assessment of the final product quality.

AI-powered technologies are revolutionizing the whole process of growing grapes and making wine by allowing early disease identification, efficient pest control, harvesting automation, precise irrigation, and nutrient supply planning. AI-driven decision-making systems lead to better production, higher quality grapes, and sustainability by using environmental, biological, and process data from the entire wine supply chain. Besides that, AI contributes to food safety and traceability by fermentation monitoring, microbiological risk prediction, and quality control from the vineyard to the consumer.

Dominant problem types are visibility and decision support (monitoring conditions, improving efficiency, strengthening governance from production to distribution). While AI by and large can be a great help in improving food safety, its application also has quite a few challenges. For example, limited availability of data, poor quality of data, and the difficulty in understanding the decisions of deep AI models may lead to inaccurate and unreliable predictions. Moreover, technical infrastructure needs, concerns about keeping data private, and regulatory issues might make the process of adopting AI-based food safety systems go even slower. Future research should be aimed at creating more understandable AI models and combining AI with technologies such as IoT and blockchain to produce safer and more efficient food supply chains (Kanicheril Ambikalekshmi et al., 2026).

Food quality monitoring and management: traceability focus

AI is mainly leveraged in traceability-related quality management, especially concerning aspects like identity, origin, and compliance with regulations. A case in point is AI-fueled systems playing a major role in confirming the geographical origin of products and ensuring compliance with certain religious or legal standards, for instance, halal authentication, by analyzing intricate

supply chain data to avert cross-contamination and secure ethical sourcing (Liu et al., 2025; Nawaz et al., 2025).

They are usually facilitated by digital records and automated classification or verification mechanisms. Here, automated classification turns to deep learning and computer vision techniques to categorize products objectively, thereby eliminating subjective manual inspections and at the same time producing quick and reliable verifications. As an illustration, these state-of-the-art visual tools are being used in the grading of meat quality or the assessment of fish freshness based on a thorough image analysis of gills and eyes (Shi et al., 2021; Yasin et al., 2023). At the same time, they depend on the unalterable digital records of blockchain technology that keeps track of every transaction in a secure way to create a transparent and tamper-proof history of a product's traceability (Femimol and Joseph, 2025; Stanescu et al., 2025).

Among the main challenges are the authentication of products and the harmonization of traceability along the different stages of the value chain. More specifically, product authentication refers to employing sophisticated instrumental methods such as biosensors, spectroscopy, and non-destructive optical techniques to authenticate scientifically the freshness and quality of seafood and meat, which are among the most perishable items (Kundu et al., 2025; Nisenbaum et al., 2025). On the other hand, harmonizing traceability is a matter of breaking through the existence of data silos by putting in place a shared digital framework and using smart contracts to guarantee not only the interoperability but also the quality consistency of tracking in the context of global networks (Singh, 2025; Stanescu et al., 2025).

Often, AI is coupled with sensing technologies and secure data infrastructures to enable complete monitoring of the product journey (Alvarez-García et al., 2024). By integrating the live data coming from IoT-enabled sensors such as biospeckle lasers for detecting contamination or spectral cameras for non-destructive testing with decentralized blockchain networks, smart systems are capable of performing anomaly detection autonomously, issuing alerts immediately, and ensuring a detailed visibility from the farm to the table (Liu et al., 2025; Nisenbaum et al., 2025).

Food quality monitoring and management: food fraud prevention

Traceability-centered AI initiatives also play a role in the prevention of food fraud indirectly. With AI, authentication and verification processes are enhanced that enable the detection of discrepancies in product identity and origination. Such measures make the overall integrity control stronger even though they are not set up as fraud detection systems independently (Li et al., 2025).

Artificial intelligence is mainly used for monitoring purposes that do not harm the product. Within the field of inspection by means of vision and sensors, AI employs non-destructive methods such as hyperspectral imaging, FT-IR (Fourier-transform infrared), and Raman spectroscopy for independent product evaluation. As an example, these techniques along with machine learning models are utilized to rapidly pinpoint the spectral signatures and thus identify hidden adulterants, such as the presence of foreign substances in high-quality edible oils or chemical contaminants in milk, all of which is done while preserving the integrity of the sample (Ahranjani et al., 2026; Aqeel et al., 2024; Lim et al., 2025). Alongside, AI is also combined with freshness and spoilage markers to accurately evaluate the state of stored goods. By extracting data from the environment in real-time and monitoring storage-induced continuous physical and chemical changes, AI models are capable of early detection of quality loss, thus enhancing preservation methods to keep freshness and avoid spoilage to the extent that products fail to reach the consumers (Zhang et al., 2025).

Besides that, AI is also an essential component in process monitoring that keeps a continuous track of various aspects during the food production cycle. These smart systems keep an eye on the

parameters of production at the moment, leading to the swift spotting of any processing irregularities and thus making sure of high standards in quality control and data integrity in the supply chain as a whole. For example, these systems are able to monitor the changes that take place during drying, mixing, or any other manufacturing processes (Gbashi and Njobeh, 2024; Li et al., 2025; Zhang et al., 2025).

The chief problem areas consist mainly of the detection of a quality decline on a real-time or almost real-time basis. Specifically, the use of AI for monitoring signals of freshness and spoilage is aimed at promptly identifying the first signs of microbial contamination or chemical breakdown so that the whole batch does not get compromised. Managing deviations in processes, on the other hand, entails the development of algorithms that are capable of quickly signaling the presence of anomalous fluctuations in highly complex manufacturing settings (Gbashi and Njobeh, 2024; Zhang et al., 2025). Usually, these kinds of applications are found more in processing and Industry-oriented environments. From the standpoint of automation, AI is radically changing how manufacturing is carried out by giving machines the capability to independently react to real-time data, thereby operating without the need for human input. At the same time, smart inspection makes use of computer vision and spectral cameras right on conveyor belts to perform continuous and non-destructive product evaluations that then help to standardize quality grading and maximize production efficiency (Aqeel et al., 2024; Gbashi and Njobeh, 2024; Li et al., 2025).

AI-based tools facilitate rapid and precise identification of food quality defects and contaminants through techniques such as image recognition and computer vision. Besides enhancing the time taken for inspections, these tools also help in realizing full compliance with food safety standards and are indispensable in real-time monitoring both during production and transportation along the supply chain (Gbashi and Njobeh, 2024). On the one hand, AI technologies enable accurate forecasting of quality problems, efficient production process management, and reduction in the numbers of products that do not conform to standards. On the other hand, predictive models are instrumental in shelf-life estimation, which, coupled with proper storage, distribution, and supply chain decisions, ensures the freshness of products (Gbashi and Njobeh, 2024).

Conclusions

In conclusion, digital technologies offer a transformative opportunity for the agri-food industry, providing significant advantages in efficient, sustainable food safety and quality. Our bibliometric analysis confirms a rapid expansion in this field, particularly between 2008 and 2025. Analysis of 70 core papers indicates that artificial intelligence, machine learning, quality control, computer vision, and food safety have been the focus of research. However, a large percentage of these papers are still review-based, suggesting that, while the potential is considered very high, empirical studies and field implementation remain substantially limited. At present, AI in the food industry primarily focuses on detection, monitoring, and traceability, and these efforts still fall short of fully autonomous systems. After analyzing the existing literature, identifying its main application areas and new areas requiring exploration, this paper serves as an excellent starting point for a more comprehensive study.

AI-powered quality control addresses public health and economic problems much more directly than laboratory measurements. Unsafe food consumption remains the leading cause of illness worldwide. In addition, product recalls and food fraud result in substantial financial losses for the industry. In contrast to traditional inspection methods, which are time-consuming and reactive, machine learning and AI-based systems offer proactive, autonomous defense mechanisms. They can identify supply chain risks early. AI-based systems, by turning reactive

into predictive models, are not only able to help reduce food waste but also to protect global food security, which is the main aim of sustainability.

For future research, the thematic map analysis conducted in this study identifies several crucial areas for exploration. 'Niche themes' such as biosensors and molecular food analysis, alongside 'emerging themes' like nanoparticle-assisted sensing and non-destructive detection technologies, represent the future focal points of both academic and industrial endeavors. The integration of AI models with non-destructive optical instruments, such as NIRS, Raman spectroscopy, HSI, and biospeckle lasers, significantly enhances real-time quality monitoring capabilities without compromising product integrity. Furthermore, the integration of deep learning with surface-enhanced Raman scattering (SERS), colorimetric biosensors, and aptasensors engineered with carbon- or metal-based nanoparticles enables rapid, molecular-level detection of trace chemical contaminants, foodborne pathogens, and food adulterants. Addressing the current literature gaps in these areas will help researchers design accurate, portable traceability networks.

Despite these highly promising developments and laboratory-scale successes, the full integration and scalability of AI in the food industry face substantial barriers. The main barrier is the scarcity of high-quality data; the natural complexity and heterogeneity of food matrices, combined with incomplete or poorly annotated datasets, severely limit the accuracy and generalizability of machine learning algorithms. Additionally, infrastructure deficits, such as the high implementation costs of IoT networks and the cost of technical hardware, hinder widespread adoption, particularly for small and medium-sized enterprises. At the same time, the collection of sensitive commercial and consumer data raises significant privacy concerns, while the “black box” nature of complex deep learning models creates a lack of transparency that complicates regulatory approval and stakeholder trust.

Overcoming these barriers requires a collaborative ecosystem involving academia, governments, and technology providers. First, the industry must establish open-access data protocols to build mutual trust. It is equally important to update current regulatory frameworks. These new rules should actively support privacy-preserving methods like federated learning, as well as transparent models like XAI. Ultimately, the digitization of food quality and safety management extends far beyond sector-specific boundaries. It fits directly into the wider shift toward Industry 4.0 and Quality 4.0. By adopting these smart systems, the agri-food industry serves as a key driver of the global smart manufacturing revolution.

References

Agrawal K., Goktas P., Holtkemper M., Beecks C., Kumar N. (2025), AI-driven transformation in food manufacturing: a pathway to sustainable efficiency and quality assurance, *Frontiers in Nutrition*, 12, 1553942, https://doi.org/10.3389/fnut.2025.1553942

Ahranjani P.J., Dehghan K., Esfandiari Z., Ahranjani P.J. (2026), A systematic review of spectroscopic techniques for detecting milk adulteration, *Critical Reviews in Analytical Chemistry*, 56(4), pp. 1071-1102, https://doi.org/10.1080/10408347.2025.2477535

Alkanan Z.T., Altemimi A.B., Awlqadr F.H., Alkaisy Q.H., Hashemi S.M.B., Pratap-Singh A. (2025), Exploring the frontiers of food science: a comprehensive review of advanced magnetic resonance applications in food analysis, Q*uality Analysis, and Safety Assessment*, 13(7), e70643, https://doi.org/10.1002/fsn3.70643

Al-Thani M.J., Hadid M., Padmanabhan R., Kerbache L., Elomri A. (2025), Smart food supply chain management: A bibliometric and systematic review, *Food and Humanity*, 5, 100736, https://doi.org/10.1016/j.foohum.2025.100736

Alvarez-García W.Y., Mendoza L., Muñoz-Vílchez Y., Nuñez-Melgar D.C., Quilcate C. (2024), Implementing artificial intelligence to measure meat quality parameters in local market

traceability processes, *International Journal of Food Science and Technology*, 59(11), pp. 8058–8068, https://doi.org/10.1111/ijfs.17546

Aqeel M., Sohaib A., Iqbal M., Rehman H.U., Rustam F. (2024), Hyperspectral identification of oil adulteration using machine learning techniques, *Current Research in Food Science*, 8, pp. 100773, https://doi.org/10.1016/j.crfs.2024.100773

Armand T.P.T., Nfor K.A., Kim J.I., Kim H.C. (2024), Applications of artificial intelligence, machine learning, and deep learning in nutrition: a systematic review, *Nutrients*, 16(7), 1073, https://doi.org/10.3390/nu16071073

Aslam M., Aslam E., Shahbaz M. (2025), Emerging trends in food safety and quality management, *Insights-Journal of Health and Rehabilitation*, 3, pp. 851–859, https://doi.org/10.71000/dtdm8185

Beck K.L., Haiminen N., Agarwal A., Carrieri A.P., Madgwick M., Kelly J., Pylro V., Kawas, B., Wiedmann M., Ganda E. (2024), Development and evaluation of statistical and artificial intelligence approaches with microbial shotgun metagenomics data as an untargeted screening tool for use in food production, *msystems*, 9(11), e00840-24, https://doi.org/10.1128/msystems.00840-24

Bhavna, Neetu, Kathuria B., Kumari A., Sindhu S.C. (2024), Global perspectives on food safety and quality control standards: A comprehensive review, *Journal of Advances in Microbiology*, 24(12), pp. 217–232, https://doi.org/10.9734/jamb/2024/v24i12885

Cao R., Li J., Ding H., Zhao T., Guo Z., Li Y., Sun X., Wang F., Qiu J. (2025), Synergistic approaches of AI and NMR in enhancing food component analysis: A comprehensive review, *Trends in Food Science & Technology*, 156, 104852, https://doi.org/10.1016/j.tifs.2024.104852

Chhetri K.B. (2024), Applications of artificial intelligence and machine learning in food quality control and safety assessment, *Food Engineering Reviews*, 16(1), pp. 1–21, https://doi.org/10.1007/s12393-023-09363-1

Dhal S.B., Kar D. (2025), Leveraging artificial intelligence and advanced food processing techniques for enhanced food safety, quality, and security: a comprehensive review, *Discover Applied Sciences*, 7(1), 75, https://doi.org/10.1007/s42452-025-06472-w

Femimol R., Joseph L.N. (2025), A comprehensive review of blockchain with artificial intelligence integration for enhancing food safety and quality control, *Innovative Food Science & Emerging Technologies*, 102, 104019, https://doi.org/10.1016/j.ifset.2025.104019

Feng Y., Soni A., Brightwell G., Reis M.M., Wang Z., Wang J., Wu Q., Ding Y. (2024), The potential new microbial hazard monitoring tool in food safety: Integration of metabolomics and artificial intelligence, *Trends in Food Science & Technology*, 149, 104555, https://doi.org/10.1016/j.tifs.2024.104555

Fodor M., Matkovits A., Benes E.L., Jókai Z. (2024), The role of Near-Infrared Spectroscopy in food quality assurance: A review of the past two decades, *Foods*, 13(21), 3501, https://doi.org/10.3390/foods13213501

Gbashi S., Njobeh P.B. (2024), Enhancing food integrity through artificial intelligence and machine learning: a comprehensive review, *Applied Sciences*, 14(8), pp. 3421, https://doi.org/10.3390/app14083421

Gu C., Wang G., Zhuang W., Hu J., He X., Zhang L., Du Z., Xu X., Yin M., Yao Y., Sun X., Hu W.W. (2026), Artificial intelligence-enabled analysis methods and their applications in food chemistry, *Critical Reviews in Food Science and Nutrition*, 66(1), pp. 206–227, https://doi.org/10.1080/10408398.2025.2521648

Hadi M.S., Sugiono B.S.R., Mizar M.A., Witjoro A., Irvan M. (2024), Enhancing low-temperature long-time milk pasteurization process with a C4.5 algorithm-driven aiot system for real-time decision-making, *Journal of Food Process Engineering*, 47(4), e14606, https://doi.org/10.1111/jfpe.14606

Hassoun A., Jagtap S., Trollman H., Garcia-Garcia G., Abdullah N.A., Goksen G., Bader F., Ozogul F., Barba F.J., Cropotova J., Munekata P.E.S., Lorenzo J.M. (2023), Food processing 4.0: Current and future developments spurred by the fourth industrial revolution, *Food Control*, 145, 109507, https://doi.org/10.1016/j.foodcont.2022.109507

Ibarra-Muñoz L.A., Resendiz-Acosta G.G., Muñoz-García R., Alvarado-Mata L.Y., Sosa-Martínez J.D., Morales-Oyervides L., Montañez J., Balagurusamy N. (2025), Artificial intelligence in the food and bioprocess industries: Addressing food security challenges, *Food and Humanity*, 5, 100818, https://doi.org/10.1016/j.foohum.2025.100818

Ince V., Bader-El-Den M., Alderton J., Arabikhan F., Sari O.F., Sansom A. (2025), Machine learning-based prediction of *Clostridium* growth in pork meat using explainable artificial intelligence, *Journal of Food Science and Technology*, 63, pp. 310–323, https://doi.org/10.1007/s13197-024-06187-7

Izquierdo-Bueno I., Moraga J., Cantoral J.M., Carbú M., Garrido C., González-Rodríguez V.E. (2024), Smart viniculture: applying artificial intelligence for improved winemaking and risk management, *Applied Sciences*, 14(22), 10277, https://doi.org/10.3390/app142210277

Jayan H., Yin L., Zhou R., Zou X., Guo Z. (2025), Future horizons of Raman spectroscopy in food science: Emerging techniques and innovations for enhanced analysis, *Food Chemistry*, 493, 145777, https://doi.org/10.1016/j.foodchem.2025.145777

Kanicheril Ambikalekshmi A., Pushparaj P., Cherian E., Rajan R., Mohan L. (2026), Advancing food safety through artificial intelligence: a detailed review of monitoring and detection technologies, *Food Safety and Health*, 4(1), pp. 82–90, https://doi.org/10.1002/fsh3.70050

Karchiyappan T., Ettiyagounder P., Selvaraj P.S., Ramanujam K. (2025), Transforming waste into value: Advancements in protein recovery and functional product development from wastewater sources, *Desalination and Water Treatment*, 321, 101044, https://doi.org/10.1016/j.dwt.2025.101044

Kilinc I., Kilinc B., Takma C., Gevrekci Y. (2025), Smart tools and artificial intelligence for enhanced quality and safety in agriculture, fisheries, and aquaculture: A review, *Iranian Journal of Fisheries Sciences*, 24(4), pp. 913–951, https://doi.org/10.22092/ijfs.2025.134035

Kim E., Kim D., Cai Y., Yang S.M., Kim J., Kim H.Y. (2025), Direct detection and differentiation of the *Vibrio harveyi* clade using MALDI-TOF MS integrated with artificial intelligence for effective outbreak management, *Food Chemistry*, 492, 145527, https://doi.org/10.1016/j.foodchem.2025.145527

Konfo T.R.C., Djouhou F.M.C., Hounhouigan M.H., Dahouenon-Ahoussi E., Avlessi F., Sohounhloue C.K.D. (2023), Recent advances in the use of digital technologies in agri-food processing: A short review, *Applied Food Research*, 3(2), 100329, https://doi.org/10.1016/j.afres.2023.100329

Koc G.D., Koc C., Koc A.U. (2026), Artificial intelligence-based pollen classification machine in apiculture: design, implementation and evaluation, *Journal of the Science of Food and Agriculture*, 106(2), pp. 1143–1158, https://doi.org/10.1002/jsfa.70238

Koushki M., Amiri-Dashatan N., Pourghadamyari H., Khodabandehloo H., Bagheri F., Farahani M., Tayebi L. (2024), An overview of the relationships between the food industry and nanotechnology, *Applied Food Biotechnology*, 11(2), e7, https://doi.org/10.22037/afb.v11i2.46737

Kumagai Y., Gilmour S., Ota E., Momose Y., Bilano V.L., Kasuga F., Sekizaki T., Shibuya K. (2015), Estimating the burden of foodborne diseases in Japan, *Bulletin of the World Health Organization*, 93, pp. 540-549, http://dx.doi.org/10.2471/BLT.14.148056

Kundu M., Vashisth A., Krishnan P. (2025), Instrumental detection of fish freshness in research and food industry: a review, *Journal of Food Science and Technology*, 63, pp. 22-50, https://doi.org/10.1007/s13197-025-06497-4

Li C., Li J., Wang Y. (2025), Data integrity of food and machine learning: Strategies, advances and prospective, *Food Chemistry*, 480, 143831, https://doi.org/10.1016/j.foodchem.2025.143831

Li D., Bai L., Wang R., Ying S. (2024), Research progress of machine learning in extending and regulating the shelf life of fruits and vegetables, *Foods*, 13(19), 3025, https://doi.org/10.3390/foods13193025

Liakos K.G., Athanasiadis V., Bozinou E., Lalas S.I. (2025), Machine learning for quality control in the food industry: A Review, *Foods*, 14(19), 3424, https://doi.org/10.3390/foods14193424

Lim H., Lee S.Y., Kim J.Y., Shin Y.J., Jang Y., Kim H., Kim B.H., Ahn S. (2025), Comparison of machine learning models for classifying edible oils using Fourier-transform infrared

spectroscopy, *Bulletin of the Korean Chemical Society,* 46(2), pp. 131-137, https://doi.org/10.1002/bkcs.12932

Liu C., Xu D., Dong X., Huang Q. (2022), A review: Research progress of SERS-based sensors for agricultural applications, *Trends in Food Science & Technology*, 128, pp. 90–101, https://doi.org/10.1016/j.tifs.2022.07.012

Liu Z., Wang S., Zhang Y., Feng Y., Liu J., Zhu H. (2023), Artificial intelligence in food safety: a decade review and bibliometric analysis, *Foods*, 12(6), 1242, https://doi.org/10.3390/foods12061242

Liu Z., Yu X., Liu N., Liu C., Jiang A., Chen L. (2025), Integrating AI with detection methods, iot, and blockchain to achieve food authenticity and traceability from farm-to-table, *Trends in Food Science & Technology*, 158, 104925, https://doi.org/10.1016/j.tifs.2025.104925

Luo Y., Zhang M., Yu Q., Mujumdar A.S., Rui L. (2025), Intelligent control for improving the quality of fresh meat products with rich lipid in cold chain logistics: research status, challenge, and potential applications, *Critical Reviews in Food Science and Nutrition*, 8877-8904, https://doi.org/10.1080/10408398.2025.2512221

Magdas D.A., Hategan A.R., David M., Berghian-Grosan C. (2025), The journey of artificial intelligence in food authentication: from label attribute to fraud detection, *Foods*, 14(10), 1808, https://doi.org/10.3390/foods14101808

Melendreras C., Montero J., Costa-Fernández J.M., Soldado A. (2026), Trends on vibrational spectroscopy tools in the agri-food sector, *Analytical and Bioanalytical Chemistry*, 418, pp.15–22, https://doi.org/10.1007/s00216-025-06166-7

Mohammadi E., Rahimian M., Panahi B. (2025), Bridging the gap: Phage manufacturing processes from laboratory to agri-food industry, *Virus Research*, 353, 199537, https://doi.org/10.1016/j.virusres.2025.199537

Mor S., Gunay B., Zanotti M., Galvani M., Pagliara S., Sangaletti L. (2025), Current opportunities and trends in the gas sensor market: a focus on e-noses and their applications in food industry, *Chemosensors*, 13(5), 181, https://doi.org/10.3390/chemosensors13050181

Moskvin G., Spakovica E. (2006), Development of intelligent technologies for consumers protection, In: *Economic Science for Rural Development Conference Proceedings*, 11, pp. 233-242.

Movahedi S., Bahramian F., Ahmadi M., Pouyanfar N., Masoudifar R., Ghalkhani M., Hussain C.M., Keçili R., Siavashy S., Ghorbani-Bidkorpeh F. (2025), Next-generation microfluidics based on artificial intelligence: Applications for food sample analysis, *Microchemical Journal*, 212, 113395, https://doi.org/10.1016/j.microc.2025.113395

Naseem S., Rizwan M. (2025), The role of artificial intelligence in advancing food safety: A strategic path to zero contamination, *Food Control*, 175, 111292, https://doi.org/10.1016/j.foodcont.2025.111292

Nawaz A., Afzal A., Khatibi A., Shankar A., Madan H., Faisal H.S., Shahbaz A., Usman I., Zulfiqar N., Saeed F., Ahmed A., Imran A., Afzaal M., Karni A., Ahmed F., Akram N., Rasheed M., Islam F. (2025), Role of artificial intelligence in halal authentication and traceability: A concurrent review, *Food Control*, 169, 111003, https://doi.org/10.1016/j.foodcont.2024.111003

Nisenbaum M., Agustinelli S.P., Guzmán M.N., Murialdo S.E. (2025), Biospeckle laser for real-time monitoring of water and food samples: Enhancing contamination detection and quality control in field applications, *Instrumentation Science & Technology*, 54(2), pp. 137-171, https://doi.org/10.1080/10739149.2025.2506110

Njiru J.M., Njeru E., Kang'iri J., Lunani I., Rotich H., Muriira G., Tombito C., Nyaboga E.N. (2025), Food fraud in selected sub-Saharan Africa countries: a wake-up call to national regulatory bodies to support enforcement and food safety, *Frontiers in Food Science and Technology*, 5, 1499271, https://doi.org/10.3389/frfst.2025.1499271

Parra-López C., Abdallah S.B., Hassoun A., Jagtap S., Garcia-Garcia G., Ben Hassen T., Trollman H., Trollman F., Carmona-Torres C. (2025), Digital and Industry 4.0 technologies in olive farming and industry: Recent applications and future outlook, *Smart Agricultural Technology*, 12, 101376, https://doi.org/10.1016/j.atech.2025.101376

Pawde S., Dave J. (2025), Applications of soft matter physics in food science: from molecular interactions to macro-scale food structures, *Sustainable Food Technology*, 3(4), pp. 979-1004, https://doi.org/10.1039/d5fb00172b

Pennells J., Watkins P., Bowler A., Watson N.J., Knoerzer K. (2025), Mapping the AI landscape in food science and engineering: A bibliometric analysis enhanced with interactive digital tools and company case studies, *Food Engineering Reviews*, 17, pp. 465–489, https://doi.org/10.1007/s12393-025-09413-w

Pereira J., Mota A., Couto P., Valente A., Serôdio C. (2025), Potential use of BME development kit and machine learning methods for odor identification: A case study, *Applied Sciences*, 15(17), 9687, https://doi.org/10.3390/app15179687

Peres F.A.P., Bondarczuk B.A., Gomes L.d.C., Jardim L.d.C., Corrêa R.G.d.F., Baierle I.C. (2025), Advances in food quality management driven by industry 4.0: A systematic review-based framework, *Foods*, 14(14), 2429, https://doi.org/10.3390/foods14142429

Radu E., Dima A., Dobrota E.M., Badea A.M., Madsen D.Ø., Dobrin C., Stanciu S. (2023), Global trends and research hotspots on HACCP and modern quality management systems in the food industry, *Heliyon*, 9(7), e18232, https://doi.org/10.1016/j.heliyon.2023.e18232

Ramachandran R.P., Clément A., Erkinbaev C. (2025), Miniaturized spectroscopy and AI-driven probes in food industry automation, *Food Research International*, 214, 116646, https://doi.org/10.1016/j.foodres.2025.116646

Revelou P.K., Tsakali E., Batrinou A., Strati I.F. (2025), Applications of machine learning in food safety and HACCP monitoring of animal-source foods, *Foods,* 14(6), 922, https://doi.org/10.3390/foods14060922

Saha D., Padhiary M., Chandrakar N. (2025), AI vision and machine learning for enhanced automation in food industry: A systematic review, *Food and Humanity*, 4, 100587, https://doi.org/10.1016/j.foohum.2025.100587

Semercioz-Oduncuogl, A.S., Luning P.A. (2025), Industry 4.0 technologies in quality and safety control systems in food manufacturing: A systematic techno-managerial analysis on benefits and barriers, *Trends in Food Science & Technology*, 163, 105144, https://doi.org/10.1016/j.tifs.2025.105144

Shan F., Liu L., Li L., Wang W., Bi Y., Li M. (2025), Management, safety, and efficacy evaluation of nutraceutical and functional food: A global perspective, *Comprehensive Reviews in Food Science and Food Safety*, 24(4), e70222, https://doi.org/10.1111/1541-4337.70222

Shi W., Chen L. (2024), Multi-scale resnet Integrated with attention mechanism for enhanced wheat freshness diagnosis based on biophotonics, *Acta Scientiarum Polonorum Technologia Alimentaria*, 23(4), pp. 525–535, https://doi.org/10.17306/J.AFS.001288

Shi Y., Wang X., Borhan M.S., Young J., Newman D., Berg E., Sun X. (2021), A review on meat quality evaluation methods based on non-destructive computer vision and artificial intelligence technologies, *Food Science of Animal Resources*, 41(4), pp. 563–588, https://doi.org/10.5851/kosfa.2021.e25

Singh D. (2025), Harnessing artificial intelligence to safeguard food quality and safety, *Journal of Food Protection*, 88(11), 100621, https://doi.org/10.1016/j.jfp.2025.100621

Stanescu S.G., Ionescu C.A., Ștefan M.C., Ionescu L., Bondac G.T., Cristea A.M. (2025), Digitalization and blockchain integration in agri-food supply chains: towards a resilient, circular, and sustainable future, *Sustainability*, 17(20), 9276, https://doi.org/10.3390/su17209276

Taneja A., Nair G., Joshi M., Sharma S., Sharma S., Jambrak A.R., Roselló-Soto E., Barba F.J., Castagnini J.M., Leksawasdi N., Phimolsiripol Y. (2023), Artificial Intelligence: Implications for the agri-food sector, *Agronomy*, 13(5), 1397, https://doi.org/10.3390/agronomy13051397

Vanaraj R., Bincy I.P., Mayakrishnan G., Kim I.S., Kim S.C. (2025), A systematic review of the applications of electronic nose and electronic tongue in food quality assessment and safety, *Chemosensors*, 13(5), 161, https://doi.org/10.3390/chemosensors13050161

Wang D., Zhang M., Mujumdar A.S., Yu D. (2022), Advanced detection techniques using artificial intelligence in processing of berries, *Food Engineering Reviews*, 14(1), pp. 176–199, https://doi.org/10.1007/s12393-021-09298-5

Wang Y., Wang Y., Wang A., Humayun M., Bououdina M. (2025), Machine learning advances in food detection technologies, *Journal of Food Composition and Analysis*, 148, 108596, https://doi.org/10.1016/j.jfca.2025.108596

WHO (World Health Organization), (2026), *Food Safety*, Available at: https://www.who.int/news-room/fact-sheets/detail/food-safety

Wu X., Liang X., Wang Y., Wu B., Sun J. (2022), Non-destructive techniques for the analysis and evaluation of meat quality and safety: A review, *Foods*, 11(22), 3713, https://doi.org/10.3390/foods11223713

Yasin E.T., Ozkan I.A., Koklu M. (2023), Detection of fish freshness using artificial intelligence methods, *European Food Research and Technology*, 249(8), pp. 1979–1990, https://doi.org/10.1007/s00217-023-04271-4

Yin B., Tan G., Muhammad R., Liu J., Bi J. (2025), AI-powered innovations in food safety from farm to fork, *Foods*, 14(11), 1973, https://doi.org/10.3390/foods14111973

Yu Q., Zhang M., Mujumdar A.S., Li J. (2024), AI-based additive manufacturing for future food: Potential applications, challenges and possible solutions, *Innovative Food Science & Emerging Technologies*, 92, 103599, https://doi.org/10.1016/j.ifset.2024.103599

Zatsu V., Shine A., Tharakan J.M., Peter D., Ranganathan T.V., Alotaibi S.S., Mugabi R., Muhsinah A.B., Waseem M., Nayik G.A. (2024), Revolutionizing the food industry: The transformative power of artificial intelligence-a review, *Food Chemistry: X*, 24, 101867, https://doi.org/10.1016/j.fochx.2024.101867

Zhang F., Alizadeh Sani M., Khezerlou A., Rezvani-Ghalhari M., Lin X., Liu R., Assadpour E., Wang X., Yang T., Wang J., Jafari S.M. (2025), Advances in aptasensors engineered with carbon nanomaterials for food safety monitoring, *Advances in Colloid and Interface Science*, 346, 103665, https://doi.org/10.1016/j.cis.2025.103665

Zhang L., Liao B., Liu D., Jiang Q., Sun Q. (2025), Artificial Intelligence empowered evolution in medicine food homology: Innovations, challenges, and future prospects, *Food Bioscience*, 69, 106928, https://doi.org/10.1016/j.fbio.2025.106928

Zhu B., Talib H.H.A., Hamamurad Q. (2024), A bibliometric analysis of quality and food safety management in the food development industry, *Journal of Infrastructure, Policy and Development*, 8(8), 5776, https://doi.org/10.24294/jipd.v8i8.5776

Ziani I., Bouakline H., El Guerraf A., El Bachiri A., Fauconnier M.L., Sher F. (2025), Integrating AI and advanced spectroscopic techniques for precision food safety and quality control, *Trends in Food Science & Technology*, 156, pp.104850, https://doi.org/10.1016/j.tifs.2024.104850

Zong B., Wu S., Yang Y., Li Q., Tao T., Mao S. (2025), Smart gas sensors: recent developments and future prospective, *Nano-Micro Letters*, 17(1), 54, https://doi.org/10.1007/s40820-024-01543-w

Cite:

Kılıç, A., Hendek, M., & Uslu, D. (2026). Bibliometric analysis of artificial intelligence applications in food quality control and safety. *Ukrainian Food Journal, 15*(2), 566–587. https://doi.org/10.24263/2304-974X-2026-15-2-17

Instructions for authors

Dear colleagues!

The Editorial Board of scientific periodical
Ukrainian Food Journal
invites you to publish your research findings in our journal

Manuscripts should present original research that has not been previously published and is not under consideration for publication elsewhere. Submission of the manuscript implies that its publication has been approved by all co-authors and by the appropriate institutional authorities at the organization where the research was conducted.

A cover letter to the editor is mandatory and should include a brief description of the research topic, its novelty and significance. The letter must also confirm that all authors agree to submit the manuscript to the Ukrainian Food Journal and that the work is original and authored solely by the listed contributors.

Manuscript requirements

Authors must prepare the manuscript according to the guide for authors. Editors reserve the right to adjust the style to certain standards of uniformity.

Language – English

Manuscripts should be submitted in Word.

Use 1.0 spacing and 2 cm margins.

Use a normal font 14-point Times New Roman for text, tables, and in the figure captions.

Present tables and figures in the text of manuscript.

Consult a recent issue of the journal for a style check.

Number all pages consecutively.

Abbreviations should be defined on first appearance in text and used consistently thereafter. No abbreviation should be used in title and section headings.

Please submit math equations as editable text and not as images (It is recommend software application MathType or Microsoft Equation Editor).

Minimal size of the article (without the Abstract and References) is 10 pages. For review article is 25 pages (without the Abstract and References).

Manuscript should include:

Title (should be concise and informative). Avoid abbreviations in it.

Authors' information: the name(s) of the author(s); the affiliation(s) of the author(s), city, country. One author has been designated as the corresponding author with e-mail address. If available, the 16-digit ORCID of the author(s) information on the title page.

Declaration of interest

Author Contribution Statement

Abstract. The **abstract** should contain the following mandatory parts:

Introduction provides a rationale for the study (2–3 lines).

Materials and methods briefly describe the materials and methods used in the study (3–5 lines).

Results and discussion describe the main findings (20–26 lines).

Conclusions provides the main conclusions (2–3 lines).

The abstract should not contain any undefined abbreviations or references to the articles.

Keywords. Immediately after the abstract provide 4 to 6 keywords.

Text of manuscript

References

Manuscripts should be divided into the following sections:

- **Introduction**
- **Materials and methods**
- **Results and discussion**
- **Conclusions**
- **References**

Introduction. Provide a background avoiding a detailed review of literature and declare the aim of the present research. Identify unexplored questions, prove the relevance of the topic. The Introduction section should not exceed 1.5 pages in length.

Materials and methods. Provide sufficient detail to enable an independent researcher to replicate the study. For methods that are already published, cite the original source and summarize the procedure briefly. Detailed descriptions are required only for new techniques or significant modifications of existing methods.

Results and discussion. Results should be presented clearly and concisely, supported by appropriate tables and/or figures. The significance of the findings should be discussed in the context of existing literature, highlighting similarities, differences, and potential implications.

Conclusions. Conclusions should be clearly derived from the study's findings and summarized briefly in a separate Conclusion section.

Acknowledgments (if necessary). Acknowledgments of individuals, grants, or funding sources should be included in a separate section. List all persons who contributed assistance during the research. Names of funding organizations must be written in full.

Organize your article into clearly defined sections and, if necessary, subsections. Each subsection should have a concise and descriptive heading.

References

Please, check references carefully.

The list of references should include works that are cited in the text and that have been published or accepted for publication.

All references mentioned in the reference list are cited in the text, and vice versa.

Citation

Cite references in the text by surname and year in parentheses:

- One author: (Smith, 2026)
- Two authors: (Smith & Jones, 2025)
- More than two authors: (Smith et al., 2021)

Some examples:

- The application of plant additives for food products is indeed a modern trend if the food industry (Ivanov et al., 2021).
- These results confirm the findings of Beker and Smith (2024).
- This effect has been widely studied (Feng et al., 2022a, b; Liu and Cheng, 2025; Lorenzo et al., 2005, 2012; Shevchenko, 2024).

Reference list

Reference list entries should be alphabetized by the last name of the first author. If available, DOIs should always be included as full DOI links (e.g., https://doi.org/xxxxx).

Journal article. Authors: surname + initials, separated by commas, & before last author; the publication year is in parentheses; the article title is in sentence case (only first word capitalized), no italics; the journal title is italicized, full name; volume number is italicized; issue number is in parentheses (not italicized); the page range (e.g., 7–36); DOI (if available) in URL format.

Example:

Ivanov, V., Shevchenko, O., Marynin, A., Stabnikov, V., Gubenia, O., Stabnikova, O., Shevchenko, A., Gavva, O., & Saliuk, A. (2021). Trends and expected benefits of the breaking edge food technologies in 2021–2030. *Ukrainian Food Journal, 10*(1), 7–36. https://doi.org/10.24263/2304-974X-2021-10-1-3

Book. Authors formatted the same as journal articles. Author, A. A. – surname followed by initials, if there are multiple authors, they are separated by commas, and an ampersand (&) is used before the last author; year of publication in parentheses, followed by a full stop (Year); book title italicized, sentence case; edition only if not first (e.g., 2nd ed., 4th ed.); place of publication required (City, Country); Publisher name written clearly (no “Inc.” or “Ltd.” if not needed).

Author, A. A. (Year). *Title of the book* (Edition). Place of publication: Publisher.

Examples:

Fellows, P. J. (2017). *Food processing technology: Principles and practice* (4th ed.). Cambridge, England: Woodhead Publishing.

Damodaran, S., & Parkin, K. L. (2017). *Fennema's food chemistry* (5th ed.). Boca Raton, FL: CRC Press.

Edited Book.

Editor, A. A. (Ed.). (Year). *Title of the book*. Place: Publisher.

Editor, A. A., & Editor, B. B. (Eds.). (Year). *Title of the book*. Place: Publisher.

Example:

Stabnikova, O., Shevchenko, O., Stabnikov, V., & Paredes-López, O. (Eds.). (2023). *Bioconversion of waste to value-added products.* Boca Raton, London, New York: CRC Press. https://doi.org/10.1201/9781003329671

Book Chapter. Author, A. A., & Author, B. B. (Year). Title of chapter. In Editor A. A. & Editor B. B. (Eds.), *Book title* (pp. xx–xx). Place: Publisher.

Example:

Topchii, O., Pasichniy, V., Marynin A., & Stabnikova, O. (2023). Biotransformation of collagen-containing meat materials into valuable product. In Stabnikova O., Shevchenko O., Stabnikov V., & Paredes-López O. (Eds.), *Bioconversion of waste to value-added products*, (pp. 37-68). Boca Raton, London, New York: CRC Press. https://doi.org/10.1201/9781003329671-2

Online document. Author, A. A. (Year). *Title of document*. Retrieved from https://xxxxxx or (if DOI is available):

Author, A. A. (Year). *Title of document*. https://doi.org/xxxxx

Examples:

Food and Agriculture Organization of the United Nations. (2019). *Food loss and waste reduction*. Retrieved from http://www.fao.org/food-loss-and-food-waste/en/

World Health Organization. (2020). *Food safety*. https://www.who.int/news-room/fact-sheets/detail/food-safet

Published conference paper (in proceedings).

Author, A. A., Author, B. B., & Author, C. C.**;** year in parentheses; paper title: sentence case, not italicized; "In" + editors (if available); *Proceedings title*, italicized; page range included (if available); Place of publication: Publisher.

Author, A. A., & Author, B. B. (Year). Title of paper. In Editor E. E. (Ed.), *Title of proceedings* (pp. xx–xx). Place: Publisher.

Example:

Marynin, A., & Pasychnyi, V. (2026). Biotechnological approaches in food packaging. In A. Brown & M. Smith (Eds.), Proceedings of the International Food Engineering Conference (pp. 120–128). London, England: Springer.

Conference paper (online proceedings). Author, A. A. (Year). Title of paper. In Title of conference proceedings. Retrieved from URL

Example:

Marynin, A., & Pasychnyi, V. (2026). Biotechnological approaches in food packaging. In *Proceedings of the International Food Engineering Conference*. Retrieved from https://www.ifec2026.org/proceedings

Dissertation retrieved from an institutional repository. Author, A. A. (Year). Title of dissertation (Doctoral dissertation or Master's thesis). Name of Institution. Retrieved from URL

Example:

Smith, J. A. (2020). *Development of biodegradable edible coatings for fresh produce preservation (*Doctoral dissertation). University of California, Davis. Retrieved from https://escholarship.org/uc/item/xxxxx

Figures

All figures must be created using a graphic editor with Arial font.

The font size on the figures and the text of the article should be the same.

Black and white graphic with no shading should be used.

The figure elements (lines, grid, and text) should be presented in black (not gray) colour.

Figure parts should be denoted by lowercase letters (a, b, etc.).

All figures are to be numbered using Arabic numerals.

Figures should be cited in text in consecutive numerical order.

Place figure after its first mentioned in the text.

Figure captions begin with the term Figure in bold type, followed by the figure number, also in bold type.

Each figure should have a caption describing what the figure depicts in bold type.

Submit all figures along with the corresponding Excel files containing the graph data as separate attachments.

If your manuscript includes figures previously published elsewhere, you must obtain permission from the copyright owner(s) prior to submission.

Tables

Number tables consecutively in accordance with their appearance in the text.

Place footnotes to tables below the table body and indicate them with superscript lowercase letters.

Place table after its first mentioned in the text.

Ensure that the data presented in tables do not duplicate results described elsewhere in the article.

Suggesting / excluding reviewers

Authors may suggest reviewers and/or request the exclusion of certain individuals when submitting their manuscripts.

When suggesting reviewers, authors should make sure they are totally independent and not connected to the work in any way. When suggesting reviewers, the Corresponding Author must provide an institutional email address for each suggested reviewer. Please note that the Journal may not use the suggestions, but suggestions are appreciated and may help facilitate the peer review process.

Submission

Email for all submissions and other inquiries:

ufj_nuft@meta.ua

Шановні колеги!

Редакційна колегія наукового періодичного видання «**Ukrainian Food Journal**» запрошує Вас до публікації результатів наукових досліджень.

Вимоги до оформлення статей

Мова статей – англійська.

Мінімальний обсяг статті – **10 сторінок** формату А4 (без врахування анотацій і списку літератури)**.**

Для всіх елементів статті шрифт – **Times New Roman**, кегль – **14**, інтервал – 1.

Всі поля сторінки – по 2 см.

Структура статті:

1. **Назва статті.**
2. Автори статті (ім'я та прізвище повністю, приклад: Денис Озерянко).
3. *Установа, в якій виконана робота.*
4. Анотація. **Обов'язкова** структура анотації:
   - Вступ (2–3 рядки).
   - Матеріали та методи (до 5 рядків)
   - Результати та обговорення (пів сторінки).
   - Висновки (2–3 рядки).
6. Ключові слова (3–5 слів, але не словосполучень).

Пункти 2–6 виконати англійською і українською мовами.

7. Основний текст статті. Має включати такі обов'язкові розділи:
   - Вступ
   - Матеріали та методи
   - Результати та обговорення
   - Висновки
   - Література.

За необхідності можна додавати інші розділи та розбивати їх на підрозділи.

8. Авторська довідка (Прізвище, ім'я та по батькові, вчений ступінь та звання, місце роботи, електронна адреса або телефон).
9. Контактні дані автора, до якого за необхідності буде звертатись редакція журналу.

Рисунки виконуються якісно. Скановані рисунки не приймаються. Розмір тексту на рисунках повинен бути **співрозмірним** (!) тексту статті. **Фотографії можна використовувати лише за їх значної наукової цінності.**

Фон графіків, діаграм – лише білий. Колір елементів рисунку (лінії, сітка, текст) – чорний (не сірий).

Рисунки та графіки EXCEL з графіками додатково подаються в окремих файлах.

Скорочені назви фізичних величин в тексті та на графіках позначаються латинськими літерами відповідно до системи СІ.

У списку літератури повинні переважати сучасні англомовні статті та монографії.

Оформлення цитат у тексті статті

Кількість авторів статті	Приклад цитування у тексті
1 автор	(Arych, 2026)
2 автора	(Kuievda and Bront, 2026)
3 і більше авторів	(Bazopol et al., 2023)

Цитати у дужках розміщуються за алфавітом.

Приклад тексту із цитуванням: It is known (Arych, 2026; Bazopol et al., 2023), the product yield depends on temperature, but, there are some exceptions (Kuievda and Bront, 2026).

Правила оформлення списку літератури

Список літератури сортується за алфавітом, літературні джерела не нумеруються.

Стаття в журналі.

Автори: прізвище та ініціали; автори відокремлюються комами; перед останнім автором ставиться знак &. Рік публікації подається в круглих дужках. Назва статті оформлюється малими літерами (з великої літери пишеться лише перше слово назви, перше слово після двокрапки та власні назви), без курсиву. Назва журналу подається повністю та курсивом, всі основні слова у назві журналу вишуться з великої літери. Номер тому виділяється курсивом. Номер випуску подається в круглих дужках без курсиву. Після цього наводиться діапазон сторінок (наприклад, 7–36). DOI (за наявності) подається у форматі URL.

Приклад:

Ivanov, V., Shevchenko, O., Marynin, A., Stabnikov, V., Gubenia, O., Stabnikova, O., Shevchenko, A., Gavva, O., & Saliuk, A. (2021). Trends and expected benefits of the breaking edge food technologies in 2021–2030. *Ukrainian Food Journal, 10*(1), 7–36. https://doi.org/10.24263/2304-974X-2021-10-1-3

Книга.

Автори оформлюються так само, як і для журнальних статей: прізвище та ініціали; автори відокремлюються комами; перед останнім автором ставиться знак **&**. Рік видання подається в круглих дужках. Назва книги виділяється **курсивом** та оформлюється у **sentence case**. Номер видання зазначається лише у випадку, якщо це не перше видання (наприклад, *2nd ed.*, *4th ed.*). Обов'язково зазначаються **місце видання** (місто, країна або штат/провінція відповідно до APA 6) та назва видавництва.

Формат:

Author, A. A. (Year). *Title of the book* (Edition). Place of publication: Publisher.

Приклади:

Fellows, P. J. (2017). *Food processing technology: Principles and practice* (4th ed.). Cambridge, England: Woodhead Publishing.

Damodaran, S., & Parkin, K. L. (2017). *Fennema's food chemistry* (5th ed.). Boca Raton, FL: CRC Press.

Книга під редакцією.

Прізвище та ініціали редактора(ів) оформлюються аналогічно до авторів. Після прізвищ зазначається **(Ed.)** для одного редактора або **(Eds.)** для кількох редакторів.

Формат:

Editor, A. A. (Ed.). (Year). *Title of the book*. Place: Publisher.

Editor, A. A., & Editor, B. B. (Eds.). (Year). *Title of the book*. Place: Publisher.

Приклад:

Stabnikova, O., Shevchenko, O., Stabnikov, V., & Paredes-López, O. (Eds.). (2023). *Bioconversion of waste to value-added products*. Boca Raton, London, New York: CRC Press. https://doi.org/10.1201/9781003329671

Розділ книги.

Автор(и) розділу оформлюються за загальними правилами APA. Після назви розділу подається слово **In**, прізвища та ініціали редакторів із позначкою **(Ed.)** або **(Eds.)**, назва книги курсивом, сторінки розділу в дужках, місце видання та видавництво.

Формат:

Author, A. A., & Author, B. B. (Year). Title of chapter. In Editor A. A. & Editor B. B. (Eds.), *Book title* (pp. xx–xx). Place: Publisher.

Приклад:

Topchii, O., Pasichniy, V., Marynin, A., & Stabnikova, O. (2023). Biotransformation of collagen-containing meat materials into valuable product. In Stabnikova, O., Shevchenko, O., Stabnikov, V., & Paredes-López, O. (Eds.), *Bioconversion of waste to value-added products* (pp. 37–68). Boca Raton, London, New York: CRC Press. https://doi.org/10.1201/9781003329671-2

Електронний документ.

За наявності URL використовується фраза **Retrieved from**. Якщо документ має DOI, він подається у форматі URL.

Формат:

Author, A. A. (Year). *Title of document*. Retrieved from https://xxxxx

або

Author, A. A. (Year). *Title of document*. https://doi.org/xxxxx

Приклади:

Food and Agriculture Organization of the United Nations. (2019). *Food loss and waste reduction*. Retrieved from http://www.fao.org/food-loss-and-food-waste/en/

World Health Organization. (2020). *Food safety*. https://www.who.int/news-room/fact-sheets/detail/food-safety

Опублікована доповідь у матеріалах конференції.

Автори оформлюються за правилами APA. Назва доповіді подається без курсиву. Після слова **In** зазначаються редактори (за наявності), назва збірника матеріалів конференції курсивом, сторінки, місце видання та видавництво.

Формат:

Author, A. A., & Author, B. B. (Year). Title of paper. In Editor E. E. (Ed.), *Title of proceedings* (pp. xx–xx). Place: Publisher.

Приклад:

Marynin, A., & Pasychnyi, V. (2026). Biotechnological approaches in food packaging. In A. Brown & M. Smith (Eds.), *Proceedings of the International Food Engineering Conference* (pp. 120–128). London, England: Springer.

Доповідь у матеріалах онлайн-конференції (Conference paper in online proceedings)

Формат:

Author, A. A. (Year). Title of paper. In *Title of conference proceedings*. Retrieved from URL

Приклад:

Marynin, A., & Pasychnyi, V. (2026). Biotechnological approaches in food packaging. In *Proceedings of the International Food Engineering Conference*. Retrieved from https://www.ifec2026.org/proceedings

Дисертація з інституційного репозитарію (Dissertation retrieved from an institutional repository)

Після назви дисертації в круглих дужках зазначається тип роботи (*Doctoral dissertation* або *Master's thesis*), далі — назва установи та URL.

Формат:

Author, A. A. (Year). *Title of dissertation* (Doctoral dissertation or Master's thesis). Name of Institution. Retrieved from URL

Приклад:

Smith, J. A. (2020). *Development of biodegradable edible coatings for fresh produce preservation* (Doctoral dissertation). University of California, Davis. Retrieved from https://escholarship.org/uc/item/xxxxx

Зверніть увагу:

- у назві статті всі слова, крім першого, пишуться з малої літери;
- у назві журналу всі основні слова пишуться з великої літери;
- у назві книги або збірника матеріалів конференції всі слова пишуться з малої літери.

Список літератури оформлюється лише латиницею.

Елементи списку українською мовою потрібно транслітерувати. Для транслітерації з українською мови використовується паспортний стандарт.

Стаття надсилається за електронною адресою:

ufj_nuft@meta.ua

УДК 663/664

Ukrainian Food Journal публікує оригінальні наукові статті, короткі повідомлення, оглядові статті, новини та огляди літератури.

Тематика публікацій в Ukrainian Food Journal:

Харчова інженерія	Процеси та обладнання
Харчова хімія	Нанотехнології
Мікробіологія	Економіка та управління
Фізичні властивості харчових продуктів	Автоматизація процесів
Якість та безпека харчових продуктів	Упаковка для харчових продуктів

Періодичність виходу журналу 4 номери на рік.

Результати досліджень, представлені в журналі, повинні бути новими, мати чіткий зв'язок з харчовою наукою і представляти інтерес для міжнародного наукового співтовариства.

Ukrainian Food Journal індексується наукометричними базами:

- Index Copernicus (2012)
- EBSCO (2013)
- Google Scholar (2013)
- UlrichsWeb (2013)
- CABI full text (2014)
- Online Library of University of Southern Denmark (2014)
- Directory of Open Access scholarly Resources (ROAD) (2014)
- European Reference Index for the Humanities and the Social Sciences (ERIH PLUS) (2014)
- Directory of Open Access Journals (DOAJ) (2015)
- InfoBase Index (2015)
- Chemical Abstracts Service Source Index (CASSI) (2016)
- FSTA (Food Science and Technology Abstracts) (2018)
- Web of Science (Emerging Sourses Citaton Index) (2018)
- Scopus (2022)

Рецензія рукопису статті. Матеріали, представлені для публікування в «Ukrainian Food Journal», проходять «Подвійне сліпе рецензування» двома вченими, призначеними редакційною колегією: один є членом редколегії і один незалежний науковець.

Авторське право. Автори статей гарантують, що робота не є порушенням будь-яких авторських прав, та відшкодовують видавцю порушення даної гарантії. Опубліковані матеріали є правовою власністю видавця «**Ukrainian Food Journal**», якщо не узгоджено інше.

Детальна інформація про Журнал, інструкції авторам, приклади оформлення статті та анотацій розміщені на сайті:

http://ufj.nuft.edu.ua

Редакційна колегія

Головний редактор:

Олена Стабнікова, д-р., *Національний університет харчових технологій, Україна*

Члени міжнародної редакційної колегії:

Агота Гедре Райшене, д-р., *Литовський інститут аграрної економіки, Литва*
В. І. Вернадського НАН України
Бао Тхи Вуронг, д-р., *Університет Меконгу, В'єтнам*
Годвін Д. Ндоссі, професор, *Меморіальний університет Хуберта Кайрукі, Дар-ес-Салам, Танзанія*
Дора Марінова, професор, *Університет Кертіна, Австралія*
Егон Шніцлер, д-р, професор, *Державний університет Понта Гросси, Бразилія*
Ейрін Марі Скйондал Бар, д-р., професор*, Норвезький університет науки і техніки, Тронхейм, Норвегія*
Йорданка Стефанова, д-р, *Пловдівський університет "Паісій Хілендарскі", Болгарія*
Кірстен Брандт, професорр, *Університет Ньюкасла, Великобританія*
Крістіна Луїза Міранда Сілва, д-р., професор, *Португальський католицький університет – Біотехнологічний коледж, Португалія*
Крістіна Попович, д-р., доцент*, Технічний університет Молдови*
Лелівельд Хуб*, асоціація «Міжнародна гармонізаційна ініціатива», Нідерланди*
Марія С. Тапіа, професор, *Центральний університет Венесуели, Каракас, Венесуела*
Мойзес Бурачик, д-р., *Інститут сільськогосподарської біотехнології Покапіо (INDEAR), Покапіо, Аргентина*
Октавіо Паредес Лопес, д-р., проф, *Центр перспективних досліджень Національного політехнічного інституту, Мексика.*
Олександр Шевченко, д.т.н., проф., *Національний університет харчових технологій, Україна*
Рана Мустафа, д-р., *Глобальний інститут продовольчої безпеки, Університет Саскачевана, Канада*
Семіх Отлес, д-р., *проф, Університет Еге, Туреччина*
Соня Амарей, д-р., *проф, Університет «Штефан чел Маре», Сучава, Румунія*
Станка Дам'янова, д.т.н., проф., *Русенський університет «Ангел Канчев», філія Разград, Болгарія*
Стефан Стефанов, д.т.н., проф., *Університет харчових технологій, Болгарія*
Тетяна Пирог, д.б.н., проф., *Національний університет харчових технологій, Україна*
Умезуруйке Лінус Опара, професор, *Стелленбошський університет, Кейптаун, Південна Африка*
Шейла Кілонзі, *Університет Каратіна, Кенія*
Юлія Дзязько, д-р. хім. наук, с.н.с., *Інститут загальної та неорганічної хімії імені В. І. Вернадського НАН України*
Юн-Хва Пеггі Хсі, д-р, професор, *Університет Флориди, США*
Юрій Білан, д-р., проф., *Університет Томаша Баті в Зліні, Чехія*
Ясміна Лукінак, д.т.н., професор, *Університет Осієка, Хорватія*
Ясміна Лукінак, д-р, проф., *Осієкський університет, Хорватія.*

Члени редакційної колегії:

Агота Гедре Райшене, д-р., *Литовський інститут аграрної економіки, Литва*
Бао Тхи Вуронг, д-р., *Університет Меконгу, В'єтнам*
Валерій Мирончук, д-р. техн. наук, проф., *Національний університет харчових технологій, Україна*
Володимир Ковбаса, д-р. техн. наук, проф., *Національний університет харчових технологій, Україна*
Галина Сімахіна, д-р. техн. наук, проф., *Національний університет харчових технологій, Україна*
Годвін Д. Ндоссі, професор, *Меморіальний університет Хуберта Кайрукі, Дар-ес-Салам, Танзанія*
Дора Марінова, професор, *Університет Кертіна, Австралія*
Егон Шніцлер, д-р, професор, *Державний університет Понта Гросси, Бразилія*
Ейрін Марі Скйондал Бар, д-р., професор*, Норвезький університет науки і техніки, Тронхейм, Норвегія*
Йорданка Стефанова, д-р, *Пловдівський університет "Паісій Хілендарскі", Болгарія*
Кірстен Брандт, професорр, *Університет Ньюкасла, Великобританія*
Крістіна Луїза Міранда Сілва, д-р., професор, *Португальський католицький університет – Біотехнологічний коледж, Португалія*
Крістіна Попович, д-р., доцент*, Технічний університет Молдови*
Лада Шерінян, д-р. екон. наук, професор., *Національний університет харчових технологій, Україна*
Лелівельд Хуб*, асоціація «Міжнародна гармонізаційна ініціатива», Нідерланди*
Марія С. Тапіа, професор, *Центральний університет Венесуели, Каракас, Венесуела*
Мойзес Бурачик, д-р., *Інститут сільськогосподарської біотехнології Покапіо (INDEAR), Покапіо, Аргентина*
Октавіо Паредес Лопес, д-р., проф, *Центр перспективних досліджень Національного політехнічного інституту, Мексика.*
Олександр Шевченко, д.т.н., проф., *Національний університет харчових технологій, Україна*
Ольга Рибак, канд. техн. наук, доц., *Тернопільський національний технічний унівреситет імені Івана Пулюя, Україна*
Рана Мустафа, д-р., *Глобальний інститут продовольчої безпеки, Університет Саскачевана, Канада*
Семіх Отлес, д-р., *проф, Університет Еге, Туреччина*
Соня Амарей, д-р., *проф, Університет «Штефан чел Маре», Сучава, Румунія*
Станка Дам'янова, д.т.н., проф., *Русенський університет «Ангел Канчев», філія Разград, Болгарія*
Стефан Стефанов, д.т.н., проф., *Університет харчових технологій, Болгарія*
Тетяна Пирог, д-р. біол. наук, проф., *Національний університет харчових технологій, Україна*
Умезуруйке Лінус Опара, професор, *Стелленбошський університет, Кейптаун, Південна Африка*
Шейла Кілонзі, *Університет Каратіна, Кенія*
Юлія Дзязько, д-р. хім. наук, с.н.с., *Інститут загальної та неорганічної хімії імені В. І. Вернадського НАН України*
Юн-Хва Пеггі Хсі, д-р, професор, *Університет Флориди, США*
Ясміна Лукінак, д-р, проф., *Осієкський університет, Хорватія.*
Олексій Губеня (відповідальний секретар), канд. техн. наук, доц., *Національний університет харчових технологій, Україна.*

Наукове видання

Ukrainian Food Journal

Volume 15 Issue 2 2026

Том 15 № 2 2026

Підп. до друку 30.06.2026 р. Формат 70х100/16.
Обл.-вид. арк. 14.42. Ум. друк. арк. 14.54.
Гарнітура Times New Roman. Друк офсетний.
Наклад 100 прим. Вид. № 12н/26.

НУХТ. 01601 Київ–33, вул. Володимирська, 68

Свідоцтво про державну реєстрацію
друкованого засобу масової інформації
КВ 18964–7754Р
видане 26 березня 2012 року.